Theoretical Fluid Dynamics

SECOND EDITION

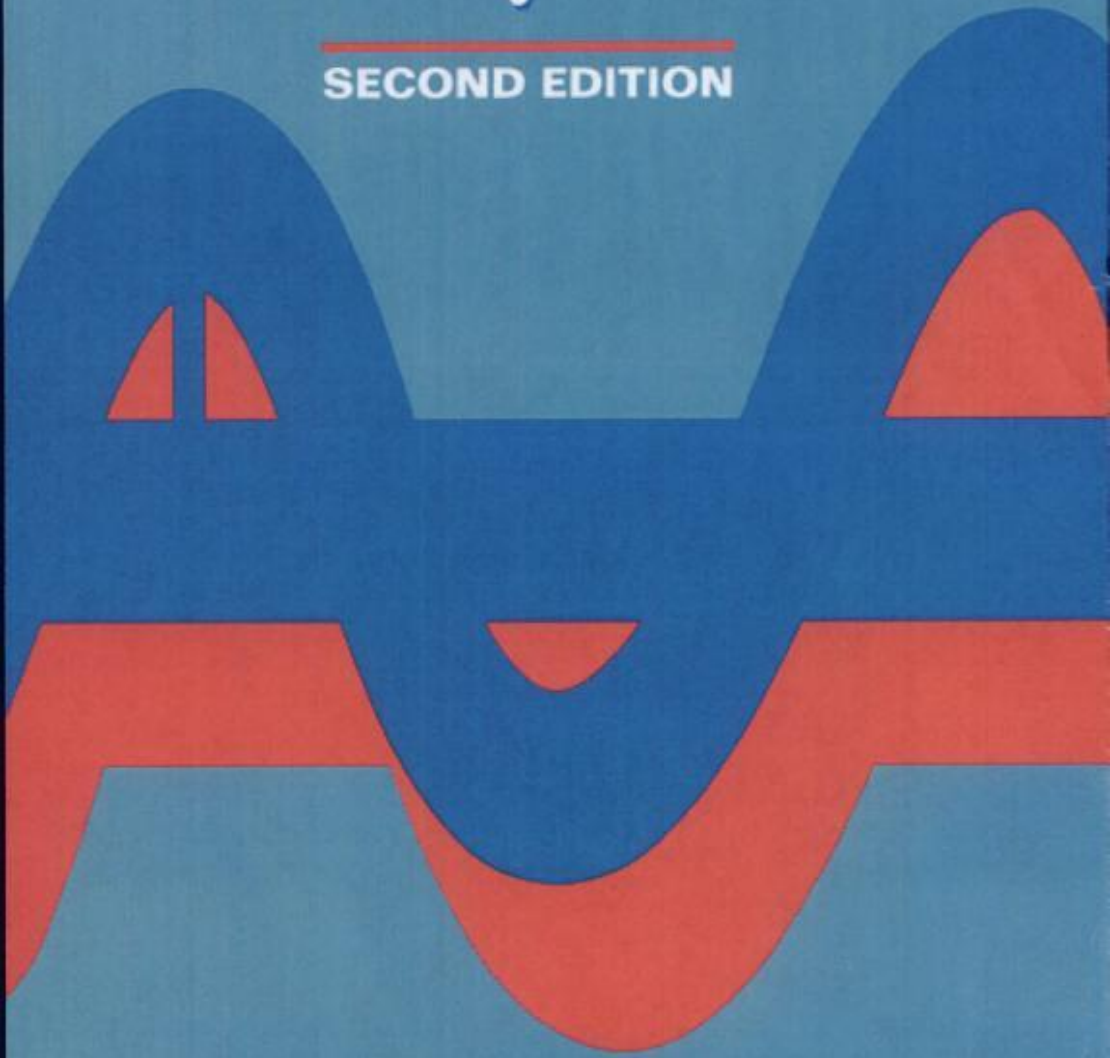

Bhimsen K. Shivamoggi

THEORETICAL FLUID DYNAMICS

This page intentionally left blank

Theoretical Fluid Dynamics

Second Edition

Bhimsen K. Shivamoggi

University of Central Florida
Orlando, Florida

A Wiley Interscience Publication
JOHN WILEY & SONS, INC.
New York • Chichester • Weinheim • Brisbane • Singapore • Toronto

This book is printed on acid-free paper.

Published simultaneously in Canada.

Library of Congress Cataloging in Publication Data:

Shivamoggi, Bhimsen K.
Theoretical fluid dynamics / Bhimsen K. Shivamoggi. — 2nd ed.
p. cm.
Includes bibliographical references and index.
ISBN 0-471-05659-6 (cloth : alk. paper)
1. Fluid dynamics. I. Title.
QA911.S463 1997
532'.05—dc21 97-10383

10 9 8 7 6 5 4 3 2 1

Seek therefore to find of what and how the world is made,
so that you may learn a better way of life.

—*Pythagoras*

TO MY MOTHER
WITH LOVE AND RESPECT

This page intentionally left blank

CONTENTS

This page intentionally left blank

Preface

Fluid flows both in nature and laboratory show many spectacular phenomena (see Professor Milton van Dyke's excellent photograph collection, An Album of Fluid Motion, Parabolic Press, Stanford, 1982). The remarkable periodicity of the vortex street in the wake of a circular cylinder, the structure and motion of vortex rings, the capillary instability of a liquid jet, convection cells in the form of hexagons, and the instability of the shear layer between two parallel streams are cases in point.

This book is concerned with a discussion of the dynamical behavior of a fluid. Drawing on a subject of enormous extent and variety, this book seeks to provide the readers with a sound and systematic account of the most important and representative types of fluid flow phenomena. At the same time, particular attention has been given to placing emphasis throughout on the most generally useful fundamental ideas of fluid dynamics. Nonetheless, some personal bias may be discernible occasionally, though I have tried to temper it by using the physical content as a criterion both in selecting a topic and in determining the extent to which it is discussed.

This book is addressed primarily to graduate students and researchers in applied mathematics and theoretical physics (graduate students and researchers in engineering will, nonetheless, find the ideas and formulations in this book very useful, as confirmed by some book reviews on the first edition). Accordingly, this book adopts a middle-of-the-road applied mathematician's approach (as opposed to the empiricism of the engineer and the abstract precision of the pure mathematician) which is, besides, thoroughly analytical.

However, even an introductory account of the main branches of fluid dynamics, like the one aimed at by this book, becomes comprehensive enough to make it difficult, if not impossible, to deal with the various topics with complete thoroughness. Consequently, many engineering details, like the skin-friction calculations in boundary layer theory (even though the skin-friction calculation was the primary objective of boundary-layer theory, in the first place), have been squeezed out of this book. Furthermore, the discussion is confined to Newtonian fluids, for which the coefficient of viscosity is independent of the rate of deformation of the fluid.

In the text, flows of an incompressible fluid have been given especially large coverage because of their central place in the subject. In the Bibliography provided at the end, I have tried to include some important papers and a few others relevant for the material in this book; this list is not to be construed as being complete. Furthermore, a few exercises have been provided at the end of each section. The

reader will find their solutions not only rewarding in enhancing, but also sometimes essential to understanding, the ideas and formulations discussed in this book.

The second edition, in addition to constituting an extensive rewrite of the text, incorporates the following features:

* refinements and additions of several mathematical developments and physical discussions
* addition of several new exercises
* updating several topics like stability and turbulence
* experimental information where pertinent
* addition of new material (Hamiltonian formulation, more on nonlinear water waves and nonlinear sound waves, more on stability of a fluid layer heated from below, Couette flow and shear flows, application of Arnol'd stability approach, equilibrium statistical mechanics of turbulence, two-dimensional turbulence, among others).

For the readership, an elementary background in fluid dynamics and some familiarity with the theory and the analytical methods (perturbation methods, in particular) of solution of differential equations are essential prerequisites.

Orlando, 1997 Bhimsen K. Shivamoggi

Acknowledgments

I wish to express my gratitude to Professor Mahinder Uberoi, who, as my former teacher, guide, and mountain-climbing partner, has been a constant source of encouragement. My gratitude is also due to Professor Willem Malkus who introduced me to hydrodynamic stability, and Professor Earl Dowell who introduced me to unsteady aerodynamics; these individuals have been sources of constant encouragement. I am very thankful to our department Chairman John Cannon for his enormous support and encouragement. Professors R. Moreau and A.S. Gupta gave detailed and helpful criticisms with the first edition of this book. The second edition of this book has benefited considerably from the helpful criticisms of the referees. The preparation of the book material has been facilitated by the visiting appointments I held in the recent years at Observatoire de Nice (France), Technische Universiteit Eindhoven (The Netherlands), Kyoto University (Japan), and University of Newcastle (Australia).

My sincere thanks are due to Jackie Callahan for the exemplary patience, dedication, and skill with which she did the whole typing job. My thanks are due to Ronee Trantham for her excellent job in doing the figures. My thanks are also due to John Wiley & Sons for their excellent editing job and splendid cooperation with this whole project. I am immensely indebted to my wife, Jayashree, and my daughters, Vasudha and Rohini, for their enormous understanding and cooperation while I was occupied with this endeavor week after week, month after month! Finally, the writing of this book (or for that matter, even my higher education and creative activity) would not have been possible without the inspiration of my beloved mother, Pramila, who could never attend college but always craved for learning and knowledge.

This page intentionally left blank

1

REVIEW OF BASIC CONCEPTS AND EQUATIONS OF FLUID DYNAMICS

1.1. Introduction to Fluid Dynamics

Fluid Model of Systems

In dealing with a fluid, one is in reality dealing with a system which has many particles which interact with one another. The main utility of fluid dynamics is the ability to develop a formalism which deals solely with a few macroscopic quantities like pressure, ignoring the details of the particle interactions. Therefore, the techniques of fluid dynamics have often been found useful in modeling systems with complicated structure where interactions (either not known or very difficult to describe) take place between the constituents. Thus, the first successful model of the fission of heavy elements was the liquid drop model of the nucleus, which treats the nucleus as a fluid and hence replaces the problem of calculating the interactions of all of the protons and neutrons with the much simpler problem of calculating the pressures and surface tension in a fluid. Of course, this treatment gives only a very rough approximation to reality, but it is nonetheless a very useful way of approaching the problem.

The Objective of Fluid Dynamics

The primary purpose is to study the causes and effects of the motion of fluids. Fluid dynamics seeks to construct a mathematical theory of fluid motion, which shall be based on the smallest number of dynamical principles and which shall be sufficiently comprehensive to correlate the different types of fluid flow so far as their macroscopic features are concerned: In many circumstances, the

incompressible and inviscid model of a fluid is sufficiently representative of its real properties to provide a satisfactory account of a great variety of types of motion. It turns out that such a model makes sufficiently accurate predictions for the airflow around *streamlined bodies* moving at low speeds. Indeed, in dealing with streamlined bodies (which minimize flow–separation) in flows of fluids of small viscosities, one may divide the flow field into two parts: a thin layer adjacent to the body and a small wake behind the body where the viscous effects are appreciable, and the rest of the flow field behaving essentially inviscid. Such a division greatly facilitates the mathematical analysis in that the inviscid flow field can first be determined independent of the boundary layer near the body, and the pressure field obtained from the inviscid–flow calculation is, then, used to calculate the flow in the boundary layer.

While amongst the attractive features of hydrodynamics is its provision of ample room for the application of many different ideas and methods of mathematical analysis, the subject is expounded in the following as a branch of theoretical physics.

The Fluid State

A fluid is a material that deforms continually upon the application of surface forces. A fluid does not have a preferred shape, and different elements of a homogeneous fluid may be rearranged freely without affecting the macroscopic properties of the fluid, i.e., the fluids are mobile. A fluid offers resistance to attempts to produce relative motions of its different elements, i.e., a deformation, and this resistance vanishes with the rate of deformation. Fluids, unlike solids, cannot support a tension or negative pressure. (Thus, the occurrence of negative pressures in a mathematical solution of a fluid flow is an indication that this solution does not correspond to a physically possible situation.) However, a thin layer of fluid can support a large normal load while offering very little resistance to tangential motion – a property which finds practical use in lubricated bearings.

A fluid is, of course, discrete on the microscopic level, and the fluid properties fluctuate violently when viewed on this level. However, in considering problems in which the dimensions of interest are very large compared with molecular distances, one may ignore the molecular structure and endow the fluid with a continuous distribution of matter. The fluid properties can, then, be taken to vary smoothly in space and time. The characteristics of a fluid which are due to molecular effects such as viscosity enter the equation of fluid flows as parameters obtained by experiment.

Fluids can exist in either of two stable phases – liquids and gases. In gases under ordinary conditions the molecules are so far apart from each other that each molecule moves independently of its neighbors except when making an occasional *collision*. In liquids, on the other hand, a molecule is continually within the strong cohesive force fields of several neighbors at all times. Gases can be compressed much more readily than liquids, and consequently, for a gas, any

motion involving appreciable variations in pressure will be accompanied by much larger changes in density. However, in cases where the fluid flows are accompanied by only slight variations in pressure, gases and liquids behave similarly.

In formulations of fluid flows, it is useful to think of a fluid particle which is small enough on a macroscopic level that it may be taken to have uniform macroscopic properties, yet it is large enough to contain sufficient molecules to diminish the molecular fluctuations and to allow one to associate with it a macroscopic property (which is a statistical average of the corresponding molecular property of large number of molecules). This is the continuum hypothesis.

As an illustration of the limiting process by which the local continuum properties are defined, consider the mass density ρ. Imagine a small volume $\delta\mathcal{V}$ surrounding a point P, let δm be the total mass of material in $\delta\mathcal{V}$ instantaneously. The ratio $\delta m/\delta\mathcal{V}$ as $\delta\mathcal{V}$ reduces to $\delta\mathcal{V}^*$, where $\delta\mathcal{V}^*$ is the volume of fluid particle is taken to give the mass density ρ at P.

Description of the Flow-Field

The continuum model affords a field description, in that the average properties in the volume $\delta\mathcal{V}^*$ surrounding the point P are assigned in the limit to the point P itself. If q represents a t fi l continuum property, then one has a fictitious continuum characterized by an aggregate of such local values of q, i.e., $q = q(\boldsymbol{x}, t)$. This enables one to consider what happens at every fixed point in space as a function of time – the so–called *Eulerian* description. In an alternative approach, called the *Lagrangian* description, the dynamical quantities, as in particle mechanics, refer more fundamentally to identifiable pieces of matter, and one looks for the dynamical history of a selected fluid element.

Imagine a fluid moving in a region Ω. Each particle of fluid follows a certain trajectory. Thus, for each point $\boldsymbol{x}_0$ in Ω, there exists a pathline $\boldsymbol{\sigma}(t)$ given by

$$\boldsymbol{\sigma}(t) : \boldsymbol{x} = \boldsymbol{\phi}(t, \boldsymbol{x}_0) \text{ with } \boldsymbol{\phi}(0, \boldsymbol{x}_0) = \boldsymbol{x}_0 \text{ and } \boldsymbol{\phi}(t+\tau, \boldsymbol{x}_0) = \boldsymbol{\phi}\big(t, \boldsymbol{\phi}(\tau, \boldsymbol{x}_0)\big), \quad (1)$$

where the mapping $\boldsymbol{\phi} : \Omega \Rightarrow \Omega$ is *one–to–one* and *onto*.

The velocity of the flow is given by

$$\boldsymbol{v}(t, \boldsymbol{x}) = \frac{d\boldsymbol{x}}{dt} = \frac{d}{dt}\, \boldsymbol{\phi}(t, \boldsymbol{x}_0). \quad (2)$$

We then have the following results.

THEOREM (*Existence*): Assume that the flow velocity $\boldsymbol{v}(t, \boldsymbol{x})$ is a C^1 function of $\boldsymbol{x}$ and t. Then for each pair $(t_0, \boldsymbol{x}_0)$ there exists a unique integral curve – the path line $\boldsymbol{\sigma}(t)$, defined on some small interval in t about t_0, such that $\boldsymbol{\sigma}(t_0) = \boldsymbol{x}_0$.

THEOREM (*Boundedness*): Consider a region Ω with a smooth boundary $\partial\Omega$. If the flow velocity v is parallel to $\partial\Omega$, then the integral curves for v, i.e., the path lines starting in Ω remain in Ω.

Streamlines $s(t)$ are obtained by holding t fixed, say $t = t_0$, and solving the differential equation

$$s'(t) = v(t_0, s(t)). \tag{3}$$

Streamlines coincide with pathlines if the flow is steady, i.e., if $v(t,x) = v(x)$.

The transformation from the Eulerian to the Lagrangian description is given by

$$V(t, x_0) = v(t,x) = v(t, \phi(t, x_0)). \tag{4}$$

Though we shall use the Eulerian description in preference to the Lagrangian description which renders the formalism cumbersome, we shall find the concept of material volumes, surfaces and lines which consist always of the same fluid particles and move with them useful even in the Eulerian description.

Volume Forces and Surface Forces

One may think of two distinct kinds of forces acting on a fluid continuum. Long–range forces such as gravity penetrate into the interior of the fluid and act on all elements of the fluid. If such a force $F(x,t)$ varies slowly in space, then the force acts equally on all the matter within a fluid particle of density ρ and volume $\delta\mathcal{V}$ and the total force on the latter is proportional to its mass and is equal to $F(x,t)\,\rho\delta\mathcal{V}$. In this sense, long–range forces are called *body forces.*

The short–range forces (which have a molecular origin) between two fluid elements, on the other hand, become effective only if they interact through direct mechanical contact. Since the short range forces on an element are determined by its surface area, one considers a plane surface element of area δA in the fluid and specifies the local short–range force as the total force exerted on the fluid on one side of the element by the fluid on the other side and equal to $\Sigma(\hat{n}, x, t)\,\delta A$ whose direction is not known *a priori* for a viscous fluid (unlike an inviscid fluid). Here, $\hat{n}$ is the unit normal to the surface element δA, and it points away from the fluid on which Σ acts. The total force exerted across δA on the fluid on the side into which $\hat{n}$ points is $-\Sigma(\hat{n}, x, t)\,\delta A = \Sigma(-\hat{n}, x, t)$ so that Σ is an odd function of $\hat{n}$. In this sense, short–range forces are called *surface forces.*

In order to determine the dependence of Σ on $\hat{n}$, consider all the forces acting instantaneously on the fluid within an element of volume $\delta\mathcal{V}$ in the shape of a tetrahedron (Figure 1.1). The three orthogonal faces have areas $\delta A_1, \delta A_2$, and δA_3 and unit outward normals $-\hat{i}, -\hat{j}, -\hat{k}$, and the fourth inclined face has area δA and unit outward normal $\hat{n}$. Surface forces will act on the fluid in the tetrahedron, across each of the four faces, and their resultant is

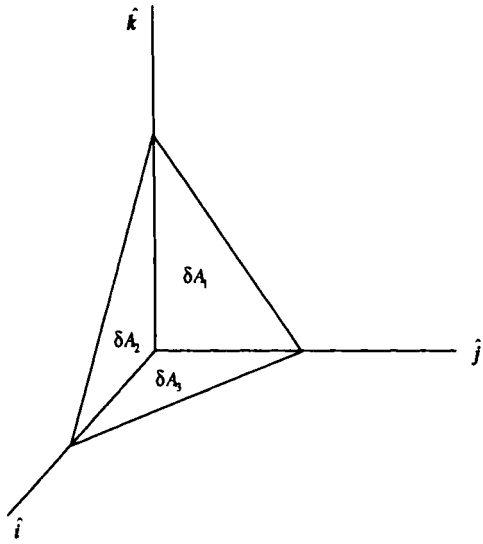

Figure 1.1. Tetrahedron–shaped fluid element.

$$\Sigma(\hat{n})\,\delta A + \Sigma\left(-\hat{i}\right)\delta A_1 + \Sigma\left(-\hat{j}\right)\delta A_2 + \Sigma\left(-\hat{k}\right)\delta A_3$$

or

$$\left\{\Sigma(\hat{n}) - \left[\hat{i}\cdot\hat{n}\,\Sigma\left(\hat{i}\right) + \hat{j}\cdot\hat{n}\,\Sigma\left(\hat{j}\right) + \hat{k}\cdot\hat{n}\,\Sigma\left(\hat{k}\right)\right]\right\}\delta A.$$

Now, since the body force and inertia force on the fluid within the tetrahedron are proportional to the volume $\delta\mathcal{V}$, they become negligible compared with the surface forces if the linear dimensions of the tetrahedron are made to approach zero without changing its shape. Then, application of Newton's second law of motion to this fluid element gives

$$\Sigma(\hat{n}) = \hat{i}\cdot\hat{n}\;\Sigma\left(\hat{i}\right) + \hat{j}\cdot\hat{n}\;\Sigma\left(\hat{j}\right) + \hat{k}\cdot\hat{n}\;\Sigma\left(\hat{k}\right). \tag{1}$$

Thus, the resultant of stress (force per unit area) across an arbitrarily oriented plane surface element with a unit normal $\hat{n}$ is related to the resultant of stress across any three orthogonal plane surface elements at the same position in the fluid as if it were a vector with orthogonal components $\Sigma\left(\hat{i}\right)$, $\Sigma\left(\hat{j}\right)$, $\Sigma\left(\hat{k}\right)$. Note that $\hat{n}$ and Σ do not depend at all on the choice of the reference axes, nor does the quantity

$$\tau = \hat{i}\,\Sigma\left(\hat{i}\right) + \hat{j}\,\Sigma\left(\hat{j}\right) + \hat{k}\,\Sigma\left(\hat{k}\right), \tag{2}$$

which is a second–order tensor called the *stress tensor* and prescribes the state of stress at a point in the fluid. This leads to the following theorem.

THEOREM (*Cauchy*): There exists a matrix function τ, such that

$$\Sigma_i(\hat{n}) = \tau_{ij}\hat{n}_j, \tag{3}$$

where τ_{ij} is the i–component of the force per unit area exerted across a plane surface element normal to the j–direction. Thus, the state of stress at a point is characterized by normal stresses (τ_{ii}) and shear stresses $(\tau_{ij},\ i \neq j)$ acting on three mutually perpendicular planes passing through the point, i.e., by nine cartesian components.

One may use an argument similar to the above to demonstrate that the nine components of the stress tensor are not all independent. This time, let us consider the moments of the various forces acting on the fluid within a volume $\delta\mathcal{V}$ of arbitrary shape. The ith component of the total moment, about a point O within this volume, exerted by the surface forces at the boundary of the volume is

$$\iint_{\delta\mathcal{A}} \varepsilon_{ijk} x_j \tau_{kl} \hat{n}_l dA,$$

where ε_{ijk} is the Levi–Civita tensor and $\boldsymbol{x}$ describes the position of the surface element $\hat{\boldsymbol{n}}dA$ relative to O. This can be written using the divergence theorem as

$$\iiint_{\delta\mathcal{V}} \varepsilon_{ijk} \frac{\partial\left(x_j \tau_{kl}\right)}{\partial x_l}\, d\boldsymbol{x} = \iiint_{\delta\mathcal{V}} \varepsilon_{ijk}\left(\tau_{kj} + x_j \frac{\partial \tau_{kl}}{\partial x_l}\right) d\boldsymbol{x}.$$

Let us now reduce the volume $\delta\mathcal{V}$ to zero without changing its shape. Equating the rate of change of angular momentum of the fluid instantaneously in $\delta\mathcal{V}$ to the total moment of the body and surface forces acting on $\delta\mathcal{V}$, dropping the terms of $O(\delta\mathcal{V})$ as $\delta\mathcal{V}$ becomes very small, one obtains

$$\varepsilon_{ijk}\tau_{jk} = 0$$

or

$$\tau_{ij} = \tau_{ji} \tag{4}$$

so that the stress tensor is symmetrical and has only six independent components.

In a fluid at rest, the shearing stresses (which are set up by a shearing motion with the parallel layers of fluid sliding relative to each other) all vanish. Further, the normal stresses are, then, all equal because a fluid is unable to withstand any tendency by applied forces to deform it without change of volume. Thus, in a fluid at rest, the stress tensor becomes isotropic,

$$\tau_{ij} = -p\delta_{ij}, \tag{5}$$

where p is called the *hydrostatic pressure*. Thus, in a fluid at rest, the stress excited across a plane surface element with unit normal $\hat{\boldsymbol{n}}$ is $-p\hat{\boldsymbol{n}}$, which is a normal force of the same magnitude for all directions of $\hat{\boldsymbol{n}}$ at a given point.

Relative Motion Near a Point

The stress tensor at a point in a fluid depends on the local deformation of the fluid caused by the motion. Therefore, as a prelude to dynamical considerations, it is necessary to analyze the relative motion in the neighborhood of any point.

Consider now the deformation of the fluid. Let (u, v, w) denote the components of the instantaneous velocity at the point $P(x, y, z)$. Then, the velocity at a neighboring point $(x + \delta x, y + \delta y, z + \delta z)$ is given by

$$\left.\begin{aligned} u + \delta u &= u + \frac{\partial u}{\partial x}\delta x + \frac{\partial u}{\partial y}\delta y + \frac{\partial u}{\partial y}\delta z + \cdots, \\ v + \delta v &= v + \frac{\partial v}{\partial x}\delta x + \frac{\partial v}{\partial y}\delta y + \frac{\partial v}{\partial y}\delta z + \cdots, \\ w + \delta w &= w + \frac{\partial w}{\partial x}\delta x + \frac{\partial w}{\partial y}\delta y + \frac{\partial w}{\partial y}\delta z + \cdots. \end{aligned}\right\} \tag{6a}$$

The geometrical character of the relative velocity $\delta \mathbf{v}$ regarded as a linear function of δx can be recognized by decomposing $\nabla \mathbf{v}$, which is a second–order tensor into symmetrical and antisymmetrical parts,

$$\left.\begin{aligned} \delta u &= \varepsilon_{xx}\delta x + \varepsilon_{xy}\delta y + \varepsilon_{xz}\delta z + \eta\delta z - \zeta\delta y, \\ \delta v &= \varepsilon_{xy}\delta x + \varepsilon_{yy}\delta y + \varepsilon_{yz}\delta z + \zeta\delta x - \xi\delta z, \\ \delta w &= \varepsilon_{xz}\delta x + \varepsilon_{yz}\delta y + \varepsilon_{zz}\delta z + \xi\delta y - \eta\delta x, \end{aligned}\right\} \tag{6b}$$

where

$$\left.\begin{aligned} &\varepsilon_{xx} = \frac{\partial u}{\partial x}, \quad \varepsilon_{yy} = \frac{\partial v}{\partial y}, \quad \varepsilon_{zz} = \frac{\partial w}{\partial z}, \\ &\varepsilon_{xy} = \frac{1}{2}\left(\frac{\partial v}{\partial x} + \frac{\partial u}{\partial y}\right), \quad \varepsilon_{yz} = \frac{1}{2}\left(\frac{\partial w}{\partial y} + \frac{\partial v}{\partial z}\right), \quad \varepsilon_{zx} = \frac{1}{2}\left(\frac{\partial u}{\partial z} + \frac{\partial w}{\partial x}\right), \\ &\xi = \frac{1}{2}\left(\frac{\partial w}{\partial y} - \frac{\partial v}{\partial z}\right), \quad \eta = \frac{1}{2}\left(\frac{\partial u}{\partial z} - \frac{\partial w}{\partial x}\right), \quad \zeta = \frac{1}{2}\left(\frac{\partial v}{\partial x} - \frac{\partial u}{\partial y}\right). \end{aligned}\right\}$$

If one imagines a rectangular fluid particle having the sides $\delta x, \delta y, \delta z$ initially, then, the total motion of the particle may be decomposed into

(1) a pure translation with velocity components (u, v, w);

(2) a mean rigid–body rotation with components (ξ, η, ζ) (each of the latter quantities defines the mean angular velocity of two mutually perpendicular fluid line–elements);

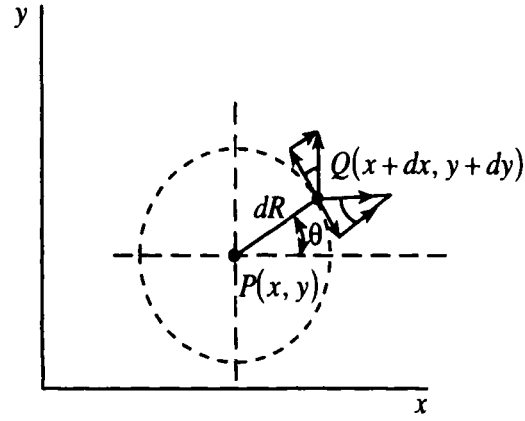

Figure 1.2. Deformation near a point in a fluid.

(3) a dilatation corresponding to the three strain rates $\varepsilon_{xx}, \varepsilon_{yy}, \varepsilon_{zz}$;

(4) a shear deformation corresponding to the three strain rates $\varepsilon_{xy}, \varepsilon_{yz}, \varepsilon_{zx}$.

In order to see these identifications, consider a two–dimensional flow. The deformation rates of a line element of fluid PQ (see Figure 1.2) are written as

$$\left.\begin{aligned} du &= -\frac{1}{2}\left(\frac{\partial v}{\partial x} - \frac{\partial u}{\partial y}\right)dy + \left[\frac{\partial u}{\partial x}dx + \frac{1}{2}\left(\frac{\partial v}{\partial x} + \frac{\partial u}{\partial y}\right)dy\right], \\ dv &= \frac{1}{2}\left(\frac{\partial v}{\partial x} - \frac{\partial u}{\partial y}\right)dx + \left[\frac{1}{2}\left(\frac{\partial v}{\partial x} + \frac{\partial u}{\partial y}\right)dx + \frac{\partial v}{\partial y}dy\right]. \end{aligned}\right\}$$

The velocity of Q relative to P is

$$V_{QP} = \left(\frac{\partial u}{\partial x}dx + \frac{\partial u}{\partial y}dy\right)\hat{i}_x + \left(\frac{\partial v}{\partial x}dx + \frac{\partial v}{\partial y}\right)\hat{i}_y.$$

The contribution of the x–component of V_{QP} to the rotational speed of PQ about P is given by

$$-\left(\frac{\partial u}{\partial x}dx + \frac{\partial u}{\partial y}dy\right)\frac{\sin\theta}{dR}$$

or

$$-\left(\frac{\partial u}{\partial x}\sin\theta\cdot\cos\theta + \frac{\partial u}{\partial y}\sin^2\theta\right).$$

Similarly, the contribution of the y–component of V_{QP} to the rotational speed of PQ about P is given by

$$\left(\frac{\partial v}{\partial x}\cos^2\theta+\frac{\partial v}{\partial y}\sin\theta\cdot\cos\theta\right).$$

Thus, as a whole, the rotational speed of PQ about P is

$$\frac{\partial v}{\partial x}\cos^2\theta-\frac{\partial u}{\partial y}\sin^2\theta+\left(\frac{\partial v}{\partial y}-\frac{\partial u}{\partial x}\right)\sin\theta\cdot\cos\theta.$$

The average rotational speed of PQ about P is then

$$\omega=\frac{1}{2\pi}\int_0^{2\pi}\left[\frac{\partial v}{\partial x}\cos^2\theta-\frac{\partial u}{\partial y}\sin^2\theta+\left(\frac{\partial v}{\partial y}-\frac{\partial u}{\partial x}\right)\sin\theta\cdot\cos\theta\right]d\theta$$

$$=\frac{1}{2}\left(\frac{\partial v}{\partial x}-\frac{\partial u}{\partial y}\right),$$

which characterizes the rotation in the neighborhood of P. Thus, this quantity evaluated at $P(x,y)$ for a given velocity field represents the instantaneous average angular speed of line segment PQ within the neighborhood of P and describes a rigid–body rotation of the fluid element at P.

Note that the vorticity Ω, defined by

$$\Omega=\frac{\partial v}{\partial x}-\frac{\partial u}{\partial y},$$

is twice the angular velocity ω.

Thus, the velocity field in the neighborhood of a point relative to the point is made up of two parts – caused, respectively, by the rigid–body rotation and the rate of straining of the element at the point.

The translation and the rigid–body rotation do not produce any change of shape of the fluid particle and result only in displacing it. On the other hand, the strain rates ε produce a deformation of the fluid particle; and since they obey the transformation laws of tensor, they form a strain order formation tensor ε_{ij} which is symmetric by construction,

$$\varepsilon_{ij}=\frac{1}{2}\left(\frac{\partial v_i}{\partial x_j}+\frac{\partial v_j}{\partial x_i}\right). \tag{7}$$

In order to see the further significance of the strain tensor ε_{ij}, consider a curve $r(s)$ in a region Ω. Under the flow $x_0 \Rightarrow \phi(t,x_0)$, this curve maps according to $r(s)\Rightarrow\phi(t,r(s))$. The tangent vector $r'(s)$ to this curve maps according to $r'(s)\Rightarrow\nabla\phi(t,r(s))\cdot r'(s)$. Indeed, any vector w at x maps according to $w\Rightarrow w(t)=\nabla\phi(t,x)\cdot w$. Further, if two vectors w_1 and w_2 at x are mapped by the flow onto $w_1(t)$ and $w_2(t)$, then the time rate of change of the inner product of $w_1(t)$ and $w_2(t)$ is given by

$$\frac{d}{dt}\boldsymbol{w}_1(t)\cdot\boldsymbol{w}_2(t)\Big|_{t=0} = \frac{d}{dt}\Big[\big(\nabla\phi(t,\boldsymbol{x})\cdot\boldsymbol{w}_1\big)\cdot\big(\nabla\phi(t,\boldsymbol{x})\cdot\boldsymbol{w}_2\big)\Big]\Big|_{t=0}$$

$$= \frac{d}{dt}\left(\frac{\partial\phi_i}{\partial x_j}w_{1_j}\frac{\partial\phi_i}{\partial x_k}w_{2_k}\right)\Bigg|_{t=0}$$

$$= \frac{\partial v_i}{\partial x_j}w_{1_j}\delta_{ik}w_{2_k} + \delta_{ij}w_{1_j}\frac{\partial v_i}{\partial x_k}w_{2_k} = 2\,\varepsilon_{ij}w_{1_i}w_{2_j} \tag{8}$$

where summation is implied on repeated indices. Equation (8) shows that the time rate of change of the inner product of two time–dependent vectors is completely characterized by the strain tensor ε_{ij}.

Note that the strain tensor can be further decomposed into the sum of a volume–preserving deformation and a shearless pure dilatation:

$$\varepsilon_{ij} = \left(\varepsilon_{ij} - \frac{\partial v_k}{\partial x_k}\delta_{ij}\right) + \frac{\partial v_k}{\partial x_k}\delta_{ij}, \tag{9}$$

which is also apparent in (6b).

Stress–Strain Relations

In a fluid at rest, as we saw previously, only normal stresses that are equal in all directions at a point exist, and the stress tensor has the isotropic form

$$\tau_{ij} = -p\delta_{ij}. \tag{5}$$

For a fluid in motion, one may write

$$\tau_{ij} = -p\delta_{ij} + d_{ij}, \tag{10}$$

where the nonisotropic part d_{ij} represents the tangential stresses that arise only in a moving fluid, and note that, for a fluid in motion,

$$p = -\frac{1}{3}\tau_{ii} \tag{11}$$

and p represents the average of the three normal stresses for any orthogonal set of axes and reduces to the hydrostatic pressure when the fluid is at rest; we shall call it the pressure in a moving fluid. Since fluid in relative motion is not in a state of thermodynamic equilibrium, p here is not a state variable in thermodynamics.

In order to relate d_{ij} to the local strain rate, first note that the local velocity gradient $\partial v_i/\partial x_j$ is a measure of the local strain rate. Let us assume that the fluid is isotropic and has no memory effects and that the strain rates are not too large, and write a linear relation,

$$d_{ij} = 2\mu\varepsilon_{ij} + \mu'\delta_{ij}\varepsilon_{kk}, \tag{12}$$

where μ and μ' are scalar coefficients. Note that in an isotropic fluid, d_{ij} cannot depend on pure rotation. Next, since $d_{ii} = 0$, (12) gives

$$2\mu + 3\mu' = 0$$

or

$$\mu' = -\frac{2}{3}\mu \tag{13}$$

so (12) becomes

$$d_{ij} = 2\mu\left(\varepsilon_{ij} - \frac{1}{3}\delta_{ij}\varepsilon_{kk}\right). \tag{14}$$

μ is called the *shear viscosity coefficient*. The effect of viscosity is to redistribute and equalize the momenta of different fluid particles.

Experiments involving a variety of fluid flows have shown that this linear relation between the strain rate and the nonisotropic part of the stress may hold over a wide range of values of the strain rates. The fluids for which this is a valid model are called *Newtonian fluids*. In this book, we shall be exclusively dealing with such fluids.

Equations of Fluid Flows

The laws governing the motion of fluids are:

(1) the law of conservation of mass;

(2) Newton's law of motion;

(3) the First Law of thermodynamics.

These laws typically refer to a system, i.e., a collection of matter of fixed identity.

In deriving equations governing the motion of fluids embodying these laws, one may hence consider a particular portion W of the fluid consisting of the same fluid particles and, hence, moving with the fluid – the Lagrangian description. The space coordinates defining W will then be functions of time since they depend on the changing locations of the fluid particles as time progresses. A typical macroscopic property is then represented by a material integral (which is one that always refers to the same fluid particles):

$$\hat{Q} = \iiint q(t,x)\,\rho\, d\mathcal{V}, \tag{15}$$

where a property q has been associated with a fluid particle of fixed identity and mass $\rho\, d\mathcal{V}$.

Alternatively, one may consider a fixed region of space called the *control volume* through which the fluid flows so that different fluid particles occupy this region at different times – the Eulerian description. A typical macroscopic

property is here represented by an integral over the control volume $\mathcal{V}$ fixed in space:

$$Q = \iiint_{\mathcal{V}} q(t,x)\, dx, \tag{16}$$

where $q(t,x)$ is a scalar field (e.g., density or a velocity component) associated with the fluid.

Thus, the value of DQ/Dt associated with the material system instantaneously occupying the control volume receives contributions from the changes with time in $\mathcal{V}$ for this material system and the flux of Q out of $\mathcal{V}$.

The Transport Theorem

THEOREM: Let $v(t,x)$ be a C^2 vector field on a region Ω, parallel to the boundary $\partial\Omega$, with flow $\phi(t,x)$, and let $q(t,x)$ be a scalar field associated with the fluid on Ω. If $\phi(t,x)$ is invertible as a function of x for a range of t, then, in this range,

$$\frac{d}{dt} \iiint_{\phi(t,W)} q(t,x)\, dx = \iiint_{\phi(t,W)} \left[\frac{\partial q}{\partial t} + \nabla \cdot (qv) \right] dx, \tag{17}$$

where W is any subregion of Ω.

LEMMA: Let $J(t,x)$ be the Jacobian determinant of the flow $\phi(t,x)$, i.e.,

$$J(t,x) = \det \left| \frac{\partial \phi_i}{\partial x_j} \right| > 0.$$

Then, if t is in the range in question, then

$$\frac{\partial}{\partial t} J(t,x) = J(t,x) \nabla \cdot v(t,x). \tag{18}$$

Proof: We have

$$\begin{aligned} \frac{\partial}{\partial t} \frac{\partial \phi_i}{\partial x_j} &= \frac{\partial}{\partial x_j} \frac{\partial}{\partial t} \phi_i(t,x) = \frac{\partial}{\partial x_j} v_i\big(t, \phi(t,x)\big) \\ &= \frac{\partial v_i}{\partial x_k} \frac{\partial \phi_k}{\partial x_j}, \qquad \text{summation on } k \\ &= \frac{\partial v_i}{\partial x_i} \frac{\partial \phi_i}{\partial x_j} \end{aligned}$$

because the nonvanishing contribution arises only for $k = i$.

Proof: We have, on using (18),

$$\frac{d}{dt}\iiint_{\phi(t,W)} q(t,x)\,dx = \frac{d}{dt}\iiint_{W} q\big(t,\phi(t,x_0)\big)\,J(t,x_0)\,dx_0$$

$$= \iiint_{W}\left(\frac{\partial q}{\partial t} + \nabla q\cdot v + q\nabla\cdot v\right) J(t,x_0)\,dx_0$$

$$= \iiint_{\phi(t,W)}\left[\frac{\partial q}{\partial t} + \nabla\cdot(qv)\right] dx. \qquad \text{Q.E.D.}$$

The Material Derivative

The time rate of change of q as one follows the given fluid particle is called the *material derivative* D/Dt of q and is given by

$$\frac{Dq}{Dt} = \frac{d}{dt}\,q\big(t,\phi(t,x_0)\big) = \frac{\partial q}{\partial t} + \nabla q\cdot v. \tag{19}$$

Thus, even in a steady flow, a fluid particle can change its properties by simply moving to a place where these properties have different values.

The Law of Conservation of Mass

Since the total amount of fluid in a control volume $\mathcal{V}$ is conserved, one has

$$\frac{d}{dt}\iiint_{\mathcal{V}} \rho\,dx = 0. \tag{20}$$

When one uses (17), (20) leads to

$$\iiint_{\mathcal{V}}\left[\frac{\partial \rho}{\partial t} + \nabla\cdot(\rho v)\right] dx = 0. \tag{21}$$

Since equation (21) must apply even to an infinitesimal control volume, one obtains

$$\frac{\partial \rho}{\partial t} + \nabla\cdot(\rho v) = 0 \tag{22a}$$

or

$$\frac{D\rho}{Dt} + \rho\nabla\cdot v = 0. \tag{22b}$$

Equation of Motion

In applying Newton's law of motion to a finite, extended mass of fluid, one equates the external resultant force to the rate of change of resultant momentum which is calculated for a mass of fluid consisting always of the same fluid particles. Thus,

$$\frac{d}{dt}\iiint_{\mathcal{V}} v\rho\,dx = \iiint_{\mathcal{V}} F\rho\,dx + \iint_{S} \tau\cdot\hat{n}\,dS, \tag{23}$$

where F is the body force per unit volume acting on the fluid, S is the control surface enclosing $\mathcal{V}$, and $\hat{n}$ is the unit outward normal to the area element dS.

Using (17), this becomes

$$\iiint_{\mathcal{V}} \left[\frac{\partial}{\partial t}(\rho \mathbf{v}) + \nabla \cdot (\rho \mathbf{v}\mathbf{v}) \right] d\mathbf{x} = \iiint_{\mathcal{V}} F\rho \, d\mathbf{x} + \oiint_{S} \boldsymbol{\tau} \cdot \hat{\mathbf{n}} \, dS. \tag{24}$$

Using Green's theorem, equation (24) may be rewritten as

$$\iiint_{\mathcal{V}} \left[\frac{\partial}{\partial t}(\rho \mathbf{v}) + \nabla \cdot (\rho \mathbf{v}\mathbf{v}) - \rho \boldsymbol{F} - \nabla \cdot \boldsymbol{\tau} \right] d\mathbf{x} = 0, \tag{25}$$

from which we have

$$\frac{\partial}{\partial t}(\rho \mathbf{v}) + \nabla \cdot (\rho \mathbf{v}\mathbf{v}) = \rho \boldsymbol{F} + \nabla \cdot \boldsymbol{\tau}. \tag{26}$$

When we use equation (22), equation (26) becomes

$$\rho \left(\frac{\partial \mathbf{v}}{\partial t} + \mathbf{v} \cdot \nabla \mathbf{v} \right) = \rho \boldsymbol{F} + \nabla \cdot \boldsymbol{\tau}. \tag{27}$$

The Energy Equation

Consider the energy balance for the fluid in the control volume $\mathcal{V}$. Work is done on this mass of fluid by both body and surface forces, and heat may also be transferred across the control surface S. Some of this work done and heat transferred shows up as an increase in the kinetic energy of the fluid, and the remainder shows up as an increase in the internal energy of the fluid (the latter is associated with the thermal motion of the molecules), according to the First law of thermodynamics. It may be noted that the additivity of these two forms of energy in the total energy of a fluid particle is valid if the fluid is only slightly dissipative.

Since a fluid flow necessarily occurs under thermodynamic nonequilibrium conditions, a revision of the definition of some of the thermodynamic quantities is necessary before proceeding further to set up an equation embodying the conservation of energy of the fluid. If one assumes that a fluid particle is passing through a succession of states in which the departure from equilibrium is small, one may define an internal energy E for this fluid particle at any instant as the value corresponding to a hypothetical equilibrium state that is attainable instantaneously by suddenly isolating the fluid particle from the surroundings and making it reach equilibrium adiabatically and without any work being done on it. Next, the density ρ may be defined as usual as the ratio of mass to instantaneous volume of the fluid particle. Knowledge of the two properties of state E and ρ at any instant then enables one to determine other quantities as in equilibrium thermodynamics.

As smooth as this procedure may look, there appears to be a small difficulty, however. The thermodynamic pressure p_{th} so calculated may not be equal to the mechanical pressure p. Indeed, one may write

$$p - p_{th} = -\kappa \varepsilon_{kk}, \tag{28}$$

where κ is a scalar coefficient called the *bulk viscosity coefficient*. Equation (28) indicates the lag in the adjustment of the mechanical pressure to the continually

changing values of ρ and E in a fluid flow. Physically, this lag is consequent to the delay in the equipartition of energy between the various modes (translational, rotational and vibrational) of a molecule.

However, in most cases the dilatation rates are very much smaller than the shear rates so that the bulk viscosity will not play an important role. We shall, therefore, neglect it and take p and p_{th} as being identical everywhere in the following.

The equation expressing the First law of thermodynamics is then

$$\frac{d}{dt}\iiint_{\mathcal{V}}\left(e+\frac{1}{2}\mathbf{v}^2+U\right)\rho\,d\mathbf{x}=\frac{DQ}{Dt}-\frac{DW}{Dt}, \tag{29}$$

where e is the internal energy of the fluid per unit mass, U is the potential energy of the fluid in a conservative body–force field $\boldsymbol{F}=-\nabla U, Q$ is the heat transfer *to* the system, and W the work delivery *from* the system.

When we use (17) and write

$$Q=\iiint_{\mathcal{V}} q d\mathbf{x}, \qquad W=\iiint_{\mathcal{V}} w d\mathbf{x}, \tag{30}$$

equation (29) becomes

$$\iiint_{\mathcal{V}}\left[\frac{\partial}{\partial t}\left\{\rho\left(e+\frac{1}{2}\mathbf{v}^2+U\right)\right\}+\nabla\cdot\left\{\rho\mathbf{v}\left(e+\frac{1}{2}\mathbf{v}^2+U\right)\right\}-\frac{Dq}{Dt}+\frac{Dw}{Dt}\right]d\mathbf{x}=0, \tag{31}$$

from which we have

$$\frac{\partial}{\partial t}\left\{\rho\left(e+\frac{1}{2}\mathbf{v}^2+U\right)\right\}+\nabla\cdot\left\{\rho\mathbf{v}\left(e+\frac{1}{2}\mathbf{v}^2+U\right)\right\}=\frac{Dq}{Dt}-\frac{Dw}{Dt}. \tag{32}$$

When we use equation (22), equation (32) becomes

$$\rho\left[\frac{\partial}{\partial t}\left(e+\frac{1}{2}\mathbf{v}^2+U\right)+\mathbf{v}\cdot\nabla\left(e+\frac{1}{2}\mathbf{v}^2+U\right)\right]=\frac{Dq}{Dt}-\frac{Dw}{Dt}. \tag{33}$$

When we use equation (10) and (27), equation (33) becomes

$$\rho\left[\frac{De}{Dt}+p\frac{D}{Dt}\left(\frac{1}{\rho}\right)\right]=\frac{Dq}{Dt}+d_{ij}\frac{\partial v_j}{\partial x_i}. \tag{34}$$

Note, from (14), that

$$d_{ij}\frac{\partial v_j}{\partial x_i}=\varepsilon_{ij}d_{ij}=2\mu\left(\varepsilon_{ij}\varepsilon_{ij}-\frac{1}{3}\varepsilon_{kk}^2\right)$$

$$=2\mu\left(\varepsilon_{ij}-\frac{1}{3}\varepsilon_{kk}\delta_{ij}\right)\left(\varepsilon_{ij}-\frac{1}{3}\varepsilon_{kk}\delta_{ij}\right)=2\mu\left(\varepsilon_{ij}-\frac{1}{3}\varepsilon_{kk}\delta_{ij}\right)^2,$$

and thus equation (34) becomes

$$\rho\left[\frac{De}{Dt}+p\frac{D}{Dt}\left(\frac{1}{\rho}\right)\right]=\frac{Dq}{Dt}+2\mu\left(\varepsilon_{ij}-\frac{1}{3}\varepsilon_{kk}\delta_{ij}\right)^2. \tag{35}$$

Note that the last term on the right–hand side in equation (35) is always positive and represents the viscous heating.

If the heat flux occurs as a consequence of molecular transport between contiguous portions of fluid across the control surface, noting that the molecular transport of heat is proportional to the local gradient of temperature T (which is a measure of the kinetic energy of the random molecular motion) of the fluid, one has

$$\iiint_{\mathcal{V}}\frac{Dq}{Dt}\,dx=\oiint_{S}K\nabla T\cdot\hat{\boldsymbol{n}}\,dS; \tag{36}$$

and using Green's Theorem, equation (36) becomes

$$\iiint_{\mathcal{V}}\frac{Dq}{Dt}\,dx=\iiint_{\mathcal{V}}\nabla\cdot(K\nabla T)\,d^3\mathcal{V} \tag{37}$$

so that, if the thermal conductivity K is constant,

$$\frac{Dq}{Dt}=K\nabla^2T. \tag{38}$$

Note that an equation of state of the form $p=p(\rho)$ is needed to close equations (22), (27), (35), and (38).

The Equation of Vorticity

Upon taking the curl of equation (27), one obtains for the vorticity $\boldsymbol{\Omega}=\nabla\times\boldsymbol{v}$,

$$\frac{\partial\boldsymbol{\Omega}}{\partial t}+(\boldsymbol{v}\cdot\nabla)\boldsymbol{\Omega}=(\boldsymbol{\Omega}\cdot\nabla)\boldsymbol{v}-\frac{1}{\rho^2}\nabla p\times\nabla\rho+\mu\left[\frac{1}{\rho}\nabla^2\boldsymbol{\Omega}-\frac{1}{\rho^2}\nabla\rho\times\left\{\nabla^2\boldsymbol{v}+\right.\right.$$
$$\left.\left.+\frac{1}{3}\nabla(\nabla\cdot\boldsymbol{v})\right\}\right]+\nabla\times\rho\boldsymbol{F}. \tag{39}$$

The second term on the right–hand side represents the baroclinic generation of vorticity which is due to the misalignment of the density and pressure gradients. This mechanism is the cause of generation of vorticity by shock waves (see Chapter 3).

For an inviscid, barotropic fluid for which $p=p(\rho)$, equation (39) becomes, in the absence of the body force $\boldsymbol{F}$,

$$\frac{D}{Dt}\left(\frac{\boldsymbol{\Omega}}{\rho}\right)=\frac{\boldsymbol{\Omega}}{\rho}\cdot\nabla\boldsymbol{v}. \tag{40}$$

The Incompressible Fluid

A fluid is said to be incompressible when the density of an element of fluid is not affected by changes of pressure, and $D\rho/Dt=0$. Equations (22), (27), (35), and (39) then become

$$\nabla \cdot \mathbf{v} = 0, \tag{41}$$

$$\rho\left[\frac{\partial \mathbf{v}}{\partial t} + \mathbf{v} \cdot \nabla \mathbf{v}\right] = \rho \boldsymbol{F} - \nabla p + \mu \nabla^2 \mathbf{v}, \tag{42}$$

$$e = \text{const.}, \tag{43}$$

$$\frac{\partial \boldsymbol{\Omega}}{\partial t} + \mathbf{v} \cdot \nabla \boldsymbol{\Omega} = \boldsymbol{\Omega} \cdot \nabla \mathbf{v} + \nabla \times \boldsymbol{F} + \nu \nabla^2 \boldsymbol{\Omega}, \tag{44}$$

where ν is the kinematic viscosity,

$$\nu \equiv \frac{\mu}{\rho}.$$

Now, in a two–dimensional flow the fluid particles move in plane paths in which all such planes are parallel, and streamline patterns are identical in each plane. For a two–dimensional flow (in the xy–plane), letting

$$\boldsymbol{\Omega} = \omega \hat{\boldsymbol{i}}_z \tag{45}$$

and assuming that the body force $\boldsymbol{F}$ is conservative, equation (44) leads to

$$\frac{\partial \omega}{\partial t} + u\frac{\partial \omega}{\partial x} + v\frac{\partial \omega}{\partial y} = \nu\left(\frac{\partial^2 \omega}{\partial x^2} + \frac{\partial^2 \omega}{\partial y^2}\right), \tag{46}$$

where

$$\mathbf{v} = (u, v, 0),$$

$$\omega = \frac{\partial v}{\partial x} - \frac{\partial u}{\partial y}. \tag{47}$$

Introducing the stream function Ψ, such that

$$u = \frac{\partial \Psi}{\partial y}, \qquad v = -\frac{\partial \Psi}{\partial x} \tag{48}$$

equation (46) leads to

$$\frac{\partial \nabla^2 \Psi}{\partial t} + \frac{\partial \Psi}{\partial y}\frac{\partial \nabla^2 \Psi}{\partial x} - \frac{\partial \Psi}{\partial x}\frac{\partial \nabla^2 \Psi}{\partial y} = \nu \nabla^4 \Psi. \tag{49}$$

The boundary conditions required in solving equations (22), (27), and (35) are that there be neither a penetration of the fluid into, nor a gap between the fluid and the boundary, at any solid boundary; this means that the fluid velocity component normal to the boundary at the boundary must be zero. When the boundary itself is in motion, the fluid velocity component normal to the boundary must equal the velocity of the boundary normal to itself. No restrictions are placed on the tangential component of fluid velocity at a boundary when inviscid fluids are considered. However, in a viscous fluid, even the tangential component of the fluid velocity at a boundary is the same as that of the boundary so that there is no slip of the fluid at a boundary.

At a boundary given by $F(x,y,z,t)=0$ moving with the fluid, one has the kinematic condition

$$\frac{DF}{Dt}=0 \tag{50}$$

so that such a boundary is always in contact with the same fluid particles.

When the fluid is set into motion by the body moving through it, a necessary condition is that the fluid at infinity remains at rest. If this were not so, it would imply that the finite forces acting on the bodies had imparted to the fluid infinite kinetic energy in finite time, which violates the principles of work and energy.

Hamiltonian Formulation of Fluid–Flow Problems

Hamiltonian formulations have traditionally played an important role in both the classical and quantum mechanics of particles and fields. Hamiltonian formulations not only offer a new perspective on familiar results, but also provide powerful tools like the conservation laws and stability theorems. However, Hamiltonian formulations were not introduced into fluid flow problems until recently. This is because of the fact that the Eulerian variables in fluid–flow problems are noncanonical (Salmon).

The Lagrangian (particle–following) variables of a fluid flow are canonical, i.e., their time evolution is given by equations of the form of Hamilton's equations. The Lagrangian equations of motion possess an additional particle–relabeling symmetry, in that the Hamiltonian is invariant under translations of fluid particles along lines of constant vorticity. Such translations are invisible in the Eulerian description; consequently, the conserved quantities are no longer related to explicit symmetries of the Hamiltonian and cannot be obtained from Noether's Theorem, but become instead Casimir invariants (see below).

Hamiltonian Dynamics of Continuous Systems

Equations of continuous systems are continuous in space and thus represent infinite–dimensional dynamical systems. Functions of state $F(u)$ then become functionals of state $\mathcal{F}(u)$, and the partial derivatives $\partial F/\partial u_i$ now become the functional (or variational) derivatives $\delta\mathcal{F}/\delta u$,[1] which is defined by

$$\begin{aligned}\delta\mathcal{F} &\equiv \mathcal{F}(u+\delta u)-\mathcal{F}(u)\\ &= \left(\frac{\delta\mathcal{F}}{\delta u},\delta u\right)+0\left(\delta u^2\right)\end{aligned} \tag{51}$$

for admissible but otherwise arbitrary variations δu, where $(\cdot,\cdot)$ is the relevant inner product for the function space $\{u\}$. If

[1]The symbol δ is used to denote an increment everywhere else in this book, but in this section it denotes the variational derivative in keeping with the standard notation.

$$\mathcal{F}(u) = \int_{x_1}^{x_2} F(x, u, u_x)\, dx, \tag{52}$$

then

$$\delta\mathcal{F} = \int_{x_1}^{x_2} \left[\frac{\partial F}{\partial u} - \frac{d}{dx}\left(\frac{\partial F}{\partial u_x} \right) \right] \delta u\, dx. \tag{53}$$

So,

$$\frac{\delta \mathcal{F}}{\delta u} = \frac{\partial F}{\partial u} - \frac{d}{dx}\left(\frac{\partial F}{\partial u_x} \right). \tag{54}$$

Consider a Hamiltonian dynamical system represented in the symplectic (i.e., nondegenerate and skew–symmetric) form

$$u_t = J \frac{\delta \mathcal{H}}{\delta u} \tag{55}$$

where $u(x,t)$ is the dynamical variable, $\mathcal{H}(u)$ is the Hamiltonian functional, and J is a sympletic operator, which is a skew–symmetric transformation from $\{u\}$ to $\{u\}$ satisfying

$$(u, Jv) = -(Ju, v). \tag{56}$$

An equivalent Poisson bracket[2] statement is

$$\frac{d\mathcal{F}}{dt} \equiv \left(\frac{\delta \mathcal{F}}{\delta u}, u_t \right) = \left(\frac{\delta \mathcal{F}}{\delta u}, J \frac{\delta \mathcal{H}}{\delta u} \right) = [\mathcal{F}, \mathcal{H}]. \tag{57}$$

Equation (7) immediately implies that the Hamiltonian $\mathcal{H}$ is an integral invariant of this system:

$$\frac{d\mathcal{H}}{dt} = \left(\frac{\delta \mathcal{H}}{\delta u}, J \frac{\delta \mathcal{H}}{\delta u} \right) = -\left(J \frac{\delta \mathcal{H}}{\delta u}, \frac{\delta \mathcal{H}}{\delta u} \right) = 0. \tag{58}$$

Now suppose that there exists some steady state $u = U$ of this system. If the Hamiltonian representation is canonical in the sense that J is invertible, it follows that the steady state $u = U$ is a conditional extremum of $\mathcal{H}$, namely,

$$J \frac{\delta \mathcal{H}}{\delta u} \Big|_{u=U} = 0, \tag{59}$$

---

[2] In the Euclidean space R^{2n} with coordinates (p,q), the Poisson bracket for a canonical system is

$$[\mathcal{F}, \mathcal{H}] = \sum_{i=1}^{n} \left(\frac{\partial \mathcal{F}}{\partial q_i} \frac{\partial \mathcal{H}}{\partial p_i} - \frac{\partial \mathcal{F}}{\partial p_i} \frac{\partial \mathcal{H}}{\partial q_i} \right) = \nabla \mathcal{F} \cdot J \nabla \mathcal{H},$$

where

$$J = \begin{pmatrix} 0 & -I & 0 \\ I & 0 & 0 \\ 0 & 0 & 0 \end{pmatrix},$$

where I is the $n \times n$ identity matrix. Note that the Poisson bracket operation is bilinear and skew-symmetric and satisfies the Jacobi identity:

$$[[\mathcal{F}, \mathcal{G}], \mathcal{H}] + [[\mathcal{G}, \mathcal{H}], \mathcal{F}] + [[\mathcal{H}, \mathcal{F}], \mathcal{G}] = 0.$$

Any system in the Hamiltonian form, with J a nonsingular, skew-symmetric matrix of constants, can be reduced locally, by a linear transformation of the dependent variable u, to a system in the canonical (Darboux) form with J given as above.

which implies

$$\frac{\delta \mathcal{H}}{\delta u}\Big|_{u=U} = 0. \tag{60}$$

If, on the other hand, the Hamiltonian representation is noncanonical, in the sense that J is singular and noninvertible, then we have instead

$$J\frac{\delta \mathcal{H}}{\delta u}\Big|_{u=U} = 0 \tag{59}$$

implying that

$$\frac{\delta \mathcal{H}}{\delta u}\Big|_{u=U} = -\frac{\delta \mathcal{C}}{\delta u}\Big|_{u=U} \tag{61}$$

for some Casimir functional $\mathcal{C}(u)$, which satisfies

$$J\frac{\delta \mathcal{C}}{\delta u} = 0. \tag{62}$$

Thus, the steady state $u = U$ is a constrained conditional extremum of $\mathcal{H}$; equivalently, it is a conditional extremum of the combined invariant $(\mathcal{H}+\mathcal{C})$.

Equation (62) implies that

$$[\mathcal{F}, \mathcal{C}] = \left(\frac{\partial \mathcal{F}}{\partial u}, J\frac{\partial \mathcal{C}}{\partial u}\right) = 0, \quad \forall\ \mathcal{F} \tag{63a}$$

and in particular,

$$[\mathcal{H}, \mathcal{C}] = 0. \tag{63b}$$

It follows immediately from (63) that Casimir functionals are integral invariants of the dynamical system, because

$$\frac{d\mathcal{C}}{dt} = [\mathcal{C}, \mathcal{H}] = 0. \tag{64}$$

The usual invariants are associated with explicit symmetries of the Hamiltonian itself. When these symmetries are continuous ones (like the translations in time and space), Noether's Theorem provides the connection between the two.

THEOREM (Noether): If $\mathcal{H}$ is invariant under translations in x, generated by the functional $\mathcal{M}$, i.e.,

$$J\frac{\delta \mathcal{M}}{\delta u} = -\frac{\partial u}{\partial x} \tag{65}$$

then $\mathcal{M}$ is invariant, i.e.,

$$\frac{d\mathcal{M}}{dt} = 0. \tag{66}$$

Proof: We have

$$\frac{d\mathcal{M}}{dt} = \left(\frac{\delta \mathcal{M}}{\delta u}, J\frac{\delta \mathcal{H}}{\delta u}\right) = -\left(J\frac{\delta \mathcal{M}}{\delta u}, \frac{\delta \mathcal{H}}{\delta u}\right)$$

$$= \left(\frac{\partial u}{\partial x}, \frac{\delta \mathcal{H}}{\delta u}\right) = \frac{\partial \mathcal{H}}{\partial x} = 0.$$

Corollary: If $\mathcal{H}$ is invariant under translations in t, then $\mathcal{H}$ is an invariant, i.e.,

$$\frac{d\mathcal{H}}{dt} = 0. \tag{67}$$

In addition to these usual invariants, noncanonical Hamiltonian systems possess Casimir invariants which cannot be obtained from Noether's Theorem. Casimir invariants are not associated with any property of the Hamiltonian function itself, but rather arise from the degenerate nature of the symplectic operator J. (Note that a canonical system has no nontrivial Casimir invariants because, when J is invertible, the condition

$$J\frac{\delta\mathcal{C}}{\delta u} = 0$$

implies

$$\frac{\delta\mathcal{C}}{\delta u} = 0$$

which, in turn, implies that $\mathcal{C}$ is simply a constant.)

Three–Dimensional Incompressible Flows

Consider a three–dimensional incompressible flow in a domain $D \subseteq R^3$. The governing equations are [see equations (41) and (42)]

$$\nabla \cdot \mathbf{v} = 0 \tag{68}$$

$$\frac{\partial \mathbf{v}}{\partial t} - \mathbf{v} \times \boldsymbol{\Omega} = -\nabla b, \tag{69}$$

where

$$b = p + \frac{1}{2}V^2, \qquad \boldsymbol{\Omega} = \nabla \times \mathbf{v}.$$

Upon taking the curl, we obtain the vorticity equation from equation (69):

$$\frac{\partial \boldsymbol{\omega}}{\partial t} - \nabla \times (\mathbf{v} \times \boldsymbol{\Omega}) = \mathbf{0}. \tag{70}$$

The Hamiltonian for this system is

$$\mathcal{H} = \frac{1}{2}\int_D \boldsymbol{\psi} \cdot \boldsymbol{\Omega}\, dx, \tag{71}$$

where

$$\mathbf{v} = \nabla \times \boldsymbol{\psi}.$$

In deriving (71), we have put $|\boldsymbol{\psi}| = 0$ on the boundary ∂D (alternatively, one may impose the preservation of circulation on ∂D, i.e., $\delta\Gamma = 0$ on ∂D), and $\boldsymbol{\psi}$ is made unique by imposing the gauge condition

$$\nabla \cdot \boldsymbol{\psi} = 0. \tag{72}$$

If one chooses $\boldsymbol{\Omega}$ to be the canonical (Darboux) variable and takes the skew–symmetric operator to be (Olver)

$$J = -\nabla \times (\boldsymbol{\Omega} \times \nabla \times (\cdot)), \tag{73}$$

Hamilton's equation is

$$\frac{\partial \boldsymbol{\Omega}}{\partial t} = J\frac{\delta \mathcal{H}}{\delta \boldsymbol{\Omega}} = -\nabla \times (\boldsymbol{\Omega} \times \nabla \times (\boldsymbol{\psi})) = \nabla \times (\mathbf{v} \times \boldsymbol{\Omega}), \tag{74}$$

which is just equation (70)! Thus, in the Hamiltonian formulation, the Euler equations describe the equations for the geodesic flow on an infinite–dimensional group of volume–preserving diffeomorphisms.

The Casimirs for this problem are the solutions of

$$J\frac{\delta \mathscr{C}}{\delta \boldsymbol{\Omega}} = -\nabla \times \left[\boldsymbol{\Omega} \times \left(\nabla \times \frac{\delta \mathscr{C}}{\delta \boldsymbol{\Omega}} \right) \right] = \mathbf{0}, \tag{75}$$

which implies that

$$\frac{\delta \mathscr{C}}{\delta \boldsymbol{\Omega}} = \mathbf{v}. \tag{76}$$

Then, a Casimir is the helicity

$$\mathscr{C} = \int_D \mathbf{v} \cdot \boldsymbol{\Omega} \, dx, \tag{77}$$

which characterizes the knottedness of the vortex line topology (Moffatt). The total helicity is not positive definite, so one cannot imagine a development of the minimum helicity state. Actually, one obtains a Beltrami flow (which has velocity parallel to vorticity) by minimizing energy while conserving the total helicity (see below).

Extremization of the Hamiltonian (71), keeping the Casimir invariant (77) fixed, leads to

$$\frac{\delta \mathscr{C}}{\delta \boldsymbol{\Omega}} = \mu \frac{\delta \mathscr{C}}{\delta \boldsymbol{\Omega}}$$

or

$$\boldsymbol{\psi} = \mu \mathbf{v}$$

or

$$\mathbf{v} = \mu \boldsymbol{\Omega} \tag{78}$$

where μ is a constant. The flows for which equations (78) are true are called *Beltrami flows*.

1.2. Surface Tension

Surface tension is a cause of the fact that small water drops in air and small gas bubbles in water take up a spherical form. Surface tension is a consequence of intermolecular cohesive forces. When one of two media in contact is a liquid phase, work must be done on a molecule approaching the interface from the interior of the liquid because this molecule experiences an unbalanced cohesive force directed away from the interface. This results in a higher potential energy for the molecules at the interface and a tendency for all molecules of the liquid near the interface to move inward. Consequently, the interface tends to contract as if it were in a state of tension like a stretched membrane. In a state of equilibrium the interface energy must be a minimum, and for a given volume the sphere is the shape with the least surface area so that a water drop in air and an air bubble in water are spherical.

Consider the interface between two stationary fluids. In order to determine the shape of the interface corresponding to a mechanical equilibrium, note that a

curved surface under tension exerts a normal stress across the surface. First, note that if the latter is described by

$$z-\zeta(x,y)=0, \tag{1}$$

the unit normal to the interface, at the origin 0, is given by

$$\hat{n}=\left(-\frac{\partial\zeta}{\partial x},\ -\frac{\partial\zeta}{\partial y},\ 1\right). \tag{2}$$

The resultant of the tensile forces acting on a portion of the interface containing 0 is

$$-T\oint\hat{n}\times d\boldsymbol{x}. \tag{3}$$

where T is the surface tension, and $d\boldsymbol{x}$ is a line element of the closed curve bounding the portion of the interface. This resultant is a force parallel to the z–axis, (which is the normal at 0) and is of magnitude

$$-T\oint\left(-\frac{\partial\zeta}{\partial x}dy+\frac{\partial\zeta}{\partial y}dx\right)=T\left(\frac{\partial^2\zeta}{\partial x^2}+\frac{\partial^2\zeta}{\partial y^2}\right)dA, \tag{4}$$

where dA is an area element of this portion of the interface.

Now, let the interface deviate only slightly from the plane $z=0$ so that ζ is everywhere small. The area S of the interface is given by

$$S=\iint\sqrt{1+\left(\frac{\partial\zeta}{\partial x}\right)^2+\left(\frac{\partial\zeta}{\partial y}\right)^2}\ dxdy\approx\iint\left[1+\frac{1}{2}\left(\frac{\partial\zeta}{\partial x}\right)^2+\frac{1}{2}\left(\frac{\partial\zeta}{\partial y}\right)^2\right]dxdy, \tag{5}$$

from which the change in the interface area on deformation is given by

$$\delta S=\iint\left[\frac{\partial\zeta}{\partial x}\frac{\partial\delta\zeta}{\partial x}+\frac{\partial\zeta}{\partial y}\frac{\partial\delta\zeta}{\partial y}\right]dxdy=-\iint\left(\frac{\partial^2\zeta}{\partial x^2}+\frac{\partial^2\zeta}{\partial y^2}\right)dxdy\delta\zeta. \tag{6}$$

Let R_1 and R_2 be the principal radii of curvature at a given point of the surface. Let dl_1 and dl_2 be two length elements on the surface which are also elements of circumference of circles with radii R_1 and R_2. Hence,

$$S=\iint dl_1\left(1+\frac{\partial\zeta}{R_1}\right)dl_2\left(1+\frac{\partial\zeta}{R_2}\right)\approx\iint dl_1dl_2\left(1+\frac{\partial\zeta}{R_1}+\frac{\partial\zeta}{R_2}\right), \tag{7}$$

from which

$$\delta S\approx\iint\delta\zeta\left(\frac{1}{R_1}+\frac{1}{R_2}\right)dx\,dy. \tag{8}$$

On comparing (6) and (8), one obtains

$$\frac{1}{R_1}+\frac{1}{R_2}=-\left(\frac{\partial^2\zeta}{\partial x^2}+\frac{\partial^2\zeta}{\partial y^2}\right). \tag{9}$$

Thus, the tension acting on a curve bounding the interface element is dynamically equivalent to a pressure at 0 on the interface of magnitude

$$T\left(\frac{\partial^2\zeta}{\partial x^2}+\frac{\partial^2\zeta}{\partial y^2}\right)=T\left(\frac{1}{R_1}+\frac{1}{R_2}\right). \tag{10}$$

Note that it is necessary to recognize R_1 and R_2 as having appropriate signs, since the contribution to the equivalent pressure on the interface is directed toward the center of curvature.

Since the interface has negligible mass, a curved interface can be in equilibrium only if the effective pressure due to surface tension is balanced by the difference between the pressures in the fluids on the two sides of the interface, i.e.,

$$\Delta p=T\left(\frac{1}{R_1}+\frac{1}{R_2}\right). \tag{11}$$

Capillary Rises in Liquids

Consider a free liquid meeting a plane vertical rigid wall (Figure 1.3). Let us determine the interface shape $z=\zeta(y)$. Noting that the principal curvatures of the interface are

$$\frac{1}{R_1}=0, \qquad \frac{1}{R_2}=\frac{\zeta''}{\left(1+\zeta'^2\right)^{3/2}} \tag{12}$$

with primes being differentials with respect to y, one has from equation (11) the following:

$$\rho g\zeta-\frac{T\zeta''}{\left(1+\zeta'^2\right)^{3/2}}=0, \tag{13}$$

where we have used the fact that

$$y\Rightarrow\infty:\ \zeta,\zeta',\zeta''\Rightarrow 0. \tag{14}$$

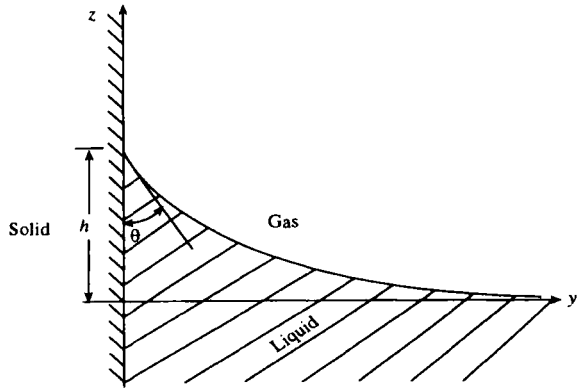

Figure 1.3. Free liquid meeting a plane vertical rigid wall.

An integration using these boundary conditions gives

$$\frac{1}{2}\rho g\zeta^2 + \frac{T}{\left(1+\zeta'^2\right)^{1/2}} = 1 \tag{15}$$

from which the rise of the liquid near the wall is given by

$$h^2 = \frac{2T}{\rho g}(1-\sin\theta). \tag{16}$$

where θ is the contact angle.

The fact that the free surface of a liquid rises or falls to meet a rigid wall leads to phenomena (called *capillarity*) which manifest themselves in small tubes.

1.3. A Program for Analysis of the Governing Equations

The set of equations governing the fluid flows given in the previous section is too complicated to render a direct mathematical approach feasible. Further, progress is possible only by isolating as much as possible the various physical features represented by these equations and then analyzing specific flow fields embodying these features separately. When assembled and interpreted appropriately, these special cases provide an insight into the totality of phenomena described by the governing equations.

Thus, as a first step, one considers a fluid as being endowed with inertia and no other physical properties – inviscid, incompressible fluid (Chapter 2). Though apparently a very restricted model, it nonetheless exhibits a wide variety of the properties of flows of a real fluid. Next, one may allow for variations in density brought about by flow–velocity variations – compressible fluid (Chapter 3). Further, one may recognize the nonzero resistance offered by a fluid to shearing deformations imposed on it – viscous fluid (Chapter 4).

EXERCISES

1. Consider a vessel containing a fluid of nonuniform subject gravity and density rotating steadily about the vertical z–axis, and assume that the fluid has taken up the same steady rotation. Show that the surfaces of constant pressure are paraboloids of revolution about the vertical axis.
2. Consider a capillary rise of a liquid in circular tube of small radius a. Find the height of the column of liquid in the tube supported by the surface tension against gravity.

This page intentionally left blank

2

DYNAMICS OF INVISCID, INCOMPRESSIBLE FLUID FLOWS

2.1. Fluid Kinematics and Dynamics

Stream Function

As discussed in Section 1.1, streamlines have the property that the instantaneous fluid velocity at any point is tangent to the streamline through that point. A surface made up entirely of streamlines instantaneously is called a *stream surface* or, when it has the appropriate shape (i.e., when the streamlines pass through a given closed curve in the fluid), a *stream tube*. The motion of a given fluid particle in space describes a pathline in space–time. In steady flow, the pathlines coincide with the instantaneous streamlines.

Streamlines are given by intersections of stream surfaces given by

$$\left.\begin{aligned} f(x,y,z) &= a, \\ g(x,y,z) &= b, \end{aligned}\right\} \tag{1}$$

or, if $\mathbf{v} = (u, v, w)$ denotes the fluid velocity, by

$$\left.\begin{aligned} uf_x + v f_y + wf_z &= 0, \\ ug_x + v g_y + wg_z &= 0, \end{aligned}\right\} \tag{2}$$

from which, one has

$$\left.\begin{aligned} u &= \lambda\left(f_y g_z - f_z g_y\right), \\ v &= \lambda\left(f_z g_x - f_x g_z\right), \\ w &= \lambda\left(f_x g_y - f_y g_x\right), \end{aligned}\right\} \tag{3}$$

where λ is an arbitrary constant.

For incompressible fluids, (3) gives

$$\mathbf{v} = \nabla f \times \nabla g \tag{4}$$

For two–dimensional flows, $g = -z$, $f = \Psi$, so that (4) leads to

$$u = -\Psi_y, \qquad v = \Psi_x. \tag{5}$$

Ψ is called the stream function because the streamlines for the flow are, in fact, the set of level curves given by $\Psi(x,y,t) = f(t)$ with $f(t)$ arbitrary. This may be seen by noting that the differential equation of the streamlines is

$$\frac{dx}{u} = \frac{dy}{v}. \tag{6}$$

When one uses equation (5), equation (6) leads to

$$\frac{\partial \Psi}{\partial x}\,dx + \frac{\partial \Psi}{\partial y}\,dy = 0$$

or

$$d\Psi = 0$$

or

$$\Psi(x,y,t) = f(t) \tag{7}$$

along a streamline.

In order to see further significance of the stream function, introduce, in a surface on which the streamlines lie, a set of orthogonal coordinates (α,β); the velocity component normal to an area element $dS = hk\,d\alpha\,d\beta$ is

$$v_n = \frac{f_\alpha g_\beta - f_\beta g_\alpha}{hk}. \tag{8}$$

Then the discharge through a portion S of the surface bounded by the traces of

$$\left.\begin{aligned} f(x,y,z) &= f_1, \quad f(x,y,z) = f_2, \\ g(x,y,z) &= g_1, \quad g(x,y,z) = g_2, \end{aligned}\right\} \tag{9}$$

is given by

$$Q = \iint_S v_n\,dS = \iint_S \left(f_\alpha g_\beta - f_\beta g_\alpha\right) d\alpha\,d\beta = \int_{g_1}^{g_2}\int_{f_1}^{f_2} df\,dg = (f_2 - f_1)(g_2 - g_1). \tag{10}$$

Note that Q is independent of the choice of the paths joining f_1 to f_2, and g_1 to g_2.

In two–dimensional flows, the discharge per unit length across an arc AB is $\Psi_B - \Psi_A$. In axisymmetric flows, the discharge across the surface generated by a revolving arc AB about the axis of symmetry is $2\pi(\Psi_B - \Psi_A)$. For the latter, $g = -\varphi$ and $F = \Psi$, and the radius and axial velocity components are given by

$$u = \frac{1}{r}\Psi_z, \qquad w = -\frac{1}{r}\Psi_r. \tag{11}$$

Here, φ is the azimuthal angle. Note that a stream tube cannot end in the interior of the fluid; it must either be closed, or end on the boundary of the fluid, or extend to infinity.

Finally, one should note the possibility that Ψ is a many–valued function of position whenever sources of mass exist in the flow field.

Equations of Motion

Referring to Section 1.1, the equation of conservation of mass is

$$\frac{\partial \rho}{\partial t} + \nabla \cdot (\rho \mathbf{v}) = 0, \tag{12}$$

where ρ is the mass density of the fluid.

The equation of motion (called *Euler's equation*) is

$$\rho\left[\frac{\partial \mathbf{v}}{\partial t} + (\mathbf{v}\cdot\nabla)\mathbf{v}\right] = \rho \boldsymbol{F} - \nabla p, \tag{13}$$

where $\boldsymbol{F}$ is the body force per unit volume, and p is the pressure.

Next, the equation of conservation of internal energy e is

$$\rho\left[\frac{\partial}{\partial t} + (\mathbf{v}\cdot\nabla)\right]\left(e + \frac{\mathbf{v}^2}{2}\right) = \rho \boldsymbol{F}\cdot\mathbf{v} - \nabla p\cdot\mathbf{v} - p\nabla\cdot\mathbf{v}; \tag{14a}$$

and when one uses equation (2), equation (14a) becomes

$$\rho\left[\frac{\partial e}{\partial t} + (\mathbf{v}\cdot\nabla)e\right] = -p\nabla\cdot\mathbf{v}. \tag{14b}$$

Integrals of Motion

Equation (2) can be written as

$$\rho\left[\frac{\partial \mathbf{v}}{\partial t} + \nabla\left(\frac{\mathbf{v}^2}{2}\right) - \mathbf{v}\times(\nabla\times\mathbf{v})\right] = \rho \boldsymbol{F} - \nabla p. \tag{15}$$

When the body force $\boldsymbol{F}$ is conservative, i.e.,

$$\boldsymbol{F} = -\nabla U$$

and the motion is steady, the integration of equation (15) is possible along a streamline, and one obtains along a streamline

$$\frac{\mathbf{v}^2}{2}+\frac{p}{\rho}+U=\text{ const.} \tag{16}$$

On the other hand, when the body force $\boldsymbol{F}$ is conservative and the flow is irrotational, i.e.,

$$\nabla\times\mathbf{v}=\mathbf{0} \quad \text{or} \quad \mathbf{v}=\nabla\Phi \tag{17}$$

(where the velocity potential Φ may be single–valued or multivalued depending on whether the region is simply connected or not, see below), the integration of equation (15) for an unsteady flow is possible in any direction, and one obtains Bernoulli's equation:

$$\frac{\partial\Phi}{\partial t}+\frac{\mathbf{v}^2}{2}+\frac{p}{\rho}+U=F(t). \tag{18}$$

In any event, for a steady flow and conservative body forces, equation (15) gives

$$\nabla\left[\frac{\mathbf{v}^2}{2}+U+\frac{p}{\rho}\right]=\mathbf{v}\times(\nabla\times\mathbf{v}). \tag{19}$$

For a two-dimensional flow, equation (16) gives

$$\left.\begin{aligned}\frac{\partial}{\partial x}\left(\frac{\mathbf{v}^2}{2}+U+\frac{p}{\rho}\right)&=v\Omega,\\ \frac{\partial}{\partial y}\left(\frac{\mathbf{v}^2}{2}+U+\frac{p}{\rho}\right)&=-u\Omega,\end{aligned}\right\} \tag{20a}$$

where

$$\boldsymbol{\Omega}\equiv\nabla\times\mathbf{v}=\Omega\hat{\boldsymbol{i}}_z.$$

Using the stream function Ψ, (20a) becomes

$$\frac{\mathbf{v}^2}{2}+U+\frac{p}{\rho}+\Omega\,\Psi=\text{ const.} \tag{20b}$$

Capillary Waves on a Spherical Drop

As an illustration of the use of the Bernoulli integral (18), consider small oscillations of a spherical drop of an incompressible fluid under the action of capillary forces. The area of surface given in spherical polar coordinates (r,θ,φ) by a function $r=r(\theta,\varphi)$ is

$$S = \int_0^{2\pi}\int_0^{\pi} \sqrt{r^2 + \left(\frac{\partial r}{\partial \theta}\right)^2 + \frac{1}{\sin^2\theta}\left(\frac{\partial r}{\partial \varphi}\right)^2}\; r \sin\theta \, d\theta \, d\varphi. \tag{21}$$

For small deviations from a spherical surface of radius R, one may write $r = R + \zeta$, $|\zeta| \ll R$, so that (21) may be approximated by

$$S \approx \int_0^{2\pi}\int_0^{\pi} \left[(R+\zeta)^2 + \left\{ \left(\frac{\partial \zeta}{\partial \theta}\right)^2 + \frac{1}{\sin^2\theta}\left(\frac{\partial \zeta}{\partial \theta}\right)^2 \right\} \sin\theta \, d\theta \, d\varphi \right], \tag{22}$$

from which the small change in the surface area is given by

$$\delta S \approx \int_0^{2\pi}\int_0^{\pi} \left[2(R+\zeta)\delta\zeta + \frac{\partial \zeta}{\partial \theta}\frac{\partial \delta\zeta}{\partial \theta} + \frac{1}{\sin^2\theta}\frac{\partial \zeta}{\partial \varphi}\frac{\partial \delta\zeta}{\partial \varphi} \right] \sin\theta \, d\theta \, d\varphi$$

$$= \int_0^{2\pi}\int_0^{\pi} \left[2(R+\zeta) - \frac{1}{\sin\theta}\frac{\partial}{\partial \theta}\left(\sin\theta \frac{\partial \zeta}{\partial \theta}\right) - \frac{1}{\sin^2\theta}\frac{\partial^2 \zeta}{\partial \varphi^2} \right] \delta\zeta \sin\theta \, d\theta \, d\varphi. \tag{23}$$

If R_1 and R_2 are the principal radii of curvature, then noting that

$$\delta S \approx \int\int \delta\zeta \left(\frac{1}{R_1} + \frac{1}{R_2}\right) R(R+2\zeta) \sin\theta \, d\theta \, d\varphi \tag{24}$$

one then obtains, on comparison with (23),

$$\frac{1}{R_1} + \frac{1}{R_2} = \frac{2}{R} - \frac{2\zeta}{R^2} - \frac{1}{R^2}\left[\frac{1}{\sin^2\theta}\frac{\partial^2 \zeta}{\partial \varphi^2} + \frac{1}{\sin\theta}\frac{\partial}{\partial \theta}\left(\sin\theta \frac{\partial \zeta}{\partial \theta}\right) \right]. \tag{25}$$

The Bernoulli integral (18) then gives

$$\rho \frac{\partial \Phi}{\partial t} + T\left[\frac{2}{R} - \frac{2\zeta}{R^2} - \frac{1}{R^2}\left\{ \frac{1}{\sin\theta}\frac{\partial}{\partial \theta}\left(\sin\theta \frac{\partial \zeta}{\partial \theta}\right) + \frac{1}{\sin^2\theta}\frac{\partial^2 \zeta}{\partial \theta^2} \right\} \right] = \text{const.}, \tag{26}$$

where T is the surface tension, and Φ is the velocity potential, given by $\mathbf{v} = \nabla\Phi$.

Differentiating (26) with respect to time and using the kinematic condition at the surface of the drop,

$$r = R: \quad \frac{\partial \zeta}{\partial t} = \frac{\partial \Phi}{\partial r} \tag{27}$$

(signifying the fact that a fluid particle on the surface of the drop always remains there), one obtains

$$r = R : \rho \frac{\partial^2 \Phi}{\partial t^2} - \frac{T}{R^2}\left[2\frac{\partial \Phi}{\partial r} + \frac{\partial}{\partial r}\left\{\frac{1}{\sin\theta}\frac{\partial}{\partial \theta}\left(\sin\theta \frac{\partial \Phi}{\partial \theta}\right) + \frac{1}{\sin^2\theta}\frac{\partial^2 \Phi}{\partial \varphi^2}\right\}\right] = 0. \tag{28}$$

One may now put

$$\Phi = e^{-i\omega t} f(r, \theta, \varphi) \tag{29}$$

with

$$f(r, \theta, \varphi) = r^{\ell} Y_{\ell m}(\theta, \varphi), \tag{30}$$

where $Y_{\ell m}(\theta, \varphi)$ are the spherical harmonics, satisfying the equation

$$\frac{1}{\sin\theta}\frac{\partial}{\partial \theta}\left(\sin\theta \frac{\partial Y_{\ell m}}{\partial \theta}\right) + \frac{1}{\sin^2\theta}\frac{\partial^2 Y_{\ell m}}{\partial \varphi^2} + \ell(\ell+1) Y_{\ell m} = 0 \tag{31}$$

and

$$\left.\begin{aligned} &Y_{\ell m}(\theta, \varphi) = P_{\ell}^{m}(\cos\theta) e^{im\varphi}, \\ &P_{\ell}^{m}(\cos\theta) = \sin^m\theta \frac{d^m P_{\ell}(\cos\theta)}{d(\cos\theta)^m}; \quad m = 0, \pm 1, \pm 2, \ldots, \pm \ell; \ \ell = 0, 1, 2, \ldots, \end{aligned}\right\} \tag{32}$$

and $P_{\ell}^{m}(\cos\theta)$ are the associated Legendre polynomials, and $P_{\ell}(\cos\theta)$ are the Legendre polynomials.

Equation (28) then gives

$$\omega^2 = \frac{T(\ell-1)(\ell+2)}{\rho R^3}. \tag{33}$$

Since, for a given ℓ, there are $(2\ell+1)$ different eigenfunctions, these frequencies have a degeneracy of $(2\ell+1)$. Note that

$$\ell = 0, 1 : \quad \omega = 0. \tag{34}$$

The case $\ell = 0$ corresponds to radial oscillations, and in an incompressible fluid such oscillations are impermissible. The case $\ell = 1$ corresponds to a translation of the drop as a whole.

Cavitation

For an incompressible fluid and for $\boldsymbol{F} = \boldsymbol{0}$, one obtains, from equation (15),

$$\nabla^2 p = -\frac{1}{2}\nabla^2 v^2 = -\rho \frac{\partial u_i}{\partial x_j}\frac{\partial u_i}{\partial x_j}. \tag{35}$$

Integrating equation (35) over a volume $\mathcal{V}$ enclosed by a surface S, one obtains

$$\int \hat{n} \cdot \nabla p \, dS = -\rho \int \frac{\partial u_i}{\partial x_j} \frac{\partial u_i}{\partial x_j} \, dx < 0 \tag{36}$$

from which, it is obvious that p can have a minimum value only at the boundary and not in the interior of the fluid. (Note, however, that the pressure can have a maximum value in the interior of the fluid.) Now, cavitation or bubble formation occurs in a fluid when the absolute pressure falls below a critical value, say, zero (such is the case near the tips of rapidly rotating turbine blades and ship propellers); since a liquid cannot withstand tension, the cavitation will occur first at some point on the boundary as the pressure everywhere is decreased. However, when the pressure in the neighborhood of a cavity rises above the vapor pressure again, the cavity collapses. The continual collapse of cavities leads to a deterioration and erosion of surfaces of solid bodies immersed in the liquid.

Rates of Change of Material Integrals

Consider the line integral of a scalar field $F(x,t)$,

$$\int_P^Q F \, dx,$$

taken along a material curve joining the points P and Q. Since this curve moves with the fluid and consists of the same fluid particles, the integral above is a function only of t. In order to determine its rate of change with time, suppose that the curve PQ moves to the curve $P'Q'$ at time $t + \delta t$ (see Figure 2.1).

Then, note that

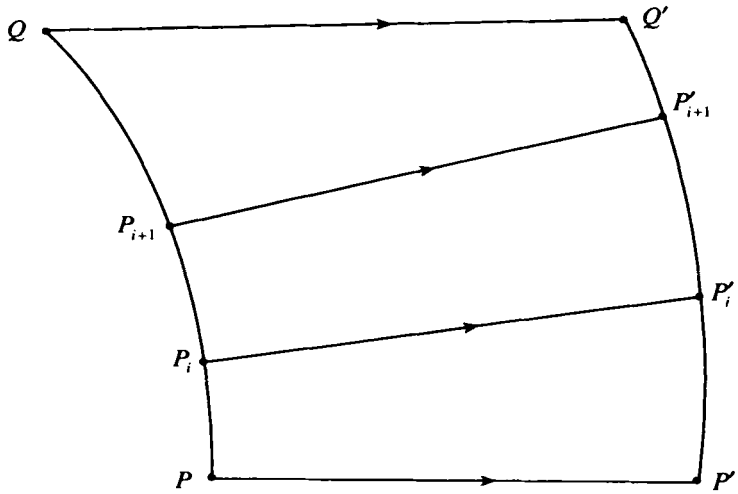

Figure 2.1. Displacement of a material curve.

$$\frac{d}{dt}\int_P^Q F(x,t)\,dx = \lim_{\delta t \Rightarrow 0} \frac{1}{\delta t}\left[\int_{P'}^{Q'} F(x',t+\delta t)\,dx - \int_P^Q F(x,t)\,dx\right]. \tag{37}$$

Dividing the curves PQ and $P'Q'$ into n segments by the points P_i and P_i', $i = 0,1,\ldots,n$, respectively, such that the segment P_iP_{i+1} of the curve PQ at time t moves to become the segment $P_i'P_{i+1}'$ of the curve $P'Q'$ at time $t+\delta t$, one has

$$\left.\begin{aligned}\int_P^Q F(x,t)dx &= \lim_{n\Rightarrow\infty}\sum_{i=1}^{n-1} F(x_i,t)\ \overrightarrow{P_iP_{i+1}},\\ \int_{P'}^{Q'} F(x',t+\delta t)dx &= \lim_{n\Rightarrow\infty}\sum_{i=1}^{n-1} F(x_i',t+\delta t)\ \overrightarrow{P_i'P_{i+1}'},\end{aligned}\right\} \tag{38}$$

where x_i and x'_i are the position vectors of P_i and P_{i+1}', respectively.

Now, writing

$$\begin{aligned}F(x_i',t+\delta t) &\approx F(x_i,t+\delta t)+\left(\overrightarrow{P_iP_i'}\cdot\nabla\right)F(x_i,t+\delta t)+0\left(\left|\overrightarrow{P_iP_i'}\right|^2\right)\\ &\approx F(x_i,t)+\frac{\partial F(x_i,t)}{\partial t}\,\delta t+v(x_i,t)\cdot\nabla F(x_i,t)+0(\delta t^2)\end{aligned}$$

$$\begin{aligned}\overrightarrow{P_i'P_{i+1}'} &\approx \overrightarrow{P_iP_{i+1}}+\left[v(x_{i+1},t)-v(x_i,t)\right]\delta t\\ &\approx \overrightarrow{P_iP_{i+1}}+\left(\overrightarrow{P_iP_{i+1}}\cdot\nabla\right)v(x_i,t)\delta t,\end{aligned} \tag{39}$$

one has

$$\begin{aligned}&F(x_i',t+\delta t)\ \overrightarrow{P_iP_{i+1}}-F(x_i,t)\ \overrightarrow{P_iP_{i+1}}\\ &\quad=\left\{\left[\frac{\partial F(x_i,t)}{\partial t}+v(x_i,t)\cdot\nabla F(x_i,t)\right]\overrightarrow{P_iP_{i+1}}\right.\\ &\qquad\left.+F(x_i,t)\left(\overrightarrow{P_iP_{i+1}}\cdot\nabla\right)v(x_i,t)\right\}\delta t+0(\delta t^2).\end{aligned} \tag{40}$$

Using (38) and (40), (37) leads to

$$\frac{d}{dt}\int_P^Q F\,dx = \int_P^Q \frac{DF}{Dt}\,dx + \int_P^Q F(dx\cdot\nabla)\,v. \tag{41}$$

If $\boldsymbol{F}(\boldsymbol{x},t)$ is a vector field,

$$\boldsymbol{F}(\boldsymbol{x},t) = F_1(\boldsymbol{x},t)\,\hat{\boldsymbol{i}}_x + F_2(\boldsymbol{x},t)\hat{\boldsymbol{i}}_y + F_3(\boldsymbol{x},t)\hat{\boldsymbol{i}}_z,$$

then one has, on successive use of equation (41),

$$\frac{d}{dt}\int_P^Q \boldsymbol{F}\cdot d\boldsymbol{x} = \int_P^Q \frac{D\boldsymbol{F}}{Dt}\cdot d\boldsymbol{x} + \int_P^Q \boldsymbol{F}\cdot(d\boldsymbol{x}\cdot\nabla)\boldsymbol{v}. \tag{42}$$

Irrotational Flow

The circulation is defined by

$$\Gamma = \oint_C \boldsymbol{v}\cdot d\boldsymbol{s} \tag{43}$$

where C is a closed curve made up of the same fluid particles. Assuming the region to be simply connected and using Stokes' Theorem, (43) becomes

$$\Gamma = \iint_S (\nabla\times\boldsymbol{v})\cdot\hat{\boldsymbol{n}}\,dS = \iint_S \boldsymbol{\Omega}\cdot\hat{\boldsymbol{n}}\,dS \tag{44}$$

where S is a surface bounded by the closed curve C, and $\hat{\boldsymbol{n}}$ is the unit normal to the surface element dS. Thus, the circulation around any reducible closed curve is equal to the integral of vorticity over an open surface bounded by the curve.

Using equation (42), one has

$$\frac{d\Gamma}{dt} = \oint_C \frac{D\boldsymbol{v}}{Dt}\cdot d\boldsymbol{s} + \oint_C \boldsymbol{v}\cdot(d\boldsymbol{s}\cdot\nabla\boldsymbol{v}). \tag{45}$$

Using equation (13), equation (45) becomes

$$\frac{d\Gamma}{dt} = \oint_C \boldsymbol{F}\cdot d\boldsymbol{s} - \oint_C \left(\frac{\nabla p}{\rho} - \nabla\left(\frac{1}{2}\boldsymbol{v}^2\right)\right)\cdot d\boldsymbol{s}. \tag{46}$$

If the body forces are conservative and the fluid is barotropic (i.e., $\nabla p/\rho$ can be written as a perfect differential), (46) gives

$$\frac{d\Gamma}{dt} = \frac{d}{dt}\iint_S \boldsymbol{\Omega}\cdot\hat{\boldsymbol{n}}\,dS = 0, \tag{47}$$

which implies that the circulation around any closed material curve and the strength of the vortex tube looped by the latter are invariants. Thus, under the action of conservative body forces, all motions of an inviscid, barotropic fluid setup from a state of rest or uniform motion are permanently irrotational.

The boundary–value problems for irrotational flows are, then, governed by the Laplace equation for the velocity potential Φ

$$\nabla^2\Phi = 0. \tag{48}$$

It is remarkable that equations (11), which are nonlinear, can be avoided in the study of kinematics of irrotational flows of an ideal fluid, which are governed by the Laplace equation. After the velocity field is determined, the pressure can be found from the Bernoulli equation [equation (18)], the only equation in which the nonlinearity of the Euler equation is manifested.

In a simply connected region, all closed curves C are reducible (i.e., they can be shrunk continuously down to a point without leaving the region), and one has

$$\Gamma = \iint_S \Omega \cdot \hat{n}\, dS = \oint_C d\Phi = 0 \tag{49}$$

so that Φ is single–valued. Whereas in a doubly connected region some closed curves C are not reducible and then Φ may be multivalued for irreducible curves C, the various values of the potential differ from one another by multiples of the circulation.

One has, from equation (48), some standard results from the potential theory, which can be readily proved:

* The potential Φ can neither have a maximum nor a minimum in the interior of the fluid.

* The solution of the Neumann exterior problem (where in the derivatives of Φ are prescribed on the boundaries) in a simply connected region is unique up to an additive constant.

* The solution of the Neumann exterior problem in a doubly connected region is uniquely determined (up to an additive constant) only when the circulation is specified.

The lack of explicit appearance of time variation in equation (48) implies that the instantaneous flow pattern depends only on the instantaneous boundary conditions and not on the history of the flow.

Thus, when a rigid body moves through a fluid which is otherwise stationary, the flow field is determined uniquely by the instantaneous velocity of the body (together with its shape); neither the acceleration nor the past history of motion of the body is relevant. (This is, of course, valid only when the compressibility of the fluid is ignored, as in equation (48), so that the speed of sound is infinity!)

Simple–Flow Patterns

Since Laplace's equation (48) is linear, it is permissible to build up some flow patterns by superposing certain singular solutions of equation (48). Let us first consider a few two–dimensional simple–flow patterns.

The Source Flow

Consider a flow directed radially from a point source (see Figure 2.2). The incompressibility condition

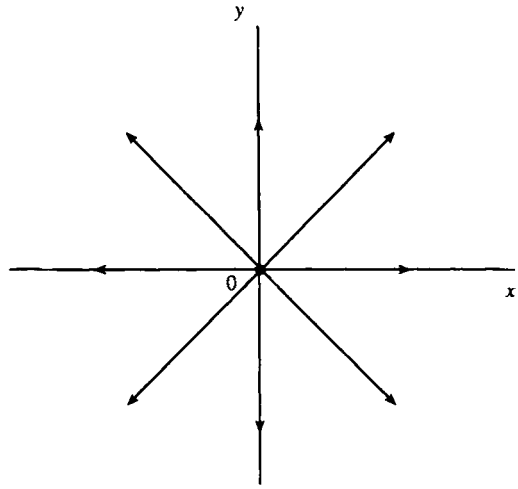

Figure 2.2. Source flow.

$$\frac{\partial}{\partial r}(ru_r) = 0 \tag{50}$$

gives

$$u_r = \frac{A}{r}, \tag{51}$$

where A is an arbitrary constant.

The conservation of mass, expressed by

$$q = \int_0^{2\pi} u_r \cdot r d\theta = \text{const.} \tag{52}$$

on using (51), gives

$$A = \frac{q}{2\pi}. \tag{53}$$

When one uses (53), (51) becomes

$$u_r = \frac{q}{2\pi r}. \tag{54}$$

Then, from the relations [see (4) and (17)]

$$u_r = \frac{\partial \Psi}{r\partial\theta} = \frac{\partial \Phi}{\partial r} \tag{55}$$

one obtains the following for the stream function Ψ and the velocity potential Φ:

$$\Psi = \frac{q\theta}{2\pi}, \qquad \Phi = \frac{q}{2\pi} \ln r \tag{56}$$

q may be called the source strength. Note that the stream function is a many-valued function of position, owing to the existence of a nonzero volume flux across a closed curve around the origin.

The Doublet Flow

Consider the superposition of a sink (strength $-q$) at $(-a,0)$, and a source (strength q) at $(0,a)$ (see Figure 2.3). From (56), one obtains the following for the velocity potential of the combined flow:

$$\Phi = \frac{q}{2\pi} \ln \sqrt{r^2 + a^2 - 2ra\cos\theta} - \frac{q}{2\pi} \ln \sqrt{r^2 + a^2 + 2ra\cos\theta}$$

$$= \frac{q}{4\pi} \ln \left[1 - \frac{4ra\cos\theta}{r^2 + a^2 + 2ra\cos\theta} \right]. \tag{57}$$

If a is small enough, (57) may be approximated by

$$\Phi \approx \frac{q}{4\pi} \left(-\frac{4a\cos\theta}{r} \right). \tag{58}$$

Consider the limit

$$\lim_{\substack{a \Rightarrow 0 \\ q \Rightarrow \infty}} q \cdot 2a = \mu = \text{finite} \tag{59}$$

so that (58) becomes, in this limit,

$$\Phi = -\frac{\mu \cos\theta}{2\pi r}. \tag{60}$$

The stream function for this flow is, then, given by

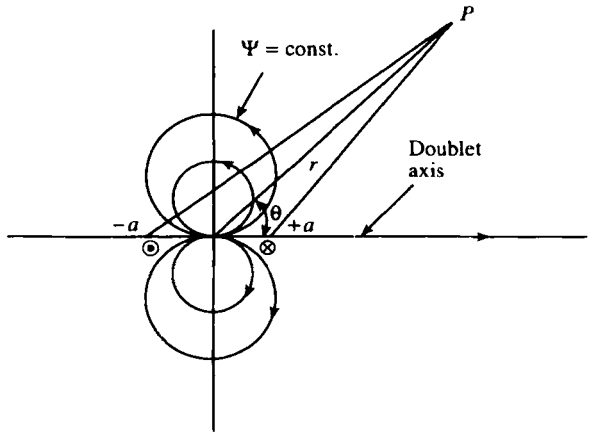

Figure 2.3. Doublet flow.

$$\Psi = \frac{\mu \sin\theta}{2\pi r}. \tag{61}$$

In cartesian coordinates, (60) and (61) become

$$\Phi = -\frac{\mu x}{2\pi\left(x^2+y^2\right)}, \qquad \Psi = \frac{\mu y}{2\pi\left(x^2+y^2\right)}. \tag{62}$$

Thus, the equipotentials given by Φ = constant are the coaxial circles

$$x^2 + y^2 = 2k_1 x,$$

and the streamlines given by Ψ = constant are the coaxial circles

$$x^2 + y^2 = 2k_2 y.$$

The first family has centers $(k_1, 0)$ and radii k_1; the second family has centers $(0, k_2)$ and radii k_2 (see Figure 2.3). The two families are mutually orthogonal.

The Vortex Flow

Consider a flow given by the streamlines in concentric circles. The velocity potential and the stream function for this flow are given by

$$\Phi = \frac{\Gamma\theta}{2\pi}, \qquad \Psi = -\frac{\Gamma}{2\pi}\ln r, \tag{63}$$

where Γ is the circulation of the flow.

Let us now build up some simple–flow patterns using these singular solutions.

Doublet in a Uniform Stream

The velocity potential and the stream function for a uniform stream with velocity (U, V) are given by

$$\left.\begin{aligned} \Phi &= Ux + Vy, \\ \Psi &= -Vx + Uy. \end{aligned}\right\} \tag{64}$$

For a doublet in a uniform stream $(U, 0)$, one obtains the following equation for the stream function:

$$\Psi = Ur\sin\theta - \frac{\mu}{2\pi}\frac{\sin\theta}{r} = U\sin\theta\left(r - \frac{\mu}{2\pi U}\frac{1}{r}\right). \tag{65}$$

The velocity components are, then, given by

$$\left.\begin{aligned} u_r &= \frac{1}{r}\frac{\partial\Psi}{\partial\theta} = U\left(1 - \frac{\mu}{2\pi U}\frac{1}{r^2}\right)\cos\theta, \\ u_\theta &= -\frac{\partial\Psi}{\partial r} = -U\left(1 + \frac{\mu}{2\pi U}\frac{1}{r^2}\right)\sin\theta, \end{aligned}\right\} \tag{66}$$

which shows the stagnation points given by $\mathbf{v} = \mathbf{0}$, at $r = \sqrt{\mu/2\pi U}$, and

$\theta = 0, \pi$. Equation (66) also shows that it represents the flow past a circular cylinder of radius

$$a = \sqrt{\frac{\mu}{2\pi U}} \tag{67}$$

because the kinematic condition

$$r = a: \quad u_r = 0 \tag{68}$$

is automatically satisfied on such a body.

The stream function (65) may, then, be rewritten as

$$\Psi = U\left(1 - \frac{a^2}{r^2}\right) r \sin\theta. \tag{69}$$

Using (69) in (18), one obtains the following condition for the pressure on the cylinder:

$$r = a: \quad \frac{p - p_\infty}{1/2\,\rho U^2} = C_p = 1 - \left(\frac{u_\theta}{U}\right)^2 = 1 - 4\sin^2\theta, \tag{70}$$

which is symmetric about the direction of streaming so that in such a flow there is neither a drag nor a lift on the cylinder.

Uniform Flow Past a Circular Cylinder with Circulation

The stream function for a uniform flow past a circular cylinder with circulation (see Figure 2.4) is, on using (63) and (69), given by

$$\Psi = Ur\sin\theta + \frac{\Gamma}{2\pi}\ln\left(\frac{r}{a}\right) - \frac{Ua^2}{r}\sin\theta, \tag{71}$$

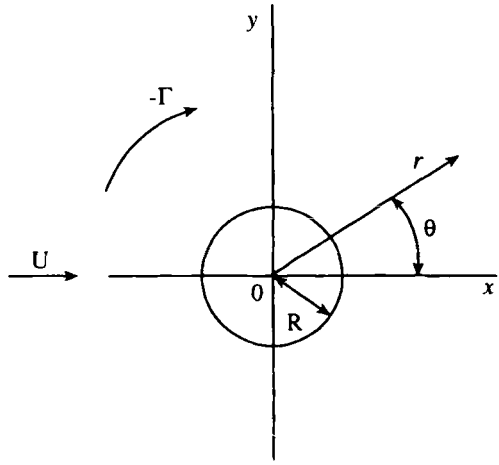

Figure 2.4. Uniform flow past a circular cylinder with circulation.

from which the velocity components are given by

$$\left.\begin{aligned} u_r &= \frac{1}{r}\frac{\partial \Psi}{\partial \theta} = U\left(1-\frac{a^2}{r^2}\right)\cos\theta, \\ u_\theta &= -\frac{\partial \Psi}{\partial r} = -U\left(1+\frac{a^2}{r^2}\right)\sin\theta - \frac{\Gamma}{2\pi r}, \end{aligned}\right\} \tag{72}$$

which shows the stagnation points given by $u_r = 0, u_\theta = 0$ at $r = a$, $\theta = \sin^{-1}\left(\Gamma/4\pi Ua\right)$. For $r \geq a$, these are given by

$$\cos\theta = 0 \quad \text{or} \quad \theta = \pm\frac{\pi}{2}$$

and

$$U\left(1+\frac{a^2}{r^2}\right) = \pm\frac{\Gamma}{2\pi r}, \tag{73}$$

which gives real values for r if $\Gamma \geq 4\pi Ua$. There are two stagnation points $r = r_1, r_2$ such that $r_1 r_2 = a^2$. Hence, one stagnation point lies outside $r = a$ and the other inside. The tangential velocity on the cylinder is, then, given by

$$r = a: \quad u_\theta = -\left(2U\sin\theta + \frac{\Gamma}{2\pi a}\right),$$

which is everywhere in the direction of Γ.

For $r = a$, from (73) the stagnation points are given by

$$\Gamma = -4\pi Ua\sin\theta. \tag{74}$$

If $\Gamma = 4\pi Ua\sin\alpha$, then the stagnation points are given by

$$-\sin\theta = \sin\alpha \quad \text{or} \quad \theta = -\alpha \text{ and } \pi+\alpha. \tag{75}$$

The flow pattern is shown in Figure 2.5.

Using (72) in (18), one obtains the following condition for the pressure on the cylinder:

$$r = a: \quad p = H - 4U^2\sin^2\theta - \frac{\Gamma^2}{4\pi a^2} - \frac{\Gamma U}{\pi a}\sin\theta \tag{76}$$

where H is an arbitrary constant.

The net force on the cylinder is directed along the y–axis, called the *lift*, and is given by

$$L = -\int_0^{2\pi} p\sin\theta \cdot a\,d\theta = \rho U\Gamma. \tag{77}$$

This result is, in fact, independent of the shape of the cross section of the cylinder (see Section 2.7).

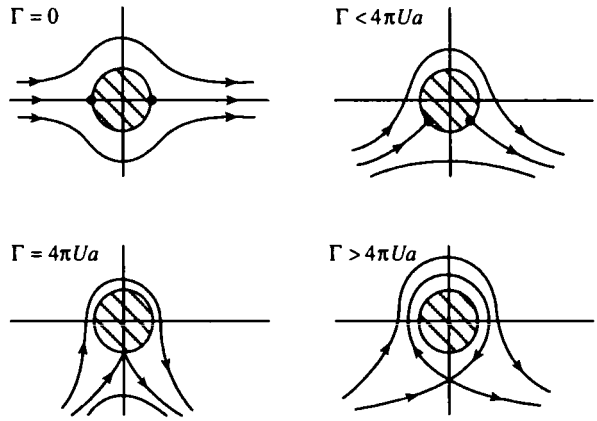

Figure 2.5. Uniform flows past a circular cylinder with various values of the circulation.

EXERCISES

1. Consider a vortex flow, as well as a doublet flow between two circular cylinders of radii R_1, R_2. Calculate the kinetic energy of the fluid between the two cylinders by a volume integral and an area integral over the boundaries separately.
2. Show that the irrotational flow of a fluid is impossible if the boundaries are fixed.[1]

2.2. The Complex–Variable Method

The Complex Potential

Since the properties exhibited by the velocity potential and stream function of a two–dimensional irrotational flow of an inviscid fluid, namely,

$$\left.\begin{aligned} &\frac{\partial^2\Phi}{\partial x^2}+\frac{\partial^2\Phi}{\partial y^2}=0, \quad \frac{\partial^2\Psi}{\partial x^2}+\frac{\partial^2\Psi}{\partial y^2}=0,\\ &\frac{\partial\Phi}{\partial x}=\frac{\partial\Psi}{\partial y}, \quad \frac{\partial\Phi}{\partial y}=-\frac{\partial\Psi}{\partial x},\\ &\frac{\partial\Phi}{\partial x}\cdot\frac{\partial\Psi}{\partial x}+\frac{\partial\Phi}{\partial y}\cdot\frac{\partial\Psi}{\partial y}=0, \end{aligned}\right\} \tag{1}$$

[1] This result implies that when the solid boundaries in motion are instantaneously brought to rest, the flow of the fluid will instantaneously cease to be irrotational but will not come to stop!

are identical to those exhibited by the real and imaginary parts of an analytic function of a complex variable, it is natural to combine Φ and Ψ into an analytic function F of a complex variable $z = x + iy$ in the region of the z–plane occupied by the flow, i.e., $F(z)$ has a unique derivative with respect to z at all points of this region. Thus, consider

$$F(z) = \Phi(x,y) + i\Psi(x,y). \tag{2}$$

This result makes all the resources of the theory of function of a complex variable available for the investigation of two–dimensional irrotational flows. From (2), one obtains for the "complex" velocity the following equation:

$$\frac{dF}{dz} \equiv W(z) = \frac{\partial \Phi}{\partial x} + i\frac{\partial \Psi}{\partial x} = \frac{\partial \Psi}{\partial y} - i\frac{\partial \Phi}{\partial y} = u - iv. \tag{3}$$

Example 1: For a uniform flow, we have

$$F(z) = Az. \tag{4}$$

Example 2: For a source flow or a vortex flow, one has

$$F(z) = A \ln z, \tag{5}$$

depending on whether A is real or imaginary.

Example 3: For a flow in a corner of angle α, one has

$$F(z) = Az^{\pi/\alpha}, \tag{6}$$

which is valid only in the neighborhood of the corner.

For illustration, consider the case $\alpha = \pi/2$, for which (6) becomes

$$F(z) = Az^2 \tag{7}$$

which describes the stagnation–point flow at a plane (by symmetry).

For the velocity potential and the stream function, (7) gives

$$\Phi = A\left(x^2 - y^2\right), \quad \Psi = 2Axy. \tag{8}$$

Thus, the equipotentials are the rectangular hyperbolae (Figure 2.6)

$$x^2 - y^2 = \text{const.}$$

with the asymptotes $y = \pm x$. The streamlines are also the rectangular hyperbolae (Figure 2.6)

$$xy = \text{const.}$$

with the axes $x = 0$, $y = 0$ as asymptotes. These two families of hyperbolae are

orthogonal to each other. Further, the only stagnation point in the flow occurs at the origin.

Now, the fact that there is no flow across a streamline implies that the flow is unaltered if any one of the streamlines is replaced by a rigid barrier. (The present case, namely $\alpha = \pi/2$, corresponds to replacing the axes $x = 0$, $y = 0$ by rigid boundaries.[2])

Example 4: For a doublet flow, upon superposing a source at $(a, 0)$ and a sink at $(-a, 0)$, one obtains

$$F(z) = \frac{q}{2\pi} \ln(z-a) - \frac{q}{2\pi} \ln(z+a) = \frac{q}{2\pi} \ln\left(1 - \frac{2a}{z+a}\right) \approx -\frac{q}{2\pi} \frac{2a}{z}. \tag{9}$$

Consider the limit

$$\lim_{\substack{a \Rightarrow 0 \\ q \Rightarrow \infty}} 2qa = \mu = \text{finite}, \tag{10}$$

so that (9) becomes

$$F(z) = -\frac{\mu}{2\pi z}. \tag{11}$$

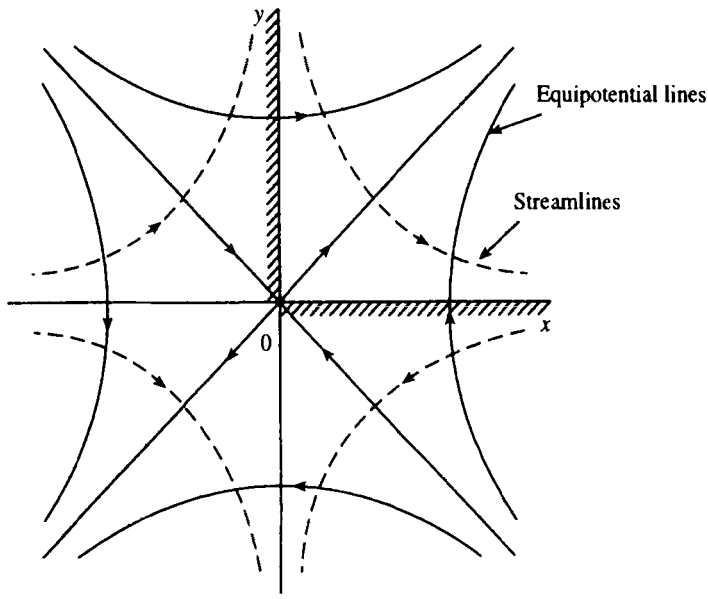

Figure 2.6. Flow in a corner of angle $\pi/2$.

[2]This implies prescribing an appropriate system of images in the barrier for the flow on the other side (see below).

Conformal Mapping of Flows

Consider a two–dimensional flow, for which the velocity potential Φ satisfies Laplace's equation:

$$\frac{\partial^2 \Phi}{\partial x^2} + \frac{\partial^2 \Phi}{\partial y^2} = 0. \tag{12}$$

Consider a transformation given by

$$\left.\begin{aligned} &(x, y) \Rightarrow [\xi(x, y),\ \eta(x, y)], \\ &\Phi(x, y) \Rightarrow \Phi(\xi, \eta). \end{aligned}\right\} \tag{13}$$

Then, equation (12) leads to

$$\begin{aligned} &\left[\left(\frac{\partial \xi}{\partial x}\right)^2 + \left(\frac{\partial \xi}{\partial y}\right)^2\right] \frac{\partial^2 \Phi}{\partial \xi^2} + \left[\left(\frac{\partial \eta}{\partial x}\right)^2 + \left(\frac{\partial \eta}{\partial y}\right)^2\right] \frac{\partial^2 \Phi}{\partial \eta^2} \\ &+ \left[\frac{\partial^2 \xi}{\partial x^2} + \frac{\partial^2 \xi}{\partial y^2}\right] \frac{\partial \Phi}{\partial \xi} + \left[\frac{\partial^2 \eta}{\partial x^2} + \frac{\partial^2 \eta}{\partial y^2}\right] \frac{\partial \Phi}{\partial \eta} \\ &+ 2\left[\frac{\partial \xi}{\partial x}\frac{\partial \eta}{\partial x} + \frac{\partial \xi}{\partial y}\frac{\partial \eta}{\partial y}\right] \frac{\partial^2 \Phi}{\partial \xi \partial \eta} = 0. \end{aligned} \tag{14}$$

If the transformation (13) is to relate the solution for one two–dimensional potential flow for one geometry with that for another geometry, i.e.,

$$\frac{\partial^2 \Phi}{\partial \xi^2} + \frac{\partial^2 \Phi}{\partial \eta^2} = 0, \tag{15}$$

then one requires, from equations (14) and (15),

$$\left.\begin{aligned} &\left(\frac{\partial \xi}{\partial x}\right)^2 + \left(\frac{\partial \xi}{\partial y}\right)^2 = \left(\frac{\partial \eta}{\partial x}\right)^2 + \left(\frac{\partial \eta}{\partial y}\right)^2 \neq 0, \\ &\frac{\partial^2 \xi}{\partial x^2} + \frac{\partial^2 \xi}{\partial y^2} = \frac{\partial^2 \eta}{\partial x^2} + \frac{\partial^2 \eta}{\partial y^2} = 0, \\ &\frac{\partial \xi}{\partial x}\frac{\partial \eta}{\partial x} + \frac{\partial \xi}{\partial y}\frac{\partial \eta}{\partial y} = 0, \end{aligned}\right\} \tag{16}$$

which are identified to be the rules governing the real and imaginary parts of an analytic function of a complex variable, i.e., $\zeta = \xi + i\eta$ is an analytical function of $z = x + iy$. If $\zeta = \zeta(z)$ describes a mapping of the z–plane onto the ζ–plane, then both the magnification ratio $|\zeta'(z)|$ and the angular rotation $\arg|\zeta'(z)|$ are the same for all curves C passing through the same point. Then, the

corresponding infinitesimal figures in the z- and ζ-planes are similar. This forms the raison d'être for the conformal mapping of flows.[3]

Example 5: Consider the flow past a parabolic cylinder (see Figure 2.7). The mapping

$$z = \zeta^2$$

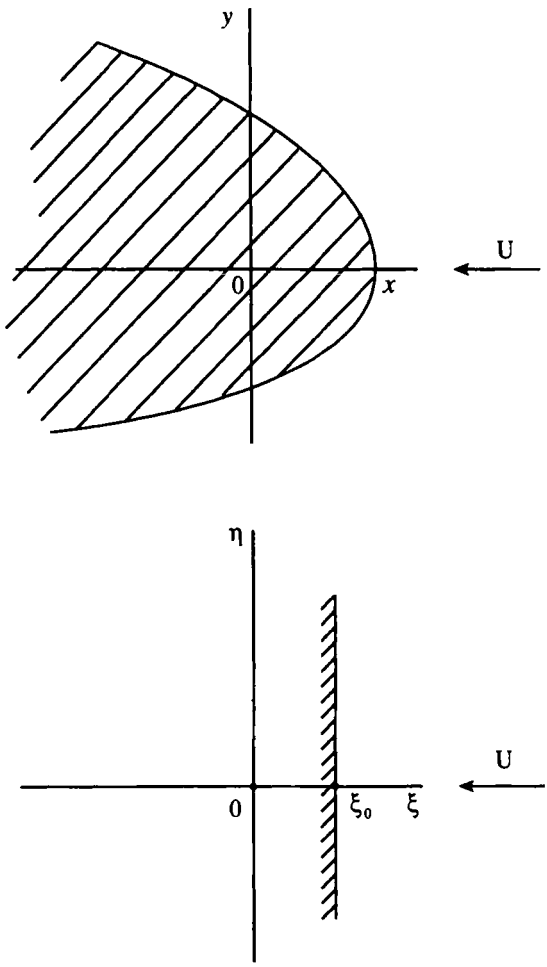

Figure 2.7. Flow past a parabolic cylinder.

[3]At a critical point of the mapping (where the latter is not conformal), the angles between two curves intersecting at this point are magnified n times, when $d^n\zeta/dz^n$ is the lowest derivative that does not vanish at this point.

maps the paraboloid in the z–plane into a plane $\xi = \xi_0$ in the ζ–plane (see Figure 2.7), since from

$$x = \xi^2 - \eta^2, \qquad y = 2\xi\eta$$

corresponding to $\xi = \xi_0$, we obtain

$$x - \xi_0^2 = -\frac{y^2}{4\xi_0^2}.$$

The flow impinging perpendicularly on a plane in the ζ–plane is given by

$$\tilde{F}(\zeta) = -A(\zeta - \zeta_0)^2$$

so that for the complex velocity in the z–plane, one obtains

$$W = \frac{d\tilde{F}/d\zeta}{dz/d\zeta} = -\frac{2A(\zeta - \xi_0)}{2\zeta}.$$

Using the boundary condition dictating that the two flows at infinity be the same, i.e.,

$$|\zeta| \Rightarrow \infty : W \Rightarrow -U$$

one obtains

$$A = U.$$

Thus, the complex velocity in the z–plane is given by

$$W = -\frac{U(\sqrt{z} - \xi_0)}{\sqrt{z}}.$$

Example 6: Consider the transformation

$$z = C\cosh\zeta,$$

which leads to the following relations:

$$\left.\begin{aligned} &\frac{x^2}{C^2\cosh^2\xi} + \frac{y^2}{C^2\sinh^2\xi} = 1, \\ &\frac{x^2}{C\cos^2\eta} - \frac{y^2}{C\sin^2\eta} = 1. \end{aligned}\right\}$$

Thus, $\xi = \xi_0$ gives an ellipse with major and minor radii, respectively:

$$a = C\cosh\xi_0, \qquad b = C\sinh\xi_0,$$

from which

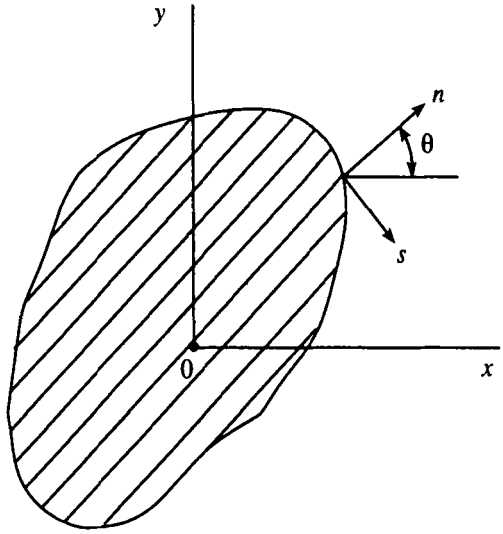

Figure 2.8. Body–fixed coordinates.

$$\left.\begin{aligned} a^2 - b^2 &= C^2, \\ a \pm b &= C e^{\pm \xi_0} \end{aligned}\right\}$$

or

$$\xi_0 = \frac{1}{2} \ln \frac{a+b}{a-b}.$$

Now, the boundary condition at the body requiring that the flow has no component normal to the body gives (see Figure 2.8)

$$-\frac{\partial \Psi}{\partial s} = -U \frac{\partial y}{\partial s},$$

from which

$$\Psi = Uy + \text{ const.}, \quad \text{at the body.}$$

Note that this prescription satisfies the boundary condition identically for any shape of the body translating in the x–direction.

Consider, for illustration, the flow in the ζ–plane to be given by

$$F = -\tilde{C} e^{-\zeta},$$

from which the velocity potential and the stream function are given by

$$\Phi = -\tilde{C} e^{-\xi} \cos \eta, \qquad \Psi = \tilde{C} e^{-\xi} \sin \eta.$$

The boundary condition at the body then gives

$$\tilde{C} = Ube^{\xi_0} = Ub\sqrt{\frac{a+b}{a-b}}$$

so that the stream function becomes

$$\Psi = Ub\sqrt{\frac{a+b}{a-b}}\, e^{-\xi} \sin\eta,$$

which gives the flow produced by a translating elliptic cylinder.

For a steady flow past an elliptic cylinder, on the other hand, the complex potential is given by

$$\tilde{F} = Ub\sqrt{\frac{a+b}{a-b}}\, e^{-\zeta} - UC\cos h\zeta.$$

Example 7: Consider a rigid body rotating about an axes through the origin. From the boundary condition at the body (see Figure 2.9), we obtain

$$-\frac{\partial\Psi}{\partial s} = \omega r\cos\theta = \omega r\frac{dr}{ds}$$

from which we obtain

$$\Psi = -\frac{1}{2}\omega r^2 + \text{const.}$$

Consider, for illustration, the flow to be given by the complex potential,

$$F = -iAz^2$$

so that the velocity potential and the stream function are given by

$$\Phi = 2Axy, \qquad \Psi = -A\left(x^2 - y^2\right).$$

The boundary condition at the body gives

$$A\left(x^2 - y^2\right) = \frac{1}{2}\omega^2\left(x^2 + y^2\right) - C$$

from which we obtain

$$\frac{x^2}{\left[C\Big/\left(\frac{\omega}{2} - A\right)\right]} + \frac{y^2}{\left[C\Big/\left(\frac{\omega}{2} + A\right)\right]} = 1,$$

which is an ellipse if $A < \omega/2$. If a and b the major and minor radii of this ellipse, i.e.,

$$a^2 = \frac{C}{\omega/2 - A}, \qquad b^2 = \frac{C}{\omega/2 + A},$$

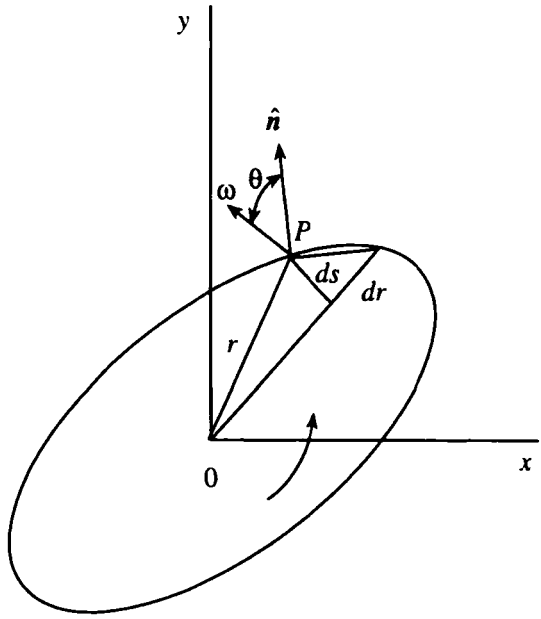

Figure 2.9. Rigid body rotating in a fluid.

then we obtain

$$A = \frac{\omega}{2}\,\frac{a^2 - b^2}{a^2 + b^2}.$$

Thus, the stream function becomes

$$\Psi = -\frac{\omega}{2}\,\frac{a^2 - b^2}{a^2 + b^2}\left(x^2 - y^2\right),$$

which represents the flow within an elliptic cylinder.

Consider next the transformation

$$z = C\cosh\zeta$$

and the flow in the ζ-plane to be given by the complex potential

$$\tilde{F} = -i\tilde{C}e^{-2\zeta}$$

so that the velocity potential and the stream function are given by

$$\Phi = -\tilde{C}e^{-2\xi}\sin 2\eta, \qquad \Psi = -\tilde{C}e^{-2\xi}\cos 2\eta.$$

The boundary condition at the body gives

$$-\tilde{C}e^{-2\xi_0}\cos 2\eta = -\frac{1}{4}C^2\omega\left(\cosh 2\xi_0 + \cos 2\eta\right) + D,$$

from which

$$\tilde{C}e^{-2\xi_0} = \frac{1}{4}C^2\omega, \qquad \frac{1}{4}C^2\omega\cos h2\xi_0 - D = 0.$$

If a and b are the major and minor radii of the elliptic cylinder given by $\xi = \xi_0$, then one obtains

$$a = C\cos h\xi_0, \qquad b = C\sin h\xi_0$$

or

$$e^{\xi_0} = \sin h\xi_0 + \cos h\xi_0 = \frac{a+b}{C}$$

so

$$\tilde{C} = (a+b)^2\frac{\omega}{4}.$$

Thus, the stream function becomes

$$\Psi = -\frac{\omega}{4}(a+b)^2 e^{-2\xi}\cos 2\eta,$$

which represents flow due to rotation of an elliptic cylinder.

Hydrodynamic Images

The hydrodynamic images are defined to be distributions of sources and vortices inside a body B, which would produce, outside B, the disturbance flow actually generated when B is placed in a field of flow. Thus, the image of a uniform stream $(U,0)$ in the circular cylinder $r = a$ is a doublet of moment $\left(-2\pi Ua^2,0\right)$ at the center $(0,0)$.

Consider a source outside a plane wall (Figure 2.10). The complex potential is given by

$$F = \frac{q}{2\pi}\left[\ln\left(z - z_0\right) + \ln\left(z + \bar{z}_0\right)\right]. \tag{17}$$

The presence of the image source ensures, on superposition with the given source, that the plane wall remains a streamline of the flow.

Let us next determine the complex potential representing motion of a fluid in the presence of an interior boundary of circular form. Let the complex potential of a given flow be given by

$$F = f(z),$$

which is free from singularities in the region $z \le a$. If now a stationary circular cylinder of radius a is placed with its center at the origin, one requires, for every singularity at z_0 of $f(z)$ (outside $z = a$), an image in the circular boundary at a^2/z_0 such that the two together will render the circle a streamline. Thus, for the

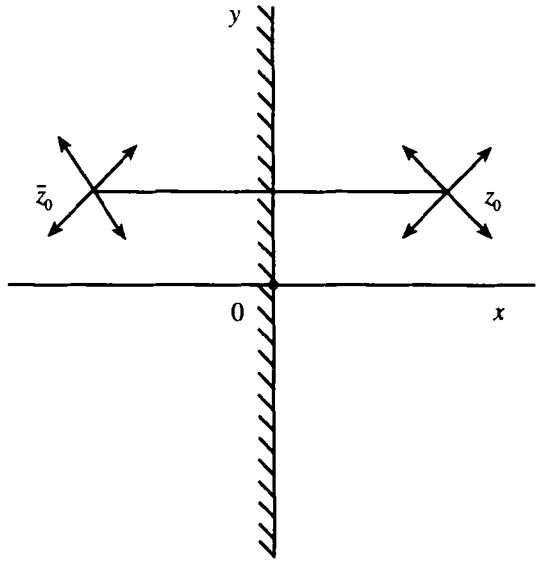

Figure 2.10. Source outside a plane wall.

complex potential for the flow in the presence of a circular cylinder, one obtains

$$f(z)+\bar{f}\left(\frac{a^2}{z}\right),$$

which is purely real on $|z|=a$, and the latter is, therefore, a streamline.

Example 8: Consider flow due to a point source of strength q at $z=z_0$; then, for the complex potential, we obtain

$$f(z)=\frac{q}{2\pi}\ln(z-z_0). \tag{18}$$

In the presence of a circular cylinder of radius $a<|z_0|$, with its center at the origin, the complex potential becomes

$$\begin{aligned} F &= \frac{q}{2\pi}\ln(z-z_0)+\frac{q}{2\pi}\ln\left(\frac{a^2}{z}-\bar{z}_0\right) \\ &= \frac{q}{2\pi}\ln(z-z_0)+\frac{q}{2\pi}\ln\left(z-\frac{a^2}{z_0}\right)-\frac{q}{2\pi}\ln z, \end{aligned} \tag{19}$$

which shows that, for a source outside the cylinder, the image system consists of (a) a source q at the inverse point $z=a^2/z_0$ and (b) a sink $-q$ at the origin.

Principles of Free–Streamline Flow

The boundary conditions imposed on the flow cases in the preceding examples do not permit separation of flow from a boundary. The assumption of free streamlines permits separation of the flow to occur at those sudden changes in direction of boundaries which otherwise cause infinite velocities. At separation points in steady flow of a fluid around a body, the streamlines leave the body. These dividing streamlines are called *free streamlines* in two–dimensional flow, and the fluid in contact with the body downstream from the separation points and separated from the main flow (assumed to be inviscid and irrotational) by the free streamlines is known as the *wake*. The fluid in the wake is assumed to be at rest in steady–flow problems. Since this is not quite so in actuality (the fluid in the wake is in a relatively slow recirculating flow), the theory yields better results if the wake contains another fluid of much less density.

If the effects of gravity are ignored, the pressure in the wake is constant, and the pressure along the free streamline must also be constant. From Bernoulli's equation [equation (18)] in Section 2.1, the velocity of the free streamline must also be constant. This somewhat alleviates the difficulty that the location of the free streamlines is not known beforehand.

The method of solution involves introducing a new complex variable

$$Q = \ln\left(\frac{1}{W}\right) = \ln q + i\theta,$$

where $W = qe^{-i\theta}$. Note that the real part of Q is constant on each free streamline and that the imaginary part of Q is constant on each straight portion of the rigid boundary, and on both of these boundaries the stream function Ψ is prescribed because they are streamlines. Consequently, the flow region is mapped onto a straight–sided figure in the Q–plane. One may then use a Schwartz–Christoffel transformation to map the interior of the straight–sided figure into the upper half of another plane.

Schwartz–Christoffel Transformation

This transformation maps the inside of a polygon in the z–plane onto the upper half of the ζ–plane. Consider the transformation given by

$$\frac{dz}{d\zeta} = C\prod_{i=1}^{n}(\zeta - a_i)^{\beta_i}, \tag{20}$$

where the a_i are real and are ordered as follows:

$$a_1 < a_2 < \cdots < a_n.$$

From equation (20), we obtain

$$\arg\left(\frac{dz}{d\zeta}\right) = \arg C + \beta_1 \arg(\zeta - a_1) + \beta_2 \arg(\zeta - a_2) + \cdots + \beta_n \arg(\zeta - a_n). \tag{21}$$

Now, since ζ is real, one has

$$\arg\left(\frac{dz}{d\zeta}\right) = \arg(dz) = \theta_i, \quad \text{in the } i\text{th interval.} \tag{22}$$

Further, when ζ lies on the real axis between a_i and a_{i+1}, note that

$$\arg(\zeta - a_k) = \begin{cases} 0, & k < i, \\ \pi, & k > i. \end{cases} \tag{23}$$

Using (22) and (23), (21) gives

$$\theta_i = \arg C + \pi(\beta_{i+1} + \beta_{i+2} + \cdots + \beta_n).$$

Thus, all points of the real axis segment $a_{i+1} - a_i$ are mappings of a line segment with slope θ_i in the z–plane (see Figure 2.11). Further,

$$\theta_{i+1} - \theta_i = -\pi\beta_{i+1}. \tag{24}$$

Noting that

$$\theta_{i+1} - \theta_i = \pi - \alpha_{i+1}, \tag{25}$$

where α_{i+1} is the interior angle at each corner (see Figure 2.11), one obtains

$$\alpha_{i+1} = \pi + \pi\beta_{i+1}$$

or

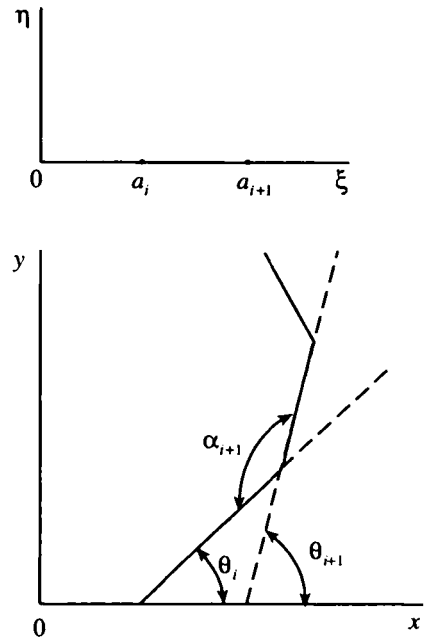

Figure 2.11. Schwartz–Christoffel mapping.

$$\beta_i = \frac{\alpha_i}{\pi} - 1. \tag{26}$$

Thus, (25) becomes

$$\frac{dz}{d\zeta} = C \prod_{i=1}^{n} (\zeta - a_i)^{(\alpha_i/\pi - 1)} \tag{27}$$

the scale factor C prescribes both the relative scale and the relative angular orientation of the two geometries. The transformation (27) transforms the real axis in the ζ–plane into the boundary of a polygon in the z–plane in such a way that the vertices of the polygon correspond to the points $a_1, a_2, \ldots$, and the interior angles of the polygon are $\alpha_1, \alpha_2, \ldots$.

Example 9: Consider a source of strength q in a channel (see Figure 2.12). One then sees, from (27), that the relation

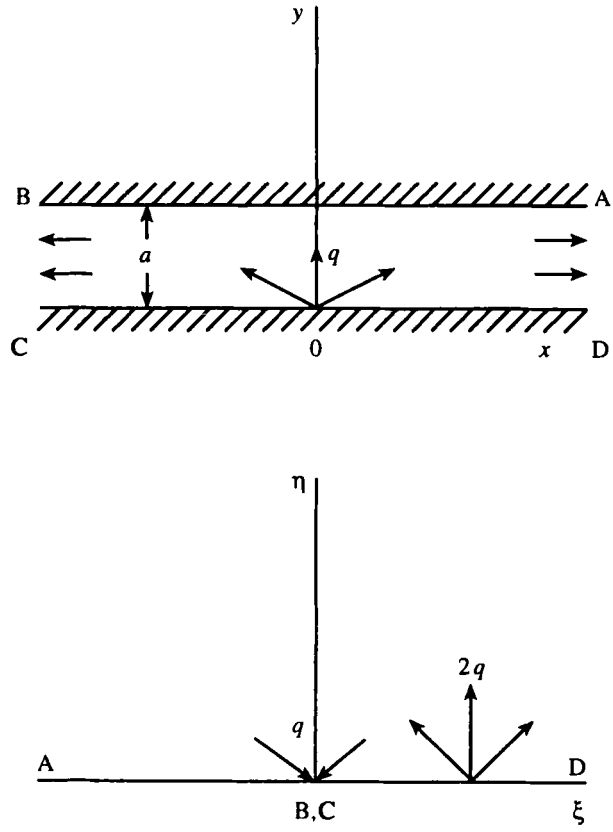

Figure 2.12. Conformal mapping for a source in a channel.

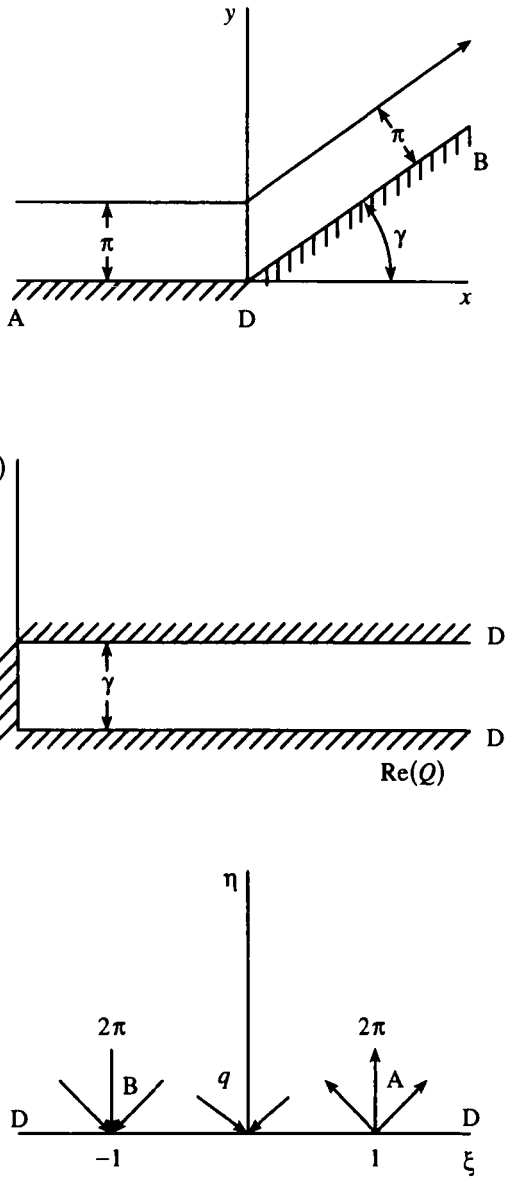

Figure 2.13. Conformal Mappings for a flow past a corner.

$$\frac{dz}{d\zeta} = \frac{C}{\zeta}$$

or

$$z = \frac{a}{\pi} \ln \zeta$$

transforms the given flow in the z–plane onto one in the ζ–plane, as shown in Figure 2.12. For the latter we obtain

$$\tilde{F}(\zeta) = \frac{2q}{2\pi} \ln(\zeta - 1) - \frac{q}{2\pi} \ln \zeta = \frac{q}{\pi} \ln \sin h \frac{\pi z}{a}.$$

Example 10: Consider the flow past a corner (see Figure 2.13). Making the hodograph transformation first, given by

$$Q = \ln\left(\frac{U}{W}\right) = \ln\left(\frac{U}{V}\right) + i\theta,$$

where U is the uniform flow speed away from the corner, the given flow maps onto a region shown in Figure 2.13. Note that the applicability of the Schwartz–Christoffel transformation depends crucially on the representation of the flow region into a polygon in the Q–plane, and this is possible only if all the solid boundaries are straight (the gravity effects on the free streamlines, of course, being neglected). Next, making the Schwartz–Christoffel transformation

$$\frac{dQ}{d\zeta} = C(\zeta + 1)^{-1/2}(\zeta - 1)^{-1/2}$$

or

$$Q = \frac{\gamma}{\pi} \cos h^{-1} \zeta$$

the given flow maps onto the one shown in Figure 2.13. The complex potential for the latter is given by

$$\tilde{F}(\zeta) = \ln(\zeta - 1) - \ln(\zeta + 1).$$

The sources at $\zeta = \pm 1$ have a strength of 2π.

Example 11: Consider a jet emerging from an orifice (see Figure 2.14). Again, one makes the hodograph transformation, first,

$$Q = \ln\left(\frac{U}{W}\right) = \ln\left(\frac{U}{V}\right) + i\theta,$$

where U is the uniform speed of the liquid on the free streamlines separating from the edges of the orifice, and this is also the speed in the interior of the jet far downstream from the orifice where the streamlines are straight and parallel.

One now makes the Schwartz–Christoffel transformation

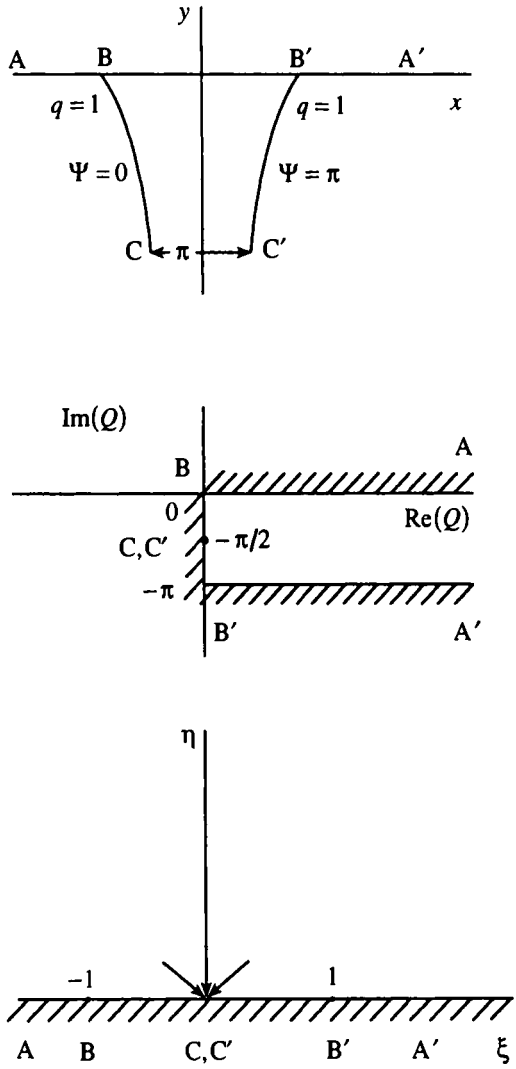

Figure 2.14. Conformal mappings for a jet emerging from an orifice.

$$\frac{dQ}{d\zeta} = C(\zeta+1)^{-1/2}(\zeta-1)^{-1/2}$$

or

$$Q = C\int \frac{d\zeta}{\sqrt{\zeta^2-1}},$$

which, on using

$$\left.\begin{aligned} \zeta = -1: \quad Q &= 0, \\ \zeta = 1: \quad Q &= -\pi i, \end{aligned}\right\}$$

becomes

$$Q = \cos h^{-1}\zeta - \pi i.$$

This transformation maps the given flow to the one shown in Figure 2.14. The complex potential for the latter is given by

$$\bar{F}(\zeta) = -\ln\zeta.$$

Note that, on the free streamline BC (see Figure 2.14), one has

$$ds = d\Phi = -\frac{d\zeta}{\zeta} = -\frac{d[\cos h(i\theta + i\pi)]}{\cos h(i\theta + i\pi)} = \frac{d(\cos\theta)}{\cos\theta} = -\tan\theta \cdot d\theta,$$

from which

$$dx = \sin\theta \cdot d\theta, \qquad dy = \frac{\sin^2\theta}{\cos\theta}\, d\theta.$$

Thus, the free streamline BC is given by

$$x = 1 - \cos\theta, \qquad y = -\sin\theta + \ln\left[\tan\left(\frac{\theta}{2} + \frac{\pi}{4}\right)\right].$$

The coefficient of contraction of the jet is, then, given by

$$\frac{2x_C}{2x_B} = \frac{\pi}{\pi + 2}.$$

Hodograph Method

This affords an alternate approach to solution of problems of free streamline flows. First, noting that

$$\left.\begin{aligned} F(z) &= \Phi + i\Psi, \\ \frac{dF}{dz} &= -qe^{-i\theta}, \end{aligned}\right\} \tag{28}$$

we obtain

$$dz = -\frac{e^{i\theta}}{q}\, dF = -\frac{e^{i\theta}}{q}\left(\frac{\partial F}{\partial q}\, dq + \frac{\partial F}{\partial \theta}\, d\theta\right). \tag{29}$$

Since dz is a perfect differential, (29) implies

$$\frac{\partial}{\partial\theta}\left(\frac{e^{i\theta}}{q}\frac{\partial F}{\partial q}\right) = \frac{\partial}{\partial q}\left(\frac{e^{i\theta}}{q}\frac{\partial F}{\partial \theta}\right), \tag{30}$$

from which we obtain

$$i\frac{\partial F}{\partial q} = -\frac{1}{q}\frac{\partial F}{\partial \theta}. \tag{31}$$

Equating real and imaginary parts of (31), we obtain

$$\frac{\partial \Phi}{\partial q} = -\frac{1}{q}\frac{\partial \Psi}{\partial \theta}, \qquad \frac{\partial \Psi}{\partial q} = \frac{1}{q}\frac{\partial \Phi}{\partial \theta} \tag{32}$$

from which we derive

$$\frac{\partial^2 \Psi}{\partial q^2} + \frac{1}{q}\frac{\partial \Psi}{\partial q} + \frac{1}{q^2}\frac{\partial^2 \Psi}{\partial \theta^2} = 0. \tag{33}$$

If it is possible to specify the boundary conditions in terms of q and θ, equation (33) enables one to solve for $\Psi(q,\theta)$. Using (32), one then solves for $\partial F/\partial q$, $\partial F/\partial \theta$. Using (29), one then determines $z = z(q,\theta)$, and next $x = x(q,\theta)$ and $y = y(q,\theta)$.

Example 12: Consider a uniform flow past a flat plate of breadth $4a$, placed broadside.

Now, the complex potential

$$F = -U\left(z + \frac{a^2}{z}\right) \tag{34}$$

represents the flow of a uniform stream U in the x–direction past a circular cylinder $|z| = a$. If the uniform stream makes an angle α with the x–direction, one has, on putting $z = e^{-i\alpha}\zeta$, for the complex potential the following:

$$F = -U\left(\zeta e^{-i\alpha} + \frac{a^2 e^{i\alpha}}{\zeta}\right). \tag{35}$$

The Joukowski transformation (see Section 2.7)

$$Z = X + iY = \zeta + \frac{a^2}{\zeta} \quad \text{or} \quad \zeta = \frac{Z + \sqrt{Z^2 - 4a^2}}{2} \tag{36}$$

transforms the circular cylinder into a flat plate leaving the direction of the uniform stream unaltered. Thus, the flow past a flat plate $-2a \le X \le 2a$, $Y = 0$ of a uniform stream U in a direction making an angle α with the X–direction is given by

$$F = -U\left[e^{-i\alpha}\frac{\left(Z+\sqrt{Z^2-4a^2}\right)}{2} + a^2 e^{i\alpha}\frac{2}{Z+\sqrt{Z^2-4a^2}}\right]$$

$$= -\frac{U}{2}\left[e^{-i\alpha}\left(Z+\sqrt{Z^2-4a^2}\right) + e^{i\alpha}\left(Z-\sqrt{Z^2-4a^2}\right)\right]$$

$$= -U\left(Z\cos\alpha - i\sqrt{Z^2-4a^2}\,\sin\alpha\right). \tag{37}$$

If $\alpha = \pi/2$, (37) becomes

$$F = iU\sqrt{Z^2-4a^2}\,. \tag{38}$$

This solution is, however, physically not acceptable because

$$Z = \pm 2a: \quad \frac{dF}{dz} \Rightarrow \infty$$

and the velocity becomes infinite at the edges of the plate. Further, the flow given by this solution is symmetrical with respect to the plane of the plate, whereas in reality the flow separates from the edges of the plate.

Instead of looking for a free–streamline flow type of solution of the problem in which the flow is divided into two regions – in one of which the fluid is at rest, while in the other it flows irrotationally – let us consider instead a somewhat simpler problem of two–dimensional jet impinging on a flat plate. The jet is supposed to originate as a uniform stream U of width $2K/U$ at $x \Rightarrow -\infty$ and is separated from the stagnant fluid by the free streamlines $\Psi = \pm K$. The x–axis is taken to be one axis of symmetry so that $\Psi = 0$ is the dividing streamline composed of the negative half of the x–axis together with the y–axis. It is sufficient to consider only the region $y \geq 0$. Referring to Figure 2.15, the points A and B represent points at infinity.

The hodograph of the free streamline AB where $\Psi = -K$ is a quadrant of the circle $q = U$ and those of the dividing streamlines OX and OY where $\Psi = 0$ are the axis OA and the ordinate OB. Noting that

$$\theta = 0, \frac{\pi}{2}: \quad \Psi = 0 \tag{39}$$

one obtains, from equation (33),

$$\Psi = \sum_s a_s q^{2s} \sin 2s\theta\,. \tag{40}$$

The boundary condition

$$\Psi(U,\theta) = -K, \quad 0 \leq \theta \leq \frac{\pi}{2} \tag{41}$$

then gives

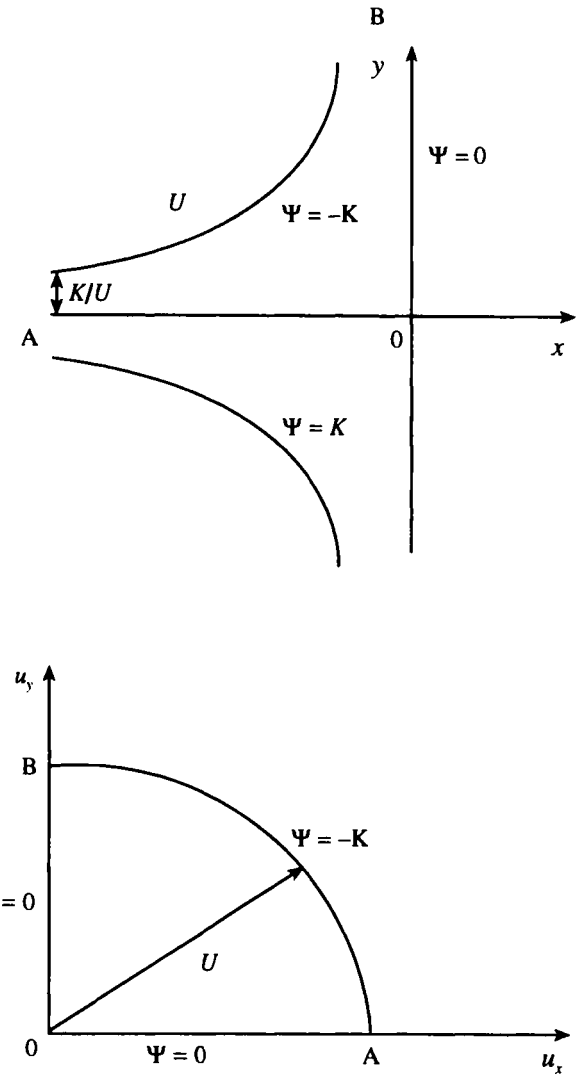

Figure 2.15. Flow impinging on a vertical wall (from Rutherford, 1959).

$$-K = \sum_s a_s U^{2s} \sin 2s\theta, \quad 0 \le \theta \le \pi/2 \tag{42}$$

from which

$$-\frac{a_s U^{2s}}{K} = \frac{4}{\pi} \int_0^{\pi/2} \sin 2st \, dt = \frac{4}{\pi} \left[\frac{1-(-1)^s}{2s} \right]. \tag{43}$$

Using (43), (40) becomes

$$\Psi = -\sum_{p=0} \frac{4K}{\pi(2p+1)} \left(\frac{q}{U}\right)^{2(2p+1)} \sin 2(2p+1)\theta. \tag{44}$$

Thus, the complex potential is given by

$$F = \frac{8K}{\pi} \sum_{p=0}^{\infty} \frac{1}{4p+2} \left(\frac{qe^{-i\theta}}{U}\right)^{4p+2} = \frac{8K}{\pi} \sum_{p=0}^{\infty} \frac{Z^{4p+2}}{4p+2}, \tag{45}$$

where

$$Z = \frac{qe^{i\theta}}{U}.$$

Noting, from (45), that

$$Udz = -\frac{dF}{Z} = -\frac{8K}{\pi} \sum_{p=0}^{\infty} Z^{4p} dZ = -\frac{8K}{\pi} \frac{dZ}{1-Z^4}, \tag{46}$$

one obtains, on integration,

$$z = -\frac{2K}{U}\left[\ln\left(\frac{1+Z}{1-Z}\right) + i \ln\left(\frac{1-iZ}{1+iZ}\right)\right]. \tag{47}$$

On the bounding streamline $\Psi = -K$, one has $q = U$ or $Z = e^{-i\theta}$. Noting, then, that

$$\left.\begin{aligned} \ln\left(\frac{1+Z}{1-Z}\right) &= -\ln\left(i \tan\frac{\theta}{2}\right) = -\frac{i\pi}{2} - \ln \tan\frac{\theta}{2}, \\ \ln\left(\frac{1-iZ}{1+iZ}\right) &= -\frac{i\pi}{2} - \ln \tan\left(\frac{\theta}{2}+\frac{\pi}{4}\right) = -\frac{i\pi}{2} - \ln\left(\frac{1+\tan\theta/2}{1-\tan\theta/2}\right), \end{aligned}\right\}$$

one obtains finally

$$z = x + iy = -\frac{2K}{\pi U}\left[-\frac{i\pi}{2} - \ln t + \frac{\pi}{2} + i \ln\left(\frac{1-t}{1+t}\right)\right], \tag{48}$$

where $t = \tan\theta/2$. Thus, for the free streamlines we have

$$x = \frac{2K}{\pi U}\left(\ln t - \frac{\pi}{2}\right), \qquad y = \frac{2K}{\pi U}\left[\frac{\pi}{2} - \ln\left(\frac{1-t}{1+t}\right)\right]. \tag{49}$$

EXERCISES

1. Find the complex potential for the flow past a wedge of angle 2α.
2. Find the complex potential due to a doublet–flow outside a circular cylinder.
3. Find the complex potential for the orifice flow shown in Figure 2.16a. Use the Schwartz–Christoffel transformation.

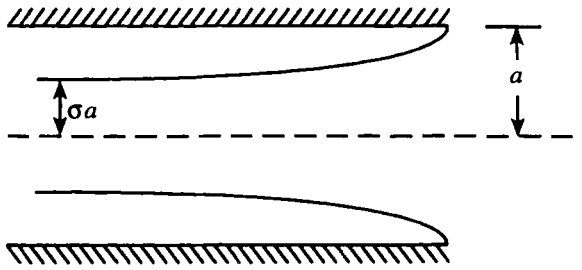

Figure 2.16a. Orifice flow.

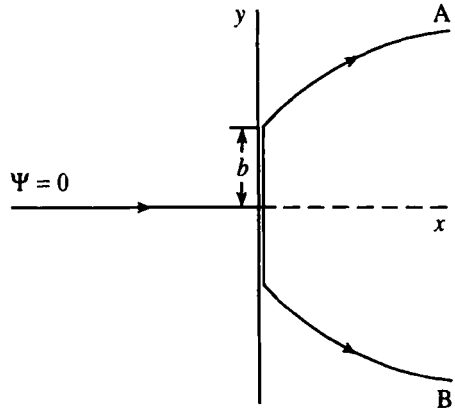

Figure 2.16b. Flow past a flat plate placed perpendicular to the flow.

4. Find the complex potential for the flow past a flat plate with a cavity of constant ambient pressure, shown in Figure 2.16b. Calculate the drag on the plate. Use the Schwartz–Christoffel transformation.

2.3. Three–Dimensional Irrotational Flows

Because of the fact that the region occupied by the fluid is necessarily doubly connected in a two–dimensional flow field and singly connected in a three–dimensional flow field, significant differences between the properties of the two flow fields may be expected to arise.

Special Singular Solutions

Just like that in two–dimensional flows, one may build up complicated three–dimensional flow fields by superposing certain singular solutions of Laplace's equation.

The Source Flow

On using the spherical polar coordinates (R, θ, φ), for the velocity potential we obtain

$$\Phi(R) = \frac{A}{R}. \tag{1}$$

Using the condition of mass conservation,

$$q = \iint_S \nabla\Phi \cdot \hat{n}\, dS = \text{const.}, \tag{2}$$

(1) gives

$$A = -\frac{q}{4\pi}. \tag{3}$$

Thus, (1) becomes

$$\Phi = -\frac{q}{4\pi R}. \tag{4}$$

From the relations

$$u_r = \frac{\partial\Phi}{\partial R} = \frac{1}{R^2 \sin\theta}\frac{\partial\Psi}{\partial\theta}, \qquad u_\theta = \frac{1}{R}\frac{\partial\Phi}{\partial\theta} = \frac{-1}{R\sin\theta}\frac{\partial\Psi}{\partial R} \tag{5}$$

we obtain, for the stream function,

$$\Psi = -\frac{q\cos\theta}{4\pi}. \tag{6}$$

Example 1: Consider a source in a uniform flow. Then for the stream function we have

$$\Psi = \frac{1}{2}UR^2\sin^2\theta - \frac{q\cos\theta}{4\pi}.$$

On noting that the stagnation point would be on the line $\theta = \pi$, the stagnation streamline is then given by

$$\Psi_0 = \frac{1}{2}UR^2\sin^2\theta - \frac{q\cos\theta}{4\pi} - \frac{q}{4\pi},$$

which represents the flow past a body of revolution of asymptotic radius (see Figure 2.17)

$$\theta \Rightarrow 0 : R\sin\theta = \sqrt{\frac{q}{\pi U}}.$$

The velocity potential for this flow is given by

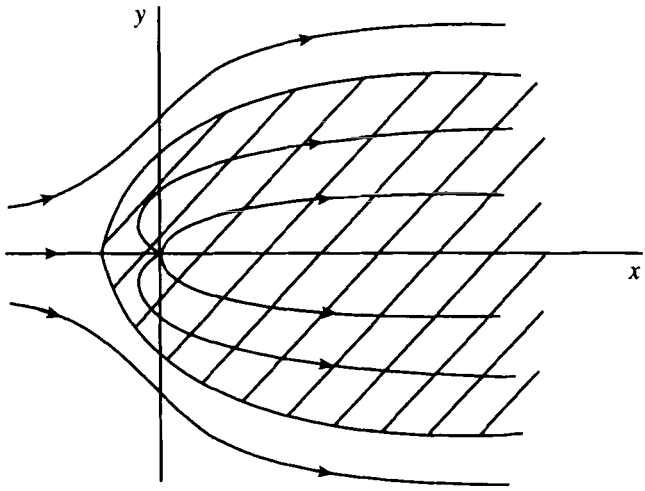

Figure 2.17. Flow past a body of revolution.

$$\Phi = UR\cos\theta - \frac{q}{4\pi R},$$

from which the velocity components are given by

$$\left.\begin{aligned} u_R &= \frac{\partial \Phi}{\partial R} = U\cos\theta + \frac{q}{4\pi R^2}, \\ u_\theta &= \frac{1}{R}\frac{\partial \Phi}{\partial \theta} = -U\sin\theta. \end{aligned}\right\}.$$

The stagnation points S is therefore at

$$\theta = \pi, \qquad R = \sqrt{\frac{q}{4\pi U}}.$$

The Doublet Flow

Note that one can generate the doublet flow from the source flow by simply differentiating the velocity potential corresponding to the source flow in a direction opposite to the doublet axis, thus, one obtains

$$\Phi = -\frac{d}{dx}\left(-\frac{q/4\pi}{\sqrt{x^2+r^2}}\right)dx = -\frac{\mu\cos\theta}{4\pi R^2}, \tag{7}$$

where

$$\mu = \lim_{\substack{dx\Rightarrow 0 \\ q\Rightarrow\infty}} q\cdot dx. \tag{8}$$

From the relations

$$\left.\begin{aligned} u_R &= \frac{\partial \Phi}{\partial R} = \frac{1}{R^2 \sin\theta}\frac{\partial \Psi}{\partial \theta}, \\ u_\theta &= \frac{1}{R}\frac{\partial \Phi}{\partial \theta} = \frac{-1}{R\sin\theta}\frac{\partial \Psi}{\partial R}, \end{aligned}\right\} \tag{9}$$

one obtains, for the stream function,

$$\Psi = \frac{\mu \sin^2\theta}{4\pi R}. \tag{10}$$

Example 2: Consider a doublet in a uniform stream. For the velocity potential, one then has

$$\Phi = UR\cos\theta + \frac{\mu\cos\theta}{4\pi R^2},$$

from which the velocity components are given by

$$\left.\begin{aligned} u_R &= \left(U - \frac{\mu}{2\pi R^3}\right)\cos\theta, \\ u_\theta &= -\left(U + \frac{\mu}{4\pi R^3}\right)\sin\theta, \end{aligned}\right\}.$$

The stream function is then given by

$$\Psi = \left(\frac{UR^2}{2} - \frac{\mu}{4\pi R}\right)\sin^2\theta,$$

from which the stagnation streamline is given by

$$R = R_0 = \left(\frac{\mu}{2\pi U}\right)^{1/3}.$$

This flow therefore represents the flow past a sphere of radius $a = R_0$. Thus, the velocity potential is given by

$$\Phi = U\left(1 + \frac{a^3}{2R^3}\right)R\cos\theta$$

with the velocity components

$$\left.\begin{aligned} u_R &= U\left(1 - \frac{a^3}{R^3}\right)\cos\theta, \\ u_\theta &= -U\left(1 + \frac{a^3}{2R^3}\right)\sin\theta. \end{aligned}\right\}.$$

The pressure on the surface of the sphere is then given by

$$R = a: \quad C_p = \frac{p - p_\infty}{\frac{1}{2}\rho U^2} = 1 - \frac{u_\theta^2}{U^2} = 1 - \frac{9}{4}\sin^2\theta,$$

which is symmetric about $\theta = 0$ and $\pi/2$, so that there is no net force exerted by the flow on the sphere – *d'Alembert's paradox.*

d'Alembert's Paradox

Example 2 appears to indicate that the zero resultant force exerted by the fluid on a sphere moving with uniform translational velocity in a quiescent unbounded ideal fluid has to do with the particular flow geometry, namely, the flow around a sphere. However, this result has greater generality and one may show, as in the following, that there is no resultant force exerted by the fluid on a finite body of arbitrary shape translating steadily through a quiescent unbounded ideal fluid.

Consider a finite body bounded by a surface S translating with constant velocity $\boldsymbol{U}$ in an unbounded fluid occupying a region $\mathcal{V}$ at rest at infinity. The boundary–value problem for the velocity potential Φ then consists of

$$\nabla^2 \Phi = 0 \quad \text{in } \mathcal{V} \tag{11}$$

along with boundary conditions

$$\left.\begin{aligned} &\frac{\partial \Phi}{\partial n} = \boldsymbol{U} \cdot \hat{\boldsymbol{n}} \quad \text{on } S, \\ &|\nabla \Phi| \Rightarrow 0 \quad \text{at infinity,} \end{aligned}\right\} \tag{12}$$

where $\hat{\boldsymbol{n}}$ is the unit normal vector to S in a direction pointing away from S.

The force exerted by the fluid on the body is given by

$$\boldsymbol{F} = -\iint_S \hat{\boldsymbol{n}}\, p\, dS \tag{13a}$$

or in the component form

$$F_j = -\iint_S n_j\, p\, dS. \tag{13b}$$

Using the Bernoulli equation [equation (18)] in Section 2.1, (13b) becomes

$$F_j = -p_\infty \iint_S n_j\, dS + \rho \iint_S n_j \frac{\partial \Phi}{\partial t} dS + \frac{1}{2}\rho \iint_S n_j (\nabla \Phi)^2\, dS, \tag{14}$$

where p_∞ is the constant pressure at infinity.

Now, one may note the following results:

$$\iint_S n_j \, dS = 0$$

$$\frac{\partial \Phi}{\partial t} = \frac{\partial \Phi}{\partial x_i} \frac{dx_i}{dt} = -\nabla\Phi \cdot \boldsymbol{U} = -U_i u_i,$$

$$\frac{\partial}{\partial x_j} (\nabla\Phi)^2 = 2u_i \frac{\partial u_j}{\partial x_i} = 2 \frac{\partial}{\partial x_i} (u_i u_j),$$

$$\begin{aligned} \iint_S n_j (\nabla\Phi)^2 \, dS &= \iiint_V \frac{\partial}{\partial x_j} (\nabla\Phi)^2 \, d\upsilon - \iint_\Sigma n_j (\nabla\Phi)^2 \, d\Sigma \\ &= 2 \iint_S n_i u_i u_j dS + 2 \iint_\Sigma n_i u_i u_j d\Sigma - \iint_\Sigma n_j (\nabla\Phi)^2 \, d\Sigma \\ &= 2U_i \iint_S n_i u_j dS, \end{aligned} \tag{15}$$

where Σ is the surface at infinity enclosing the region $\mathcal{V}$, and the boundary conditions (12) have been used in deriving the last result.

Using (15), (14) becomes

$$\begin{aligned} F_j &= \rho U_i \iint_S \left(n_i u_j - n_j u_i \right) dS \\ &= \rho U_i \iint_S \left(\frac{\partial u_j}{\partial x_i} - \frac{\partial u_i}{\partial x_j} \right) dS + \rho U_i \iint_\Sigma \left(n_i u_j - n_j u_i \right) d\Sigma \\ &= 0 \end{aligned} \tag{16}$$

on noting the boundary conditions (12) and that the velocity field is irrotational, i.e., $\nabla \times \boldsymbol{\upsilon} = \boldsymbol{0}$. Thus, a finite body of arbitrary shape translating steadily through a quiescent unbounded ideal fluid experiences no resultant force exerted by the fluid. This result is called *d'Alembert's paradox* because it is contrary to experience. It is to be noted that the fallacy is less related to the neglect of viscous effects than to the assumption that there is no vorticity in the fluid outside the body. Thus, the above result is applicable to a streamlined body for which there is only a thin wake containing vorticity.

Image of a Source in a Sphere

Let us find the image of a source of strength m at $(0,0,a)$ in the sphere of radius $b (b < a)$ with center at the origin. In the absence of the sphere, the potential for the source is (see Figure 2.18) $m/\sqrt{r^2 + a^2 - 2ar\cos\theta}$, so that for the flow in the presence of the sphere we may write,

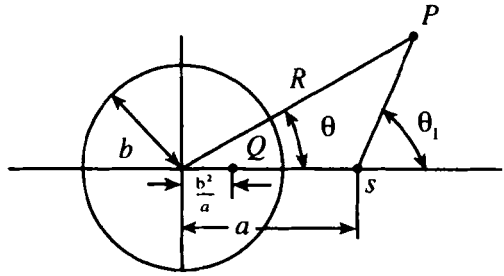

Figure 2.18. Source outside a sphere.

$$\phi = \phi_1 + \frac{m}{\sqrt{r^2 + a^2 - 2ar\cos\theta}}, \tag{17}$$

where

$$\left.\begin{aligned} r > b: \quad & \nabla^2\phi_1 = 0, \\ r \Rightarrow \infty: \quad & \nabla\phi \Rightarrow 0. \end{aligned}\right\} \tag{18}$$

One may write

$$\phi_1 = \sum_{n=0}^{\infty} \frac{B_n}{r^{n+1}} P_n(\cos\theta), \tag{19}$$

where $P_n(z)$ are the Legendre polynomials. Thus from (17) and (19), for $r < a$, one has

$$\phi = \sum_{n=0}^{\infty} \left[\frac{B_n}{r^{n+1}} P_n(\cos\theta) + \frac{mr^n}{a^{n+1}} P_n(\cos\theta) \right]. \tag{20}$$

The boundary condition on the sphere,

$$r = b: \quad \frac{\partial\phi}{\partial r} = 0, \tag{21}$$

then gives

$$B_n = \frac{mn}{b(n+1)} \left(\frac{b^2}{a}\right)^{n+1}. \tag{22}$$

Using (22), (20) becomes

$$\phi_1 = \sum_{n=0}^{\infty} \frac{m}{b}\left(1 - \frac{1}{n+1}\right)\left(\frac{b^2}{a}\right)^{n+1} \frac{1}{r^{n+1}} P_n(\cos\theta). \tag{23}$$

Note that the first term on the right in (23) can be written as

$$\sum_{n=0}^{\infty} \frac{m}{b}\left(\frac{b^2}{a}\right)^{n+1} \frac{1}{r^{n+1}} P_n(\cos\theta) = \frac{mb}{a} \sum_{n=0}^{\infty} \left(\frac{b^2}{a}\right)^n \frac{1}{r^{n+1}} P_n(\cos\theta)$$

$$= \frac{(mb/a)}{\sqrt{r^2 + (b^2/a)^2 - 2r(b^2/a)\cos\theta}},$$

which corresponds to a source of strength mb/a located at $(0,0,b^2/a)$. Next, the second term on the right in (23) can be written as

$$-\sum_{n=0}^{\infty} \frac{m}{b(n+1)}\left(\frac{b^2}{a}\right)^{n+1} \frac{1}{r^{n+1}} P_n(\cos\theta) = -\frac{m}{b} \sum_{n=0}^{\infty} \int_0^{b^2/a} \frac{z^n P_n(\cos\theta)\, dz}{r^{n+1}}$$

$$= -\frac{m}{b} \int_0^{b^2/a} \frac{dz}{\sqrt{r^2 + z^2 - 2rz\cos\theta}},$$

which corresponds to a uniform line sink of strength m/b per unit length stretching from $(0,0,0)$ to $(0,0,b^2/a)$. The image system consists of a source mb/a at $(0,0,b^2/a)$ and this line sink.

Flow Past an Arbitrary Body

Let us use Green's Theorem for the region $\mathcal{V}$ between the body and an infinite sphere enclosing the body. It turns out that the nonvanishing contribution to the velocity potential from the surface integral on the infinite sphere is a constant; one then has (on ignoring the latter contribution)

$$\iint_{S_0} (\Phi_1 \nabla\Phi_2 - \Phi_2 \nabla\Phi_1) \cdot \hat{n}\, dS = \iiint_{\mathcal{V}} (\Phi_1 \nabla^2\Phi_2 - \Phi_2 \nabla^2\Phi_1)\, d\boldsymbol{x}\,., \tag{24}$$

where S_0 is the surface of the body.

If one takes

$$\Phi_1 = \frac{1}{R}, \quad \Phi_2 = \Phi, \quad \text{with } \nabla^2\Phi = 0, \tag{25}$$

where $R = |\boldsymbol{x} - \boldsymbol{x}'|$ is the distance between the point of interest $P(\boldsymbol{x})$ and an element of area $dS(\boldsymbol{x}')$ on the body, then (24) becomes

$$\iint_{S_0} \left[\frac{1}{R}\nabla\Phi - \Phi\nabla\left(\frac{1}{R}\right)\right] \cdot \hat{n}\, dS = \iiint_{\mathcal{V}} \left[\frac{1}{R}\nabla^2\Phi - \Phi\nabla^2\left(\frac{1}{R}\right)\right] d\boldsymbol{x}. \tag{26}$$

If the point $P(\boldsymbol{x})$ is not in $\mathcal{V}$, then (26) gives

$$\iint_{S_0}\left[\frac{1}{R}\nabla\Phi-\Phi\nabla\left(\frac{1}{R}\right)\right]\cdot\hat{n}\,dS=0. \tag{27}$$

If the point $P(x)$ is within $\mathcal{V}$, enclose it by a small sphere ε, then (26) gives

$$-\iint_{\varepsilon}\left(\frac{1}{R}\frac{\partial\Phi}{\partial R}+\frac{\Phi}{R^2}\right)dS+\iint_{S_0}\left[\frac{1}{R}\nabla\Phi-\Phi\nabla\left(\frac{1}{R}\right)\right]\cdot\hat{n}\,dS=0.$$

As $\varepsilon\Rightarrow 0$, this gives

$$\Phi(P)=\frac{1}{4\pi}\iint_{S_0}\left[\frac{1}{r}\nabla\Phi-\Phi\nabla\left(\frac{1}{R}\right)\right]\cdot\hat{n}\,dS, \tag{28}$$

which shows explicitly how Φ is determined throughout the fluid by conditions on the body.

One may write

$$\frac{1}{R}=\frac{1}{r}-x_i'\frac{\partial}{\partial x_i}\left(\frac{1}{r}\right)+\frac{1}{2}x_i'x_j'\frac{\partial^2}{\partial x_i\partial x_j}\left(\frac{1}{r}\right)+\cdots, \tag{29}$$

which is convergent for $r'<r$; here $|x|=r$, $|x'|=r'$.

Using (29), (28) gives

$$\Phi(P)=\frac{c}{r}+c_i\frac{\partial}{\partial x_i}\left(\frac{1}{r}\right)+c_{ij}\frac{\partial^2}{\partial x_i\partial x_j}\left(\frac{1}{r}\right)+\cdots, \tag{30}$$

where

$$c=-\frac{1}{4\pi}\iint_{S_0}\hat{n}\cdot\nabla\Phi\,dS$$

$$c_i=\frac{1}{4\pi}\iint_{S_0}\left(x_i'\hat{n}\cdot\nabla\Phi-\hat{n}_i\Phi\right)dS$$

$$c_{ij}=\frac{1}{4\pi}\iint_{S_0}\left(-\frac{1}{2}x_i'x_j'\hat{n}\cdot\nabla\Phi+x_i'\hat{n}_j\Phi\right)dS,$$

etc.

Thus, the flow field at large distances from a moving body can be expressed as that due to a sum of multipole flow fields where the coefficients are certain integrals on the given body. At such large distances, the dominant action of the moving body on the fluid is equivalent to the exertion of a point force, with the detailed distribution of the surface forces on the moving body being unimportant.

Unsteady Flows

As an example of unsteady flows, consider an infinite mass of fluid initially at rest and having a spherical cavity of radius $\hat{R}_0$. The fluid is made to move outwards by a pressure applied uniformly over the surface of the cavity; there is no pressure at infinity and no body forces act.[4] Since the motion is spherically symmetric, Laplace's equation for the velocity potential takes the form

$$\frac{\partial}{\partial R}\left(R^2 \frac{\partial \Phi}{\partial R}\right) = 0 \tag{31}$$

while the kinematic condition at the surface of the cavity is

$$R = \hat{R}(t): \quad \frac{\partial \Phi}{\partial R} = \frac{d\hat{R}}{dt}. \tag{32}$$

Equation (32) implies that the radius of the cavity increases at a rate equal to the local fluid velocity, so that no fluid ever crosses the cavity surface, and the latter always consists of the same fluid particles.

From (31) and (32), one obtains

$$\Phi(R,t) = -\frac{R^2(t)}{R}\,\hat{R}', \tag{33}$$

where the primes denote differentiation with respect to t.

Using (33), the Bernoulli equation, namely (18) in Section 2.1, then gives

$$p + \frac{1}{2}\left(\frac{\hat{R}^2\hat{R}'}{R^2}\right)^2 - \frac{\hat{R}^2\hat{R}'' + 2\hat{R}\hat{R}'^2}{R} = 0. \tag{34}$$

Using the adiabatic equation of state (see Chapter 3),

$$\frac{p_1}{p_0} = \left(\frac{\hat{R}_0^3}{\hat{R}_1^3}\right)^{\gamma}, \tag{35}$$

where γ is the ratio of specific heats of the gas in the cavity and p_1 is the pressure at $R = \hat{R}_1$, one obtains from (34), for $R = \hat{R}$,

$$\hat{R}\hat{R}'' + \frac{3}{2}\hat{R}'^2 = \frac{p_0}{\rho_0}\left(\frac{\hat{R}_0}{\hat{R}}\right)^{3\gamma}. \tag{36}$$

Upon integrating (36) and using

$$\hat{R} = \hat{R}_0: \quad \hat{R}' = 0, \tag{37}$$

[4]The cavity dynamics takes different characters depending on whether the cavity consists of a permanent noncondensable gas or the vapor of the surrounding fluid. In the former case, the inertia of the surrounding fluid plays a dominant role, while in the latter case the latent heat flow associated with boiling phenomena plays a dominant role.

one obtains

$$\hat{R}'^2 = \frac{2a_0^2}{3(\gamma-1)}\left[\left(\frac{\hat{R}_0}{\hat{R}}\right)^3 - \left(\frac{\hat{R}_0}{\hat{R}}\right)^{3\gamma}\right], \tag{38}$$

where

$$a_0 = \sqrt{\frac{\gamma p_0}{\rho_0}}$$

is the speed of sound in the gas.

According to (38), the velocity approaches infinity as $R \Rightarrow 0$, which implies that the approximations underlying the derivation of (38) will break down as the collapse process develops.

Added Mass of Bodies Moving Through a Fluid

The reaction of the fluid to a body translating through it is to change the inertia of the body. As an example, consider a sphere of radius a translating unsteadily through a fluid with velocity $\boldsymbol{U} = U\hat{\boldsymbol{i}}_x$. Thus for the velocity potential we obtain

$$\Phi = \frac{U(t)a^3}{2}\frac{\cos\theta}{R^2} = \frac{1}{2}a^3\frac{(\boldsymbol{U}\cdot\boldsymbol{R})}{R^3}. \tag{39}$$

The kinetic energy of the fluid set into motion by this translating sphere is given by

$$T = \frac{1}{2}\rho\iiint_V (\nabla\Phi)^2\,d\boldsymbol{x} = -\frac{1}{2}\rho\oiint_S \Phi\frac{\partial\Phi}{\partial n}\,dS, \tag{40}$$

where S denotes the surface of the sphere, and the normal $\hat{\boldsymbol{n}}$ points into the fluid.

Using (39), (40) leads to

$$T = -\frac{\rho}{2}\oiint_S \frac{U_a\cos\theta}{2}(-U\cos\theta)\,dS = \frac{1}{2}\left(\frac{2\pi a^3\rho}{3}\right)U^2. \tag{41}$$

It is obvious from (41) that one may view the kinetic energy of the fluid as an *added mass*

$$m_a = \frac{2\pi\rho a^3}{3} \tag{42}$$

for the body moving through the fluid. Note that this *added mass* is half the mass of the fluid displaced by the sphere.

In order to see the dynamical significance of the added mass further, let us calculate the force exerted by the fluid on the sphere.

Using (39) and noting that

$$\frac{\partial \Phi}{\partial t} = \frac{1}{2} a^3 \left[\frac{\dot{U} \cos\theta}{R^2} + \frac{U^2}{R^3} - \frac{3U^2 \cos^2\theta}{R^3} \right]$$

with

$$\frac{\partial \boldsymbol{R}}{\partial t} = \boldsymbol{U},$$

the Bernoulli equation (namely, (18) in Section 2.1) gives the following equation for the pressure at a point on the sphere:

$$p\Big|_{R=a} = p_\infty - \frac{\rho}{8} U^2 \left(4\cos^2\theta + \sin^2\theta\right) - \frac{\rho}{2}\left(\dot{U} a \cos\theta + U^2 - 3U^2 \cos^2\theta\right). \quad (43)$$

where p_∞ is the constant pressure at infinity.

The force exerted by the fluid on the sphere is thus given by

$$\boldsymbol{F} = \iint_S \hat{\boldsymbol{n}}\, p \Big|_{R=a}\, dS = -\hat{\boldsymbol{i}}_x \iint_S p \Big|_{R=a} \cos\theta\, dS - \hat{\boldsymbol{i}}_y \iint_S p \Big|_{R=a} \sin\theta\, dS; \quad (44)$$

and on using (43) we obtain

$$\boldsymbol{F} = -\left(\frac{2\pi\rho a^3}{3}\right) \dot{U}\, \hat{\boldsymbol{i}}_x, \quad (45)$$

which is simply the inertia force of the accelerating fluid matter of mass equal to the added mass given in (42) and is in the direction opposing the motion of the sphere.

EXERCISES

1. Find the velocity potential for a doublet–flow outside a sphere when the axis of the doublet passes through the center of the sphere.
2. A spherical bubble of gas of radius R_0 and at a pressure p_0 starts to expand in an infinite mass of fluid of density ρ with zero pressure at infinity. Suppose that the gas is initially at rest and that its pressure and volume $\mathcal{V}$ are related to one another by the equation of state $p\mathcal{V}^{4/3}$ = constant. Show that the bubble radius becomes double the original value R_0 in time $(28R_0/15)\sqrt{2\rho p_0}$.
3. Calculate the added mass of a plate (length 4ℓ) moving normal to its plane in a fluid. Use the Joukowski transformation (see Section 2.7).
4. Calculate the added mass of a sphere moving through a fluid inside a bigger hollow sphere.
5. Determine the flow past a nearly spherical surface given by

$$R = a\left(1 - \varepsilon \sin^2 \theta\right), \qquad \varepsilon \ll 1$$

the flow at infinity being uniform with a velocity U in the x–direction.

2.4. Vortex Flows

Vortex Tubes

The Euler equations of motions for an incompressible fluid are

$$\nabla \cdot \mathbf{v} = 0, \tag{1}$$

$$\frac{\partial \mathbf{v}}{\partial t} + (\mathbf{v} \cdot \nabla)\mathbf{v} = -\frac{1}{\rho} \nabla p. \tag{2}$$

The vorticity is given by

$$\boldsymbol{\Omega} = \nabla \times \mathbf{v}. \tag{3}$$

The vortex lines are those which are tangential everywhere to the local vorticity vector. The surface in the fluid formed by all the vortex lines passing through a given reducible closed curve drawn in the fluid is a vortex tube. Consider the integral of vorticity over an open surface S bounded by this same closed curve and lying entirely in the fluid

$$\iint_S \boldsymbol{\Omega} \cdot \hat{\boldsymbol{n}}\, dS,$$

where $\hat{\boldsymbol{n}}\, dS$ is an element of area of this surface. From (3) one obtains

$$\nabla \cdot \boldsymbol{\Omega} = 0, \tag{4}$$

from which it follows that this integral has the same value for any such open surface lying in the fluid and bounded by any closed curve lying on the vortex tube and passing around it once and is called the strength of the vortex tube. Thus, the vortex tubes are constant in strength and are either closed tubes or end nowhere in the interior of the fluid. Further, since a vortex tube consists always of the same fluid particle, its volume is conserved. Consequently, any stretching of the vortex tube would intensify the local vorticity.

For the vorticity, equation (2) gives

$$\frac{\partial \boldsymbol{\Omega}}{\partial t} = \nabla \times (\mathbf{v} \times \boldsymbol{\Omega}), \tag{5a}$$

which, on using equation (1), becomes

$$\frac{\partial \boldsymbol{\Omega}}{\partial t} + (\mathbf{v} \cdot \nabla) = (\boldsymbol{\Omega} \cdot \nabla)\, \mathbf{v}. \tag{5b}$$

Now, if $d\ell$ is an infinitesimal material line element, one has the following kinematical equation governing the stretching and reorientation of this element (see Section 2.1):

$$\left[\frac{\partial}{\partial t}+(\mathbf{v}\cdot\nabla)\right] d\ell=(d\ell\cdot\nabla)\,\mathbf{v}. \tag{6}$$

Thus it follows from equation (5b) that $\boldsymbol{\Omega}$ changes like the vector representing a material line element which coincides instantaneously with an element of the local vortex line. Consequently, vortex lines move with the fluid.

The terms on the right–hand side in equation (5b) represents the vortex–line stretching. This leads to a concentration and intensification of vorticity, no matter how dispersed the vorticity may be initially. An example is the bath–plug vortex wherein the extension due to the draining motion of the vortex lines produces a concentration of the vorticity.

For a two–dimensional flow, equation (5) gives

$$\frac{\partial\Omega}{\partial t}+(\mathbf{v}\cdot\nabla)\,\Omega=0, \tag{7}$$

where Ω is the component of vorticity normal to the flow.

Induced Velocity Field

Noting, from equation (1), that the velocity field is solenoidal, one may write

$$\mathbf{v}=-\nabla\times\boldsymbol{A}. \tag{8}$$

Then, the vorticity is given by

$$-\boldsymbol{\Omega}=\nabla\times\mathbf{v}=\nabla\times(\nabla\times\boldsymbol{A})=\nabla(\nabla\cdot\boldsymbol{A})-\nabla^2\boldsymbol{A}. \tag{9}$$

Now, note that the vector potential $\boldsymbol{A}$ is not uniquely determined by (8) when the velocity $\mathbf{v}$ is known. In fact,

$$\boldsymbol{A}'=\boldsymbol{A}+\nabla\chi \tag{10}$$

represents the same field. But, it is always possible to choose χ such that

$$\nabla^2\chi=\nabla\cdot\boldsymbol{A} \tag{11}$$

so that

$$\nabla\cdot\boldsymbol{A}'=0 \tag{12}$$

and, consequently, (9) gives

$$\nabla\cdot\boldsymbol{A}=\boldsymbol{\Omega}, \tag{13}$$

from which we have

$$\boldsymbol{A}=\frac{1}{4\pi}\iiint_V\frac{\Omega(\boldsymbol{r}',t)}{|\boldsymbol{r}-\boldsymbol{r}'|}\,d^3V(\boldsymbol{r}'). \tag{14}$$

One may, in fact, verify that $\nabla \cdot \boldsymbol{A} = 0$, in accordance with equation (12), if the vorticity vanishes at infinity. Finally, using (14) in (8), one has the following equation for the velocity field:

$$\boldsymbol{v} = \frac{1}{4\pi} \nabla_r \times \iiint_V \frac{\boldsymbol{\Omega}(\boldsymbol{r}', t)}{|\boldsymbol{r} - \boldsymbol{r}'|} \, d^3V(\boldsymbol{r}'). \tag{15}$$

Biot–Savart's Law

From (14), note that for a vortex tube shown in Figure 2.19, one has

$$\delta \boldsymbol{A}(r) = \frac{1}{4\pi} \frac{\boldsymbol{\Omega}(\boldsymbol{r}', t)}{|\boldsymbol{r} - \boldsymbol{r}'|} (\hat{\boldsymbol{n}} \delta S \cdot d\ell). \tag{16}$$

Noting that

$$d\boldsymbol{\ell} = \frac{\boldsymbol{\Omega}}{|\boldsymbol{\Omega}|} d\ell, \qquad \Gamma = \hat{\boldsymbol{n}} \cdot \boldsymbol{\Omega} \, dS, \tag{17}$$

where Γ is the circulation about the vortex tube, (16) becomes

$$\delta \boldsymbol{A}(\boldsymbol{r}) = \frac{\Gamma}{4\pi} \frac{d\boldsymbol{\ell}}{|\boldsymbol{r} - \boldsymbol{r}'|}. \tag{18}$$

Using (18), (8) gives

$$\delta \boldsymbol{v}(\boldsymbol{r}) = \nabla_r \times \frac{\Gamma}{4\pi} \frac{d\boldsymbol{\ell}}{|\boldsymbol{r} - \boldsymbol{r}'|}, \tag{19a}$$

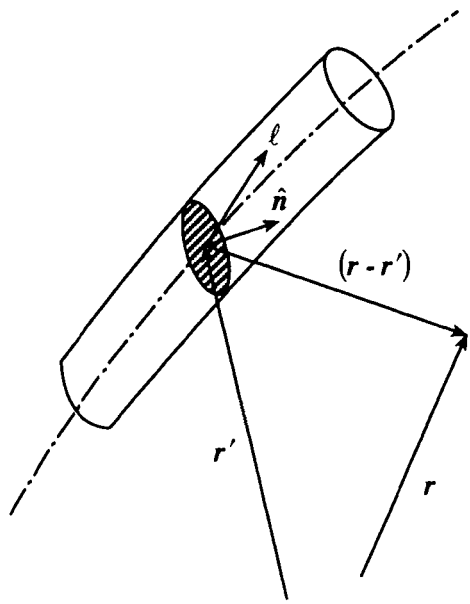

Figure 2.19. Vortex tube in a fluid.

from which

$$\mathbf{v}(\mathbf{r}) = \frac{\Gamma}{4\pi} \iiint_{\mathcal{V}} \frac{d\boldsymbol{\ell} \times (\mathbf{r} - \mathbf{r}')}{|\mathbf{r} - \mathbf{r}'|^3}. \tag{19b}$$

Example 1: Consider a line vortex of finite length ℓ (Figure 2.20). Examples of such a concentration of vorticity are tornadoes, whirlpools, etc.

Let

$$\mathbf{r}_1 = \mathbf{r} - \mathbf{r}'.$$

Thus we obtain (see Figure 2.20)

$$d\mathbf{r}' \times \mathbf{r}_1 = r_1 dr' \sin\theta\, \hat{e},$$

where $\hat{e}$ is the unit vector pointing into the plane of the paper.

Hence, (19b) gives

$$\mathbf{v}(\mathbf{r}) = \hat{e}\, \frac{\Gamma}{4\pi} \int_0^{\ell} \frac{\sin\theta}{r_1^2}\, dr'.$$

Noting, from Figure 2.20, that

$$r_1 = h \operatorname{cosec} \theta, \qquad r_0 - r' = h \cot\theta,$$

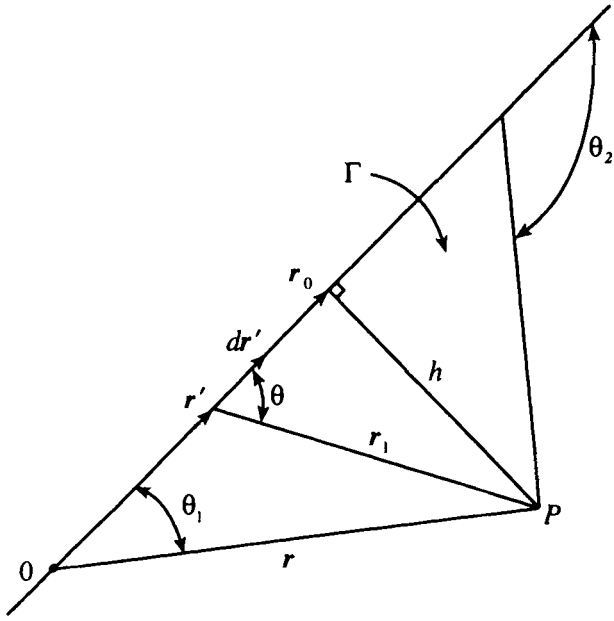

Figure 2.20. A line vortex.

one obtains

$$\mathbf{v}(\mathbf{r}) = \hat{\boldsymbol{e}}\,\frac{\Gamma}{4\pi}\int_{\theta_1}^{\theta_2}\sin\theta\,d\theta = e\,\frac{\Gamma}{4\pi h}\left(\cos\theta_1 - \cos\theta_2\right).$$

Example 2: Consider a closed vortex filament. Then, on using Stokes' Theorem, (19) gives,

$$\mathbf{v}(\mathbf{r}) = -\frac{\Gamma}{4\pi}\nabla_r \times \iint_S \left[\nabla_{r'}\left(\frac{1}{|\mathbf{r}-\mathbf{r}'|}\right)\right] \times \hat{\boldsymbol{n}}\,dS(\mathbf{r}')$$

$$= -\frac{\Gamma}{4\pi}\iint_S \hat{\boldsymbol{n}}\cdot\nabla_r\left[\nabla_{r'}\left(\frac{1}{|\mathbf{r}-\mathbf{r}'|}\right)\right] dS(\mathbf{r}') = -\frac{\Gamma}{4\pi}\nabla\omega,$$

where

$$\omega \equiv \iint_S \frac{(\mathbf{r}-\mathbf{r}')\cdot\hat{\boldsymbol{n}}}{|\mathbf{r}-\mathbf{r}'|^3}\,dS(\mathbf{r}')$$

which is the solid angle subtended by the line vortex at $\boldsymbol{r}$.

Example 3: Consider a vortex between two perpendicular planes (Figure 2.21). The image system corresponding to the given vortex at A consists of vortices at A_1, A_2, A_3 as shown in Figure 2.21. The velocity induced at A by the image system is (on using the results of Example 1)

$$\left.\begin{aligned} \dot{r} &= \frac{\Gamma}{2\pi}\left(\frac{\cos\theta}{AA_3} - \frac{\sin\theta}{AA_1}\right) = \frac{\Gamma\cot 2\theta}{2\pi r}, \\ r\dot{\theta} &= \frac{\Gamma}{2\pi}\left(\frac{1}{AA_2} - \frac{\cos\theta}{AA_1} - \frac{\sin\theta}{AA_3}\right) = -\frac{\Gamma}{4\pi r}, \end{aligned}\right\}$$

from which

$$\frac{1}{r}\frac{dr}{d\theta} = -2\cot 2\theta$$

or

$$r\sin 2\theta = \text{const.}$$

Putting

$$u = \frac{1}{r}$$

one obtains

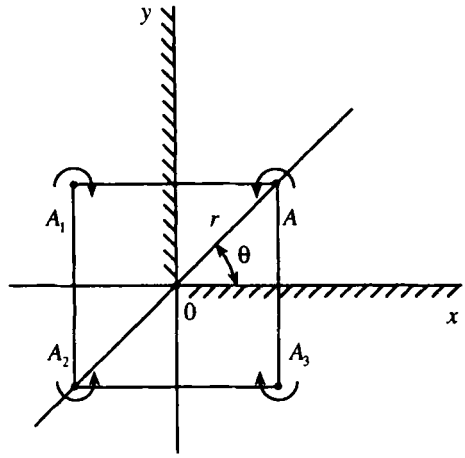

Figure 2.21. A line vortex between two perpendicular planes.

$$\frac{d^2u}{d\theta^2} + u = -3u,$$

which implies that the radial acceleration of the vortex A is $3\Gamma^2/16\pi^2 r^3$ and that the transverse acceleration is zero. Therefore, the vortex A moves as if it were under a repulsion from the origin, inversely proportional to r^3.

Example 4: Consider an infinite system of equal parallel rectilinear vortices each of strength Γ arranged along the x–axis at $x = 0, \pm a, \pm 2a, \ldots$. Then, the complex potential for the resulting flow is given by (see Section 2.2)

$$F(z) = \sum_{n=-\infty}^{\infty} -\frac{i\Gamma}{2\pi} \ln(z - na) = \frac{i\Gamma}{2\pi} \ln\left[(z) \cdot \left(z^2 - a^2\right) \cdot \left(z^2 - 4a^2\right) \ldots\right]$$

$$= -\frac{i\Gamma}{2\pi} \ln\left[\frac{\pi z}{a}\left(1 - \frac{z^2}{a^2}\right)\left(1 - \frac{z^2}{4a^2}\right)\ldots\right] - \frac{i\Gamma}{2\pi} \ln\left[\frac{a}{\pi}\left(-a^2\right)\left(-4a^2\right)\ldots\right]$$

$$= -\frac{i\Gamma}{2\pi} \ln\left(\sin\frac{\pi z}{a}\right),$$

where we have used the result

$$\frac{\sin z}{z} = \prod_{n=1}^{\infty}\left(1 - \frac{z^2}{n^2\pi^2}\right).$$

Now, recall that any particular vortex will move with the fluid so that the motion of any particular line vortex in the above row cannot take place in isolation and has to be induced by the other line vortices in the row. The complex potential at the mth line vortex due to all the others is

$$F^{(m)}(z) = -\frac{i\Gamma}{2\pi} \sum_{\substack{n=-\infty \\ n\neq m}}^{\infty} \ln(z-na) \Big|_{z=ma} .$$

The corresponding complex velocity at the mth line vortex is, then, given by

$$W^{(m)}(z) = -\frac{i\Gamma}{2\pi} \sum_{\substack{n=-\infty \\ n\neq m}}^{\infty} \frac{d}{dz} \ln(z-na) \Big|_{z=ma} = -\frac{i\Gamma}{2\pi} \sum_{\substack{n=-\infty \\ n\neq m}}^{\infty} \frac{1}{(m-n)a} = 0,$$

so that all line vortices in the row are at rest.

The streamlines for this flow are given by

$$\Psi = \frac{\Gamma}{2i}\left[F(z) - \bar{F}(z)\right] = -\frac{\Gamma}{4\pi} \ln\left(\sin\frac{\pi z}{a} \cdot \sin\frac{\pi \bar{z}}{a}\right)$$

$$= -\frac{\Gamma}{4\pi} \ln\left[\frac{\cos\frac{\pi(\bar{z}-z)}{a} - \cos\frac{\pi(\bar{z}+z)}{a}}{2}\right]$$

$$= -\frac{\Gamma}{4\pi} \ln\left[\cos h\frac{2\pi y}{a} - \cos\frac{2\pi x}{a}\right] + \frac{\Gamma}{4\pi} \ln 2 = \text{const.}$$

Next, for the velocity components we obtain

$$\left.\begin{aligned} u &= \frac{\partial \Psi}{\partial y} = -\frac{\Gamma}{2a} \frac{\sin h\,\frac{2\pi y}{a}}{\cos h\,\frac{2\pi y}{a} - \cos\frac{2\pi x}{a}}, \\ v &= -\frac{\partial \Psi}{\partial x} = \frac{\Gamma}{2a} \frac{\sin\frac{2\pi x}{a}}{\cos h\,\frac{2\pi y}{a} - \cos\frac{2\pi x}{a}}. \end{aligned}\right\}$$

Note that

$$\left.\begin{aligned} &\frac{y}{a} \gg 1: \quad u \approx \mp\frac{\Gamma}{2a} \quad \text{for} \quad y \gtrless 0 \\ &x = \frac{1}{2}a, a, \frac{3}{2}a, \ldots : \quad v = 0. \end{aligned}\right\}$$

If, now, one places another row of vortices, which are similar, but of opposite sign, at the points

$$\left(\pm\frac{1}{2}a, b\right), \left(\pm\frac{3}{2}a, b\right), \ldots$$

a typical vortex of the new set has a velocity, induced by the first set, given by

$$\left.\begin{aligned} u &= -\frac{\Gamma}{2a}\,\frac{\sin h\,\dfrac{2\pi b}{a}}{\cos h\,\dfrac{2\pi b}{a}+1} = -\frac{\Gamma}{2a}\tan h\,\frac{\pi b}{a}, \\ v &= 0. \end{aligned}\right\}$$

From symmetry considerations, the first set must have exactly the same velocity, so that the whole double row of vortices, called a *Kármán vortex sheet*, moves with speed $\Gamma/2a \tan h\, \pi b/a$ in the negative x–direction. Such a vortex sheet can be used to represent the wake behind a body moving slowly through a fluid.[5]

Vortex Ring

In an axisymmetric flow with cylindrical polar coordinates (r, θ, z), the velocity field is given by

$$\boldsymbol{v} = u_r(r,z,t)\,\hat{\boldsymbol{i}}_r + u_z(r,z,t)\,\hat{\boldsymbol{i}}_z. \tag{20}$$

Thus streamlines lie in planes θ =const and the vorticity is given by $\boldsymbol{\Omega} = \Omega \hat{\boldsymbol{i}}_\theta$, where

$$\Omega = \frac{\partial u_r}{\partial z} - \frac{\partial u_z}{\partial r}. \tag{21}$$

In an axisymmetric flow, the vortex tubes are, therefore, ring–shaped around the axis of symmetry. During their motion with the fluid, the vortex rings will expand and contract about the axis of symmetry. However, since the fluid is incompressible, the volume of these rings must remain constant so that the vorticity Ω will be proportional to the length of the ring $2\pi r$. In fact, for the present situation, equation (5b) becomes

$$\frac{D}{Dt}\left(\frac{\Omega}{r}\right) = 0. \tag{22}$$

Consider now an arbitrarily thin circular vortex filament. Upon introducing the axisymmetric stream function Ψ according to

$$u_r = -\frac{1}{r}\frac{\partial \Psi}{\partial z}, \qquad u_z = \frac{1}{r}\frac{\partial \Psi}{\partial r} \tag{23}$$

one obtains, from (21),

---

[5]For the flow past a body such a cylinder, when the flow speed is small, the streamline pattern is essentially symmetrical both fore and aft of the cylinder, but as the flow speed increases, asymmetry of the flow develops. Eddies are observed to form in regions of separated flow attached to the downstream side of the cylinder. With further increase in the flow speed, these eddies detach from the cylinder and are carried downstream. The eddies are shed alternately from the top and bottom of the cylinder on its downstream side, which then give a chase to the cylinder and their pattern is closely simulated by the *Kármán vortex Sheet*. Observations of *Kármán vortex sheet* date back to several centuries – they are clearly visible in Lionardo da Vinci's sketches.

$$\frac{\partial^2 \Psi}{\partial z^2} + \frac{\partial^2 \Psi}{\partial r^2} - \frac{1}{r}\frac{\partial \Psi}{\partial r} + r\Omega = 0. \tag{24}$$

Outside the ring, one has an irrotational flow, so that equation (24) leads to

$$\frac{\partial^2 \Psi'}{\partial z^2} + \frac{\partial^2 \Psi'}{\partial r^2} - \frac{1}{r}\frac{\partial \Psi'}{\partial r} = 0. \tag{25}$$

Putting

$$\Psi = \chi r, \quad \Psi' = \chi' r, \tag{26}$$

equations (24) and (25) lead to

$$\frac{\partial^2 \chi}{\partial z^2} + \frac{\partial^2 \chi}{\partial r^2} + \frac{1}{r}\frac{\partial \chi}{\partial r} - \frac{\chi}{r^2} + \Omega = 0, \tag{27}$$

$$\frac{\partial^2 \chi'}{\partial z^2} + \frac{\partial^2 \chi'}{\partial r^2} + \frac{1}{r}\frac{\partial \chi'}{\partial r} - \frac{\chi'}{r^2} = 0, \tag{28}$$

which imply that $\chi \cos\theta$ is the potential of a distribution of matter of density $\Omega \cos\theta/4\pi$ which occupies the same region of space as the vortex ring.

Then (see Figure 2.22) one obtains

$$\chi \cos\theta = \frac{r_0 \Omega \sigma}{4\pi} \int_{\theta}^{2\pi+\theta} \frac{\cos\theta' \, d\theta'}{\left[(z-z')^2 + r^2 + r_0^2 - 2rr_0 \cos(\theta - \theta')\right]^{1/2}}, \tag{29}$$

where σ is the cross section of the core of the ring, and r_0 is the radius of the ring.

Putting

$$\theta' - \theta = \varepsilon, \tag{30}$$

(29) becomes

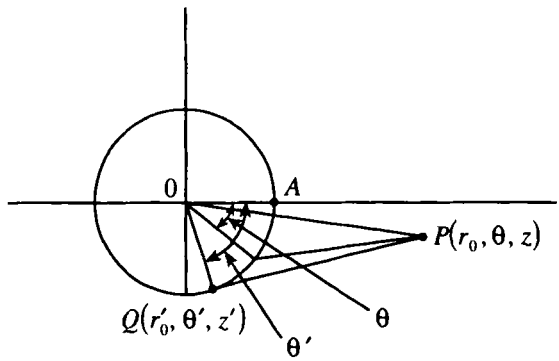

Figure 2.22. A vortex ring.

$$\chi \cos\theta = \frac{\sigma\Omega r_0}{2\pi} \int_0^{\pi} \frac{\cos\varepsilon d\varepsilon}{\left[(z-z')^2 + r^2 + r_0^2 - 2rr_0\cos\varepsilon\right]^{1/2}}. \tag{31a}$$

So, from (26), one obtains

$$\Psi = \frac{\sigma\Omega rr_0}{2\pi} \int_0^{\pi} \frac{\cos\varepsilon d\varepsilon}{\left[(z-z')^2 + r^2 + r_0^2 - 2rr_0\cos\varepsilon\right]^{1/2}}. \tag{31b}$$

Putting

$$\left.\begin{aligned} k &= \frac{2(rr_0)^{1/2}}{\left[(z-z')^2 + (r+r_0)^2\right]^{1/2}}, \\ 2\eta &= \varepsilon, \end{aligned}\right\} \tag{32}$$

(31) becomes

$$\Psi = \sigma\Omega \frac{(rr_0)^{1/2}}{\pi} \int_0^{\pi/2} \frac{\left(2\cos^2\eta - 1\right)}{\left(1 - k^2\cos^2\eta\right)^{1/2}} d\eta \tag{33}$$

or

$$\Psi = \sigma\Omega \frac{(rr_0)^{1/2}}{\pi} \left[\left(\frac{2}{k} - k\right) K(k) - \frac{2}{k} E(k)\right], \tag{34}$$

where

$$K(k) = \int_0^{\pi/2} \frac{d\eta}{\left(1 - k^2\cos^2\eta\right)^{1/2}}, \qquad E(k) = \int_0^{\pi/2} \left(1 - k^2\cos^2\eta\right)^{1/2} d\eta$$

are the elliptic integrals of first and second kinds.

The streamline pattern for this flow is sketched in Figure 2.23.

Noting that, on the surface of the ring, $z \sim z'$, $r \sim r_0, k \sim 1$, so that

$$\left.\begin{aligned} K(k) &= \ln\frac{4}{\left(1-k^2\right)^{1/2}} + \frac{1}{2}\left(1-k^2\right)^{1/2}\left[\ln\frac{4}{\left(1-k^2\right)^{1/2}} - 1\right], \\ E(k) &= 1 + \frac{1}{2}\left(1-k^2\right)\left[\ln\frac{4}{\left(1-k^2\right)^{1/2}} - \frac{1}{2}\right], \end{aligned}\right\} \tag{35}$$

we obtain, from (34), for the velocity components

$$u_r = \frac{\Gamma}{\pi}\left[\frac{2r_0}{a} - \frac{3a}{4r_0}\left(\ln\frac{8r_0}{a} - \frac{3}{2}\right)\right]\frac{z-z'}{2r_0 a}, \tag{36}$$

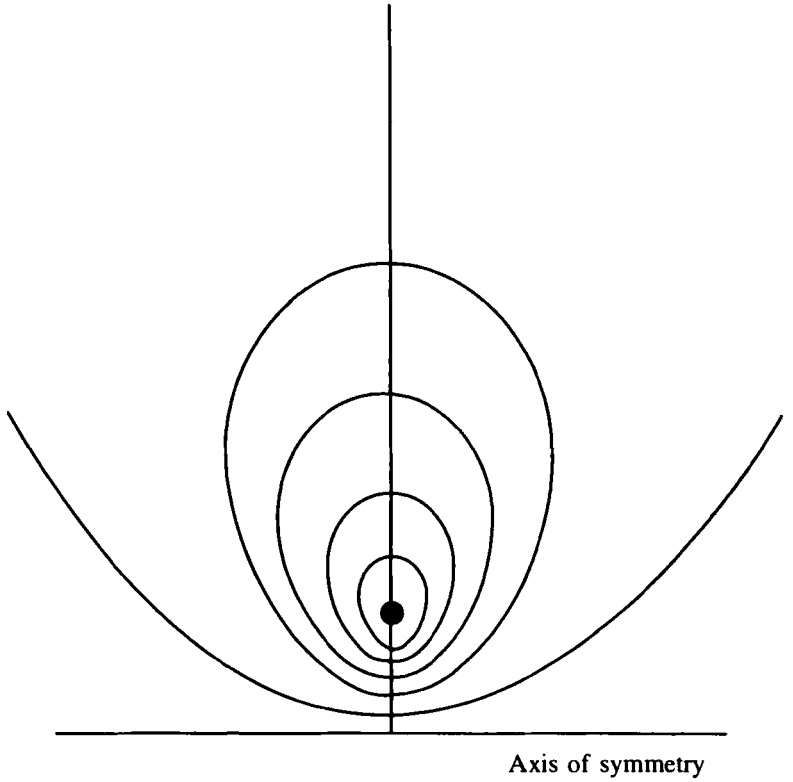

Figure 2.23. Streamline pattern near a vortex ring (from Batchelor, 1967).

$$u_z = \frac{\Gamma}{2\pi r_0}\left(\ln\frac{8r_0}{a} - 1\right), \tag{37}$$

where a is the radius of the vortex core, and $\Gamma = r_0\Omega$. Note that at $z = z'$, $u_r = 0$, so that radius of the ring remains unchanged.

Thus, an isolated vortex ring in an unbounded ideal fluid will move without noticeable change of size in a direction perpendicular to its plane with a constant velocity. Equation (37) also shows that the axial speed is greater for small values of r_0. In order to illustrate the consequences of the latter, consider two similar vortex rings at same distance apart on a common axis of symmetry. The velocity field induced by the vortex ring in the rear has a radially outward component at the position of the vortex ring in the front so that the radius of the latter gradually increases. According to (37), this leads to a decrease in its speed of motion, and conversely, there is a corresponding increase in the speed of motion of the vortex ring in the rear, which subsequently passes through the larger vortex ring in the front and becomes the front vortex ring. This "leap–frogging" sequence keeps repeating itself.

Hill's Spherical Vortex

Hill's spherical vortex corresponds to a flow configuration in which the vorticity is confined to the interior of a sphere of radius a, say. Here, the vortex lines are circles about an axis passing through the center of the sphere while the streamlines lie in meridional planes. The flow outside the sphere is irrotational.

The equations of continuity and vorticity transport for a steady axisymmetric flow in cylindrical polar coordinates are

$$\frac{\partial(u_r r)}{\partial r} + \frac{\partial(u_z r)}{\partial z} = 0, \tag{38}$$

$$\frac{\partial(u_r \Omega)}{\partial r} + \frac{\partial(u_z \Omega)}{\partial z} = 0, \tag{39}$$

from which we derive

$$u_r \frac{\partial}{\partial r}\left(\frac{\Omega}{r}\right) + u_z \frac{\partial}{\partial z}\left(\frac{\Omega}{r}\right) = 0 \tag{22}$$

or, in terms of a streamfunction Ψ,

$$\frac{1}{r}\frac{\partial \Psi}{\partial z}\frac{\partial}{\partial r}\left(\frac{\Omega}{r}\right) - \frac{1}{r}\frac{\partial \Psi}{\partial r}\frac{\partial}{\partial z}\left(\frac{\Omega}{r}\right) = 0. \tag{40}$$

Equation (40) implies that

$$\frac{\Omega}{r} = f(\Psi). \tag{41}$$

Using equation (41), equation (24) becomes in spherical polar coordinates (R, θ, φ):

$$\frac{\partial}{\partial R}\left(\frac{1}{\sin\theta}\frac{\partial \Psi}{\partial R}\right) + \frac{\partial}{\partial \theta}\left(\frac{1}{R^2 \sin\theta}\frac{\partial \Psi}{\partial \theta}\right) = R^2 \sin\theta \cdot f(\Psi). \tag{42}$$

If $f(\Psi) = \text{constant} = A$, putting

$$\Psi = F(R)\sin^2\theta, \tag{43}$$

then equation (42) gives

$$R^2 F'' - 2F = AR^4, \tag{44}$$

where primes denote differentiation with respect to the argument. Thus,

$$F(R) = \frac{B}{R} + CR^2 + \frac{AR^4}{10}. \tag{45}$$

Equations (43) and (44) describe the motion within a fixed sphere of radius a; i.e., the surface of this sphere is a material surface if Ψ is well-behaved for $R < a$, and the normal velocity of this flow vanishes at the boundary, i.e., if

$$B = 0$$

and

$$-\left(\frac{1}{R\sin\theta}\frac{\partial\Psi}{R\partial\theta}\right)_{R=a} = 0. \tag{46}$$

Using (43) and (45), (46) gives

$$C = -\frac{Aa^2}{10}. \tag{47}$$

Using (45), (46), and (47), (43) leads to

$$R < a: \ \Psi = -\frac{A}{10}\left(a^2 - R^2\right)R^2\sin^2\theta. \tag{48}$$

Figure 2.24 shows the streamlines in the meridian plane. The vortex lines are circles perpendicular to the axis of symmetry.

If such a vortex is immersed in an irrotational flow of a fluid with a uniform speed U_∞, then one obtains a uniformly translating spherical vortex:

$$\begin{aligned} R < a: &\quad \Psi = -\frac{A}{10}\left(a^2 - R^2\right)R^2\sin^2\theta, \\ R > a: &\quad \Psi = \frac{1}{2}U_\infty R^2\sin^2\theta\cdot\left(1 - \frac{a^3}{R^3}\right). \end{aligned} \tag{49}$$

The continuity of the tangential velocity $\partial\Psi/\partial R$, at $R = a$, leads to

$$A = \frac{15}{2}\frac{U_\infty}{a^2}. \tag{50}$$

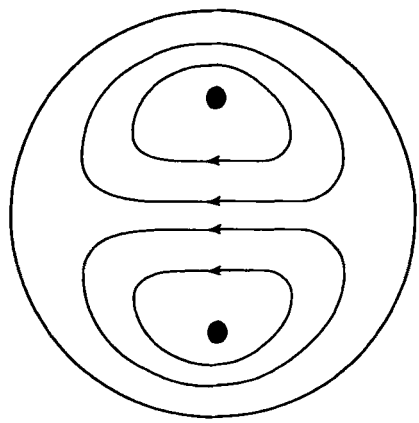

Figure 2.24. Streamline pattern in Hill's vortex.

Vortex Sheet

Surfaces on which the vorticity is infinite and the tangential component of the velocity field is discontinuous are not only kinematically possible but also can exist in the limit of vanishing viscosity as long as the discontinuities are consistent with the integral forms of the Euler equations of flow.

An example of a surface concentration of vorticity is the flow field behind an airplane wing (see Section 2.7). Let

$$\lim_{\varepsilon \Rightarrow 0} \int_{\varepsilon} \boldsymbol{\Omega}\, dn = \boldsymbol{\Gamma} = \text{const.}, \tag{51}$$

where n is the distance normal to the sheet and the integral is over some small range ε containing the surface. Using (51), (19) gives

$$\mathbf{v}(\mathbf{r}) = -\frac{1}{4\pi} \int \frac{(\mathbf{r}-\mathbf{r}') \times \boldsymbol{\Gamma}(\mathbf{r}')}{|\mathbf{r}-\mathbf{r}'|^3}\, dS(\mathbf{r}'). \tag{52}$$

For a single plane sheet of uniform vorticity, (52) becomes

$$\mathbf{v}(\mathbf{r}) = \frac{\boldsymbol{\Gamma}}{4\pi} \times \int_S \frac{(\mathbf{r}-\mathbf{r}')}{|\mathbf{r}-\mathbf{r}'|^3}\, dS(\mathbf{r}')$$

or

$$\mathbf{v}(\mathbf{r}) = \frac{\boldsymbol{\Gamma}}{4\pi} \times \hat{\mathbf{n}} \left[\int_S \frac{\hat{\mathbf{n}} \cdot (\mathbf{r}-\mathbf{r}')}{|\mathbf{r}-\mathbf{r}'|^3}\, dS(\mathbf{r}') \right] = \frac{1}{2}\, \boldsymbol{\Gamma} \times \hat{\mathbf{n}}, \tag{53}$$

where $\hat{\mathbf{n}}$ is the unit normal to the sheet directed to the side on which the point $\mathbf{r}$ lies. Thus, the fluid velocity produced by the vortex sheet is uniform and parallel to the sheet on each side, but in opposite direction on the two sides.[6]

Note that even if $\boldsymbol{\Gamma}$ is not constant, and the sheet were not plane, one has, from (52), the following equation for the local jump across the sheet in the induced flow velocity:

$$[\mathbf{v}] = \boldsymbol{\Gamma} \times \hat{\mathbf{n}}. \tag{54}$$

Consider next a vortex sheet in the form of a cylinder of arbitrary cross section, over which $\boldsymbol{\Gamma}$ defined in (51) is uniform and $\boldsymbol{\Gamma}$ is everywhere at right angles to the generators of the cylinder (so that the vortex lines are plane curves, all of the same shape, passing round the cylinder). Equation (52), then, gives

$$\mathbf{v}(\mathbf{r}) = -\frac{\boldsymbol{\Gamma}}{4\pi} \oint_C \int_{-\infty}^{\infty} \frac{(\mathbf{r}-\mathbf{r}') \times d\boldsymbol{\ell}(\mathbf{r}')}{|\mathbf{r}-\mathbf{r}'|^3}\, ds(\mathbf{r}'), \tag{55a}$$

[6]The application of integral form of Euler's equation to an element of the vortex sheet shows that the pressure as well as the normal component of the velocity field are continuous across the vortex sheet.

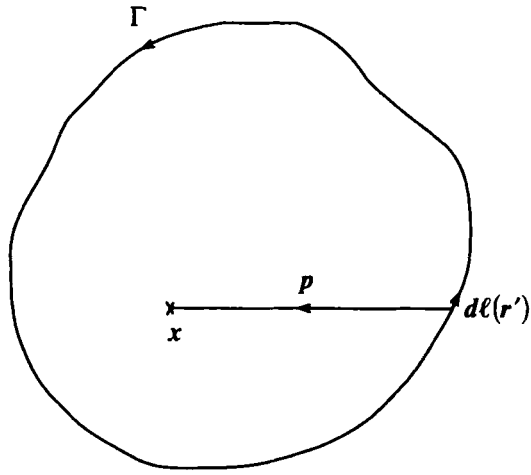

Figure 2.25. Sectional view of a cylindrical vortex sheet (from Batchelor, 1967).

where $ds(\boldsymbol{r}')$ is an element of length of a generator and $d\boldsymbol{\ell}(\boldsymbol{r}')$ a vector element of length of a vortex line (Figure 2.25). The component of $(\boldsymbol{r}-\boldsymbol{r}')$ parallel to the generators makes no contribution to the integral with respect to s so that (55a) becomes

$$\boldsymbol{v}(\boldsymbol{r}) = -\frac{\Gamma}{2\pi}\nabla \oint_C \frac{\boldsymbol{p}\times d\boldsymbol{\ell}(\boldsymbol{r}')}{p^2}, \tag{55b}$$

where $\boldsymbol{p}$ is the projection of $(\boldsymbol{r}-\boldsymbol{r}')$ on a cross-sectional plane. $|\boldsymbol{p}\times d\boldsymbol{\ell}(\boldsymbol{r}')|/p^2$ is the angle subtended at $\boldsymbol{r}$ by $d\boldsymbol{\ell}$ in this cross-sectional plane so that, at any point $\boldsymbol{r}$ within the cylinder, $\boldsymbol{v}$ is parallel to the generators and has a uniform magnitude Γ, while at any point $\boldsymbol{r}$ outside the cylinder $\boldsymbol{v}$ is zero.

Example 5: Consider n equal rectlinear vortex filaments arranged symmetrically as the generators of a circular cylinder of radius a. For the complex potential of this flow, one has

$$F(z) = \frac{i\Gamma}{2\pi}\sum_{s=0}^{n-1}\ln\left(z-ae^{2\pi si/n}\right) = \frac{i\Gamma}{2\pi}\ln\prod_{s=0}^{n-1}\left(z-ae^{2\pi si/n}\right) = \frac{i\Gamma}{2\pi}\ln\left(z^n-a^n\right).$$

The stream function Ψ of this flow is, then, given by

$$2i\Psi = F - \overline{F}$$

or

$$e^{4\pi\Psi/\Gamma} = z^n\bar{z}^n - a^n\left(z^n+\bar{z}^n\right)+a^{2n} = r^{2n} - 2a^n r^n\cos n\theta + a^{2n} = \text{const.}$$

The velocity components are, further, given by

$$\left.\begin{aligned} u_r &= -\frac{1}{r}\frac{\partial \Psi}{\partial \theta} = \frac{-\Gamma n a^n r^{n-1} \sin n\theta}{2\pi\left(r^{2n} - 2a^n r^n \cos n\theta + a^{2n}\right)}, \\ u_\theta &= \frac{\partial \Psi}{\partial r} = \frac{\Gamma n\left(r^{2n-1} - a^n r^{n-1} \cos n\theta\right)}{2\pi\left(r^{2n} - 2a^n r^n \cos n\theta + a^{2n}\right)}. \end{aligned}\right\}$$

For $n \gg 1$ and $r \gg a$, these give

$$u_r \approx 0, \qquad u_\theta \approx \frac{\Gamma n}{2\pi r};$$

and for $n \gg 1$ and $r < a$, these give

$$u_r \approx 0, \qquad u_\theta \approx 0.$$

One obtains a cylindrical vortex sheet by letting $n \Rightarrow \infty$ and keeping $n\Gamma$ =constant. Outside this sheet, therefore, the fluid moves as if all the vorticity were concentrated along its own axis; inside the sheet the fluid is stagnant.

The Vortex Breakdown: Brooke Benjamin's Theory

Vortex breakdown refers to major structural changes undergone by a concentrated vortex core embedded in a decelerating irrotational flow. Typically, this involves the formation of an internal stagnation point on the vortex axis, followed by a localized reversed axial flow. Downstream of the breakdown region, a new vortex structure with an expanded core develops. As a model of the vortex breakdown process consider an otherwise cylindrical vortex, embedded in a decelerating irrotational flow, that passes through a region of noncylindrical flow; at some distance downstream, the cylindrical state (i.e., no variations in the flow properties along the axis) prevails again. Initially, one has

$$\begin{aligned} r \le a: \quad & u_z = U_1, \qquad u_\theta = \omega r, \\ r \ge a: \quad & u_z = U_1, \qquad u_\theta = \frac{\omega a^2}{r}, \end{aligned} \tag{56a}$$

and finally one has

$$r \ge b: \quad u_z = U_2, \qquad u_\theta = \frac{\omega b^2}{r}. \tag{56b}$$

In the theoretical models the principal mechanism underlying the vortex breakdown process are assumed to exist in axisymmetric flow conditions (this is, however, known now to be inaccurate). Note that, for an axisymmetric flow, the vorticity components are given by

$$\Omega_z = \frac{1}{r}\frac{\partial\left(r u_\theta\right)}{\partial r}, \qquad \Omega_r = -\frac{\partial u_\theta}{\partial z}, \qquad \Omega_\theta = \frac{\partial u_r}{\partial z} - \frac{\partial u_z}{\partial r} \tag{57}$$

while the velocity components are given by

$$u_r = -\frac{1}{r}\frac{\partial \Psi}{\partial z}, \qquad u_z = \frac{1}{r}\frac{\partial \Psi}{\partial r}. \tag{23}$$

Using (23), (57) leads to

$$\Omega_\theta = -\frac{1}{r}\left(\frac{\partial^2 \Psi}{\partial z^2} + \frac{\partial^2 \Psi}{\partial r^2} - \frac{1}{r}\frac{\partial \Psi}{\partial r}\right). \tag{58}$$

Next, the equations of motion give, for a steady axisymmetric flow,

$$u_r \Omega_\theta - u_\theta \Omega_r = \frac{\partial H}{\partial z}, \tag{59}$$

$$u_\theta \Omega_z - u_z \Omega_\theta = \frac{\partial H}{\partial r}, \tag{60}$$

$$u_z \Omega_r - u_r \Omega_z = 0, \tag{61}$$

where

$$H = \frac{1}{2}\left(u_r^2 + u_\theta^2 + u_z^2\right) + \frac{p}{\rho}.$$

From equations (57) and (61), one obtains

$$\frac{D}{Dt}\left(r u_\theta\right) = 0, \tag{62}$$

which implies that

$$r u_\theta = C(\Psi). \tag{63}$$

When one uses (63), (57) gives

$$\Omega_z = u_z \frac{dC}{d\Psi}, \qquad \Omega_r = u_r \frac{dC}{d\Psi}. \tag{64}$$

When one uses (64), (59) gives

$$\frac{\Omega_\theta}{r^2} = \frac{C}{r^2}\frac{dC}{d\Psi} - \frac{dH}{d\Psi}. \tag{65}$$

When one uses (65), (58) gives

$$\frac{\partial^2 \Psi}{\partial z^2} + \frac{\partial^2 \Psi}{\partial r^2} - \frac{1}{r}\frac{\partial \Psi}{\partial r} = r^2 \frac{dH}{d\Psi} - C\frac{dC}{d\Psi}. \tag{66}$$

The functions H and C are arbitrary and must be prescribed to suit a given flow. They can be determined uniquely by the flow properties on open streamlines extending to upstream infinity where the flow properties are uniform along the axis. The functional forms so determined will then apply to all regions of the flow permeated by these streamlines. At upstream infinity, one has, on using (63),

$$\frac{1}{\rho}\frac{dp}{dr} = \frac{u_\theta^2}{r} = \frac{C^2}{r^3}. \tag{67}$$

Using (67), one obtains

$$H(\Psi) = \frac{1}{2}\left(u_r^2 + u_\theta^2 + u_z^2\right) + \int \frac{C^2}{r^3}\,dr$$

or

$$H(\Psi) = \frac{1}{2}\left(u_r^2 + u_z^2\right) + \int \frac{C^2}{r^3}\frac{dC}{dr}\,dr. \tag{68}$$

If the flow far upstream has an axial velocity U_1 and rotates as a rigid body with angular velocity ω, then one has

$$\Psi = \frac{1}{2}\,U_1 r^2, \qquad C = \omega r^2. \tag{69}$$

When one uses (69), (68) becomes

$$H(\Psi) = \frac{1}{2}\,U_1^2 + \omega^2 r^2. \tag{70}$$

When one uses (69) and (70), the upstream conditions may be alternately written as

$$C(\Psi) = \frac{2\omega}{U_1}\,\Psi, \qquad H(\Psi) = \frac{1}{2}\,U_1^2 + \frac{2\omega^2}{U_1}\,\Psi. \tag{71}$$

When one uses (71), (66) becomes

$$\frac{\partial^2 \Psi}{\partial z^2} + \frac{\partial^2 \Psi}{\partial r^2} - \frac{1}{r}\frac{\partial \Psi}{\partial r} = \frac{2\omega^2}{U_1}\,r^2 - \frac{4\omega^2}{U_1^2}\,\Psi \tag{72}$$

which is linear!

When one uses

$$\Psi(z,r) = \frac{1}{2}\,U_1 r^2 + rF(z,r), \tag{73}$$

equation (72) leads to

$$\frac{\partial^2 F}{\partial z^2} + \frac{\partial^2 F}{\partial r^2} + \frac{1}{r}\frac{\partial F}{\partial r} + \left(k^2 - \frac{1}{r^2}\right)F = 0, \tag{74}$$

where

$$k = \frac{2\omega}{U_1}.$$

When one uses the boundary condition (56b), (73) leads to

$$r = b : F = \frac{1}{2} U_1 \left(\frac{a^2 - b^2}{b} \right). \tag{75}$$

From equations (74) and (75), one obtains

$$F = \frac{1}{2} U_1 \left(\frac{a^2}{b^2} - 1 \right) \frac{bJ_1(kr)}{J_1(kb)}, \tag{76}$$

where $J_n(x)$ is Bessel's function of order n.

When one uses (73) and (76), (23) gives

$$u_z = U_1 + \frac{1}{2} U_1 \left(\frac{a^2}{b^2} - 1 \right) \frac{kbJ_0(kr)}{J_1(kb)}, \tag{77}$$

from which

$$\left(\frac{u_z}{U_2} \right)_{r=0} = \frac{U_1}{U_2} \left[1 + \left(\frac{a^2}{b^2} - 1 \right) \frac{\frac{1}{2} kb}{J_1(kb)} \right] \tag{78}$$

$$\left(\frac{U_2}{U_1} \right) = 1 + \left(\frac{a^2}{b^2} - 1 \right) \frac{\frac{1}{2} kbJ_0(kb)}{J_1(kb)}. \tag{79}$$

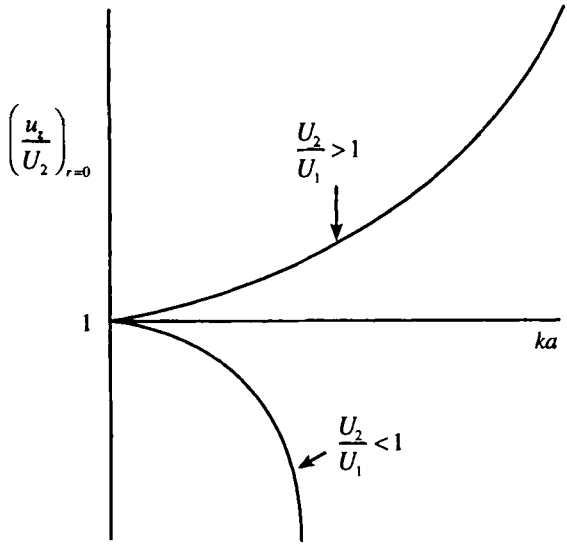

Figure 2.26. Variation of the axial velocity in the vortex core with the radius of the vortex filament (from Batchelor, 1967).

Equation (78) shows that a change in the axial velocity in the irrotational flow surrounding a vortex produces significant changes (see Figure 2.26) in the structure of the vortex (particularly, when the external fluid is decelerated).

Figure 2.27 shows the way in which kb varies with $U_1/U_2(>1)$ for a given value ka [$0 \le ka \le 2,4$, the first zero of $J_0(x)$] according to (79). One observes that the increased thickening of the vortex due to deceleration of the external stream becomes catastrophic at a critical value $(U_2/U_1)^*$ of (U_2/U_1) – an event identified to be the vortex breakdown.

Figure 2.27 predicts the possibility of a finite transition from a state on the lower part to a state on the upper part. Indeed, Brooke Benjamin proposed that the vortex breakdown be viewed as such a finite transition between dynamically conjugate states of axisymmetric flow. The transition is from a supercritical flow, which cannot support standing waves, to a subcritical flow, which can. In support of Brooke Benjamin's proposal were Harvey's experimental results that

* the breakdown can be made axisymmetric, whereas the original flow is of a kind that is highly stable to axisymmetric disturbances;
* the breakdown can then comprise an abrupt expansion of the stream surfaces near the axis;
* the above configuration can be made approximately steady.

Typically, the transitional breakdown region occupies a small length so that the oncoming and emerging regions may be thought of as joined by a sudden jump. The jump conditions connecting these two regions follow from the continuity of the fluxes of mass and momentum:

$$U_1 a^2 = U_2 b^2 \tag{80}$$

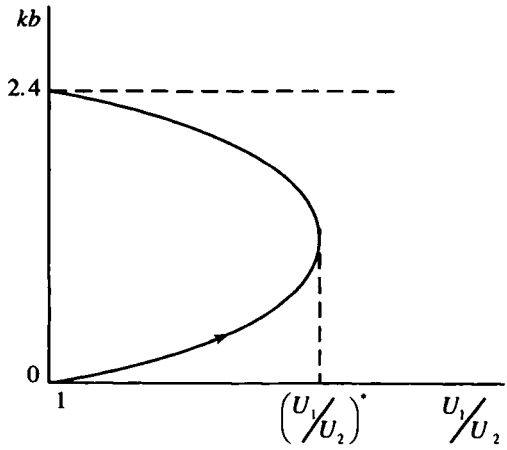

Figure 2.27. Variation of the size of the vortex with the axial flow (from Batchelor, 1967).

$$2\pi \int_0^a \left(p_1 + \rho U_1^2 + \rho u_\theta^2\right) r\,dr = 2\pi \int_0^b \left(p_2 + \rho U_2^2 + \rho u_\theta^2\right) r\,dr, \tag{81}$$

from which we obtain

$$\left.\begin{aligned} U_1^2 &= \frac{1}{2}\,\Omega^2 \frac{b^3}{a}, \\ U_2^2 &= \frac{1}{2}\,\Omega^2 \frac{a^3}{b}. \end{aligned}\right\} \tag{82}$$

The energy fluxes on both sides of the transition are not the same, and their difference is the amount of energy dissipated in the transition. Thus,

$$\Delta\varepsilon = 2\pi\rho \int_0^a U_1 H_1 r\,dr - 2\pi\rho \int_0^b U_2 H_2 r\,dr \tag{83a}$$

or

$$\Delta\varepsilon = \frac{2Q\Omega^2}{4a^2b^2}\left(b^4 + b^3a - \frac{b^2a^2}{3} + ba^3 + a^4\right)(b-a), \tag{83b}$$

where

$$H = \frac{p}{\rho} + \frac{1}{2}\left(U^2 + u_\theta^2\right), \qquad Q = \pi a^2 \rho U_1$$

and it is easy to verify that

$$b^4 + b^3a - \frac{b^2a^2}{3} + ba^3 + a^4 > 0.$$

Then, $\Delta\varepsilon > 0$ implies

$$b > a. \tag{84}$$

Therefore, in such a transition the vortex always expands.

Next, from equation (77), it is seen that there is a maximum value for b/a only below which it is possible to preserve axisymmetry in the flow downstream of the transition. From equation (74), it is seen that the presence of a wavemotion downstream of the transition increases this maximum value of b/a. In other words, a wavemotion promotes the possibility of axisymmetric flow downstream of the transition.

EXERCISES

1. Find the velocity induced on the axis of a vortex ring.

2. Find the motion of the line vortices of equal and opposite strengths $\pm\Gamma$ located at $z = \pm a$.

3. Consider a two–dimensional incompressible flow bounded by perpendicular rigid walls $0X, 0Y$, with a line vortex of strength Γ at a point (x, y) in the fluid. Show that this line vortex moves along a path given by

$$x^2 + y^2 = Cx^2y^2.$$

2.5. Rotating Flows

The dominance of Coriolis forces in a rotating flow can lead to interesting consequences. One example is when the flow is steady relative to the rotating axes; there occurs a strong tendency in the flow toward two–dimensionality. In general, rotation imparts some kind of rigidity to the flow. Rotation also confers a certain elasticity on the fluid that makes possible the propagation of waves in a rotating fluid.

Governing Equations and Elementary Results

When the motion of a uniformly rotating fluid is referred to a frame of reference that rotates with the fluid, the equation of motion of the fluid is changed only by the addition of an apparent body force,

$$\frac{\partial \mathbf{v}}{\partial t} + \frac{1}{2}\nabla(\mathbf{v}\cdot\mathbf{v}) + (\nabla\times\mathbf{v})\times\mathbf{v} + 2\boldsymbol{\Omega}\times\mathbf{v} + \boldsymbol{\Omega}\times(\boldsymbol{\Omega}\times\mathbf{r}) = -\frac{1}{\rho}\nabla p, \tag{1}$$

where $\boldsymbol{\Omega}$ is the angular velocity of the fluid.

The centrifugal force $\boldsymbol{\Omega}\times(\boldsymbol{\Omega}\times\mathbf{r})$ plays a significant role only when the density ρ is nonuniform. On the other hand, if ρ is uniform, the centrifugal force is conservative and is equivalent to an effective radial pressure gradient and may be transformed away by incorporating this effective pressure in the actual pressure.

Thus, when we put

$$P = \frac{1}{\rho}\left[p - \frac{1}{2}|\boldsymbol{\Omega}\times\mathbf{r}|^2\right], \tag{2}$$

equation (1) becomes

$$\frac{\partial \mathbf{v}}{\partial t} + \frac{1}{2}\nabla(\mathbf{v}\cdot\mathbf{v}) + (\nabla\times\mathbf{v})\times\mathbf{v} + 2\boldsymbol{\Omega}\times\mathbf{v} = -\nabla P, \tag{3}$$

so that the effects of rotation are contained only in the term $2\boldsymbol{\Omega}\times\mathbf{v}$, called the Coriolis force. The Coriolis force does no work on the fluid but serves only to change the direction of velocity of the latter.

Taylor–Proudman Theorem

If equation (3) is written in a dimensionless form by introducing reference lenght and velocity scales L and U, one finds that the following dimensionless parameter, called by Rossby number,

$$R_0 = \frac{U}{\Omega L}, \tag{4}$$

occurs. The Rossby number measures the importance of the nonlinear convective acceleration term relative to the Coriolis term. For small Rossby number flows (like the steady large–scale circulations of the oceans and atmospheres) the inertia forces are negligible, and equation (3) reduces to a balance between the Coriolis term and the pressure–gradient term:

$$2\boldsymbol{\Omega} \times \boldsymbol{v} = -\nabla p. \tag{5}$$

This is called the *geostrophic approximation.*[7]

Taking the curl of equation (5), one obtains

$$-(2\boldsymbol{\Omega} \cdot \nabla)\boldsymbol{v} = \boldsymbol{0}. \tag{6}$$

Thus, the velocity components of such a flow do not vary in the direction of the angular velocity. This leads to the Taylor–Proudman Theorem:

THEOREM: All steady, slow motions in a rotating inviscid fluid are very nearly two–dimensional.

In fact, experimentally, if a solid cylinder of finite height and horizontal ends is towed steadily and horizontally in a fluid rotating about the vertical axis, then a fluid column coaxial with the solid cylinder is found to move along with the latter. This is due to the fact that when the lateral velocity is made to vanish at a point along the direction of the angular velocity by a small obstruction, this velocity will vanish at all points along the direction of the angular velocity. The fluid will, then, flow two–dimensionally around this so–called Taylor column.[8]

If we take the angular velocity $\boldsymbol{\Omega}$ to be along the z–direction, say $\boldsymbol{\Omega} = (f/z)\,\hat{\boldsymbol{i}}_z$, and include a body force $-\nabla\Phi$, $(\Phi = gz)$, due to gravity, then, equation (5) gives

$$\frac{1}{\rho}\frac{\partial p}{\partial x} - fv = 0, \tag{7}$$

---

[7]Geostrophic flows are governed by equation (5), which is mathematically degenerate, being of lower order than the complete equation of motion, namely, equation (3), and consequently incapable of solution under all the necessary initial/boundary conditions. Therefore, boundary layers characterized by highly nongeostrophic flows necessarily appear in geostrophic flows.

[8]Taylor demonstrated this dramatically moving a rather short cylinder, standing on end, slowly across the bottom of a rotating slab of water and coloring matter appropriately introduced into the water. The streamlines were then observed to flow discretely around the column of water directly above the cylinder – apparently almost as if this column is impenetrable (see Figure 2.28).

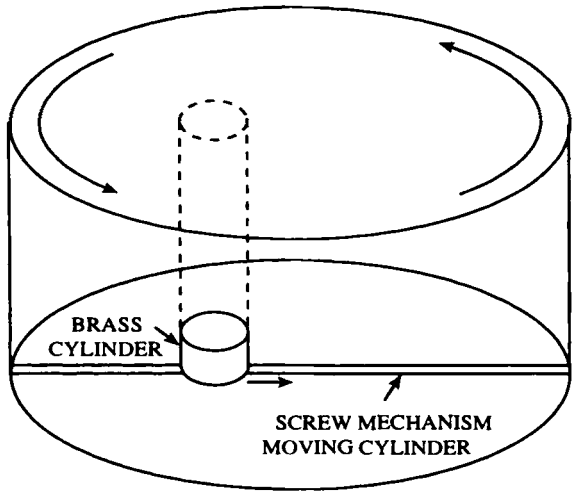

Figure 2.28. "Taylor column" experimental arrangement.

$$\frac{1}{\rho}\frac{\partial p}{\partial y} + fu = 0, \tag{8}$$

$$\frac{1}{\rho}\frac{\partial p}{\partial z} + g = 0. \tag{9}$$

Equation (9) is simply the hydrostatic approximation, while equations (7) and (8) can be combined to give

$$u\frac{\partial p}{\partial x} + v\frac{\partial p}{\partial y} = 0. \tag{10}$$

Equation (10) shows that the horizontal streamlines of a steady geostrophic flow are perpendicular to the (horizontal) pressure gradient or are along the isobars.

On the other hand, elimination of p from equations (7) and (8) gives

$$\frac{\partial u}{\partial x} + \frac{\partial v}{\partial y} = 0, \tag{11}$$

which shows that the strong Coriolis forces oppose any nonsolenoidal flow in a lateral plane.

Propagation of Waves in a Rotating Fluid

Thanks to a certain elasticity conferred on a fluid by rotation, a restoring mechanism becomes available in the fluid to sustain the propagation of waves. This restoring force arises from the tendency of the Coriolis forces to oppose any lack of solenoidal flow in the lateral plane associated with perturbations on a rigid–body rotation.

One has

$$\frac{\partial v_i}{\partial t} + v_j \frac{\partial v_i}{\partial x_j} = -\frac{\partial P}{\partial x_i} + 2\varepsilon_{ijk} v_j \Omega_k , \tag{12}$$

$$\frac{\partial v_i}{\partial x_i} = 0. \tag{13}$$

Seeking solutions of the form

$$e^{i(k_j x_j + nt)}, \tag{14}$$

equations (12) and (13) give

$$inv_i + ik_j v_j v_i = -ik_i P + 2\varepsilon_{ijk} v_j \Omega_k , \tag{15}$$

$$k_j v_j = 0. \tag{16}$$

Multiplying equation (15) by v_i, k_i, Ω_i, one obtains

$$nv_i^2 = 0, \tag{17}$$

$$k^2 P + 2i\varepsilon_{ijk} k_i v_j \Omega_k = 0, \tag{18}$$

$$nv_i \Omega_i + Pk_i \Omega_i = 0. \tag{19}$$

When we let

$$\boldsymbol{\Omega} = (\Omega_x, 0, \Omega_z), \qquad \boldsymbol{k} = (0, 0, k), \tag{20}$$

(16) gives

$$kv_z = 0 \quad \text{or} \quad v_z \equiv 0. \tag{21}$$

When we use (20) and (21), equations (17)–(19) become

$$n\left(v_x^2 + v_y^2\right) = 0, \tag{22}$$

$$2i\Omega_x v_y = kP, \tag{23}$$

$$n\Omega_x v_x = -kP\Omega_z , \tag{24}$$

from which

$$n\left(1 - \frac{n^2}{4\Omega_z^2}\right) v_x^2 = 0$$

or

$$n = \pm 2\Omega_z . \tag{25}$$

When we use (25), equations (22)–(24) give

$$v_x = \pm i v_y , \tag{26}$$

which implies that the waves are transverse, and circularly polarized.

Plane Inertial Flows

Having just seen that small disturbances in a uniformly rotating, incompressible fluid can propagate as wavemotions, let us now go on to study some special features of wave propagation in a rotating fluid. For the linearized motion in a rotating fluid, one has

$$\nabla \cdot \mathbf{v} = 0, \tag{27}$$

$$\frac{\partial \mathbf{v}}{\partial t} + 2\boldsymbol{\Omega} \times \mathbf{v} = -\nabla p. \tag{28}$$

When we look plane wave solutions of the form

$$\left.\begin{aligned} \mathbf{v} &= \boldsymbol{V} e^{i(\boldsymbol{k}\cdot\boldsymbol{x}-\sigma t)}, \\ p &= P e^{i(\boldsymbol{k}\cdot\boldsymbol{x}-\sigma t)}, \end{aligned}\right\} \tag{29}$$

equation (27) gives

$$\boldsymbol{V} \cdot \boldsymbol{k} = 0; \tag{30}$$

i.e., the velocity is perpendicular to the propagation direction and the waves are transverse. This is the only possible type of motion in an incompressible fluid. Equation (28) gives

$$-i\omega \mathbf{v} \cdot \mathbf{v} = 0. \tag{31}$$

When we put

$$\mathbf{v} = \boldsymbol{a} + i\boldsymbol{b}, \tag{32}$$

equation (31), in turn, gives

$$a^2 = b^2 \quad \text{and} \quad \boldsymbol{a} \cdot \boldsymbol{b} = 0, \tag{33}$$

which implies that the waves are circularly polarized and that $\boldsymbol{a}, \boldsymbol{b}, \boldsymbol{k}$ form an orthogonal triad.

Equation (22) also lends to the following dispersion relation:

$$\sigma = \pm 2\boldsymbol{\Omega} \cdot \hat{\boldsymbol{k}}, \tag{34}$$

where

$$\hat{\boldsymbol{k}} = \frac{\boldsymbol{k}}{|\boldsymbol{k}|}.$$

The phase velocity of the wave moving in the direction $\hat{\boldsymbol{k}}$ is

$$\boldsymbol{C}_p = 2\frac{\boldsymbol{\Omega} \cdot \hat{\boldsymbol{k}}}{|\boldsymbol{k}|}\hat{\boldsymbol{k}}. \tag{35}$$

Equation (35) implies that the phase speed is inversely proportional to the magnitude of the wave vector and that the waves are, in general, dispersive and

anisotropic. The long waves (small $|k|$) travel fastest and the short waves slowest, like the surface waves on water (see Section 2.6).

The group velocity of the waves is the velocity of energy propagation and is given by

$$C_g = \nabla_k \sigma(k) = \frac{2}{|k|}\,\Omega - 2\,\frac{\Omega\cdot\hat{k}}{|k|}\,\hat{k} \tag{36a}$$

or

$$C_g = \frac{2}{|k|}\,\hat{k}\times\left(\Omega\times\hat{k}\right), \tag{36b}$$

which shows that the energy transport is at right angles to the phase velocity.

When $\sigma \sim \Omega\cdot\hat{k} \approx 0$, the phase velocity C_p is zero; however, there is a steady propagation of wave energy along the axis of rotation with a group velocity $C_g = 2\Omega/|k|$. This leads to the formation of Taylor columns in a rotating fluid.

Consider now wave propagation in a flow field which otherwise has a rigid rotation with angular velocity Ω and a uniform streaming motion with velocity U. For linearized wave motion in this flow field, one has

$$\nabla\cdot v = 0, \tag{27}$$

$$\frac{\partial v}{\partial t} + U\cdot\nabla v + 2\Omega\times v = -\nabla p. \tag{37}$$

Looking for plane wave solution of the form (29), we note that equation (37) gives

$$\sigma = \pm 2\Omega\cdot\hat{k} + U\cdot k. \tag{38}$$

The phase velocity is

$$C_p = \left(\pm 2\frac{\Omega\cdot\hat{k}}{|k|} + U\cdot k\right)\hat{k}, \tag{39}$$

and the group velocity is

$$C_g = \pm\,\frac{2}{|k|}\,\hat{k}\times\left(\Omega\times\hat{k}\right) + U. \tag{40}$$

Note that the frequency is corrected for a Doppler shift, and the wavespeeds are augmented by the free-stream convection.

Suppose U were in a direction opposite to that of Ω. Then, energy can be transmitted upstream, against the streaming flow if $C_g\cdot\Omega > 0$, i.e., if

$$\frac{2}{k\Omega}\left[\Omega^2 - \left(\Omega\cdot\hat{k}\right)^2\right] > U.$$

Thus, waves with wavenumber k can propagate against the streaming flow if $U < 2\Omega/k$.

Forced Wavemotion in a Rotating Fluid

Consideration of forced wavemotion in a rotating fluid shows that the equation governing the waves is elliptic, parabolic, or hyperbolic, depending on whether the frequency of forcing oscillation ω is greater than, equal to, or less than twice the angular velocity Ω of the fluid. Further, in the hyperbolic case, there exist real characteristic surfaces in the flow (similar to the Mach cones in gas dynamics, see Chapter 3) across which the disturbances become discontinuous. The experiments have confirmed the predicted dependence of the apex angle of the cone on the forcing frequency. We will give here a linearized calculation of the motion induced by an oscillatory point source in a rotating incompressible, inviscid fluid. (Since the flow velocities near the source are large, the linearization of the equations governing the flow is valid only at distances far away from the source.) The solutions in the elliptic and hyperbolic cases are obtained using the Fourier–transform method. In the hyperbolic case, an appropriate radiation condition has to be imposed to find the correct solution. We will find that in the elliptic case, the flow is continuous everywhere; in the hyperbolic case, a cone with vertex at the source and axis along the axis of rotation becomes a surface of discontinuity dividing the flow into three separate regions with different characteristic features.

Consider the motion induced by an oscillatory point source of strength $\rho_0 q e^{i\omega t}$ and placed at the origin in an inviscid, incompressible fluid rotating with a constant angular velocity about the x–direction through the origin. The linearized equations for this flow, when referred to a frame rotating with the fluid, are

$$\frac{\partial u'}{\partial x} + \frac{\partial v'}{\partial y} + \frac{\partial w'}{\partial z} = q e^{i\omega t}\delta(x)\delta(y)\delta(z), \tag{41}$$

$$\frac{\partial u'}{\partial t} = \frac{\partial P'}{\partial x}, \tag{42}$$

$$\frac{\partial v'}{\partial t} - 2\Omega w' = \frac{\partial P'}{\partial z}, \tag{43}$$

$$\frac{\partial w'}{\partial t} + 2\Omega v' = \frac{\partial P'}{\partial y}, \tag{44}$$

where

$$P' \equiv \frac{p'}{\rho}.$$

The primes denote the disturbances, the subscript 0 refers to the basic state of the fluid, and for the latter we obtain

$$\left.\begin{aligned} -\Omega^2 y &= -\frac{\partial p_0}{\partial y}, \\ -\Omega^2 z &= -\frac{\partial p_0}{\partial z}. \end{aligned}\right\} \tag{45}$$

Using equations (41)–(44), one obtains

$$\frac{\partial^2}{\partial t^2}\nabla^2 P' + 2\Omega\frac{\partial^2}{\partial t^2}\left(\frac{\partial w'}{\partial y} - \frac{\partial v'}{\partial z}\right) = -i\omega^3 q e^{i\omega t}\delta(x)\delta(y)\delta(z). \tag{46}$$

Using equations (43) and (44), one has

$$\frac{\partial^2}{\partial t^2}\left(\frac{\partial w'}{\partial y} - \frac{\partial v'}{\partial z}\right) = -2\Omega\frac{\partial}{\partial t}\left(\frac{\partial v'}{\partial y} + \frac{\partial w'}{\partial z}\right),$$

which, on using equations (41) and (42), becomes

$$\frac{\partial^2}{\partial t^2}\left(\frac{\partial w'}{\partial y} - \frac{\partial v'}{\partial z}\right) = -2\Omega i\omega q e^{i\omega t}\delta(x)\delta(y)\delta(z) + 2\Omega\frac{\partial^2 P'}{\partial x^2}. \tag{47}$$

Using equation (47), equation (46) becomes

$$\frac{\partial^2}{\partial t^2}\nabla^2 P' + 4\Omega^2\frac{\partial^2 P'}{\partial x^2} = i\omega\left(4\Omega^2 - \omega^2\right) q e^{i\omega t}\delta(x)\delta(y)\delta(z). \tag{48}$$

Upon Fourier–transforming, according to

$$F(\ell, m, n)\, e^{i\omega t} = \frac{1}{(2\pi)^{3/2}}\int_{-\infty}^{\infty}\int\int\int e^{i(\ell x + my + nz)} f(x, y, z, t)\, dxdydz, \tag{49}$$

equation (52) gives, on inversion,

$$P' = \frac{e^{i\omega t}}{8\pi^3}\int_{-\infty}^{\infty}\int\int\int \frac{iq\omega\left(4\Omega^2 - \omega^2\right)}{-\ell^2\left(4\Omega^2 - \omega^2\right) + \omega^2\left(m^2 + n^2\right)} e^{i(\ell x + my + nz)}\, d\ell dmdn. \tag{50}$$

We shall evaluate the integral in (50) by first performing the ℓ–integration by the method of residues, and then, the m,n integrations by changing the variables. Two cases are distinguished:

$$\begin{aligned} B_1^2 &\equiv \omega^2 - 4\Omega^2 > 0: \quad \text{elliptic case} \\ B_2^2 &\equiv 4\Omega^2 - \omega^2 > 0: \quad \text{hyperbolic case.} \end{aligned} \tag{51}$$

The Elliptic Case

The poles of the integrand in (50) now occur at,

$$\ell = \pm\frac{i\omega s}{B_1}, \tag{52}$$

where

$$s^2 \equiv m^2 + n^2.$$

For $x > 0$, the path of ℓ–integration along the $\mathrm{Re}(\ell)$–axis is closed by a large semicircle in the upper–half of the ℓ–plane. The contribution to the integral in (50) then comes from the positive values in (52), and one obtains

$$P' = -\frac{iqB_1 e^{i\omega t}}{8\pi^2} \int_{-\infty}^{\infty}\int_{-\infty}^{\infty} \frac{1}{s} e^{-\omega xs/B_1 + imy + inz}\, dmdn. \tag{53}$$

When we change the variables according to

$$\left.\begin{aligned} &x = r\cos\theta, \quad y = r\sin\theta\cos\phi, \quad z = r\sin\theta\sin\phi, \\ &m = s\cos\psi, \quad n = s\sin\psi, \end{aligned}\right\} \tag{54}$$

(53) becomes

$$P' = -\frac{iqB_1 e^{i\omega t}}{8\pi^2} \int_0^{\infty}\int_0^{2\pi} \frac{1}{s} e^{-s\omega r\cos\theta/B_1}\; e^{ir\sin\theta\cdot s\cos(\psi-\phi)} s\, dsd\psi,$$

$$= -\frac{iqB_1 e^{i\omega t}}{4\pi} \int_0^{\infty} \frac{1}{s} e^{-s\omega r\cos\theta/B_1}\; J_0(r\sin\theta\cdot s)\, s\, ds, \tag{55}$$

where $J_\upsilon(x)$ is the Bessel function of order υ. Upon carrying out the integration in (55) further, one obtains

$$P' = -\frac{iqB_1^2 e^{i\omega t}}{4\pi r\sqrt{\omega^2 - 4\Omega^2\sin^2\theta}}. \tag{56}$$

Equation (56) shows that the flow is continuous everywhere.

The Hyperbolic Case

The poles of the integrand in (50) now occur at

$$\ell = \pm\frac{\omega s}{B_2}. \tag{57}$$

For $x > 0$, the path of ℓ–integration along the $\mathrm{Re}\,(\ell)$–axis is closed again by a large semicircle in the upper half of the ℓ–plane. In order to determine which of the two poles in (57) contributes to the integral in (50), one imposes an appropriate radiation condition by giving ω a small negative imaginary part $-i\varepsilon(\varepsilon \Rightarrow 0^+)$. (This is equivalent to posing a more realistic initial–value problem, rather than a steady–wave problem as in the foregoing, with the applied steady source being switched–on at time $t = 0$.) The contribution to the integral in (50), then, comes from the negative value in (57), and one obtains, upon changing the variables, according to (54),

$$P' = -\frac{qB_2 e^{i\omega t}}{8\pi^2} \int_0^{\infty} \int_0^{2\pi} \frac{1}{s} e^{-is\omega r \cos\theta/B_2} \; e^{ir \sin\theta \cdot s \cos(\psi-\phi)} s \, ds d\psi$$

$$= -\frac{qB_2 e^{i\omega t}}{4\pi} \int_0^{\infty} \frac{1}{s} e^{-is\omega r \cos\theta/B_2} \; J_0(r \sin\theta \cdot s) s \, ds. \tag{58}$$

Upon carrying out the integration in (58) further, one obtains

$$P' = \begin{cases} \dfrac{iqB_2^2 e^{i\omega t}}{4\pi r \sqrt{\omega^2 - 4\Omega^2 \sin^2\theta}}, & \dfrac{\omega}{2\Omega} > \sin\theta, \\ \dfrac{qB_2^2 e^{i\omega t}}{4\pi r \sqrt{4\Omega^2 \sin^2\theta - \omega^2}}, & \dfrac{\omega}{2\Omega} < \sin\theta. \end{cases} \tag{59}$$

Equation (59) shows that the pressure becomes infinity on the cone $\omega/2\Omega = \sin\theta$ with vertex at the source and axis along the axis of rotation which is a surface of discontinuity in the flow dividing the latter into three separate regions with different characteristic features. Observe that the solution inside the cone resembles that of the elliptic case. The adjustment of the flow from inside the cone to the outside is made through thin viscous shear layers about the surface of the cone.

Note that when $\omega = 2\Omega$ the pressure vanishes everywhere except on the cone of discontinuity, which now becomes a plane through the source and perpendicular to the axis of rotation.

Slow Motion Along the Axis of Rotation

Let us consider a simple case of transient evolution of inertial waves to illustrate the process by which these waves organize to form a Taylor column ahead of the body producing the waves. Specifically, consider a finite disk of radius r_0 that is initially rotating rigidly with an infinite body of fluid. The disk is then moved slowly perpendicular to itself along the axis of rotation. Since only the projected shape of a body on a plane perpendicular to the axis of rotation is important as far as steady longitudinal motion of the body is concerned, it appears that a body of any shape in slow forward motion is related to a disk of the same projected cross-sectional area.

The linearized problem for the slow forward motion of the disk in a rotating frame of cylindrical coordinates with the z-axis along the axis of rotation is governed by

(60)

$$\frac{\partial \mathbf{v}}{\partial t} + 2\Omega \times \mathbf{v} = -\frac{1}{\rho} \nabla p \tag{61}$$

with

$$\left.\begin{aligned} t \geq 0: \quad & \mathbf{v} \cdot \hat{\mathbf{k}} = U \quad \text{on} \quad r \leq r_0, z = 0 \\ & \mathbf{v} \Rightarrow 0 \quad \text{as} \quad |r| \Rightarrow \infty \end{aligned}\right\} \tag{62}$$

$$t \leq 0: \quad \mathbf{v} \equiv 0. \tag{63}$$

We shall apply the Laplace and Hankel transforms consecutively to reduce the above partial differential equation to ordinary differential equations with z as the independent variable. If (u_r, u_θ, u_z) denote the velocity components along the (r, θ, z)–directions, let us first introduce a stream function ψ, through

$$u_r = \frac{1}{r}\frac{\partial \psi}{\partial z}, \quad u_z = -\frac{1}{r}\frac{\partial \psi}{\partial r}, \tag{64}$$

so that equation (60) is identically satisfied. Upon Laplace transforming, according to

$$\overline{\psi} = \int_0^\infty e^{-st} \psi \, dt, \tag{65}$$

equation (61) leads to

$$r \frac{\partial}{\partial r}\frac{1}{r}\frac{\partial \overline{\psi}}{\partial r} + \left(1 + \frac{4\Omega^2}{s^2}\right)\frac{\partial^2 \overline{\psi}}{\partial z^2} = 0, \tag{66}$$

with (62) giving

$$\left.\begin{aligned} & z = 0, \; r \leq r_0: \quad -\frac{1}{r}\frac{\partial \overline{\psi}}{\partial r} = \frac{U}{s}, \\ & z \Rightarrow \infty: \quad \overline{\psi} \Rightarrow 0. \end{aligned}\right\}. \tag{67}$$

One solves equation (66) by applying the Hankel transform to obtain

$$\overline{\psi} = r \int_0^\infty A(k) J_1(kr) e^{-k|z|/\sqrt{1+4\Omega^2/s^2}} \, dk. \tag{68}$$

Then, (67) gives

$$\left.\begin{aligned} r \leq r_0: \quad & \int_0^\infty kA(k) J_0(kr) \, dk = -\frac{U}{s}, \\ r > r_0: \quad & \int_0^\infty kA(k) J_1(kr) \, dk = 0, \end{aligned}\right\} \tag{69}$$

from which we have

$$kA(k) = \frac{2U}{\pi s}\left(\cos k - \frac{\sin k}{k}\right). \tag{70}$$

When one uses (70), (68) leads to

$$\overline{\psi} = \frac{2Ur}{\pi} \int_0^\infty \frac{J_1(kr)}{k} \left(\cos k - \frac{\sin k}{k} \right) \cdot \frac{1}{s} e^{-(kz)/\left(\sqrt{1+4\Omega^2/s^2}\right)} dk, \tag{71}$$

and equation (60) gives

$$u_\theta = \frac{4U\Omega}{\pi} \int_0^\infty J_1(kr) \cdot \left(\cos k - \frac{\sin k}{k} \right) \frac{e^{-(kz)/\left(\sqrt{1+4\Omega^2/s^2}\right)}}{s^2 \sqrt{1+4\Omega^2/s^2}} dk. \tag{72}$$

Let us now find an asymptotic approximation for large t. In inverting the Laplace transform, note that there is a simple pole at $s = 0$ and two branch points at $s = \pm 2i\Omega$, and a branch cut is introduced between the latter. Further, the condition that a certain minimum time must elapse before waves of a given wavenumber arrive at a given location on the axis of rotation implies that one requires

$$t > \frac{z}{C_g}, \tag{73}$$

where

$$C_g = \frac{2\Omega}{k},$$

is the group velocity of plane waves of wavenumber k whose phase velocity is in a direction perpendicular to the axis of rotation; the group velocity is, therefore, along the latter direction. Thus, inversion of (71) and (72) leads to

$$\psi \sim \frac{2Ur}{\pi} \int_0^{2\Omega t/z} \frac{J_1(kr)}{k} \left(\cos k - \frac{\sin k}{k} \right) dk, \tag{74}$$

$$u_\theta \sim \frac{2U\Omega}{\pi} \int_0^{2\Omega t/z} J_1(kr) \left(\cos k - \frac{\sin k}{k} \right) dk. \tag{75}$$

In the frame of reference moving with the disk, the stream function is

$$\Psi = \frac{1}{2} Ur^2 + \psi \tag{76}$$

and u_θ is unchanged. Figure 2.29 shows the instantaneous streamlines Ψ about the disk. Observe the appearance of a stagnation point in the flow, the broad bluff front, and the reverse cellular flow behind it. This is similar to the flow about an imaginary obstacle of the same projected cross–sectional area as the disk, but of a constantly increasing dimension along the axis of rotation, and represents, of course, the formation and development of a Taylor column. Note that the latter cannot form if the waves are convected downstream by a stream flowing with a speed exceeding their group velocities.

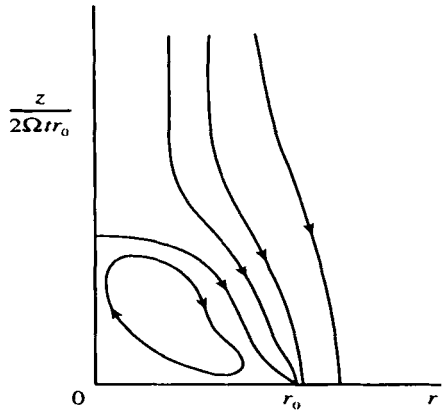

Figure 2.29. Instantaneous streamline pattern about a rotating disk moving slowly perpendicular to itself along the axis of rotation (from Greenspan, 1968).

Figure 2.30 shows the variation of the azimuthal velocity u_θ with r for different values of $2\Omega t r_0/z$. Observe the formation of a velocity discontinuity across the cylinder circumscribing the disk, with the generators parallel to the axis of rotation. This implies simply the existence of a thin viscous shear layer there. In this layer, the Taylor–Proudman Theorem does not apply, and there is, in fact, some interchange of fluid between the interior and the exterior of the Taylor column.

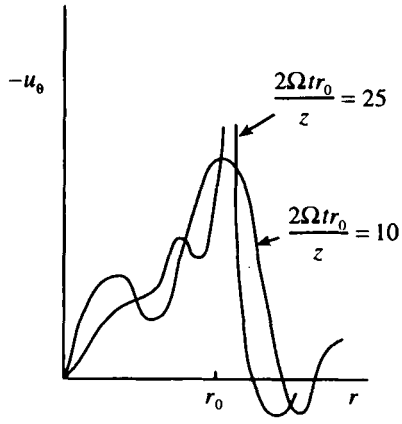

Figure 2.30. Variation of the azimuthal velocity with radius for different values of $2\Omega t r_0/z$ (from Greenspan, 1968).

Rossby Waves

Rossby waves occur in oceans and atmospheres and are transverse waves propagating in a plane perpendicular to the earth's angular velocity $\mathbf{\Omega}$. Rossby waves arises due to the variation of the vertical component of $\mathbf{\Omega}$ with latitude, i.e., $\partial\Omega_z/\partial y \neq 0$. If one assumes that $\partial\Omega_z/\partial y =$ constant $\neq 0$, this approximation simulates, in the tangent plane, the first–order effect of the planet's curvature and supplies a steady gradient of planetary vorticity Ω_z along a meridian. The law of vorticity conservation, then, implies that a displaced fluid element is subjected to a restoring torque.

In order to study large–scale motions in a layer of fluid on a rotating globe, one makes further the following assumptions:

* The upper boundary of the layer of fluid remains spherical.
* The bulk motion of the fluid is nearly horizontal, and is uniform across the layer.[9]

Thus the equations of motion in spherical polar coordinates are

$$\frac{Dv_\theta}{Dt} - \frac{v_\varphi^2 \cot\theta}{R} - fv_\varphi = -\frac{1}{\rho R}\frac{\partial P}{\partial \theta}, \tag{77}$$

$$\frac{Dv_\varphi}{Dt} - \frac{v_\theta v_\varphi \cot\theta}{R} + fv_\theta = -\frac{1}{\rho R \sin\theta}\frac{\partial P}{\partial \varphi}, \tag{78}$$

where f is the vertical component of the angular velocity $\mathbf{\Omega}$,

$$f = 2\Omega\cos\theta, \tag{79}$$

the complementary latitude angle θ is measured from the north pole,

$$\frac{D}{Dt} = \frac{\partial}{\partial t} + \frac{v_\theta}{R}\frac{\partial}{\partial\theta} + \frac{v_\varphi}{R\sin\theta}\frac{\partial}{\partial\varphi},$$

and P is the effective pressure that includes the centrifugal force arising from rotation of the coordinate system [see (2)]. Equation (79) expresses the fact that the angular velocity $\mathbf{\Omega}$ of the rotating sphere makes different angles with the vertical at different latitudes.

The radial component of the vorticity of the motion of the fluid relative to the globe is

$$\omega = \frac{1}{R\sin\theta}\left\{\frac{\partial\left(v_\varphi \sin\theta\right)}{\partial\theta} - \frac{\partial v_\theta}{\partial\varphi}\right\} \tag{80}$$

and one obtains, from equations (77) and (78),

---

[9] It turns out, essentially because of the density stratification, no matter how small, and because the layer is thin, that the geophysical flows normally have a horizontal scale that is large compared with the vertical scale and have velocity vectors that are nearly horizontal, and in such cases the vertical component alone of the angular velocity $\mathbf{\Omega}$ influences the motion.

$$\frac{D\omega}{Dt} = -\frac{v_\theta}{R}\frac{df}{d\theta} - \frac{1}{R\sin\theta}\left\{\frac{\partial(v_\theta \sin\theta)}{\partial\theta} + \frac{\partial v_\varphi}{\partial\varphi}\right\}(f+\omega). \tag{81}$$

Now, from the conservation of mass, one has

$$\frac{1}{R\sin\theta}\left[\frac{\partial(v_\theta \sin\theta)}{\partial\theta} + \frac{\partial v_\varphi}{\partial\varphi}\right] = -\frac{1}{H}\frac{DH}{Dt}, \tag{82}$$

where H is the thickness of the layer. We consider here flows with a horizontal characteristic length L large compared with the layer thickness H.

Using equation (81), equation (82) gives

$$\frac{D}{Dt}\left(\frac{f+\omega}{H}\right) = 0 \tag{83}$$

According to equation (83), the absolute vorticity of each individual column of fluid changes whenever the latter moves to a place where the height of the fluid column is different. Equation (83) also implies that a fluid column of constant height will experience a decreasing (increasing) cyclonic rotation when displaced towards higher (lower) latitudes, where the cyclonic vertical component of the earth's angular velocity is stronger (weaker).

Localized motions, near the latitude $\theta = \theta_0$, say, whose scale is relatively small compared with the earth's radius, may be modeled by a plane layer flow. Thus, we have a plane horizontal layer of fluid rotating about a vertical axis with angular velocity equal to the vertical component $f = 2\Omega \sin\theta_0$ of the earth's angular velocity. Introducing

$$\left.\begin{aligned} x &= R\sin\theta\cdot\varphi, \quad \text{the eastward coordinate} \\ y &= R(\theta-\theta_0), \quad \text{the northward coordinate,} \end{aligned}\right\} \tag{84}$$

one has, for the material derivative,

$$\frac{D}{Dt} = \frac{\partial}{\partial t} + u\frac{\partial}{\partial x} + v\frac{\partial}{\partial y}.$$

One may improve upon this approximation by including the variation of the vertical component f of the earth's angular velocity $\boldsymbol{\Omega}$ with latitude. Thus, one may write

$$f = f_0 + \beta y, \tag{85}$$

where

$$\beta = \frac{2\Omega\sin\theta_0}{R}.$$

Thus, the flow field may now be regarded as occurring in a plane layer with a normal rotation vector f whose magnitude varies linearly in the y–direction. This is called the *β–plane approximation.*

Let us demonstrate the existence of Rossby waves in a plane layer of fluid of uniform thickness, and with f varying linearly. For such a wave in a fluid otherwise at rest, we have for the stream function

$$\psi \sim e^{i(kx+\ell y-\sigma t)}. \tag{86}$$

The concomitant relative vorticity is

$$\omega = -\nabla^2 \psi = \left(k^2 + \ell^2\right)\psi. \tag{87}$$

Then, the invariance of the absolute vorticity of a material element set forth by equation (83) leads to

$$-\frac{\partial \psi}{\partial x}\frac{df}{dy} + \left(k^2 + \ell^2\right)\frac{\partial \psi}{\partial t} = i\psi\left[-\beta k - \sigma\left(k^2 + \ell^2\right)\right] = 0, \tag{88}$$

from which

$$\sigma = -\frac{\beta k}{k^2 + \ell^2}. \tag{89}$$

These are transverse waves, for which the fluid velocity is everywhere at right angles to the wave vector (k, ℓ). Rossby waves propagate toward west, opposite to the direction of earth's rotation, and have far lower frequency than that of the inertial waves for which $\sigma > 2\Omega$ [see (38)].

Let us now consider the Rossby wave generation in a setting that includes in the basic state a horizontal flow perpendicular to the planetary vorticity gradient. Such a situation arises in the atmosphere when zonal winds move past a topographical obstale. Thus, consider next the steady flow over a ridge in the form of a step along a north–south line at $x = 0$ (Figure 2.31). Let the oncoming stream have a uniform velocity U_0 along the x–direction and zero relative vorticity. Thus, from the conservation of mass and absolute vorticity, one has over the ridge,

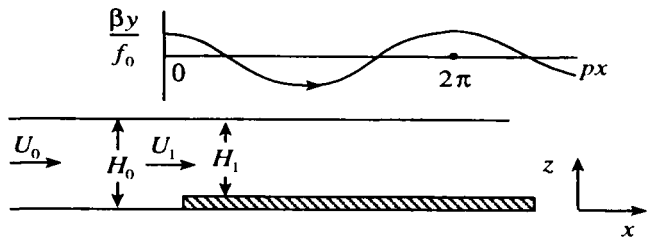

Figure 2.31. Streamline pattern for steady flow over a ridge in the form a step along the north–south line at $x = 0$ (from Batchelor, 1967).

$$U_1 = \frac{U_0 H_0}{H_1}, \qquad \omega = \left(f_0 + \beta y\right) \frac{H_1 - H_0}{H_0}. \tag{90}$$

Now, at $x = 0$, one has for the stream function $\Psi = U_1 y$, so from (90) one has

$$f + \omega = \frac{H_1}{H_0}\left(f_0 + \frac{\beta}{U_1}\,\Psi\right). \tag{91}$$

Thus, in the region $x > 0$, one has

$$\nabla^2 \Psi = -\omega = f - \frac{H_1}{H_0}\left(f_0 + \frac{\beta}{U_1}\,\Psi\right) \tag{92}$$

or

$$\nabla^2 \Psi = f_0\left(\frac{H_0 - H_1}{H_0}\right) + \beta y - p^2 \Psi, \tag{93}$$

where

$$p^2 \equiv \frac{\beta H_1}{U_1 H_0}.$$

When we put

$$\Psi = \left(y + \frac{f_0}{\beta}\right) F(x) + \left\{f_0\left(\frac{H_0 - H_1}{H_0}\right) + \beta y\right\} \frac{1}{p^2}, \tag{94}$$

equation (93) leads to

$$\frac{d^2 F}{dx^2} + p^2 F = 0. \tag{95}$$

The boundary conditions are

$$x = 0: \quad F + \frac{\beta}{p^2} = U_1, \qquad \frac{dF}{dx} = 0. \tag{96}$$

When we use (95) and (96), (94) becomes

$$\Psi = U_1 y + U_1\left(\frac{H_0 - H_1}{H_1}\right)\left(f_0 + \beta y\right) \frac{1 - \cos px}{\beta}, \tag{97}$$

which is sketched in Figure 2.32.

Note that the existence of the waves is associated with nonuniformity of the Coriolis parameter. Further, the effect of the bottom topography is to generate a relative vorticity at $x = 0$ and then turn the flow toward the south.

EXERCISE

1. For the steady case, find an integral of motion for a rotating flow of a fluid.

2.6. Water Waves

The phenomenon of water waves has provided a great deal of impetus and background for the development of theory of dispersive waves. The purpose of this chapter is to give a brief account of the mathematical theory of wavemotion in liquids with a free surface and subjected to gravitational and other forces.

There are two types of surface–wave motions. Shallow–water waves arise when the wavelength of the oscillations is much greater than the depth of the liquid. The vertical acceleration of the liquid is small in comparison with the horizontal acceleration in the case of shallow–water waves. Surface waves correspond to disturbances that do not extend far below the surface. The wavelength is much less than the depth of the liquid, and the vertical acceleration is then no longer negligible.

The features that make an analysis of surface waves difficult are

* the presence of nonlinearities;
* the free surface being unknown *a priori*, besides being variant with time.

In order to make progress with the theory of surface waves, it is usually necessary to simplify the model by making special hypothesis of one kind or another which suggest themselves on the basis of general physical circumstances contemplated in a given class of problems. Thus, two approximate theories result when

* the amplitude of the surface waves is considered small or
* the depth of the water is considered small with respect to wavelength.

The first hypothesis leads to a linear theory and to boundary–value problems of nearly classical type; while the second leads to a nonlinear theory for initial–value problems, which, in the lowest order, is of the type corresponding to wave propagation in compressible fluids (see Chapter 3).

Governing Equations

The equilibrium configuration of a liquid in a container of finite size is one of rest with a plane surface. One may produce a wavemotion on the surface which is due to the action of gravity that acts in the direction of restoring the undisturbed state of rest. If the wavemotion is assumed to have started from rest relative to the undisturbed state of flow, which is itself assumed irrotational, then the wavemotions will be irrotational. The wave propagation is taken to occur along

the x–direction, and the gravity acts opposite to the z–direction. For the velocity potential Φ we have

$$\frac{\partial^2 \Phi}{\partial x^2} + \frac{\partial^2 \Phi}{\partial z^2} = 0 \tag{1}$$

and at a rigid stationary boundary we have

$$\frac{\partial \Phi}{\partial n} = 0. \tag{2}$$

If $z = \xi(x,t)$ denotes the displacement of the free surface from its mean position (or equilibrium position), since a fluid particle on that surface will remain there, we have the following kinematic condition expressing the fact that the free surface remains a material surface:

$$\frac{D}{Dt}(z - \xi) = 0 \tag{3}$$

and upon linearizing, (3) gives

$$\frac{\partial \Phi}{\partial z} = \frac{\partial \xi}{\partial t}. \tag{4}$$

The dynamic condition at the free surface is

$$p = -T\left(\frac{1}{R_1} + \frac{1}{R_2}\right), \tag{5}$$

where R_1 and R_2 are the two principal radii at the free surface, counted positive when the center of curvature is above the surface (see Section 1.2), and T is the surface tension. Upon linearizing, (5) gives

$$p = -T\frac{\partial^2 \xi}{\partial x^2}. \tag{6}$$

The Bernoulli equation

$$\frac{p}{\rho} = -\frac{\partial \Phi}{\partial t} - gz - \frac{u^2 + w^2}{2} + f(t), \tag{7}$$

upon linearization and combining with (4) and (6), gives

$$z = 0 : \frac{\partial^2 \Phi}{\partial t^2} = \left(\frac{T}{\rho}\frac{\partial^2}{\partial x^2} - g\right)\frac{\partial \Phi}{\partial z}. \tag{8}$$

Here, the fluid velocity is $\mathbf{v} = (u, v, w)$.

The neglect of the no–slip condition at the bottom wall and the shear stress of the free surface imply that there must be boundary layers (see Chapter 4) at the bottom wall and the free surface which are contaminated by vorticity. However, if the viscosity of the fluid is small, these boundary layers are thin and thus may be neglected in the following.

Surface Waves in a Semi-infinite Liquid

If the liquid fills the semi-infinite space, $-\infty < z \leq 0$, $-\infty < x < \infty$, with a free surface at $z = 0$, then one requires

$$z \Rightarrow -\infty: \quad \frac{\partial \Phi}{\partial z} \Rightarrow 0. \tag{9}$$

From (1) and (9), one finds

$$\Phi = Ce^{kz} \cos k(x - ct). \tag{10}$$

When one uses (10) in (8), there follows the dispersion relation

$$c^2 = \frac{g}{k} + \frac{kT}{\rho}. \tag{11}$$

For long waves, gravity effects dominate and (11) yields

$$c^2 \approx \frac{g}{k}. \tag{12}$$

For short waves, capillary effects dominate and (11) yields

$$c^2 \approx \frac{kT}{\rho}. \tag{13}$$

Both (12) and (13) show that the waves are dispersive.

Surface Waves in a Liquid Layer of Finite Depth

One requires now on the bottom surface (which is taken to be rigid and stationary)

$$z = -h_0: \quad \frac{\partial \Phi}{\partial z} = 0. \tag{2}'$$

Any irrotational-flow solution so obtained involves a nonzero tangential velocity at the boundary, which in a viscous fluid has to be reconciled with the exact boundary condition of zero fluid velocity at a stationary solid surface through the intervention of a boundary layer (see Chapter 4) between the irrotational flow and the surface.

From (1) and (2)′, one obtains

$$\Phi = C \cos hk(z + h_0) \cos k(x - ct). \tag{14}$$

When one uses (14) in (8), there follows

$$c^2 = \left(g + \frac{kT}{\rho}\right) \frac{\tan hkh_0}{k}, \tag{15}$$

which is sketched in Figure 2.32.

For long waves, (15) gives

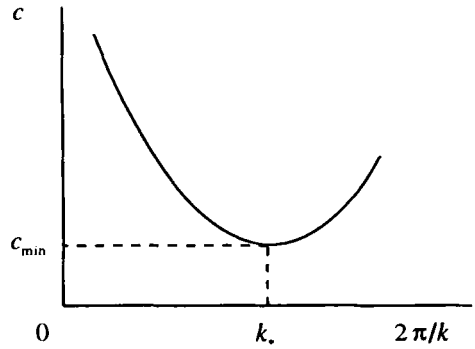

Figure 2.32. Dispersion curve for surface waves.

$$c^2 \approx gh_0. \tag{16}$$

For short waves, (15) gives, on the other hand,

$$c^2 \approx \frac{kT}{\rho}. \tag{17}$$

The fluid velocity components are given, from (14), by

$$u = \frac{\partial \Phi}{\partial x} = -kC \cosh k(z + h_0) \sin k(x - ct), \tag{18}$$

$$w = \frac{\partial \Phi}{\partial z} = kC \sinh k(z + h_0) \cos k(x - ct). \tag{19}$$

For long waves $w \approx 0$, so that the vertical acceleration is negligible and the pressure distribution in the liquid is then nearly hydrostatic.

The locus of a material particle is given by

$$u = \frac{dX}{dt}, \qquad w = \frac{dZ}{dt}, \tag{20}$$

so, on using (18) and (19), this leads to

$$\left.\begin{aligned} X &= -\frac{C}{c} \cosh k(z + h_0) \cos k(x - ct), \\ Z &= -\frac{C}{c} \sinh k(z + h_0) \sin k(x - ct). \end{aligned}\right\} \tag{21}$$

It is obvious that the locus is an ellipse in a vertical plane,

$$\frac{X^2}{A^2} + \frac{Z^2}{B^2} = 1, \tag{22}$$

where

$$A = \frac{C}{c}\cosh k\left(z + h_0\right), \qquad B = \frac{C}{c}\sinh k\left(z + h_0\right).$$

Note that, at $z = -h_0$, the ellipse degenerates into a horizontal line segment. Consequently, the particles on the bottom surface move only to and fro and do not rise and fall. For infinite depth, the locus is a circle, since

$$\lim_{h_0 \to \infty} \frac{A}{B} = 1. \tag{23}$$

Shallow–Water Waves

It was seen in the foregoing that if the wavelength is large compared with the depth, the horizontal velocity at any section normal to the direction of propagation is very nearly constant, and that the pressure distribution is nearly hydrostatic due to very small vertical accelerations. Then, the fluid particles originally in a vertical plane remain so.

One has, for the two–dimensional flow in a layer of liquid over a rigid surface at bottom,

$$u_x + w_z = 0, \tag{24}$$

$$z = \xi: \quad \xi_t + u\xi_x - w = 0, \tag{25}$$

$$z = \xi: \quad p = 0, \tag{26}$$

$$z = -h_0: \quad uh_{0_x} + w = 0, \tag{27}$$

where we have allowed for a spatial variation in the bottom topography.

From (24), (25), and (27), one obtains

$$\int_{-h_0}^{\xi} u_x dz + \xi_t + u\Big|_{\xi} \cdot \xi_x + u\Big|_{-h_0} \cdot h_{0_x} = 0$$

or

$$\frac{\partial}{\partial x}\int_{-h_0}^{\xi} u\, dz = -\xi_t. \tag{28}$$

The shallow–water wave theory results from an assumption that the vertical acceleration of the fluid is negligible so that the pressure behaves hydrostatically as

$$p = \rho g\left(\xi - z\right). \tag{29}$$

When we use (29), the equation of motion becomes

$$u_t + uu_x = -g\xi_x. \tag{30}$$

Equation (28) gives, upon integration,

$$\left[u\left(\xi + h_0\right)\right]_x \approx -\xi_t. \tag{31}$$

If $h_0 = \text{const.}$, (30) and (31) give, upon linearization,

$$u_{xx} - \frac{1}{gh_0} u_{tt} = 0. \tag{32}$$

Thus, the solution of a problem of elliptic type is approximated in the lowest order by the solution of a problem of hyperbolic type.

Analogy with Gas Dynamics: It turns out that the equations of shallow–water wave theory become analogous to those of one–dimensional gas flows (see Chapter 3). Introducing

$$\bar{\rho} = \rho\left(\xi + h_0\right), \tag{33}$$

$$\bar{p} = \int_{-h_0}^{\xi} p\, dz \tag{34}$$

and using (29), one obtains

$$\bar{p} = \frac{\rho g}{2}\left(\xi + h_0\right)^2 = \frac{g}{2\rho}\,\bar{\rho}^2. \tag{35}$$

Using (35), the equation of motion, then leads to

$$\bar{\rho}\left(u_t + uu_x\right) = -\bar{p}_x = g\bar{\rho}\bar{\rho}_x \tag{36}$$

and (31) leads to

$$\left(\bar{\rho}u\right)_x = -\bar{\rho}_t. \tag{37}$$

If $h_0 = \text{const.}$, the speed of the waves, in analogy with gas dynamics (see Chapter 3), is given by

$$c = \sqrt{\frac{d\bar{p}}{d\bar{\rho}}} = \sqrt{g\left(\xi + h_0\right)}. \tag{38}$$

Breaking of Waves: The nonlinear shallow–water equations which neglect dispersion altogether lead to breaking of the typical hyperbolic kind (see Chapter 3), with the development of a vertical slope and a multivalued profile. In particular, noting that

$$\omega^2 = k^2 g\left(\xi + h_0\right),$$

one observes that a wave crest will travel faster than a trough, and any wave profile will gradually steepen until it ultimately falls over forward, as is seen in the breaking of waves on the sea shore when they reach shallow water.

Water Waves Generated by an Initial Displacement Over a Localized Region

Consider water waves generated by an initial displacement over a localized region near the origin, according to

$$t=0: \quad \xi = f(x), \quad \frac{\partial \xi}{\partial t} = 0. \tag{39}$$

If

$$f(x) = f(-x), \tag{40}$$

then one has the Fourier transform

$$f(x) = \sqrt{\frac{2}{\pi}} \int_0^\infty \phi(k) \cos kx \, dk, \tag{41}$$

where

$$\phi(k) = \sqrt{\frac{2}{\pi}} \int_{-\infty}^{\infty} f(x) \cos kx \, dx. \tag{42}$$

The solution for ξ, for $x > 0$, at any subsequent position and time, with the initial conditions (39), is

$$\xi = \frac{1}{\sqrt{2\pi}} \int_{-\infty}^{\infty} \phi(k) \cos(kx - \omega t) \, dk. \tag{43}$$

Since $\omega/k = h(k)$, waves of different wavenumber propagate at different velocities. Consequently, the overall wave profile, represented by (43), changes its shape as it moves.

As an example, let us take

$$f(x) = \begin{cases} \dfrac{A}{2a}, & -a < x < a, \\ 0, & \text{otherwise.} \end{cases} \tag{44}$$

Then, one has, from (42),

$$\phi(k) = \sqrt{\frac{2}{\pi}} \int_{-a}^{a} \frac{A}{2a} \cos kx \, dx = \sqrt{\frac{2}{\pi}} \frac{A \sin ka}{ka}. \tag{45}$$

Consider the asymptotic behavior of (43) as $t \Rightarrow \infty$, with x/t held fixed. Write (43) as

$$\xi = \frac{1}{\sqrt{2\pi}} \operatorname{Re}\left[\int \phi(k) e^{-i\chi(k)t} dk\right], \tag{46}$$

where

$$\chi(k) = \omega(k) - k\frac{x}{t},$$

and x/t is presently a fixed parameter. This integral is evaluated by using the method of stationary phase. This is based on the fact that wave components with nearly same phase will reinforce, and those differing in phase will annul each other due to mutual interference. Therefore, one looks for positions and times at which a large number of harmonic components have the same phase.

If $\chi(k)$ possesses no stationary point and if $\chi'(k) \neq 0$, one may use Cauchy's Theorem to deform the path of integration from the real–k axis, on which $\chi(k)$ is real, to a path on which $\chi(k)$ has a negative imaginary part (if $\chi'(k) > 0$, lower the path of integration from the real–k axis and vice versa); this will reduce the modulus of the integrand for $t \Rightarrow \infty$ so that the integral becomes exponentially small.

However, if $\chi(k)$ possesses a stationary point at $k = k_0$, where

$$\chi'(k_0) = \omega'(k_0) - \frac{x}{t} = 0 \tag{47}$$

on one side of k_0 where $\chi'(k_0) < 0$, the path of integration must be raised; and on the other side, where $\chi'(k_0) > 0$, it must be lowered. In order to preserve continuity, the path of integration must go through $k = k_0$ wherein the imaginary part of $\chi(k)$ is zero and, therefore, the main nonvanishing contribution to the integral comes from the neighborhood of the stationary point at $k = k_0$. (Physically, the stationary phase condition corresponds to maximum constructive interference of the various Fourier components, which occurs when the latter are nearly in phase with each other.) Thus, as $t \Rightarrow \infty$, the integral takes an asymptotic form determined entirely in terms of values of k where the phase $\chi(k)$ is stationary, i.e., by the value of k where $\chi'(k) = 0$.

For $k \approx k_0$, one writes

$$\left.\begin{aligned} \phi(k) &\approx \phi(k_0), \\ \chi(k) &\approx \chi(k_0) + \frac{1}{2}(k - k_0)^2 \chi''(k_0), \end{aligned}\right\} \tag{48}$$

provided that $\chi''(k_0) \neq 0$.

From (46), one then has

$$\xi(x,t) \approx \frac{1}{\sqrt{2\pi}} \operatorname{Re}\left[\phi(k_0) e^{-i\chi(k_0)t} \int_{-\infty}^{\infty} e^{-i/2(k-k_0)^2 \chi''(k_0)t} dk\right]. \tag{49}$$

This approximation becomes valid and accurate as $t \Rightarrow \infty$. The remaining integral is reduced to the real error integral

$$\int_{-\infty}^{\infty} e^{-\alpha z^2} dx = \sqrt{\frac{\pi}{\alpha}} \tag{50}$$

by rotating the path of integration through $\pm\pi/4$ [the sign being that of $\chi''(k_0)$]; this corresponds to changing to the path of steepest descents.

Thus, the asymptotic form of ξ, for $t \Rightarrow \infty$, is

$$\xi(x,t) \approx \mathrm{Re}\left[\phi(k_0)\sqrt{\frac{1}{t|\chi''(k_0)|}}\, e^{-i[\chi(k_0)t+\pi/4\,\mathrm{sgn}\,\chi''(k_0)]}\right]$$

$$\approx \phi(k_0)\sqrt{\frac{1}{t|\omega''(k_0)|}}\cos\left[k_0 x - \omega(k_0)t - \frac{\pi}{4}\mathrm{sgn}\,\omega''(k_0)\right]. \tag{51}$$

From (51), one has, for the wave amplitude,

$$a = F(k_0)\sqrt{\frac{1}{t|\omega''(k_0)|}}\, e^{-i(\pi/4)\,\mathrm{sgn}\,\omega''(k_0)}. \tag{52}$$

Consider

$$Q(t) = \int_{x_1}^{x_2} |a|^2\, dx. \tag{53}$$

When one uses (52), (53) may be rewritten as

$$Q(t) = \int_{x_1}^{x_2} \frac{F(k_0)F^*(k_0)}{t|\omega''(k_0)|}\, dx = \int_{k_{01}}^{k_{02}} F(k_0)F^*(k_o)\, dk_0. \tag{54}$$

If we let

$$x_1 = \omega'(k_{01})t, \qquad x_2 = \omega'(k_{02})t \tag{55}$$

and hold k_{01} and k_{02} fixed, as t varies, then $Q(t)$ remains constant. Thus, the total amount of $|a|^2$ between points x_1 and x_2 moving with the group velocity remains unchanged. Thus,

$$\frac{dQ}{dt} = \int_{x_1}^{x_2} \frac{\partial q}{\partial t}\, dx + C_2 q_2 - C_1 q_1 = \int_{x_1}^{x_2}\left[\frac{\partial q}{\partial t} + \frac{\partial}{\partial x}\{C(k)q\}\right] dx = 0, \tag{56}$$

where

$$q = |a|^2, \qquad C = \omega'(k_0).$$

Equation (56) implies that

$$\frac{\partial q}{\partial t} + \frac{\partial}{\partial x}[C(k)q] = 0 \tag{57a}$$

or

$$\frac{\partial}{\partial t}\left(|a|^2\right)+\frac{\partial}{\partial x}\left[C(k)|a|^2\right]=0. \tag{57b}$$

In this sense, $|a|^2$ (which may be proportional to energy in some simple cases) propagates with the group velocity.

Thus, in the special case of a wavepacket where the initial disturbance is localized around $x=0$ and contains appreciable amplitude only in wavenumbers close to some value $k_0=K_0$, say, the resulting disturbance will evolve as a group around $k_0=K_0$ and the above wavepacket as a whole moves with the particular group velocity $\omega'(K_0)$.

For gravity waves, one has [see (11)],

$$\omega=\sqrt{gk}. \tag{58}$$

When one uses (45) and (58), (51) becomes

$$\xi\approx\frac{A}{a}\sqrt{\frac{2x}{\pi gt^2}}\sin\frac{gt^2a}{4x^2}\cos\left(\frac{gt^2}{4x}-\frac{\pi}{4}\right). \tag{59}$$

Now, consider the initial disturbance to be an infinite displacement concentrated at the origin, i.e., let $a\Rightarrow 0$. Equation (58) then becomes

$$\xi\approx\frac{At}{4}\sqrt{\frac{2g}{\pi x^3}}\cos\left(\frac{gt^2}{4x}-\frac{\pi}{4}\right). \tag{69a}$$

On the other hand, for very large x, (54) becomes

$$\xi\approx\frac{At}{4}\sqrt{\frac{2g}{\pi x^3}}\cos\left(\frac{gt^2}{4x}-\frac{\pi}{4}\right). \tag{60b}$$

From the identity between (60a) and (60b), one finds that the asymptotic behavior of water waves very far away from a finite localized region of their generation around the origin corresponds to that of water waves generated by an infinite line displacement concentrated at the origin.

Water Waves Generated by a Finite Train of Harmonic Waves

Consider water waves generated by an initial displacement consisting of a limited train of harmonic waves. Let

$$t=0:\quad \xi=f(x),\qquad \frac{\partial\xi}{\partial t}=0. \tag{61}$$

If $f(x)$ is symmetrical with respect to the origin, then, as before,

$$\left.\begin{aligned} f(x) &= \sqrt{\frac{2}{\pi}} \int_0^\infty \phi(k) \cos kx \, dk, \\ \phi(k) &= \sqrt{\frac{2}{\pi}} \int_{-\infty}^{\infty} f(x) \cos kx \, dx. \end{aligned}\right\} \tag{62}$$

Further, if $f(x)$ is zero except for a range of $(2n+1/2)\,2\pi/k' > x > 0$, within which it is $\cos k'x$, then one has

$$\phi(k) = \sqrt{\frac{2}{\pi}} \int_0^{(2n+1/2)2\pi/k'} \cos k'x \cos kx \, dx = \sqrt{\frac{2k'}{\pi}} \frac{\cos\left[\left(2n+\frac{1}{2}\right)\frac{\pi k}{k'}\right]}{k'^2 - k^2}. \tag{63}$$

The solution for ξ, for $x > 0$, at $t > 0$, with the initial conditions (61), is then given, on using (63) in (43), by

$$\xi(x,t) = \frac{k'}{\pi} \int_0^\infty \frac{\cos\left(2n+\frac{1}{2}\right)\frac{\pi k}{k'}}{k'^2 - k^2} \cos(kx - \omega t)\, dk. \tag{64}$$

As $t \Rightarrow \infty$, x/t remaining constant, one finds, from (64), by using the method of steepest descent,

$$\xi(x,t) \approx \frac{16\sqrt{\frac{g}{\pi}}\, k'x^{5/2} t}{16k'^2x^4 - g^2t^4} \cos\left[\left(2n+\frac{1}{2}\right)\frac{\pi g t^2}{4k'x^2}\right] \cos\left(\frac{gt^2}{4x} - \frac{\pi}{4}\right). \tag{65}$$

The variation of the amplitude A [the coefficient of $\cos\left(gt^2/4x - \pi/4\right)$] with k is shown in Figure 2.33.

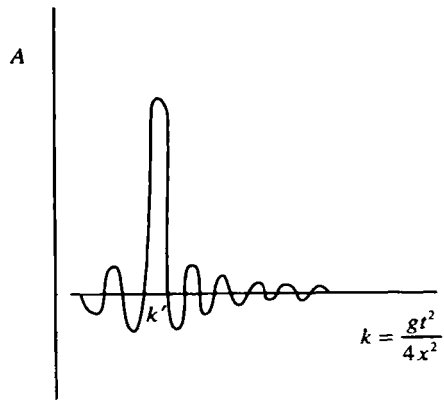

Figure 2.33. Variation of the amplitude with wavenumber for waves generated by an initial displacement.

The main undulatory disturbance appears as a simple group around $k = k'$, moving forward with $d\omega/dk = 1/2\ \omega/k$. But in advance of this main group of undulations there are two or three subsidiary groups of appreciable amplitude and larger wavelengths. In the rear of the main group, a series of alternating groups show up, following each other much more quickly, and their wavelengths and velocities are less separated out than those in advance of the main group. Hence the disturbance in the rear, close to the origin, may be expected to consist of small, irregular motions resulting from the superposition of this latter system of groups.

Waves on a Steady Stream

We now study the waves which stand steady in a uniform stream of velocity U. We take the source to be an external steady pressure applied to the surface of the stream, rather than a prescribed displacement, since this represents the effect of a floating body more correctly.

In solving steady–wave problems by Fourier transforms, one has to impose an appropriate radiation condition to ensure uniqueness. One may avoid this by posing a more realistic unsteady problem with suitable initial conditions applied at some finite time in the past – $t = -t_0$, say – and then let $t_0 \Rightarrow \infty$ in the solution.

We take the applied pressure on $z = 0$ to be

$$\frac{p - p_0}{\rho} = f(x,y)e^{\varepsilon t}, \qquad \varepsilon > 0. \tag{66}$$

One, then, has the following boundary–value problem for the velocity potential Φ:

$$z < 0: \quad \nabla^2 \Phi = 0 \tag{67}$$

$$z = 0: \quad \xi_t + U\xi_x = \Phi_z \tag{68}$$

$$z = 0: \quad \Phi_t + U\Phi_x + g\xi - \frac{T}{\rho}\left(\xi_{xx} + \xi_{yy}\right) = -f(x,y)e^{\varepsilon t} \tag{69}$$

$$z \Rightarrow -\infty: \quad \Phi \Rightarrow 0. \tag{70}$$

Upon Fourier transforming according to

$$\Phi = \frac{e^{\varepsilon t}}{2\pi} \int_{-\infty}^{\infty} B(k)e^{i(k_x x + k_y y) + kz}\, dk,$$

$$\xi = \frac{e^{\varepsilon t}}{2\pi} \int_{-\infty}^{\infty} A(k)e^{i(k_x x + k_y y)}\, dk, \tag{71}$$

$$f = \frac{e^{\varepsilon t}}{2\pi} \int_{-\infty}^{\infty} F(k)e^{i(k_x x + k_y y)}\, dk,$$

one finds, from (67)–(70),

$$\xi(x,t)=\frac{e^{\varepsilon t}}{2\pi}\int_{-\infty}^{\infty}\frac{kF(k)e^{i(k_x x+k_y y)}dk}{(k_x U-i\varepsilon)^2-\omega_0^2(k)}, \tag{72}$$

where

$$\omega_0^2=gk+\frac{T}{\rho}k^3, \qquad k=\sqrt{k_x^2+k_y^2}.$$

The poles of the integrand in (72) lie at

$$k_x^2U^2-\omega_0^2(k)\approx 0, \tag{73}$$

which is also the condition for the waves to stand steady in the stream.

One-Dimensional Gravity Waves

One has, for the one-dimensional gravity waves, from (72),

$$\xi(x,t)=\frac{e^{\varepsilon t}}{2\pi}\int_{-\infty}^{\infty}\frac{k_xF(k_x)dk_x}{(k_xU-i\varepsilon)^2-gk_x}. \tag{74}$$

If the applied pressure is localized around $x=0$, i.e.,

$$f(x)=P\delta(x), \tag{75}$$

then from (71) we have

$$F(k_x)=P. \tag{76}$$

When one uses (76), (74) becomes

$$\xi(x,t)=\frac{Pe^{\varepsilon t}}{2\pi}\int_{-\infty}^{\infty}\frac{k_xe^{ik_xx}}{(k_xU-i\varepsilon)^2-gk_x}dk_x \tag{77}$$

or

$$\frac{2\pi\xi(x,t)}{P}=\lim_{\varepsilon\Rightarrow 0}\int_{-\infty}^{\infty}\frac{e^{ik_xx}}{k_xU^2-2i\varepsilon U-g}dk_x. \tag{78}$$

For $x>0$, the path of k_x-integration along the $\mathrm{Re}(k_x)$-axis is closed by a large semicircle in the upper half of the k_x-plane. Thus (78) becomes

$$\frac{U^2\xi(x,t)}{P}=-e^{iKx}, \qquad x>0, \tag{79}$$

where

$$K\equiv\frac{g}{U^2}.$$

For $x<0$, the path of integration is fixed the other way, and one then obtains

$$\frac{U^2\xi(x,t)}{P} = 0. \tag{80}$$

Therefore, standing gravity waves appear downstream $(x > 0)$ of the applied pressure disturbance.

One–Dimensional Capillary–Gravity Waves

Upon including the surface tension, (78) becomes

$$\frac{2\pi\xi(x,t)}{P} = \lim_{\varepsilon \Rightarrow 0^+} \int_{-\infty}^{\infty} \frac{e^{ik_x x}\,dk_x}{k_x U^2 - 2i\varepsilon U - g - \dfrac{T}{\rho}k_x^2}. \tag{81}$$

The poles of the integrand in (81) lie at

$$k_x U^2 \approx g + \frac{T}{\rho}k_x^2 \quad \text{or} \quad U \approx c(k_x), \tag{82}$$

which is again the condition for the waves to stand steady in the stream. If $U < c_{\min}$, then there are no real roots for k_x, so there is no standing wave pattern. If $U > c_{\min}$ (see Figure 2.32), there are two real roots:

$$k_x = k_{x_s},\ k_{x_T}, \tag{83}$$

where

$$k_{x_T} > k_{x_s},$$

and the poles will lie at

$$k_x \approx k_{x_s} + \frac{2\rho U}{\left(k_{x_T} - k_{x_s}\right)T}\,i\varepsilon, \qquad k_x = k_{x_T} - \frac{2\rho U}{\left(k_{x_T} - k_{x_s}\right)T}\,i\varepsilon. \tag{84}$$

For $x > 0$, the path of integration for the first integral may be fixed as before. Contributions then come from the poles at $k_x \approx k_{x_s}$. Consequently, gravity waves appear downstream of the source. For $x < 0$, the paths of integration may be fixed the other way, and one then obtains capillary waves upstream of the source. Thus, one obtains

$$\xi(x,t) \sim \begin{cases} \dfrac{-2P\rho}{\left(k_{x_T} - k_{x_s}\right)T}\sin k_{x_s}x, & x > 0, \\ \dfrac{-2P\rho}{\left(k_{x_T} - k_{x_s}\right)T}\sin k_{x_T}x, & x < 0. \end{cases} \tag{85}$$

Ship Waves

Consider the wave pattern produced by a ship traveling with uniform velocity U in the negative x–direction on the surface of deep water. Consider a reference frame in which the ship is fixed, and so there is a uniform stream with velocity U in the x–direction. In this frame, the ship is equivalent to an applied pressure localized at $x = 0$, $y = 0$, i.e.,

$$f(x,y) = P\delta(x,y), \tag{86}$$

so that one has, from (71),

$$F(k) = P. \tag{87}$$

When one uses (87), (74) gives

$$\frac{4\pi^2 U^2 \xi(x,t)}{P} = e^{\varepsilon t} \int_{-\infty}^{\infty}\int_{-\infty}^{\infty} \frac{k e^{i(k_x x + k_y y)}}{\left(k_x - \dfrac{i\varepsilon}{U}\right)^2 - \dfrac{gk}{U^2}}\, dk_x dk_y. \tag{88}$$

When one puts

$$\left.\begin{aligned} x &= r\cos\alpha, \quad & y &= r\sin\alpha \\ k_x &= -k\cos\chi, \quad & k_y &= k\sin\chi \end{aligned}\right\} \tag{89}$$

and note that the contribution from the range $\pi/2 < \chi < 3\pi/2$ is the conjugate of the range $-\pi/2 < \chi < \pi/2$, (88) becomes

$$\frac{2\pi^2 U^2 \xi(x,t)}{P} = \mathrm{Re}\left[\lim_{\varepsilon \Rightarrow 0^+} \int_{-\pi/2}^{\pi/2} \frac{d\chi}{\cos^2\chi} \int_0^{\infty} \frac{k e^{-ikr\cos(\alpha+\chi)}}{k - k_0}\, dk\right], \tag{90}$$

where

$$k_0 = \frac{g}{U^2\cos^2\chi} - \frac{2i\varepsilon}{U\cos\chi}.$$

The pattern is symmetrical about the x–axis, so it is sufficient to consider the range $0 < \alpha < \pi$. When $\cos(\alpha+\chi) > 0$, i.e., $-\pi/2 < \chi < \pi/2 - \alpha$, the path of integration in the k–plane may be closed by a large semicircle in the upper half of the k–plane, and the pole at $k = k_0$ contributes (physically this implies that the ship can feed energy continuously to a wave only when its bow travels with the crest of the wave, which is like the "surf–riding" condition!); when $\cos(\alpha+\chi) < 0$, i.e., $-\pi/2 > \chi > \pi/2 - \alpha$, the path of integration is fixed the other way, and the pole at $k = k_0$ does not contribute. Thus,

$$\xi(x,t) \sim \frac{gP}{\pi U^4}\,\mathrm{Im}\left[\int_{-\pi/2}^{\pi/2-\alpha} \frac{e^{-ik_0 r\cos(\alpha+\chi)}}{\cos^4\chi}\, d\chi\right]. \tag{91}$$

The exponent in (91), namely,

$$s(\chi) = k_0\cos(\alpha+\chi) = \frac{g\cos(\alpha+\chi)}{U^2\cos^2\chi},$$

has a stationary point at $\chi = \psi$, where

$$\tan(\alpha+\psi) = 2\tan\psi,$$

so by using the method of stationary phase we obtain

$$\xi(x,t) \sim \frac{gP}{\pi U^4} \operatorname{Im}\left[\sqrt{\frac{2\pi}{r|s''(\psi)|}}\, e^{-irs(\psi)-\pi i/4 \operatorname{sgn} s''(\psi)}\right] \tag{92}$$

or

$$\xi(x,t) \sim -\sqrt{\frac{2g}{\pi r}}\, \frac{P}{U^3 \cos^3 \psi}\, \frac{(1+4\tan^2\psi)^{1/4}}{|1-2\tan^2\psi|^{1/2}} \times \sin\left[kr\cos(\alpha+\psi)+\frac{\pi}{4}\operatorname{sgn} s''(\psi)\right], \tag{93}$$

where

$$k = k_0 = \frac{g}{U^2 \cos^2 \psi}.$$

Note that the amplitude is singular at the maximum wedge angle $\alpha = \alpha_{\max} = 19.5^\circ$ where $\tan \psi = 1/\sqrt{2}$. This is where the lateral and transverse crests meet at a cusp (see Figure 2.34) and corresponds in the analysis to the confluence of the two stationary point of the exponent $s(\chi)$. Thus, the wave pattern is confined to a wedge–shaped region spreading out behind the ship, and the semivertex angle of the wedge is 19.5°. Note that this result is independent of the ship velocity U, provided that the latter is constant. It depends only on the fact that the ratio of the group velocity and the phase velocity for deep water waves is 1/2 (see (12))!

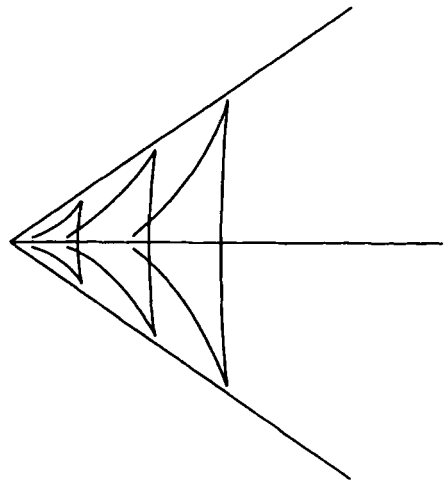

Figure 2.34. Ship–wave pattern.

Gravity Waves in a Rotating Fluid

Consider wavemotions in a liquid of depth h_0, rotating with an angular velocity Ω about a vertical axis (along the z–direction). Consider long waves for which the vertical accelerations are negligible, and one may assign, for the pressure, the hydrostatic value corresponding to the distance from the free surface given by $z = h_0 + \xi$. Thus, one has the following linearized equations in the rotating frame:

$$\frac{\partial u}{\partial t} - \Omega v = -g\frac{\partial \xi}{\partial x}, \tag{94}$$

$$\frac{\partial V}{\partial t} + \Omega u = -g\frac{\partial \xi}{\partial y}, \tag{95}$$

$$\frac{\partial \xi}{\partial t} = -h_0\frac{\partial u}{\partial x} - h_0\frac{\partial v}{\partial y}. \tag{96}$$

Considering one–dimensional waves, one obtains, from equations (94)–(96),

$$\frac{\partial^2 u}{\partial t^2} + \Omega^2 u = c^2\frac{\partial^2 u}{\partial x^2}, \tag{97}$$

where c is the phase velocity of long surface waves in water of depth L [see (16)],

$$c = \sqrt{gh_0}.$$

Let us prescribe the initial conditions:

$$t = 0: \quad u = u_0, \ \frac{\partial u}{\partial t} = s_0. \tag{98}$$

Consider traveling waves of the form $e^{i(kx \mp \omega t)}$, for which equation (97) yields the dispersion relation

$$\omega = c\sqrt{k^2 + \Omega^2/c^2}. \tag{99}$$

Upon Fourier transforming, according to

$$\left.\begin{aligned} u_0(x) &= \frac{1}{\sqrt{2\pi}}\int_{-\infty}^{\infty} a(k)e^{ikx}\,dk, \\ s_0(k) &= \frac{1}{\sqrt{2\pi}}\int_{-\infty}^{\infty} b(k)e^{ikx}\,dk, \end{aligned}\right\} \tag{100}$$

one obtains, from equation (97),

$$u(x,t) = \frac{1}{\sqrt{2\pi}}\int_{-\infty}^{\infty} A(k)e^{i(kx-\omega t)} + \frac{1}{\sqrt{2\pi}}\int_{-\infty}^{\infty} B(k)e^{i(kx+\omega t)}\,dk, \tag{101}$$

where

$$\left.\begin{aligned} A(k) &\equiv \frac{1}{2}\left[a(k)+\frac{i}{\omega(k)}\,b(k)\right], \\ B(k) &\equiv \frac{1}{2}\left[a(k)-\frac{i}{\omega(k)}\,b(k)\right]. \end{aligned}\right\}$$

Thus,

$$u(x,t)=\frac{1}{\sqrt{2\pi}}\int_{-\infty}^{\infty}a(k)\,e^{ikx}\cos\left(\sqrt{k^2+\Omega^2/c^2}\;ct\right)dk$$

$$+\frac{1}{c}\,\frac{1}{\sqrt{2\pi}}\int_{-\infty}^{\infty}b(k)\,e^{ikx}\,\frac{\sin\left(\sqrt{k^2+\Omega^2/c^2}\;ct\right)}{\sqrt{k^2+\Omega^2/c^2}}\,dk$$

or

$$u(x,t)=\frac{1}{\pi}\int_{-\infty}^{\infty}u_0(\xi)\,d\xi\int_{0}^{\infty}\cos\,k(x-\xi)\cos\left(\sqrt{k^2+\Omega^2/c^2}\;ct\right)dk$$

$$+\frac{1}{\pi c}\int_{-\infty}^{\infty}s_0(\xi)\,d\xi\int_{0}^{\infty}\cos k(x-\xi)\,\frac{\sin\left(\sqrt{k^2+\Omega^2/c^2}\;ct\right)}{\sqrt{k^2+\Omega^2/c^2}}\,dk. \tag{102}$$

Equation (102) may be written as

$$u(x,t)=\frac{1}{\pi c}\,\frac{\partial}{\partial t}\int_{-\infty}^{\infty}G(x-\xi,ct)\,u_0(\xi)\,d\xi+\frac{1}{\pi c}\int_{-\infty}^{\infty}G(x-\xi,ct)\,s_0(\xi)\,d\xi, \tag{103}$$

where

$$G(x,\tau)\equiv\int_{0}^{\infty}\cos\zeta x\,\frac{\sin\left(\sqrt{\zeta^2+\Omega^2/c^2}\;\tau\right)}{\sqrt{\zeta^2+\Omega^2/c^2}}\,d\zeta, \tag{104}$$

which can, in turn, be written as

$$G(x,\tau)=\frac{1}{2}\int_{-\infty}^{\infty}e^{i\zeta x}\,\frac{\sin\left(\sqrt{\zeta^2+\Omega^2/c^2}\;\tau\right)}{\sqrt{\zeta^2+\Omega^2/c^2}}\,d\zeta. \tag{105}$$

If we put

$$\zeta=\frac{\Omega}{c}\sin\,h\varphi, \tag{106}$$

(105) becomes

$$G(x,\tau)=\frac{1}{2}\int_{-\infty}^{\infty}e^{i(\Omega/c)x\sin h\varphi}\sin\left(\frac{\Omega\tau}{c}\cos\,h\varphi\right)d\varphi.$$

Thus,

$$G(x,\tau)=\begin{cases}\dfrac{\pi}{2}J_0\left(\dfrac{\Omega}{c}\sqrt{\tau^2-x^2}\right), & \tau>x,\\ 0, & \tau<x,\end{cases} \tag{107}$$

which implies that $G(x,\tau)$ assumes the role as the propagator of causal effects from the source region. Here, $J_n(x)$ is Bessel's function of first kind of order n. When one uses (107), (103) gives

$$u(x,t)=\frac{1}{2c}\frac{\partial}{\partial t}\int_{x-ct}^{x+ct} J_0\left[\frac{\Omega}{c}\sqrt{c^2t^2-(x-\xi)^2}\right]u_0(\xi)\,d\xi$$

$$+\frac{1}{2c}\int_{x-ct}^{x+ct} J_0\left[\frac{\Omega}{c}\sqrt{c^2t^2-(x-\xi)^2}\right]s_0(\xi)\,d\xi$$

or

$$u(x,t)=\frac{1}{2}\left[u_0(x-ct)+u_0(x+ct)\right]$$

$$-\frac{1}{2}\Omega t\int_{x-ct}^{x+ct}\frac{J_1\left[\dfrac{\Omega}{c}\sqrt{c^2t^2-(x-\xi)^2}\right]}{\sqrt{c^2t^2-(x-\xi)^2}}u_0(\xi)d\xi$$

$$+\frac{1}{2c}\int_{x-ct}^{x+ct} J_0\left[\frac{\Omega}{c}\sqrt{c^2t^2-(x-\xi)^2}\right]s_0(\xi)\,d\xi. \tag{108}$$

Let us now assume an excitation moving with a speed c, i.e.,

$$s_0(x)=-c\frac{du_0}{dx}. \tag{109}$$

Equation (108) then becomes

$$u(x,t)=u_0(x-ct)$$

$$-\frac{\Omega}{2c}\int_{x-ct}^{x+ct}\frac{J_1\left[\dfrac{\Omega}{c}\sqrt{c^2t^2-(x-\xi)^2}\right]}{\sqrt{c^2t^2-(x-\xi)^2}}\left[ct+(x-\xi)\right]u_0(\xi)\,d\xi. \tag{110}$$

If the excitation is localized around $x=0$, i.e.,

$$u_0(x)=A\delta(x), \tag{111}$$

(110) becomes

$$u(x,t)=A\delta(x-ct)-\frac{A\Omega}{2c}\frac{ct+x}{\sqrt{c^2t^2-x^2}}J_1\left(\frac{\Omega}{c}\sqrt{c^2t^2-x^2}\right). \tag{112}$$

The excitation represented by this expression comprises a sharp front advancing in the x–direction at the speed c, behind which a wavetrain extends over the steadily

widening range $|x| < ct$, with an amplitude that diminishes as the trailing edge $x = -ct$ is approached. As $t \Rightarrow \infty$, this wavetrain is described by

$$u(x,t) \sim A \sqrt{\frac{\Omega}{2\pi c}} \frac{(ct+x)}{\left(c^2t^2 - x^2\right)^{3/4}} \cos\left[\frac{\Omega}{c}\sqrt{c^2t^2 - x^2} + \frac{\pi}{4}\right]. \tag{113}$$

Theory of Tides

The tides are periodic rise and fall of the free level of water in the oceans caused by the lunar gravitational attraction. Let us consider here the equatorial tides.

In the long–wave approximation, one has the following equations for the flow:

$$\rho \frac{\partial u}{\partial t} = -\frac{\partial p}{\partial x} + \rho F_x, \tag{114}$$

$$0 = -\frac{\partial p}{\partial z} - \rho g \quad \text{or} \quad p = p_0 + \rho g\left(h + \xi - z\right), \tag{115}$$

$$\frac{\partial u}{\partial x} + \frac{\partial w}{\partial z} = 0 \quad \text{or} \quad w = -h\frac{\partial u}{\partial x}, \tag{116}$$

$$z = 0 : \frac{\partial \xi}{\partial t} = w, \tag{117}$$

where h is the depth of water and F_x is the gravitational force (see Figure 2.35). From (114)–(117), one obtains

$$\frac{\partial^2 \xi}{\partial t^2} = gh\frac{\partial^2 \xi}{\partial x^2} - h\frac{\partial F_x}{\partial x}. \tag{118}$$

The net potential due to lunar gravitation at P on earth (see Figure 2.35) is given by

$$\Omega = -\frac{GM_m}{\left(D^2 + a^2 - 2aD\cos\phi\right)^{1/2}} + \frac{GM_m}{D - a\cos\phi}, \tag{119}$$

where a is the radius of the earth, and D the distance to moon. Here, we have noted that the gravitational field due to moon at the center of earth is nearly uniform and is directed along the line joining the latter to the moon and has the potential

$$\frac{GM_m}{D - a\cos\phi}.$$

Since $a/D \ll 1$, (119) can be approximated by

$$\Omega \approx \frac{GM_m a^2}{2D^3}\left(1 - 3\cos^2\phi\right). \tag{120}$$

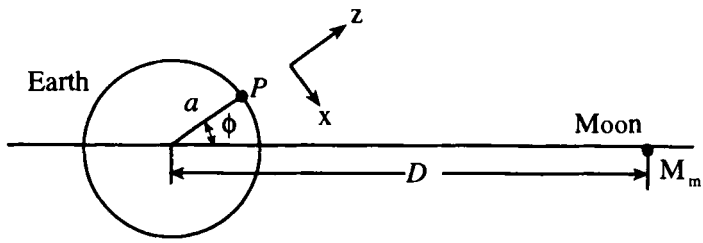

Figure 2.35. The earth–moon system.

Let us neglect the dynamical effects of the earth's rotation (i.e., neglect centrifugal and Coriolis forces), and let the only effect of this rotation be an apparent revolution of the moon (as seen by an observer) around the earth once each day. Let us assume further that the earth is a uniform sphere covered with a static ocean of uniform depth, and ignore the presence of land masses.

When we use (120), the tidal force F_x is given by

$$F_x = -\frac{\partial \Omega}{\partial x} = -\frac{\partial \Omega}{a \partial \phi} = \frac{3}{2} \frac{G M_m a}{D^3} \sin 2\phi. \tag{121}$$

When we use (121), (118) becomes

$$\frac{\partial^2 \xi}{\partial t^2} - \frac{gh}{a^2} \frac{\partial^2 \xi}{\partial \phi^2} = \frac{3 G M_m h}{D^3} \cos 2\phi. \tag{122}$$

Let ω be the frequency of the moon about the earth, as observed from the point P; then

$$\phi = \omega t, \tag{123}$$

so that (122) gives

$$\frac{\partial^2 \xi}{\partial t^2} = \frac{3 G M_m a h}{D^3 \left(1 - \dfrac{gh}{\omega^2 a^2}\right)} \cos 2\omega t, \tag{124}$$

from which

$$\xi = \frac{3 G M_m a^2 h}{4 D^3 \left(gh - \omega^2 a^2\right)} \cos 2\omega t. \tag{125}$$

Note from (125) that

* the tides are semidiurnal, i.e., the water level at a particular point will reach its maximum value twice a day – even though the moon traverses its path only once in the same period of time;
* since $gh \ll \omega^2 a^2$, the tide is inverted, i.e., one has a low tide when the moon is directly overhead.

Nonlinear Shallow Water Waves

Nonlinear effects in a train of surface waves lead to many essential observed phenomena. In deep water, the wave profile becomes distorted, with the crests slightly sharper than the troughs and the phase speed increasing slightly with increasing wave slope. In shallow water, the nonlinear effects are stronger and thus more easily observed; consequently, the linearized model here entails much more stringent conditions on the wave amplitude than that in deep water.

Consider small (but finite)–amplitude long waves of amplitude a and wavelength λ in shallow water of depth h so that

$$\alpha \equiv \frac{a}{h} \ll 1 \quad \text{and} \quad \beta \equiv \frac{h}{\lambda} \ll 1. \tag{126}$$

Two limiting cases arise for such waves depending on whether the parameter $S \equiv \alpha/\beta^2 = a\lambda^2/h^3$ is much greater than one (the *Stokes* approximation) or is near one (the *Boussinesq* approximation). The first case leads to nonlinear periodic waves, while the second case affords a balance between nonlinearity and dispersion and leads to solitary waves.

Consider a homogeneous, incompressible fluid whose undisturbed depth above a rigid horizontal boundary is h_0. Let the disturbed free surface be at a height $h(x,t)$ (see Figure 2.36). We will assume that the flow is two–dimensional and that there is no dependence on the transverse horizontal coordinate.

Thus one has the following boundary–value problem for the velocity potential ϕ:

$$\frac{\partial^2 \phi}{\partial x^2} + \frac{\partial^2 \phi}{\partial z^2} = 0, \tag{127}$$

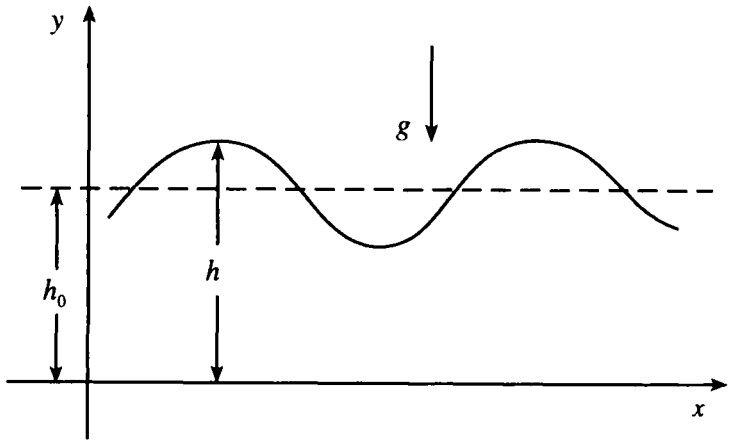

Figure 2.36. Surface waves on water of mean depth h_0.

$$z=0: \quad \frac{\partial \phi}{\partial z}=0, \tag{128}$$

$$z=h: \quad \frac{\partial \Phi}{\partial z}=\frac{\partial h}{\partial t}+\frac{\partial \Phi}{\partial x}\frac{\partial h}{\partial x}, \tag{129}$$

$$\frac{\partial \Phi}{\partial t}+\frac{1}{2}\left[\left(\frac{\partial \Phi}{\partial x}\right)^2+\left(\frac{\partial \Phi}{\partial z}\right)^2\right]+g\left(h-h_0\right)=0. \tag{130}$$

Consider propagation of waves moving only to the right and introduce

$$\xi=\sqrt{\varepsilon}\left(x-c_0 t\right), \quad \tau=\varepsilon^{3/2}t, \quad \psi=\varepsilon^{1/2}\Phi,$$

$$c_0=\sqrt{g h_0}, \quad \varepsilon \ll 1, \tag{131}$$

so that (127)–(130) become

$$\varepsilon\frac{\partial^2 \psi}{\partial \xi^2}+\frac{\partial^2 \psi}{\partial z^2}=0, \tag{132}$$

$$z=0: \quad \frac{\partial \psi}{\partial z}=0, \tag{133}$$

$$z=h: \quad \frac{\partial \psi}{\partial z}=\varepsilon^2\frac{\partial h}{\partial \tau}+\varepsilon\left(\frac{\partial \psi}{\partial \xi}-c_0\right)\frac{\partial h}{\partial \xi}, \tag{134}$$

$$\varepsilon^2\frac{\partial \psi}{\partial \tau}-\varepsilon c_0\frac{\partial \psi}{\partial \xi}+\frac{1}{2}\left[\varepsilon\left(\frac{\partial \psi}{\partial \xi}\right)^2+\left(\frac{\partial \psi}{\partial z}\right)^2\right]+\varepsilon g\left(h-h_0\right)=0. \tag{135}$$

If we put

$$\left.\begin{aligned} h &= h_0+\varepsilon h_1+\varepsilon^2 h_2+\cdots, \\ \psi &= \varepsilon\psi_1+\varepsilon^2\psi_2+\cdots, \end{aligned}\right\} \tag{136}$$

equation (132) leads to

$$\frac{\partial^2 \psi_1}{\partial z^2}=0, \tag{137}$$

$$\frac{\partial^2 \psi_n}{\partial z^2}+\frac{\partial^2 \psi_{n-1}}{\partial \xi^2}=0, \quad n>1. \tag{138}$$

One obtains, from equations (137) and (138), on using (133),

$$\psi_1=\psi_1(\xi,\tau),$$

$$\psi_2=-\frac{1}{2}z^2\frac{\partial^2 \psi_1}{\partial \xi^2},$$

$$\psi_3 = \frac{1}{24} z^4 \frac{\partial^4 \psi_1}{\partial \xi^4},$$

etc. (139)

The boundary conditions (134) and (135) are imposed at a boundary which is unknown without the solution and varies slightly with the perturbation parameter ε. If the solution is analytic in spatial coordinates, the transfer of the boundary conditions to the basic configuration of the boundary corresponding to $\varepsilon = 0$ is effected by expanding the solution in a Taylor series about the values at the basic configuration. Thus, (134) and (135) give

$$z = h_0: \quad \frac{\partial \psi_2}{\partial z} = -c_0 \frac{\partial h_1}{\partial \xi}$$

$$\frac{\partial \psi_3}{\partial z} + h_1 \frac{\partial^2 \psi_2}{\partial z^2} = \frac{\partial h_1}{\partial \tau} - c_0 \frac{\partial h_2}{\partial \xi} + \frac{\partial \psi_1}{\partial \xi} \frac{\partial h_1}{\partial \xi},$$

etc. (140)

and

$$-c_0 \frac{\partial \psi_1}{\partial \xi} + g h_1 = 0,$$

$$\frac{\partial \psi_1}{\partial \tau} - c_0 \frac{\partial \psi_2}{\partial \xi} + \frac{1}{2}\left(\frac{\partial \psi_1}{\partial \xi}\right)^2 + g h_2 = 0,$$

etc. (141)

From (139)–(141), one derives

$$\frac{\partial h_1}{\partial \tau} + \frac{3c_0}{2h_0} h_1 \frac{\partial h_1}{\partial \xi} = -\frac{c_0 h_0^2}{6} \frac{\partial^3 h_1}{\partial \xi^3}, \tag{142}$$

which is the Korteweg–deVries equation.

Recall the linear dispersive relation for water waves

$$\omega^2 = gk \tan hkh_0, \tag{15}'$$

from which, for shallow–water waves, one has

$$kh_0 \ll 1 : \omega = kc_0 \left[1 - \frac{h_0^2 k^2}{6} + \cdots\right]. \tag{143}$$

Observe that the coefficient of the dispersive term on the right–hand side of the Korteweg–deVries equation (142) is the same as the coefficient of k^3 in the linear dispersion relation (143)!

Solitary Waves

Write the Korteweg–deVries equation (142) in the form

$$\phi_t + \kappa \phi \phi_x + \phi_{xxx} = 0. \tag{144}$$

Looking for steady, progressing, and localized wave solutions of the form

$$\phi(x,t) = \phi(\xi), \qquad \xi = x - Ut, \tag{145}$$

equation (144) gives

$$\phi_\xi(\kappa\phi - U) + \phi_{\xi\xi\xi} = 0,$$

$$|\xi| \Rightarrow \infty : \phi, \phi_\xi, \phi_{\xi\xi} \Rightarrow 0. \tag{146}$$

Upon integrating, equation (146) gives

$$\phi_{\xi\xi} = U\phi - \frac{\kappa}{2}\phi^2 \tag{147}$$

and again equation (147) gives

$$\frac{1}{2}\phi_\xi^2 = \frac{U}{2}\phi^2 - \frac{\kappa}{6}\phi^3, \tag{148}$$

from which

$$\int_{\phi_{max}}^{\phi} \frac{d\phi}{\sqrt{\frac{U}{2}\phi^2 - \frac{\kappa}{6}\phi^3}} = \sqrt{2}\,\xi. \tag{149}$$

The integral in (149) is of the form

$$I = \int \frac{d\phi}{\phi\sqrt{1-\sigma\phi}}. \tag{150}$$

If we put

$$\psi = \sqrt{1-\sigma\phi}, \quad \sigma \equiv \frac{\kappa}{3U}, \tag{151}$$

(150) becomes

$$I = -2\int \frac{d\psi}{1-\psi^2} = \ln\frac{1-\psi}{1+\psi}. \tag{152}$$

When we use (152), (149) leads to

$$\frac{1-\psi}{1+\psi} = e^{\sqrt{U}\,\xi}, \tag{153}$$

from which

$$\psi = \frac{1 - e^{\sqrt{U}\,\xi}}{1 + e^{\sqrt{U}\,\xi}}. \tag{154}$$

Noting, from (151), that

$$\phi = \frac{1-\psi^2}{\sigma}, \tag{151}'$$

one obtains, on using (154),

$$\phi = \frac{1}{\sigma}\frac{4e^{\sqrt{U}\xi}}{\left(1+e^{\sqrt{U}\xi}\right)^2} = \frac{1}{\sigma}\operatorname{sech}^2\frac{\sqrt{U}\,\xi}{2} = \frac{3U}{\kappa}\operatorname{sech}^2\left[\frac{\sqrt{U}}{2}(x-Ut)\right], \quad (155)$$

which represents a unidirectional solitary wave. Equation (155) shows that

- this solitary wave moves with a velocity larger than the speed of the gravity waves, viz., c_0, by an amount proportional to the square root of its amplitude (this is a consequence of the nonlinearity of the wave);
- the width of the solitary wave is inversely proportional to the square root of its amplitude (this is a consequence of the spreading of the wave due to dispersion); this result, of course, confirms the condition $\alpha \sim \beta^2$ discussed before [see (126)]!

Solitary waves are localized waves propagating without change of shape and velocity.[10] The essential quality of a solitary wave is the balance between nonlinearity, which tends to steepen the wavefront in consequence of the increase of the wavespeed with amplitude, and dispersion, which tends to spread the wavefront. Solitary waves are found to preserve their identity and to be stable in processes of mutual collisions (see Figure 2.37). Solitary waves are strictly nonlinear phenomena with no counterparts in linear theory.

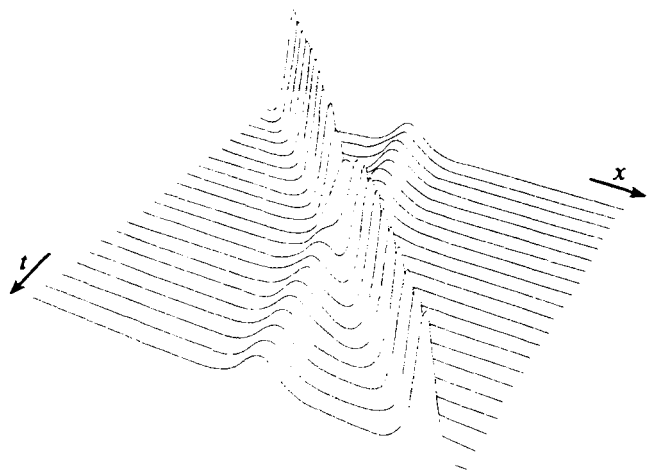

Figure 2.37. Numerical solution of the Korteweg–deVries equation describing the overtaking collision of the solitary waves (from Dodd et al., 1982).

[10]Solitary waves were first observed by J. Scott Russell on the Edinburgh-Glasgow canal in 1834. Russell also performed laboratory experiments on solitary waves and empirically deduced that the speed u of the solitary wave is given by

$$u^2 = g(h_0 + a).$$

where a is the amplitude of the wave and h_0 is the undisturbed depth of water.

Stability of solitary waves has been demonstrated with respect to one–dimensional perturbations (Jeffrey and Kakutani, Benjamin) and two–dimensional perturbations (Kadomtsev and Petviashvili, Oikawa et al.).

Periodic Cnoidal Waves

Korteweg–deVries equation also possesses periodic cnoidal–wave solutions given in terms of Jacobi elliptic functions. Consider the Korteweg–deVries equation in the form

$$\phi_t + \kappa\phi\phi_x + \phi_{xxx} = 0 \tag{144}$$

and look for stationary solutions of the form

$$\phi(x,t) = \phi(\xi), \quad \xi = x - Ut. \tag{145}$$

Equation (144) leads to

$$-U\phi_\xi + \kappa\phi\phi_\xi + \phi_{\xi\xi\xi} = 0. \tag{156}$$

Integrating equation (156) twice, one obtains

$$-\frac{1}{2}U\phi^2 + \frac{\kappa}{6}\phi^3 + \frac{1}{2}\phi_\xi^2 = A\phi + B, \tag{157}$$

where A and B are constants of integration.

Equation (157) may be written in the form

$$\frac{3}{\kappa}\phi_\xi^2 = -\phi^3 + \frac{3U}{\kappa}\phi^2 + \frac{6A}{\kappa}\phi + \frac{6B}{\kappa} \equiv f(\phi). \tag{158}$$

Under certain conditions, equation (158) may give a periodic solution between two consecutive real zeros of $f(\phi)$, where $f(\phi) \geq 0$. Note that $f(\phi)$ is a cubic and therefore has three zeros. Hence one has two separate cases to consider:

(a) Only one zero is real (Figure 2.38).

For a real solution, one has to restrict ϕ to $\phi \leq \sigma_1$. In this region, one obtains, from equation (158),

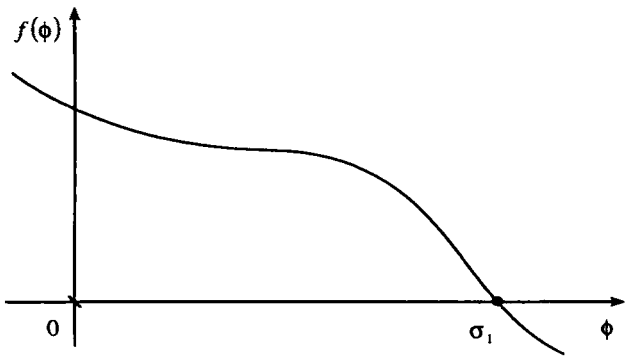

Figure 2.38. The case with one real zero.

$$\frac{d\phi}{d\xi} = \pm\sqrt{\frac{\kappa}{3}f(\phi)}. \tag{159}$$

However, note that this solution becomes unbounded, since

$$\phi \Rightarrow -\infty: \quad f(\phi) \Rightarrow \infty.$$

(b) All three zeros are real (Figure 2.39). Here, one has three subcases:

(b1) all three real roots α, β, γ are distinct (curve A);

(b2) two roots are equal $\beta = \gamma$ (curve B);

(b3) two roots are equal $\beta = \alpha$ (curve C).

Writing

$$f(\phi) = (\phi - \gamma)(\phi - \beta)(\alpha - \phi), \tag{160}$$

one has from (158)

$$\left.\begin{aligned} \frac{1}{3}(\alpha + \beta + \gamma) &= \frac{U}{\kappa}, \\ -\frac{1}{6}(\alpha\beta + \beta\gamma + \gamma\alpha) &= \frac{A}{\kappa}, \\ \frac{1}{6}\alpha\beta\gamma &= \frac{B}{\kappa}. \end{aligned}\right\} \tag{161}$$

For the solution to be real and bounded, one requires $\beta < \phi < \alpha$ for curve A and $\beta = \gamma < \phi < \alpha$ for curve B. For curve C, $\phi \leq \gamma$ appears acceptable, but the solution becomes unbounded as in case (a).

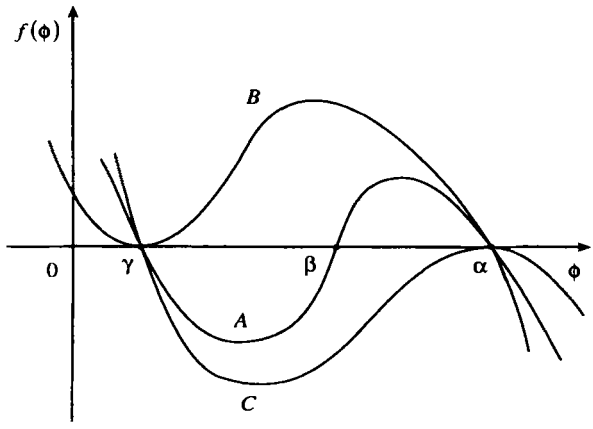

Figure 2.39. The cases with three real zeros.

Incidentally, one has from (161)

$$U^2+2A\kappa=\frac{\kappa^2}{18}\left[(\alpha-\beta)^2+(\beta-\gamma)^2+(\gamma-\alpha)^2\right], \tag{162}$$

from which, in order that the zeros α, β, and γ are real, one requires

$$U^2+2A\kappa\geq 0. \tag{163}$$

(b1) Here, there is a local maximum at α (since $f'(\alpha)<0$) and a local minimum at β (since $f'(\beta)>0$). Thus, ϕ' will change sign at these points and since the behavior near them is algebraic, consecutive points $\phi=\alpha$, $\phi=\beta$ will be a finite distance apart, and hence, $(\alpha-\beta)$ can be considered as a measure of the amplitude of the wave. One has, from (159) and (160),

$$-\frac{d\phi}{\left[(\phi-\gamma)(\phi-\beta)(\alpha-\phi)\right]^{1/2}}=\frac{d\xi}{\sqrt{3/\kappa}}. \tag{164}$$

If we put

$$p^2\equiv\alpha-\phi, \tag{165}$$

(164) becomes

$$\frac{d\xi}{\sqrt{3/\kappa}}=\frac{2dp}{\left[\left\{(\alpha-\gamma)-p^2\right\}\left\{(\alpha-\beta)-p^2\right\}\right]^{1/2}}. \tag{166}$$

Further, if we put

$$q=\frac{p}{\sqrt{(\alpha-\beta)}}, \tag{167}$$

(166) becomes

$$\sqrt{(\alpha-\gamma)}\,\frac{d\xi}{\sqrt{3/\kappa}}=\frac{2dq}{\left[\left(1-s^2q^2\right)\left(1-q^2\right)\right]^{1/2}}, \tag{168}$$

where

$$\left.\begin{aligned} s^2&=\frac{\alpha-\beta}{\alpha-\gamma},\quad 0<s^2<1,\\ q&=\frac{p}{\sqrt{(\alpha-\beta)}}=\sqrt{\frac{\alpha-\phi}{\alpha-\beta}}. \end{aligned}\right\} \tag{169}$$

Recall that, here, $\beta<\phi<\alpha$, and from (165) and (167), note that

$$\left.\begin{aligned} &\phi=\alpha:\quad q=0,\\ &\phi=\beta:\quad q=1. \end{aligned}\right\}.$$

If we take

$$q = 0: \quad \xi = 0, \tag{170}$$

(168) gives

$$\xi = \sqrt{\frac{12}{\kappa(\alpha-\gamma)}}\left[\int_0^q \frac{dq}{\sqrt{\left(1-s^2q^2\right)\left(1-q^2\right)}}\right] = \sqrt{\frac{12}{\kappa(\alpha-\gamma)}}\, sn^{-1}(q,s), \tag{171}$$

from which

$$\phi(\xi) = \beta + (\alpha-\beta)\, cn^2\left(\xi\sqrt{\frac{\kappa(\alpha-\gamma)}{12}}, s\right), \tag{172}$$

where sn and cn are the Jacobian elliptic functions.

The period of $\phi(\xi)$ (which is the period of cn^2) is given by

$$P = 2\sqrt{\frac{12}{\kappa(\alpha-\gamma)}}\int_0^1 \frac{dq}{\sqrt{\left(1-s^2q^2\right)\left(1-q^2\right)}} = 4\sqrt{\frac{3}{\kappa(\alpha-\gamma)}}\, K\left(s^2\right), \tag{173}$$

where $K(s^2)$ is the complete elliptic integral of the first kind. Thus, the bounded solution of the Korteweg–deVries equation represents a periodic wave. Figure 2.40 shows the cnoidal wave solutions for $s^2 = 0$, 0.6, and 0.9. Observe that the crests become narrower and the troughs become wider as s^2 increases. The actual wave profile is a curve called *trochoid.*

Note that the linear case corresponds to the limit $s^2 \Rightarrow 0$ [see (169)]; noting, further, that

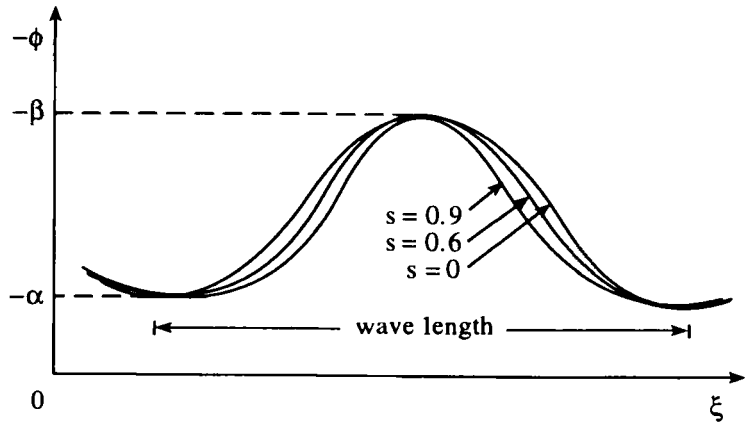

Figure 2.40. One period of the cnoidal wave for $s = 0, 0.6$, and 0.9. All three waves have been normalized so that the amplitudes and wavelengths are the same (from Drazin and Johnson, 1989).

$$cn(\zeta,0) \approx \cos\zeta,$$

we see that (172) leads to

$$\phi(\xi) = \beta + (\alpha-\beta)\cos^2\left(\sqrt{\frac{\kappa(\alpha-\gamma)}{12}}\,\xi\right), \tag{174}$$

as to be expected!

(b2) One has now, from (159) and (160),

$$d\xi = \sqrt{\frac{3}{\kappa}}\,\frac{d\phi}{(\phi-\gamma)\sqrt{(\alpha-\phi)}}, \tag{175}$$

which leads to the solitary wave:

$$\phi(\xi) = \gamma + (\alpha-\gamma)\,\mathrm{sech}^2\left(\sqrt{\frac{\kappa(\alpha-\gamma)}{12}}\,\xi\right).^{11} \tag{176}$$

The period of this wave, from (173), is given by

$$P = 4\sqrt{\frac{3}{\kappa(\alpha-\gamma)}}\int_0^1 \frac{dq}{1-q^2} = \infty, \tag{177}$$

as to be expected!

Noting, from (176), that

$$\xi \Rightarrow \pm\infty : \phi \Rightarrow \gamma, \tag{178}$$

one recognizes that $\phi_\infty = \gamma$ denotes the uniform state corresponding to $\xi \Rightarrow \pm\infty$. Therefore, one may write

$$a \equiv \alpha - \gamma \tag{179}$$

and interpret a as the amplitude of the wave. Thus, (176) may be rewritten as

$$\phi(\xi) - \phi_\infty = a\,\mathrm{sech}^2\left[\sqrt{\frac{a\kappa}{12}}\left\{x - \left(\phi_\infty\kappa + \frac{a\kappa}{3}\right)t\right\}\right], \tag{180}$$

which (on identifying a with $3U/\kappa$) precisely is the solitary wave solution (155), as we obtained before!

---

[11] Alternatively, note that this case corresponds to $s^2 = 1$ [see (169)] – the "most nonlinear" case; noting further that

$$cn(\zeta,1) = \mathrm{sech}\,\zeta,$$

we see that (172) leads to

$$\phi(\xi) = \gamma + (\alpha-\gamma)\,\mathrm{sech}^2\left(\sqrt{\frac{\kappa(\alpha-\gamma)}{12}}\,\xi\right),$$

as in (176)!

Interacting Solitary Waves

We will now consider the behavior of two interacting solitary waves by using a method due to Hirota. This method involves transforming the Korteweg–deVries equation into homogeneous bilinear forms, and then developing the bilinear equations in series expansions which "self–truncate." Consider Korteweg–deVries equation in the form,

$$\phi_t + \kappa\phi\phi_x + \phi_{xxx} = 0. \tag{181}$$

If we put

$$\phi = \frac{12}{\kappa}(\ln F)_{xx}, \tag{182}$$

equation (181) gives

$$F(F_t + F_{xxx})_x - F_x(F_t + F_{xxx}) + 3(F_{xx}^2 - F_x F_{xxx}) = 0. \tag{183}$$

When we look for a solution of the form

$$F = 1 + \varepsilon F_1 + \varepsilon^2 F_2 + \cdots, \quad \varepsilon \ll 1, \tag{184}$$

equation (183) leads to the following hierarchy of equations:

$$(F_{1t} + F_{1xxx})_x = 0, \tag{185}$$

$$(F_{2t} + F_{2xxx})_x = -3(F_{1xx}^2 - F_{1x} F_{1xxx}), \tag{186}$$

$$(F_{3t} + F_{3xxx})_x = -F_1(F_{2t} + F_{2xxx})_x + F_{1x}(F_{2t} + F_{2xxx}) - 3(2F_{1xx} F_{2xx} - F_{1x} F_{2xxx} - F_{2x} F_{1xxx}), \tag{187}$$

$$(F_{4t} + F_{4xxx})_x = -F_2(F_{2tx} + F_{2xxxx}) + F_{2x}(F_{2t} + F_{2xxx}) - 3(F_{2x}^2 - F_{2x} F_{2xxx}), \tag{188}$$

etc.

Equation (185) has the solution

$$F_1 = f_1 + f_2, \quad f_j = e^{-\alpha_j(x - s_j) + \alpha_j^3 t}, \quad j = 1, 2. \tag{189}$$

When we use equation (189), equation (186) becomes

$$(F_{2t} + F_{2xxx})_x = 3\alpha_1\alpha_2(\alpha_2 - \alpha_1)^2 f_1 f_2, \tag{190}$$

from which

$$F_2 = \frac{(\alpha_2 - \alpha_1)^2}{(\alpha_2 + \alpha_1)^2} f_1 f_2. \tag{191}$$

When we use equations (189) and (191), equation (187) becomes

$$
\begin{aligned}
\left(F_{3t}+F_{3xxx}\right)_x &= \frac{\left(\alpha_2-\alpha_1\right)^2}{\left(\alpha_2+\alpha_1\right)^2}\Big[-\left(f_1+f_2\right)\left\{\left(f_1f_2\right)_{tx}+\left(f_1f_2\right)_{xxxx}\right\} \\
&\quad +\left(f_{1x}+f_{2x}\right)\left\{\left(f_1f_2\right)_t+\left(f_1f_2\right)_{xxx}\right\}-3\Big\{2\left(f_{1xx}+f_{2xx}\right) \\
&\quad \times\left(f_1f_2\right)_{xx}-\left(f_{1x}+f_{2x}\right)\left(f_1f_2\right)_{xxx}-\left(f_1f_2\right)_x\left(f_{1xxx}+f_{2xxx}\right)\Big\}\Big] \\
&= \frac{\left(\alpha_2-\alpha_1\right)^2}{\left(\alpha_2+\alpha_1\right)^2}\Big[-\left(f_1+f_2\right)\left(6f_{1xx}f_{2xx}+3f_{1x}f_{2xxx}+3f_{1xxx}f_{2x}\right) \\
&\quad +\left(f_{1x}+f_{2x}\right)\left(3f_{1x}f_{2xx}+3f_{1xx}f_{2x}\right)-3\Big\{2\left(f_{1xx}+f_{2xx}\right) \\
&\quad \times\left(f_{1xx}f_2+2f_{1x}f_{2x}+f_1f_{2xx}\right)-\left(f_{1x}+f_{2x}\right) \\
&\quad \times\left(f_{1xxx}f_2+3f_{1xx}f_{2x}+3f_{1x}f_{2xx}+f_1f_{2xxx}\right) \\
&\quad -\left(f_{1x}f_2+f_1f_{2x}\right)\left(f_{1xxx}+f_{2xxx}\right)\Big\}\Big] \\
&= \frac{\left(\alpha_2-\alpha_1\right)^2}{\left(\alpha_2+\alpha_1\right)^2}\,f_1f_2\Big[-3\alpha_1\alpha_2\left(\alpha_1+\alpha_2\right)\left(f_1+f_2\right) \\
&\quad +3\alpha_1\alpha_2\left(\alpha_1f_1+\alpha_2f_2\right)-3\Big\{2\left(\alpha_1+\alpha_2\right)\left(\alpha_1^2f_1+\alpha_2^2f_2\right) \\
&\quad -\left(\alpha_1+\alpha_2\right)^2\left(\alpha_1f_1+\alpha_2f_2\right)-\left(\alpha_1^3f_1+\alpha_2^3f_2\right)\Big\}\Big] \\
&= 0, \qquad (192)
\end{aligned}
$$

so that

$$F_3 = 0. \qquad (193)$$

When we use equations (189), (191) and (193), equation (188) becomes

$$\left(F_{4t}+F_{4xxx}\right)_x = 0, \qquad (194)$$

so that

$$F_4 = 0. \qquad (195)$$

Thus,

$$F_n = 0, \quad n>2. \qquad (196)$$

Therefore, (184), (189), (191), and (196) imply that

$$F = 1+\varepsilon\left(f_1+f_2\right)+\varepsilon^2\frac{\left(\alpha_2-\alpha_1\right)^2}{\left(\alpha_2+\alpha_1\right)^2}\,f_1f_2 \qquad (197)$$

is an exact solution! Consequently, one may put $\varepsilon = 1$.

Thus, one has from (182) and (197)

$$\frac{\kappa}{12}\phi = \frac{\left[\left(\alpha_1^2 f_1 + \alpha_2^2 f_2\right) + 2\left(\alpha_2 - \alpha_1\right)^2 f_1 f_2 + \dfrac{\left(\alpha_2 - \alpha_1\right)^2}{\left(\alpha_2 + \alpha_1\right)^2}\left(\alpha_2^2 f_1^2 f_2 + \alpha_1^2 f_1 f_2^2\right)\right]}{\left[1 + \left(f_1 + f_2\right) + \dfrac{\left(\alpha_2 - \alpha_1\right)^2}{\left(\alpha_2 + \alpha_1\right)^2} f_1 f_2\right]^2}. \tag{198}$$

Note, from (198), that a single solitary wave is given by

$$\frac{\kappa}{12}\phi = \frac{\alpha^2 f}{(1+f)^2}.$$

Note that

$$\phi = \phi_{\max} = \frac{3\alpha^2}{\kappa}$$

occurs on

$$f = 1, \quad x = s + \alpha^2 t.$$

Next, note that

$$\left.\begin{aligned} &f_1 \approx 1,\ f_2 \ll 1 : \frac{\kappa}{12}\phi \approx \frac{\alpha_1^2 f_1}{\left(1+f_1\right)^2}, \\ &f_1 \approx 1,\ f_2 \gg 1 : \frac{\kappa}{12}\phi \approx \frac{\alpha_1^2 \tilde{f}_1}{\left(1+\tilde{f}_1\right)^2},\quad \tilde{f}_1 = \frac{\left(\alpha_2 - \alpha_1\right)^2}{\left(\alpha_2 + \alpha_1\right)^2} f_1. \end{aligned}\right\}$$

The latter is a solitary wave with s_1 replaced by $\tilde{s}_1$, where

$$\tilde{s}_1 = s_1 - \frac{1}{\alpha_1} \ln\left(\frac{\alpha_2 + \alpha_1}{\alpha_2 - \alpha_1}\right)^2,$$

which signifies a finite displacement of the profile in the x–direction. Similarly, when $f_2 \approx 1$ and f_1 is either large or small, one has the solitary wave α_2 with or without a shift in s_2. Where $f_1 \approx 1$ and $f_2 \approx 1$, one has the interaction region. Where f_1 and f_2 are both small or large, one has $\phi \approx 0$.

In order to consider the behavior of two interacting solitary waves, let $\alpha_2 > \alpha_1 > 0$; the solitary wave α_2 is bigger and thus moves faster than the wave α_1. As $t \Rightarrow -\infty$, one has

$$\left.\begin{aligned} &f_1 \approx 1,\ f_2 \ll 1: \quad \text{wave } \alpha_1 \text{ on } x = s_1 + \alpha_1^2 t \\ &f_2 \approx 1,\ f_1 \gg 1: \quad \text{wave } \alpha_2 \text{ on } x = s_2 - \frac{1}{\alpha_2} \ln\left(\frac{\alpha_2 + \alpha_1}{\alpha_2 - \alpha_1}\right)^2 + \alpha_2^2 t \end{aligned}\right\}$$

and elsewhere $\phi \approx 0$.

As $t \Rightarrow \infty$, one has

$$\left.\begin{aligned} &f_1 \approx 1,\ f_2 \gg 1: \quad \text{wave } \alpha_1 \text{ on } x = s_1 - \frac{1}{\alpha_1} \ln\left(\frac{\alpha_2+\alpha_1}{\alpha_2-\alpha_1}\right)^2 + \alpha_1^2 t \\ &f_2 \approx 1,\ f_1 \ll 1: \quad \text{wave } \alpha_2 \text{ on } x = s_2 + \alpha_2^2 t \end{aligned}\right\}$$

and elsewhere $\phi \approx 0$.

Thus, the solitary waves emerge unchanged in form with the original parameters α_1 and α_2, with the faster wave α_2 now being ahead of the slower wave α_1. The only remnant of the collision process is a forward shift

$$\frac{1}{\alpha_2} \ln\left(\frac{\alpha_2+\alpha_1}{\alpha_2-\alpha_1}\right)^2$$

for the wave α_2, and a backward shift

$$\frac{1}{\alpha_1} \ln\left(\frac{\alpha_2+\alpha_1}{\alpha_2-\alpha_1}\right)^2$$

for the wave α_1, from where they would have been in the absence of a collision.

Zabusky and Kruskal introduced the term *soliton* to describe such remarkably stable nonlinear structures.

Stokes Waves

Irrotational, steady, progressive waves were considered first by Stokes and are called *Stokes waves*. The Korteweg–deVries equation (144) can be written as

$$\frac{\partial h_1}{\partial t} + c_0\left(1 + \frac{3}{2}\frac{h_1}{h_0}\right)\frac{\partial h_1}{\partial x} + \gamma \frac{\partial^3 h_1}{\partial x^3} = 0, \tag{199}$$

where

$$\gamma = \frac{c_0 h_0^2}{6}.$$

Let us find the next approximation to the linear periodic wave train using the method of strained parameters. Thus let

$$\left.\begin{aligned} &\frac{h_1}{h_0} = \varepsilon h_1^{(1)}(\theta) + \varepsilon^2 h_1^{(2)}(\theta) + \varepsilon^3 h_1^{(3)}(\theta) + \cdots \\ &\omega = \omega_0(k) + \varepsilon\,\omega_1(k) + \varepsilon^2 \omega_2(k) + \cdots, \end{aligned}\right\} \tag{200}$$

where

$$\theta \equiv k\,x - \omega\,t.$$

When we use (200), (199) leads to the following hierarchy of equations:

$$\left(\omega - c_0 k\right) h_1^{(1)'} - \gamma k^3 h_1^{(1)'''} = 0, \tag{201}$$

$$\left(\omega - c_0 k\right) h_1^{(2)'} - \gamma k^3 h_1^{(2)'''} = \frac{3}{2} c_0 k h_1^{(1)} h_1^{(1)'} - \omega_1 h_1^{(1)'}, \tag{202}$$

$$\left(\omega - c_0 k\right) h_1^{(3)'} - \gamma k^3 h_1^{(3)'''} = \frac{3}{2} c_0 k \left(h_1^{(1)} h_1^{(2)}\right)' - \omega_2 h_1^{(1)'}, \tag{203}$$

etc.

Equation (201) gives the linear result:

$$h_1^{(1)} = \cos\theta, \qquad \omega_0(k) = c_0 k - \gamma k^3. \tag{204}$$

When we use (204), the removal of secular terms on the right–hand side in (202) requires

$$\omega_1 = 0. \tag{205}$$

When we use (204) and (205), (202) gives

$$h_1^{(2)} = \frac{c_0}{8\gamma k^2} \cos 2\theta. \tag{206}$$

When we use (204)–(206), the removal of secular terms on the right–hand side in (203) requires

$$\omega_2 = \frac{3c_0^2}{32\gamma k}. \tag{207}$$

Thus,

$$\left.\begin{aligned} \frac{h_1}{h_0} &= \varepsilon \cos\theta + \frac{3\varepsilon^2}{4k^2 h_0^2} \cos 2\theta + \cdots \\ \frac{\omega}{c_0 k} &= 1 - \frac{1}{6} k^2 h_0^2 + \frac{9\varepsilon^2}{16 k^2 h_0^2} + \cdots \end{aligned}\right\} \tag{208}$$

Equation (208) exhibits two essential effects of nonlinearities:

* Periodic solutions of the form $e^{i(kx-\omega t)}$ may exist, but they are no longer sinusoidal.
* The amplitude appears in the dispersion relation.

Stokes showed that the Stokes waves have a limiting form with a sharp crest enclosing an angle of 120°. A simple and accurate analytical approximation to the Stokes wave profile was given by Longuet–Higgins:

$$\frac{dh}{dx} = \tan x.$$

It should be mentioned that the two–dimensional waves described by the Korteweg–deVries equation are more likely to be found only under controlled

conditions in the laboratory than in a natural setting where depth variations, nonuniform currents, and other effects lead to three–dimensional wave patterns. The propagation of three–dimensional, finite–amplitude, long waves is described by the Kadomtsev–Petviashvili equation, which is a generalization of the Korteweg–deVries equation to incorporate weak three–dimensional effects. This equation provides a suitable framework to describe oblique interactions of solitary waves (Miles) and periodic waves (Segur and Finkel).

Modulational Instability and Envelope Solitons

Let us superimpose a slowly varying weak modulation on a stationary weakly nonlinear wave, and study the evolution of such a modulation. Let us assume that the basic wave can be taken to be sinusoidal, i.e.,

$$\psi = a_0 \cos\theta_0, \qquad \theta_0 = k_0 x - \omega_0 t. \tag{209}$$

Because of the nonlinearities, the dispersion relation is of the form [see (208)]

$$\omega_0 = \omega_0\left(k_0, a_0^2\right). \tag{210}$$

Consequent to the superimposition of the modulation, let us assume that the wave is still plane periodic, but with the amplitude and phase varying slowly in x and t:

$$\left.\begin{aligned} a &= a(x,t), \\ \theta(x,t) &= k_0 x - \omega_0 t + \varphi(x,t). \end{aligned}\right\} \tag{211}$$

Thus, one may define a generalized frequency and wavenumber

$$\left.\begin{aligned} \omega(x,t) &= -\theta_t = \omega_0 - \varphi_t, \\ k(x,t) &= \theta_x = k_0 + \varphi_x. \end{aligned}\right\} \tag{212}$$

For weak modulations, one may write

$$\omega = \omega_0 + \frac{\partial\omega}{\partial a_0^2}\left(a^2 - a_0^2\right) + \frac{\partial\omega}{\partial k_0}\cdot\left(k - k_0\right) + \frac{\partial^2\omega}{\partial k_0^2}\cdot\left(k - k_0\right)^2 + \cdots \tag{213}$$

so that using (212), one obtains

$$\varphi_t + u_0\varphi_x + \frac{u_0'}{2}\,\varphi_x^2 + \left(\frac{\partial\omega}{\partial a_0^2}\right)\cdot\left(a^2 - a_0^2\right) = 0, \tag{214}$$

where u_0 is the group velocity,

$$u_0 \equiv \frac{\partial\omega}{\partial k_0}.$$

Next, note, from (212), that

$$u \equiv \frac{\partial\omega}{\partial k} = u_0 + u_0' \cdot \varphi_x. \tag{215}$$

Further, since the given wave has been assumed to be weakly nonlinear, we may make use of the result

$$\frac{\partial}{\partial t}\left(a^2\right)+\frac{\partial}{\partial x}\left(ua^2\right)=0. \tag{57}$$

When we use (215), (57) leads to

$$\frac{\partial}{\partial t}\left(a^2\right)+u_0\frac{\partial}{\partial x}\left(a^2\right)+u_0'\frac{\partial}{\partial x}\left(\varphi_x a^2\right)=0. \tag{216}$$

When we introduce

$$\xi=x-u_0t, \qquad \tau=u_0't, \tag{217}$$

equations (214) and (216) become

$$\varphi_\tau+\frac{1}{2}\varphi_\xi^2+\frac{1}{u_0'}\left(\frac{\partial\omega}{\partial a_0^2}\right)\left(a^2-a_0^2\right)=0, \tag{218}$$

$$\left(a^2\right)_\tau+\left(a^2\varphi_\xi\right)_\xi=0. \tag{219}$$

If we let

$$\varphi,\left(a^2-a_0^2\right)\sim e^{i(\chi\xi-\Omega\tau)}, \tag{220}$$

one then obtains, on linearizing equations (218) and (219),

$$\Omega^2=\frac{a_0^2}{u_0'}\frac{\partial\omega}{\partial a_0^2}\chi^2. \tag{221}$$

Therefore, instability arises if

$$\frac{1}{u_0'}\frac{\partial\omega}{\partial a_0^2}<0. \tag{222}$$

If in (213), one replaces $\left(\omega-\omega_0\right)$ by the operator $i\left(\partial/\partial t\right)$ and $\left(k-k_0\right)$ by $-i\left(\partial/\partial x\right)$, one obtains the so–called nonlinear Schrödinger equation:

$$i\left[\frac{\partial a}{\partial t}+\left(\frac{\partial\omega}{\partial k_0}\right)\frac{\partial a}{\partial x}\right]+\frac{1}{2}\left(\frac{\partial^2\omega}{\partial k_0^2}\right)\frac{\partial^2 a}{\partial x^2}-\frac{\partial\omega}{\partial a_0^2}\left(|a|^2-|a_0|^2\right)a=0. \tag{223}$$

In the frame of reference moving with the group velocity, equation (223) becomes

$$i\frac{\partial\tilde{a}}{\partial\tau}+\frac{1}{2}\frac{\partial^2\tilde{a}}{\partial\xi^2}+\kappa|a|^2\tilde{a}=0, \tag{224}$$

where we have put $a=\tilde{a}\,e^{i\left(\partial\omega/\partial a_0^2\right)t}$, and

$$\xi=x-\frac{\partial\omega}{\partial k_0}t, \qquad \tau=\frac{\partial^2\omega}{\partial k_0^2}t, \qquad \kappa\equiv-\frac{\partial\omega/\partial a_0^2}{\partial^2\omega/\partial k_0^2}.$$

Plane–wave solutions of equation (224) are modulationally unstable if $\kappa > 0$, i.e., a ripple on the envelope of the wave will tend to grow.

In order to see why the sign of κ matters, consider a ripple on the envelope (see Figure 2.41). Suppose $\partial\omega/\partial a_0^2 < 0$. Then, the phase velocity $\omega/k = c$ becomes somewhat smaller in the region of high intensity. This causes the wave crests to pile up on the left in Figure 2.41 and to spread out on the right. If $\partial^2\omega/\partial k^2 > 0$, the group velocity $u = \partial\omega/\partial k$ will be larger on the left than on the right, so the wave energy will pile up into a smaller space. Thus, the ripple on the envelope will become narrower and larger and an instability ensues. On the other hand, if $\partial\omega/\partial a_0^2$ and $\partial^2\omega/\partial k^2$ were of the same sign, this modulational instability will not develop. Alternatively, one may regard equation (224) as the Schrödinger equation for "quasi–particles" whose wave function is given by a and which are trapped by a self–generated localized potential well $\mathcal{V} = \kappa|a|^2$. If $\kappa > 0$, this potential has an attractive sign. Therefore, if the "quasi–particle" density $|a|^2$ increases, the potential depth increases, and if $\kappa > 0$, more "quasi–particles" are attracted, leading to a further increase in the potential depth. In this sense, the instability may be regarded as a consequence of the self–trapping of the "quasi–particles."

Let us now construct a localized stationary solution of equation (224). When we put

$$\tilde{a} = v(\xi - U\tau)e^{i(\gamma\xi - s\tau)}, \tag{225}$$

equation (224) gives

$$\frac{1}{2}v'' + \frac{i}{2}(2\gamma - U)v' + \left(s - \frac{\gamma^2}{2}\right)v + \kappa|v|^2 v = 0. \tag{226}$$

When we let

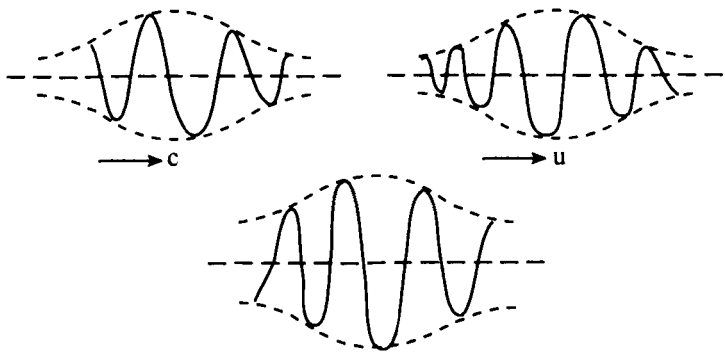

Figure 2.41. Modulational instability.

$$\gamma = \frac{U}{2}, \quad s = \frac{U^2}{2} - \frac{\alpha}{2}, \tag{227}$$

equation (226) becomes

$$v'' - \alpha v + 2\kappa v^3 = 0. \tag{228}$$

Upon integrating once, equation (228) gives

$$v'^2 = \alpha v^2 - \kappa v^4, \tag{229}$$

from which

$$\int \frac{dv}{v\sqrt{\alpha - \kappa v^2}} = (\xi - U\tau). \tag{230a}$$

If we put

$$w = \sqrt{1 - \frac{\kappa v^2}{\alpha}}, \tag{231}$$

(230a) leads to

$$\frac{1}{\sqrt{\alpha}} \int \frac{dw}{1 - w^2} = (\xi - U\tau), \tag{230b}$$

from which

$$\frac{1}{2} \ln \frac{1 - w}{1 + w} = \sqrt{\alpha}\,(\xi - U\tau). \tag{232}$$

If $\kappa > 0$, $\alpha > 0$, one obtains, from (232),

$$v = \sqrt{\frac{\alpha}{\kappa}}\, \operatorname{sech} \sqrt{\alpha}\,(\xi - U\tau), \tag{233}$$

which represents an envelope soliton (Figure 2.42) that propagates unchanged in shape and with constant velocity. The latter result arises because the nonlinearity and dispersion exactly balance each other – a result which turns out to be unique

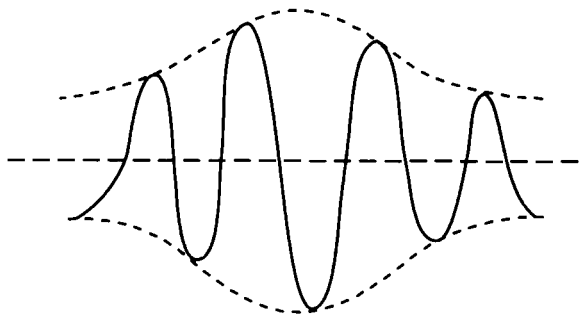

Figure 2.42. An envelope soliton.

to one–dimensional solutions. Further, if the wave energy is to move along with the above envelope, the latter must move near the group velocity u of the wave in question.

Note that this solution is possible only if modulational instability occurs, i.e., if $\kappa > 0$. This suggests that the end result of an unstable wavetrain subject to small modulations is a series of envelope solitons.

For nonlinear gravity waves in water, according to (208), one has

$$\frac{\partial \omega}{\partial a_0^2} > 0, \qquad \frac{\partial^2 \omega}{\partial k_0^2} < 0 \tag{234}$$

so that according to (222), such waves are unstable to small modulations. Indeed, careful experiments of Benjamin and Feir on waves in wavetanks showed that consequent to such a modulational instability, an originally almost uniform wavetrain degenerates into a series of wavegroups. Figure 2.43 shows the experimental traces of waveheight as a function of distances from the wave–making device at one end of the wavetank. At 200 feet the amplitude of the wave was almost uniform, while at 400 feet it was not.

It is found that the above modulational instabilities exhibit a nonergodic behavior in their long–time evolution. The numerical solution of the nonlinear Schrödinger equation (224) with periodic boundary conditions and with a modulationally unstable initial condition shows that (Lake et al.) a state of maximum modulation is reached by the unstable wave system. After that, the solution demodulates and eventually returns to an unmodulated state. This process is repeated in time. Thus, the end state is neither random (no thermalization) nor steady, but consists of a time–periodic spreading and regrouping of wave energy initially confined to carrier wavenumber and its linearly unstable harmonics and

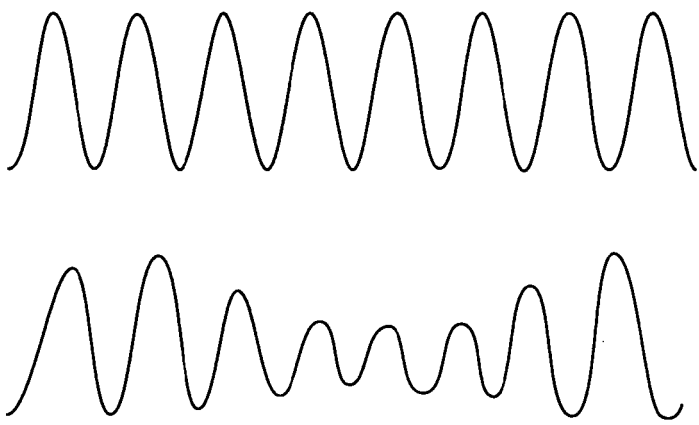

Figure 2.43. Experimental traces of wave height as a function of time. Upper trace: 200 feet from the wavemaker. Lower trace, 400 feet from the wavemaker (from Benjamin, 1967).

sidebands (Figure 2.44). This is similar to the Fermi–Pasta–Ulam recurrence observed in oscillations of an anharmonic lattice. This is due to the fact that the actively participating modes in this long–time evolution are few and clearly identifiable (with those which are modulationally unstable), and these linearly unstable modes nonlinearly evolve into a superperiodic state.

According to (222), a finite–amplitude uniform wavetrain is unstable to infinitesimal modulations with sufficiently long wavelengths while it is stable to modulations with short wavelengths so that a threshold for instability exists. The long–time behavior of the linearly unstable modulation near this threshold for instability shows that (Janssen) the nonlinear effects stabilize the linearly unstable modulations and produce a periodic motion. For this purpose, let us put

$$a = e^{-i\kappa|\phi_0|^2 t} + \phi \tag{235}$$

and first write equation (224) in the form

$$i\frac{\partial \phi}{\partial t} + \frac{1}{2}\frac{\partial^2 \phi}{\partial \xi^2} + \kappa\left(|\phi|^2 - |\phi_0|^2\right)\phi = 0. \tag{236}$$

In order to investigate the modulational instability of the wavetrain whose evolution is governed by equation (236), one puts

$$\phi = \rho^{1/2} e^{i\sigma}, \tag{237}$$

so that equation (236) gives

$$\rho_t + (\rho\sigma_x)_x = 0, \tag{238}$$

$$\sigma_t + \frac{1}{2}\sigma_x^2 + \frac{1}{8\rho^2}\rho_x^2 - \frac{1}{4\rho}\rho_{xx} - \kappa(\rho - \rho_0) = 0. \tag{239}$$

In order to perform the linear stability analysis, one puts next

$$\begin{pmatrix} \rho \\ \sigma \end{pmatrix} = \begin{pmatrix} \rho_0 \\ 0 \end{pmatrix} + \begin{pmatrix} \rho_1 \\ \sigma_1 \end{pmatrix} e^{i(Kx - \Omega t)}, \tag{240}$$

where K is the wavenumber and Ω is the frequency of the modulation. Assuming that $|\rho_1| \ll |\rho_0|$, and keeping only the terms linear in ρ_1 and σ_1, we obtain, from equations (238) and (239),

$$\Omega^2 = \frac{1}{4}K^2\left(K^2 - 4\kappa\rho_0\right). \tag{241}$$

Figure 2.44. Recurring modulation and demodulation of the wave envelope (from Lake et al., 1977).

Thus, if $\kappa > 0$, Ω^2 is negative for $|K| < \sqrt{4\kappa\rho_0}$.

We will now consider the nonlinear development of the initially linearly unstable modulation. For this purpose, we consider the initial–value problem for modulations with wavenumbers near the threshold for instability given by $K^2 = 4\kappa\rho_0$.

We look for a solution of the following form:

$$\left.\begin{aligned} \rho(x,t) &= \rho_0 + \varepsilon\rho_1(x,\tau) + \varepsilon^2\rho_2(x,\tau) + \cdots \\ \sigma(x,t) &= \varepsilon\sigma_1(x,\tau) + \varepsilon^2\sigma_2(x,\tau) + \cdots \\ K^2 &= 4\rho_0\kappa + \varepsilon^2\chi + \cdots, \end{aligned}\right\} \tag{242}$$

where ε is a small parameter that characterizes the departure of K^2 from the linear stability threshold value $4\rho_0\kappa$, and $\tau = \varepsilon t$ is a slow time scale characterizing slow time evolutions near the stability threshold. We have introduced an explicit detuning parameter χ in (242).

Substituting (242) into equations (238) and (239), we obtain the following systems of equations to various orders in ε:

$$O(\varepsilon^n): \quad L\begin{pmatrix}\rho_n \\ \sigma_n\end{pmatrix} = S_n\left(\rho_0, \rho_1, \ldots, \rho_{n-1}; \sigma_1, \ldots, \sigma_{n-1}\right), \quad n = 1, 2, \ldots, \tag{243}$$

where

$$L \equiv \begin{bmatrix} 0 & \rho_0 \dfrac{\partial^2}{\partial x^2} \\ \dfrac{1}{4}\dfrac{\partial^2}{\partial x^2} + \kappa\rho_0 & 0 \end{bmatrix}$$

and the function S_n depends on the solutions up to $O(\varepsilon^{n-1})$.

We obtain, from equation (243), to $O(\varepsilon)$:

$$L\begin{pmatrix}\rho_1 \\ \sigma_1\end{pmatrix} = 0 \tag{244}$$

the solution which corresponds to the neutrally stable case of the linear problem:

$$\left.\begin{aligned} \rho_1 &= A(\tau)e^{iKx} + \text{c.c.}, \\ \sigma_1 &= \alpha(\tau), \\ K^2 &= 4\rho_0\kappa, \end{aligned}\right\} \tag{245}$$

where c.c. means complex conjugate.

Using (241), we obtain, from equation (243), to $O(\varepsilon^2)$:

$$L\begin{pmatrix}\rho_2\\ \sigma_2\end{pmatrix}=\begin{bmatrix}-\dfrac{dA}{d\tau}e^{iKx}+\text{c.c.},\\ -\kappa|A|^2+\rho_0\dfrac{d\alpha}{d\tau}+\left\{-\dfrac{3}{2}\kappa A^2e^{2iKx}+\text{c.c.}\right\},\end{bmatrix} \tag{246}$$

from which

$$\left.\begin{aligned}\rho_2&=\frac{1}{\kappa}\frac{d\alpha}{d\tau}-|A|^2+\frac{A^2}{2\rho_0}e^{2iKx}+\text{c.c.},\\ \sigma_2&=\frac{1}{4\rho_0^2\kappa}\frac{dA}{d\tau}e^{iKx}+\text{c.c.}\end{aligned}\right\} \tag{247}$$

Using (245) and (247), we obtain, from equation (243), to $0(\varepsilon^3)$:

$$L\begin{pmatrix}\rho_3\\ \sigma_3\end{pmatrix}=\begin{bmatrix}-\dfrac{1}{\kappa}\dfrac{d^2\alpha}{d\tau^2}+\dfrac{d|A|^2}{d\tau}\\ \left\{\dfrac{1}{4\rho_0\kappa}\dfrac{d^2A}{d\tau^2}+\dfrac{1}{4}\chi A+\dfrac{\kappa}{2\rho_0}|A|^2A+\right.\\ \left.-2\kappa A^2\left(\dfrac{1}{\kappa}\dfrac{d\alpha}{d\tau}-|A|^2\right)\right\}e^{iKx}+\text{c.c.}\end{bmatrix}+\text{nonsecular terms.} \tag{248}$$

Removal of the secular terms in the first member of equation (248) requires

$$\frac{1}{\kappa}\frac{d\alpha}{d\tau}-|A|^2=\text{const.} \tag{249}$$

Let us take the constant above to be zero. Thus, removal of the secular terms in the second member of equation (248) then requires

$$\frac{d^2A}{d\tau^2}+\left(\rho_0\kappa\chi+2\kappa^2|A|^2A\right)=0. \tag{250}$$

If we impose the following initial conditions,

$$\tau=0:\quad A=\hat{A},\quad \frac{dA}{d\tau}=0, \tag{251}$$

and take A to be real, we obtain, from equation (250),

$$\left(\frac{dA}{d\tau}\right)^2=\kappa^2\left(\hat{A}^2-A^2\right)\left(A^2-\beta\right), \tag{252}$$

where

$$\beta\equiv-\frac{\rho_0\chi}{\kappa}-\hat{A}^2.$$

Equation (252) shows that A is bounded and oscillates between $\hat{A}$ and $\sqrt{\beta}$ if $\beta > 0$ and oscillates between 0 and $\hat{A}$ if $\beta < 0$. This demonstrates the nonlinear saturation of the linearly unstable modulation $(\chi < 0)$ near the linear–instability threshold.

Nonlinear Three–Wave Resonant Interactions of Capillary–Gravity Waves

When two waves with frequencies ω_3, ω_2 and wavevectors k_3, k_2 respectively, are present, the nonlinear terms in the equations of fluid flow may contain the product of the wave amplitudes, viz.,

$$e^{i(k_3-k_2)\cdot x - i(\omega_3-\omega_2)t},$$

which is a beat–frequency wave. If the frequency $\omega_3 - \omega_2 = \omega_1$ and the wave vector $\boldsymbol{k}_3 - \boldsymbol{k}_2 = \boldsymbol{k}_1$ of the beat happen to be a normal mode of the fluid, then this mode will be generated by the interaction of the first two waves. An exchange of energy and momentum takes place between these waves and the process is called *resonant wave interaction.* Thus, the interactions are selective in that only certain combinations of wave components are capable of significant energy exchange. Further, if the wave amplitudes are small, the interactions are weak because, even for the resonant combinations, the interaction time is large compared with a typical wave period. However, although the secondary interactions among wave components are given by a perturbation term that is algebraically smaller than that representing the primary interaction, their cumulative dynamical effect is much more pronounced because of the existence of resonant wavenumbers and frequencies with the concomitant growth in time of one or more of the wave amplitudes. The wave amplitudes show a slow modulation in time, with the modulation envelopes being given in terms of the Jacobian elliptic functions.

Consider an initially quiescent water of infinite depth whose mean surface level is given by $y = 0$. The water is assumed to be inviscid and is subjected to a gravity $\boldsymbol{g} = -g\boldsymbol{i}_y$ acting normal to the surface and directed toward the water. Let us consider the wave propagation to be two–dimensional. If $y = \eta(x,t)$ denotes the disturbed shape of the surface, one has the following boundary value problem:

$$y < \eta: \quad \phi_{xx} + \phi_{yy} = 0, \tag{253a}$$

$$y = \eta: \quad \phi_y = \eta_t + \phi_x \eta_x, \tag{254}$$

$$y = \eta: \quad \phi_t + \frac{1}{2}\left(\phi_x^2 + \phi_y^2\right) + g\eta - \frac{T}{\rho}\eta_{xx}\left(1+\eta_x^2\right)^{-3/2} = 0, \tag{255}$$

$$y \Rightarrow -\infty: \quad \phi_y \Rightarrow 0. \tag{256}$$

Let us now transfer the boundary conditions (254) and (255) from the actual location of the surface $y = \eta$ to the mean location of the surface $y = 0$. This is

accomplished by an expansion of $\phi(x,y,t)$ in Taylor's series about the values at $y=0$. Let us retain the nonlinearities only of quadratic order since we shall consider only the second–order interactions. The system (253)–(256) now becomes

$$y<0: \quad \phi_{xx}+\phi_{yy}=0, \tag{253b}$$

$$y=0: \quad \phi_y-\eta_t=-\phi_{yy}\eta+\phi_x\eta_x, \tag{257}$$

$$y=0: \quad \phi_t+g\eta-\frac{T}{\rho}\eta_{xx}=-\phi_{ty}\eta-\frac{1}{2}\left(\phi_x^2+\phi_y^2\right), \tag{258}$$

$$y\Rightarrow-\infty: \quad \phi_y\Rightarrow 0, \tag{256}$$

where the left–hand sides represent the linear problem and the right–hand sides contain the nonlinearities that produce the interaction between the waves.

Let us consider unidirectional wave propagation since this case is well suited for experimental verification, and consider waves of the form

$$\left.\begin{aligned}\phi(x,y,t)&\sim e^{ky-ikx},\\ \eta(x,t)&\sim e^{-ikx},\end{aligned}\right\} \tag{259}$$

where we have noted (253) and (256). Let us now introduce

$$a=\eta-\frac{ik}{\omega}\phi, \tag{260}$$

where

$$\omega^2=gk+\frac{T}{\rho}k^3.$$

Using the linear parts in (257) and (258), one then obtains

$$\frac{\partial a}{\partial t}=i\omega a, \tag{261}$$

so that a is a normal mode of the linearized problem associated with (253)–(256). When the nonlinear terms are included, one obtains, from (257) and (258),

$$\frac{\partial a}{\partial t}-i\omega a=\phi_{yy}\eta-\phi_x\eta_x+\frac{ik}{\omega}\left[\phi_{ty}\eta+\frac{1}{2}\left(\phi_x^2+\phi_y^2\right)\right]. \tag{262}$$

Let us now consider two capillary-gravity waves of the form $e^{i(\omega_3 t-k_3 x)}$ and $e^{i(\omega_2 t-k_2 x)}$ propagating in the x-direction with

$$\left.\begin{aligned}\omega_3^2&=gk_3+\frac{T}{\rho}k_3^3,\\ \omega_2^2&=gk_2+\frac{T}{\rho}k_2^3.\end{aligned}\right\}. \tag{263}$$

Due to nonlinear interaction between these two waves, let another capillary–gravity wave of the form $e^{i(\omega_1 t - k_1 x)}$, propagating in the x–direction, be excited such that

$$\omega_3 - \omega_2 = \omega_1, \qquad k_3 - k_2 = k_1.^{12} \tag{264}$$

For the linearized problem, one obtains

$$\left.\begin{aligned} \eta &= \frac{a}{2}, \\ \phi &= \frac{i\omega}{2k} a, \\ a &= a(t) e^{i(\omega t - kx)} + a^*(t) e^{-i(\omega t - kx)}, \end{aligned}\right\} \tag{265}$$

where $a(t)$ is a slowly varying function of time.

Using (265), equation (262) gives, upon keeping only the resonant terms [according to (264)] on its right hand side,

$$\frac{\partial a_3}{\partial t} - i\omega_3 a_3 = \frac{ik_3\omega_1\omega_2}{2\omega_3} a_1 a_2, \tag{266}$$

$$\frac{\partial a_2}{\partial t} - i\omega_2 a_2 = -\frac{ik_2\omega_3\omega_1}{2\omega_2} a_3 a_1^*, \tag{267}$$

$$\frac{\partial a_1}{\partial t} - i\omega_1 a_1 = -\frac{ik_1\omega_3\omega_2}{2\omega_1} a_3 a_2^*, \tag{268}$$

and in terms of the ϕ, equations (266)–(268) become

$$\frac{\partial \phi_3}{\partial \tilde{t}} = (k_1 k_2)\phi_1\phi_2 \tag{269}$$

$$\frac{\partial \phi_2}{\partial \tilde{t}} = -(k_3 k_1)\phi_3\phi_1^*, \tag{270}$$

$$\frac{\partial \phi_1}{\partial \tilde{t}} = -(k_3 k_2)\phi_3\phi_2^*, \tag{271}$$

where $\partial/\partial\tilde{t}$ characterizes only the slow variations in the amplitude suffered by the waves undergoing resonant interactions.

---

[12] It may be noted that whether or not solutions of (264) exist depends upon the form of the dispersion relation involved. Thus, it turns out that three-wave resonant interactions are not possible for deep-water gravity waves, which allow instead four-wave resonant interactions to occur with the concomitant matching conditions (Phillips:

$$\omega_1 + \omega_2 = \omega_3 + \omega_4,$$

$$k_1 + k_2 = k_3 + k_4.$$

For some prescribed initial values of the amplitudes of the three waves, equations (269)–(271) can be solved by quadratures and the general solution can be expressed in terms of Jacobi elliptic functions. As an illustration, let us consider a case wherein only the modes ϕ_1 and ϕ_2 are present initially, and mode ϕ_3 is then absent, i.e., let

$$t = t_0: \quad \phi_{1,2} = \phi_{1,2}^{(0)}, \quad \phi_3 = 0. \tag{272}$$

Equations (267)–(271) then indicate the generation and growth of the mode ϕ_3 at the expense of the modes ϕ_1 and ϕ_2.

One obtains, from equations (267)–(271)

$$\frac{d}{d\tilde{t}}\left(\frac{|\phi_1|^2}{k_2k_3} + \frac{|\phi_3|^2}{k_1k_2}\right) = 0$$

or

$$|\phi_1|^2 = |\phi_1^{(0)}|^2\left(1 - \frac{k_3}{k_1}\frac{|\phi_3|^2}{|\phi_1^{(0)}|^2}\right). \tag{273}$$

Similarly,

$$|\phi_2|^2 = |\phi_2^{(0)}|^2\left(1 - \frac{k_3}{k_2}\frac{|\phi_3|^2}{|\phi_2^{(0)}|^2}\right). \tag{274}$$

When one uses equations (273) and (274), equation (269) becomes

$$\left|\frac{\partial\phi_3}{\partial\tilde{t}}\right|^2 = |\phi_1^{(0)}|^2|\phi_2^{(0)}|^2 k_1^2k_2^2\left(1 - \frac{k_3}{k_1}\frac{|\phi_3|^2}{|\phi_1^{(0)}|^2}\right)\left(1 - \frac{k_3}{k_2}\frac{|\phi_3|^2}{|\phi_2^{(0)}|^2}\right), \tag{275}$$

from which

$$\phi_3 = \phi_2^{(0)}\sqrt{\frac{k_2}{k_3}}\, sn(\Sigma/m), \tag{276}$$

where

$$\left.\begin{aligned}\Sigma &= \phi_1^{(0)}k_1\sqrt{k_2k_3}\,(t - t_0),\\ m &= \frac{k_2|\phi_2^{(0)}|^2}{k_1|\phi_1^{(0)}|^2}.\end{aligned}\right\} \tag{277}$$

Let us assume that $m \le 1$. Noting that

$$\frac{\dfrac{\partial}{\partial \bar{t}}\left|\dfrac{\phi_1}{\phi_1^{(0)}}\right|^2}{\dfrac{\partial}{\partial \bar{t}}\left|\dfrac{\phi_2}{\phi_2^{(0)}}\right|^2} = \frac{k_2\left|\phi_2^{(0)}\right|^2}{k_1\left|\phi_1^{(0)}\right|^2} = m, \tag{278}$$

we may regard m as measuring the extent to which resonant partners participate in the interaction. In particular, $m \leq 1$ implies that the mode k_2 is decreasing at a rate faster than the mode k_1.

When we use equation (276), equations (273) and (274) give

$$\phi_2 = \phi_2^{(0)}\, cn(\Sigma/m), \tag{279}$$

$$\phi_1 = \phi_1^{(0)}\, dn(\Sigma/m). \tag{280}$$

Here, sn, cn, and dn are Jacobian elliptic functions with real parameter. The solutions (276), (279), and (280) represent a system for which energy is transferred around periodically among the three waves k_1, k_2, k_3. Initially, the energy in mode k_3 increases at the expense of both modes k_1 and k_2. Eventually, the energy in mode k_2 vanishes (since we have assumed the mode k_2 to decay at a faster rate than the mode k_1). Then, the direction of energy transfer is reversed, modes k_1 and k_2 now increase at the expense of the mode k_3 until the initial state is reached again, and this sequence of energy transfer repeats itself. The period of this energy transfer is

$$T_E = \frac{2K(m)}{k_1\sqrt{\left|\phi_1^{(0)}\right|^2 k_2 k_3}}, \tag{281}$$

where $K(m)$ is the complete elliptic integral of the first kind.

The case $k_1 = k_2 = \sqrt{g/2T} = k_3/2$, which corresponds to the second harmonic resonance, is a degenerate case of the triad resonances for which two members of the triad are identical, the closure being their second harmonic. Since $m = 1$ for this case and we have

$$m = 1: \quad K(m) \sim \ln \frac{2}{\sqrt{1-m}} \Rightarrow \infty, \tag{282}$$

the period of the energy transfer from (281) is infinite, and the interaction takes on an asymptotic character. Thus, (276), (279), and (280) become

$$\phi_3 = \phi_2^{(0)} \sqrt{\frac{k_2}{k_3}}\, \tanh \Sigma, \tag{283}$$

$$\phi_1 = \phi_1^{(0)}\, \operatorname{sech} \Sigma, \tag{284}$$

$$\phi_2 = \phi_2^{(0)}\, \operatorname{sech} \Sigma. \tag{285}$$

We will discuss the second-harmonic resonance in detail below.

Second-Harmonic Resonance

If a typical surface disturbance is characterized by a sinusoidal traveling wave with amplitude a' and wavelength λ', then let us nondimensionalize all physical quantities in the following with respect to a reference length $(\lambda'/2\pi)$ and a time $(\lambda'/2\pi g')^{1/2}$, where g' denotes the acceleration due to gravity; the primes here denote the dimensional quantities. The potential function of the motion of the liquid is taken to be $g'^{1/2}(\lambda'/2\pi)^{3/2}\phi$. If $y = \eta$ denotes the disturbed shape of the surface (whose mean level is given by $y = 0$), one has the following boundary-value problem:

$$y < \eta: \quad \phi_{xx} + \phi_{yy} = 0, \tag{286}$$

$$y = \eta: \quad \phi_y = \eta_t + \eta_x \phi_x, \tag{287}$$

$$\phi_t + \frac{1}{2}\left(\phi_x^2 + \phi_y^2\right) + \eta = k^2 \eta_{xx}\left(1 + \eta_x^2\right)^{-3/2}, \tag{288}$$

$$y \Rightarrow -\infty: \quad \phi_y \Rightarrow 0, \tag{289}$$

where

$$k^2 \equiv \left(\frac{2\pi}{\lambda'}\right)^2 \frac{T'}{\rho' g'}.$$

Let us look for traveling waves and introduce

$$\xi = x - ct, \tag{290}$$

so that (206)–(209) become

$$y < \eta: \quad \phi_{\xi\xi} + \phi_{yy} = 0, \tag{291}$$

$$y = \eta: \quad \phi_y = \left(\phi_\xi - c\right)\eta_\xi, \tag{292}$$

$$\eta = c\phi_\xi - \frac{1}{2}\left(\phi_\xi^2 + \phi_y^2\right) + k^2 \eta_{\xi\xi}\left(1 + \eta_\xi^2\right)^{-3/2}, \tag{293}$$

$$y \Rightarrow -\infty: \quad \phi_y \Rightarrow 0. \tag{289}$$

Seek solutions to (209), (211)–(213) of the form

$$\left.\begin{aligned} \phi(\xi, y; \varepsilon) &= \sum_{n=1}^{\infty} \varepsilon^n \phi_n(\xi, y), \\ \eta(\xi; \varepsilon) &= \sum_{n=1}^{\infty} \varepsilon^n \eta_n(\xi), \\ c(k; \varepsilon) &= \sum_{n=0}^{\infty} \varepsilon^n c_n(k), \\ k(\varepsilon) &= \sum_{n=0}^{\infty} \varepsilon^n k_n, \end{aligned}\right\} \tag{294}$$

where

$$\varepsilon \equiv a' \cdot \frac{2\pi}{\lambda'} \ll 1.$$

Using (294), one obtains from (289), (291)–(293) the following hierarchy of boundary–value problems:

$0(\varepsilon)$:

$$y < 0: \quad \phi_{1\xi\xi} + \phi_{1yy} = 0, \tag{295}$$

$$y = 0: \quad \phi_{1y} = -c_0 \eta_{1\xi}, \tag{296}$$

$$\eta_1 = c_1 \phi_{1\xi} + k_0^2 \eta_{1\xi\xi}, \tag{297}$$

$$y \Rightarrow -\infty: \quad \phi_{1y} \Rightarrow 0. \tag{298}$$

$0(\varepsilon^2)$:

$$y < 0: \quad \phi_{2\xi\xi} + \phi_{2yy} = 0, \tag{299}$$

$$y = 0: \quad \phi_{2y} + \phi_{1yy}\eta_1 = -c_0 \eta_{2\xi} + \left(\phi_{1\xi} - c_1\right)\eta_{1\xi}, \tag{300}$$

$$\eta_2 = c_0\left(\phi_{2\xi} + \phi_{1\xi y}\eta_1\right) - \frac{1}{2}\left(\phi_{1\xi}^2 + \phi_{1y}^2\right) + c_1\phi_{1\xi} + k_0^2\eta_{2\xi\xi} + 2k_0k_1\eta_{1\xi\xi}, \tag{301}$$

$$y \Rightarrow -\infty: \quad \phi_{2y} \Rightarrow 0. \tag{302}$$

$0(\varepsilon^3)$:

$$y < 0: \quad \phi_{3\xi\xi} + \phi_{3yy} = 0, \tag{303}$$

$$\begin{aligned} y = 0: \quad & \phi_{3y} + \phi_{2yy}\eta_1 + \phi_{1yy}\eta_2 + \frac{1}{2}\phi_{1yyy}\eta_1^2, \\ & = -c_0\eta_{3\xi} + \left(\phi_{1\xi} - c_1\right)\eta_{2\xi} + \left(\phi_{2\xi} + \phi_{1\xi y}\eta_1 - c_2\right)\eta_{1\xi}. \end{aligned} \tag{304}$$

$$\begin{aligned} \eta_3 = {} & c_0\left(\phi_{3\xi} + \phi_{2\xi y}\eta_1 + \phi_{1\xi y}\eta_2 + \frac{1}{2}\phi_{1\xi yy}\eta_1^2\right) \\ & + c_1\left(\phi_{2\xi} + \phi_{1\xi y}\eta_1\right) + c_2\phi_{1\xi} \\ & - \phi_{1\xi}\left(\phi_{2\xi} + \phi_{1\xi y}\eta_1\right) - \phi_{1y}\left(\phi_{2y} + \phi_{1yy}\eta_1\right) + k_0^2\eta_{3\xi\xi} \\ & + 2k_0k_1\eta_{2\xi\xi} + 2k_0k_2\eta_{1\xi\xi} - \frac{3}{2}k_0^2\eta_{1\xi\xi}\eta_{1\xi}^2, \end{aligned} \tag{305}$$

$$y \Rightarrow -\infty: \quad \phi_{3y} \Rightarrow 0. \tag{306}$$

Let

$$\eta_1 = A\cos\xi. \tag{307}$$

Then, from (295)–(298), one obtains

$$\phi_1(\xi, y) = Ac_0 e^y \sin\xi, \tag{308}$$

$$c_0^2 = 1 + k_0^2. \tag{309}$$

Next, letting

$$\eta_2 = B\cos 2\xi \tag{310}$$

and using (307)–(310), one then obtains, from (299), (300), and (302),

$$\phi_2(\xi, y) = c_0\left(B - \frac{A^2}{2}\right) e^{2y} \sin 2\xi + c_1 A e^y \sin\xi. \tag{311}$$

Using (307)–(311), one finds that the removal of secular terms in (301) requires

$$k_1 = c_1 = 0 \tag{312}$$

and then

$$B = \frac{c_0^2}{2\left(1 - 2k_0^2\right)} A^2. \tag{313}$$

The case $k_0 = \pm\sqrt{1/2}$, where the above solution breaks down, corresponds to the second–harmonic resonance, which we shall treat shortly.

Using (307)–(313), one obtains, from (303), (304), and (306),

$$\phi_3(\xi, y) = A\left[-c_0 A^2\left(\frac{c_0^2/4}{1 - 2k_0^2} + \frac{3}{8}\right) + c_2\right] e^y \sin\xi + \text{higher harmonics}. \tag{314}$$

Using (307)–(314), one finds that the removal of secular terms in (305) requires

$$c_2 = \frac{c_0}{2}\left(\frac{c_0^2/2}{1 - 2k_0^2} + \frac{1}{2} - \frac{3}{8}\frac{k_0^2}{c_0^2}\right) A^2, \qquad k_2 = 0, \tag{315}$$

which is again not valid for $k_0 = \pm\sqrt{1/2}$.

In order to treat the case of second–harmonic resonance, wherein $k = \pm\sqrt{1/2}$, first note that for this case, the fundamental component

$$\left.\begin{aligned} \eta_1^{(1)} &= A\cos\xi, \\ \phi_1^{(1)} &= Ac_0 e^y \sin\xi \end{aligned}\right\}$$

and its second harmonic

$$\left.\begin{aligned} \eta_1^{(2)} &= \hat{B}\cos 2\xi, \\ \phi_1^{(2)} &= \hat{B}c_0 e^{2y} \sin 2\xi \end{aligned}\right\}$$

have the same linear wave velocity c_0, so that the two can interact resonantly with each other. In order to treat this nonlinear resonant interaction, put

$$\eta_1 = A\cos\xi + \hat{B}\cos 2\xi, \tag{316}$$

$$\phi_1 = c_0\left(Ae^{y}\sin\xi + \hat{B}e^{2y}\sin 2\xi\right). \tag{317}$$

Using (316) and (317), one obtains, from (299), (300), and (302),

$$\phi_2(\xi, y) = \left(-\frac{3A\hat{B}}{2}c_0 + Ac_1\right)e^{y}\sin\xi$$

$$+\left(-A^2c_0 + 2\hat{B}c_1\right)\frac{1}{2}e^{2y}\sin 2\xi + \text{ higher harmonics.} \tag{318}$$

Using (316)–(318), one finds that the removal of secular terms in (301) requires

$$-c_0^2\hat{B} + 2c_0c_1 - 2k_0k_1 = 0, \tag{319}$$

$$-\frac{1}{2}c_0^2A + 4c_0\hat{B}c_1 - 8k_0k_1\hat{B} = 0, \tag{320}$$

from which

$$\hat{B} = \frac{k_0k_1}{c_0^2} \pm \sqrt{\frac{A^2}{4} - c_0^2k_1^2}, \tag{321}$$

$$c_1 = \frac{k_1\left(3k_0 + c_0^2/k_0^2\right)}{2c_0} \pm \frac{c_0}{2}\sqrt{\frac{A^2}{4} - c_0^2k_1^2}, \tag{322}$$

which show that purely phase–modulated waves are possible for wavenumbers near the second–harmonic resonant values.

Hydraulic Jump

Flow in a channel downstream of a sluice gate experiences a sudden transition from a supercritical ($V > \sqrt{gh}$, where h is the water depth) flow to a subcritical $\left(V < \sqrt{gh}\right)$ flow. Under these conditions, infinitesimal disturbances cannot travel upstream, but finite disturbances can travel with a speed equal to V to make a stationary jump possible. The free surface rises sharply and is usually covered with a mass of foam beneath which there is a violent turbulent motion; this is called a hydraulic jump, which is analogous to a shock wave in supersonic gas flows (see Section 3.3). The relations between the values of the flow variables on either side of the discontinuity can be obtained from the conditions of continuity of fluxes of mass and momentum. The mass flux density is ρVh. The momentum flux density is

$$\int_0^n \left(p + \rho V^2\right)dz = \rho V^2h + \frac{1}{2}\rho gh^2, \tag{323}$$

where we have noted that for a shallow water $p = \rho gz$. If the states upstream and downstream of the discontinuity are denoted by subscripts 1 and 2, then one has the following conditions:

$$V_1 h_1 = V_2 h_2, \tag{324}$$

$$V_1^2 h_1 + \frac{1}{2} g h_1^2 = V_2^2 h_2 + \frac{1}{2} g h_2^2. \tag{325}$$

The energy fluxes on the two sides of the discontinuity are not the same, and their difference accounts for the rate of energy dissipated in the discontinuity. The energy flux density is

$$\int_0^h \left(p + \frac{1}{2} V^2 \right) \rho V \, dz = \frac{1}{2} \rho V_1 h_1 \left(gh + V^2 \right), \tag{326}$$

so that its drop is

$$\frac{\rho V_1 h_1}{4 h_1 h_2} \left(h_1^2 + h_2^2 \right) \left(h_2 - h_1 \right).$$

Thus, $h_2 > h_1$, or the liquid attains a higher surface level across such a jump.

The Froude numbers $F \equiv V/\sqrt{gh}$ upstream and downstream of the jump are given by

$$\left.\begin{aligned} F_1 &= \frac{V_1}{\sqrt{g h_1}} = \frac{\sqrt{(h_1 + h_2) h_2}}{\sqrt{2}\, h_1}, \\ F_2 &= \frac{V_2}{\sqrt{g h_2}} = \frac{\sqrt{(h_1 + h_2) h_1}}{\sqrt{2}\, h_2}. \end{aligned}\right\} \tag{327}$$

Thus the result $h_2 > h_1$ then gives

$$F_1 > 1 \text{ and } F_2 < 1, \tag{328}$$

as with the Mach numbers upstream and downstream of the shock wave in supersonic gas flows (see Section 3.3).

EXERCISES

1. Show that the wavelength λ of stationary waves on a stream of depth h and flow speed U is given by

$$U^2 = \frac{g\lambda}{2\pi} \tan h \frac{2\pi h}{\lambda}$$

and hence deduce that such stationary waves exist provided that $U < \sqrt{gh}$.

2. Show that the semivertex angle of the shipwave pattern is 19.5° by merely in invoking the fact that the ratio of the group velocity and the phase velocity for deep–water waves is 1/2.

3. The linear dispersion relation $\omega^2 = gk$ for gravity waves in deep water can be generalized to the two–dimensional case by interpreting k as the magnitude of the wavevector $\boldsymbol{k} = (\ell, m)$. This leads to the nonlinear dispersion relation

$$\omega^2 = g\sqrt{\ell^2 + m^2} + \frac{1}{2}\sqrt{g}\left(\ell^2 + m^2\right)^{5/4} a^2.$$

Expanding this about $\boldsymbol{k}_0 = (k_0, 0)$ with perturbation (k_1, k_2), show that

$$\omega = \omega_0 + \frac{\omega_0}{2k_0} k_1 - \frac{\omega_0}{8k_0^2} k_1^2 + \frac{\omega_0}{4k_0^2} k_2^2 + \frac{1}{2}\omega_0 k_0^2 a^2$$

where $\omega_0 = \sqrt{gk_0}$. Show that this relation, then, leads, to the following nonlinear Schrödinger equation describing the evolution of the two–dimensional modulated gravity waves (Zakharov):

$$i\left(\frac{\partial a}{\partial t} + \frac{\omega_0}{2k_0}\frac{\partial a}{\partial x}\right) - \frac{\omega_0}{8k_0^2}\frac{\partial^2 a}{\partial x^2} + \frac{\omega_0}{4k_0^2}\frac{\partial^2 a}{\partial y^2} - \frac{1}{2}\omega_0 k_0^2\left(|a|^2 - |a_0|^2\right)a = 0.$$

Investigate the stability of the three–dimensional modulations by putting

$$a = \left[\rho(\xi, \eta, t)\right]^{1/2} e^{i\sigma(\xi,\eta,t)}, \quad \xi = x - \frac{\omega_0}{2k_0}t, \eta = y,$$

$$\rho = \rho_0 + \rho_1(\xi, \eta, t), \quad \sigma = \sigma_1(\xi, \eta, t),$$

$$\rho_1(\xi, \eta, t) \text{ and } \sigma_1(\xi, \eta, t) \sim e^{i(K_1\xi + K_2\eta - \Omega t)};$$

and by linearizing in ρ_1 and σ_1, show that the growth rate Ω is given by

$$\Omega^2 = \frac{\omega_0}{8k_0^2}\left(K_1^2 - 2K_2^2\right)\left(\frac{K_1^2}{8k_0^2} - \frac{K_2^2}{4k_0^2} - k_0^2|a_0|^2\right),$$

which shows that the instability region for three–dimensional modulations, unlike that for two–dimensional modulations, is unbounded in (K_1, K_2)–space!

2.7. Applications to Aerodynamics

We shall now deal with the aerodynamic forces which act on a lifting surface in flight. This information is required for performance and structural–strength calculations or, in the unsteady case, for purposes of stability and control.

Though ideal–fluid aerodynamics assumes that the fluid is inviscid, it does recognize and account for the gross features of the flow which would not be present if the fluid were truly inviscid.[13] The circulation about an airfoil, the Kutta condition, and the shedding of free vorticies at the trailing edge of the wing whenever the circulation varies along the wing span are cases in point. One may assume that the viscous processes involving boundary–layer separation and the shedding of vortices into the flow occur so rapidly upon a change of flow conditions that the Kutta condition at the trailing edge can be taken to be satisfied at each instant. The success of the two–dimensional airfoil theory for unsteady flows (e.g., flows over oscillating airfoils) where one supposes the vorticity in the wake to be concentrated into a plane vortex sheet, adjusting itself with zero delay time to the requirement of smooth flow at the trailing edge, indicates that such adjustment is, in fact, very rapid.

Airfoil Theory: Method of Complex Variables

Consider a wing of infinite aspect ratio, whose generators are parallel to the z–axis. The cross section of the wing is the same in all planes parallel to the x, y–plane, and it will therefore suffice to consider the conditions in that plane only. Since the third dimension z no longer appears, z may be reassigned to mean something else, as in the following.

Force and Moments on an Arbitrary Body

In a classical approach the force exerted on a fluid by a moving body is calculated by first calculating the momentum in the fluid and then differentiating the latter with respect to time. This method fails when applied to bodies in uniform steady motion because the fluid would have then received an infinite momentum from the constant force acting on it for an infinite time. A more workable approach is to calculate the forces in steady motion by integration of the pressures on the moving body.

THEOREM (*Blasius*): Let C be a simple closed curve in R^2 which constitutes the trace of an arbitrary body in the x, y–plane (Figure 2.45). Let $\mathbf{v}$ be a steady two–dimensional velocity field defined on the exterior of C such that $\mathbf{v}$ is parallel to C on C. The force exerted by the fluid on the body is given by

$$X - iY = \frac{i\rho}{2} \oint_C [W(z)]^2 \, dz, \tag{1}$$

where

$$W(z) = Ve^{-i\theta}, \qquad z = x + iy.$$

Proof: We have, on using the Bernoulli integral,

---

[13] In an attached flow past a wing, the viscous effects are actually confined to a thin boundary layer adjacent to the wing surface and the wake. The presence of the boundary layer changes the effective cross section of the wing, and therefore, it influences the pressure distribution over the

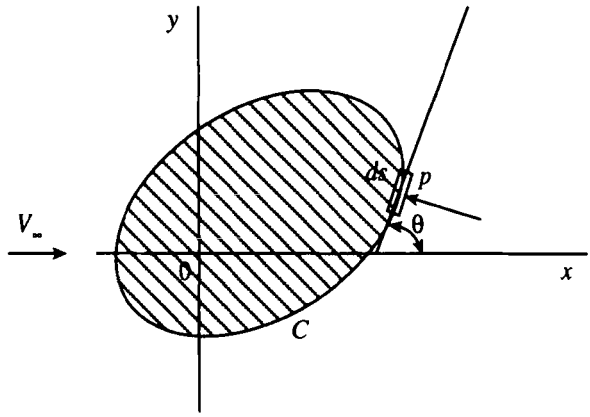

Figure 2.45. Force exerted by a fluid on a body.

$$X - iY = \int_C p(-dy - idx) = \frac{\rho}{2} \int_C (u^2 + v^2)(idx + dy)$$

$$= \frac{i\rho}{2} \int_C (u - iv)^2 (dx + idy) = \frac{i\rho}{2} \int_C [W(z)]^2 \, dz,$$

where we have noted that $\mathbf{v}$ on C is parallel to C so that $u\,dy = v\,dx$.

The moment about 0, exerted by the fluid on the body, is given by

$$M = \oint_C p(-y \sin\theta + x \cos\theta)\, ds = -\frac{\rho}{2} \operatorname{Re} \oint_C [W(z)]^2 \, z\, dz, \tag{2}$$

where the moment M is reckoned positive when clockwise.

Using Cauchy's integral Theorem, the integration may be carried out around an infinitely large circle S enclosing C, provided that there are no singularities between S and C.

As an example, consider the flow with velocity V_∞ in the x–direction and a clockwise circulation Γ past a cylinder of arbitrary cross section. Then, $W(z)$ is regular except possibly at or inside the contour of the body. Therefore, it can be expanded into a Laurent series

$$W(z) = \sum_{n=0}^{\infty} \frac{A_n}{z^n}, \tag{3}$$

where

$$A_0 = V_\infty, \qquad A_1 = -\frac{i\Gamma}{2\pi}.$$

Thus,

$$[W(z)]^2 = \sum_{n=0}^{\infty} \frac{B_n}{z^n}, \tag{4}$$

---

wing. However, the inviscid theory affords the correct first approximation for most of the flow field, provided that the flow remains attached over most of the airfoil.

where

$$B_0 = A_0^2, \quad B_1 = 2A_0A_1, \quad B_2 = A_1^2 + 2A_0A_2, \ldots.$$

Using (4), (1) gives the following equation for the forces exerted by the fluid on the body:

$$X - iY = \frac{i\rho}{2} \cdot 2\pi i B_1 = i\rho V_\infty \Gamma; \tag{5a}$$

thus the lift is given, as before, by

$$Y = \rho V_\infty \Gamma. \tag{5b}$$

Next, using (4), (2) gives the following equation for the moment, about 0, exerted by the fluid on the body:

$$M = -\frac{\rho}{2} \operatorname{Re}(2\pi i B_2) = -2\rho V_\infty \operatorname{Re}(iA_2). \tag{6}$$

Flow Past an Arbitrary Cylinder

In order to calculate flow past an arbitrary cylinder, one first writes down the complex potential of the flow past a circular cylinder in an auxiliary ζ-plane and then tries to find a suitable complex transformation that maps the region outside the circle onto the region outside the cross section of the given cylinder (Figure 2.46). Such a transformation is possible only when referred to axes fixed in the interior boundaries.

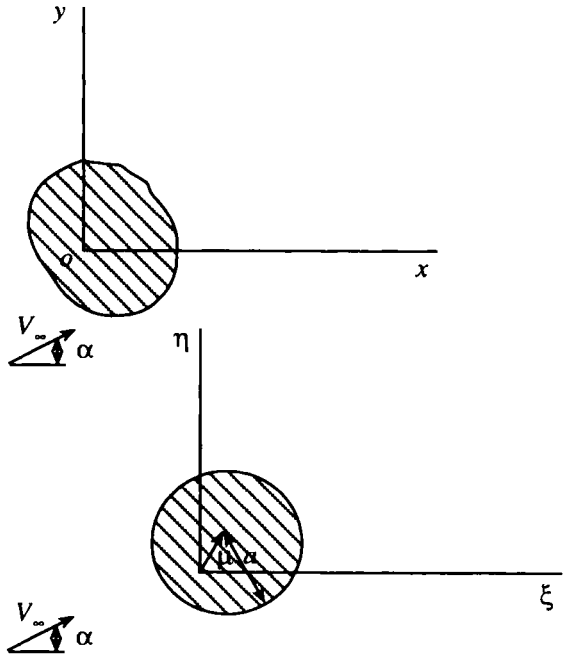

Figure 2.46. Conformal mapping of a flow past an arbitrary cylinder on to a flow past a circular cylinder.

From the relation

$$\tilde{W}(\zeta)=\frac{W(z)}{d\zeta/dz} \tag{7}$$

and the condition that the flow upstream infinity, for the two cases, is the same, one requires, for the transformation $\zeta=\zeta(z)$,

$$\zeta\Rightarrow\infty:\quad \frac{d\zeta}{dz}\Rightarrow 1. \tag{8}$$

Thus, this transformation changes the shape of the interior boundary and the flow in its neighborhood. Noting that $z(\zeta)$ is an analytic function everywhere in the region in the ζ–plane outside the circle of radius a and satisfies (8), one may write

$$z=\zeta+\sum_{n=1}^{\infty}\frac{C_n}{\zeta^n}, \tag{9}$$

from which

$$\frac{dz}{d\zeta}=1-\sum_{n=1}^{\infty}\frac{nC_n}{\zeta^{n+1}}$$

or

$$\frac{1}{dz/d\zeta}\approx 1+\sum_{n=1}^{\infty}\frac{nC_n}{\zeta^{n+1}}. \tag{10}$$

For the flow in the ζ–plane, one has, for the complex potential,

$$\hat{F}(\hat{\zeta})=V_\infty\left(\hat{\zeta}+\frac{a^2}{\hat{\zeta}}\right)+\frac{i\Gamma}{2\pi}\ln\frac{\hat{\zeta}}{a}, \tag{11}$$

where, referring to Figure 2.46, one has

$$\hat{\zeta}=(\zeta-\mu)e^{-i\alpha},$$

where α is the angle of attack. Thus,

$$\tilde{F}(\zeta)=V_\infty(\zeta-\mu)e^{-i\alpha}+\frac{i\Gamma}{2\pi}\ln\frac{(\zeta-\mu)}{ae^{i\alpha}}+V_\infty\frac{a^2e^{i\alpha}}{\zeta-\mu}, \tag{12}$$

from which

$$\tilde{W}(\zeta)=\frac{d\tilde{F}}{d\zeta}=V_\infty e^{-i\alpha}+\frac{i\Gamma}{2\pi}\frac{1}{(\zeta-\mu)}-\frac{V_\infty a^2e^{i\alpha}}{(\zeta-\mu)^2}. \tag{13}$$

Using the expansions

$$\left.\begin{aligned}\frac{1}{\zeta-\mu}&=\frac{1}{\zeta}+\frac{\mu}{\zeta^2}+\frac{\mu^2}{\zeta^3}+\cdots,\\ \frac{1}{(\zeta-\mu)^2}&=\frac{1}{\zeta^2}+\frac{2\mu}{\zeta^3}+\cdots,\end{aligned}\right\}$$

(13) may be written as

$$\tilde{W}(\zeta)=A_0+\frac{A_1}{\zeta}+\frac{A_2}{\zeta^2}+\cdots, \tag{14}$$

where

$$A_0=V_\infty e^{-i\alpha},$$

$$A_1=\frac{i\Gamma}{2\pi},$$

$$A_2=\frac{i\Gamma}{2\pi}\mu-V_\infty a^2 e^{i\alpha},$$

etc.

Thus,

$$\left[\tilde{W}(\zeta)\right]^2=B_0+\frac{B_1}{\zeta}+\frac{B_2}{\zeta^2}+\cdots, \tag{15}$$

where

$$B_0=A_0^2=V_\infty^2 e^{-2i\alpha},$$

$$B_1=2A_0A_1=\frac{i\Gamma}{\pi}V_\infty e^{-i\alpha},$$

$$B_2=\left(2A_0A_2+A_1^2\right)=\frac{iV_\infty e^{-i\alpha}\mu\Gamma}{\pi}-2V_\infty^2 a^2-\frac{\Gamma^2}{4\pi^2},$$

etc.

When we use (7) and (15), (1) gives, for the lift,

$$\mathbb{L}=\rho V_\infty \Gamma \tag{16}$$

and (2) gives, for the moment about 0,

$$\begin{aligned}M_0&=-\frac{\rho}{2}\mathrm{Re}\left[2\pi i\left(2B_0C_1+B_2\right)\right]\\ &=\mathrm{Re}\left(\mathbb{L}\mu e^{-i\alpha}-i2\pi\rho V_\infty^2 C_1 e^{-2i\alpha}\right).\end{aligned} \tag{17}$$

When we put

$$\mu=me^{i\delta},\qquad C_1=\xi^2 e^{2i\gamma}, \tag{18}$$

(17) becomes

$$M_0=\mathbb{L}m\cos\left(\delta-\alpha\right)+2\pi\rho V_\infty^2\xi^2\sin 2\left(\gamma-\alpha\right). \tag{19}$$

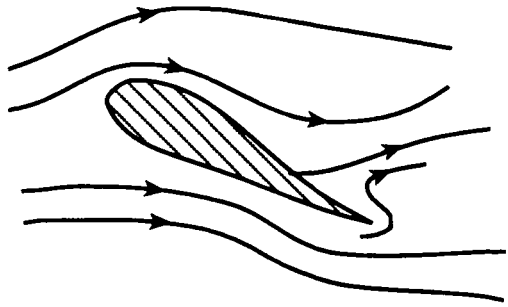

Figure 2.47. Flow near the trailing edge of an airfoil.

Flow Around a Flat Plate

The flow past an airfoil at an angle of attack (see Figure 2.47) near the trailing edge resembles that around a flat plate (see Figure 2.48). One has, for the latter (see Section 2.2),

$$W(z) = Az^{1/2}, \tag{20}$$

from which

$$\Psi = Ar^{1/2} \sin\frac{\theta}{2}. \tag{21}$$

It turns out that the very low pressure near the sharp edge produces a nonzero total force on the boundary. One may see this by calculating the force on a boundary coinciding with a streamline $\Psi = \Psi_0$ (which is a parabola) and then allowing $\Psi_0 \Rightarrow 0$. The total force exerted by the fluid on the finite portion of this boundary lying within the circle $r = R$, say, is parallel to the x–axis $(\theta = 0)$ by symmetry, and the x–component is

$$F_x = \int p\, dy, \tag{22}$$

with the integral being taken over the section of the curve defined by

$$Ar^{1/2} \sin\frac{\theta}{2} = \Psi_0 \quad \text{or} \quad y = 2\left(\frac{\Psi_0}{A}\right)^2 \cot\frac{\theta}{2} \tag{23}$$

that lies between $\theta = \varepsilon$ and $\theta = 2\pi - \varepsilon$, where

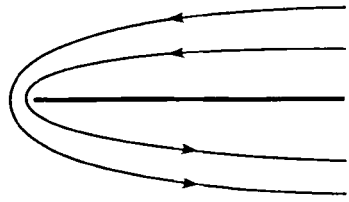

Figure 2.48. Flow around a flat plate.

$$\sin\frac{\varepsilon}{2} = \frac{\Psi_0}{Ar^{1/2}}.$$

Using the Bernoulli integral, we obtain

$$p = p_0 - \rho\frac{\partial\Phi}{\partial t} - \frac{1}{2}\rho|\nabla\Phi|^2 \tag{24}$$

Thus, (22) gives

$$F_x = \int_{\varepsilon}^{2\pi-\varepsilon}\left(p_0 - \rho\frac{A^4}{8\Psi_0^2}\sin^2\frac{\theta}{2}\right)\frac{\Psi_0^2}{A^2}\operatorname{cosec}^2\frac{\theta}{2}\,d\theta,$$

from which

$$F_x \sim -\frac{1}{4}\pi\rho A^2 \quad \text{as} \quad \varepsilon \Rightarrow 0, \tag{25}$$

which represents a suction force concentrated at the sharp trailing edge and parallel to the plate and pointing upstream. The effect of this suction force is to make the drag force on the plate zero, while the latter still experiences a lift even though the existence of a lift would imply the existence of a drag because the pressure on either side of the plate acts in a direction normal to the plate.

Flow Past an Airfoil

For an airfoil with a sharp trailing edge, the angle ψ_z at the trailing edge is not equal to ψ_ζ at the corresponding point on the circle in the ζ–plane (see Figure 2.49), so that the mapping is not conformal at the trailing edge. If the first $(n-1)$ derivatives of the transformation function $z = z(\zeta)$ vanish at $\zeta = \zeta_T$, then, since $\psi_\zeta = \pi$, one has

$$\psi_z = n\pi,$$

so that

$$\tau = 2\pi - n\pi = \pi(2-n) \approx 0$$

gives

$$n = 2.$$

Therefore,

$$\zeta = \zeta_T : \frac{dz}{d\zeta} = 0. \tag{26}$$

For an airfoil with a sharp cusped trailing edge aligned parallel to the direction of motion of the airfoil, the flow separation at the rear of the airfoil caused by the presence of a stagnation point there would be reduced so that the streams of fluid on the two sides would flow toward the sharp edge and join there smoothly. If the stagnation point is not located at the sharp edge itself but is located, instead, on the upper surface, flow occurs around it with infinite velocity and experiences an

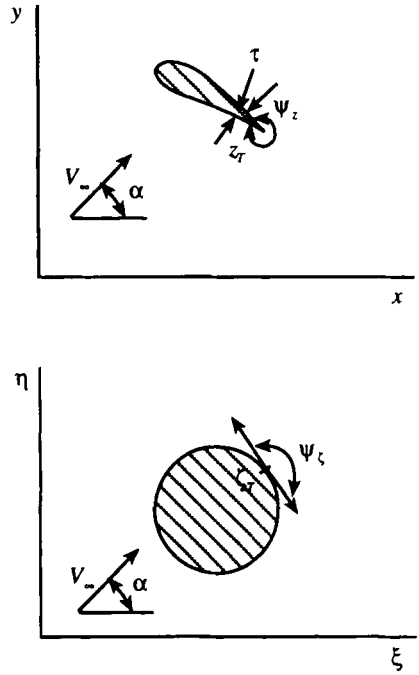

Figure 2.49. Conformal mapping of the flow near the trailing edge of an airfoil (from Karamcheti, 1966).

enormous adverse pressure gradient so that boundary–layer separation (see Section 4.3) and vorticity shedding occur at the trailing edge which continue until the stagnation point has moved to the trailing edge. These transient flow adjustments brought about by viscous effects (!) occur rapidly, and one ultimately has a steady flow with the flow velocity finite and tangential to the airfoil at the trailing edge; this is called the *Kutta condition.*[14] From (26) and (7), this requires

$$\zeta = \zeta_T: \quad \tilde{W}(\zeta) = 0. \tag{27}$$

Using (13), (27) gives

$$\Gamma = 4\pi a V_\infty \sin(\alpha + \beta), \tag{28}$$

where

$$\zeta_T - \mu = ae^{-i\beta},$$

[14]However, for a flat plate airfoil, the velocity at the leading edge remains infinite. In designing an airplane wing section, it is, therefore, necessary to round off the leading edge to reduce the velocity there. However, it is desirable to sharpen the trailing edge since this reduces the size of the wake and reduces the drag in a real fluid.

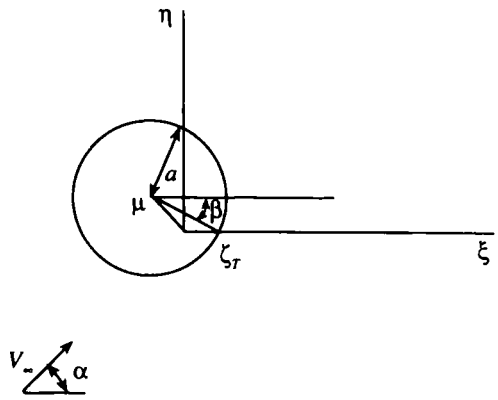

Figure 2.50. Flow past a circular cylinder in the mapped ζ-plane (from Karamcheti, 1966).

which is represented in Figure 2.50. Equation (27) implies that the circulation setup around an airfoil should be of a strength just sufficient to make the flow leave the airfoil smoothly at the trailing edge. Thus, for uniform irrotational flow past an airfoil with a sharp trailing edge there is just one value of the circulation Γ, for which the velocity is finite everywhere. The starting process by which this circulation is generated involves shedding of vorticity into the fluid. This may be seen by applying Kelvin's circulation Theorem (see Section 2.1) to a closed path enclosing the initial position and the present position of the airfoil and noting that the circulation around this path must remain zero. As a result, a starting vortex, of opposite sense to the circulation round the airfoil, is left at the place from which it started. If the viscous effects are negligible, the starting vortex would remain there forever!

Now, from (19), the moment about any point z is given by

$$M_z = M_\mu + \mathbb{L} h \cos(\varphi - \alpha), \tag{29a}$$

where

$$\left.\begin{aligned} M_\mu &= -2\pi\rho V_\infty^2 \xi^2 \sin 2(\gamma - \alpha) \\ z - \mu &= he^{i\varphi} \end{aligned}\right\}.$$

Using (16) and (28), (29a) may be written as

$$M = 2\pi\rho V_\infty^2 \xi^2 \left[\sin 2(\alpha - \gamma) - \frac{ah}{\xi^2}\left\{\sin(\beta + \varphi) + \sin(2\alpha + \beta - \varphi)\right\}\right]. \tag{29b}$$

Equation (29b) shows that the aerodynamic center, i.e., the point about which the moment is independent of the angle of attack, is given by

$$h = \frac{\xi^2}{a}, \qquad \varphi = \beta + 2\gamma \tag{30}$$

and that the moment about the aerodynamic center is given by

$$M_{AC} = 2\pi\rho V_\infty^2 \xi^2 \sin 2(\gamma + \beta), \tag{31}$$

which can be verified, from (19), to be the same as that corresponding to zero lift, as indeed it must be.

The Joukowski Transformation

In order to generate airfoil–like profiles from a circle, one considers a transformation

$$z = \zeta + \sum_{n=1}^{\infty} \frac{C_n}{\zeta^n}, \tag{9}$$

from which

$$\frac{dz}{d\zeta} = 1 - \frac{C_1}{\zeta^2} - \frac{2C_2}{\zeta^3} + \cdots.$$

If one writes

$$\frac{dz}{d\zeta} = \left(1 - \frac{\zeta_1}{\zeta}\right)\left(1 - \frac{\zeta_2}{\zeta}\right)\cdots\left(1 - \frac{\zeta_k}{\zeta}\right),$$

then one has, on comparison,

$$\sum_{i=1}^{k} \zeta_i = 0.$$

The Joukowski transformation is given by

$$\frac{dz}{d\zeta} = \left(1 - \frac{\zeta_T}{\zeta}\right)\left(1 + \frac{\zeta_T}{\zeta}\right) = 1 - \frac{\zeta_T^2}{\zeta^2}, \tag{32}$$

so that

$$z = \zeta + \frac{\zeta_T^2}{\zeta} = \zeta + \frac{C^2}{\zeta}, \text{ say.} \tag{33}$$

The inverse of equation (33) is

$$\zeta = \frac{1}{2} z + \sqrt{\frac{1}{4} z^2 - C^2}$$

which shows that there are branch points at $z = \pm 2C$. In order to eliminate the multivalued nature of the above expression, we cut the z–plane along the real axis between $z = -2C$ and $z = 2C$, and interpret $\sqrt{1/4\, z^2 - C^2}$ as meaning that branch of the function, which behaves like $1/2\, z$ as $|z| \Rightarrow \infty$. The latter ensures that $\zeta \sim z$ as $|z| \Rightarrow \infty$.

Note that the transformation (33) maps the circle $\zeta = Ce^{i\theta}$ into the strip $-2C \le x \le 2C$. Thus, one generates a flat–plate airfoil (see Figure 2.51) by putting $\mu = 0$, $C = a$, and $\beta = 0$.

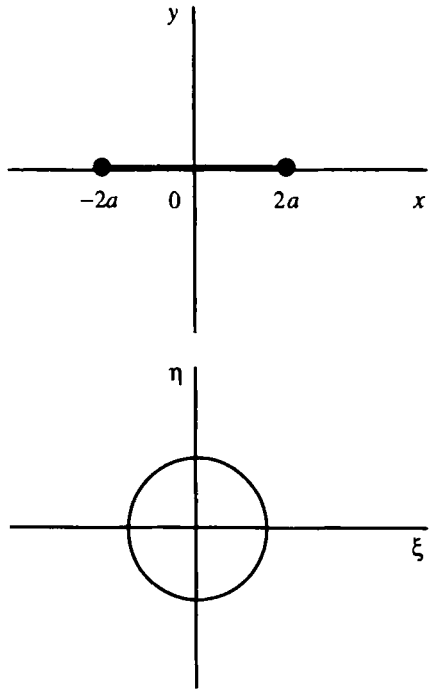

Figure 2.51. Conformal mapping of a strip on to a circle.

Equation (13) then becomes

$$\tilde{W}(\zeta) = V_\infty e^{-i\alpha} + \frac{i\Gamma}{2\pi\zeta} - \frac{V_\infty a^2 e^{i\alpha}}{\zeta^2}, \tag{34}$$

where

$$\Gamma = 4\pi a V_\infty \sin\alpha.$$

Then (7) gives

$$W(z) = \frac{V_\infty e^{-i\alpha} + \dfrac{i\Gamma}{2\pi\zeta} - \dfrac{V_\infty a^2 e^{i\alpha}}{\zeta^2}}{1 - C^2/\zeta^2} \tag{35}$$

and on the plate, (35) becomes

$$W(z) = \frac{[\sin\alpha - \sin(\alpha - \theta)]}{\sin\theta} V_\infty = \frac{V_\infty \cos\left(\alpha - \dfrac{\theta}{2}\right)}{\cos\dfrac{\theta}{2}}. \tag{36}$$

Noting that

$$x = 2C\cos\theta \tag{37}$$

from (36), the stagnation points on the plate are given by

$$\frac{x^2}{4C} - \frac{x\sin^2\alpha}{C} + \left(\sin^2\alpha - \cos^2\alpha\right) = 0. \tag{38}$$

The velocity at the trailing edge, from (36), is given by

$$W = V_\infty \cos\alpha.$$

From (30), the aerodynamic center is at 1/4 of the chord (chord is the straight segment from leading to trailing edge), from the leading edge. Also, at zero incidence, from (19), the moment acting on the plate (about any point) vanishes (since the pressure is constant everywhere), and so the moment about the aerodynamic center vanishes at all incidence. This means that the force on the plate acts through the aerodynamic center.

By putting $\mu = me^{i\pi/2}$, $a = C\sec\beta$, and $\beta \neq 0$, one generates a circular–arc airfoil because, from (33), one derives

$$\frac{z-2C}{z+2C} = \frac{(\zeta - C)^2}{(\zeta + C)^2}.$$

Thus, if

$$\arg\left(\frac{\zeta - C}{\zeta + C}\right) = \varphi, \tag{39}$$

then (see Figure 2.52)

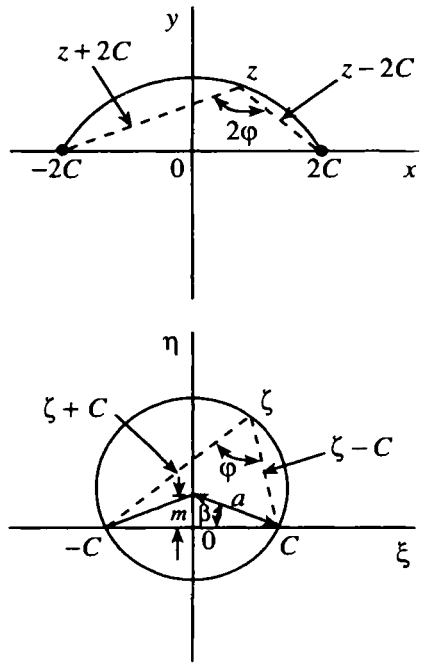

Figure 2.52. Conformal mapping of a circular arc on to a circle (from Karamcheti, 1966).

$$\arg\left(\frac{z-2C}{z+2C}\right)=2\varphi. \tag{40}$$

Next, by putting $\mu = me^{i\pi}$, $\beta = 0$, one generates a symmetric airfoil (see Figure 2.53) given by

$$z=\left(ae^{i\theta}-m\right)+\frac{C^2}{\left(ae^{i\theta}-m\right)}, \tag{41}$$

from which

$$x = 2C\cos\theta, \quad y = C\varepsilon\left(2\sin\theta-\sin 2\theta\right), \tag{42}$$

where

$$a = m + C = C(1+\varepsilon).$$

Thus, by displacing the center μ of the circle in the ζ–plane along the η–axis from the origin, one produces a camber (the camber line is the locus of mid–points of segments cut out by the airfoil on the straight lines perpendicular to the chord, and the camber is the maximum distance of the camber line from the chord) for the airfoil in the z–plane, and by displacing μ along the ξ–axis from the origin one produces thickness for the airfoil in the z–plane.

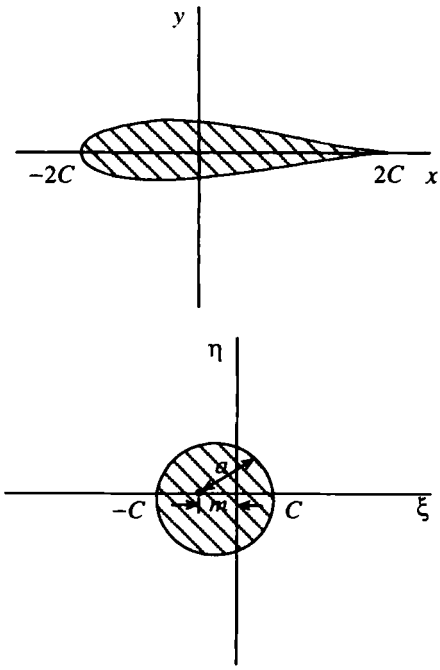

Figure 2.53. Conformal mapping of a symmetric profile on to a circle (from Karamcheti, 1966).

Thin Airfoil Theory

We will now consider the more difficult problem of determining the pressure distribution on an airfoil of given profile. The theory in the following gives only an approximate solution to the problem and involves determination of the singularity distribution representing the airfoil, which satisfies the kinematic boundary conditions in the presence of a wake or a trail of free vortices.

Consider a steady flow past a stationary airfoil. Then, one has the boundary–value problem for the velocity potential Φ:

$$\nabla^2 \Phi = 0 \tag{43}$$

$$\nabla \Phi \cdot \nabla F = 0 \quad \text{on} \quad F(x,y) = 0 \tag{44}$$

$$|\nabla \Phi| \Rightarrow V_\infty \text{ at infinity} \tag{45}$$

$$\text{Kutta condition at trailing edge,} \tag{46}$$

where the airfoil profile is given by

$$F(x,y) = \varepsilon \eta(x) - y = 0, \quad \varepsilon \ll 1. \tag{47}$$

The kinematic condition (44) indicates that the flow should occur tangential to the surface of the body, and implies that

$$\left.\begin{aligned} \frac{\Phi_y}{\Phi_x} &= \varepsilon \frac{d\eta_u}{dx} \quad \text{on} \quad y = \varepsilon \eta_u(x), \\ \frac{\Phi_y}{\Phi_x} &= \varepsilon \frac{d\eta_l}{dx} \quad \text{on} \quad y = \varepsilon \eta_l(x), \end{aligned}\right\} \tag{48}$$

where the subscripts u and l refer to the upper and the lower parts of the profile (see Figure 2.54). Note that

$$\left.\begin{aligned} \eta_u(x) &= [\eta_t(x) + \eta_c(x)] - \alpha x, \\ \eta_l(x) &= [-\eta_t(x) + \eta_c(x)] - \alpha x, \end{aligned}\right\} \tag{49}$$

where the subscripts t and c refer to the thickness part and the camber part, respectively.

When we put

$$\Phi = V_\infty x + \varepsilon \phi(x,y), \tag{50}$$

(43), (45), and (48) give, upon linearization,

$$\phi_{xx} + \phi_{yy} = 0, \tag{51}$$

$$y = 0^+: \quad \phi_y = V_\infty \frac{d\eta_u}{dx}, \tag{52}$$

$$y = 0^-: \quad \phi_y = V_\infty \frac{d\eta_l}{dx}, \tag{53}$$

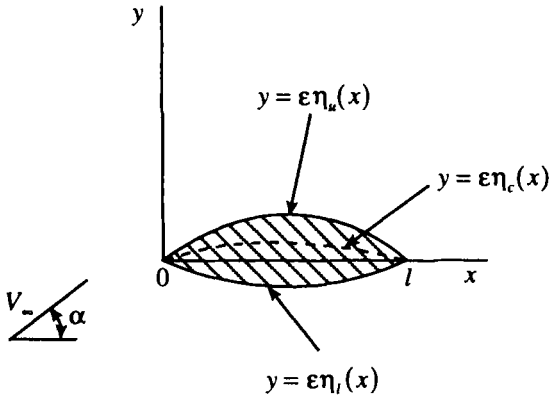

Figure 2.54. Airfoil section and camberline.

$$\phi_x, \phi_y \Rightarrow 0 \text{ at infinity.} \tag{54}$$

The assumption of small perturbations requires that both the angle of attack and the airfoil thickness be sufficiently small.

One now splits (51)–(54) into three simpler problems: Let

$$\phi = \phi_1 + \phi_2 + \phi_3,$$

where

(i)
$$\nabla^2\phi_1 = 0, \tag{55}$$

$$y = 0^{\pm} : \phi_{1y} = \pm V_\infty \frac{d\eta_t}{dx}, \quad 0 \le x \le l, \tag{56}$$

$$|\nabla\phi_1| \Rightarrow 0 \text{ at infinity;} \tag{57}$$

(ii)
$$\nabla^2\phi_2 = 0, \tag{58}$$

$$y = 0^{\pm} : \phi_{2y} = V_\infty \frac{d\eta_c}{dx}, \quad 0 \le x \le l, \tag{59}$$

$$|\nabla\phi_2| \Rightarrow 0 \text{ at infinity,} \tag{60}$$

$$\text{Kutta condition at } x = l; \tag{61}$$

(iii)
$$\nabla^2\phi_3 = 0, \tag{62}$$

$$y = 0^{\pm} : \phi_{3y} = -V_\infty \alpha, \quad 0 \le x \le l, \tag{63}$$

$$|\nabla\phi_3| \Rightarrow 0, \tag{64}$$

$$\text{Kutta condition at } x = l. \tag{65}$$

In the kinematic condition (56), the ± signs correspond to the upper and lower surfaces. Thus, ϕ_1 corresponds to the thickness problem, ϕ_2 to the camber problem, and ϕ_3 to the angle of attack problem.

The pressure on the airfoil is given (in terms of the pressure coefficient) by

$$C_p = \frac{p - p_\infty}{\frac{1}{2}\rho V_\infty^2} = 1 - \frac{V^2}{V_\infty^2} = -\frac{2}{V_\infty}\phi_x. \tag{66}$$

Thickness Problem

This corresponds to a symmetrical airfoil at zero angle of attack.

One has

$$\nabla^2\phi = 0, \tag{55}$$

$$y = 0^{\pm}: \quad \phi_y = \pm V_\infty \frac{d\eta_t}{dx}, \quad 0 \le x \le l, \tag{56}$$

$$|\nabla\phi_1| \Rightarrow 0 \text{ at infinity.} \tag{57}$$

There is no Kutta condition because there is no circulation around the airfoil in the thickness problem.

The thickness problem is equivalent to a superposition of uniform stream and a source distribution (see Figure 2.55), so that one may write

$$\phi(x,y) = \frac{1}{2\pi}\int_0^l q(\xi)\ln\left[(x-\xi)^2 + y^2\right]^{1/2} d\xi, \tag{67}$$

from which the velocity components are given by

$$\left.\begin{aligned} u(x,y) &= \frac{1}{2\pi}\int_0^l \frac{q(\xi)\cdot(x-\xi)}{(x-\xi)^2 + y^2}\, d\xi, \\ v(x,y) &= \frac{1}{2\pi}\int_0^l \frac{q(\xi)\cdot y}{(x-\xi)^2 + y^2}\, d\xi. \end{aligned}\right\} \tag{68}$$

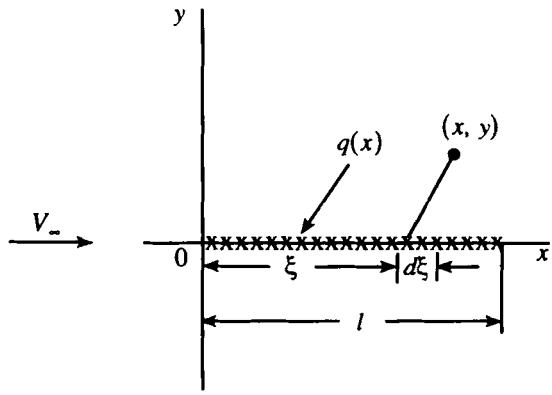

Figure 2.55. Superposition of a uniform stream and a source distribution.

When we use (68), (56) – the kinematic condition – gives

$$v(x,0^+) = \lim_{y\Rightarrow 0} \pm\left[\frac{1}{2\pi}\int_0^l \frac{q(\xi)\cdot y}{(x-\xi)^2+y^2}\,d\xi\right] = \pm V_\infty \frac{d\eta_t}{dx}, \quad 0\le x\le l. \qquad (56)'$$

When we put

$$\eta = \frac{\xi - x}{y},$$

(56)′ becomes

$$v(x,0^+) = \lim_{y\Rightarrow 0} \pm\frac{1}{2\pi}\int_{\eta_0}^{\eta_l} \frac{q(\xi)\,d\eta}{1+\eta^2} = \pm V_\infty \frac{d\eta_t}{dx},$$

where

$$\eta_{0,l} = \eta(x = 0, l).$$

Thus,

$$v(x,0^+) = \mp\frac{1}{2\pi}\,q(x)\int_{-\infty}^{\infty}\frac{d\eta}{1+\eta^2} = \pm V_\infty \frac{d\eta_t}{dx},$$

from which

$$\frac{1}{2}q(x) = V_\infty \frac{d\eta_t}{dx}. \qquad (69)$$

Note that at any point of the strip, the jump in v across the strip is equal to the source strength at the point. Thus, (68) becomes

$$\phi(x,y) = \frac{V_\infty}{\pi}\int_0^l \frac{d\eta_t}{dx}(\xi)\,\ln\left[(x-\xi)^2+y^2\right]^{1/2} d\xi. \qquad (70)$$

If one introduces

$$\left.\begin{aligned} x &= \frac{l}{2}(1+\cos\theta), \quad -\pi\le\theta\le\pi, \\ \xi &= \frac{l}{2}(1+\cos\varphi), \end{aligned}\right\} \qquad (71)$$

(68), evaluated at $y = 0$, namely,

$$u(x,0) = \frac{V_\infty}{\pi}\int_0^l \frac{d\eta_t}{dx}(\xi)\,\frac{d\xi}{x-\xi}, \quad 0\le x\le l,$$

gives

$$u(\theta) = -\frac{V_\infty}{\pi}\int_0^\pi \frac{d\eta_t}{dx}(\varphi)\,\frac{\sin\varphi}{\cos\varphi-\cos\theta}\,d\varphi. \qquad (72)$$

Noting that $d\eta_t/dx(\theta)$ is an odd function of θ, one may write

$$\frac{d\eta_t}{dx}(\theta) = \sum_{n=1}^{\infty} A_n \sin n\theta. \tag{73}$$

Equation (73) shows that $d\eta_t/dx$ vanishes at $\theta = 0,\ \pi$, and

$$A_n = \frac{2}{\pi}\int_0^{\pi} \frac{d\eta_t}{dx}(\theta) \sin n\theta\, d\theta.$$

When we use (73), (72) becomes

$$\frac{u(\theta)}{V_\infty} = \sum_{n=1}^{\infty} A_n \cos n\theta, \tag{74}$$

where we have used the result

$$\frac{1}{\pi}\int_0^{\pi} \frac{\sin n\varphi \cdot \sin \varphi}{\cos\theta - \cos\varphi}\, d\varphi = \cos n\theta. \tag{75}$$

Note that $u(\theta)$ is an even function of θ.

Camber Problem

This corresponds to a camber profile at zero angle of attack (see Figure 2.56).

One has

$$\nabla^2\phi = 0, \tag{58}$$

$$y = 0^{\pm}: \quad \phi_y = V_\infty \frac{d\eta_c}{dx}, \tag{59}$$

$$|\nabla\phi| \Rightarrow 0 \text{ at infinity}, \tag{60}$$

$$\text{Kutta condition at } x = l. \tag{61}$$

The camber problem is equivalent to a superposition of uniform stream and a vortex distribution so that one may write

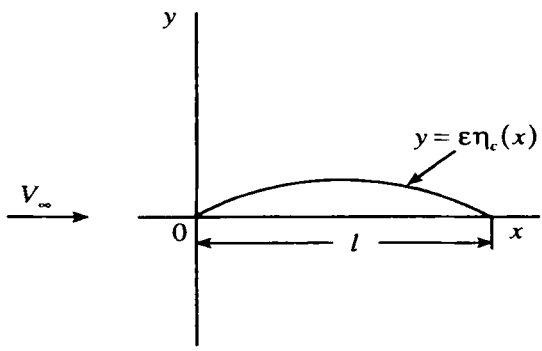

Figure 2.56. Flow past a cambered profile at zero angle of attack.

$$\phi(x,y)=\frac{1}{2\pi}\int_0^l \gamma(\xi)\tan^{-1}\frac{y}{x-\xi}\,d\xi \tag{76}$$

from which, the velocity components are given by

$$\left.\begin{aligned} u(x,y)&=\frac{1}{2\pi}\int_0^l \frac{\gamma(\xi)\cdot y}{(x-\xi)^2+y^2}\,d\xi \\ v(x,y)&=-\frac{1}{2\pi}\int_0^l \frac{\gamma(\xi)\cdot(x-\xi)}{(x-\xi)^2+y^2}\,d\xi \end{aligned}\right\}. \tag{77}$$

Note, from (77), that

$$u(x,0^{\pm})=\lim_{y\Rightarrow 0}\pm\frac{1}{2\pi}\int_0^l \frac{\gamma(\xi)\cdot y}{(x-\xi)^2+y^2}\,d\xi=\pm\frac{\gamma(x)}{2} \tag{78}$$

so that, at any point on the strip, the jump in u across the strip is equal to the vortex strength at that point.

Using (77), the kinematic condition (59) gives

$$\lim_{y\Rightarrow 0}\pm\left[-\frac{1}{2\pi}\int_0^l \frac{\gamma(\xi)\cdot(x-\xi)}{(x-\xi)^2+y^2}\,d\xi\right]=V_\infty\frac{d\eta_c}{dx},\quad 0\le x\le l, \tag{79}$$

from which

$$-\frac{1}{2\pi}\int_0^l \frac{\gamma(\xi)}{x-\xi}\,d\xi=V_\infty\frac{d\eta_c}{dx},\quad 0\le x\le l; \tag{80}$$

and the Kutta condition requiring that there be no jump in u at $x=l$ implies, from (78), that $\gamma(\ell)=0$.

Introducing again

$$\left.\begin{aligned} x&=\frac{l}{2}(1+\cos\theta),\quad -\pi\le\theta\le\pi, \\ \xi&=\frac{l}{2}(1+\cos\varphi), \end{aligned}\right\} \tag{71}$$

(80) becomes

$$\frac{1}{\pi}\int_0^\pi \frac{\gamma(\varphi)}{2V_\infty}\frac{\sin\varphi}{\cos\varphi-\cos\theta}\,d\varphi=\frac{d\eta_c}{dx}(\theta). \tag{81}$$

Noting that $d\eta_c/dx(\theta)$ is an even function of θ, one may write

$$\frac{d\eta_c}{d\theta}(\theta)=\frac{B_0}{2}+\sum_{n=1}^{\infty}B_n\cos n\theta, \tag{82}$$

where

$$B_n = \frac{2}{\pi}\int_0^{\pi} \frac{d\eta_c}{dx}(\theta)\cos n\theta \cdot d\theta.$$

Let

$$\gamma(\theta) = \gamma_1(\theta) + \gamma_2(\theta) + \frac{K}{\sin\theta}, \tag{83}$$

where, noting that

$$\int_0^{\pi} \frac{d\varphi}{\cos\varphi - \cos\theta} = 0,$$

one sees that the last term on the right hand side in (83) represents the homogeneous solution to (81).

When one uses (83) in (81), one may choose γ_1 and γ_2 such that

$$\frac{1}{\pi}\int_0^{\pi} \frac{\gamma_1(\varphi)}{2V_\infty} \frac{\sin\varphi}{\cos\varphi - \cos\theta} d\varphi = \sum_{n=1}^{\infty} B_n \cos n\theta, \tag{84}$$

$$\frac{1}{\pi}\int_0^{\pi} \frac{\gamma_2(\varphi)}{2V_\infty} \frac{\sin\varphi}{\cos\varphi - \cos\theta} d\varphi = \frac{B_0}{2}. \tag{85}$$

When one uses (75), (84) leads to

$$\gamma_1(\theta) = -2V_\infty \sum_{n=1}^{\infty} B_n \sin n\theta. \tag{86}$$

When one has

$$\frac{1}{\pi}\int_0^{\pi} \frac{\cos\varphi}{\cos\varphi - \cos\theta} d\varphi = 1, \tag{87}$$

(85) gives

$$\gamma_2(\theta) = V_\infty B_0 \frac{\cos\theta}{\sin\theta}. \tag{88}$$

When one uses (86) and (88), (83) becomes

$$\gamma(\theta) = -2V_\infty \sum_{n=1}^{\infty} B_n \sin n\theta + V_\infty B_0 \frac{\cos\theta}{\sin\theta} + \frac{K}{\sin\theta}. \tag{89}$$

Applying the Kutta condition

$$\gamma(x = l) = \gamma(\theta = 0) = 0 \tag{61}$$

so that there is no jump in u at $x = l$, one obtains, from (89),

$$K = -V_\infty B_0. \tag{90}$$

When one uses (90), (89) becomes

$$\gamma(\theta) = -2V_\infty \left(\frac{B_0}{2} \frac{1-\cos\theta}{\sin\theta} + \sum_{n=1}^{\infty} B_n \sin n\theta \right). \tag{91}$$

Next, the pressure on the airfoil, using (78), is given by

$$C_p\left(x,0^\pm\right) = -\frac{2u\left(x,0^\pm\right)}{V_\infty} = \mp \frac{\gamma(x)}{V_\infty} \tag{92}$$

and using (91), (92) becomes

$$C_p(\theta) = 2\left[\frac{B_0}{2} \cdot \frac{1-\cos\theta}{\sin\theta} + \sum_{n=1}^{\infty} B_n \sin n\theta \right]. \tag{93}$$

The lift on the airfoil is given by

$$\mathbb{L} = \frac{\rho V_\infty^2}{2} \int_0^l \left[C_p\left(x,0^-\right) - C_p\left(x,0^+\right) \right] dx;$$

and on using (92), this becomes

$$\mathbb{L} = \rho V_\infty \int_0^l \gamma(x)\, dx. \tag{94a}$$

The moment (about the leading edge) is given by

$$M = -\rho V_\infty \int_0^l \gamma(x)\, x\, dx. \tag{95a}$$

When one uses (71), (94a) and (95a) become

$$\mathbb{L} = \frac{\rho l}{2V_\infty} \int_0^\pi \gamma(\theta) \sin\theta\, d\theta, \tag{94b}$$

$$M = -\frac{\rho l^2}{4V_\infty} \int_0^\pi \gamma(\theta) \cdot (1+\cos\theta) \sin\theta\, d\theta. \tag{95b}$$

Using (91), one see that (94b) and (95b) become

$$\mathbb{L} = -\left(B_0 + B_1\right) \pi \cdot \frac{\rho l}{2}, \tag{96}$$

$$M = \frac{\rho l^2}{4} \left[\frac{\pi}{4} B_0 + \frac{\pi}{2} B_1 + \frac{\pi}{4} B_2 \right]. \tag{97a}$$

Writing (97a) as

$$M = \frac{\rho l^2}{4} \left[\frac{\pi}{4} \left(B_0 + B_1\right) + \frac{\pi}{4} \left(B_1 + B_2\right) \right] \tag{97b}$$

and using (96), one has

$$M = -\frac{\mathbb{L}}{4} + \frac{\rho l^2}{4} \frac{\pi}{4} \left(B_1 + B_2\right), \tag{98}$$

which shows the lift acting at the 1/4–chord point – the aerodynamic center.

Flat Plate at an Angle of Attack

One has

$$\nabla^2\phi = 0, \tag{62}$$

$$y = 0^{\pm}: \quad \phi_{3_y} = -V_\infty \alpha, \quad 0 \le x \le l, \tag{63}$$

$$|\nabla\phi_3| \Rightarrow 0 \text{ at infinity}, \tag{64}$$

$$\text{Kutta condition at } x = l. \tag{65}$$

The angle of attack problem, like the camber problem, is equivalent to superposition of uniform stream and a vortex distribution, so that one may write

$$\phi(x,y) = -\frac{1}{2\pi}\int_0^l \gamma(\xi)\tan^{-1}\frac{y}{(x-\xi)}\,d\xi, \tag{99}$$

from which the velocity components are given by

$$\left.\begin{aligned} u(x,y) &= \frac{1}{2\pi}\int_0^l \frac{\gamma(\xi)\cdot y}{(x-\xi)^2+y^2}\,d\xi, \\ v(x,y) &= -\frac{1}{2\pi}\int_0^l \frac{\gamma(\xi)\cdot(x-\xi)}{(x-\xi)^2+y^2}\,d\xi. \end{aligned}\right\} \tag{100}$$

When one uses (100), the kinematic condition (63) gives

$$\lim_{y\Rightarrow 0^{\pm}}\left[-\frac{1}{2\pi}\int_0^l \frac{\gamma(\xi)\cdot(x-\xi)}{(x-\xi)^2+y^2}\,d\xi\right] = -V_\infty\alpha, \quad 0 \le x \le l,$$

from which

$$\frac{1}{2\pi}\int_0^l \frac{\gamma(\xi)}{x-\xi}\,d\xi = V_\infty\alpha, \quad 0 \le x \le l. \tag{101}$$

When one reintroduces

$$\left.\begin{aligned} x &= \frac{l}{2}(1+\cos\theta), \quad -\pi \le \theta \le \pi, \\ \xi &= \frac{l}{2}(1+\cos\varphi), \end{aligned}\right\} \tag{71}$$

(101) becomes

$$\frac{1}{\pi}\int_0^{\pi} \frac{\gamma(\varphi)\sin\varphi}{\cos\varphi - \cos\theta}\,d\varphi = -2V_\infty\alpha. \tag{102}$$

Equation (102) implies that

$$\gamma(\theta) = \frac{K}{\sin\theta} - 2V_\infty \alpha \frac{\cos\theta}{\sin\theta}. \tag{103}$$

The Kutta condition $\gamma(0) = 0$ gives, from (103),

$$K = 2V_\infty \alpha. \tag{104}$$

When one uses (104), (103) becomes

$$\gamma(\theta) = \frac{2V_\infty \alpha}{\sin\theta}(1 - \cos\theta). \tag{105}$$

The pressure on the airfoil is then given, from (92), by

$$C_p(\theta) = -\frac{\gamma(\theta)}{V_\infty} = -2\alpha\left(\frac{1-\cos\theta}{\sin\theta}\right). \tag{106}$$

Thus, the lift on the airfoil and the moment (about the leading edge) are given by

$$\mathbb{L} = \frac{\rho l/2}{V_\infty}\int_0^\pi \gamma(\theta)\sin\theta\, d\theta = \pi\alpha\rho l, \tag{107}$$

$$M = -\frac{2}{V_\infty}\frac{\rho l^2}{4}\int_0^\pi \gamma(\theta)(1+\cos\theta)\sin\theta\, d\theta = -\frac{\rho l^2}{4}\pi\alpha = -\frac{\mathbb{L}}{4}. \tag{108}$$

Equation (108) shows that the force system on the flat plate is again equivalent to a lift force acting at the quarter chord point. This point is, therefore, the aerodynamic center.

Combined Aerodynamic Characteristics

One thus has from (73) and (82)

$$\frac{d\eta}{dx}(\theta) = \frac{B_0}{2} + \sum_{n=1}^{\infty} B_n \cos n\theta + \sum_{n=1}^{\infty} A_n \sin n\theta, \tag{109}$$

where

$$B_n = \frac{2}{\pi}\int_0^\pi \frac{d\eta}{dx}(\theta)\cos n\theta\, d\theta,$$

$$A_n = \frac{2}{\pi}\int_0^\pi \frac{d\eta}{dx}(\theta)\sin n\theta\, d\theta.$$

Using (74), (93), and (106), one obtains for the pressure on the airfoil

$$C_p = 2\left[\frac{B_0}{2}\frac{1-\cos\theta}{\sin\theta} + \sum_{n=1}^{\infty} B_n \sin n\theta - \alpha\left(\frac{1-\cos\theta}{\sin\theta}\right) - \sum_{n=1}^{\infty} A_n \cos n\theta\right], \tag{110}$$

from which the lift on the airfoil and the moment (about the leading edge) are given by

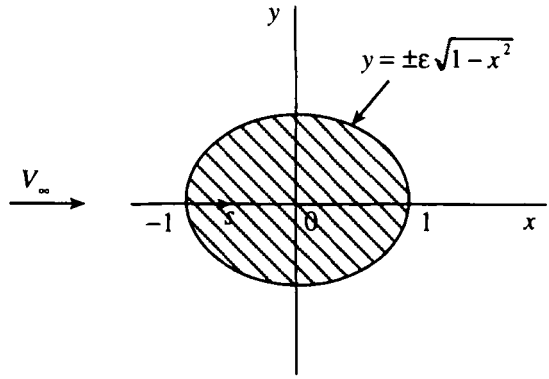

Figure 2.57. Uniform flow past a thin elliptic airfoil.

$$\mathbb{L} = \frac{\rho l}{2}\left[2\pi\alpha - \pi\left(B_0 + B_1\right)\right], \tag{111}$$

$$M = \frac{\rho l^2}{4}\left[-\frac{\pi\alpha}{2} + \frac{\pi}{4}\left(B_0 + B_1\right) + \frac{\pi}{4}\left(B_1 + B_2\right)\right] = -\frac{\mathbb{L}}{4} + \frac{\rho l^2}{4}\left[\frac{\pi}{4}\left(B_1 + B_2\right)\right]. \tag{112}$$

Note that the quarter chord point is again the aerodynamic center.

The Leading-Edge Problem of a Thin Airfoil

The foregoing theory breaks down at the stagnation points (such as one at the leading edge) because of the violation of the assumption of small disturbances there. In order to see how one can handle the leading-edge problem, consider a uniform flow past a thin elliptic airfoil (see Figure 2.57). If the fluid velocity is given by

$$\boldsymbol{v} = V_\infty \nabla \Phi,$$

then one has the following boundary-value problem,

$$\Phi_{xx} + \Phi_{yy} = 0 \tag{113}$$

$$\frac{\Phi_y}{\Phi_x} = \mp\,\varepsilon\,\frac{x}{\sqrt{1-x^2}} \quad \text{at} \quad y = \pm\,\varepsilon\,\sqrt{1-x^2} = \varepsilon T(x), \tag{114}$$

$$\Phi \sim x + 0(1) \quad \text{as} \quad \left(x^2 + y^2\right) \Rightarrow \infty. \tag{115}$$

Seeking a solution of the form

$$\Phi(x, y; \varepsilon) = x + \varepsilon\phi_1 + \varepsilon^2\phi_2 + \cdots, \quad \varepsilon \ll 1, \tag{116}$$

(113)-(115) lead to the following hierarchy of problems:

$0(\varepsilon)$:

$$\phi_{1xx} + \phi_{1yy} = 0 \quad , \tag{117}$$

$$y = 0^{\pm}: \quad \phi_{1y} = \mp \frac{x}{\sqrt{1-x^2}}, \tag{118}$$

$$\phi_1 = 0(1) \quad \text{as} \quad \left(x^2 + y^2\right) \Rightarrow \infty; \tag{119}$$

$0\left(\varepsilon^2\right)$:

$$\phi_{2xx} + \phi_{2yy} = 0 \ , \tag{120}$$

$$y = 0^{\pm}: \quad \phi_{2y} = \mp \frac{x}{\sqrt{1-x^2}}\, \phi_{1x} + \mp \sqrt{1-x^2}\ \phi_{1yy};$$

or

$$\phi_{2y} = \pm \frac{\partial}{\partial x}\left[\sqrt{1-x^2}\ \phi_{1x}\right], \tag{121}$$

$$\phi_2 = 0(1) \quad \text{as} \quad \left(x^2 + y^2\right) \Rightarrow \infty. \tag{122}$$

The flow speed at the airfoil is then given by

$$\frac{V}{V_\infty} = \left[\left\{1 + \varepsilon\left(\phi_{1x} + \varepsilon T \phi_{1xy}\right) + \varepsilon^2 \phi_{2x} + \cdots\right\}^2 + \left\{\varepsilon \phi_{1y} + \varepsilon^2 \phi_{2y} + \cdots\right\}^2\right]_{y=0}^{1/2}. \tag{123}$$

When one uses (118) and (121), (123) becomes

$$\frac{V}{V_\infty} = 1 + \varepsilon \phi_{1x}(x,0) + \varepsilon^2 \left[\phi_{2x}(x,0) - \frac{1}{\left(1-x^2\right)} + \frac{1}{2}\,\frac{x^2}{\left(1-x^2\right)} + \cdots\right]. \tag{124}$$

Representing the body by a distribution of sources along the axis, one has from (68), on nondimensionalizing the lengths using the semichord length l,

$$\left.\begin{aligned} \phi_{nx}(x,y) &= \frac{1}{\pi}\int_{-1}^{1} \frac{(x-\xi)\phi_{ny}\left(\xi,0^{\pm}\right)d\xi}{(x-\xi)^2 + y^2}, \\ \phi_{nx}(x,y) &= \frac{1}{\pi}\int_{-1}^{1} \frac{y\,\phi_{ny}\left(\xi,0^{\pm}\right)d\xi}{(x-\xi)^2 + y^2}, \qquad n = 1,2,\ldots; \end{aligned}\right\} \tag{125}$$

and on the surface, (125) gives

$$\phi_{nx}(x,0) = \frac{1}{\pi}\int_{-1}^{1} \frac{\phi_{ny}\left(\xi,0^{\pm}\right)\,d\xi}{x-\xi}. \tag{126}$$

When one uses the kinematic condition (118), (126) gives

$$\phi_{1x}(x,0) = -\frac{1}{\pi}\int_{-1}^{1} \frac{\xi d\xi}{\sqrt{1-\xi^2}\,(x-\xi)}, \tag{127}$$

from which

$$y=0: \quad \phi_{1x}=\begin{cases} 1, & x^2<1, \\ 1-\sqrt{\dfrac{x}{x^2-1}}, & x^2>1. \end{cases} \tag{128}$$

Note that the problem for ϕ_2 is identical with that of ϕ_1, and thus the flow speed on the airfoil is, from (124), given by

$$\frac{V}{V_\infty}=1+\varepsilon-\varepsilon^2\,\frac{x^2/2}{1-x^2}+\cdots. \tag{129}$$

When one puts

$$s=1+x \tag{130}$$

(129) gives, in the neighborhood of the leading edge $x=-1$, where $s \ll 1$,

$$V=V_\infty(1+\varepsilon)\left[1-\frac{\varepsilon^2}{4s(1+\varepsilon)}+\cdots\right]. \tag{131}$$

Note that the assumption of small disturbances has been violated at the stagnation points (such as at $x=-1$), so that (131) breaks down there locally. Note that the region of nonuniformity is of order ε^2.

One way to remove this singularity is to sum the patently divergent series in (131) by pretending that the latter is not divergent, i.e., $s \sim 0(1)$, though this is not justified. Thus, (131) becomes

$$V \approx \frac{V_\infty(1+\varepsilon)}{1+\varepsilon^2/4s} \approx \frac{V_\infty(1+\varepsilon)}{\sqrt{1+\varepsilon^2/2s}} \approx V_\infty(1+\varepsilon)\sqrt{\frac{s}{s+\varepsilon^2/2}}, \tag{132}$$

which is an exact result that corresponds to a uniform flow of speed $V_\infty(1+\varepsilon)$ past a parabola of nose radius ε^2! This is how the flow appears near the leading edge for this problem, and the latter result ensues from the leading-edge value of the exact expression for the flow speed on the airfoil (which can be obtained by the method of complex variables, see Van Dyke),

$$\frac{V}{V_\infty}=\frac{1+\varepsilon}{\sqrt{1+\varepsilon^2\left(\dfrac{x^2}{1-x^2}\right)}}. \tag{133}$$

Another way of removing the singularity in (131) is to write a multiplicative correction factor converting the formal thin-airfoil solution V for the flow speed on an airfoil of nose radius ε^2 into a uniformly valid approximation $\bar{V}$:

$$\bar{V}=\frac{\sqrt{\dfrac{s}{s+\varepsilon^2/2}}}{\left(1-\dfrac{\varepsilon^2}{4s}+\cdots\right)}\,V, \tag{134}$$

which gives the result that near the leading edge the flow speed on the airfoil is nearly that on the osculating parabola, and far from the leading edge the correction factor approaches unity, so that the thin-airfoil solution for the airfoil is recovered. One may write (134) as

$$\frac{\bar{V}}{V_\infty} = \sqrt{\frac{s}{s+\varepsilon^2/2}}\left(\frac{V}{V_\infty} + \frac{\varepsilon^2}{4s}\right) \tag{135a}$$

or

$$\frac{\bar{V}}{V_\infty} = \sqrt{\frac{1+x}{1+x+\varepsilon^2/2}}\left(1+\varepsilon+\frac{\varepsilon^2}{4}\frac{1-2x}{1-x}\right). \tag{135b}$$

Although the singularity at the leading edge has been removed, the one at the trailing edge remains. The latter too can be removed by applying the above correction again with $\tilde{s} = 1 - x$. Thus one obtains the fully uniform result

$$\frac{\bar{V}}{V_\infty} = \sqrt{\frac{1-x^2}{1-x^2+\varepsilon^2+\varepsilon^4/4}}\left(1+\varepsilon+\frac{\varepsilon^2}{2}\right). \tag{136}$$

Slender-Body Theory

Slender-body theory is concerned with the calculation of flows past bodies whose lateral dimensions change slowly with distance parallel to the flow direction.

One chooses a singularity distribution along the axis of symmetry of a slender body in such a way that the potential flow associated with these singularities in combination with a uniform stream satisfies approximately the condition of zero normal component of velocity at the surface of the body of given shape. Thus, for a uniform stream past a slender body (of length l) simulated by a doublet distribution of strength $m(x)$, with x being the distance along the axis of symmetry, one has

$$\Phi = -V_\infty x + \frac{1}{4\pi}\int_0^l \frac{m(\xi)}{\sqrt{(x-\xi)^2+r^2}}\,d\xi, \tag{137}$$

from which the velocity components are given by

$$\left.\begin{aligned} u &\equiv -\frac{\partial\Phi}{\partial r} = \frac{1}{4\pi}\int_0^l \frac{m(\xi)\cdot r}{\left[(x-\xi)^2+r^2\right]^{3/2}}\,d\xi, \\ w &\equiv -\frac{\partial\Phi}{\partial x} = V_\infty + \frac{1}{4\pi}\int_0^l \frac{m(\xi)\cdot(x-\xi)}{\left[(x-\xi)^2+r^2\right]^{3/2}}\,d\xi. \end{aligned}\right\} \tag{138}$$

One may write (138) as

$$u = \frac{1}{4\pi r} \int_{-x/r}^{(l-x)/r} \frac{m(\xi)}{\left[\left(\frac{\xi - x}{r}\right)^2 + 1\right]^{3/2}} d\left(\frac{\xi - x}{r}\right). \tag{139}$$

For a slender body, r is very small; thus (139) may be approximated by

$$u \approx \frac{1}{4\pi r} m(x) \int_{-\infty}^{\infty} \frac{d\eta}{\left(\eta^2 + 1\right)^{3/2}} = \frac{1}{2\pi r} m(x). \tag{140}$$

When one uses (140), the boundary condition at the surface of the body $r = F(x)$,

$$r = F(x): \quad u = V_\infty \frac{dF}{dx}, \tag{141}$$

gives

$$m(x) = 2\pi V_\infty F \frac{dF}{dx}. \tag{142}$$

When one uses (142), (137) becomes

$$\Phi = -V_\infty x + \frac{V_\infty}{2} \int_0^l \frac{F(\xi) \frac{dF(\xi)}{d\xi}}{\sqrt{(x-\xi)^2 + r^2}} d\xi. \tag{143}$$

Lifting–Line Theory for Wings

For wings of finite span, one has to take into account the three–dimensional effects. This is handled satisfactorily by the lifting–line theory to Prandtl, provided that

* the wing is of sufficiently large aspect ratio (which is span/chord);
* the wing section (made by a plane perpendicular to the span) does not vary too rapidly along the span.

The lifting–line model envisages the following simplifying conditions:

1. The variation (which is taken to be symmetric about the center line of the wing) of circulation Γ around a wing section along the wing span leads to the shedding of the vorticity from the wing; this forms a sheet of trailing vortices, which extends downstream from the trailing edges of the wing; this sheet may be supposed to consist of line vortices, which are parallel to the direction of flow; this sheet is unstable and rolls up at the edges, which is here, however, ignored; the circulation is presumed to drop to zero at the wing–tips, i.e.,

$$\Gamma = \Gamma(y), \qquad \Gamma(+y) = \Gamma(-y), \qquad \Gamma\left(\pm\frac{b}{2}\right) = 0. \tag{144}$$

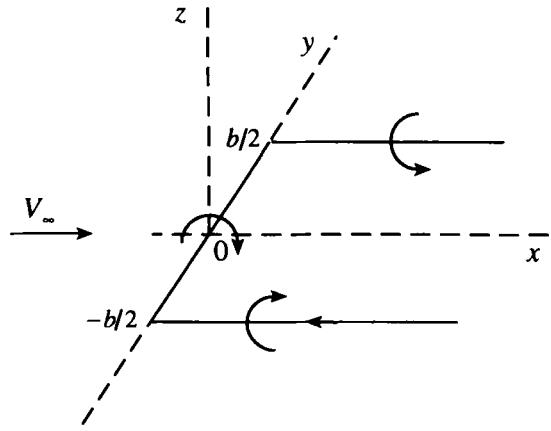

Figure 2.58. Lifting–line configuration (from Karamcheti, 1966).

2. The span b of the wing is sufficiently large compared with the chord l so that the variation of the velocity in the spanwise direction is small compared with the variation in a plane normal to the span.
3. The wing for a very large aspect ratio is replaced by a lifting line (see Figure 2.58) having the same distribution of lifting forces along the span as the wing; the disturbances caused by the lifting line are small.
4. The velocity field induced at the wing by the trailing vortices consists of a small downwash for wings of large aspect ratio; as a consequence, the flow at each sectional plane can be considered as two–dimensional flow around an airfoil; the only additional feature for the flow in the sectional plane is the modification of the angle of attack (see Figure 2.59) as defined by the undisturbed flow, on account of the induced velocity.

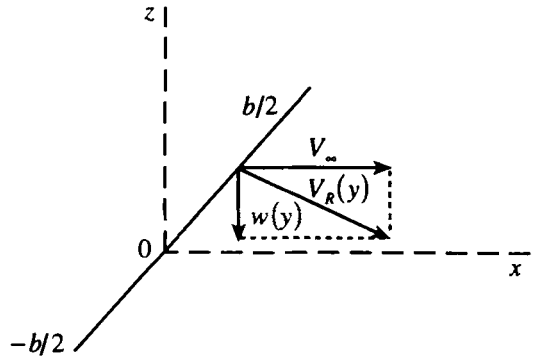

Figure 2.59. Flow at a sectional plane perpendicular to the lifting line (from Karamcheti, 1966).

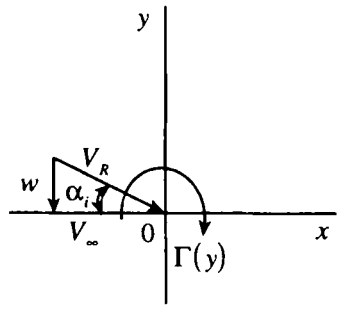

Figure 2.60. The trailing vortex sheet (from Karamcheti, 1966).

The flow situation at a wing section is represented in Figure 2.60. Now, from the thin airfoil theory, namely, (28), one has

$$\Gamma(y) = \pi l(y) V_R(y) \alpha_R(y), \tag{145}$$

where the effective angle of attack $\alpha_R(y)$ (taken to be small) is given by

$$\alpha_R(y) = \alpha(y) - \tan^{-1} \frac{w(y)}{V_\infty}. \tag{146}$$

The velocity induced by an element of trailing vortex sheet of strength $\gamma(\eta)$ (see Figure 2.61) is given by (see Section 2.4)

$$\delta w(y) = \frac{1}{4\pi} \frac{\gamma(\eta)}{\eta - y}, \tag{147}$$

where, by the conservation of vorticity, the strength $\gamma(\eta)$ of the vortex sheet is given by

$$\gamma(\eta) = -\frac{d\Gamma}{dy}(\eta) d\eta. \tag{148}$$

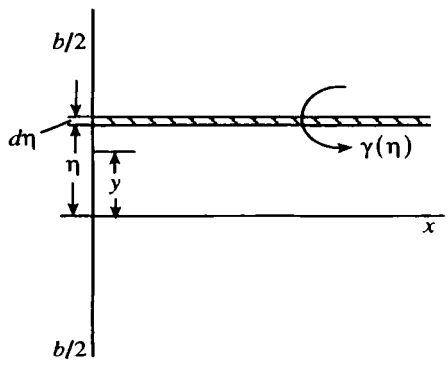

Figure 2.61. Flow situation in a wing section (from Karamcheti, 1966).

Thus, for the whole trailing vortex sheet, one obtains

$$w(y)=\frac{1}{4\pi}\int_{-b/2}^{b/2}\frac{d\Gamma}{dy}(\eta)\,\frac{d\eta}{y-\eta}. \tag{149}$$

When one uses (146) and (149) and assumes $w/V_\infty \ll 1$, (145) gives an integral equation for $\Gamma(y)$,

$$\Gamma(y)\approx \pi l(y)\left[V_\infty\alpha(y)-\frac{1}{4\pi}\int_{-b/2}^{b/2}\frac{d\Gamma}{dy}(\eta)\,\frac{d\eta}{y-\eta}\right] \tag{150}$$

with the boundary condition

$$\Gamma\left(\pm\frac{b}{2}\right)=0. \tag{144}$$

The force on a section dy is given by

$$\delta \boldsymbol{F}(y)=\rho \boldsymbol{V}_R(y)\times\Gamma(y)\,dy\,\hat{\boldsymbol{i}}_y, \tag{151}$$

from which the lift and the induced drag on the wing element at y are given by

$$\delta\mathbb{L}(y)\approx \rho V_\infty\Gamma(y)\,dy, \tag{152}$$

$$\delta D_i(y)\approx \rho w(y)\Gamma(y)\,dy. \tag{153}$$

Thus, for the whole wing, one obtains

$$\mathbb{L}=\rho V_\infty\int_{-b/2}^{b/2}\Gamma(y)\,dy, \tag{154}$$

$$D_i=\rho\int_{-b/2}^{b/2}w(y)\Gamma(y)\,dy. \tag{155}$$

An essential biproduct with lift on a three–dimensional body is the existence of a trailing vertex sheet. Energy spent by the body constantly in maintaining these trailing vortices shows up as the induced drag.

The moment on the wing is given by

$$\boldsymbol{M}=\int_{-b/2}^{b/2}y\hat{\boldsymbol{i}}_y\times\left(\hat{\boldsymbol{i}}_x\delta D_i+\hat{\boldsymbol{i}}_z\delta\mathbb{L}\right)=-\hat{\boldsymbol{i}}_z\int_{-b/2}^{b/2}y\delta D_i+\boldsymbol{i}_x\int_{-b/2}^{b/2}y\delta\mathbb{L}=\boldsymbol{M}_y+\boldsymbol{M}_R; \tag{156}$$

the first term $\boldsymbol{M}_y$ on the right–hand side in (156) corresponds to yawing of the wing and the second term $\boldsymbol{M}_R$ to rolling.

Consider a loading on the wing given by

$$\Gamma(\theta)=2bV_\infty\sum_{n=1}^{\infty}A_n\sin n\theta, \tag{157}$$

where

$$y=\frac{b}{2}\cos\theta \tag{158}$$

and the boundary conditions (144) have been incorporated.

When one uses (157), (149) gives

$$w(\theta) = V_\infty \sum_{n=1}^{\infty} nA_n \frac{\sin n\theta}{\sin \theta}. \tag{159}$$

When one uses (157)–(159), (154)–(156) give the following equations for the lift, induced drag, and moments on the wing:

$$\mathbb{L} = \rho V_\infty^2 b^2 \frac{\pi}{2} A_1, \tag{160}$$

$$D_i = \rho V_\infty^2 b^2 \frac{\pi}{2} \sum_{n=1}^{\infty} nA_n^2, \tag{161}$$

$$M_R = -\frac{\pi}{8} \rho V_\infty^2 b^3 A_2, \tag{162}$$

$$M_Y = \frac{\pi}{2} \rho V_\infty^2 b^3 \sum_{n=1}^{\infty} (2n+1)\, A_n A_{n+1}. \tag{163}$$

For a body of minimum induced drag, one has, from (161),

$$A_n = 0 \quad \text{for} \quad n > 1, \tag{164}$$

which, from (157), corresponds to an elliptic lift distribution.

Further, equation (150) gives, on using (164),

$$l(\theta)\left[\frac{\pi\alpha}{2b} - \frac{\pi A_1}{2b}\right] = A_1 \sin\theta$$

or

$$l(\theta) \sim \sin\theta$$

or

$$l(y) \sim \sqrt{1-(2y/b)^2}, \tag{165}$$

which corresponds an elliptic plan form for the wing.

Thus, for a wing with elliptic platform and an elliptic lift distribution, namely,

$$\Gamma(y) = \Gamma_0 \sqrt{1-(2y/b)^2},$$

$$l(y) = l_0 \sqrt{1-(2y/b)^2}, \tag{166}$$

equation (150) gives

$$\Gamma_0 = \pi l_0 \left[V_\infty \alpha - \frac{\Gamma_0}{2b}\right]$$

or

$$\Gamma_0 = \frac{2\pi b V_\infty \alpha}{1 + \dfrac{2b}{\pi l_0}}, \tag{167}$$

which reduces to the two–dimensional airfoil result, namely (28), in the limit $b/l_0 \Rightarrow \infty$.

Oscillating Thin–Airfoil Theory: Theodorsen's Theory

The unsteady airfoil theory has important applications, like in the flutter problem and the forces experienced by airplanes flying through gusts.

When an airfoil performs oscillations around a given mean position, the circulation around the airfoil also undergoes periodic variations. This, in conjunction with the total vorticity conservation constraint, leads to the shedding of free vorticity from the trailing edge. This vorticity is equal in strength but opposite in sign to the change in the circulation around the airfoil and is carried downstream by the flow. The velocity field induced around the airfoil by these free vortices causes changes in the instantaneous angles of attack of the airfoil with the consequence that the oscillating part of the lift lags behind the motion of the airfoil.

Within the framework of a linearized theory, solutions may be superposed to generate another solution. The solution of an oscillating airfoil with finite but small thickness and camber at a given mean angle of attack can, therefore, be obtained by a superposition of an unsteady motion for an oscillating airfoil of zero thickness and zero camber at zero mean angle of attack, along with a steady–state solution for an airfoil of the given thickness and camber at the given mean angle of attack.

One has, for a uniform flow past an oscillating airfoil (see Figure 2.62), the following boundary–value problem:

$$\nabla^2 \phi = 0, \tag{168}$$

$$z = 0: \quad w = w_a = \frac{\partial z_a}{\partial t} + V_\infty \frac{\partial z_a}{\partial x}, \qquad -b \le x \le b, \tag{169}$$

$$x = b: \text{ Kutta condition.} \tag{170}$$

Here, $z = z_a(x,t)$ describes the surface of the airfoil, and the subscript a refers to the latter location. In (170), we overlook any possibility of lag in the adjustment of flow at the trailing edge.[1]

In order to find a solution to (168)–(170) one chooses an appropriate distribution of sources and sinks just above and below the line $z = 0$, and a pattern of vortices on this line with countervortices along the wake to infinity in

[1]The success of this model, as it turns out, indicates that such adjustment is, in fact, very rapid.

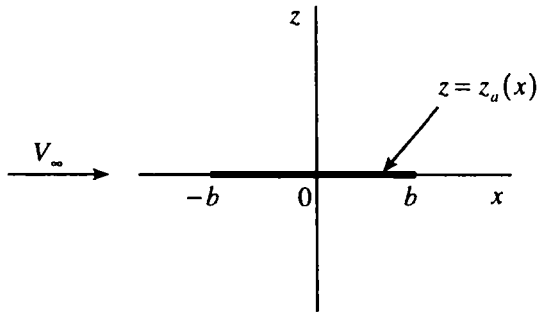

Figure 2.62. Uniform flow past an oscillating airfoil.

such a way that Kutta's condition is fulfilled without disturbing the boundary conditions at the surface of the airfoil. The flow components due to the sources and vortices are most conveniently obtained by using Joukowski's conformal transformation, namely (33), to map a circle of radius $b/2$ onto the projection of the airfoil. It is

$$x + iz = (X + iZ) + \frac{b^2/4}{(X + iZ)}. \tag{171}$$

On the surface of the airfoil and its mapped image, one has, from (171),

$$r = \frac{b}{2} e^{i\theta}, \qquad x = b\cos\theta, \qquad z = 0, \qquad 0 \le \theta \le \pi \tag{172}$$

and the complex velocity,

$$u - iw = \frac{q_x - iq_z}{2\sin\theta e^{i\theta}} = \frac{q_\theta - iq_r}{2\sin\theta}. \tag{173}$$

Since the transformation (171) is conformal, (173) gives

$$u = -\frac{q_\theta}{2\sin\theta}, \qquad w = \frac{q_r}{2\sin\theta}, \qquad 0 \le \theta \le \pi. \tag{174}$$

Distribute sources on the upper half of the circle, and distribute sinks of equal strength on the lower half. Corresponding to the source sheet on the airfoil in the x, z–plane, one has

$$\phi(x, z, t) = \frac{1}{4\pi} \int_{-b}^{b} H^-(\xi, t) \ln\left[(x - \xi)^2 + z^2\right] d\xi, \tag{175}$$

from which the velocity component along z–direction, on the upper surface of the airfoil, is given by

$$w(x,0^+,t)=\frac{1}{2\pi}\lim_{z\Rightarrow 0^+}\int_{-b}^{b}\frac{H^+(\xi,t)z}{\left[(x-\xi)^2+z^2\right]}\,d\xi$$

$$=\frac{1}{2\pi}H^+(x,t)\lim_{\substack{z\Rightarrow 0^+\\ \varepsilon\Rightarrow 0}}\left[\tan^{-1}\left(\frac{\varepsilon}{z}\right)-\tan^{-1}\left(-\frac{\varepsilon}{z}\right)\right]$$

$$=\frac{1}{2}H^+(x,t). \tag{176a}$$

Similarly, the velocity component along the z–direction on the lower surface of the airfoil is given by

$$w(x,0^-,t)=-\frac{1}{2}H^-(x,t). \tag{176b}$$

In the X, Z–plane, from (174) and (176), one has

$$\left.\begin{aligned} H^+\left(\frac{b}{2},\theta,t\right)&=2q_r=4w_a\sin\theta,\\ H^-\left(\frac{b}{2},\theta,t\right)&=-4w_a\sin\theta. \end{aligned}\right\} \tag{177}$$

Corresponding to a source of strength $H^+(b/2)d\varphi$ at $\theta=\varphi$ (see Figure 2.63), one has at P the flow speed

$$\left|dq^+\right|=\frac{H^+\frac{b}{2}d\varphi}{2\pi b\sin\left(\frac{\varphi-\theta}{2}\right)}=\frac{w_a\sin\varphi\,d\varphi}{\pi\sin\left(\frac{\varphi-\theta}{2}\right)}; \tag{178}$$

similarly, for a sink of strength $H^-(b/2)d\varphi$ at $\theta=-\varphi$, one has at P the flow speed

$$\left|dq^-\right|=\frac{w_a\sin\varphi\,d\varphi}{\pi\sin\left(\frac{\varphi+\theta}{2}\right)}. \tag{179}$$

Noting

$$\left.\begin{aligned} dq_\theta&=-\left|dq^+\right|\cos\left(\frac{\varphi-\theta}{2}\right)-\left|dq^-\right|\cos\left(\frac{\varphi+\theta}{2}\right),\\ dq_r&=\left|dq^+\right|\sin\left(\frac{\varphi-\theta}{2}\right)-\left|dq^-\right|\sin\left(\frac{\varphi+\theta}{2}\right), \end{aligned}\right\} \tag{180}$$

and using (178) and (179), one has the following equation for the flow velocity components at P:

$$dq_\theta=\frac{2w_a\sin^2\varphi\,d\varphi}{\pi(\cos\varphi-\cos\theta)} \tag{181}$$

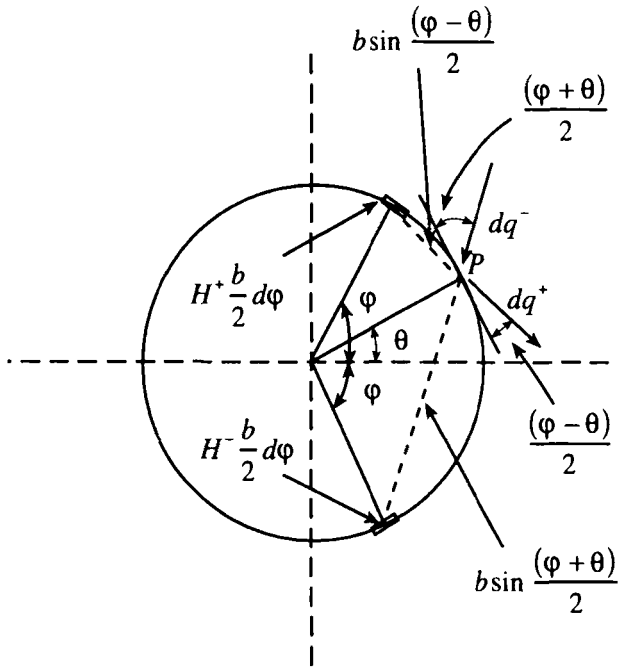

Figure 2.63. Source and sink distribution on the circle generated by Joukowski's mapping of the airfoil (from Bisplinghoff, Ashley, and Halfman, 1955).

$$dq_r = 0. \tag{182}$$

Equation (182) implies that the circle is a streamline.

One obtains, from (181), for the whole airfoil,

$$q_\theta = \frac{2}{\pi}\int_0^\pi \frac{w_a \sin^2\varphi\, d\varphi}{(\cos\varphi - \cos\theta)}. \tag{183}$$

Now, one has

$$\phi(\pi,t) - \phi^+(\theta,t) = \int_\theta^\pi q_\theta \frac{b}{2} d\theta, \tag{184}$$

where

$$\phi(\pi,t) = 0 \quad \text{since} \quad \phi^-(-\theta,t) = -\phi^+(\theta,t). \tag{185}$$

When one uses (183) and (185), (184) gives the following equation for the noncirculatory part of the flow:

$$\phi^+_{NC}(\theta,t) = -\frac{b}{\pi}\int_\theta^\pi\int_0^\pi \frac{w_a \sin^2\varphi\, d\varphi\, d\theta}{(\cos\varphi - \cos\theta)}. \tag{186}$$

On the airfoil, one has, from the Bernoulli equation, upon using (185), the following equation for the pressure jump across the airfoil:

$$\left(p^+ - p^-\right) = -2\rho\left(V_\infty \frac{\partial \phi^+}{\partial x} + \frac{\partial \phi^+}{\partial t}\right).$$

Further, on using (172), one obtains

$$\left(p^+ - p^-\right) = -2\rho\left(\frac{\partial \phi^+}{\partial t} - \frac{V_\infty}{b \sin\theta}\frac{\partial \phi^+}{\partial \theta}\right). \tag{187}$$

The lift and the moment on the airfoil corresponding to the noncirculatory part of the flow are, then, given by

$$\left(\mathbb{L}\right)_{NC} = -\int_{-b}^{b}\left(p^+ - p^-\right)dx = 2\rho b\frac{\partial}{\partial t}\int_0^\pi \phi^+ \sin\theta\, d\theta, \tag{188}$$

$$\begin{aligned}\left(M_y\right)_{NC} &= \int_{-b}^{b}\left(p^+ - p^-\right)(x - ba)\,dx \\ &= 2\rho V_\infty \int_{-b}^{b}\phi^+ dx - 2\rho\frac{\partial}{\partial t}\int_{-b}^{b}\phi^+ \cdot (x - ba)\,dx \\ &= 2\rho V_\infty b\int_0^\pi \phi^+ \sin\theta\, d\theta - 2\rho b^2\frac{\partial}{\partial t}\int_0^\pi \phi^+ \cdot (\cos\theta - a)\sin\theta\, d\theta,\end{aligned} \tag{189}$$

where $0 \le a \le 1$.

Now, the temporal variation of the total circulation around the airfoil generates a wake of two–dimensional countervortices along the x–axis from the trailing edge to infinity. The latter are continually moving away from the airfoil at the free–stream velocity. By pairing with each wake vortex a bound one of opposite circulation at the image position inside the circle, one ensures that the circle and the airfoil slit remain streamlines of the vortex flow so that the boundary conditions remain undisturbed.

Consider the flow due to a single bound vortex of strength Γ and its image $-\Gamma$ (see Figure 2.64). At P one has, by the Biot–Savart Law (see Section 2.4),

$$\begin{aligned}q_\theta &= \left|q^-\right|\cos\left(\theta_2 - \theta\right) - \left|q^+\right|\cos\left(\theta_1 - \theta\right) \\ &= \frac{\Gamma}{2\pi}\left[\frac{r_2\cos\left(\theta_2 - \theta\right)}{r_2^2} - \frac{r_1\cos\left(\theta_1 - \theta\right)}{r_1^2}\right].\end{aligned} \tag{190}$$

Since, from Figure 2.55,

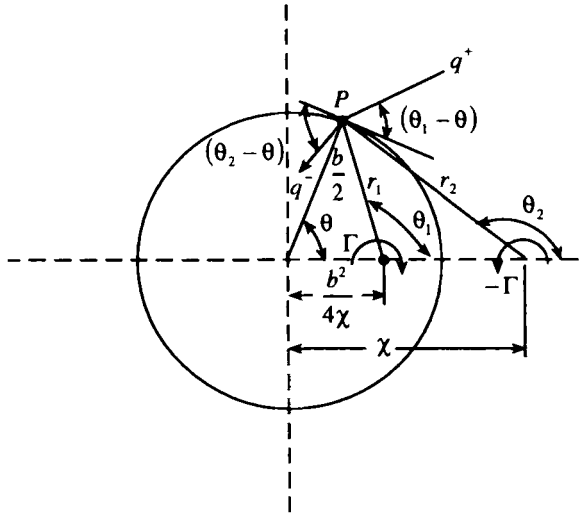

Figure 2.64. Flow generated by a system of wake vortices and image vortices in the circle (from Bisplinghoff, Ashley, and Halfman, 1955).

$$r_1^2 = \left(\frac{b^2}{4\chi}\right)^2 + \left(\frac{b}{2}\right)^2 - 2\frac{b^2}{4\chi}\cdot\frac{b}{2}\cos\theta,$$

$$r_2^2 = \chi^2 + \left(\frac{b}{2}\right)^2 - 2\chi\cdot\frac{b}{2}\cos\theta,$$

$$r_2\cos(\theta_2-\theta) = \frac{b}{2} - \chi\cos\theta,$$

$$r_1\cos(\theta_1-\theta) = \frac{b}{2} - \frac{b^2}{4\chi}\cos\theta, \tag{191}$$

(190) becomes

$$q_\theta = -\frac{\Gamma}{\pi b}\left[\frac{\chi^2-(b/2)^2}{\chi^2+(b/2)^2-\chi b\cos\theta}\right]. \tag{192}$$

Using (192) and (185), one has, from (184),

$$\phi_c^+(\theta,t) = \frac{\Gamma\left[\chi^2-(b/2)^2\right]}{2\pi}\int_0^\pi \frac{d\theta}{\chi^2+(b/2)^2-\chi b\cos\theta}$$

$$= \frac{\Gamma}{\pi}\tan^{-1}\left[\frac{\chi-b/2}{\chi+b/2}\sqrt{\frac{1+\cos\theta}{1-\cos\theta}}\right]. \tag{193}$$

Noting that, if ξ is the distance of a countervortex from the origin the x, y–plane, one has

$$\xi = \chi + \frac{b^2}{4\chi}, \qquad \frac{d\xi}{dt} = V_\infty \tag{194}$$

from which

$$\sqrt{\frac{\xi - b}{\xi + b}} = \frac{\chi - b/2}{\chi + b/2}. \tag{195}$$

When one uses (195), (193) becomes

$$\phi_c^+(\theta, t) = \frac{\Gamma}{\pi} \tan^{-1} \sqrt{\frac{(\xi - b)(1 + \cos\theta)}{(\xi + b)(1 - \cos\theta)}}. \tag{196}$$

When one uses (196), the Bernoulli equation, namely (187),

$$\left(p^+ - p^-\right)_\Gamma = -2\rho \left[\frac{\partial \phi_c^+}{\partial \xi} \frac{d\xi}{dt} - \frac{V_\infty}{b \sin\theta} \frac{\partial \phi_c^+}{\partial \theta} \right],$$

gives the following equation for the pressure jump across the airfoil,

$$\left(p^+ - p^-\right)_\Gamma = -\frac{\rho V_\infty \Gamma (\xi + b \cos\theta)}{\pi b \sin\theta \cdot \sqrt{\xi^2 - b^2}}. \tag{197}$$

The corresponding lift and the moment on the airfoil are given by

$$(\mathbb{L})_\Gamma = -\int_0^\pi b \sin\theta \cdot d\theta \cdot \left(p^+ - p^-\right)_\Gamma = \frac{\rho V_\infty \Gamma \xi}{\sqrt{\xi^2 - b^2}}, \tag{198}$$

$$\left(M_y\right)_\Gamma = \int_0^\pi (b \cos\theta - ba)\, b \sin\theta \cdot d\theta \cdot \left(p^+ - p^-\right)_\Gamma = \frac{\rho V_\infty \Gamma b^2}{\sqrt{\xi^2 - b^2}} \left(\frac{\xi}{b} a - \frac{1}{2} \right). \tag{199}$$

Note that, as $\xi \Rightarrow \infty$, the flow approaches that of a single–bound vortex Γ. The lift $\rho V_\infty \Gamma$, then, acts at midchord.

For the complete wake, one obtains the following equations for the circulatory flow, from (197)–(199):

$$\left(p^+ - p^-\right)_c = \frac{\rho V_\infty}{\pi b \sin\theta} \int_b^\infty \left[\frac{\xi}{\sqrt{\xi^2 - b^2}} (1 - \cos\theta) + \sqrt{\frac{\xi + b}{\xi - b}} \cos\theta \right] \gamma_w(\xi, t)\, d\xi \tag{200}$$

$$(\mathbb{L})_c = -\rho V_\infty \int_b^\infty \frac{\xi}{\sqrt{\xi^2 - b^2}} \gamma_w(\xi, t)\, d\xi \tag{201}$$

$$\left(M_y\right)_c = \rho V_\infty b \int_b^\infty \left[\frac{1}{2}\sqrt{\frac{\xi+b}{\xi-b}} - \left(a+\frac{1}{2}\right)\frac{\xi}{\sqrt{\xi^2-b^2}}\right] \gamma_w(\xi,t)\, d\xi. \tag{202}$$

Here we have replaced Γ by $\gamma_w d\xi$, where γ_w is the circulation per unit length of the wake.

From (174), one has the Kutta condition at $\theta = 0$:

$$q_\theta = 0. \tag{203}$$

When one uses (186) and (196), (203) leads to

$$\frac{2}{\pi}\int_0^\pi \frac{w_a \sin^2\varphi\, d\varphi}{\cos\varphi - 1} + \frac{1}{\pi b}\int_b^\infty \sqrt{\frac{\xi+b}{\xi-b}}\, \gamma_w(\xi,t)\, d\xi = 0, \tag{204}$$

which is an integral equation for γ_w.

When we put

$$\xi^* = \cos\varphi, \tag{205}$$

(204) becomes

$$\frac{2}{\pi}\int_{-1}^{1} \frac{\sqrt{1-\xi^{*2}}}{\left(\xi^*-1\right)} w_a\left(\xi^*,t\right) d\xi^* + \frac{1}{\pi b}\int_b^\infty \sqrt{\frac{\xi+b}{\xi-b}}\, \gamma_w(\xi,t)\, d\xi = 0. \tag{206}$$

Note that for the bound vortices distributed on the airfoil, one has the total circulation,

$$\Gamma_0(t) = \int_{-b}^{b} \gamma_0(x,t)\, dx. \tag{207}$$

The velocity induced by this vortex distribution is given by (see Section 2.4)

$$w_0(x) = -\frac{1}{2\pi}\int_{-b}^{b} \frac{\gamma(x_1)}{x - x_1}\, dx_1. \tag{208}$$

Now, in order to invert

$$w_0(x) = -\frac{1}{2\pi}\int_0^{\ell} \frac{\gamma(x_1)}{x - x_1}\, dx_1 \tag{209}$$

one may write

$$\gamma(x) = \int_0^{\ell} dx_1\, w_0(x_1)\, \psi(x, x_1). \tag{210}$$

When one uses (210), (209) implies that

$$-\frac{1}{2\pi}\int_0^{\ell} dx_1 \frac{\psi(\xi, x_1)}{x - x_1} = \delta(x - \xi), \tag{211}$$

from which we have

$$x\,\delta(x-\xi) = -\frac{1}{2\pi}\int_0^{\ell} dx_1\ \psi(\xi,x_1) - \frac{1}{2\pi}\int_0^{\ell} dx_1\ \frac{x_1\,\psi(\xi,x_1)}{x-x_1},$$

$$\xi\delta(x-\xi) = -\frac{1}{2\pi}\int_0^{\ell} dx_1\ \frac{\xi\psi(\xi,x_1)}{x-x_1}. \tag{212}$$

Equation (212), in turn, gives

$$-\frac{1}{2\pi}\int_0^{\ell} dx_1\ \frac{(x_1-\xi)\,\psi(\xi,x_1)}{x-x_1} = \frac{1}{2\pi}\int_0^{\ell} dx_1\ \psi(\xi,x_1). \tag{213}$$

Let

$$(x_1-\xi)\ \psi(\xi,x_1) = A(\xi)\gamma_1(x_1) \tag{214}$$

with

$$-\frac{1}{2\pi}\int_0^{\ell}\frac{\gamma_1(x_1)}{x-x_1}\,dx_1 = 1. \tag{215}$$

Equation (215) implies that

$$\gamma_1(x_1) = 2\sqrt{\frac{x_1}{\ell-x_1}}. \tag{216}$$

When one uses (214) and (215), (213) gives

$$A(\xi) = \frac{1}{2\pi}\int_0^{\ell} dx_1\ \psi(\xi,x_1). \tag{217}$$

Consider

$$\int_0^{\ell}\gamma_1(\ell-x)\,\delta(x-\xi)\,dx = \int_0^{\ell}\left(-\frac{1}{2\pi}\right)\int_0^{\ell} dx_1\,\frac{\gamma_1(\ell-x)\,\psi(\xi,x_1)}{x-x_1}\,dx, \tag{218}$$

from which we have

$$\gamma_1(\ell-\xi) = \frac{1}{2\pi}\int_0^{\ell} dx_1\ \psi(\xi,x_1)\left[-\int_0^{\ell} dx\,\frac{\gamma_1(\ell-x)}{x-x_1}\right]. \tag{219}$$

When one uses (215) and (217), (219) becomes

$$\gamma_1(\ell-\xi) = -2\pi A(\xi). \tag{220}$$

Using (210), (214), (216), and (220), one obtains

$$\gamma(x) = -\frac{2}{\pi}\sqrt{\frac{\ell-x}{x}}\int_0^{\ell} dx_1\ \frac{w_0(x_1)}{x_1-x}\sqrt{\frac{x_1}{\ell-x_1}}. \tag{221}$$

Thus,

$$\gamma_0(x,t) = \frac{2}{\pi}\sqrt{\frac{1-x}{1+x}} \oint_{-1}^{1} \sqrt{\frac{1+\xi^*}{1-\xi^*}}\, \frac{w_a(\xi^*,t)}{x-\xi^*}\, d\xi^*. \tag{222}$$

When one uses (222), (207) gives

$$\Gamma_0(t) = -2b \int_{-1}^{1} \sqrt{\frac{1+\xi^*}{1-\xi^*}}\, w_a(\xi^*,t)\, d\xi^*. \tag{223}$$

When one uses (223), (206) becomes

$$\Gamma_0(t) + \int_{b}^{\infty} \sqrt{\frac{\xi+b}{\xi-b}}\, \gamma_w(\xi,t) d\xi = 0. \tag{224}$$

Example 1: Consider an airfoil in vertical translation $h(t)$, and a rotation about an axis at $x = ba$, through an angle α. One then has

$$w_a(x,t) = -\dot{h} - V_\infty \alpha - \dot{\alpha}(x - ba). \tag{225}$$

When one uses (225), (186) gives

$$\begin{aligned}\phi_{NC}^{+}(\theta,t) &= \frac{b}{\pi}\left(\dot{h} + V_\infty \alpha\right) \int_{\theta}^{\pi}\int_{0}^{\pi} \frac{\sin^2\varphi\, d\varphi\, d\theta}{(\cos\varphi - \cos\theta)} \\ &\quad + \frac{b^2\dot{\alpha}}{\pi} \int_{\theta}^{\pi}\int_{0}^{\pi} \frac{\sin^2\varphi \cdot (\cos\varphi - a)\, d\varphi\, d\theta}{(\cos\varphi - \cos\theta)} \\ &= b\left(\dot{h} + V_\infty \alpha\right) \sin\theta + b^2\dot{\alpha}\, \sin\theta \cdot \left(\frac{\cos\theta}{2} - a\right).\end{aligned} \tag{226}$$

When one uses (226), (188) and (189) give, for the lift and the moment on the airfoil corresponding to the noncirculatory part of the flow,

$$(\mathbb{L})_{NC} = \pi\rho b^2 \left(\ddot{h} + V_\infty \dot{\alpha} - ba\ddot{\alpha}\right), \tag{227}$$

$$\left(M_y\right)_{NC} = \pi\rho b^2 \left[V_\infty \dot{h} + ba\ddot{h} + V_\infty^2\, \alpha - b^2\left(\frac{1}{8} + a^2\right)\ddot{\alpha}\right]. \tag{228}$$

In order to calculate the corresponding quantities for the circulatory part of the flow, let us take

$$w_a(x,t) = \overline{w}_a(x) e^{i\omega t} \tag{229}$$

so that one has for the wake vortices

$$\gamma_w(\xi,t) = \overline{\gamma}_w\, e^{i\omega(t - \xi/V_\infty)}. \tag{230}$$

When one uses (230), note that

$$\frac{\int_b^\infty \frac{\xi}{\sqrt{\xi^2-b^2}}\,\gamma_w(\xi,t)\,d\xi}{\int_b^\infty \sqrt{\frac{\xi+b}{\xi-b}}\,\gamma_w(\xi,t)\,d\xi} = \frac{\int_1^\infty \frac{\xi^*}{\sqrt{\xi^{*2}-1}}\,e^{-ik\xi^*}\,d\xi}{\int_1^\infty \sqrt{\frac{\xi^*+1}{\xi^*-1}}\,e^{-ik\xi^*}\,d\xi},$$

$$= \frac{H_1^{(2)}(k)}{H_1^{(2)}(k)+iH_0^{(2)}(k)} \equiv C(k), \text{ say,} \tag{231}$$

where $H_n^{(2)}(x)$ is Hankel's function of second kind, and

$$k \equiv \frac{\omega b}{V_\infty}, \qquad \xi^* \equiv \frac{\xi}{b}.$$

In order to ensure the convergence of the integrals in $C(k)$, one needs to impose an appropriate radiation condition, namely, that k is a complex quantity with a negative imaginary part.

When one uses (225), the Kutta condition (224) leads to

$$-\frac{1}{\pi b}\int_b^\infty \sqrt{\frac{\xi+b}{\xi-b}}\,\gamma_w(\xi,t)\,d\xi$$

$$= \frac{2}{\pi}\int_0^\pi (1+\cos\varphi)\left[\dot h + V_\infty\alpha + \dot\alpha b(\cos\varphi - a)\right]d\varphi$$

$$= 2\left[\dot h + V_\infty\alpha + b\left(\frac{1}{2}-a\right)\dot\alpha\right]. \tag{232}$$

Thus, using (227), (228), (201), (202), (231) and (232), one obtains the following equations for the total lift and the moment on the airfoil:

$$\mathbb{L} = (\mathbb{L})_{NC} + (\mathbb{L})_c = \pi\rho b^2\left(\dot h + V_\infty\dot\alpha - ba\ddot\alpha\right)$$

$$+ 2\pi\rho V_\infty b C(k)\left[\dot h + V_\infty\alpha + b\left(\frac{1}{2}-a\right)\dot\alpha\right], \tag{233}$$

$$M_y = (M_y)_{NC} + (M_y)_c$$

$$= \pi\rho b^2\left[ba\ddot h - V_\infty b\left(\frac{1}{2}-a\right)\dot\alpha - b^2\left(\frac{1}{8}+a^2\right)\ddot\alpha\right]$$

$$= 2\pi\rho V_\infty b^2\left(a+\frac{1}{2}\right)C(k)\left[\dot h + V_\infty\alpha + b\left(\frac{1}{2}-a\right)\dot\alpha\right]. \tag{234}$$

In deriving (234), note that certain cancellations have occurred between circulatory and noncirculatory parts of the moment expressions.

EXERCISES

1. Using the Joukowski transformation, calculate the flow about an elliptic cylinder with its major axis aligned with the flow direction, and also calculate the moment about the leading edge acting on the cylinder.
2. Calculate the flow at the trailing edge of a symmetric airfoil (with $\mu = me^{i\pi}$, $\beta = 0$) at zero incidence in a uniform flow.
3. Calculate the camber–line shape of an airfoil, given the loading $\gamma(\theta) = \text{const.} = k$, by thin–airfoil theory.
4. Using equation (150), solve for the coefficients A_n in the prescription

$$\Gamma(\theta) = 2bU \sum_{n=1}^{\infty} A_n \sin n\theta .$$

3

DYNAMICS OF INVISCID, COMPRESSIBLE FLUID FLOWS

3.1. Review of Thermodynamics

The laws of thermodynamics apply to equilibrium states of matter in bulk. Thermodynamics is concerned with connecting the initial and final states of a system undergoing a process rather than the detailed evolution of the system during the process. Equilibrium thermodynamics is directly applicable to the mechanics of ideal fluids. But the mechanics of real fluids has to include the various transport phenomena which upset the state of thermodynamic equilibrium.

Thermodynamic System and Variables of State

A thermodynamic system is a quantity of matter isolated from the surroundings for the purpose of observation. The system we consider is a simple, homogeneous system composed of a single fluid.

An isolated system reaches a state of equilibrium, i.e., the macroscopic state becomes steady. Variables of state determine the state of the system. For a simple system, one has an equation of state of the form

$$p = p(V, T), \tag{1}$$

where p is the pressure, V the volume, and T the temperature. The Zeroth law of thermodynamics states that there exists a variable of state, the temperature T; two systems that are in thermal contact are in equilibrium only if T is the same in both.

In the context of exchange of work or heat of a system with its surroundings, one introduces another variable of state, the internal energy E, which measures the

energy stored in the system. Furthermore, it is necessary to introduce another variable of state, the entropy S, which determines whether a state is in stable equilibrium.

The equations of state are

$$E = E(V,T),$$
$$S = S(V,T). \tag{2}$$

A variable of state is uniquely defined for any equilibrium state of the system and is independent of the process by which system arrived at that state in the first place.

An extensive variable of state depends on the mass of the system, e.g.., E,V,S. An intensive variable of state does not depend on the mass of the system, e.g., p,T.

The First Law of Thermodynamics; Reversible and Irreversible Processes

The First law of thermodynamics asserts mutual equivalence between heat energy and mechanical work. If a system is transformed from a state of equilibrium A to another one, B, by a process in which a certain amount of work W is done by the surroundings, and a certain quantity of heat Q leaves the surroundings, then one defines the internal energy E by

$$E_A - E_B = Q + W. \tag{3}$$

The internal energy E measures the energy stored in the system. For a small change of state (so that the process is reversible and the system passes through a succession of equilibrium states; the pressure in the fluid remains uniform), (3) gives

$$dE = dQ + dW = dQ - pdV, \tag{4}$$

or, in terms of specific quantities,

$$de = dq - pd\upsilon.$$

Note that E is a variable of state, whereas Q and W depend on the process followed in changing the state.[1]

---

[1] This may be seen by considering a perfect gas for which equation (5) becomes

$$dq = C_\upsilon dT + pd\upsilon = \frac{C_\upsilon}{R} d(p\upsilon) + pd\upsilon$$
$$= \left(1 + \frac{C_\upsilon}{R}\right) pd\upsilon + \frac{C_\upsilon}{R} \upsilon dp = \frac{C_p}{R} pd\upsilon + \frac{C_\upsilon}{R} \upsilon dp$$

on using (6), (8), and (10). This shows that dq is not an exact differential because

$$\frac{\partial}{\partial p}\left(\frac{C_p}{R} p\right) \neq \frac{\partial}{\partial \upsilon}\left(\frac{C_\upsilon}{R} \upsilon\right)$$

on account of $C_p \neq C_\upsilon$. Therefore, Q is not a variable of state.

The First law of thermodynamics dictates only the magnitude of the change of state of a system by (4), but does not dictate the direction of this change of state.

However, all natural or spontaneous processes are irreversible. Note that during an irreversible process the system deviates from equilibrium.

A perfect gas is taken to have no interparticle forces of repulsion or attraction, and although the particles have mass, they occupy no space. A perfect gas is described by the equation of state

$$p = \rho RT \tag{6}$$

where, R is the gas constant, ρ the density of the gas.

One may define the specific heats at constant volume and constant pressure according to

$$\begin{aligned} C_\upsilon &= \left(\frac{\partial q}{\partial T}\right)_\upsilon, \\ C_p &= \left(\frac{\partial q}{\partial T}\right)_p. \end{aligned} \tag{7}$$

Using equation (5), one obtains

$$\begin{aligned} C_\upsilon &= \left(\frac{\partial e}{\partial T}\right)_\upsilon, \\ C_p &= \left[p + \left(\frac{\partial e}{\partial \upsilon}\right)_T\right]\left(\frac{\partial \upsilon}{\partial T}\right) + \left(\frac{\partial e}{\partial T}\right)_\upsilon = \frac{\partial h}{\partial T} \end{aligned} \tag{8}$$

where h is the enthalpy,

$$h = e + p\upsilon. \tag{9}$$

Using (6), one has

$$C_p = C_\upsilon + R. \tag{10}$$

For an adiabatic, reversible (also called isentropic) process, one has, from (5) and (9),

$$\begin{aligned} de &= -pd\upsilon \\ dh &= \upsilon dp \end{aligned} \tag{11}$$

or

$$\begin{aligned} \frac{\partial e}{\partial \upsilon} d\upsilon + \frac{\partial e}{\partial T} dT &= -pd\upsilon, \\ \frac{\partial h}{\partial p} dp + \frac{\partial h}{\partial T} dT &= \upsilon\, dp. \end{aligned} \tag{12}$$

When one uses (8), (12) leads to

$$\frac{dT}{dv} = -\frac{1}{C_v}\left(\frac{\partial e}{\partial v} + p\right),$$
$$\frac{dT}{dp} = -\frac{1}{C_p}\left(\frac{\partial h}{\partial p} - v\right). \tag{13}$$

For a perfect gas, given by (6), (13) yields

$$\frac{v}{T}\frac{dT}{dv} = -\frac{R}{C_v},$$
$$\frac{p}{T}\frac{dT}{dp} = \frac{R}{C_p}. \tag{14}$$

Furthermore, (14) leads to

$$\frac{v}{p}\frac{dp}{dv} = -\frac{C_p}{C_v} \tag{15}$$

from which

$$\frac{p}{v^\gamma} = \text{const.}, \tag{16}$$

where

$$\gamma \equiv \frac{C_p}{C_v}.$$

Consider next irreversible processes. For an isolated system, one has the following equation for the two end states denoted by A and B,

$$e_B - e_A = 0. \tag{17}$$

For an adiabatic flow, on the other hand, one has

$$e_B + p_B v_B = e_A + p_A v_A. \tag{18}$$

The Second Law of Thermodynamics

The evolution of a system is dictated by certain natural tendencies, and all natural or spontaneous processes are irreversible. There is considerable departure from equilibrium in the latter. By contrast, a system remains in equilibrium during a reversible process. In this context, one introduces a new variable of state, called the entropy S.

First note that the internal energy has the character of a potential energy; for an adiabatic reversible change of state of a system, one has from (4)

$$p = -\left(\frac{\partial E}{\partial V}\right)_S. \tag{19}$$

When one defines

$$T = -\left(\frac{\partial E}{\partial S}\right), \tag{20}$$

the equation of state

$$E = E(V, S) \tag{21}$$

gives

$$dE = \frac{\partial E}{\partial V} dV + \frac{\partial E}{\partial S} dS. \tag{22}$$

When one uses (19) and (20), equation (22) becomes

$$dE = -pdV + TdS. \tag{23}$$

On comparing (23) with (4), we have

$$TdS = dQ. \tag{24}$$

By virtue of the manner of definition, S, a variable of state,[2] is defined only for a system in equilibrium, or for reversible changes of state.

For an irreversible process, one has

$$S_B - S_A \geqslant \int_A^B \frac{dQ}{T}, \tag{25}$$

where the equality prevails for a reversible process. Thus, for an adiabatic irreversible process, the entropy can only increase.

A system has reached a state of equilibrium if no further spontaneous processes are possible, for which

$$dS \geq \frac{dQ}{T}.$$

On the other hand, the system is in stable equilibrium if, for every process compatible with the constraints of the system, one has

$$\delta S \leq \frac{\delta Q}{T}.$$

For an isolated system, this gives

$$\delta S \leq 0;$$

i.e., the entropy for an isolated system reaches a maximum.

One obtains from equation (23)

---

[2]This may be seen by noting (see footnote 1) that, for a perfect gas,

$$dS = \frac{dq}{T} = \frac{C_p}{v} dv + \frac{C_v}{p} dp,$$

which shows that dS is a perfect differential because

$$\frac{\partial}{\partial p}\left(\frac{C_p}{v}\right) = \frac{\partial}{\partial v}\left(\frac{C_v}{p}\right) = 0.$$

$$S = \int \frac{de}{T} + \int p \frac{dv}{T} + \text{const.} \tag{26}$$

When one considers a perfect gas given by (6) and uses (8), equation (26) leads to

$$S = \int C_v \frac{dT}{T} + R \ln v + \text{const.} \tag{27}$$

or, alternatively,

$$S = \int C_p \frac{dT}{T} - R \ln p + \text{const.} \tag{28}$$

If the specific heats C_p, C_v are constants, then (28) leads to

$$S_2 - S_1 = C_p \ln\left(\frac{T_2}{T_1}\right)\left(\frac{p_2}{p_1}\right)^{-(\gamma-1)/\gamma}. \tag{29}$$

Next, when one considers a perfect gas given by (6) and uses (8), (23) leads to

$$dS = C_v \frac{dp}{p} + C_p \frac{dv}{v} \tag{30}$$

and, on integrating, (30) gives

$$\ln \frac{p}{p_0} + \frac{C_p}{C_v} \ln \frac{v}{v_0} = \frac{S - S_0}{C_v}; \tag{31}$$

or in terms of the mass density $\rho \equiv 1/v$, (31) becomes

$$p = k\rho^{\gamma}, \tag{32}$$

where

$$k = \frac{p_0 e^{(S-S_0)/C_v}}{\rho_0^{\gamma}}.$$

Note that, for an isentropic process, (32) gives

$$p \sim \rho^{\gamma}, \tag{33}$$

in agreement with (16).

Liquid and Gaseous Phases

A given material may exist in the liquid phase for some values of the two parameters of state (p and v, say) and in the gaseous phase for other values. The manner in which the intermolecular force varies with molecular spacing is responsible for the occurrence of these two distinct phases.

At low temperature and high pressures, the molecules in a gas are brought so close together that in many cases, actual condensation to the liquid state and the formation of a free surface separating vapor and liquid sets in, but above a certain temperature, no amount of compression can produce such an interface.

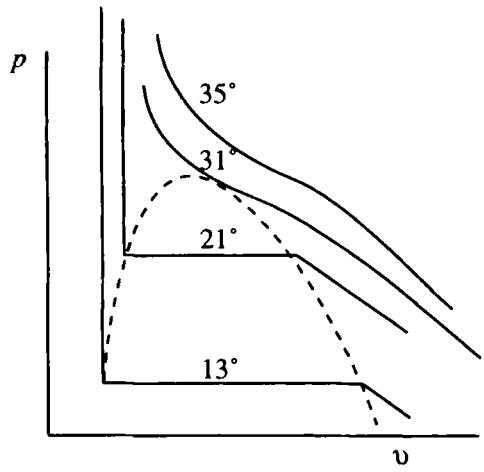

Figure 3.1. Isothermals for CO_2.

Figure 3.1 shows the isothermals for CO_2. The lower curves all pass through a horizontal step, which signifies a change in volume at constant pressure. To the left of this step, one has a liquid state, wherein it takes a large increase of pressure to produce a small change of volume, implying that liquids are nearly incompressible. To the right is the vapor or gaseous region, these curves eventually become hyperbolas: $p\upsilon$ =constant. The constant pressure on an isothermal through the polyphase region is the saturated vapor pressure p_v, i.e., the pressure existing in pure vapor which is in contact with the liquid at the given temperature. The effect of reducing the pressure of a liquid below the saturated vapor pressure is of importance in fluid dynamics, since this leads to the formation of vapor packets distributed throughout the liquid. The occurrence of such vapor packets, called *cavitation*, has important mechanical consequences on objects placed in such flows, (see Section 2.1).

At 31°C, for CO_2, the constant pressure step is reduced to a pause in passing, and above this temperature, the isothermal passes steadily from high to low pressure with no marked distinction between gas and liquid; 31.5°C is called the *critical temperature* for CO_2.

Application of Thermodynamics to Fluid Flows

Classical thermodynamics deals with a uniform, static system whose state is specified by certain variables of state and which exchanges energy with its surroundings. In applying classical thermodynamics to fluid flows, a fluid particle, small enough to be assumed uniform, is taken to be the system in *local* thermodynamic equilibrium. (The conditions of equilibrium cannot be strictly attained in a real, nonuniform flow, since a fluid particle must adjust itself continuously to the new conditions that it encounters; the rate at which the

adjustments must be made depends on the gradients in the flow and is a measure of the departure from equilibrium.) One may then ascribe state variables $(T, \rho, p, h, s, \text{etc.})$ to the fluid particle and, as before, relate them to each other by equations of state. Here, p is the thermodynamic pressure if the fluid is compressible, while it is simply an independent dynamical variable otherwise.

3.2. Isentropic Flows

The Energy Equation

The conservation of energy of a fluid particle in an adiabatic flow may be expressed by the energy equation

$$h + \frac{1}{2} V^2 = \text{const.} \tag{1}$$

For a perfect gas, one has

$$h = C_p T = \frac{C_p}{R} \frac{p}{\rho} = \frac{\gamma}{\gamma - 1} \frac{p}{\rho} = \frac{a^2}{\gamma - 1}, \tag{2}$$

where

$$a \equiv \sqrt{\left(\frac{dp}{d\rho}\right)_s} = \sqrt{\frac{\gamma p}{\rho}} = \sqrt{\gamma RT} \tag{3}$$

is the speed of sound in the gas. The disturbances produced in a fluid by a sound wave are so small that each fluid particle undergoes a nearly isentropic process. Besides, the frequencies of the sound wave are assumed to be not so great as to allow large departures from thermodynamic equilibrium.

When one uses equation (2), equation (1) gives

$$\frac{a^2}{\gamma - 1} + \frac{V^2}{2} = \text{const} = \frac{a_0^2}{\gamma - 1}, \tag{4}$$

where the subscript 0 refers to the stagnation values. The latter are the values that would result if the fluid particle were brought to rest isentropically, and they are different from the values measured by an observer moving with the particle, (called the *static properties*). This is due to the exchanges occurring between the kinetic energy, the internal energy, and the potential energy (due to the pressure) of the fluid particle with those of the surrounding fluid particles.

One obtains from equation (4), upon using (3),

$$\frac{T_0}{T} = \left(1 + \frac{\gamma - 1}{2} M^2\right), \tag{5}$$

where M is the Mach number,

$$M^2 \equiv \frac{V^2}{a^2}.$$

Using (5), one obtains the following relations:

$$\frac{p_0}{p} = \left(1 + \frac{\gamma - 1}{2} M^2\right)^{\gamma/(\gamma-1)}, \quad \frac{\rho_0}{\rho} = \left(1 + \frac{\gamma - 1}{2} M^2\right)^{1/(\gamma-1)} \tag{6a,b}$$

If $M = V/a \ll 1$, (6a) leads to the following expansion:

$$\frac{p_0}{p} = 1 + \frac{1}{2}\gamma M^2 + \frac{1}{8}\gamma M^4 + \cdots$$

or

$$p_0 - p = \frac{1}{2}\rho q^2 \left(1 + \frac{1}{4} M^2\right) + \cdots, \tag{7}$$

so that, when $M \ll 1$, one obtains

$$p_0 \approx p + \frac{1}{2}\rho q^2, \tag{8}$$

the same as for the incompressible flow.

Let $a = a^*$ correspond to the location where $V = a$, then for a^*, equation (4) gives

$$a^{*2} = \frac{2}{\gamma + 1} a_0^2. \tag{9}$$

Stream–Tube Area and Velocity Relations

The conservation of mass for steady flow in a stream tube requires

$$\rho V A = \text{const.}, \tag{10}$$

where A is the cross–sectional area of the stream tube. One may write equation (10), alternatively, as

$$\frac{d\rho}{\rho} + \frac{dV}{V} + \frac{dA}{A} = 0. \tag{11}$$

The equation of motion of the fluid in the stream tube is

$$V\frac{dV}{dx} = -\frac{1}{\rho}\frac{dp}{dx} = -\frac{a^2}{\rho}\frac{d\rho}{dx}, \tag{12}$$

where x is the distance along the stream–tube, and we have assumed the flow to be one–dimensional.

When one uses equation (12), equation (11) gives

$$\frac{dA}{A} = \frac{dV}{V}\left(M^2 - 1\right), \tag{13}$$

which shows that, in subsonic flow $(M < 1)$, an increase in speed is produced by a decrease in the stream–tube area, and in a supersonic flow $(M > 1)$, an increase in speed is produced by an increase in area. This is so because in supersonic flows, the decrease in density overweighs the increase in velocity. Also, note that the acceleration of a fluid from a subsonic speed to a supersonic speed requires that the flow pass through a throat, where the flow is sonic $(M = 1)$.

Noting, from (29) (Section 3.1), that, for an isentropic flow,

$$\frac{p}{p_0} = \left(\frac{T}{T_0}\right)^{\gamma/(\gamma-1)} = \left[1 - \frac{\gamma-1}{2}\left(\frac{V}{a_0}\right)^2\right]^{\gamma/(\gamma-1)}, \tag{14}$$

one obtains

$$V = \sqrt{\frac{2\gamma RT_0}{\gamma-1}\left[1 - \left(\frac{p}{p_0}\right)^{(\gamma-1)/\gamma}\right]}. \tag{15}$$

The mass flux is then given by

$$G = \rho V = \rho_0\sqrt{\frac{2\gamma RT_0}{\gamma-1}\left[\left(\frac{p}{p_0}\right)^{2/\gamma} - \left(\frac{p}{p_0}\right)^{(\gamma+1)/\gamma}\right]}, \tag{16}$$

which reaches its maximum at

$$\frac{dG}{d(p/p_0)} = 0,$$

i.e., at

$$\left(\frac{p}{p_0}\right)_C = \left(\frac{2}{\gamma+1}\right)^{\gamma/(\gamma-1)}$$

or

$$V_C = \sqrt{\frac{2\gamma RT_0}{\gamma+1}} = a^*,$$

i.e., at the throat.

In order to show that the flow is indeed sonic at the throat, note, from (5), that

$$a^2 = \frac{dp}{d\rho} = k\gamma\rho^{\gamma-1} = a_0^2 - \frac{1}{2}(\gamma-1)V^2, \tag{17}$$

where we have used

$$\frac{p}{\rho^\gamma} = k = \text{const.}$$

When we use equation (17), equation (10) gives

$$A^{\gamma-1}\left[a_0^2-\frac{1}{2}(\gamma-1)V^2\right]V^{\gamma-1}=\text{const.} \tag{18}$$

Differentiating equation (18) with respect to V, one obtains

$$(\gamma-1)A^{\gamma-2}\frac{dA}{dV}\left[a_0^2-\frac{1}{2}(\gamma-1)V^2\right]V^{\gamma-1}$$
$$+A^{\gamma-1}\left[(\gamma-1)a_0^2V^{\gamma-2}-\frac{1}{2}(\gamma^2-1)V^{\gamma}\right]=0, \tag{19}$$

which shows that

$$\frac{dA}{dV}=0:\quad a_0^2=\frac{1}{2}(\gamma+1)V^2\quad\text{or}\quad V=a^*, \tag{20}$$

as also shown by (13). Further, at $V=a^*$, (19) gives, upon one more differentiation,

$$\left.\frac{d^2A}{dV^2}\right|_{V=a^*}\cdot\left[a_0^2-\frac{1}{2}(\gamma-1)V^2\right]V-A(\gamma+1)V=0,$$

from which

$$\left.\frac{d^2A}{dV^2}\right|_{V=a^*}=\frac{A(\gamma+1)}{a_0^2-\frac{1}{2}(\gamma-1)a^{*2}}=\frac{A(\gamma+1)^2}{2a_0^2}>0, \tag{21}$$

so that A reaches a minimum at $V=a^*$.

Next, from

$$\rho VA=\rho^*V^*A^*=\left(\frac{2}{\gamma+1}\right)^{(\gamma-1)/2(\gamma+1)}\rho_0a_0A^*,$$

one obtains

$$\frac{A}{A^*}=\frac{1}{M}\left[\frac{2}{\gamma+1}\left(1+\frac{\gamma-1}{2}M^2\right)\right]^{(\gamma+1)/2(\gamma-1)}, \tag{22}$$

which, for a given value of (A/A^*), in general, gives two values of M, one subsonic and the other supersonic, except at $A/A^*=1$, where the two roots for M coalesce at $M=1$.

EXERCISES

1. Show that at very-small Mach-number flows, the changes in the flow velocity are much larger than those in the speed of sound in the fluid, and the reverse is true at very-large Mach-number flows.

3.3. Shock Waves

It turns out that (see Section 3.7), in the absence of dissipative effects such as viscosity and heat conductivity, propagation and convection of compressional disturbances with speeds increasing with compression leads to a continual steepening of waveforms that eventually can no longer be expressed by single-valued functions of position. One then has to introduce into the flow a discontinuity to get over this difficulty. A shock wave is a surface in a flow field across which the flow variables change discontinuously. The existence of shock waves is also necessary in order that one may admit certain types of boundary conditions that could not be satisfied in a continuous flow pattern.

Of course, a real fluid cannot sustain an actual discontinuity, so that the latter is only an idealization of the sharp gradients in the flow variables that occur in reality in a shock wave. Consequent to these flow gradients, various transport processes such as those due to viscosity and heat conductivity show up inside the shock. One can in fact give an explicit solution for the flow structure within the shock when viscosity and heat conductivity are included for the particular Prandtl number $\mu C_p/k = 3/4$ (see Section 4.1).[3]

The Normal Shock Wave

The changes in flow properties which occur across a shock wave may be determined without reference to the specific dissipation processes occurring within the shock wave. The dissipation processes influence only the structure within the shock wave. Consider a stationary shock wave with its plane normal to the flow.

For a one-dimensional flow of gas, one has

$$\frac{\partial \rho}{\partial t} + u\frac{\partial \rho}{\partial x} + \rho\frac{\partial u}{\partial x} = 0, \tag{1}$$

$$\rho\left(\frac{\partial u}{\partial t} + u\frac{\partial u}{\partial x}\right) + \frac{\partial p}{\partial x} = 0, \tag{2}$$

$$\frac{\partial S}{\partial t} + u\frac{\partial S}{\partial x} = 0, \tag{3a}$$

or

[3]It may be noted that real gas effects can provide additional thermodynamics relaxation processes to support the flow gradients in a shock wave. In the case of the very weakest shocks, the process with the longest relaxation time is adequate to support the concomitant flow gradient. But, when the shock becomes stronger, the next longest relaxation-time process is called into play to sustain the main shock transition, followed by a slower relaxation involving only the longer relaxation-time process. Finally, when the shock becomes so strong that all these thermodynamic relaxations are insufficient to support the steep flow gradients occurring inside the shock, strongest dissipative processes like viscosity and thermal conductivity are called into play to sustain the main shock transition, followed by slower thermodynamic relaxations.

$$\frac{\partial e}{\partial t}+u\frac{\partial e}{\partial x}-\frac{p}{\rho^2}\left(\frac{\partial \rho}{\partial t}+u\frac{\partial \rho}{\partial x}\right)=0, \tag{3b}$$

which may be rewritten in conservation form

$$\frac{\partial \rho}{\partial t}+\frac{\partial}{\partial x}(\rho u)=0, \tag{4}$$

$$\frac{\partial}{\partial t}(\rho u)+\frac{\partial}{\partial x}\left(\rho u^2+p\right)=0, \tag{5}$$

$$\frac{\partial}{\partial t}\left(\frac{1}{2}\rho u^2+\rho e\right)+\frac{\partial}{\partial x}\left[\left(\frac{1}{2}\rho u^2+\rho e\right)u+pu\right]=0. \tag{6}$$

Equations (4)–(6) can be represented by

$$\frac{\partial q}{\partial t}+\frac{\partial}{\partial x}\left[f(q)\right]=0, \tag{7}$$

which may be rewritten as

$$\nabla\cdot\boldsymbol{F}=0, \tag{8}$$

where

$$\begin{aligned}\boldsymbol{F}&=\left(f(q),q\right),\\ \nabla&=\hat{\boldsymbol{i}}_x\frac{\partial}{\partial x}+\hat{\boldsymbol{i}}_t\frac{\partial}{\partial t}.\end{aligned} \tag{9}$$

If φ is a smooth function with compact support in the (x,t) plane, then equation (8) is equivalent to

$$\int\int \varphi\nabla\cdot\boldsymbol{F}\,dxdt=0, \quad \forall\varphi. \tag{10}$$

On integrating by parts, equation (10) leads to

$$\int\int \nabla\varphi\cdot\boldsymbol{F}\,dxdt=0. \tag{11}$$

If q is smooth, equations (8) and (11) are, of course, equivalent. However, if q is not smooth, equation (11) may remain valid even when equation (8) does not. In fact, a weak solution of equation (8) is defined to be a function q that satisfies equation (11) for all smooth functions φ with compact support. Note that a weak solution is capable of exhibiting a discontinuous behavior.

Let us now consider properties of a weak solution q of equation (8) near a jump discontinuity across a smooth curve Σ in the (x,t) plane. If φ is a smooth function vanishing outside the region S that is divided into S_1 and S_2 by the curve Σ (see Figure 3.2), so $S=S_1\cup S_2$, one has, from equation (11),

$$\iint_S \nabla\varphi\cdot\boldsymbol{F}\,dxdt=\iint_{S_1} \nabla\varphi\cdot\boldsymbol{F}\,dxdt+\iint_{S_2} \nabla\varphi\cdot\boldsymbol{F}\,dxdt=0. \tag{12}$$

Note that

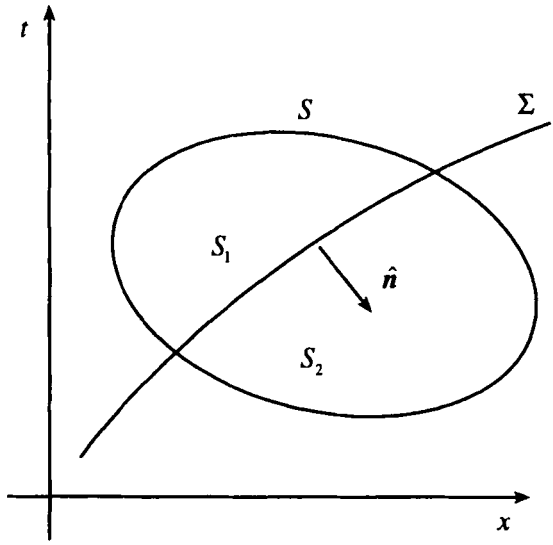

Figure 3.2. Jump discontinuity of a weak solution q across the curve Σ.

$$\iint_{S_1} \nabla\varphi \cdot \boldsymbol{F}\, dxdt = \iint_{S_1} \nabla\cdot(\varphi \boldsymbol{F})\, dxdt - \iint_{S_1} \varphi \nabla\cdot \boldsymbol{F}\, dxdt.$$

If q is assumed to be smooth in S_1, then equation (8) prevails in S_1, and one obtains

$$\iint_{S_1} \nabla\varphi \cdot \boldsymbol{F}\, dxdt = \int_{\Sigma} \varphi \boldsymbol{F}_1 \cdot \hat{n}\, ds,$$

where $\boldsymbol{F}_1$ denotes the value taken by $\boldsymbol{F}$ on Σ as the limit is taken from the region S_1. Similarly, one obtains

$$\iint_{S_2} \nabla\varphi \cdot \boldsymbol{F}\, dxdt = -\int_{\Sigma} \varphi \boldsymbol{F}_2 \cdot \hat{n}\, ds,$$

where the negative sign on the right hand side corresponds to the fact that the outward normal $\hat{n}$ for S_1 is the inward normal for S_2.

When one substitutes these results, equation (12) leads to

$$\int_{\Sigma} \varphi(\boldsymbol{F}_1 - \boldsymbol{F}_2)\cdot \hat{n}\, ds = 0, \qquad \forall\varphi,$$

from which the jump condition is obtained:

$$[\boldsymbol{F}\cdot\hat{n}] = 0 \quad \text{on} \quad \Sigma, \tag{13}$$

where the rectangular bracket denotes the jump of the contents across Σ.

If the curve Σ is parameterized by t and is given by $x = x(t)$, one has

$$\hat{n} = \frac{(1,-U)}{\sqrt{1+U^2}},$$

where $U = dx/dt$ is the speed of the discontinuity. Equation (13) then becomes

$$-U[q]+[f(q)]=0 \quad \text{on} \quad \Sigma. \tag{14}$$

Thus, a weak solution q satisfies equation (7) where possible and (14) across a jump discontinuity.

Applying the jump conditions (14) to equations (4)–(6), one obtains the following jump conditions across a discontinuity Σ in the (x,t)–plane, like a shock wave, moving with speed $dx/dt = U$,

$$-U[\rho]+[\rho u]=0, \tag{15}$$

$$-U[\rho u]+[\rho u^2+p]=0, \tag{16}$$

$$-U\left[\frac{1}{2}\rho u^2+\rho e\right]+\left[\left(\frac{1}{2}\rho u^2+\rho e\right)u+pu\right]=0. \tag{17}$$

Transforming to a frame of reference moving with the shock wave, i.e., putting

$$v = U-u, \tag{18}$$

equations (7)–(9) become

$$[\rho v]=0, \tag{19}$$

$$\left[p+\rho v^2-\rho vU\right]=0, \tag{20}$$

$$\left[\rho v\left(h+\frac{1}{2}v^2\right)-\left(p+\rho v^2\right)U+\frac{1}{2}\rho vU^2\right]=0, \tag{21}$$

or

$$[\rho v]=0, \tag{22}$$

$$\left[p+\rho v^2\right]=0, \tag{23}$$

$$\left[h+\frac{1}{2}v^2\right]=0, \tag{24}$$

which merely highlight (compare with equations (15)–(17)) the fact that equations (1)–(3) are Galilean–invariant. Thus,

$$\rho_1 V_1 = \rho_2 V_2, \tag{25}$$

$$p_1+\rho_1 V_1^2 = p^2+\rho_2 V_2^2, \tag{26}$$

$$h_1+\frac{1}{2}V_1^2 = h_2+\frac{1}{2}V_2^2, \tag{27}$$

where the subscripts 1 and 2 refer to the flow conditions in front of and behind the shock. Equations (17)–(19) are called the *Rankine–Hugoniot relations*.

The Rankine–Hugoniot relations are not sufficient to determine a unique, physically correct weak solution of equations (1)–(3); one needs to impose further conditions, like the causality condition, for this purpose. The causality condition stipulates that, when a shock separates characteristics of one family[4] (see below), the characteristics on each side can be traced back to the initial data so that the shock is determined by the given initial data and not by future events. For a perfect gas, the causality condition is equivalent to the thermodynamic entropy condition (see below) which stipulates that the entropy increases across a shock, making the flow transition across a shock an irreversible process.

From equations (25) and (26), one obtains

$$V_2^2 - V_1^2 = (p_1 - p_2)\left(\frac{1}{\rho_1} + \frac{1}{\rho_2}\right). \tag{28}$$

When one uses equation (28), equation (27) gives

$$\frac{(p_1 - p_2)}{2}\left(\frac{1}{\rho_1} + \frac{1}{\rho_2}\right) = \frac{\gamma}{\gamma - 1}\left(\frac{p_1}{\rho_1} - \frac{p_2}{\rho_2}\right),$$

from which we have

$$\frac{p_2}{p_1} = \frac{\left(\frac{\gamma+1}{\gamma-1}\right)\frac{\rho_2}{\rho_1} - 1}{\left(\frac{\gamma+1}{\gamma-1}\right) - \frac{\rho_2}{\rho_1}} \tag{29a}$$

and

$$\frac{\rho_2}{\rho_1} = \frac{\left(\frac{\gamma+1}{\gamma-1}\right)\frac{p_2}{p_1} + 1}{\frac{p_2}{p_1} + \left(\frac{\gamma-1}{\gamma+1}\right)} \quad \text{or} \quad \frac{p_2 - p_1}{\rho_2 - \rho_1} = \gamma\frac{p_2 + p_1}{\rho_2 + \rho_1}, \tag{29b}$$

which is represented (called the *Hugoniot curve*) along with an isentrope (for which $p \sim \rho^\gamma$) in Figure 3.3. Note that

$$\frac{p_2}{p_1} \gg 1: \quad \frac{\rho_2}{\rho_1} \Rightarrow \frac{\gamma+1}{\gamma-1}. \tag{30}$$

Next, one has, from equation (27),

[4] A discontinuity separates a family of characteristics if, through each point of the graph of the discontinuity in the (x,t) plane, there exist two characteristics, both of which either point forward in time or can be traced backward in time.

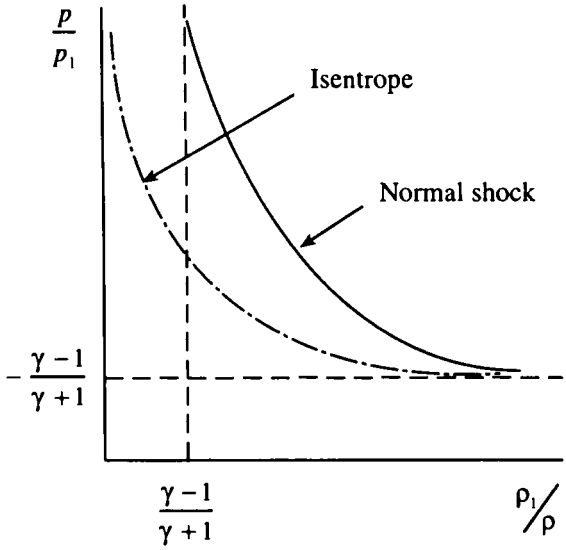

Figure 3.3. The Hugoniot curve.

$$\frac{T_2}{T_1} = \frac{1 + \dfrac{\gamma - 1}{2} M_1^2}{1 + \dfrac{\gamma - 1}{2} M_2^2}, \tag{31}$$

and from the perfect gas equation of state and equation (25), one has

$$\frac{T_2}{T_1} = \frac{p_2}{p_1} \cdot \frac{\rho_1}{\rho_2} = \frac{p_2}{p_1} \cdot \frac{V_2}{V_1} = \frac{p_2}{p_1} \cdot \frac{M_2}{M_1} \sqrt{\frac{T_2}{T_1}}. \tag{32}$$

Using (31) and (32), one obtains

$$\frac{p_2}{p_1} = \frac{M_1 \sqrt{1 + \left(\dfrac{\gamma - 1}{2}\right) M_1^2}}{M_2 \sqrt{1 + \left(\dfrac{\gamma - 1}{2}\right) M_2^2}}. \tag{33}$$

Also from equation (26), one obtains

$$\frac{p_2}{p_1} = \frac{1 + \gamma M_1^2}{1 + \gamma M_2^2}. \tag{34}$$

From (33) and (34), one obtains

$$M_2^2 = \frac{1 + \dfrac{\gamma - 1}{2} M_1^2}{\gamma M_1^2 - \left(\dfrac{\gamma - 1}{2}\right)}. \tag{35}$$

When one uses (35), (34) gives

$$\frac{p_2}{p_1} = 1 + \frac{2\gamma}{\gamma+1}\left(M_1^2 - 1\right). \tag{36}$$

On using (36), we obtain the following equation from (29b) and (25):

$$\frac{\rho_2}{\rho_1} = \frac{\left(\frac{\gamma+1}{2}\right)M_1^2}{1+\left(\frac{\gamma-1}{2}\right)M_1^2} = \frac{V_1}{V_2}. \tag{37}$$

Noting, from (5) and (9) in Section 3.2, that

$$M_1^{*2} = \frac{V_1^2}{a_1^{*2}} = \frac{\left(\frac{\gamma+1}{2}\right)M_1^2}{1+\left(\frac{\gamma-1}{2}\right)M_1^2}$$

and using (37), one obtains the Prandtl relation

$$V_1 V_2 = a^{*2} \quad \text{or} \quad M_1^* M_2^* = 1, \tag{38}$$

so that if the flow ahead of the normal shock is supersonic, the flow behind is subsonic.

Next, the entropy change across the shock wave is given by [see equation (31)] in Section 3.1)

$$\left(S_2 - S_1\right) = C_v \ln\left(\frac{p_2}{p_1}\right)\left(\frac{\rho_1}{\rho_2}\right)^{\gamma}. \tag{39}$$

When we use (29a), (39) becomes

$$S_2 - S_1 = C_v \ln\left[\frac{(\gamma+1)\left(\frac{\rho_2}{\rho_1}\right)-(\gamma-1)}{(\gamma+1)\left(\frac{\rho_2}{\rho_1}\right)^{\gamma}-(\gamma-1)\left(\frac{\rho_2}{\rho_1}\right)^{\gamma+1}}\right]. \tag{40}$$

Now, the dissipative effects associated with the transport processes inside a shock wave would raise the entropy of the fluid, so that from (40) we require

$$g\left(\frac{\rho_2}{\rho_1}\right) = (\gamma-1)\left(\frac{\rho_2}{\rho_1}\right)^{\gamma+1} - (\gamma+1)\left(\frac{\rho_2}{\rho_1}\right)^{\gamma} + (\gamma+1)\left(\frac{\rho_2}{\rho_1}\right) - (\gamma-1) > 0. \tag{41}$$

The function $g(\rho_2/\rho_1)$ is sketched in Figure 3.4. It is seen that

$$\begin{aligned} g(\rho_2/\rho_1) > 0 \quad &\text{if} \quad \rho_2/\rho_1 > 1 \\ &\text{or,} \quad \text{if} \quad M_1 > 1, \quad \text{from (37),} \\ &\text{i.e.,} \quad \text{if} \quad M_2 < 1, \quad \text{from (35),} \end{aligned} \tag{42}$$

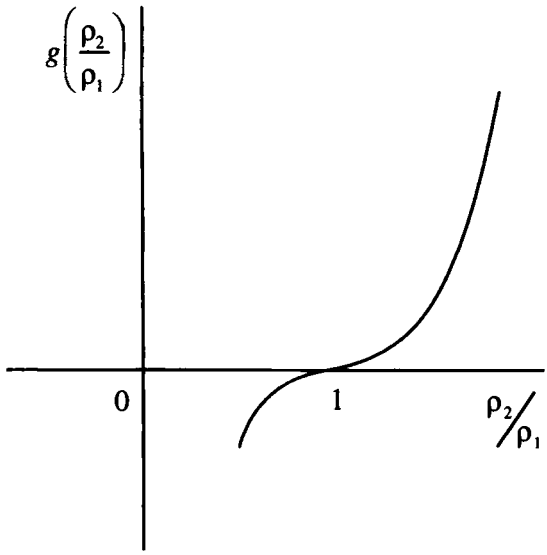

Figure 3.4. Entropy variation across a shock.

so that only the compression shocks are admissible and the expansion shocks are not.

Let us consider weak shock waves next. One has [see equation (23) in Section 3.1]

$$T\Delta S = h - h_1 - \int_{p_1}^{p} \frac{dp}{\rho}. \tag{43}$$

Using equations (27) and (28), one has

$$h - h_1 = \frac{1}{2}(p - p_1)\left(\frac{1}{\rho} + \frac{1}{\rho_1}\right). \tag{44}$$

In order to evaluate the integral in (43), note the trapezoidal rule,

$$\int_{x_1}^{x_2} f(x)\,dx = \frac{1}{2}(x_2 - x_1)\left[f(x_1) + f(x_2)\right] - \frac{1}{12}(x_2 - x_1)^3 f''(x_1) + 0\left[(x_2 - x_1)^4\right] \quad \text{as} \quad x_2 \Rightarrow x_1, \tag{45}$$

so that

$$\int_{p_1}^{p} \frac{dp}{\rho} = \frac{1}{2}\left(\frac{1}{\rho} + \frac{1}{\rho_1}\right)(p - p_1) - \frac{1}{12}\left[\frac{\partial^2}{\partial p^2}\left(\frac{1}{\rho}\right)\right]_1 (p - p_1)^3 + 0\left[(p - p_1)^4\right]. \tag{46}$$

When one uses equations (44) and (46), equation (43) becomes

$$T\Delta S = \frac{1}{12}\left[\frac{\partial^2}{\partial p^2}\left(\frac{1}{\rho}\right)\right]_1 (p-p_1)^3 + 0\left[(p-p_1)^4\right]. \tag{47}$$

This means that the Hugoniot curve for the normal shock and the isentrope in Figure 3.2 have the same tangent and curvature at the point (p_1, ρ_1).

Further, since for a weak shock, equations (25)–(27) reduce to

$$\rho dV + V d\rho = 0, \tag{48}$$

$$dp + \rho V dV = 0, \tag{49}$$

$$C_p dT + V dV = 0, \tag{50}$$

one has

$$\begin{aligned} \frac{\rho-\rho_1}{\rho_1} &\approx \frac{1}{\gamma}\frac{p-p_1}{p_1}, \\ \frac{V-V_1}{V_1} &\approx -\frac{1}{\gamma}\frac{p-p_1}{p_1}, \\ \frac{T-T_1}{T_1} &\approx \frac{\gamma-1}{\gamma}\frac{p-p_1}{p_1}. \end{aligned} \tag{51}$$

Comparison of equations (51) with equation (47) shows that one may treat the weak shock waves to a good approximation as being isentropic.

The Oblique Shock Wave

Consider a stationary shock wave with its plane now oblique to the flow direction. The equations expressing the conservation of mass, momenta tangential and normal to the shock, and energy are

$$\rho_1 V_{n_1} = \rho_2 V_{n_2}, \tag{52}$$

$$\left(\rho_1 V_{n_1}\right) V_{t_1} = \left(\rho_2 V_{n_2}\right) V_{t_2}, \tag{53}$$

$$p_1 + \rho_1 V_{n_1}^2 = p_2 + \rho_2 V_{n_2}^2, \tag{54}$$

$$h_1 + \frac{V_1^2}{2} = h_2 + \frac{V_2^2}{2}, \tag{55}$$

where the subscripts n and t denote the values perpendicular and parallel to the shock wave.

From equation (53), it follows that

$$\frac{p_1}{\rho_1} = \left[\frac{\gamma+1}{2\gamma}a^{*2} - \frac{\gamma-1}{2\gamma}\left(V_{n_1}^2 + V_{t_1}^2\right)\right] \tag{56}$$

$$\frac{p_2}{\rho_2} = \left[\frac{\gamma+1}{2\gamma}a^{*2} - \frac{\gamma-1}{2\gamma}\left(V_{n_2}^2 + V_{t_2}^2\right)\right]. \tag{57}$$

Using equation (56) and (57), equation (54) gives

$$V_{n_1}V_{n_2} = a^{*2} - \frac{\gamma-1}{\gamma+2}V_t^2. \tag{58}$$

Since the superposition of a uniform velocity V_t does not affect the static properties of the flow, the normal-shock jump relations can be carried over merely by replacing M_1 by $M_1 \sin\sigma$ (see Figure 3.4). Thus, we have, from (35)–(37),

$$\frac{\rho_2}{\rho_1} = \frac{\left(\frac{\gamma+1}{2}\right)M_1^2 \sin^2\sigma}{\left(\frac{\gamma-1}{2}\right)M_1^2 \sin^2\sigma + 1}, \tag{59}$$

$$\frac{p_2}{p_1} = 1 + \frac{2\gamma}{\gamma+1}\left(M_1^2 \sin^2\sigma - 1\right), \tag{60}$$

$$M_1^2 \sin^2\sigma = \frac{1 + \left(\frac{\gamma-1}{2}\right)M_1^2 \sin^2\sigma}{\gamma M_1^2 \sin^2\sigma - \left(\frac{\gamma-1}{2}\right)}. \tag{61}$$

Noting, from equation (52) and Figure 3.5, that

$$\frac{\rho_2}{\rho_1} = \frac{V_{n_1}}{V_{n_2}} = \frac{\tan\sigma}{\tan(\sigma-\delta)} \tag{62}$$

and using equation (59), one obtains the following equation for the flow deflection across the shock:

$$\tan\delta = \frac{\left(M_1^2 \sin^2\sigma - 1\right)\cot\sigma}{1 + M_1^2\left(\frac{\gamma+1}{2} - \sin^2\sigma\right)}. \tag{63}$$

Now since

$$M_1 \sin\sigma > 1,$$

one requires

$$\sin^{-1}\left(\frac{1}{M_1}\right) \le \sigma \le \frac{\pi}{2}. \tag{64}$$

Equation (63) shows that

$$\sigma = \frac{\pi}{2}, \ \sin^{-1}\left(\frac{1}{M_1}\right) : \ \delta = 0. \tag{65}$$

For $\sin^{-1}(1/M_1) \le \sigma \le \pi/2, \delta$ is positive and reaches a maximum (see Figure 3.6). δ_{max} is the maximum angle of flow deflection for which there can exist an

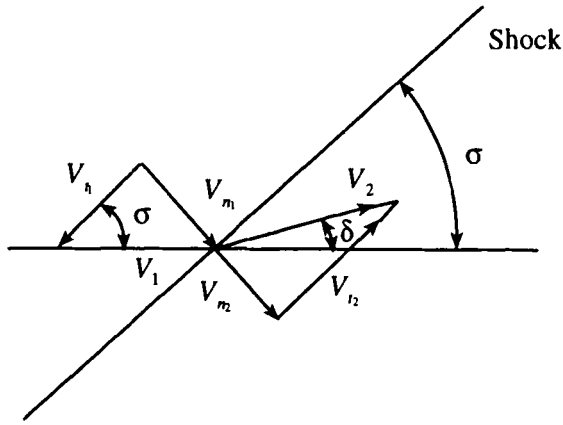

Figure 3.5. The oblique shock.

attached shock. Further, as indicated by (63), δ_{max} increases with M_1. Note that for $\delta < \delta_{max}$ for each value of δ and M_1 there are two possible shock waves corresponding to two different values of σ – one a strong shock $(M_2 < 1)$, and the other a weak shock $(M_2 > 1)$.

Consider now weak oblique shock waves. Equation (63) then gives

$$M_1^2 \sin^2 \sigma - 1 \approx \frac{\gamma+1}{2} \frac{M_1^2}{\sqrt{M_1^2 - 1}} \delta. \tag{66}$$

When one uses (66), (60) gives

$$\frac{p - p_1}{p_1} \approx \frac{\gamma M_1^2}{\sqrt{M_1^2 - 1}} \delta. \tag{67}$$

Noting, from (51), that

$$(p - p_1) \approx \rho_1 V_1 (V - V_1),$$

one obtains from (67)

$$\frac{V - V_1}{V_1} \approx -\frac{\delta}{\sqrt{M_1^2 - 1}}. \tag{68}$$

A centered-fan of such weak oblique waves may be used to simulate the flow past a gentle convex corner – the Prandtl–Meyer flow (see Section 3.5).

Blast Waves: Sedov's Solution

Consider the propagation of a very strong spherical shock wave produced by a strong explosion, i.e., from the instantaneous release of a large quantity of energy

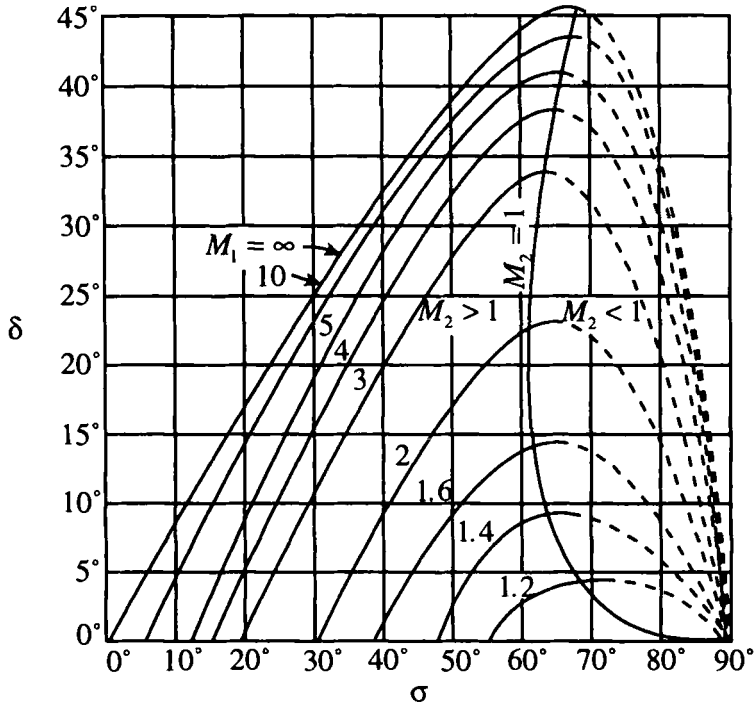

Figure 3.6. Variation of flow–deflection angle with the inclination of the shock to the incoming flow (from Liepmann and Roshko, 1957).

E in a small volume. Let us consider the wave at distances small enough from the source so that its amplitude is still large, but at distances large enough compared with the dimensions of the source so that the latter can be taken to be a point. Since the shock wave is strong, one may neglect the pressure p_1 of the undisturbed stagnant gas in front of it in comparison with the pressure p_2 immediately behind it, and the density ratio ρ_2/ρ_1 then approaches its limiting value $(\gamma+1)/(\gamma-1)$. Thus, as Taylor argued, the gas flow pattern is essentially determined by two parameters, E and ρ_1; this enables one to find some self–similar solutions to the flow. First, let us form a dimensionless parameter

$$\xi = R\left(\frac{\rho_1}{Et^2}\right)^{1/5}, \tag{69}$$

where R is the radial distance.

It turns out that such a choice leads to a constance of the total energy (which follows it one neglects p_1),

$$E = \int_0^{\infty}\left(\frac{p}{\gamma-1}+\frac{1}{2}\rho V^2\right)4\pi R^2\,dR, \tag{70}$$

of the gas within the sphere bounded by the shock if one assumes that p, ρ, V are all functions only of ξ.

The position of the shock wave corresponds to a certain constant ξ_0 of ξ, and if $R = R_0$ denotes the shock radius at time t, one has

$$R_0 = \xi_0 \left(\frac{Et^2}{p_1} \right)^{1/5}, \tag{71a}$$

from which the rate of propagation of the shock wave is given by

$$u_1 = \frac{dR_0}{dt} = \frac{2R_0}{5t}. \tag{72}$$

Equation (71) implies, as Taylor deduced, that

$$R_0 \sim t^{2/5}. \tag{71b}$$

This relationship was confirmed in an impressive manner by the observations of the mushroom cloud generated by the explosion of the first atomic bomb (see Figure 3.7).

The state of the gas immediately behind the shock is given by (on using the results from Exercise 1)

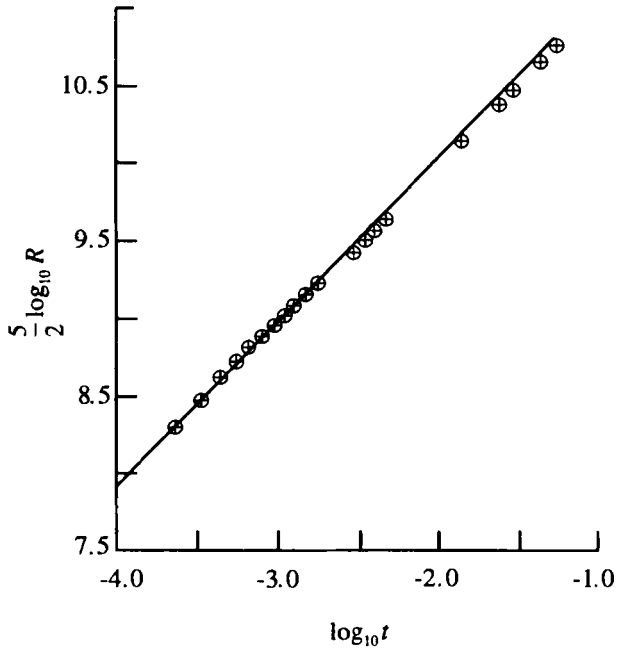

Figure 3.7. Variation with time of the radius R_0 of a strong spherical shock wave (from Faber, 1995). The straight line corresponds to (71b), while the crosses correspond to the observations.

$$V_2 = u_1 - u_2 = \frac{2u_1}{\gamma+1}, \quad p_2 = 2\rho_1 \frac{u_1^2}{\gamma+1},$$

$$\rho_2 = \rho_1 \frac{\gamma+1}{\gamma-1}. \tag{73}$$

In order to determine the gas flow throughout the region behind the shock, let us make a similarity transformation:

$$V = \frac{4}{5(\gamma+1)} \frac{R}{t} V'(\xi), \quad \rho = \frac{\gamma+1}{\gamma-2} \rho_1 \rho'(\xi),$$

$$p = \frac{8\rho_1}{25(\gamma+1)} \frac{R^2}{t^2} p'(\xi); \tag{74}$$

and on the shock wave, one has

$$\xi = \xi_0: \quad V', \ p', \ \rho' = 1. \tag{75}$$

The equations governing the flow are

$$\frac{\partial V}{\partial t} + V \frac{\partial V}{\partial R} = -\frac{1}{\rho} \frac{\partial p}{\partial R}, \tag{76}$$

$$\frac{\partial \rho}{\partial t} + \frac{\partial}{\partial R}(\rho V) + \frac{2\rho V}{R} = 0, \tag{77}$$

$$\left(\frac{\partial}{\partial t} + V \frac{\partial}{\partial R}\right) \ln\left(\frac{p}{\rho^\gamma}\right) = 0; \tag{78}$$

and when one uses equation (74), equations (76)–(78) become ordinary differential equations:

$$\xi\left[\left(V' - \frac{2}{5}\right)\frac{dV'}{d\xi'} + \frac{p'}{\rho'}\right] = -V'(V'-1) - 2\frac{p'}{\rho'}, \tag{79}$$

$$\xi\left[\frac{dV'}{d\xi} + \left(V' - \frac{2}{5}\right)\frac{1}{\rho'}\frac{d\rho'}{d\xi}\right] = -3V', \tag{80}$$

$$\xi\left(V' - \frac{2}{5}\right)\left(\frac{1}{p'}\frac{dp'}{d\xi} - \frac{\gamma}{\rho'}\frac{d\rho'}{d\xi}\right) = -2(V'-1). \tag{81}$$

The integration of equations (79)–(81) is facilitated by noting the existence of another integral. This is obtained from the constance of the total energy between any two similarity lines $R/t^{2/5} = \text{const.}$, i.e., from

$$\left(\frac{p}{\gamma-1} + \frac{1}{2}\rho V^2\right)\left(V - \frac{2R}{5t}\right) + pV = 0 \tag{82a}$$

or

$$\frac{p'}{\rho'} = \frac{\gamma+1-2V'}{2\gamma V' - (\gamma+1)} V'^2. \tag{82b}$$

An ingenious solution of equations (79)–(83) was given by Sedov,

$$\left(\frac{\xi_0}{\xi}\right)^5 = V'^2\left[\frac{5(\gamma+1)-2(3\gamma-1)V'}{7-\gamma}\right]^{\nu_1}\left[\frac{2\gamma V'-(\gamma+1)}{\gamma-1}\right]^{\nu_2}$$

$$\rho' = \left[\frac{2\gamma V'-(\gamma+1)}{\gamma-1}\right]^{\nu_3}\left[\frac{5(\gamma+1)-2(3\gamma-1)V'}{7-\gamma}\right]^{\nu_4}\left[\frac{\gamma+1-2V'}{\gamma-1}\right]^{\nu_5}, \tag{83}$$

where

$$\nu_1 = \frac{13\gamma^2-7\gamma+12}{(3\gamma-1)(2\gamma+1)}, \quad \nu_2 = -\frac{5(\gamma-1)}{2\gamma+1}, \quad \nu_3 = \frac{3}{2\gamma+1},$$

$$\nu_4 = \frac{13\gamma^2-7\gamma+12}{(2-\gamma)(3\gamma-1)(2\gamma+1)}, \quad \nu_5 = \frac{1}{\gamma-2}.$$

The constant ξ_0 is determined from the condition (70):

$$\frac{32\pi\xi_0^5}{25(\gamma^2-1)}\int_0^1\left(\xi^4\rho'V'^2+\xi^9\rho'\right)d\xi = 1. \tag{84}$$

One has from (83)

$$\frac{R}{R_0}\Rightarrow 0: \quad \frac{V}{V_2}\sim\frac{R}{R_0}, \quad \frac{\rho}{\rho_2}\sim\left(\frac{R}{R_0}\right)^{3/(\gamma-1)}. \tag{85}$$

Figure 3.8 shows V/V_2, p/p_2, ρ/ρ_2 vs. R/R_0, as given by (75), for air $(\gamma=1.4)$. Observe the sharp fall of the density away from the shock front, and note that the gas is almost completely concentrated in a thin layer behind the shock.

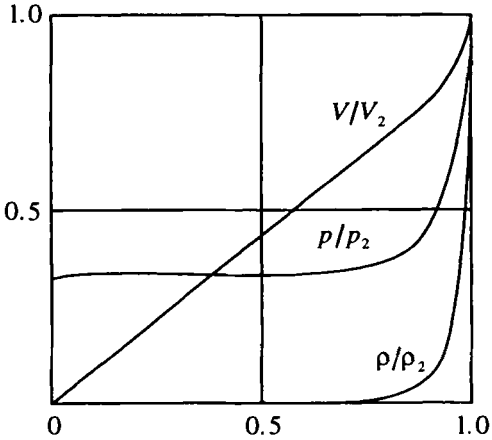

Figure 3.8. Variation of flow properties behind a blast wave (from Sedov, 1959).

EXERCISE

1. Study the nature of flow transitions across a very strong shock wave.

3.4. Flows with Heat Transfer

Rayleigh Flow

Consider a steady one–dimensional flow with a heat transfer. The latter may be caused by external agents or some chemical reactions in the flow. One has (see equation (23) in Section 3.1),

$$TdS = dQ = dh - \frac{dp}{\rho} = \frac{\gamma R}{\gamma - 1} dT - \frac{dp}{\rho}. \tag{1}$$

When one uses the perfect–gas equation of state,

$$p = \rho RT, \tag{2}$$

equation (1) becomes

$$TdS = dQ = \frac{\gamma RT}{\gamma - 1}\left(\frac{dp}{p} - \frac{d\rho}{\rho}\right) - \frac{dp}{\rho}. \tag{3}$$

When one uses the continuity equation

$$\rho V = \text{const.}, \tag{4}$$

equation (3) becomes

$$TdS = dQ = \frac{\gamma RT}{\gamma - 1}\left(\frac{dp}{p} + \frac{dV}{V}\right) - \frac{dp}{\rho}. \tag{5}$$

When one uses the equation of motion,

$$\rho V dV = -dp, \tag{6}$$

equation (5) becomes

$$TdS = dQ = \frac{dp}{\rho M^2 (\gamma - 1)}\left(M^2 - 1\right). \tag{7}$$

Equation (7) shows that the heat addition $(dQ > 0)$ will accelerate a subsonic flow and decelerate a supersonic flow.

In order to see this effect a little better, consider the steady one–dimensional flow in a variable–area $(A = A(x))$ stream tube. For this flow, one then has

$$\frac{1}{V}\frac{dV}{dx} + \frac{1}{\rho}\frac{d\rho}{dx} + \frac{1}{A}\frac{dA}{dx} = 0, \tag{8}$$

$$V\frac{dV}{dx} + \frac{1}{\rho}\frac{dp}{dx} = 0, \tag{9}$$

$$T\frac{dS}{dx}=\frac{dQ}{dx}=\frac{dh}{dx}-\frac{1}{\rho}\frac{dp}{dx}. \tag{10}$$

From equations (8)–(10), one derives

$$\frac{1}{V}\frac{dV}{dx}=\frac{1}{1-M^2}\left[\frac{1}{A}\frac{dA}{dx}-\frac{1}{C_pT}\frac{dQ}{dx}\right], \tag{11}$$

which shows that the heat addition $(dQ>0)$ acts, in general, like a narrowing of the stream tube. This explains why the heat addition accelerates a subsonic flow and decelerates a supersonic flow.

Detonation and Deflagration Waves

The rate at which a chemical reaction takes place in a mixture of gases depends on the temperature of the gases and increases with this temperature. If the reaction is exothermic, i.e., if heat is released as the reaction proceeds, the temperature will rise and increase the rate of reaction, so that such a reaction is self–sustaining. This is called *combustion of the mixture*, and the zone of reaction is called a *flame*. The speed of a flame is usually very small, and its rate of propagation depends primarily on the thermal conductivity, which enables heat to be transferred from the hot products to the unburnt gas. If the combustion zone is very thin, then the flame can be treated as a discontinuous front separating the burnt products from the unburnt gas.

Detonation wave is composed of a shock wave followed by a chemical reaction zone (the shock wave raises the temperature of the gases sufficiently to start off a chemical reaction, and the latter is assumed to occur instantaneously across the sharp front). It moves with a supersonic velocity relative to the unburnt gas, and it is sustained by the energy released in the chemical reaction.

Consider a detonation wave moving through a gas with speed U (Figure 3.9); the gas behind the wave is set into motion with a speed u_2 with respect to a stationary observer. The Rankine–Hugoniot relations now have to be modified to allow for the liberation of chemical energy across the wave. Thus,

$$\rho_1U=\rho_2(U-u_2), \tag{12}$$

$$p_1+\rho_1U^2=p_2+\rho_2(U-u_2)^2, \tag{13}$$

$$\frac{p_1}{\rho_1}+e_1+\frac{1}{2}U^2+q=\frac{p_2}{\rho_2}+e_2+\frac{1}{2}(U-u_2)^2, \tag{14}$$

where q is the quantity of heat per unit mass of the gas released on passage through the wave front.

One derives from equations (12) and (13)

$$p_2-p_1=\frac{u_2^2}{1/\rho_1-1/\rho_2}. \tag{15}$$

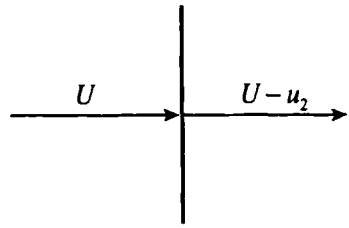

Figure 3.9. Flow through a detonation wave.

From (15), the shock waves with $p_2 > p_1$ and $\rho_2 > \rho_1$ are called *detonations*, and those with $p_2 < p_1$ and $\rho_2 < \rho_1$ are called *deflagrations* (see Figure 3.10).

The Hugoniot curve (see Figure 3.10) for the combustion wave is displaced from the Hugoniot curve for a normal shock wave because of the fact that $dQ > 0$ for the former and $dQ = 0$ for the latter. The Hugoniot curve for the combustion wave consists of two separate branches, exhibiting the fact that the conservation laws are compatible with two quite distinct types of processes – detonation and deflagration.

At points D and C, called the *Chapman–Jouguet points*, on the Hugoniot curve for the combustion wave, a straight line from $0'$ (the point representing the initial state of the gas), is tangential to the latter (see Figure 3.10), so that one has there

$$\frac{dp}{d(1/\rho)} = \frac{p - p_1}{1/\rho - 1/\rho_1} = -\rho^2 a^2. \tag{16}$$

Now,

$$TdS = dh - \frac{dp}{\rho}. \tag{17}$$

Now (recall equation (21) in Section 3.3),

$$h - h_1 = -\frac{(p - p_1)}{2}\left(\frac{1}{\rho_1} + \frac{1}{\rho}\right), \tag{18}$$

from which

$$dh = -\frac{dp}{2}\left(\frac{1}{\rho_1} + \frac{1}{\rho}\right) + \frac{(p - p_1)}{2}\frac{d\rho}{\rho^2}. \tag{19}$$

When one uses (16) and (19), (17) gives

$$TdS = 0,$$

so that the transitions corresponding to the Chapman–Jouguet points D and C are isentropic.

Next, one obtains from (12) and (13)

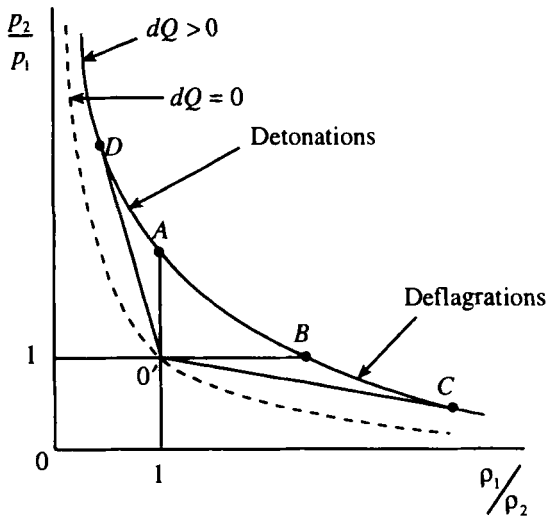

Figure 3.10. The Hugoniot curve for the combustion wave.

$$U = \mp \sqrt{\frac{\rho}{\rho_1}\frac{p - p_1}{\rho - \rho_1}}, \tag{20}$$

and when one uses (16), (20) becomes

$$U = \mp a\frac{\rho}{\rho_1}. \tag{21}$$

Also, when one uses (16), (15) gives

$$u_2 = \mp a\left(\frac{\rho}{\rho_1} - 1\right). \tag{22}$$

When one uses (21), (22) becomes

$$u_2 = U \pm a \quad \text{at} \quad D, C; \tag{23}$$

so that corresponding to the transitions represented by the Chapman–Jouguet points D and C, the burnt gas behind the combustion wave travels at the speed of sound relative to the wave front.

Now, corresponding to the region AB on the Hugoniot curve for a combustion wave, one has (see Figure 3.8)

$$\frac{p_2}{p_1} > 1, \qquad \frac{\rho_1}{\rho_2} > 1;$$

so that from (15), u_2 will be imaginary for that region. This means that the transitions corresponding to the region AB on the Hugoniot curve for a combustion wave are forbidden.

Experimentally, while many different detonational wave speeds have been observed, the detonation wave, after a very short period, evolves into a state represented by the Chapman–Jouguet point *D*. This is understandable because, only for a detonation wave corresponding to the Chapman–Jouguet point *D*, the wave moves with the speed of sound relative to the burnt gas and is so out of reach of the disturbances originating from the burnt gas and is stable. In contrast, a detonation wave corresponding to a point to the left of the Chapman–Jouguet point *D* moves with a subsonic speed relative to the burnt gas and is thus within the reach of the disturbances originating from the burnt gas which weaken it until it reaches a state represented by the Chapman–Jouguet point *D*. On the other hand, a deflagration wave corresponding to a point to the right of the Chapman–Jouguet point *C* moves with supersonic speed relative to the burnt gas and subsonic speed relative to the unburnt gas; it is, therefore, excluded by the *causality* condition (rather than the *thermodynamic entropy* condition).

EXERCISE

1. Obtain the expressions for changes in pressure, density, and temperature of the fluid in a Rayleigh flow.

3.5. Potential Flows

Governing Equations

The equations expressing the conservation of mass, momentum, and energy are

$$\frac{\partial \rho}{\partial t} + \frac{\partial}{\partial x_j}\left(\rho v_j\right) = 0, \tag{1}$$

$$\frac{\partial v_i}{\partial t} + v_j \frac{\partial v_i}{\partial x_j} = -\frac{1}{\rho}\frac{\partial p}{\partial x_j}, \tag{2}$$

$$\frac{\partial}{\partial t}\left(e + \frac{v^2}{2}\right) + v_j \frac{\partial}{\partial x_j}\left(e + \frac{v^2}{2}\right) = -\frac{1}{\rho}\frac{\partial}{\partial x_i}\left(p v_i\right). \tag{3a}$$

Equation (3) may be expressed alternatively as

$$\frac{\partial e}{\partial t} + v_j \frac{\partial e}{\partial x_j} = -\frac{p}{\rho}\frac{\partial v_i}{\partial x_i}, \tag{3b}$$

$$\frac{\partial}{\partial t}\left(h + \frac{v^2}{2}\right) + v_j \frac{\partial}{\partial x_j}\left(h + \frac{v^2}{2}\right) = \frac{1}{\rho}\frac{\partial p}{\partial t}, \tag{3c}$$

$$\frac{\partial h}{\partial t} + v_j \frac{\partial h}{\partial x_j} = \frac{1}{\rho}\left(\frac{\partial p}{\partial t} + v_j \frac{\partial p}{\partial x_j}\right). \tag{3d}$$

For a potential flow, one may write

$$v_i = \frac{\partial \Phi}{\partial x_i}; \tag{4}$$

then equations (1) and (2) become

$$\frac{1}{\rho}\frac{\partial \rho}{\partial t} + \frac{\partial^2 \Phi}{\partial x_i \partial x_i} + \frac{1}{\rho} v_j \frac{\partial \rho}{\partial x_j} = 0, \tag{5}$$

$$-\frac{v_j}{a^2}\left(\frac{\partial v_j}{\partial t} + v_k \frac{\partial v_j}{\partial x_k}\right) = \frac{v_j}{a^2 \rho}\frac{\partial p}{\partial x_j} = \frac{v_j}{\rho}\frac{\partial \rho}{\partial x_j}, \tag{6}$$

where a is the speed of sound.

The Bernoulli integral of equation (2), viz.,

$$\frac{\partial \Phi}{\partial t} + \frac{v^2}{2} + \int \frac{dp}{\rho} = \text{const.}, \tag{7}$$

gives

$$\frac{\partial^2 \Phi}{\partial t^2} + v_j \frac{\partial v_j}{\partial t} + \frac{a^2}{\rho}\frac{\partial \rho}{\partial t} = 0. \tag{8}$$

Using equations (6) and (8), equation (5) gives the potential–flow equation

$$\left(1 - \frac{\Phi_x^2}{a^2}\right)\Phi_{xx} + \left(1 - \frac{\Phi_y^2}{a^2}\right)\Phi_{yy} + \left(1 - \frac{\Phi_z^2}{a^2}\right)\Phi_{zz} - 2\frac{\Phi_x \Phi_y}{a^2}\Phi_{xy}$$
$$-2\frac{\Phi_y \Phi_z}{a^2}\Phi_{yz} - 2\frac{\Phi_z \Phi_x}{a^2}\Phi_{zx} = \frac{1}{a^2}\left(\Phi_{tt} + 2\Phi_x \Phi_{xt} + 2\Phi_y \Phi_{yt} + 2\Phi_z \Phi_{zt}\right). \tag{9}$$

For an adiabatic process with the relation

$$p/\rho^\gamma = \text{const.}, \tag{10}$$

(7) leads to

$$a^2 + \frac{\gamma - 1}{2}\left(\Phi_x^2 + \Phi_y^2 + \Phi_z^2\right) + (\gamma - 1)\Phi_t = \text{const.} = a_0^2. \tag{11}$$

Streamline Coordinates

Consider a two–dimensional situation in streamline coordinates (see Figure 3.11). The equations expressing the conservation of mass and momentum in a steady flow are

$$\frac{1}{\rho}\frac{\partial \rho}{\partial s} + \frac{1}{V}\frac{\partial V}{\partial s} + \frac{1}{\Delta n}\frac{\partial \Delta n}{\partial s} = 0, \tag{12}$$

$$\rho V \frac{\partial V}{\partial s} = -\frac{\partial p}{\partial s}, \tag{13}$$

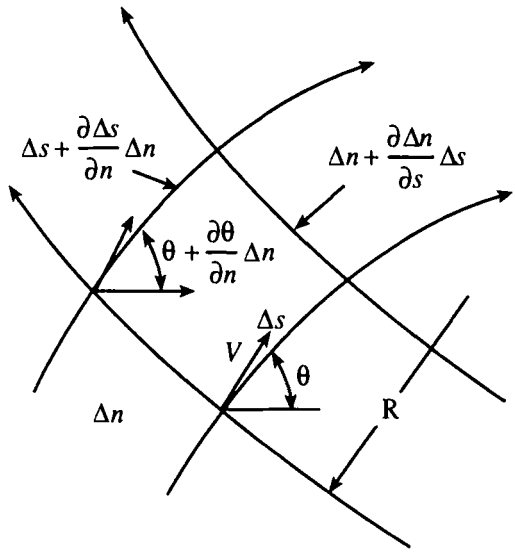

Figure 3.11. The streamline coordinate system.

$$\frac{\rho V^2}{R} = \frac{\partial p}{\partial n}. \tag{14}$$

When one uses that (see Figure 3.9)

$$\frac{1}{\Delta n}\frac{\partial \Delta n}{\partial s} = \frac{\partial \theta}{\partial n}, \tag{15}$$

equations (12) and (13) give

$$\left(\frac{V^2}{a^2} - 1\right)\frac{1}{V}\frac{\partial V}{\partial s} - \frac{\partial \theta}{\partial n} = 0. \tag{16}$$

Next, the energy–conservation equation is (see equation (23) in Section 3.1)

$$\frac{\partial h}{\partial n} = T\frac{\partial S}{\partial n} + \frac{1}{\rho}\frac{\partial p}{\partial n} \tag{17a}$$

or

$$\frac{\partial h_0}{\partial n} = T\frac{\partial S}{\partial n} + V\Omega, \tag{17b}$$

where h_0 is the stagnation enthalpy, and Ω is the vorticity

$$\Omega = \frac{\partial V}{\partial n} - \frac{V}{R}, \tag{18}$$

where R is the radius of curvature of the streamline in question. Equation (17) shows that the variation of total enthalpy and entropy across streamlines is related to the vorticity in the flow. An example of a flow with vorticity is the flow downstream of a curved shock wave. Since the inclination of the shock wave

relative to the oncoming flow determines its strength (see Section 3.3) and hence the entropy change experienced by the fluid, the entropy continually varies on the downstream side. This leads to the production of vorticity in the flow there.

Conical Flows

In cylindrical–polar coordinates for a steady flow, equation (9) becomes

$$\left(a^2-\frac{\Phi_\theta^2}{r^2}\right)\frac{\Phi_{\theta\theta}}{r^2}-2\Phi_r\Phi_\theta\frac{\Phi_{r\theta}}{r^2}+\left(a^2-\Phi_r^2\right)\Phi_{rr}+\frac{\Phi_r}{r}\left(a^2+\frac{\Phi_\theta^2}{r^2}\right)=0. \quad (19)$$

For a conical flow (say, if the flow properties are constant on the rays from the origin), one has

$$\Phi_{rr}=0, \quad (20)$$

while the irrotationality condition gives

$$\frac{1}{r}\Phi_\theta=\Phi_{r\theta}. \quad (21)$$

It follows from (20) and (21) that

$$\Phi(r,\theta)=r\varphi(\theta). \quad (22)$$

When one uses (20) and (21), equation (19) gives

$$\left(\Phi_r+\frac{\Phi_{\theta\theta}}{r}\right)\left(a^2-\frac{\Phi_\theta^2}{r^2}\right)=0$$

or

$$\frac{\Phi_\theta}{r}=a. \quad (23)$$

Noting that

$$\Phi_r=\sqrt{V^2-\frac{\Phi_\theta^2}{r^2}}=\sqrt{V^2-a^2}=V\sqrt{1-\frac{a^2}{V^2}}=V\cos(r,V), \quad (24)$$

one has

$$\sin(r,V)=\frac{a}{V}, \quad (25)$$

so that the radius vector intersects the streamline at the Mach angle and hence must be a Mach line. The Prandtl–Meyer flow (Figure 3.12) is such an example. This flow consists of two regions of uniform flow separated by a fan–shaped region of expansion where the positive characteristics (see below) are all straight lines through the corner 0.

Note that using (23), one obtains from energy conservation (see equation (4) in Section 3.2)

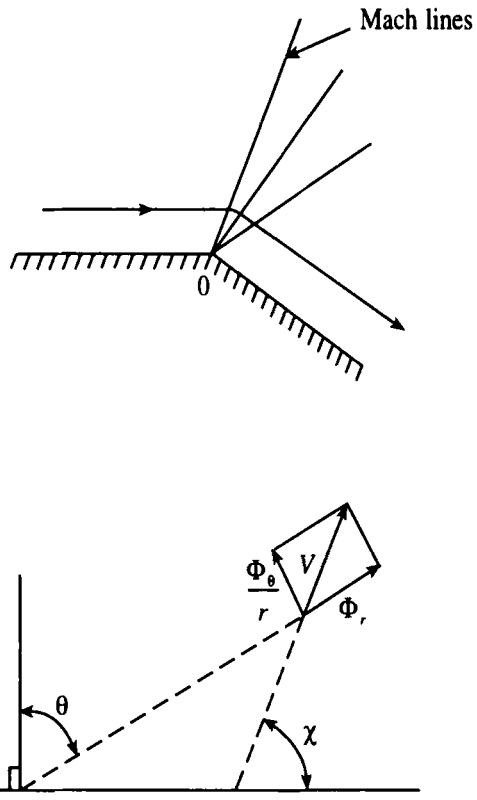

Figure 3.12. The Prandtl–Meyer flow.

$$\frac{\Phi_\theta^2}{r^2} = \frac{\gamma-1}{\gamma+1}\left(V_{\max}^2 - \Phi_r^2\right). \tag{26}$$

When one uses (22) and (23), (26) gives

$$\Phi_r = V_{\max} \sin\sqrt{\frac{\gamma-1}{\gamma+1}}\left(\frac{\pi}{2}-\theta\right),$$

$$\frac{\Phi_\theta}{r} = a = V_{\max}\sqrt{\frac{\gamma-1}{\gamma+1}}\cos\sqrt{\frac{\gamma-1}{\gamma+1}}\left(\frac{\pi}{2}-\theta\right). \tag{27}$$

Note that, according to (27), the streamlines become radial when

$$\theta = \theta_{\max} = -\frac{\pi}{2}\left(\sqrt{\frac{\gamma+1}{\gamma-1}}-1\right). \tag{28}$$

If the angle turned through by the streamline is larger than $\theta_{\max}$, then a region of zero pressure will form between the fluid and the wall. Referring to Figure 3.12, the angle turned by a streamline from $M_1 = 1$ to $M > 1$ is given by

$$\chi = \left(\frac{\pi}{2} - \theta\right) + \tan^{-1}\frac{\Phi_\theta / r}{\Phi_r}$$

$$= \left(\frac{\pi}{2} - \theta\right) + \tan^{-1}\left[\sqrt{\frac{\gamma-1}{\gamma+1}}\cot\sqrt{\frac{\gamma-1}{\gamma+1}}\left(\frac{\pi}{2} - \theta\right)\right]$$

$$= \tan^{-1}\sqrt{M^2 - 1} + \tan^{-1}\left[\sqrt{\frac{\gamma-1}{\gamma+1}}\sqrt{M^2 - 1}\right]. \tag{29}$$

Small Perturbation Theory

Consider small disturbances introduced into a steady stream by a small body placed in it. Let

$$\Phi = U_\infty x + \phi(x, y, z). \tag{30}$$

When one uses (30), (9) gives, on linearization in ϕ,

$$\left(1 - M_\infty^2\right)\phi_{xx} + \phi_{yy} + \phi_{zz} = 0, \tag{31}$$

where

$$M_\infty^2 \equiv \frac{U_\infty^2}{a_\infty^2}$$

and the subscript ∞ denotes conditions in the free stream.

The pressure is given by

$$C_p \equiv \frac{p - p_\infty}{\frac{1}{2}\rho_\infty U_\infty^2} = \frac{2}{\gamma M_\infty^2}\left(\frac{p}{p_\infty} - 1\right) = \frac{2}{\gamma M_\infty^2}\left[\left(\frac{T}{T_\infty}\right)^{\gamma/\gamma-1} - 1\right]. \tag{32}$$

When one uses the energy conservation equation (see equation (4) in Section 3.2)

$$\frac{\left(U_\infty + \phi_x\right)^2 + \phi_y^2 + \phi_z^2}{2} + \frac{a^2}{\gamma - 1} = \frac{a_\infty^2}{\gamma - 1} + \frac{U_\infty^2}{2}, \tag{33}$$

(32) can be expanded as

$$C_p = -\left[\frac{2\phi_x}{U_\infty} + \left(1 - M_\infty^2\right)\frac{\phi_x^2}{U_\infty^2} + \frac{\phi_y^2 + \phi_z^2}{U_\infty^2} + \cdots\right]. \tag{34}$$

Note that this expansion is not valid either when $M_\infty \approx 1$ or when $M_\infty \gg 1$.

The requirement that the streamline near the surface of the body be tangential to it leads to the boundary condition, upon linearization,

$$y = 0: \quad \frac{\phi_y}{U_\infty} = \frac{\partial f}{\partial x}, \tag{35}$$

where $y = f(x, z)$ describes the surface of the body.

Example 1: Consider the flow past a wavy wall given by

$$y = \varepsilon \sin \alpha x = f(x), \tag{36}$$

for which we have the following boundary–value problem:

$$\left.\begin{aligned} &\left(1 - M_\infty^2\right)\phi_{xx} + \phi_{yy} = 0, \\ &y = 0: \quad \phi_y = \varepsilon U_\infty \alpha \cos \alpha x. \end{aligned}\right\} \tag{37}$$

For the case $M_\infty < 1$, (37) has the solution

$$\phi(x, y) = -\frac{\varepsilon U_\infty}{\sqrt{1 - M_\infty^2}} \exp\left(-y\alpha\sqrt{1 - M_\infty^2}\right) \cos \alpha x, \tag{38}$$

so that

$$y = 0: \quad C_p = -\frac{2\varepsilon \alpha}{\sqrt{1 - M_\infty^2}} \sin \alpha x. \tag{39}$$

On the other hand, for the case $M_\infty > 1$, (37) has the solution

$$\phi(x, y) = -\frac{\varepsilon U_\infty}{\sqrt{M_\infty^2 - 1}} \sin \alpha\left(x - y\sqrt{M_\infty^2 - 1}\right), \tag{40}$$

so that

$$y = 0: \quad C_p = \frac{2\varepsilon \alpha}{\sqrt{M_\infty^2 - 1}} \cos \alpha x. \tag{41}$$

Note the differences between the subsonic–flow and the supersonic–flow solutions, as indicated by (38)–(41):

1. The disturbances in a supersonic flow propagate unattenuated to infinity, whereas those in a subsonic flow attenuate at infinity,
2. The pressure changes in a supersonic flow are proportional to the slope of the boundary, whereas those in a subsonic flow are proportional to the curvature of the boundary,
3. As a consequence of point 2, a nonzero drag force exists on the wavy wall in a supersonic flow, whereas there is no drag force on the wavy wall in a subsonic flow,
4. Thanks to the limited upstream influence in a supersonic flow, the analysis of the latter becomes simpler than that of a subsonic flow.

Characteristics

One distinguishing property of hyperbolic equations is the existence of certain characteristic surfaces across which there can exist discontinuities in the normal derivatives of the dependent variables. The governing system of partial differential equations imposes certain restrictions on the relative magnitudes of these jumps.

These relations form a linear, homogeneous system, and the solvability condition for this system produces restrictions on the possible orientations of the characteristic surface. Thanks to the admissibility of discontinuities in the normal derivatives of the velocity on the characteristic surfaces, it is possible to patch different flows together at these surfaces, the only restriction being that the velocity itself must be continuous. Furthermore, the fact that the dependent variables satisfy certain compatibility relations of the characteristic surfaces can be made the basis of a graphical procedure to compute the flow. Such a computational aid is not possible for an elliptic problem wherein the region of computation must be completely bounded and each point is influenced by all other points in the region.

For steady two–dimensional potential flow, one has

$$\left(a^2 - \Phi_x^2\right)\Phi_{xx} + \left(a^2 - \Phi_y^2\right)\Phi_{yy} - 2\Phi_x\Phi_y\Phi_{xy} = 0. \tag{42}$$

Consider a system of partial differential equations,

$$\begin{aligned} &A\Phi_{xx} + 2B\Phi_{xy} + C\Phi_{yy} = 0, \\ &d\Phi_x = \Phi_{xx}dx + \Phi_{xy}dy, \\ &d\Phi_y = \Phi_{yx}dx + \Phi_{yy}dy, \end{aligned} \tag{43}$$

from which we have

$$\Phi_{xy} = \frac{\begin{vmatrix} A & 0 & C \\ dx & d\Phi_x & 0 \\ 0 & d\Phi_y & dy \end{vmatrix}}{\begin{vmatrix} A & 2B & C \\ dx & dy & 0 \\ 0 & dx & dy \end{vmatrix}} \equiv \frac{\Delta_1}{\Delta_2}, \tag{44}$$

so that the physical (f,g) characteristics are given by

$$\Delta_2 = 0$$

or

$$\left(\frac{dy}{dx}\right)_{g,f} = \frac{B \pm \sqrt{B^2 - AC}}{A} \tag{45}$$

and the hodograph (f,g) characteristics, which are the images of the physical characteristics in the hodograph plane, are given by

$$\Delta_1 = 0$$

or

$$\left(\frac{d\Phi_y}{d\Phi_x}\right)_{g,f} = -\frac{A}{C}\left(\frac{dy}{dx}\right)_{g,f}. \tag{46}$$

When one uses (45), (46) becomes

$$\left(\frac{d\Phi_y}{d\Phi_x}\right)_{g,f} = -\frac{B \pm \sqrt{B^2 - AC}}{C}. \tag{47}$$

For equation (42), the physical and the hodograph characteristics are then given by

$$\left(\frac{dy}{dx}\right)_{f,g} = \frac{-\dfrac{\Phi_x \Phi_y}{a^2} \mp \sqrt{\dfrac{\Phi_x^2 + \Phi_y^2}{a^2} - 1}}{1 - \Phi_x^2/a^2}, \tag{48}$$

$$\left(\frac{d\Phi_y}{d\Phi_x}\right)_{f,g} = \frac{-\dfrac{\Phi_x \Phi_y}{a^2} \mp \sqrt{\dfrac{\Phi_x^2 + \Phi_y^2}{a^2} - 1}}{1 - \Phi_y^2/a^2}. \tag{49}$$

According to (48) and (49), the characteristics can exist only in a supersonic flow. Also, note that

$$\left(\frac{dy}{dx}\right)_{f,g}\left(\frac{d\Phi_y}{d\Phi_x}\right)_{g,f} = -1. \tag{50}$$

When one puts

$$\Phi_x = V\cos\theta, \qquad \Phi_y = V\sin\theta, \tag{51}$$

(48) becomes

$$\begin{aligned}\left(\frac{dy}{dx}\right)_{f,g} &= \frac{-M^2\sin\theta\cdot\cos\theta \mp \sqrt{M^2-1}}{1 - M^2\cos^2\theta} \\ &= \frac{\left(1 \mp \sqrt{M^2-1}\cot\theta\right)}{\left(1 \mp \sqrt{M^2-1}\cot\theta\right)} \frac{\left[-M^2\left(1-\cos^2\theta\right)\cot\theta \mp \sqrt{M^2-1}\right]}{1 - M^2\cos^2\theta} \\ &= \frac{-\cot\theta \pm \sqrt{M^2-1}}{1 \mp \sqrt{M^2-1}\cot\theta} \\ &= \tan(\theta \pm \mu),\end{aligned} \tag{52}$$

where

$$\tan\mu = \frac{1}{\sqrt{M^2-1}}.$$

Equation (52) shows that the Mach lines are the physical characteristics.

Similarly, (49) becomes

$$\left(\frac{d\Phi_y}{d\Phi_x}\right)_{f,g} = \left(\frac{dV}{Vd\theta}\right)_{f,g} = \pm\tan\mu. \tag{53}$$

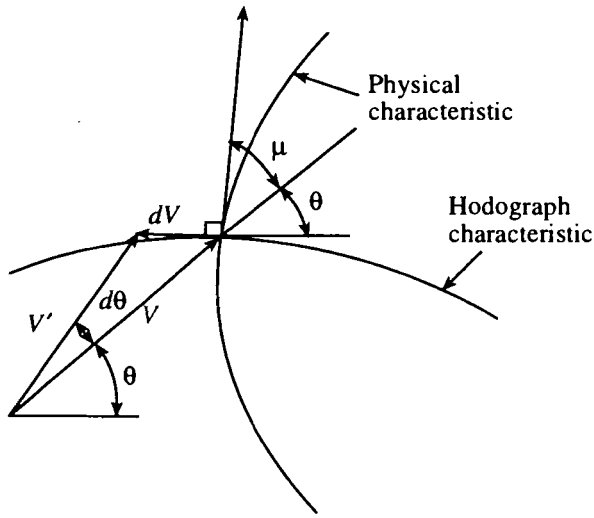

Figure 3.13. Physical and hodograph characteristics.

The physical and the hodograph characteristics are sketched in Figure 3.13.

Next, it turns out that along the characteristics, the dependent variables satisfy some compatibility relations. In order to determine the latter, recall that, in streamline coordinates, the equation of motion is (recall equation (16))

$$\frac{\cot^2 \mu}{V}\frac{\partial V}{\partial s} - \frac{\partial \theta}{\partial n} = 0, \tag{54}$$

while one has from the geometry (see Figure 3.11)

$$\frac{1}{V}\frac{\partial V}{\partial n} - \frac{\partial \theta}{\partial s} = 0. \tag{55}$$

When one puts

$$dv = \cot \mu \cdot \frac{dV}{V}, \tag{56}$$

equations (54) and (55) become

$$\frac{\partial v}{\partial s} - \tan \mu \cdot \frac{\partial \theta}{\partial n} = 0, \tag{57}$$

$$\tan \mu \cdot \frac{\partial v}{\partial n} - \frac{\partial \theta}{\partial s} = 0. \tag{58}$$

From equations (57) and (58), one has

$$\frac{\partial}{\partial s}(v \mp \theta) \pm \tan \mu \cdot \frac{\partial}{\partial n}(v \mp \theta) = 0. \tag{59}$$

If η and ξ measure distances along the two characteristics, then

$$\frac{\partial}{\partial \eta}, \frac{\partial}{\partial \xi} = \frac{\partial}{\partial s} \pm \tan\mu \cdot \frac{\partial}{\partial n}$$

and equation (59) implies that

$$\nu \mp \theta = \text{const. along } (f,g) \text{ characteristics,} \tag{60}$$

which are called the *Riemann invariants* (see Section 3.7).[5,6]

---

[5]For a general first-order quasilinear hyperbolic system in one dimension we have

$$\boldsymbol{u}_t + \boldsymbol{A}(x,t,\boldsymbol{u}) \cdot \boldsymbol{u}_x = \boldsymbol{B}(x,t,\boldsymbol{u})$$

where $\boldsymbol{u} = \boldsymbol{u}(x,t)$ is an n-component vector function of x and t, $\boldsymbol{B}(x,t,\boldsymbol{u})$ is a nonlinear vector function of $\boldsymbol{u}$, and $\boldsymbol{A}$ is an $n \times n$ matrix function of x, t, and $\boldsymbol{u}$ that has n distinct real eigenvalues $\lambda_1,\ldots,\lambda_n$; and therefore n linearly independent eigenvectors, the Riemann invariants $h_1,\ldots,h_n$ that are constant along the characteristics associated with the eigenvalues $\lambda_1,\ldots,\lambda_n$, respectively, are given by

$$\boldsymbol{A}^T \cdot \frac{\partial h_k}{\partial \boldsymbol{u}} = \lambda_k \frac{\partial h_k}{\partial \boldsymbol{u}}, \text{ no sum on } k.$$

Note that if the characteristic associated with the eigenvalue λ_k is given by

$$t = t(s_k), \quad x = x(s_k); \quad k = 1,\ldots,n$$

with

$$\frac{dt}{ds_k} = 1 \text{ and } \frac{dx}{ds_k} = \lambda_k; \quad k = 1,\ldots,n,$$

then

$$\begin{aligned}
\frac{\partial h_k}{\partial s_k} &= \sum_{\ell=1}^{n} \frac{\partial h_k}{\partial u_\ell} \frac{\partial u_\ell}{\partial s_k} = \sum_{\ell=1}^{n} \frac{\partial h_k}{\partial u_\ell} \left[\frac{\partial u_\ell}{\partial t} + \frac{\partial u_\ell}{\partial x} \frac{dx}{ds_k} \right] \\
&= \sum_{\ell=1}^{n} \frac{\partial h_k}{\partial u_\ell} \left[-\sum_{m=1}^{n} A_{\ell m} \frac{\partial u_m}{\partial x} + \lambda_k \frac{\partial u_\ell}{\partial x} \right] \\
&= \sum_{\ell=1}^{n} \left[-\sum_{m=1}^{n} A_{m\ell}^T \frac{\partial h_k}{\partial u_m} \right] \frac{\partial u_\ell}{\partial x} + \sum_{\ell=1}^{n} \lambda_k \frac{\partial h_k}{\partial u_\ell} \frac{\partial u_\ell}{\partial x} \\
&= \sum_{\ell=1}^{n} \left[-\lambda_k \frac{\partial h_k}{\partial u_\ell} \frac{\partial u_\ell}{\partial x} + \lambda_k \frac{\partial h_k}{\partial u_\ell} \frac{\partial u_\ell}{\partial x} \right] = 0.
\end{aligned}$$

[6]One may find an explicit expression for ν as follows. Using the relation

$$a = V \sin\mu$$

in the energy-conservation equation

$$\frac{V^2}{2} + \frac{a^2}{\gamma - 1} = \text{const.},$$

one obtains

$$\frac{dV}{V} + \frac{2\sin\mu\cos\mu}{(\gamma-1) + 2\sin^2\mu} d\mu = 0.$$

When one uses (56), this equation becomes

$$d\nu = -\frac{2\cot^2\mu}{(\gamma-1)\cot^2\mu + (\gamma+1)} d\mu.$$

When one puts

$$t = \cot\mu,$$

this equation, in turn, becomes

Now, the fact that each equation in characteristic form involves a particular linear combination of the derivatives can be used to gain insight into the structure of solutions of the equations, such as the correct number of boundary conditions and the domain of dependence, by considering a construction of the solution at successive small time increments. In order to see this, let us express the equations in the characteristic form

$$\frac{d\psi_k}{dt} + f_k(x,t,\psi) = 0 \quad \text{on} \quad \frac{dx}{dt} = c_k(x,t,\psi). \tag{61}$$

Consider the initial value problem in $x > 0$, $t > 0$, with data prescribed on the x–axis (which is transverse to the characteristics, i.e., nowhere tangent to them) at $t = 0$.[7] If P and Q_k are two neighboring points on the kth characteristic, then one obtains from (61)

$$\psi_k(P) - \psi_k(Q_k) + f_k(Q_k)\left[t(P) - t(Q_k)\right] = 0,$$
$$x(P) - x(Q_k) = c_k(Q_k)\left[t(P) - t(Q_k)\right].$$

Further, the values at P will depend only on the data between P_1 and P_2 on the x–axis where PP_1 and PP_2 are the two characteristics through P (see Figure 3.14). In other words, P_1P_2 is the domain of dependence of P. Thus, for the full initial problem, with ψ_k given on $t = 0$, $-\infty < x < \infty$, the solution can be constructed in $t > 0$ and it is unique.

Therefore, it is as if the characteristics carry information from the boundaries into the region concerned. Physically, the characteristics correspond to paths of waves propagating with the velocities c_k.

A Singular–Perturbation Problem for Hyperbolic Systems

Consider

$$\varepsilon\left(\frac{\partial^2 v}{\partial x^2} - \frac{\partial^2 v}{\partial t^2}\right) = a\frac{\partial v}{\partial x} + b\frac{\partial v}{\partial t}, \tag{62}$$

which has real characteristics (see Figure 3.15),

$$r = t - x, \qquad s = t + x. \tag{63}$$

The characteristics serve to define the region of influence, propagating into the future, of a disturbance at a point Q (see Figure 3.15). The manner of

---

$$dv = \left[\frac{1}{\left(\frac{\gamma-1}{\gamma+1}\right)t^2 + 1} - \frac{1}{t^2+1}\right],$$

from which we obtain

$$v = \sqrt{\frac{\gamma+1}{\gamma-1}}\tan^{-1}\left(\sqrt{\frac{\gamma-1}{\gamma+1}}\cot\mu\right) - \tan^{-1}(\cot\mu) + \text{const.}$$

[7] If data are prescribed on the characteristic, the differential equation does not determine the solution at any point *not* on the characteristic.

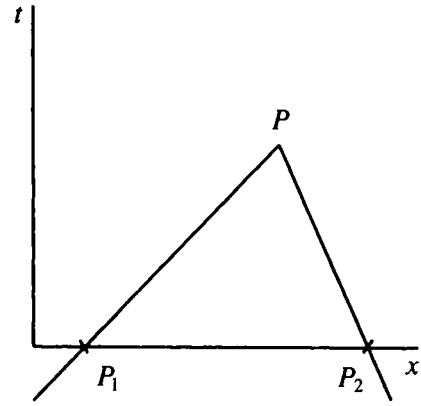

Figure 3.14. Characteristics through a point.

specification of boundary conditions on an arc for a fully posed boundary–value problem depends on the nature of the arc with respect to the characteristic directions of propagation. One boundary condition is specified on the time–like arc (see Figure 3.16) corresponding to one characteristic leading into the adjacent region in which the solution is defined. Two boundary conditions are given on the space–like arc (see Figure 3.16) corresponding to the two characteristics leading into the adjacent domain. When the boundary curves are along the characteristic curves, only one condition can be prescribed, and the characteristic relations must hold. The characteristic–initial–value problem describes one condition each on AB and on AC to define the solution in $ABCD$ (see Figure 3.17).

Consider the initial–value problem corresponding to equation (62) in $-\infty < x < \infty$ with

$$t = 0: \quad v = F(x), \qquad v_t = G(x). \tag{64}$$

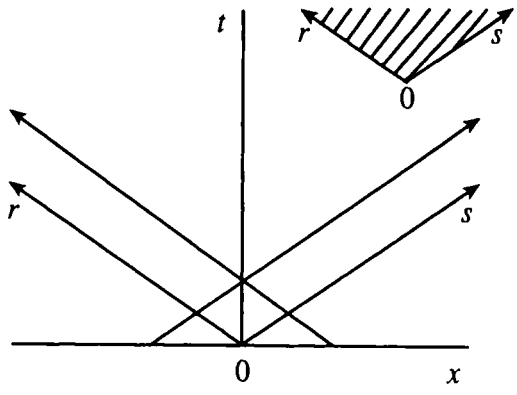

Figure 3.15. Characteristics and region of influence (from Kevorkian and Cole, 1980).

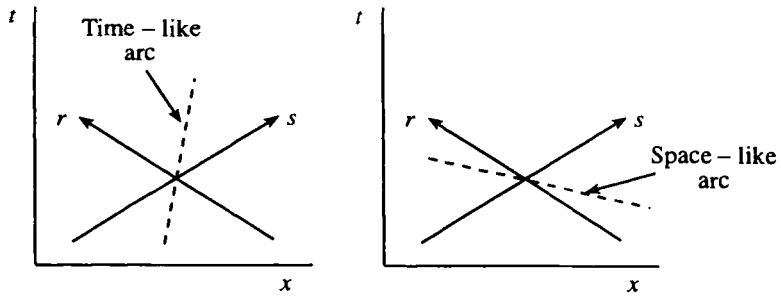

Figure 3.16. Time–like arc and space–like arc (from Kevorkian and Cole, 1980).

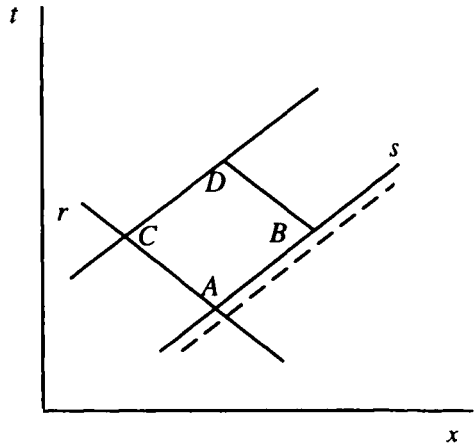

Figure 3.17. Domain of influence in a characteristic initial–value problem (from Kevorkian and Cole, 1980).

According to the general theory of characteristics, the solutions at a point $P(x,t)$ (see Figure 3.18) can depend only on that part of the initial data which can send a signal to P. This is part of the initial line contained between the backward running characteristics through $P, (x_1 < x < x_2)$.

Now, corresponding to $\varepsilon = 0$, equation (62) gives

$$a\frac{\partial v^{(0)}}{\partial x} + b\frac{\partial v^{(0)}}{\partial t} = 0, \tag{65}$$

from which

$$v^{(0)}(x,t) = f\left(x - \frac{a}{b}t\right). \tag{66}$$

In the limit $\varepsilon \Rightarrow 0$ the solution $v(x,t)$ depends only on the data connected to P along a subcharacteristic of equation (62) given by

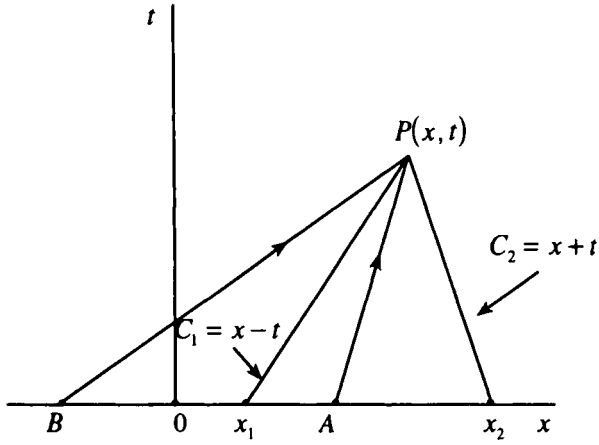

Figure 3.18. Domain of influence and time–like and space–like subcharacteristics (from Kevorkian and Cole, 1980).

$$bx - at = \text{const.} \tag{67}$$

Now the subcharacteristic, reaching P, originates at point A between x_1, x_2 if $|b/a| > 1$, i.e., if it is time–like. Then the limit $\varepsilon \Rightarrow 0$ preserves the domain of influence. However, if $|b/a| < 1$, the subcharacteristic reaching P is space–like and lies outside the domain of influence, originating at B (see Figure 3.18). In this case, the limit $\varepsilon \Rightarrow 0$ increases the domain of influence – a behavior that is not physically permissible.

It turns out that even the issue of stability of the solutions $v(x,t)$ is related to whether the subcharacteristics are time–like or space–like. In order to see that, note that in terms of the characteristic coordinates (63), equation (62) becomes

$$-4\varepsilon \frac{\partial^2 v}{\partial r \partial s} = (b-a)\frac{\partial v}{\partial r} + (b+a)\frac{\partial v}{\partial s}. \tag{68}$$

Consider the propagation of a jump in $\partial v/\partial r$ along $r = r_0 = \text{const.}$

Let

$$K \equiv \left[\frac{\partial v}{\partial r}\right]_{r=r_0} \equiv \left(\frac{\partial v}{\partial r}\right)_{r_0^+} - \left(\frac{\partial v}{\partial r}\right)_{r_0^-}. \tag{69}$$

Assuming that v itself is continuous across $r = r_0$, one finds from equation (68)

$$-4\varepsilon \frac{\partial K}{\partial s} = (b-a)K,$$

from which

$$K = K_0 \exp\left[-\left(\frac{b-a}{4s}\right)(s - s_0)\right]. \tag{70}$$

Now, a jump across a characteristic propagates to infinity along that characteristic. When one uses (69) and (70), this implies

$$\begin{aligned}(b-a)>0 &\Rightarrow \text{stability},\\ (b-a)<0 &\Rightarrow \text{instability}.\end{aligned} \tag{71}$$

Similarly, a consideration of a jump in $\partial v/\partial s$ across a characteristic $s=s_0$ gives

$$\begin{aligned}(b+a)>0 &\Rightarrow \text{stability},\\ (b+a)<0 &\Rightarrow \text{instability}.\end{aligned} \tag{72}$$

From (71) and (72), one obtains

$$|b/a|>1 \qquad \text{for stability.} \tag{73}$$

We restrict further discussion to the stable case.

Now, note that the solutions $v^{(0)}(x,t)$ given in (66) can only satisfy one initial condition, so that one may expect the existence of boundary layer on the line $t=0$.

Assume an initially valid expansion

$$v^{(i)}\left(x,\tilde{t};\varepsilon\right)=v_0^{(i)}\left(x,\tilde{t}\right)+\beta_1(\varepsilon)v_1^{(i)}\left(x,\tilde{t}\right)+\cdots, \tag{74}$$

where

$$\tilde{t}=\frac{t}{\delta(\varepsilon)}$$

and

$$\beta_1,\delta\Rightarrow 0 \quad \text{as} \quad \varepsilon\Rightarrow 0$$

with the associated inner limit process $\varepsilon\Rightarrow 0, x, \tilde{t}$ held fixed. If one takes

$$\beta_1(\varepsilon)=\delta(\varepsilon), \tag{75}$$

(64) gives

$$\begin{aligned}&\tilde{t}=0: v_0^{(i)}=F(x), \qquad v_n^{(i)}=0 \quad \text{for} \quad n>0\\ &\tilde{t}=0: \frac{\partial v_0^{(i)}}{\partial\tilde{t}}=0, \qquad \frac{\partial\tilde{v}_1^{(i)}}{\partial\tilde{t}}=G(x),\\ &\qquad\qquad \frac{\partial v_n^{(i)}}{\partial\tilde{t}}=0 \quad \text{for} \quad n>1.\end{aligned} \tag{76}$$

When one chooses $\delta(\varepsilon)=\varepsilon$ and substitutes (74) and (75), (62) gives

$$\frac{\partial^2 v_0^{(i)}}{\partial\tilde{t}^{\,2}}+b\frac{\partial v_0^{(i)}}{\partial\tilde{t}}=0 \tag{77}$$

$$\frac{\partial^2 v_1^{(i)}}{\partial \tilde{t}^2} + b\frac{\partial v_1^{(i)}}{\partial \tilde{t}} = -a\frac{\partial v_0^{(i)}}{\partial x}. \tag{78}$$

Notice that the boundary–layer equations (77) and (78) are ordinary–differential equations, which is a feature of the boundary layers that do not occur on a subcharacteristic. This is true for any hyperbolic–initial value problem, since a space–like arc can never be a subcharacteristic.

Using (76), equations (77) and (78) give

$$v_0^{(i)}(x,\tilde{t}) = F(x), \tag{79}$$

$$v_1^{(i)}(x,\tilde{t}) = \left[G(x) + \frac{a}{b}F'(x)\right]\left[1 - \exp(-\tilde{t})\right] - \frac{a}{b}\tilde{t}F'(x), \tag{80}$$

so that

$$v^{(i)}(x,\tilde{t};\varepsilon) = F(x) + \varepsilon\left[\left\{G(x) + \frac{a}{b}F'(x)\right\}\left\{1 - \exp(-\tilde{t})\right\} - \frac{a}{b}\tilde{t}F'(x)\right] + \cdots. \tag{81}$$

Note that (81) possesses terms that persist in the limit $t \Rightarrow \infty$, as well as terms that decay in time which are typical of a boundary layer (further details of this are found in Section 4.3).

Next, construct an outer expansion, with the associated outer limit process $\varepsilon \Rightarrow 0, x, t$ held fixed,

$$v^{(0)}(x,t,\varepsilon) = v_0^{(0)}(x,t) + \varepsilon v_1^{(0)}(x,t) + \cdots, \tag{82}$$

so that equation (82) gives

$$a\frac{\partial v_0^{(0)}}{\partial x} + b\frac{\partial v_0^{(0)}}{\partial t} = 0, \tag{83}$$

$$a\frac{\partial v_1^{(0)}}{\partial x} + b\frac{\partial v_1^{(0)}}{\partial t} = \left(\frac{\partial^2 v_0^{(0)}}{\partial x^2} - \frac{\partial^2 v_0^{(0)}}{\partial t^2}\right). \tag{84}$$

One obtains from equation (83)

$$v_0^{(0)} = f(\xi), \qquad \xi = x - \frac{a}{b}t. \tag{85}$$

When one uses (85), (84) becomes

$$a\frac{\partial v_1^{(0)}}{\partial x} + b\frac{\partial v_1^{(0)}}{\partial t} = \left(1 - \frac{a^2}{b^2}\right)f''(\xi), \tag{86}$$

from which

$$v_1^{(0)} = \frac{a}{b^2}\frac{b^2 - a^2}{b^2 + a^2}\left(x + \frac{b}{a}t\right)f''(\xi) + f_1(\xi), \tag{87}$$

so that

$$v^{(0)}(x,t;\varepsilon)=f(\xi)+\varepsilon\left[f_1(\xi)+\frac{a}{b^2}\frac{b^2-a^2}{b^2+a^2}\left(x+\frac{b}{a}t\right)f''(\xi)\right]+\cdots. \tag{88}$$

The asymptotic matching between $v^{(i)}$ and $v^{(0)}$ requires (see Section 4.3)

$$v^{(0)}(x,0;\varepsilon)+\varepsilon\tilde{t}\,v_t^{(0)}(x,0;\varepsilon)+\cdots=v^{(i)}(x,\infty;\varepsilon). \tag{89}$$

When one uses (81) and (88), (89) gives

$$f(x)=F(x),$$

$$f_1(x)+\frac{a}{b^2}\frac{b^2-a^2}{b^2+a^2}xf''(x)=G(x)+\frac{a}{b}F'(x), \tag{90}$$

so that (88) becomes

$$v^{(0)}(x,t;\varepsilon)=F\left(x-\frac{a}{b}t\right)+\varepsilon\left[\frac{b^2-a^2}{b^3+ba^2}tF''\left(x-\frac{a}{b}t\right)+\frac{a}{b}F'\left(x-\frac{a}{b}t\right)+G\left(x-\frac{a}{b}t\right)\right]+\cdots. \tag{91}$$

Consider, next, a radiation problem in which boundary conditions are prescribed on a time–like arc and propagate into the quiescent medium in $x>0$ (Figure 3.19). When the boundary condition is prescribed for instance, at $x=0$, one has to distinguish two cases depending on whether the subcharacteristics run into or out of the boundary $x=0$. Recall, from (67), that the subcharacteristics are given by

$$\xi=x-\frac{a}{b}t=\text{const.} \tag{67}$$

Note that the characteristics are incoming or outgoing according as $a\lessgtr 0$. Let the boundary condition be

$$x=0:\quad v=F(t),\qquad t>0. \tag{92}$$

Outgoing Characteristics: Assume an outer solution,

$$v^{(0)}(x,t;\varepsilon)=v_0^{(0)}(x,t)+\varepsilon v_1^{(0)}(x,t)+\cdots, \tag{93}$$

where

$$v_0^{(0)}=f(\zeta),\qquad \zeta=t-\frac{b}{a}x. \tag{66}$$

When one substitutes (92), (66) gives

$$v_0^{(0)}=\begin{cases}0, & t<\dfrac{b}{a}x,\\ F\left(t-\dfrac{b}{a}x\right), & t>\dfrac{b}{a}x.\end{cases} \tag{94}$$

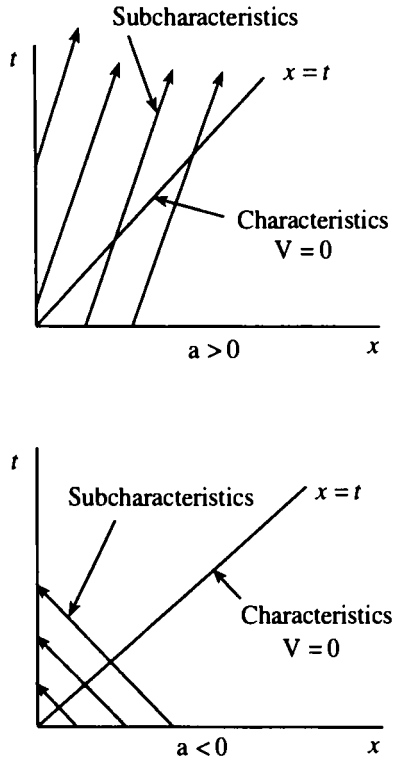

Figure 3.19. Radiation problem with boundary conditions prescribed on a finite portion of the boundary (from Kevorkian and Cole, 1980).

This solution obviously has a discontinuity on the particular subcharacteristic through the origin. However, such a discontinuity is not permitted in the solution to equation (62) with $\varepsilon \neq 0$. Thus, in order to obtain a uniformly valid solution, a suitable boundary layer must be introduced on the particular subcharacteristic $\zeta = 0$ which supports the discontinuity in the outer solution $v^{(0)}$. Assume an inner expansion

$$v^{(i)}(\tilde{x}, \tilde{t}; \varepsilon) = v_0^{(i)}(\tilde{x}, \tilde{t}) + \mu(\varepsilon) v_1^{(i)}(\tilde{x}, \tilde{t}) + \cdots,$$

where

$$\tilde{x} = \frac{x - \frac{a}{b} t}{\delta(\varepsilon)}, \tag{95}$$

$$\tilde{t} = t,$$

and

$$\delta \Rightarrow 0 \quad \text{as} \quad \varepsilon \Rightarrow 0,$$

with an associated inner limit process $\varepsilon \Rightarrow 0, (\tilde{x}, \tilde{t})$ held fixed. When one chooses

$$\delta = \sqrt{\varepsilon}$$

and substitutes (95), (62) gives in the limit $\varepsilon \Rightarrow 0$

$$K \frac{\partial^2 v_0^{(i)}}{\partial \tilde{x}^2} = \frac{\partial v_0^{(i)}}{\partial \tilde{t}}, \tag{96}$$

where

$$K \equiv \frac{1 - \frac{a^2}{b^2}}{b} > 0,$$

which ensures that $\tilde{t} = t$ is a positive timelike variable so that (96) is a diffusion equation that describes the spreading of the discontinuity in the outer expansion $v^{(0)}$ on the subcharacteristic $\zeta = 0$. Matching $v^{(i)}$ to $v^{(0)}$ asymptotically, as before, one obtains

$$v_0^{(i)}(\tilde{x}, \tilde{t}) = \frac{F(0^+)}{2} erfc\left(\frac{\tilde{x}}{2\sqrt{\tilde{t}}}\right). \tag{97}$$

Incoming Characteristics: Assume an outer expansion

$$v^{(0)}(x, t; \varepsilon) = v_0^{(0)}(x, t) + \varepsilon v_1^{(0)}(x, t) + \cdots. \tag{98}$$

Since the disturbances now propagate along the subcharacteristics from the quiescent region to the boundary, one has

$$v^{(0)} \equiv 0. \tag{99}$$

Then the discontinuity in $v^{(0)}$ occurs at the boundary $x = 0$, so that one has a boundary layer at $x = 0$. Since the line $x = 0$ is not a subcharacteristic, the boundary layer equations should now be ordinary differential equations. Assume an inner expansion

$$v^{(i)}(\tilde{x}, \tilde{t}; \varepsilon) = v_0^{(i)}(\tilde{x}, \tilde{t}) + \nu_1(\varepsilon) v_1^{(i)}(\tilde{x}, \tilde{t}) + \cdots, \tag{100}$$

where

$$\tilde{x} = \frac{x}{\delta(\varepsilon)}, \quad \tilde{t} = t, \quad \text{and} \quad \nu_1 \Rightarrow 0 \quad \text{as} \quad \varepsilon \Rightarrow 0 \tag{101}$$

with an associated inner limit process $\varepsilon \Rightarrow 0, \tilde{x}, \tilde{t}$ held fixed. If one chooses $\delta = \varepsilon$, (62) gives, on substituting (100),

$$\frac{\partial^2 v_0^{(i)}}{\partial \tilde{x}^2} = a \frac{\partial v_0^{(i)}}{\partial \tilde{x}} \tag{102}$$

from which, on using (92), one obtains

$$v_0^{(i)}(\tilde{x}, \tilde{t}) = F(\tilde{t}) \exp(a\tilde{x}), \qquad a < 0. \tag{103}$$

EXERCISES

1. Show that the rate of change of circulation Γ around a closed curve C made up of the same fluid particles, for nonisentropic cases, is

$$\frac{D\Gamma}{Dt} = \int_C T\,dS, \text{ Bjerknes' Theorem.}$$

2. Show that one can produce the Prandtl–Meyer solution starting from the flow–deflection formula for a weak oblique shock.
3. Show that the hodograph curve described by (29) is an epicycloid.
4. Derive the compatibility conditions for flow variables in the nonisentropic cases (to emphasize the utility of characteristics in calculating more general flows as well) along the characteristics.

3.6. The Hodograph Method

It turns out that the problem of plane steady potential flow of a gas becomes linear when the velocity components are used as independent variables. However, the advantages of linearity are somewhat offset by

(1) the practical difficulty of fulfilling boundary conditions prescribed in the physical plane;

(2) the fact that the shape of the body cannot be prescribed in advance, unless they have a simple representation in the hodograph, such as wedges;

(3) the fact that the shape of the body changes if either the freestream Mach number or the thickness ratio is altered.

The Hodograph Transformation

Recall that the equations of motion in the streamline coordinates for a two-dimensional steady potential flow are (equations (54) and (55) in Section 3.5)

$$\left(1-M^2\right)\frac{1}{V}\frac{\partial V}{\partial s}+\frac{\partial \theta}{\partial n}=0, \tag{1}$$

$$\frac{1}{V}\frac{\partial V}{\partial n}-\frac{\partial \theta}{\partial s}=0. \tag{2}$$

When one puts

$$V=\frac{\partial \Phi}{\partial s}, \qquad \frac{\rho V}{\rho_0}=\frac{\partial \Psi}{\partial n}, \tag{3}$$

equations (1) and (2) become

$$\frac{\rho V}{\rho_0}\frac{\partial \theta}{\partial \Psi}+\left(1-M^2\right)\frac{\partial V}{\partial \Phi}=0, \tag{4}$$

$$V\frac{\partial\theta}{\partial\Phi}-\frac{\rho}{\rho_0}\frac{\partial V}{\partial\Psi}=0. \tag{5}$$

Now, from

$$\left.\begin{aligned} d\Phi &= \frac{\partial\Phi}{\partial V}dV+\frac{\partial\Phi}{\partial\theta}d\theta,\\ d\Psi &= \frac{\partial\Psi}{\partial V}dV+\frac{\partial\Psi}{\partial\theta}d\theta, \end{aligned}\right\} \tag{6}$$

one obtains

$$\left.\begin{aligned} dV &= \frac{1}{\Delta}\left(\frac{\partial\Psi}{\partial\theta}d\Phi-\frac{\partial\Phi}{\partial\theta}d\Psi\right),\\ d\theta &= \frac{1}{\Delta}\left(-\frac{\partial\Psi}{\partial V}d\Phi+\frac{\partial\Phi}{\partial V}d\Psi\right), \end{aligned}\right\} \tag{7}$$

where Δ is the Jacobian of the transformation from Φ,Ψ to V,θ:

$$\Delta\equiv\begin{vmatrix}\dfrac{\partial\Phi}{\partial V} & \dfrac{\partial\Phi}{\partial\theta}\\[2ex] \dfrac{\partial\Psi}{\partial V} & \dfrac{\partial\Psi}{\partial\theta}\end{vmatrix}.$$

When one uses equation (7), equations (4) and (5) give

$$\frac{\rho V}{\rho_0}\frac{\partial\Phi}{\partial V}+\left(1-M^2\right)\frac{\partial\Psi}{\partial\theta}=0, \tag{8}$$

$$V\frac{\partial\Psi}{\partial V}-\frac{\rho}{\rho_0}\frac{\partial\Phi}{\partial\theta}=0. \tag{9}$$

When one puts

$$\frac{dW}{W}=\sqrt{1-M^2}\,\frac{dV}{V}, \tag{10}$$

equations (8) and (9) become

$$W\frac{\partial\Phi}{\partial W}=-\frac{\rho_0}{\rho}\sqrt{1-M^2}\,\frac{\partial\Psi}{\partial\theta}, \tag{11}$$

$$\frac{\partial\Phi}{\partial\theta}=\frac{\rho_o}{\rho}\sqrt{1-M^2}\,\frac{\partial\Psi}{\partial W}W. \tag{12}$$

Let us now make the *tangent–gas* approximation, i.e., let

$$\left(\frac{\rho_0}{\rho}\right)^2\left(1-M^2\right)=1, \tag{13a}$$

which may be rewritten as

$$\left[1-\left(\frac{\rho}{\rho_0}\right)^2\right]\frac{dp}{d\rho}=V^2. \tag{13b}$$

When one differentiates with respect to ρ, (13b) gives

$$\left[1-\left(\frac{\rho}{\rho_0}\right)^2\right]\frac{d^2p}{d\rho^2}-2\left(\frac{\rho}{\rho_0}\right)\frac{1}{\rho_0}\frac{dp}{d\rho}=2V\frac{dV}{d\rho}. \tag{14}$$

When one uses the momentum–conservation relation,

$$V\frac{dV}{d\rho}+\frac{1}{\rho}\frac{dp}{d\rho}=0, \tag{15}$$

equation (14) becomes

$$\left[1-\left(\frac{\rho}{\rho_o}\right)^2\right]\left[\frac{d^2p}{d\rho^2}+\frac{2}{\rho}\frac{dp}{d\rho}\right]=0, \tag{16}$$

from which

$$\frac{d^2p}{d\rho^2}+\frac{2}{\rho}\frac{dp}{d\rho}=0. \tag{17}$$

The solution of equation (17) is

$$p=A-\frac{B}{\rho}. \tag{18}$$

This amounts to replacing the isentrope by a tangent to it at a certain point; let us choose the free stream for the latter, (see Figure 3.20). This is the von Kármán–Tsien approximation. Equation (13) and (18) then lead to the following relations:

$$\begin{aligned}
&p-p_\infty=\rho_\infty a_\infty^2\left(\frac{1}{\rho_\infty}-\frac{1}{\rho}\right),\\
&U_\infty^2-a_\infty^2=V^2-a^2,\\
&\frac{\rho_0}{\rho}=\sqrt{1+\left(\frac{V}{a_0}\right)^2},\\
&\rho^2a^2=\rho_\infty^2a_\infty^2,
\end{aligned} \tag{19}$$

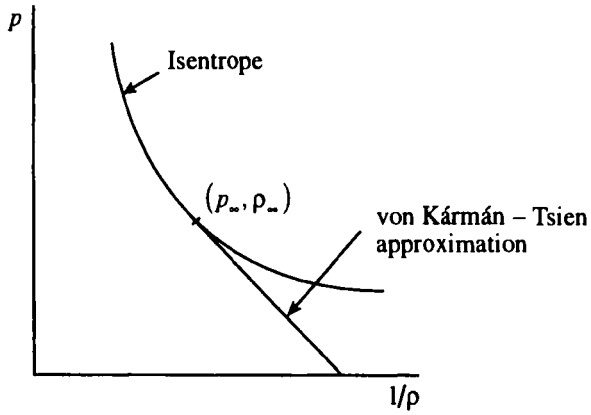

Figure 3.20. The tangent–gas approximation.

where the subscript ∞ denotes the conditions in the free stream.

Using (19), one has from (10)

$$W = \frac{2V}{1+\sqrt{1+(V/a_0)^2}}, \qquad V = \frac{4a_0^2 W}{4a_0^2 - W^2}. \tag{20}$$

Next, in order to relate the geometries in the compressible physical plane and the incompressible hodograph plane, note

$$\left.\begin{aligned} d\Phi &= \frac{\partial \Phi}{\partial x}dx + \frac{\partial \Phi}{\partial y}dy, \\ d\Psi &= \frac{\partial \Psi}{\partial x}dx + \frac{\partial \Psi}{\partial y}dy, \end{aligned}\right\} \tag{21}$$

where

$$\left.\begin{aligned} \frac{\partial \Phi}{\partial x} &= V\cos\theta, \qquad \frac{\partial \Phi}{\partial y} = V\sin\theta, \\ \frac{\partial \Psi}{\partial x} &= -\frac{\rho V}{\rho_0}\sin\theta, \qquad \frac{\partial \Psi}{\partial y} = \frac{\rho V}{\rho_0}\cos\theta, \end{aligned}\right\} \tag{22}$$

so that

$$\left.\begin{aligned} dx &= \frac{1}{D}\left(\frac{\rho V}{\rho_0}\cos\theta \cdot d\Phi - V\sin\theta \cdot d\Psi\right), \\ dy &= \frac{1}{D}\left(\frac{\rho V}{\rho_0}\sin\theta \cdot d\Phi + V\cos\theta \cdot d\Psi\right), \end{aligned}\right\} \tag{23}$$

where D is the Jacobian of the transformation from Φ, Ψ to V, θ:

$$D = \begin{vmatrix} V\cos\theta & V\sin\theta \\ -\dfrac{\rho V}{\rho_0}\sin\theta & \dfrac{\rho V}{\rho_0}\cos\theta \end{vmatrix} = \frac{\rho}{\rho_0}V^2.$$

Thus,

$$\left.\begin{aligned} dx &= \frac{1}{V^2}\left[\Phi_x d\Phi + \left(\frac{\rho_0}{\rho}\right)^2 \Psi_x d\Psi\right], \\ dy &= \frac{1}{V^2}\left[\Phi_y d\Phi + \left(\frac{\rho_0}{\rho}\right)^2 \Psi_y d\Psi\right]. \end{aligned}\right\} \tag{24}$$

When one uses (10), (24) may be written alternatively as

$$\left.\begin{aligned} dx &= \frac{U_1}{W^2}\left(1 - \frac{W^2}{4a_0^2}\right)d\Phi - \frac{U_2}{W^2}\left(1 + \frac{W^2}{4a_0^2}\right)d\Psi, \\ dy &= \frac{U_2}{W^2}\left(1 - \frac{W^2}{4a_0^2}\right)d\Phi + \frac{U_1}{W^2}\left(1 + \frac{W^2}{4a_0^2}\right)d\Psi, \end{aligned}\right\} \tag{25}$$

where

$$U_1 = W\cos\theta, \quad U_2 = W\sin\theta.$$

If

$$z = x + iy, \quad q = U_1 + iU_2, \quad F = \Phi + i\Psi, \quad q = \frac{d\overline{F}}{d\zeta}, \tag{26}$$

then (25) may be rewritten as

$$dz = \frac{dF}{\bar{q}} - \frac{q}{4a_0^2}d\overline{F} = d\zeta - \frac{q^2}{4a_0^2}d\zeta, \tag{27}$$

which gives a relation between the geometries in the physical plane and the hodograph plane.

The Lost Solution

The hodograph transformation is degenerate when $V = V(\theta)$, i.e.,

$$\frac{\partial(V,\theta)}{\partial(\Phi,\Psi)} = \begin{vmatrix} \dfrac{\partial V}{\partial \Phi} & \dfrac{\partial V}{\partial \Psi} \\ \dfrac{\partial \theta}{\partial \Phi} & \dfrac{\partial \theta}{\partial \Psi} \end{vmatrix} = \frac{\partial V}{\partial \theta}\begin{vmatrix} \dfrac{\partial \theta}{\partial \Phi} & \dfrac{\partial \theta}{\partial \Psi} \\ \dfrac{\partial \theta}{\partial \Phi} & \dfrac{\partial \theta}{\partial \Psi} \end{vmatrix} = 0. \tag{28}$$

Such a situation prevails for a Prandtl–Meyer flow, for example, whereby the nonuniform flow is represented by just a line in the hodograph plane. Equations (1) and (2) now become

$$\frac{\partial\theta}{\partial n}+\left(1-M^2\right)\frac{1}{V}\frac{dV}{d\theta}\frac{\partial\theta}{\partial s}=0, \tag{29}$$

$$\frac{\partial\theta}{\partial s}-\frac{1}{V}\frac{dV}{d\theta}\frac{\partial\theta}{\partial n}=0, \tag{30}$$

from which

$$\frac{\partial\theta}{\partial n}\left[1+\left(1-M^2\right)\frac{1}{V}\left(\frac{dV}{d\theta}\right)^2\right]=0 \tag{31}$$

or

$$\frac{dV}{V}=\pm\frac{d\theta}{\sqrt{M^2-1}}, \tag{32}$$

so that the hodograph transformation is degenerate when the hodograph curve becomes tangential locally to a characteristic.

The Limit Line

Recall the relations

$$\left.\begin{aligned} dx&=\frac{\cos\theta}{V}d\Phi-\frac{\rho_0}{\rho}\frac{\sin\theta}{V}d\Psi,\\ dy&=\frac{\sin\theta}{V}d\Phi+\frac{\rho_0}{\rho}\frac{\cos\theta}{V}d\Psi. \end{aligned}\right\} \tag{23}$$

When one uses (6), (23) becomes

$$\begin{aligned} dx&=\left[\frac{\cos\theta}{V}\left(\frac{\partial\Phi}{\partial V}\right)-\frac{\rho_0}{\rho}\frac{\sin\theta}{V}\left(\frac{\partial\Psi}{\partial V}\right)\right]dV\\ &\quad+\left[\frac{\cos\theta}{V}\left(\frac{\partial\Phi}{\partial\theta}\right)-\frac{\rho_0}{\rho}\frac{\sin\theta}{V}\left(\frac{\partial\Psi}{\partial\theta}\right)\right]d\theta\\ dy&=\left[\frac{\sin\theta}{V}\left(\frac{\partial\Phi}{\partial V}\right)+\frac{\rho_0}{\rho}\frac{\cos\theta}{V}\left(\frac{\partial\Psi}{\partial V}\right)\right]dV\\ &\quad+\left[\frac{\sin\theta}{V}\left(\frac{\partial\Phi}{\partial\theta}\right)+\frac{\rho_0}{\rho}\frac{\cos\theta}{V}\left(\frac{\partial\Psi}{\partial\theta}\right)\right]d\theta. \end{aligned} \tag{33}$$

When one uses (8) and (9), (33) becomes

$$dx = \frac{\rho_0}{\rho}\frac{1}{V}\left[-\left\{\left(1-M^2\right)\frac{\cos\theta}{V}\frac{\partial\Psi}{\partial\theta}+\sin\theta\frac{\partial\Psi}{\partial V}\right\}dV\right.$$
$$\left.+\left\{V\cos\theta\frac{\partial\Psi}{\partial V}-\sin\theta\frac{\partial\Psi}{\partial\theta}\right\}d\theta\right]$$
$$dy = \frac{\rho_0}{\rho}\frac{1}{V}\left[-\left\{\left(1-M^2\right)\frac{\sin\theta}{V}\frac{\partial\Psi}{\partial\theta}-\cos\theta\frac{\partial\Psi}{\partial V}\right\}dV\right.$$
$$\left.+\left\{V\sin\theta\frac{\partial\Psi}{\partial V}+\cos\theta\frac{\partial\Psi}{\partial\theta}\right\}d\theta\right]. \tag{34}$$

On the streamlines, (34) becomes

$$\left.\begin{aligned} dx &= -\frac{\rho_0\cos\theta}{\rho V^2\Psi_\theta}\left[V^2\Psi_V^2-\left(M^2-1\right)\Psi_\theta^2\right]dV,\\ dy &= -\frac{\rho_0\sin\theta}{\rho V^2\Psi_\theta}\left[V^2\Psi_V^2-\left(M^2-1\right)\Psi_\theta^2\right]dV. \end{aligned}\right\} \tag{35}$$

Note the Jacobian of the transformation from x, y to V, θ:

$$J = \frac{\partial(x,y)}{\partial(V,\theta)} = \frac{\partial(\Phi,\Psi)/\partial(V,\theta)}{\partial(\Phi,\Psi)/\partial(x,y)} = -\left(\frac{\rho_0}{\rho}\right)^2\frac{1}{V^3}\left[V^2\Psi_V^2-\left(M^2-1\right)\Psi_\theta^2\right]. \tag{36}$$

Solutions of hodograph equations correspond to real flows only when $J \neq 0$, so that the transformation is one–to–one. The case $J = 0$ corresponds to the limit line and can occur only in a sonic or supersonic flow $(M \geq 1)$.

The fluid acceleration f on a streamline is given, on using (7), by

$$f = \left(V\frac{\partial V}{\partial s}\right)_\Psi = \left(V^2\frac{\partial V}{\partial\Phi}\right) = \frac{1}{\Delta}V^2\frac{\partial\Psi}{\partial\theta}, \tag{37}$$

which shows that the fluid acceleration becomes infinite on a limit line.

Note that dx, dy change their signs across the lines $J = 0$, whereas the slope of the streamlines does not change across $J = 0$. Thus, the streamline must have a cusp there. The solution there is no longer physically possible: this is known as the *limit line*. At a point on the limit line, the streamline is locally tangential to a hodograph characteristic; thus the limit line which exists only in supersonic flows must be the envelope of one family of Mach waves. Physically, the existence of a limit line implies that the assumption of isentropic processes has broken down.

Example 2: Consider the case

$$\Psi = \Psi(V), \quad \frac{\rho_0}{\rho}\frac{d\Psi}{dV} = \frac{K_1}{V}, \quad K_1 = \text{const.}$$

Then, one obtains from equations (8), (9), and (33)

$$\frac{\partial x}{\partial V} = -K_1 \frac{\sin\theta}{V^2}, \qquad \frac{\partial x}{\partial \theta} = K_1 \frac{\cos\theta}{V},$$

$$\frac{\partial y}{\partial V} = K_1 \frac{\cos\theta}{V^2}, \qquad \frac{\partial y}{\partial \theta} = K_1 \frac{\sin\theta}{V}.$$

On integrating, one obtains

$$x = K_1 \frac{\sin\theta}{V}, \qquad y = K_1 \frac{\cos\theta}{V},$$

so that the streamlines are circles. Choosing $K_1 = r^* a^*$, one obtains

$$\frac{r}{r^*} = \frac{a^*}{V},$$

which represents a vortex flow. Note that $r = r^*$ represents a limit line.

Example 3: Consider the case

$$\Psi = \Psi(\theta).$$

Equations (8) and (9) then give

$$\Psi_{\theta\theta} = 0$$

or

$$\Psi = K_1\theta + K_2.$$

Using this, equations (8) and (9) give

$$\Phi_\theta = 0, \qquad \Phi_V = -\frac{\rho_0}{\rho}\frac{K_1}{V}\left(1 - M^2\right)$$

and (33) gives

$$\frac{\partial x}{\partial \theta} = -\frac{\rho_0}{\rho}\frac{K_1}{V}\sin\theta,$$

$$\frac{\partial y}{\partial \theta} = \frac{\rho_0}{\rho}\frac{K_1}{V}\cos\theta.$$

On integrating, one obtains

$$x = K_1 \frac{\rho_0}{\rho}\frac{\cos\theta}{V} + K_3,$$

$$y = K_1 \frac{\rho_0}{\rho}\frac{\sin\theta}{V} + K_4,$$

from which, on choosing $K_3, K_4 = 0, K_1 = \left(\rho^*/\rho_0\right)a^* r^*$,

$$\frac{r}{r^*} = \frac{\rho^*}{\rho}\frac{a^*}{V}.$$

Note that $r = r^*$ represents the limit line.

Next, consider the acceleration

$$V\frac{dV}{dr} = \frac{V}{dr/dV},$$

where now

$$\frac{dr}{dV} = \frac{\rho r^* a^*}{\rho}\left(-\frac{1}{\rho V}\frac{d\rho}{dV} - \frac{1}{V^2}\right).$$

Using the tangent–gas approximation (19),

$$\frac{1}{\rho V}\frac{d\rho}{dV} = \frac{1}{a_0^2 + V^2},$$

one obtains

$$\frac{dr}{dV} = \frac{r^*\rho^* a^*}{\rho}\left[\frac{-a_0^2}{V^2\left(a_0^2 + V^2\right)}\right] = \frac{r^*\rho^* a^*}{\rho}\left(\frac{M^2 - 1}{V^2}\right),$$

where (19) has been used again. Thus,

$$V\frac{dV}{dr} = \pm\frac{\rho V^3}{r^*\rho^* a^*\left(M^2 - 1\right)},$$

so that the acceleration becomes infinite at the limit line $(M = 1)$.

This solution represents a source flow and is confined to the region $r > r^*$.

Example 4: Note that

$$\Phi = \frac{\rho_0}{\rho V}\cos\theta, \qquad \Psi = \frac{\sin\theta}{V}$$

is a particular integral of equations (8) and (9), which is called *Ringleb's solution*.

Using (23), one obtains along the streamlines

$$dx = \frac{\cos\theta}{V}d\Phi, \qquad dy = \frac{\sin\theta}{V}d\Phi.$$

Now, noting

$$d\Phi = \frac{\partial\Phi}{\partial V}dV + \frac{\partial\Phi}{\partial\theta}d\theta$$

and using equations (8) and (9), one obtains

$$d\Phi = -\frac{\rho_0}{\rho V^2}\left(1-M^2\right)\cos\theta \cdot dV - \frac{\rho_0}{\rho V}\sin\theta \cdot d\theta .$$

Now, along the streamlines, one has

$$d\Psi = -\frac{\sin\theta}{V^2}dV + \frac{\cos\theta}{V}d\theta = 0$$

so that

$$d\Phi = -\frac{\rho_0}{\rho V}\left[\frac{\cos^2\theta}{\sin\theta}\left(1-M^2\right)+\sin\theta\right]d\theta .$$

Thus, the streamlines are given by

$$dx = -\frac{\rho_0}{\rho V^2}\left[\cot^2\theta\cdot\left(1-M^2\right)+1\right]\sin\theta\cdot\cos\theta\cdot d\theta,$$

$$dy = -\frac{\rho_0}{\rho V^2}\left[\cot^2\theta\cdot\left(1-M^2\right)+1\right]\sin^2\theta\cdot d\theta.$$

For $M \Rightarrow 0$, this gives

$$dx = -k^2\frac{\cot\theta}{\sin^2\theta}d\theta,$$

$$dy = -\frac{k^2}{\sin^2\theta}d\theta,$$

where

$$k = \frac{\sin\theta}{V} = \text{const. along the streamlines.}$$

Thus,

$$x = \frac{k^2}{2\sin^2\theta}, \qquad y = k^2\cot\theta$$

or

$$y^2 = k^4\left(\frac{2x}{k^2}-1\right),$$

which represents a family of confocal parabolic symmetrical curves about the x–axis with focus at the origin. Thus, in the $M \Rightarrow 0$ limit, the above solution represents the flow past a semi–infinite wall.

The limit line is given by

$$\left(1-M^2\right)\left(\frac{\partial\Psi}{\partial\theta}\right)^2 + V^2\left(\frac{\partial\Psi}{\partial V}\right)^2 = 0,$$

where

$$M^2 = \frac{V^2}{a^2} = \frac{V^2}{a_0^2 - \left(\frac{\gamma-1}{2}\right)V^2} = \frac{\left(\frac{\sin^2\theta}{k^2}\right)}{a_0^2 - \left(\frac{\gamma-1}{2}\right)\left(\frac{\sin^2\theta}{k^2}\right)}.$$

Thus, the limit line is given by

$$\sin^4\theta - \frac{\gamma+1}{2}\sin^2\theta + k^2a_0^2 = 0,$$

from which

$$\sin^2\theta = \left(\frac{\gamma+1}{4}\right) \pm \sqrt{\left(\frac{\gamma+1}{4}\right)^2 - k^2a_0^2}.$$

In order that a streamline does not cross a limit line, one requires

$$k^2 > \left(\frac{\gamma+1}{4a_0}\right)^2,$$

so that a smooth transition from $M<1$ to $M>1$ then again to $M<1$ is possible if $M < M_{\max}$, where

$$M_{\max} = \left[\left(\frac{\gamma+1}{4}\right)^2 - \left(\frac{\gamma-1}{2}\right)\right]^{-1}.$$

Such a smooth transition is similar to that which can occur on the upper surface of an airfoil in transonic flow.

EXERCISE

1. In Example 4, derive the range of values for k in which a streamline can have an encounter with a limit line.

3.7. Nonlinear Theory of Plane Sound Waves

In linear acoustics (Section 3.5), one considers the disturbances on a constant ambient state to be small so that the governing equations are linearized by retaining only the first–order terms in the small disturbances. The latter then satisfy the classical wave equation. One would then inquire, How does this linear solution relate to the original nonlinear equations? Further, one wants to know what were the essential nonlinear features that were lost in the linearization of the original equations.

Riemann Invariants

Consider a one–dimensional propagation of plane waves in a fluid. The equations expressing the conservation of mass and momentum are

$$\frac{\partial \rho}{\partial t} + \frac{\partial}{\partial x}(\rho u) = 0, \tag{1}$$

$$\rho\left(\frac{\partial u}{\partial t} + u\frac{\partial u}{\partial x}\right) = -\frac{\partial p}{\partial x}. \tag{2}$$

When one introduces

$$P = \int_o^\rho a\frac{d\rho}{\rho}, \qquad a^2 = \left(\frac{\partial p}{\partial \rho}\right)_S, \tag{3}$$

equation (1) and (2) give

$$\frac{\partial P}{\partial t} + u\frac{\partial P}{\partial x} + a\frac{\partial u}{\partial x} = 0, \tag{4}$$

$$\frac{\partial u}{\partial t} + u\frac{\partial u}{\partial x} + a\frac{\partial P}{\partial x} = 0, \tag{5}$$

from which

$$\frac{\partial}{\partial t}(u \pm P) + (u \pm a)\frac{\partial}{\partial x}(u \pm P) = 0. \tag{6}$$

Equation (6) gives the Riemann invariants[8]

$$u \pm P = \text{ const. along } C_\pm: \quad \frac{dx}{dt} = u \pm a. \tag{7}$$

The lines $dx/dt = u \pm a$ are called the characteristics $C_\pm$.

---

[8]Equation (7) may also be derived alternatively by noting that equations (1) and (2) may be rewritten as follows

$$\begin{pmatrix} \rho \\ u \end{pmatrix}_t + \boldsymbol{A} \cdot \begin{pmatrix} \rho \\ u \end{pmatrix}_x = 0,$$

where

$$\boldsymbol{A} = \begin{bmatrix} u & \rho \\ a^2/\rho & u \end{bmatrix}.$$

The Riemann invariants $h_\pm$ are then given by (see footnote 5)

$$\begin{bmatrix} u & a^2/\rho \\ \rho & u \end{bmatrix}\begin{bmatrix} \partial h_\pm/\partial \rho \\ \partial h_\pm/\partial u \end{bmatrix} = (u \pm a)\begin{bmatrix} \partial h_\pm/\partial \rho \\ \partial h_\pm/\partial u \end{bmatrix},$$

where we have noted that the eigenvalues of $\boldsymbol{A}$ are $u \pm a$. Thus,

$$\begin{bmatrix} \partial h_\pm/\partial \rho \\ \partial h_\pm/\partial u \end{bmatrix} = \begin{bmatrix} \pm a/\rho \\ 1 \end{bmatrix},$$

from which

$$h_\pm = u \pm \int a\frac{d\rho}{\rho},$$

as in equation (7).

The existence of two families of characteristics greatly facilitates solution of hyperbolic systems. For a linear problem, the characteristics are found by simple integration, and a knowledge of the Riemann invariants along the characteristics then completes the solution. But, this is not possible for equations (4) and (5), which are nonlinear and depend on unknown variables u and a, making integration impossible. Nonetheless, in certain special geometries with the concomitant special boundary conditions, one family of characteristics reduces to a set of straight lines and one of the Riemann invariants is constant everywhere (i.e., it takes the same constant value on every characteristic of its family) and integration of equations (4) and (5) becomes possible. Suppose, for instance, that the condition

$$u - \int a \frac{d\rho}{\rho} = \text{const.} \tag{8}$$

holds everywhere. Then, since $u + \int a(d\rho/\rho)$ is constant on a given characteristic $dx/dt = u + a$, it follows that, on this characteristic, u and $\int a(d\rho/\rho)$ must separately be constant. If the flow is homentropic,[9] then $a = a(\rho)$, and, therefore, a is constant on this characteristic. Thus, $u + a$ is also constant on it, and the characteristic is a straight line. The family of characteristics $dx/dt = u + a$, therefore, consists of straight lines, and, since one of these passes through each point of (x,t) space (as does one of the other family), the solutions of equations (1) and (2) for this region called the *simple wave region* takes the form

$$u = f[x - (u + a)t]. \tag{9}$$

If one has the initial condition

$$t = 0: \quad u = u_0(x), \tag{10}$$

then (9) becomes

$$u = u_0[x - (u + a)t]. \tag{11}$$

If $u_0(x) \geq 0$, $u + a$ will be positive everywhere. Thus, the family of characteristics carrying the wave has positive slope in the (x,t) plane, and the wave is said to be forward-progressing.

If the time history of the velocity of a fluid particle is known at a particular place, say,

$$x = 0: \quad u = g(t), \tag{12}$$

the solution is

$$u = g\left(t - \frac{x}{\beta u \pm a_0}\right), \tag{13}$$

[9] A flow is called *homentropic* is the entropy of each fluid particle is the same and remains so for all times.

where

$$\beta = \frac{\gamma+1}{2}.$$

Thus, a simple wave situation with one family of straight-line characteristics occurs when all the members of the other family come from a region of uniform flow conditions in the (x,t) plane (as, for example, at infinity upstream in a uniform flow of infinite extent). An example of this is the Prandtl–Meyer expansion of a supersonic flow around a convex corner; if the corner is sharp the straight-line characteristics bunch into a fan centered on the corner itself (Section 3.5).

Example 5: Consider an initial-value problem wherein all the fluid except that in a finite interval BF of x is undisturbed (see Figure 3.21).

One has from (7)

$$u = P(\rho) = \int_0^\rho a\frac{d\rho}{\rho} \quad \begin{matrix} \text{ahead of } C_-^F, \\ \text{behind } C_-^B, \end{matrix} \Bigg\}$$

$$u = -P(\rho) = -\int_0^\rho a\frac{d\rho}{\rho} \quad \begin{matrix} \text{behind } C_+^B, \\ \text{ahead of } C_+^F, \end{matrix} \Bigg\}.$$

Note that ahead of C_+^F and behind C_-^B, $u = P(\rho) \equiv 0$. Also, ahead of C_-^F and behind C_+^B, $u = P(\rho) \equiv 0$. During the time $0 < t < t^*$ (Figure 3.21), the disturbances become disentangled and thereafter propagate as two simple waves (one forward and one backward) with an undisturbed region in between.

Consider the region ahead of C_-^F between C_+^B and C_+^F. Since $u+P$ is constant along each C_+ which becomes $2u = \text{const}$ in this region along each C_+. This means $\rho = \text{const}$ or $a = \text{const}$ along each C_+ in this region or

$$u + a = \text{cons.t along } C_+,$$

so that the characterstics $dx = (u+a)\,dt$ are straight lines in this region.

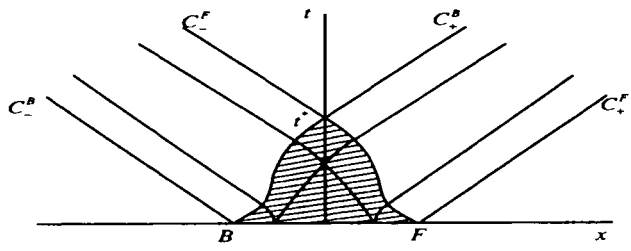

Figure 3.21. The initial-value problem with the initial perturbation prescribed on a finite portion of the boundary (from Lighthill, 1978).

Example 6: Consider plane sound waves in a perfect gas. One has

$$\frac{p}{p_0} = \left(\frac{\rho}{\rho_0}\right)^{\gamma},$$

so that

$$a^2 = \frac{dp}{d\rho} = \frac{\gamma p}{\rho}.$$

Hence

$$\frac{a}{a_0} = \left(\frac{\rho}{\rho_0}\right)^{(\gamma-1)/2}.$$

When one uses this, (3) gives

$$P = \int_{\rho_0}^{\rho} \frac{a}{\rho}\, d\rho = 2\left(\frac{a - a_0}{\gamma - 1}\right).$$

Then, for a simple wave, the relation

$$u = P$$

gives

$$a = a_0 + \frac{1}{2}(\gamma - 1)u,$$

so that

$$\frac{\rho}{\rho_0} = \left[1 + \frac{1}{2}(\gamma - 1)\frac{u}{a_0}\right]^{2/(\gamma-1)}.$$

Now the signal is propagated at the velocity

$$\frac{dx}{dt} = u + a = a_0 + \frac{1}{2}(\gamma + 1)u,$$

which implies that the characteristics would intersect and the solution then becomes multivalued unless a shock is introduced to prevent it. Thus, finite-amplitude compressive waves continually steepen with time (see Figure 3.22) until a discontinuity develops. One then has to include the effects of viscosity and heat conductivity (see Section 4.1) so as to produce balance between the effects of nonlinear steepening and dissipative spreading, leading to a steady profile. It turns out that the transition layer over which this balance takes effect has a thickness of the order of a few mean free paths. One then obtains a shock wave. This shock region is, however, idealized into a discontinuity in the inviscid theory, and one simply adds the jump conditions across the discontinuity of the flow variables to the inviscid theory, as done in Section 3.3.

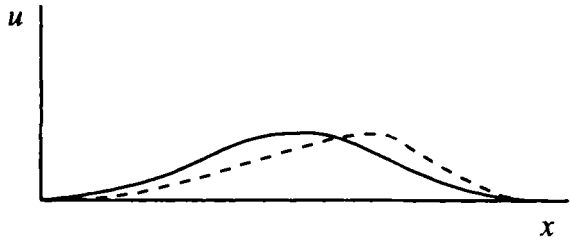

Figure 3.22. Nonlinear steepening of plane waves.

It turns out that the isentropic flow considered above possesses an exact explicit solution (due to Fubini–Ghiron). First, note that using the relation (see Example 6)

$$a = a_0 + \frac{1}{2}(\gamma - 1)u$$

(9) becomes

$$u = f\left[x - \left(a_0 + \frac{\gamma+1}{2}u\right)t\right]. \tag{14}$$

Consider the initially sinusoidal motion defined by the condition

$$t = 0: \quad u = u_0 \sin kx. \tag{15}$$

Then, (14) becomes

$$u = u_0 \sin k\left[x - \left(a_0 + \frac{\gamma+1}{2}u\right)t\right]. \tag{16}$$

If one expands u/u_0 in a Fourier series

$$\frac{u}{u_0} = \sum_{n=1}^{\infty} B_n \sin n(kx - \omega t), \tag{17}$$

where

$$B_n = \frac{1}{\pi}\int_0^{2\pi} \frac{u}{u_0} \sin n(kx - \omega t)\, d(kx - \omega t), \tag{18}$$

one has

$$B_n = \frac{1}{\pi}\int_0^{2\pi} \sin\zeta \cdot \sin\left(n\zeta - n\frac{\gamma+1}{2}t \cdot \sin\zeta\right)\cdot\left(1 - \frac{\gamma+1}{2}t\cos\zeta\right)d\zeta$$

$$= \frac{\gamma+1}{nt} J_n\left(\frac{2nt}{\gamma+1}\right), \tag{19}$$

where J_n is the Bessel function of the first kind of order n. Hence,

$$u = 2u_0 \sum_{n=1}^{\infty} \frac{J_n\left(\frac{2nt}{\gamma+1}\right)}{\left(\frac{2nt}{\gamma+1}\right)} \sin n(kx - \omega t), \quad t < \frac{\gamma+1}{2}. \tag{20}$$

Example 7: Consider the waves produced by the prescribed motion of a piston at the end of a long tube. The gas is assumed to be at rest with a uniform state $u = 0$, $a = a_0$ in $x \geq 0$ at $t = 0$. Since the piston is itself a particle path, all particle paths originate on the x–axis in the uniform region, and the flow is isentropic.

The C_- characteristics start on the x–axis in the uniform region, and on each of them we have

$$\frac{2a}{\gamma-1} - u = \frac{2a_0}{\gamma-1} = \text{const.},$$

which holds throughout the flow.

The C_+ characteristics start on the piston, and on each of them we have

$$\frac{2a}{\gamma-1} + u = \text{const.}$$

or

$$u = \text{const. on } \frac{dx}{dt} = a_0 + \frac{\gamma+1}{2}u,$$

so that the C_+ characteristics will be a family of straight lines (see Figure 3.23). The leading C_+ characteristic starts on the x–axis and is given by $x = a_0 t$.

Note that since the C_+ are straight lines with slope dx/dt increasing with u, these characteristics will overlap if u ever increases on the piston. This is the typical nonlinear breaking that is resolved by the introduction of shocks. This happens in the compressive parts of the disturbance.

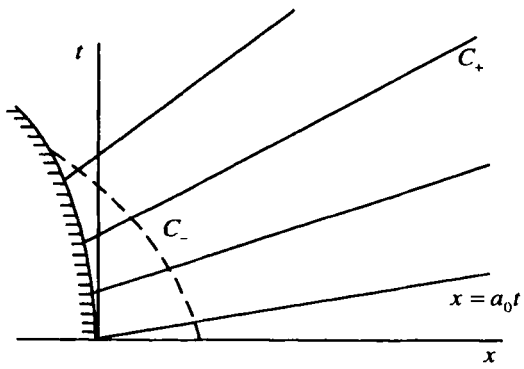

Figure 3.23. Loci of wave fronts produced by the motion of a piston.

Nonlinear Propagation of a Sound Wave

Consider unidirectional propagation of sound waves in an ideal fluid. The governing equations are

$$\frac{\partial \rho}{\partial t} + \frac{\partial}{\partial x}(\rho u) = 0, \tag{21}$$

$$\rho\left(\frac{\partial u}{\partial t} + u\frac{\partial u}{\partial x}\right) = -\frac{\partial p}{\partial x}, \tag{22}$$

$$\frac{\partial}{\partial t}\left(\frac{p}{\rho^{\gamma}}\right) + u\frac{\partial}{\partial x}\left(\frac{p}{\rho^{\gamma}}\right) = 0. \tag{23}$$

Noting, from equation (23), that

$$\left(\frac{a}{a_0}\right) = \left(\frac{\rho}{\rho_0}\right)^{\frac{\gamma-1}{2}} \tag{24}$$

and putting

$$\rho = \rho_0(1+\hat{\rho})$$

and nondimensionalizing u, x and t, suitably, equations (21) and (22) become

$$\frac{\partial \hat{\rho}}{\partial t} + \frac{\partial u}{\partial x} = -u\frac{\partial \hat{\rho}}{\partial x} - \hat{\rho}\frac{\partial u}{\partial x}, \tag{25}$$

$$\frac{\partial u}{\partial t} + \frac{\partial \hat{\rho}}{\partial x} = -u\frac{\partial u}{\partial x} + (2-\gamma)\frac{\hat{\rho}}{1+\hat{\rho}}\frac{\partial \hat{\rho}}{\partial x}. \tag{26}$$

Let us now treat equations (25) and (26) by using a method based on perturbing the characteristics (Lin and Fox). Thus, look for a solution of the form,

$$\begin{aligned} u(x,t;\varepsilon) &= \varepsilon u_1(s_1, s_2, \tilde{t}) + \varepsilon^2 u_2(s_1, s_2, \tilde{t}) + \cdots, \\ \hat{\rho}(x,t;\varepsilon) &= \varepsilon \hat{\rho}_1(s_1, s_2, \tilde{t}) + \varepsilon^2 \hat{\rho}_2(s_1, s_2, \tilde{t}) + \cdots, \end{aligned} \tag{27}$$

where

$$s_{1,2} = t \mp x. \tag{28}$$

Here, $\varepsilon \ll 1$ represents the amplitude of the sound wave and $\tilde{t} = \varepsilon t$ represents the slow time scale characterizing the modulation of the given sound wave.

Substituting equations (27) and (28) in equations (25) and (26), one obtains the following conditions upon equating coefficients of equal powers of ε to zero:

$O(\varepsilon)$:

$$\left(\frac{\partial}{\partial s_2} + \frac{\partial}{\partial s_1}\right)\hat{\rho}_1 + \left(\frac{\partial}{\partial s_2} - \frac{\partial}{\partial s_1}\right)u_1 = 0, \tag{29}$$

$$\left(\frac{\partial}{\partial s_2}+\frac{\partial}{\partial s_1}\right)u_1+\left(\frac{\partial}{\partial s_2}-\frac{\partial}{\partial s_1}\right)\hat{\rho}_1=0, \tag{30}$$

$0(\varepsilon^2)$:

$$\left(\frac{\partial}{\partial s_2}+\frac{\partial}{\partial s_1}\right)\hat{\rho}_2+\left(\frac{\partial}{\partial s_2}-\frac{\partial}{\partial s_1}\right)u_2$$

$$=-\frac{\partial\hat{\rho}_1}{\partial\tilde{t}}\,u_1\left(\frac{\partial}{\partial s_2}-\frac{\partial}{\partial s_1}\right)\hat{\rho}_1-\hat{\rho}_1\left(\frac{\partial}{\partial s_2}-\frac{\partial}{\partial s_1}\right)u_1,$$

$$\left(\frac{\partial}{\partial s_2}+\frac{\partial}{\partial s_1}\right)u_2+\left(\frac{\partial}{\partial s_2}-\frac{\partial}{\partial s_1}\right)\hat{\rho}_2 \tag{31}$$

$$=-\frac{\partial u_1}{\partial\tilde{t}}-u_1\left(\frac{\partial}{\partial s_2}-\frac{\partial}{\partial s_1}\right)u_1+(2-\gamma)\hat{\rho}_1\left(\frac{\partial}{\partial s_2}-\frac{\partial}{\partial s_1}\right)\hat{\rho}_1. \tag{32}$$

One has from equations (29) and (30)

$$4\frac{\partial^2 u_1}{\partial s_1\partial s_2}=0. \tag{33}$$

Assuming the given wave to be a right–running wave, one has from equation (33)

$$u_1=f(s_1,\tilde{t})=\hat{\rho}_1. \tag{34}$$

Using equation (34), one has from equations (31) and (32)

$$4\frac{\partial^2 u_2}{\partial s_1\partial s_2}=(\gamma+1)\left[f\frac{\partial^2 f}{\partial s_1^2}+\left(\frac{\partial f}{\partial s_1}\right)^2\right]-2\frac{\partial^2 f}{\partial s_1\partial\tilde{t}}. \tag{35}$$

Removal of the secular terms on the right–hand side in equation (35) requires

$$(\gamma+1)\left[f\frac{\partial^2 f}{\partial s_1^2}+\left(\frac{\partial f}{\partial s_1}\right)^2\right]-2\frac{\partial^2 f}{\partial s_1\partial\tilde{t}}=0$$

or

$$\frac{\partial f}{\partial\tilde{t}}-\left(\frac{\gamma+1}{2}\right)f\frac{\partial f}{\partial s_1}=0, \tag{36}$$

from which

$$f=F\left(s_1+\frac{\gamma+1}{2}\,f\tilde{t}\right). \tag{37}$$

Thus, from equation (34),

$$u \approx \varepsilon F\left[\left(1+\frac{\gamma+1}{2}u\right)t - x\right]. \tag{38}$$

Equation (38) implies that the uniformly valid first–order solution for the nonlinear problem is simply the solution for the corresponding linear problem, with the respective characteristic replaced by the characteristic calculated by including the first–order nonlinearities in the problem. In other words, the solution to the linear problem, when the first–order nonlinearities are included, may still have the right form, but not quite at the right place.

Incidentally, as we saw before (equation (9)), (38) becomes the exact result if one considers *simple* waves for which

$$u + \int a\frac{d\rho}{\rho} \quad \text{or} \quad u - \int a\frac{d\rho}{\rho}$$

is constant for all x.

Nonlinear Resonant Three–Wave Interactions of Sound Waves

Sound waves are nondispersive in the linear regime, so the frequency and wave vector matching conditions (see (45) below) imply that resonant wave interaction in a triad of sound waves occurs when the wavevectors are collinear (Shivamoggi).

Consider again unidirectional propagation of sound waves in an ideal fluid. The equations governing this situation are equations (21)–(23). Putting,

$$\rho = \rho_0\left(1+\hat{\rho}\right)$$

and using the relation

$$a = a_0 + \frac{\gamma-1}{2}u$$

equations (21) and (22) may be rewritten as

$$\frac{\partial\hat{\rho}}{\partial t} + \frac{\partial u}{\partial x} = -u\frac{\partial\hat{\rho}}{\partial x} - \hat{\rho}\frac{\partial u}{\partial x}, \tag{25}$$

$$\frac{\partial u}{\partial t} + a_0^2\frac{\partial\hat{\rho}}{\partial x} = -u\frac{\partial u}{\partial x} + a_0^2\frac{\left[\hat{\rho} - (\gamma-1)\dfrac{u}{a_0}\right]}{1+\hat{\rho}}\frac{\partial\hat{\rho}}{\partial x}. \tag{39}$$

Observe that, in equations (25) and (39), the left–hand sides represent the linear problem and the right–hand sides contain the nonlinearities that give rise to the interactions among the sound waves.

Consider the waves of the form

$$u(x,t) \text{ and } \hat{\rho}(x,t) \sim e^{i(kx-\omega t)}, \tag{40}$$

where $\omega/k = c_0$. Let us use the method of Section 2.6 to treat the nonlinear three–wave resonant interactions of sound waves. In this method, one introduces an auxiliary variable

$$a = u + \frac{\omega}{k}\hat{\rho}, \tag{41}$$

which turns out to be a normal mode of the linearized problem associated with equations (25) and (39). This may be verified by noting that the linear parts in equations (25) and (39) leads to

$$\frac{\partial a}{\partial t} + i\omega a = 0. \tag{42}$$

The nonlinear analysis of the wave–wave interactions, as will be seen below, becomes very convenient when formulated in terms of this auxiliary variable a. When the nonlinear terms are included, one obtains from equations (25) and (39)

$$\frac{\partial a}{\partial t} + i\omega a = -u\frac{\partial u}{\partial x} + \frac{\omega^2}{k^2}\left[\hat{\rho} - (\gamma - 1)\frac{u}{c_0}\right](1-\hat{\rho})\frac{\partial \hat{\rho}}{\partial x} + \frac{\omega}{k}\left(-u\frac{\partial \hat{\rho}}{\partial x} - \hat{\rho}\frac{\partial u}{\partial x}\right). \tag{43}$$

Let us now consider two sound waves of the form $e^{i(k_3x-\omega_3t)}$ and $e^{i(k_2x-\omega_2t)}$ propagating in the x–direction with

$$\frac{\omega_3}{k_3} = \frac{\omega_2}{k_2} = c_0. \tag{44}$$

Due to nonlinear interaction between these two waves, let another sound wave of the form $e^{i(k_1x-\omega_1t)}$, propagating in the x–direction, be excited such that

$$\omega_3 - \omega_2 = \omega_1, \quad k_3 - k_2 = k_1, \tag{45}$$

where $\omega_1/k_1 = c_0$.

If one puts

$$a_j(x,t) = \tilde{a}_j(t)e^{i(k_jx-\omega_jt)} + \tilde{a}_j^*(t)e^{-i(k_jx-\omega_jt)}, \tag{46}$$

then the nonlinear terms on the right hand side in equation (43), which represent coupling of these sound waves, lead to slow variations with time in the amplitudes $\tilde{a}_j(t)$.

Now, note that we have from the linearized problem associated with equations (25) and (39),

$$u = \frac{a}{2}, \quad \hat{\rho} = \frac{k}{2\omega}a. \tag{47}$$

Using (47) on the right hand side in equation (43) and keeping only the resonant terms (according to (45)) thereof, we obtain from this equation

$$\frac{\partial \tilde{a}_3}{\partial t} = \frac{i/4}{\omega_1\omega_2 k_3}\left[\omega_3 k_2(\omega_3 k_1 - \omega_1 k_3) - \omega_2 k_3(\omega_3 k_1 + \omega_1 k_3)\right.$$
$$\left. -(\gamma-1)\omega_3(\omega_1 k_2^2 + \omega_2 k_1^2)\right]\tilde{a}_1\tilde{a}_2, \tag{48}$$

$$\frac{\partial \tilde{a}_2}{\partial t} = \frac{-i/4}{\omega_3\omega_1 k_2}\left[\omega_2 k_1(\omega_2 k_3 - \omega_3 k_2) - \omega_1 k_2(\omega_2 k_3 + \omega_3 k_2)\right.$$
$$\left. -(\gamma-1)\omega_2(\omega_3 k_1^2 + \omega_1 k_3^2)\right]\tilde{a}_3\tilde{a}_1^*, \tag{49}$$

$$\frac{\partial \tilde{a}_1}{\partial t} = \frac{-i/4}{\omega_2\omega_3 k_1}\left[\omega_1 k_3(\omega_1 k_2 - \omega_2 k_1) - \omega_3 k_1(\omega_1 k_2 + \omega_2 k_1)\right.$$
$$\left. -(\gamma-1)\omega_1(\omega_2 k_3^2 + \omega_3 k_2^2)\right]\tilde{a}_3\tilde{a}_2^*. \tag{50}$$

When we express $\tilde{a}_j$ in terms of $\tilde{\hat{\rho}}_j$, recall (44), and put,

$$\tilde{\hat{\rho}}_j(t) = \left(i\frac{2}{\gamma+1}\sqrt{\omega_j}\right)\tilde{\phi}_j(\hat{t}), \quad \hat{t} = \sqrt{\omega_1\omega_2\omega_3}\,t, \tag{51}$$

equations (48)–(50) become

$$\frac{\partial \tilde{\phi}_3}{\partial \hat{t}} = \tilde{\phi}_1\tilde{\phi}_2, \tag{52}$$

$$\frac{\partial \tilde{\phi}_2}{\partial \hat{t}} = -\tilde{\phi}_3\tilde{\phi}_1^*, \tag{53}$$

$$\frac{\partial \tilde{\phi}_1}{\partial \hat{t}} = -\tilde{\phi}_3\tilde{\phi}_2^*. \tag{54}$$

Equations (52)–(54) show that the three sound waves have positive energy, which means that the wave interactions under consideration are nonexplosive.

One obtains from equations (52)–(54) the following Manley–Rowe relations:

$$\frac{d}{d\hat{t}}\left(\left|\tilde{\phi}_1\right|^2 + \left|\tilde{\phi}_3\right|^2\right) = 0, \tag{55}$$

$$\frac{d}{d\hat{t}}\left(\left|\tilde{\phi}_2\right|^2 + \left|\tilde{\phi}_3\right|^2\right) = 0, \tag{56}$$

$$\frac{d}{d\hat{t}}\left(\left|\tilde{\phi}_1\right|^2 - \left|\tilde{\phi}_2\right|^2\right) = 0. \tag{57}$$

Equations (55)–(57) imply a periodic exchange of energy among the three sound waves $\tilde{\phi}_1, \tilde{\phi}_2$ and $\tilde{\phi}_3$. Consider, for instance, a case wherein only the low-frequency modes $\tilde{\phi}_1$ and $\tilde{\phi}_2$ are present initially and the high-frequency mode $\tilde{\phi}_3$ is absent, i.e.,

$$\hat{t} = \hat{t}_0: \quad \tilde{\phi}_{1,2} = \tilde{\phi}_{1,2}^{(0)}, \ \tilde{\phi}_3 = 0. \tag{58}$$

Suppose $\left|\tilde{\phi}_2^{(0)}\right|^2 < \left|\tilde{\phi}_1^{(0)}\right|^2$. Equations (55) and (56) then show that initially the energy in mode $\tilde{\phi}_3$ increases at the expense of both modes $\tilde{\phi}_1$ and $\tilde{\phi}_2$. Eventually, the energy in mode $\tilde{\phi}_2$ vanishes $\left(\text{since } \left|\tilde{\phi}_2^{(0)}\right|^2 < \left|\tilde{\phi}_1^{(0)}\right|^2\right)$. Then the direction of energy transfer is reversed: Modes $\tilde{\phi}_1$ and $\tilde{\phi}_2$ now increase at the expense of the mode $\tilde{\phi}_3$ until the initial state is attained again, and this sequence of energy transfer repeats itself.

Explicit solutions of equations (52)–(54), for the initial condition (58), can be given as follows:

$$\left.\begin{aligned} \tilde{\phi}_3 &= \tilde{\phi}_2^{(0)} \operatorname{sn}(\xi|m), \\ \tilde{\phi}_2 &= \tilde{\phi}_2^{(0)} \operatorname{cn}(\xi|m), \\ \tilde{\phi}_1 &= \tilde{\phi}_1^{(0)} \operatorname{dn}(\xi|m), \end{aligned}\right\} \tag{59}$$

where sn, cn, and dn are Jacobian elliptic functions with real parameter, and

$$\left.\begin{aligned} \xi &= \left|\tilde{\phi}_1^{(0)}\right|(\hat{t}-\hat{t}_0), \\ m &= \left|\frac{\tilde{\phi}_2^{(0)}}{\tilde{\phi}_1^{(0)}}\right|^2 < 1; \end{aligned}\right\} \tag{60}$$

m may be regarded as a measure of the extent to which resonant partners participate in the interaction. In particular, $m < 1$ implies that the mode $\tilde{\phi}_2$ is decreasing at a rate faster than the mode $\tilde{\phi}_1$. Using the solutions (59) and (60), the period of the resonant energy exchange among the three modes $\tilde{\phi}_1, \tilde{\phi}_2$, and $\tilde{\phi}_3$ is given by

$$\hat{T} = \frac{2}{\left|\tilde{\phi}_1^{(0)}\right|} K(m), \tag{61}$$

where $K(m)$ is the complete elliptic integral of the first kind.

The case $\omega_1 = \omega_2 = \omega_3/2$ and $\tilde{\phi}_1^{(0)} = \tilde{\phi}_2^{(0)}$ constitutes the degenerate case of the triad resonances for which two members of the triad are identical, with the closure being their second harmonic. Since $m = 1$ for this case and we have

$$m = 1 : K(m) \sim \ln \frac{4}{\sqrt{1-m}} \approx \infty, \tag{62}$$

the period of the energy transfer from (61) is

$$\hat{T} \Rightarrow \infty. \tag{63}$$

The resonant interactions now take on an asymptotic character, and (26) then becomes

$$\left.\begin{aligned}\tilde{\phi}_3 &= \tilde{\phi}_1^{(0)} \tanh \xi, \\ \tilde{\phi}_2 &= \tilde{\phi}_1 = \tilde{\phi}_1^{(0)} \operatorname{sech} \xi.\end{aligned}\right\} \tag{64}$$

Equations (52)–(54) also indicate the development of a nonlinear saturation state under certain conditions. In order to see this, we first derive, from equations (52)–(54), the following equations:

$$\frac{\partial^2 \tilde{\phi}_3}{\partial \hat{t}^2} + \left(\left| \tilde{\phi}_2 \right|^2 + \left| \tilde{\phi}_1 \right|^2 \right) \tilde{\phi}_3 = 0, \tag{65}$$

$$\frac{\partial^2 \tilde{\phi}_2}{\partial \hat{t}^2} + \left(\left| \tilde{\phi}_1 \right|^2 - \left| \tilde{\phi}_3 \right|^2 \right) \tilde{\phi}_2 = 0, \tag{66}$$

$$\frac{\partial^2 \tilde{\phi}_1}{\partial \hat{t}^2} + \left(\left| \tilde{\phi}_2 \right|^2 - \left| \tilde{\phi}_3 \right|^2 \right) \tilde{\phi}_1 = 0. \tag{67}$$

Consider now the case wherein the high–frequency mode $\tilde{\phi}_3$ is initially much stronger than the low–frequency modes $\tilde{\phi}_1$ and $\tilde{\phi}_2$, i.e.,

$$\hat{t} = \hat{t}_0 : \quad \left| \tilde{\phi}_3 \right| >> \left| \tilde{\phi}_1 \right| \text{ and } \left| \tilde{\phi}_2 \right|. \tag{68}$$

One may then take $\tilde{\phi}_3$ to be constant for small times subsequent to $\hat{t} = \hat{t}_0$ in the evolution of $\tilde{\phi}_1$ and $\tilde{\phi}_2$. If we further assume

$$\tilde{\phi}_1 \text{ and } \tilde{\phi}_2 \sim e^{\gamma \hat{t}} \tag{69}$$

we obtain from equations (66) and (67)

$$\gamma = \left| \tilde{\phi}_3 \right|. \tag{70}$$

Equations (69) and (70) show that, for small times following $\hat{t} = \hat{t}_0$, the high–frequency mode $\tilde{\phi}_3$ undergoes a decay instability into two low–frequency modes $\tilde{\phi}_1$ and $\tilde{\phi}_2$ which grow exponentially until the nonlinear regime is reached where a saturation state develops. In this nonlinear saturation state, the amplitudes of the three modes are

$$\left| \tilde{\phi}_1 \right| = \left| \tilde{\phi}_2 \right| = \left| \tilde{\phi}_3 \right|. \tag{71}$$

Thus, nonlinear resonant three–wave interactions of sound waves exhibits two different evolution scenarios depending on the particular set of initial conditions:

(1) a periodic exchange of energy among three sound waves (an exception occurring for the degenerate case with two members of the triad identical, for which the period of the energy exchange becomes infinite);

(2) a decay instability of the high-frequency mode into two low-frequency modes followed by a nonlinear saturation state.

Burgers' Equation

A real gas cannot sustain an actual discontinuity mentioned above, so that the latter is only an idealization of the sharp gradients in the flow variables that occur in reality in a shock wave. Consequent to these flow gradients, various transport processes such as those due to viscosity and heat conductivity show up inside the shock. The evolution of the flow structure within the shock when viscosity and heat conductivity are included can in fact be satisfactorily described by an approximate model represented by Burgers' equation. We will now divert from the inviscid fluid model concerned with in this chapter to give here a discussion of the Burgers' equation, since this is otherwise the most appropriate place for this topic.

Let us consider here weak shock waves so that flow of interest is a perturbation on a uniform sonic flow of velocity a^*. The equations governing the flow are those describing the conservation of mass, momentum, and energy

$$\frac{D\rho}{Dt}+\rho\frac{\partial u}{\partial x}=0, \tag{72}$$

$$\rho\frac{Du}{Dt}=-\frac{\partial p}{\partial x}-\frac{4}{3}\mu\frac{\partial^2 u}{\partial x^2}, \tag{73}$$

$$\frac{1}{\gamma-1}\frac{Dp}{Dt}-\frac{\gamma p/\rho}{\gamma-1}\frac{D\rho}{Dt}=\frac{4}{3}\mu\left(\frac{\partial u}{\partial x}\right)^2+K\frac{\partial^2 T}{\partial x^2}, \tag{74}$$

where μ is the coefficient of viscosity, and K is the coefficient of heat conductivity; μ and K are taken to be constants, and

$$\frac{D}{Dt}\equiv\frac{\partial}{\partial t}+u\frac{\partial}{\partial x}.$$

Using equation (72), one can rewrite equation (74) as

$$\frac{Dp}{Dt}+a^2\rho\frac{\partial u}{\partial x}-(\gamma-1)K\frac{\partial^2 T}{\partial x^2}-\frac{4}{3}\mu(\gamma-1)\left(\frac{\partial u}{\partial x}\right)^2=0. \tag{75}$$

When one uses the approximate relations

$$\begin{aligned} dp &= -\rho u du, \\ C_p dT &= -u du \end{aligned} \tag{76}$$

and drops $(\partial u/\partial x)^2$ in comparison with $\left[u\left(\partial^2 u/\partial x^2\right)\right]$, equation (75) gives

$$-\rho u\frac{\partial u}{\partial t}+u\frac{\partial p}{\partial x}+\rho a^2\frac{\partial u}{\partial x}+\frac{K}{C_p}(\gamma-1)u\frac{\partial^2 u}{\partial x^2}=0. \tag{77}$$

Now, when one multiplies through by u, equation (73) gives

$$\rho u \frac{\partial u}{\partial t} + \rho u^2 \frac{\partial u}{\partial x} + u \frac{\partial p}{\partial x} - \frac{4}{3} \mu u \frac{\partial^2 u}{\partial x^2} = 0. \tag{78}$$

One obtains from equations (77) and (78)

$$2\rho u \frac{\partial u}{\partial t} + \rho \left(u^2 - a^2\right) \frac{\partial u}{\partial x} - \frac{4}{3} \mu u \left(1 + \frac{\gamma - 1}{\mathrm{Pr}}\right) \frac{\partial^2 u}{\partial x^2} = 0, \tag{79}$$

where

$$\mathrm{Pr} \equiv \frac{\mu C_p}{K}.$$

For weak shocks, one may write (see Section 3.2)

$$u^2 - a^2 \approx (\gamma + 1) u \left(u - a^*\right),$$

so that equation (79) becomes

$$\frac{\partial u}{\partial t} + \left(\frac{\gamma + 1}{2}\right)\left(u - a^*\right) \frac{\partial u}{\partial x} = \nu \frac{\partial^2 u}{\partial x^2}, \tag{80}$$

where

$$\nu \equiv \frac{2}{3} \frac{\mu}{\rho} \left(1 + \frac{\gamma - 1}{\mathrm{Pr}}\right).$$

When one puts

$$W \equiv \frac{u}{2(\gamma + 1)}, \qquad X = x - \left(\frac{\gamma + 1}{2}\right) a^* t, \tag{81}$$

equation (80) becomes

$$\frac{\partial W}{\partial t} + W \frac{\partial W}{\partial X} = \nu \frac{\partial^2 W}{\partial X^2}, \tag{82}$$

which is Burgers' equation. Burgers' equation is the simplest equation combining the nonlinear propagation effects and the dissipative diffusion effects.

An explicit solution to Burgers' equation can in fact be found, thanks to the Hopf–Cole transformation. On putting

$$W = -2\nu \frac{\psi_x}{\psi}, \tag{83}$$

one finds that equation (82) gives the heat equation:

$$\psi_t = \nu \psi_{xx}. \tag{84}$$

Let us prescribe an initial condition

$$t = 0: \quad W = F(X); \tag{85}$$

and from (83), this gives

$$t=0: \quad \psi=\Psi(X)=\exp\left(-\frac{1}{2\nu}\int_0^x F(\eta)\,d\eta\right). \tag{86}$$

One may now solve equation (84), using (86), to obtain

$$\psi(x,t)=\frac{1}{\sqrt{4\pi\nu t}}\int_{-\infty}^{\infty}\Psi(\eta)\exp\left[-\frac{(X-\eta)^2}{4\nu t}\right]d\eta. \tag{87}$$

Thus,

$$W(X,t)=\frac{\displaystyle\int_{-\infty}^{\infty}\left(\frac{X-\eta}{t}\right)\exp\left(-\frac{G}{2\nu}\right)d\eta}{\displaystyle\int_{-\infty}^{\infty}\exp\left(-\frac{G}{2\nu}\right)d\eta}, \tag{88}$$

where

$$G(\eta)=\int_{0^+}^{\eta}F(\eta')\,d\eta'+\frac{(X-\eta)^2}{2t}. \tag{89}$$

As an example, let us consider a single–hump solution, $F(X)=A\delta(X)$. Then, one obtains

$$G(\eta)=\begin{cases}\dfrac{(X-\eta)^2}{2t}, & \eta>0,\\[2ex] \dfrac{(X-\eta)^2}{2t}-A, & \eta<0,\end{cases} \tag{90}$$

so that (88) gives

$$W=\sqrt{\frac{\nu}{t}}\,\frac{\left(e^R-1\right)\exp\left(-\dfrac{X^2}{4\nu t}\right)}{\sqrt{\pi}+\left(e^R-1\right)\displaystyle\int_{X/\sqrt{4\nu t}}^{\infty}e^{-\zeta^2}d\zeta}, \tag{91}$$

where

$$R\equiv\frac{A}{2\nu}.$$

Note, from (91), that

$$R\ll 1: \quad W\approx\sqrt{\frac{\nu}{\pi t}}\,R\exp\left(-\frac{X^2}{4\nu t}\right). \tag{92}$$

In order to investigate the limit $R\gg 1$, first introduce

$$Z\equiv\frac{X}{\sqrt{2At}} \tag{93}$$

so that (91) becomes

$$W = \sqrt{\frac{2A}{t}}\,\frac{\left(e^R-1\right)}{2\sqrt{R}}\,\frac{e^{-Z^2R}}{\sqrt{\pi}+\left(e^R-1\right)\int_{Z\sqrt{R}}^{\infty} e^{-\zeta^2}d\zeta}. \tag{94}$$

Now, note, from (94), that

$$\begin{aligned} R \gg 1:\quad & Z<0:\ W \sim \sqrt{\frac{2A}{t}}\,\frac{1}{\sqrt{R}}, \\ & Z>0:\ W \sim \sqrt{\frac{2A}{t}}\,\frac{Z}{1+2Z\sqrt{\pi R}\,e^{R\left(Z^2-1\right)}}, \end{aligned} \tag{95}$$

where we have used the results

$$\int_{-\infty}^{\infty} e^{-\zeta^2}d\zeta = \sqrt{\pi}, \quad \int_{\eta}^{\infty} e^{-\zeta^2}d\zeta \approx \frac{e^{-\eta^2}}{2\eta} \quad \text{as} \quad \eta \Rightarrow \infty.$$

Thus, for $R \gg 1$, we have

$$\begin{aligned} 0<Z<1:\quad & W \sim \sqrt{\frac{2A}{t}}\,Z \\ Z>1:\quad & W \Rightarrow 0 \end{aligned} \tag{96a}$$

or

$$W \sim \begin{cases} X/t, & 0<X<\sqrt{2At}, \\ 0, & \text{outside}, \end{cases} \tag{96b}$$

which represents a shock at $X=\sqrt{2At}$ with velocity $V=\sqrt{A/2t}$. Observe that the shock amplitude at large times is independent of the source strength signifying that the saturation has been reached.

Let us next find a stationary solution of equation (82) with

$$W(X,t) = W(\xi), \tag{97}$$

where

$$\xi \equiv x - Ut. \tag{98}$$

Equation (82) now becomes

$$-UW_{\xi} + WW_{\xi} = \nu W_{\xi\xi}. \tag{99}$$

When one integrates once, equation (99) gives

$$\frac{1}{2}W^2 - UW + C = \nu W_{\xi}, \tag{100}$$

where C is an arbitrary constant.

Let us impose infinity conditions

$$\xi \Rightarrow \pm\infty: \quad W \Rightarrow W_{1,2}. \tag{101}$$

When one uses equation (101), equation (100) gives

$$U = \frac{1}{2}(W_1 + W_2), \quad C = \frac{1}{2} W_1 W_2. \tag{102}$$

When one uses equation (102), equation (100) becomes

$$(W - W_1)(W_2 - W) = -2\nu W_\xi, \tag{103}$$

from which

$$\frac{\xi}{\nu} = \frac{2}{W_2 - W_1} \ln \frac{W_2 - W}{W - W_1} \tag{104a}$$

or

$$W = W_1 + \frac{W_2 - W_1}{1 + \exp\left(\dfrac{W_2 - W_1}{2\nu}\right)(X - Ut)}, \tag{104b}$$

which represents a shock wave connecting two different uniform states

$$W(X \Rightarrow \mp\infty) \Rightarrow W_1, W_2.$$

Thus, the diffusive term on the right hand side in equation (82) prevents the development of steep wave profiles and tends to spread the sharp discontinuities into smooth profiles.

EXERCISES

1. A source of finite duration produces a wavemotion only in the plane case. Show that in the spherical case, the time–integral of the wave–amplitude at any fixed location vanishes.

2. Consider the waves produced by a piston moving, for time $t > 0$, with a constant velocity u_0 out of a semi–infinite tube containing gas at rest at $t = 0$. Show that the ensuing flow consists of two uniform regions in the (x,t)–plane, joined by an expansion fan for $-a_0 t < x < \left((\gamma+1)/2\ u - a_0\right)t$.

   Further, deduce that the latter region has a similarity solution, depending only on the variable x/t, and is given by

$$u = \frac{2}{\gamma+1}\left(a_0 + \frac{x}{t}\right), \quad a = \frac{2a_0}{\gamma+1} - \left(\frac{\gamma-1}{\gamma+1}\right)\frac{x}{t}.$$

3. Consider the piston problem, in which a piston at rest begins at time $t = 0$ to move smoothly with a given displacement $X(t)$, so that one has the boundary condition

$$x = X(t): \quad u = X'(t)h(t).$$

Show that the solution of this problem is given by

$$u = X'(\phi)h\left(t \mp \frac{x}{a_0}\right),$$

where

$$\phi = t - \frac{x - X(\phi)}{\beta X'(\phi) \pm a_0}, \quad \beta = \frac{\gamma + 1}{2}.$$

Note that the parameter ϕ represents the time at which a given signal left the piston.

3.8. Applications to Aerodynamics

Thin Airfoil Theory

Thin Airfoil in a Linearized Supersonic Flows

If the airfoil is thin and at a small angle of attack, one may make use of the small–perturbation theory. With the assumption of small disturbances, the vorticity generated by any shock wave standing on the airfoil will be small, and if, in addition, the flow around the airfoil is assumed to be attached, the vorticity generated by viscous effects in the boundary layer will be confined to the latter region, so the flow may be assumed to be irrotational. From equation (40), Section 3.5, the general solution to the linearized potential–flow equation is of the form

$$\phi(x, y) = f(x - \lambda y) + g(x + \lambda y), \tag{1}$$

where $\lambda = \sqrt{M^2 - 1}$. Since the disturbances are carried only along downstream–running Mach lines (see Figure 3.24), one has for the airfoil

$$\phi = \begin{cases} f(x - \lambda y), & y > 0, \\ g(x + \lambda y), & y < 0. \end{cases} \tag{2}$$

The boundary conditions at the airfoil surface $y = F(x)$ are

$$\begin{aligned} y = 0^+: \quad & \phi_y = -\lambda f'(x) = U_\infty \frac{dF_u}{dx}, \\ y = 0^-: \quad & \phi_y = \lambda g'(x) = U_\infty \frac{dF_l}{dx}, \end{aligned} \tag{3}$$

where the subscripts u and l denote the upper surface and the lower surface of the airfoil, and U_∞ is the free–stream velocity.

Thus, the pressure on the airfoil is then given by

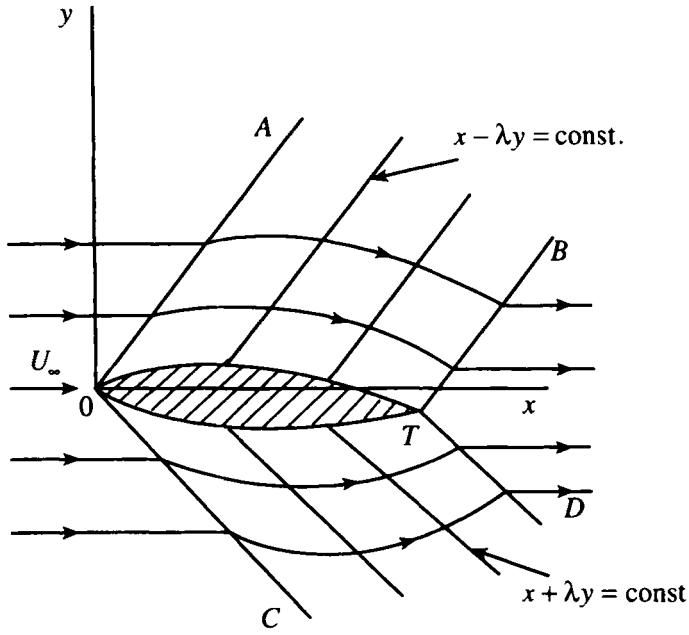

Figure 3.24. Supersonic flow past an airfoil.

$$C_p=\frac{p-p_\infty}{\frac{1}{2}\rho_\infty U_\infty^2}=-\frac{2\phi_x}{U_\infty}=\begin{cases}-\dfrac{2f'(x)}{U_\infty}, & y>0,\\ \dfrac{2g'(x)}{U_\infty}, & y<0.\end{cases} \tag{4}$$

Now note that the potential ϕ is constant outside the wavezone $0<x-\lambda y<c$ (c being the chordlength of the airfoil), and from (4) there is a jump of pressure, for example, across $x=\lambda y$ if $F'(0)\neq 0$. This jump is a linearized version of a shock wave.

Further, equation (3) implies that

$$\phi_y=U_\infty F_u'(x-\lambda y) \quad \text{for } y>0,\ 0<x-\lambda y<c$$

so that in the wavezone $0<x-\lambda y<c$, the slope of the streamlines (ϕ_y/U_∞ in the linearized theory) is $F_u'(x-\lambda y)$, which is constant along lines $x-\lambda y=\text{const}$. Thus, inside the wavezone $0<x-\lambda y<c$, each streamline has the same shape as that of the airfoil profile.

When one uses (3), (4) becomes

$$C_p = \begin{cases} \dfrac{2\left(\dfrac{dF_u}{dx}\right)}{\sqrt{M_\infty^2 - 1}}, & y > 0, \\ -\dfrac{2\left(\dfrac{dF_l}{dx}\right)}{\sqrt{M_\infty^2 - 1}}, & y < 0. \end{cases} \tag{5}$$

If the airfoil is at an angle of attack α, then one obtains

$$C_p = \begin{cases} \dfrac{2\left(\dfrac{dF_u}{dx} - \alpha\right)}{\sqrt{M_\infty^2 - 1}}, & y > 0, \\ \dfrac{2\left(-\dfrac{dF_l}{dx} + \alpha\right)}{\sqrt{M_\infty^2 - 1}}, & y < 0. \end{cases} \tag{6}$$

The lift of the airfoil is given by

$$C_L = \frac{\int_0^c \left(C_{p_u} - C_{p_l}\right) dx}{c} = \frac{4\alpha}{\sqrt{M_\infty^2 - 1}} \tag{7}$$

and the drag of the airfoil is given by

$$C_D = \frac{1/c}{\sqrt{M_\infty^2 - 1}} \left[\int_0^c \left(C_{p_u}\right)\left(\frac{dF_u}{dx} - \alpha\right) dx + \int_0^c \left(C_{p_l}\right)\left(-\frac{dF_l}{dx} + \alpha\right) dx \right]$$

$$= \frac{2}{\sqrt{M_\infty^2 - 1}} \left[\bar{\sigma}_u^2 + \bar{\sigma}_l^2 + 2\alpha^2\right], \tag{8}$$

where

$$\bar{\sigma}_{u,l}^2 = \frac{1}{c} \int_0^c \left(\frac{dF_{u,l}}{dx}\right)^2 dx .$$

Note that sharp corners do not cause any difficulty in supersonic flows. Recall from Section 2.7 that for subsonic flows, on the other hand, the negative pressures at the sharp corners tended to become infinitely large. Further, note that, thanks to the absence of upstream influence in supersonic flows, one does not impose the Kutta condition in supersonic flows, unlike the case with subsonic flows.

Far–Field Behavior of Supersonic Flow Past a Thin Airfoil

Consider a supersonic flow past a thing airfoil. The solution given in (2) is based on the linear equation

$$\phi_{yy} - \lambda^2 \phi_{xx} = 0 .$$

Although the solution of this equation is a valid first approximation at or near the airfoil, it fails at large distances from the airfoil since it predicts disturbances propagating undiminished along the free–stream Mach lines to infinity, whereas in reality the Mach lines are neither straight or parallel, and shock waves arise and decay. The latter is brought about by the cumulative effect of the nonlinear terms in the full potential flow equation.

For the corresponding nonlinear problem (from equations (9) and (30) in Section 3.5), one has

$$\phi_{yy} - \lambda^2 \phi_{xx} = M_\infty^2 \left[\frac{\gamma - 1}{2} \left(2\phi_x + \phi_x^2 + \phi_y^2 \right) \left(\phi_{xx} + \phi_{yy} \right) + \left(2\phi_x + \phi_x^2 \right) \phi_{xx} \right.$$
$$\left. + 2\left(1 + \phi_x \right) \phi_y \phi_{xy} + \phi_y^2 \phi_{yy} \right]. \tag{9}$$

The boundary condition at the airfoil is

$$y = \varepsilon F(x): \quad \frac{\phi_y}{1 + \phi_x} = \varepsilon F'(x), \quad 0 \le x \le c, \quad \varepsilon \ll 1, \tag{10}$$

and at upstream infinity we have

$$\phi(x, y) \Rightarrow 0. \tag{11}$$

It is convenient to transfer the boundary condition (10) from $y = \varepsilon F(x)$ to $y = 0$ by using the following Taylor's expansion

$$\phi(x, \varepsilon F) = \phi(x, 0) + \varepsilon F \phi_y(x, 0) + \frac{1}{2} \varepsilon^2 F^2 \phi_{yy}(x, 0) + \cdots \tag{12}$$

so that (10) gives

$$\frac{\phi_y(x, 0) + \varepsilon F \phi_{yy}(x, 0) + \cdots}{1 + \phi_x(x, 0) + \cdots} = \varepsilon F(x). \tag{13}$$

Seek solutions to (9), (11), and (13) of the form

$$\phi = \varepsilon \phi_1 + \varepsilon^2 \phi_2 + \cdots, \tag{14}$$

so that one obtains the following equations upon equating coefficients of equal powers of ε to zero.

$O(\varepsilon)$:

$$\phi_{1yy} - \lambda^2 \phi_{1xx} = 0 \tag{15}$$

$$y = 0: \quad \phi_{1y} = F'(x), \quad 0 \le x \le c, \tag{16}$$

$$\text{upstream:} \quad \phi_1 \Rightarrow 0; \tag{17}$$

$O(\varepsilon^2)$:

$$\phi_{2yy} - \lambda^2 \phi_{2xx} = M_\infty^2 \left[(\gamma + 1) \phi_{1x} \phi_{1xx} + (\gamma - 1) \phi_{1x} \phi_{1yy} + 2\phi_{1y} \phi_{1xy} \right], \tag{18}$$

$$y = 0: \quad \phi_{2y} = \phi_{1x} F'(x) - \phi_{1yy} F(x), \quad 0 \le x \le c, \tag{19}$$

$$\text{upsteam:} \quad \phi_2 \Rightarrow 0. \tag{20}$$

Equations (15)–(17) give

$$\phi_1(x,y) = -\frac{1}{\lambda} F(x-\lambda y). \tag{21}$$

When one uses equation (21), equation (18) becomes

$$\phi_{2yy} - \lambda^2 \phi_{2xx} = \frac{M_\infty^4(\gamma+1)}{\lambda^2} F'(x-\lambda y) F''(x-\lambda y). \tag{22}$$

Put

$$\xi = x - \lambda y, \qquad \eta = x + \lambda y \tag{23}$$

so that equation (23) becomes

$$\frac{\partial^2 \phi_2}{\partial \xi \partial \eta} = -\frac{M_\infty^4(\gamma+1)}{4\lambda^2} F'(\xi) F''(\xi), \tag{24}$$

from which

$$\phi_2 = -\frac{M_\infty^4(\gamma+1)}{8\lambda^2} \left[f'(\xi)\right]^2 \eta + G(\xi). \tag{25}$$

When one uses (25), (19) gives

$$G'(\xi) = \frac{M_\infty^2(\gamma+1)}{4\lambda^4} \xi F'F'' + \frac{1}{\lambda^2}\left[1 - \frac{M_\infty^4(\gamma+1)}{8\lambda^2}\right] F'^2 - F'F''. \tag{26}$$

Using (14), (21), (25), and (26), one obtains

$$\frac{u}{U_\infty} = \frac{\phi_x}{U_\infty} = 1 - \varepsilon \frac{F'(\xi)}{\lambda} + \varepsilon^2 \left[\frac{1}{\lambda^2}\left(1 - \frac{\gamma+1}{4}\frac{M_\infty^2}{\lambda^2}\right)\left\{F'(\xi)\right\}^2 - \frac{\gamma+1}{2}\frac{M_\infty^4}{\lambda^3} yF'(\xi)F''(\xi) - F(\xi)F''(\xi)\right] + 0(\varepsilon^3). \tag{27}$$

Observe that (27) is not uniformly valid and that it becomes inaccurate in the far field.

In order to remove this nonuniformity, let us use Lighthill's method of strained coordinates in a modified form due to Pritulo. Thus, set

$$\xi = \xi_0 + \varepsilon \xi_1 + 0(\varepsilon^2) \tag{28}$$

so that (27) can be written as

$$\frac{u}{U_\infty} = 1 - \varepsilon \frac{F'(\xi_0)}{\lambda} + \varepsilon^2 \left[\frac{1}{\lambda^2}\left(1 - \frac{\gamma+1}{4}\frac{M_\infty^2}{\lambda^2}\right)\left\{F'(\xi_0)\right\}^2 - \left\{\frac{\gamma+1}{2}\frac{M_\infty^4}{\lambda^2} yF'(\xi_0) + \xi_1\right\}\frac{F''(\xi_0)}{\lambda} - F(\xi_0)F''(\xi_0)\right] + 0(\varepsilon^3); \tag{29}$$

thus the nonuniform term can be eliminated by simply choosing

$$\xi_1 = -\frac{\gamma+1}{2}\frac{M_\infty^4}{\lambda^2} yF'(\xi_0). \tag{30}$$

Then, to first approximation, (29) gives

$$\frac{u}{U} = 1 - \varepsilon \frac{F'(\xi_0)}{\lambda} + \cdots, \tag{31}$$

where

$$\xi_0 = \xi + \varepsilon\frac{\gamma+1}{2}\frac{M_\infty^4}{\lambda^2} yF'(\xi) + \cdots. \tag{32}$$

Thus, as we saw in Section 3.7, the uniformly valid first–order solution for the nonlinear problem is simply the solution for the corresponding linear problem, with the respective characteristic replaced by the characteristic calculated by including the first–order nonlinearities in the problem.

Thin Airfoil in Transonic Flows

The term *transonic* refers to flows in which the free–stream Mach number M_∞ is not too far removed from 1. The need for a special theory for transonic flows arises from the fact that the foregoing linearized treatment (that was valid for supersonic flows) breaks down when applied to transonic flows. The difficulties is solving the transonic flow–field arise from the facts that the governing partial differential equation turns out to be nonlinear and of mixed elliptic–hyperbolic type.

In order to appreciate the latter situation physically, consider the flow pattern past a symmetrical airfoil as the free–stream Mach number M is increased from a subsonic value. When the free–stream Mach number M reaches a critical Mach number M^* the maximum local Mach number in the flow near the airfoil becomes unity. For $M > M^*$, a supersonic region appears on the airfoil which is then terminated by a shock wave across which the flow is retarded back to a subsonic one. As M increases further, the shock wave moves aft and the size of the supersonic region as well as the strength of the shock wave increase (see Figure 3.25).

Shock waves in transonic flows are, however, necessarily weak. Along any streamline, recall, from Section 3.3, that the change in entropy through a normal shock is proportional to $\left(M_\infty^2 - 1\right)^3$. This means that outside the shock waves and boundary layers, the flow can be considered irrotational.

For simplicity, let us consider only airfoils that are symmetric about the x–axis. For a two–dimensional potential flow (see Section 3.5), one has

$$\left(a^2 - \Phi_x^2\right)\Phi_{xx} + \left(a^2 - \Phi_y^2\right)\Phi_{yy} - 2\Phi_{xy}\Phi_x\Phi_y = 0, \tag{33}$$

$$\frac{a^2}{\gamma-1} + \frac{1}{2}\left(\Phi_x^2 + \Phi_y^2\right) = \frac{a_\infty^2}{\gamma-1} + \frac{U_\infty^2}{2}, \tag{34}$$

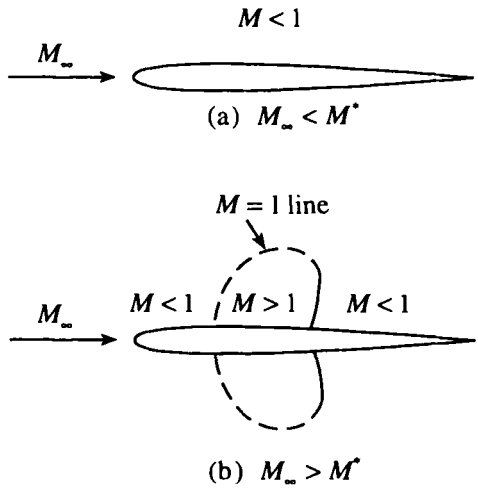

Figure 3.25. Influence of the free–stream Mach number on the flow past a symmetrical airfoil.

$$y = \delta F(x) : \frac{\Phi_y}{\Phi_x} = \delta F'(x), \tag{35}$$

$$\Phi \Rightarrow Ux \quad \text{at upstream infinity,} \tag{36}$$

where δ is a small parameter characterizing the thin nature of the airfoil.

In order to treat cases with $M_\infty \approx 1$, put

$$M_\infty^2 = 1 + \alpha\nu(\delta), \tag{37}$$

where

$$\lim_{\delta \Rightarrow 0} \nu(\delta) \Rightarrow 0$$

and α is going to be made $0(1)$ in a distinguished limit. Seek a solution of the form

$$\Phi(x, y; M_\infty, \delta) = U_\infty\left[x + \varepsilon(\delta)\phi(x, \tilde{y}, \alpha) + \cdots\right], \tag{38}$$

where

$$\tilde{y} = \lambda(\delta)\, y, \qquad \lambda = \sqrt{M_\infty^2 - 1},$$

$$\lim_{\delta \Rightarrow 0} \varepsilon(\delta), \qquad \lambda(\delta) \Rightarrow 0.$$

The spatial scalings in (38) are motivated by the fact that, in the limit $M_\infty \Rightarrow 1$, the linearized supersonic–flow theory (see Section 3.5) indicates that the disturbances are propagated practically undiminished to infinity in the y–direction, but are restricted to a small width in the x–direction.

Using (37) and (38), equation (33) becomes

$$-\nu\varepsilon\alpha\phi_{xx} + \varepsilon\lambda^2\phi_{\tilde{y}\tilde{y}} = (\gamma+1)\varepsilon^2\phi_x\phi_{xx} + \text{higher-order terms.} \tag{39}$$

A distinguished limit occurs if

$$\varepsilon\lambda^2 = \varepsilon\nu = \varepsilon^2$$

or

$$\lambda = \sqrt{\varepsilon}, \quad \nu = \varepsilon. \tag{40}$$

Then, equation (15) gives

$$\left[\alpha + (\gamma+1)\phi_x\right]\phi_{xx} - \phi_{\tilde{y}\tilde{y}} = 0. \tag{41}$$

This equation is expected to contain the essential features of mixed subsonic–supersonic flow with embedded shock waves.

Next, using (38), (35) becomes

$$\tilde{y} = \lambda\delta F(x): \quad \varepsilon^{3/2}\phi_{\tilde{y}} = \delta F'(x),$$

from which

$$\varepsilon = \delta^{2/3}. \tag{42}$$

When one uses (40) and (42), (37) gives

$$\alpha = \frac{M_\infty^2 - 1}{\delta^{2/3}}, \tag{43}$$

which is the so–called transonic similarity parameter.

The parabolic nature of the transonic–flow equation (41) allows no upstream influence, so only the region $0 \le x \le c$ is of interest. Furthermore, it means that the flow in the region $y \ge 0$ is independent of that for $y \le 0$.

The nonlinear nature of equation (41) makes it very difficult to solve it exactly. As a first approximation, one may propose a linearized model for transonic flows. But then the calculated flow does not exhibit the mixed–flow character that is essential of a transonic flow, because the differential equation so obtained by assuming ϕ_{xx} to be constant in the nonlinear term is everywhere parabolic when $M_\infty = 1$ rather than being so only on the sonic line. Some steps have been taken in the literature to improve upon this method, but they are not a lot more rigorous, though more successful.

Slender Bodies of Revolution

Let us adopt cylindrical coordinates (x, r, θ), with the x–axis aligned with the axis of the body of revolution (Figure 3.26)

$$\left(1 - M_\infty^2\right)\frac{\partial^2\phi}{\partial x^2} + \frac{\partial^2\phi}{\partial r^2} + \frac{1}{r}\frac{\partial\phi}{\partial r} = 0. \tag{44}$$

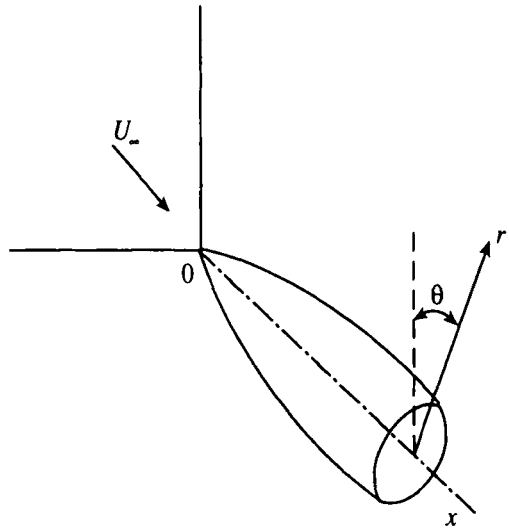

Figure 3.26. Uniform flow past a slender body of revolution.

In order to derive the boundary condition at the surface of the body, note that whereas in plane flows the normal velocity at the chord differs little from that at the airfoil surface, in axisymmetric flows the radial velocity becomes infinite at the axis in order that it becomes finite at the body surface. The latter follows from the continuity equation

$$\frac{\partial u}{\partial x}+\frac{1}{r}\frac{\partial}{\partial r}(\upsilon r)=0, \tag{45}$$

which shows that the product (υr) stays finite. Thus, one writes the boundary condition at surface of the body given by $r=R(x)$ in the form

$$r=R(x): \quad R\frac{dR}{dx}=\frac{(\upsilon r)_{r=0}}{(U_\infty+u)}. \tag{46}$$

The pressure is then given by (see Section 3.5)

$$C_p=-\frac{2u}{U_\infty}-\frac{\upsilon^2}{U_\infty^2}, \tag{47}$$

where we have retained the term quadratic in υ since the latter is of a lower order than u near the axis.

Let us construct the solution to (44) and (46) as a superposition of the singular source solution to equation (44). Thus, for a subsonic flow we have

$$\phi(x,r)=-\int_0^L \frac{f(\xi)\,d\xi}{\sqrt{(x-\xi)^2+m^2r^2}}, \qquad m^2=1-M_\infty^2>0. \tag{48}$$

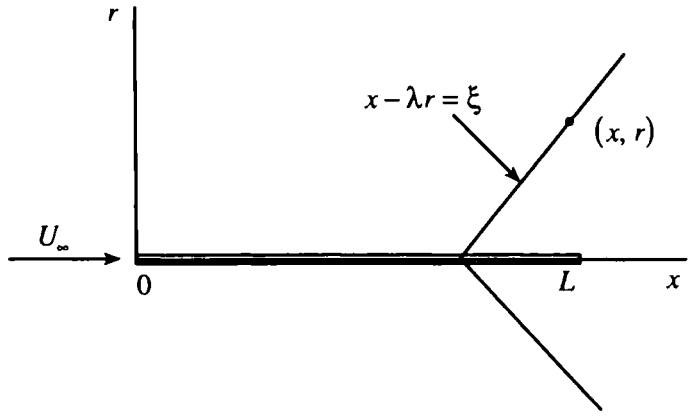

Figure 3.27. Domain of influence in supersonic flows.

In a supersonic flow, note that the flow conditions at a point (x,r) are affected by the sources on the body only up to $\xi = x - \lambda r$ since, for the sources downstream of the latter point, the point (x,r) lies ahead of their Mach cones (see Figure 3.27) and such sources have no effect on the flow conditions at (x,r). Thus,

$$\phi(x,r) = -\int_0^{x-\lambda r} \frac{f(\xi)\,d\xi}{\sqrt{(x-\xi)^2 - \lambda^2 r^2}}, \qquad \lambda^2 = M_\infty^2 - 1 > 0. \tag{49}$$

The region of influence of the body in the three–dimensional case extends over the whole fluid downstream of the Mach cone $x - \lambda r = 0$. (By contrast, in the two–dimensional case the region of influence of the body is bounded by the Mach lines at the leading and trailing edges of the body because the effect of the body is felt only on these Mach lines.)

In order to obtain the velocity components from (49), note that the integrand in (49) diverges at the upper limit, so that one introduces

$$\xi = x - \lambda r \cosh\sigma. \tag{50}$$

Then, (49) becomes

$$\phi(x,r) = -\int_0^{\cosh^{-1}(x/\lambda r)} f(x - \lambda r \cosh\sigma)\,d\sigma, \tag{51}$$

from which, if $f(0) = 0$, one obtains

$$\phi_x = -\int_0^{\cosh^{-1}(x/\lambda r)} f'(x - \lambda r \cosh\sigma)\,d\sigma,$$

$$\phi_r = -\int_0^{\cosh^{-1}(x/\lambda r)} f'(x-\lambda r\cosh\sigma)\cdot(-\lambda\cosh\sigma)\,d\sigma, \tag{52}$$

so that

$$\phi_x = -\int_0^{x-\lambda r} \frac{f'(\xi)\,d\xi}{\sqrt{(x-\xi)^2-\lambda^2 r^2}},$$

$$\phi_r = \frac{1}{r}\int_0^{x-\lambda r} \frac{(x-\xi)f'(\xi)\,d\xi}{\sqrt{(x-\xi)^2-\lambda^2 r^2}}. \tag{53}$$

Example 8: Consider a supersonic flow past a cone, with $f(\xi)=a\xi$. Thus, (51) gives

$$\phi(x,r) = -\int_0^{\cosh^{-1}(x/\lambda r)} (ax - a\lambda r\cosh\sigma)\,d\sigma$$

or

$$\phi(x,r) = -ax\left[\cosh^{-1}\frac{x}{\lambda r} - \sqrt{1-\left(\frac{\lambda r}{x}\right)^2}\right],$$

from which, on the surface of the cone, one has

$$\phi_x = -a\cosh^{-1}\frac{x}{\lambda r}, \qquad \phi_r = a\lambda\sqrt{\left(\frac{x}{\lambda r}\right)^2 - 1}.$$

Note that both ϕ_x and ϕ_r are functions of x/r, i.e., constant along each ray from the origin; such a flow is called *conical* (see Section 3.5). (The solution for the flow past a nonslender cone may therefore be constructed by fitting a conical flow to a conical shock.)

When one uses these expressions for ϕ_x and ϕ_r, (46) gives

$$\frac{a\sqrt{\cot^2\delta - \lambda^2}}{U_\infty - a\cosh^{-1}\left(\dfrac{\cot\delta}{\lambda}\right)} = \tan\delta,$$

from which, for $\delta \ll 1$ (δ being the semivertex angle of the cone), one obtains

$$a \approx U_\infty \delta^2,$$

thus

$$\phi = -U_\infty \delta^2 x\,\ln\frac{2x}{\lambda r} - 1,$$

from which the pressure on the cone is given, on using (74), by

$$C_p = 2\delta^2\left(\ln\frac{2}{\lambda\delta} - \frac{1}{2}\right).$$

Note that for a supersonic flow past a thin wedge of nose angle 2δ, the pressure rise occurs completely at the nose shock, and one has from (4)

$$C_p = \frac{2\delta}{\lambda}.$$

Observe that the pressure rise on the cone is much less than that on the wedge – a result traceable to the three–dimensional flow effect for the cone, and occurs continuously downstream of the Mach cone at the nose.

Let us now evaluate the integral in (49) for $\lambda r/x \ll 1$. Since the integrand is singular near the upper limit of integration, it proves convenient to write

$$\phi = I_1 + I_2, \tag{54}$$

where

$$I_1 = -\int_0^{x-\lambda r-\varepsilon} \frac{f(\xi)\,d\xi}{\sqrt{(x-\xi)^2 - \lambda^2 r^2}},$$

$$I_2 = -\int_{x-\lambda r-\varepsilon}^{x-\lambda r} \frac{f(\xi)\,d\xi}{\sqrt{(x-\xi)^2 - \lambda^2 r^2}}, \qquad \varepsilon \Rightarrow 0^+.$$

In I_1, one may expand the integrand in powers of $\lambda^2 r^2$,

$$\frac{f(\xi)}{\sqrt{(x-\xi)^2 - \lambda^2 r^2}} = f(\xi)\left[\frac{1}{(x-\xi)} + \frac{\lambda^2 r^2}{2}\frac{1}{(x-\xi)^3} + \cdots\right].$$

Then, integration term by term gives, as $\lambda r \Rightarrow 0^+$,

$$I_1 = f(x)\ln\varepsilon - \int_0^{x-\varepsilon} f'(\xi)\,\ln(x-\xi)\,d\xi + \cdots, \tag{55}$$

where we have noted that

$$f(0) = 0.$$

In order to evaluate I_2, introducing

$$\xi = x - \lambda r\cosh\sigma, \tag{50}$$

one obtains

$$I_2 = -\int_0^{\cosh^{-1}\left(\frac{\lambda r+\varepsilon}{\lambda r}\right)} f(x - \lambda r\,\cosh\sigma)\,d\sigma.$$

Expanding the integrand in powers of λr, one obtains

$$I_2 = -f(x) \int_0^{\cosh^{-1}\left(\frac{\lambda r+\varepsilon}{\lambda r}\right)} d\sigma + \lambda r \int_0^{\cosh^{-1}\left(\frac{\lambda r+\varepsilon}{\lambda r}\right)} f'(x)\cosh\sigma\, d\sigma + \cdots$$

which, as $\lambda r \Rightarrow 0^+$, leads to

$$I_2 = -f(x)\ln\frac{2}{\lambda r} - f(x)\ln\varepsilon + \cdots. \tag{56}$$

Using (55) and (56), (54) leads to

$$\phi \approx -f(x)\ln\frac{2}{\lambda r} - \int_0^x f'(\xi)\ln(x-\xi)\,d\xi. \tag{57}$$

The boundary condition at the surface of the body given by $r = R(x)$ then becomes

$$r = R: \quad \frac{\partial\phi}{\partial r} = \frac{f(x)}{R} = U\frac{dR}{dx}$$

or

$$f(x) = \frac{U}{2\pi}\frac{dA}{dx}, \tag{58}$$

where

$$A \equiv \pi R^2.$$

Equation (58) implies that the source strength is proportional only to the rate of change of area of the body.

When one uses (58), (57) becomes

$$\phi \approx -\frac{U}{2\pi}A'(x)\ln\frac{2}{\lambda r} - \frac{U}{2\pi}\int_0^x A''(\xi)\ln(x-\xi)\,d\xi. \tag{59}$$

Consider next the flow past a body of revolution at an angle of attack (see Figure 3.28). Even though the flow is no longer axisymmetric, the linearity of the potential-flow equation permits one to write

$$\phi(x,r,\theta) = \phi_a(x,r) + \phi_c(x,r,\theta), \tag{60}$$

where the subscripts a and c denote the axial flow and the cross flow, respectively, and one has

$$\frac{\partial^2\phi_a}{\partial r^2} + \frac{\partial\phi_a}{r\partial r} - \lambda^2\frac{\partial^2\phi_a}{\partial x^2} = 0, \tag{61}$$

$$\frac{\partial^2\phi_c}{\partial r^2} + \frac{\partial\phi_c}{r\partial r} + \frac{1}{r^2}\frac{\partial^2\phi_c}{\partial\theta^2} - \lambda^2\frac{\partial^2\phi_c}{\partial x^2} = 0. \tag{62}$$

From equations (61) and (62), it is easy to verify that

$$\phi_c = \cos\theta\cdot\frac{\partial\phi_a}{\partial r}, \tag{63}$$

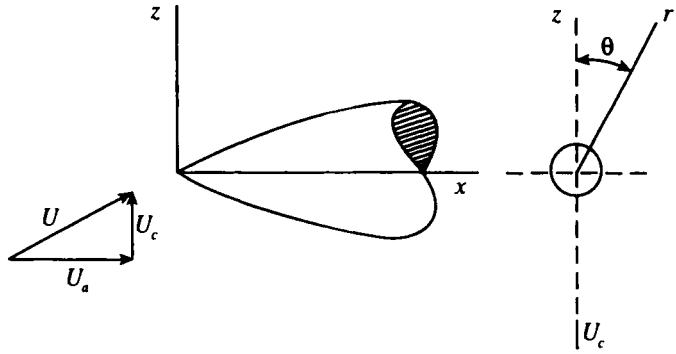

Figure 3.28. Uniform flow past a slender body of revolution at an angle of attack.

so that, on using (53), one obtains

$$\phi_c(x,r,\theta)=\frac{\cos\theta}{r}\int_0^{x-\lambda r}\frac{m(\xi)\cdot(x-\xi)\,d\xi}{\sqrt{(x-\xi)^2-\lambda^2 r^2}}. \tag{64}$$

The boundary conditions are

$$r=R(x):\ \left(r\frac{\partial\phi_a}{\partial r}\right)=R\frac{dR}{dx}u_a,$$

$$\frac{\partial\phi_c}{\partial r}=-U_c\cos\theta. \tag{65}$$

Alternatively, one has, from (64), as $r\Rightarrow 0^+$,

$$\phi_c\approx\frac{\sigma(x)}{r}\cos\theta, \tag{66}$$

where $\sigma(x)$, on using (65), is given by

$$\sigma(x)=U_c\left[R(x)\right]^2, \tag{67}$$

so that the doublet strength modeling the cross flow is proportional to the local section area. This implies that the cross flow at any section is the same as if the latter were part of an infinite cylinder normal to a uniform flow. Thus,

$$\phi_c\approx U_\infty\sin\alpha\,\frac{\left[R(x)\right]^2}{r}\cos\theta,\quad \text{as } r\Rightarrow 0^+, \tag{68}$$

which simply represents the incompressible flow normal to an infinitely long cylinder. This means that in a linearized approximation, the cross flow prevails under incompressible conditions, at least near the body. This is to be expected if the cross flow at a cross section is independent of the cross flow at other sections.

Oscillating Thin Airfoil in Subsonic Flows: Possio's Theory

Further complications arise due to compressibility effects because of the facts:

1. Additional phase lags appear,
2. Flow patterns do not adjust themselves immediately to changing boundary conditions; thus the flow properties do not just depend on the instantaneous accelerations and velocities of the body, but are affected by their time history.

For a linearized unsteady subsonic flow past a thin airfoil (see Section 3.5), one has

$$\frac{1}{a^2}\frac{\partial^2\phi}{\partial t^2}+\frac{2M_\infty}{a}\frac{\partial^2\phi}{\partial x\partial t}-\beta^2\frac{\partial^2\phi}{\partial x^2}=\frac{\partial^2\phi}{\partial y^2}, \tag{69}$$

where

$$\beta=\sqrt{1-M_\infty^2}\,.$$

When one puts

$$\tau=t+\frac{M_\infty}{\beta^2 a}x\equiv t+\alpha x,$$

$$\xi=\frac{x}{\beta^2 a},\qquad \eta=\frac{y}{\beta a}, \tag{70}$$

equation (69) becomes

$$\phi_{\tau\tau}=\phi_{\xi\xi}+\phi_{\eta\eta}. \tag{71}$$

When one puts

$$\xi=r'\cos\theta,\qquad \eta=r'\sin\theta, \tag{72}$$

equation (71) becomes

$$\phi_{\tau\tau}=\phi_{r'r'}+\frac{1}{r'}\phi_{r'}+\frac{1}{r'^2}\phi_{\theta\theta}. \tag{73}$$

When one lets

$$\phi=e^{i\omega\tau}\begin{Bmatrix}\sin n\theta\\ \cos n\theta\end{Bmatrix}R(r'), \tag{74}$$

equation (73) gives

$$\frac{d^2R}{dr'^2}+\frac{1}{r'}\frac{dR}{dr'}+\left(\omega^2-\frac{n^2}{r'^2}\right)R=0, \tag{75}$$

from which

$$R=A_n\begin{Bmatrix}H_n^{(1)}(\omega r')\\ H_n^{(2)}(\omega r')\end{Bmatrix}. \tag{76}$$

$H_n^{(1)}(x)$ and $H_n^{(2)}(x)$ are Hankel's functions of the first kind and second kind.

Note that (76) gives a source at the origin for $n = 0$ and a doublet for $n = 1$.

Let us now introduce what is called the *acceleration potential*, which makes the formulation in the following more simple. The equation of motion is

$$\frac{Dv_i}{Dt} = -\frac{1}{\rho}\frac{\partial p}{\partial x_i}. \tag{77}$$

Let

$$\frac{Dv_i}{Dt} \equiv \frac{\partial \varphi}{\partial x_i}, \tag{78}$$

where

$$\varphi + \int_{p_0}^{p} \frac{dp}{\rho} = \text{const}. \tag{79}$$

For a barotropic fluid and thin airfoils, φ will be continuous everywhere. (When the wake is idealized into a thin surface, the velocity potential is discontinuous across that surface, but φ is continuous; this means that one would have in the equation for φ no source terms arising from the wake due to the vorticity shed from the trailing edges.)

Consider small disturbances in an otherwise uniform, rectilinear, steady flow. Let

$$\rho = \rho_\infty + \rho', \quad p = p_\infty + p', \quad \rho' \ll \rho_\infty, \quad p' \ll p_\infty; \tag{80}$$

one then obtains from (79)

$$\varphi = -\frac{p'}{\rho_\infty}. \tag{81}$$

Since the pressure may be considered to be a potential for the acceleration field, from (81), one may call φ the acceleration potential.

Now, the discontinuity of the pressure field across an oscillating airfoil can be represented by a layer of doublets, the strength of which of course varies with time. Thus, for a line distribution of doublets (with vertical axes), upon noting (74) and that, for a linearized flow, φ satisfies the same equation as that for ϕ, viz. equation (69), one has

$$\varphi(x, y, t) = e^{i\omega t} \int_0^c B(x') \sin\theta \, H_1^{(2)}(\omega r') e^{i\omega\alpha(x-x')} \, dx', \tag{82}$$

where we have chosen $H_1^{(2)}(\omega r')$ rather than $H_1^{(1)}(\omega r')$ in accordance with the radiation condition (see Section 2.6), and

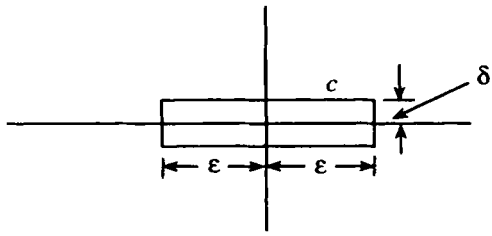

Figure 3.29. An element of the airfoil.

$$r' = \frac{1}{\beta^2 a}\sqrt{(x-x')^2 + \beta^2 y^2},$$

$$\theta = \tan^{-1}\left(\frac{\beta y}{x-x'}\right).$$

Consider a small element of length 2ε, at $x = \xi$ (see Figure 3.29). If L is the lift per unit length at $(x,0)$, applying the force balance, one finds

$$\begin{aligned} 2\varepsilon L(\xi,t) = \int_C p'dx &= -\rho_\infty \int_C \varphi(x,y,t)\,dx \\ &= 2\rho_\infty \lim_{\delta\Rightarrow 0} \int_{\xi-\varepsilon}^{\xi+\varepsilon} \varphi(x,\delta,t)\,dx. \end{aligned} \tag{83}$$

From (82), note that

$$\lim_{\delta\Rightarrow 0} \int_{x-\varepsilon}^{x+\varepsilon} \varphi(x,\delta,t)\,dx = e^{i\omega t} B(x) \int_{x-\varepsilon}^{x+\varepsilon} \lim_{\delta\Rightarrow 0} \sin\theta\, H_1^{(2)}(\omega r')\,dx', \tag{84}$$

where

$$H_1^{(2)}(z) \sim \frac{2i}{\pi z} \quad \text{for} \quad |z| \ll 1,$$

$$\sin\theta = \frac{\beta y}{\sqrt{(x-x')^2 + \beta^2 y^2}}.$$

Thus,

$$\begin{aligned} \lim_{\delta\Rightarrow 0} \varphi(x,\delta,t) &= e^{i\omega t} B(x) \lim_{\delta\Rightarrow 0} \int_{x-\varepsilon}^{x+\varepsilon} \frac{2i}{\pi}\,\frac{\beta^3 a}{\omega}\,\frac{\delta}{\left[(x-x')^2 + \beta^2\delta^2\right]}\,dx' \\ &= \frac{4i}{\pi}\,\frac{\beta^2 a}{\omega}\, e^{i\omega t} B(x) \lim_{\delta\Rightarrow 0} \tan^{-1}\frac{\varepsilon}{\beta\delta} \\ &= \frac{2i\beta^2 a}{\omega}\, e^{i\omega t} B(x). \end{aligned} \tag{85}$$

When one uses (85), (83) gives

$$L(\xi,t)=\frac{4i\rho_\infty\beta^2 a}{\omega}\,e^{i\omega t}B(\xi). \tag{86}$$

Consider next the velocity field. From the linearized equation of motion,

$$\frac{\partial\varphi}{\partial y}=\frac{\partial v}{\partial t}+U_\infty\frac{\partial v}{\partial x} \tag{87a}$$

with

$$v,\varphi\sim e^{i\omega t}, \tag{87b}$$

one obtains

$$v(x,y)=\frac{1}{U_\infty}\exp\left(-\frac{i\omega x}{U_\infty}\right)\int_{-\infty}^{x}\frac{\partial\varphi}{\partial y'}\exp\left(\frac{i\omega x'}{U_\infty}\right)dx'. \tag{88}$$

Without loss of generality, one may put the doublet at the origin. Then, (88) leads to

$$v(x,y,t)=\frac{1}{U_\infty}\exp\left(-\frac{i\omega x}{U_\infty}\right)\int_{-\infty}^{x}Be^{i\omega(t+Kx')}\frac{\partial}{\partial y'}\left[\sin\theta\cdot H_1^{(2)}(\omega r')\right]dx', \tag{89}$$

where

$$K=\alpha+\frac{1}{U_\infty}=\frac{1}{U_\infty\beta^2}.$$

When one notes that

$$\begin{aligned}&\frac{\partial\theta}{\partial y}=\frac{\cos\theta}{\beta ar'},\quad \frac{\partial\theta}{\partial x}=-\frac{\sin\theta}{\beta^2 ar'},\quad \frac{\partial r'}{\partial y}=\frac{\sin\theta}{\beta a},\quad \frac{\partial r'}{\partial x}=\frac{\cos\theta}{\beta^2 a},\\ &\frac{n}{z}H_n(z)-H_n'(z)=H_{n+1}(z),\end{aligned} \tag{90}$$

(89) becomes

$$v(x,y,t)=-\frac{B\beta a}{U_\infty\omega}\exp\left[i\omega\left(t-\frac{x}{U_\infty}\right)\right]\int_{-\infty}^{\infty}e^{i\omega Kx'}\frac{\partial^2}{\partial y'^2}\left[H_0^{(2)}(\omega r')\right]dx', \tag{91}$$

which is divergent when $y=0,\ x\geq 0$.

When one notes that

$$\frac{\partial^2}{\partial y'^2}\left[H_0^{(2)}(\omega r')\right]=-\frac{\omega^2}{\beta^2 a^2}H_0^{(2)}(\omega r')-\beta^2\frac{\partial^2}{\partial x'^2}\left[H_0^{(2)}(\omega r')\right], \tag{92}$$

(91) becomes

$$v(x,y,t)=A\int_{-\infty}^{x}e^{i\omega Kx'}\left[\frac{\omega^2}{\beta^2 a^2}H_0^{(2)}(\omega r')+\beta^2\frac{\partial^2}{\partial x'^2}H_0^{(2)}(\omega r')\right]dx'\equiv I_1+I_2, \tag{93}$$

where

$$A = \frac{B\beta a}{U_\infty \omega} \exp\left[i\omega\left(t - \frac{x}{U_\infty} \right) \right] = \frac{L}{4i\rho_\infty \beta U_\infty} \exp\left(-\frac{i\omega x}{U_\infty} \right)$$

on using (86).

When one notes that

$$I_2 = A\beta^2 \left\{ \omega \left[-H_1^{(2)}(\omega r') \frac{\cos\theta}{\beta^2 a} - iKH_0^{(2)}(\omega r') \right] \right.$$
$$\left. \times e^{i\omega Kx} - \omega^2 K^2 \int_{-\infty}^{x} e^{i\omega Kx} H_0^{(2)}(\omega r')\, dx' \right\}, \tag{94}$$

(93) becomes

$$v(x,y,t) = A\beta^2 \omega e^{i\omega Kx} \left\{ -H_1^{(2)}(\omega r') \frac{\cos\theta}{\beta^2 a} + iKH_0^{(2)}(\omega r') \right\}$$
$$+ A\left(\frac{1}{\beta^2 a^2} - \beta^2 K^2 \right) \omega^2 \int_{-\infty}^{x} e^{i\omega Kx'} H_0^{(2)}(\omega r')\, dx', \tag{95}$$

from which

$$v(x,0,t) = -\frac{iA\omega e^{i\omega Kx}}{U_\infty} \left\{ -iM_\infty H_1^{(2)}(|W|) \frac{W}{|W|} + H_0^{(2)}(|W|) \right\}$$
$$- \frac{A\omega^2}{U_\infty^2} \int_{-\infty}^{x} e^{i\omega Kx'} H_0^{(2)}\left(\omega \frac{|x'|}{\beta^2 a} \right) dx', \tag{96}$$

where

$$W \equiv \frac{\omega}{\beta^2 a} x = \omega M_\infty K x .$$

Consider

$$I = \int_0^\infty e^{-i\omega Kx'} H_0^{(2)}\left(\frac{\omega}{\beta^2 a} x' \right) dx' = \frac{U_\infty \beta^2}{\omega} \int_0^\infty e^{-iu} H_0^{(2)}(M_\infty u)\, du, \tag{97}$$

where

$$u \equiv \omega K x' .$$

When one notes that

$$\int_1^\infty e^{-ix\xi} \frac{d\xi}{\sqrt{\xi^2 - 1}} = -\frac{i\pi}{2} H_0^{(2)}(x), \quad x > 0, \tag{98}$$

(97) becomes

$$I = \frac{2U_\infty \beta^2}{\pi\omega} \int_1^\infty \frac{d\xi}{\sqrt{\xi^2 - 1}\,(1 + M_\infty \xi)}. \tag{99}$$

When one puts

$$\xi = \cosh \eta,$$

(99) becomes

$$I = \frac{2U_\infty \beta^2}{\pi\omega} \int_1^\infty \frac{d\eta}{1 + M_\infty \cosh \eta}. \tag{100}$$

When one notes that

$$\int \frac{dx}{1 + \cos\alpha \cosh x} = 2 \operatorname{cosec}\alpha \tanh^{-1}\left(\tanh\frac{x}{2}\tan\frac{\alpha}{2}\right), \tag{101}$$

(100) becomes

$$I = \frac{2U_\infty \beta^2}{\pi\omega} \frac{2}{\sqrt{1 - M_\infty^2}} \tanh^{-1}\left(\sqrt{\frac{1 - M_\infty}{1 + M_\infty}} \tanh\frac{\eta}{2}\right)\Bigg|_0^\infty$$

or

$$I = \frac{4U_\infty \beta}{\pi\omega} \tanh^{-1}\sqrt{\frac{1 - M_\infty}{1 + M_\infty}} = \frac{2U_\infty \beta}{\pi\omega} \ln\frac{1 + \sqrt{1 - M_\infty^2}}{M_\infty}. \tag{102}$$

When one uses (97) and (102), (96) becomes

$$v(x,0,t) = \frac{\omega L}{\rho_\infty U_\infty^2} \kappa(M_\infty, x), \tag{103}$$

where

$$\kappa(M_\infty, x) = \frac{1}{4\beta} e^{iM_\infty W} \left\{ iM_\infty \frac{W}{|W|} H_1^{(2)}(|W|) - H_0^{(2)}(|W|) \right\} + \frac{i\beta}{4} \exp\left(-\frac{i\omega x}{U_\infty}\right)$$
$$\times \left\{ \frac{2}{\pi\beta} \ln\frac{1 + \beta}{M_\infty} + \int_0^{W/M_\infty} e^{iu} H_0^{(2)}(M_\infty |u|\, du) \right\}.$$

Thus, for the whole airfoil, one obtains an integral equation

$$v(x,0,t) = \frac{\omega}{\rho_\infty U_\infty^2} \oint_0^c L(\xi,t)\, \kappa(M_\infty, x - \xi)\, d\xi \tag{104}$$

with the Kutta condition in the form of continuity of the pressure at the trailing edge:

$$\xi = c: \quad L = 0. \tag{105}$$

Note that $\kappa(M_\infty, x - \xi)$ has a singularity at $x = \xi$.

Oscillating Thin Airfoils in Supersonic Flows: Stewartson's Theory

The treatment of oscillating thin airfoils in supersonic flows becomes simpler than that in subsonic flows because, in the supersonic case, the flows above and below the airfoil are independent of each other, and the flow over the airfoil is independent of the conditions in the wake.

For the linearized unsteady potential flows,[10] one has

$$\begin{aligned} &\left(1-M_\infty^2\right)\phi_{xx}+\phi_{yy}-2M_\infty^2\,\phi_{xt}-M_\infty^2\,\phi_{tt}=0,\\ &y=0:\quad \phi_y=v_0(x,t),\qquad x\geq 0. \end{aligned} \tag{106}$$

When one assumes a harmonic time dependence,

$$v_0(x,t)=v_0(x)e^{i\omega t},\quad \phi(x,y,t)=\phi(x,y)e^{i\omega t}, \tag{107}$$

(106) becomes

$$\begin{aligned} &\left(M_\infty^2-1\right)\phi_{xx}-\phi_{yy}+2M_\infty^2\,i\omega\phi_x-M_\infty^2\,\omega^2\phi=0,\\ &y=0:\quad \phi_y=v_0(x),\qquad x\geq 0. \end{aligned} \tag{108}$$

Upon Laplace–transforming according to

$$\tilde{\phi}(s,y)=\int_0^\infty e^{-sx}\phi(x,y)\,dx, \tag{109}$$

(108) becomes

$$\begin{aligned} &\tilde{\phi}_{yy}-\mu^2\tilde{\phi}=0,\\ &y=0:\quad \tilde{\phi}=\tilde{v}_0(s), \end{aligned} \tag{110}$$

where

$$\mu^2=s^2\left(M_\infty^2-1\right)+2M_\infty^2\,i\omega s-\omega^2M_\infty^2.$$

One obtains from (110)

$$\tilde{\phi}(s,y)=-\frac{\tilde{v}_0(s)}{\mu}e^{-\mu y},\qquad y\geq 0^+. \tag{111}$$

When one inverts the Laplace transform, (111) gives

[10]Even though transonic flows are patently nonlinear, the nonlinear characteristics in an unsteady situation manifest themselves only in low-frequency airfoil motions. For sufficiently high frequencies, even the unsteady transonic flow problem becomes a linear one like the subsonic- and supersonic-flow cases!

$$\phi(x,y) = -\frac{1}{\sqrt{M_\infty^2 - 1}} \int_0^{x-\sqrt{M_\infty^2-1}\,y} v_0(x_1) \exp\left[-\frac{iM_\infty^2\omega}{M_\infty^2 - 1}(x - x_1)\right] \times J_0\left[\frac{M_\infty \omega}{M_\infty^2 - 1}\sqrt{(x-x_1)^2 - (M_\infty^2 - 1)y^2}\right] dx_1. \tag{112}$$

As $M_\infty \Rightarrow 1$ or $\omega \Rightarrow \infty$, note that (112) becomes

$$\phi(x,y) \approx -\int_0^x v_0(x_1) \frac{\exp\left[-\frac{i\omega}{2}\left\{(x-x_1) + \frac{y^2}{(x-x_1)}\right\}\right]}{\sqrt{2\pi i\omega(x-x_1)}} dx_1. \tag{113}$$

Using (112), the Bernoulli integral gives the pressure on the airfoil,

$$p(x,0) = \frac{1}{\sqrt{M_\infty^2 - 1}}\left[v_0(x) - \int_0^x v_0(x_1)\frac{\partial G}{\partial x_1} dx_1 + i\omega\int_0^x v_0(x_1) G(x_1) dx_1\right], \tag{114}$$

where

$$G(x, x_1) = \exp\left[-i\frac{M_\infty^2\,\omega}{M_\infty^2 - 1}(x - x_1)\right] J_0\left[\frac{M_\infty \omega}{M_\infty^2 - 1}(x - x_1)\right].$$

Example 9: Consider a sharp–edged gust, given by

$$v_g = \begin{cases} 0, & x > t, \\ V, & x < t, \end{cases} \tag{115}$$

so that

$$v(\omega) = \int_0^\infty v_g(t) e^{i\omega t} dt = \frac{iV}{\omega} e^{i\omega x}, \tag{116}$$

from which

$$2\pi v_g(t) = iV \int_{-\infty}^{\infty} \frac{e^{i\omega(x-t)}}{\omega} d\omega. \tag{117}$$

When one uses (117), (114) becomes

$$p(\omega, x) = \frac{e^{-i\omega t}}{\sqrt{M_\infty^2 - 1}}\left[\frac{iV}{\omega} e^{i\omega x} - \int_0^x \frac{iV}{\omega} e^{i\omega x_1}\frac{\partial G}{\partial x_1} dx_1 + i\omega\int_0^x \frac{iV}{\omega} e^{i\omega x_1} G(x_1) dx_1\right], \tag{118}$$

from which

$$p(x,t) = \frac{1}{2\pi}\int_{-\infty}^{\infty} p(\omega, x)\, d\omega. \tag{119}$$

EXERCISES

1. Estimate the error incurred in writing the boundary condition (46).
2. Obtain the solution for a supersonic flow past a cone by starting with the assumption that the flow is conical (and not using the slender axisymmetric body theory).
3. Linearize the transonic–flow equation using the hodograph transformation, and investigate the prospects of its solvability.
4. Set up the boundary–value problem for a nonlinear axisymmetric flow past a cone, and investigate its prospects of solvability.

4

DYNAMICS OF VISCOUS FLUID FLOWS

4.1. Exact Solutions to Equations of Viscous Fluid Flows

The mathematical theory of ideal–fluid flow given so far provides a powerful approach to the solution of several problems and gives satisfactory descriptions of such characteristics of flows of the real fluid as (a) the main characteristics of wave motion and (b) the pressure field on streamlined bodies placed in flows. However, this theory is unable to indicate how nearly the flow field (the whole or part of it) will be irrotational. Therefore, application of the results from this theory requires the clarification of the circumstances in which the ideal–fluid assumption is valid. Basically, the ideal–fluid assumption is useful insofar as it may describe the behavior of a real fluid in the limit of vanishing viscosity. However, because of the contamination by vorticity within a boundary layer near a solid surface, the ideal–fluid theory does not give a correct description of the flows near solid boundaries and cannot describe such things as skin friction and form drag of a body placed in a flow. In order to remove these discrepancies, an understanding and inclusion of the effects of viscosity of a real fluid is essential.

Among the effects produced by the fluid viscosity are

(1) generation of shearing stresses in the fluid;

(2) maintenance of a zero slip–velocity of the fluid at a solid boundary.

In the following, we shall consider only the Newtonian fluids for which the coefficient of viscosity μ is independent of the rate of deformation of the fluid. Furthermore, we shall restrict ourselves to laminar flows wherein the viscous processes have their origin in the molecular transport processes.

Channel Flows

One has for a steady, unidirectional flow in a channel bounded by rigid wall the

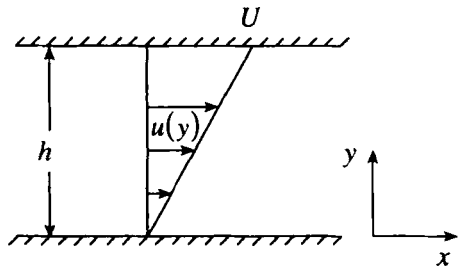

Figure 4.1. Couette flow.

equation of motion (Chapter 1)

$$\frac{dp}{dx} = \mu \frac{d^2u}{dy^2}. \tag{1}$$

For this case, the nonlinear convective term in the equation of motion vanishes identically, and the latter becomes linear.

For a Couette flow (see Figure 4.1), for which

$$\begin{aligned} y = 0: &\quad u = 0 \\ y = h: &\quad u = U, \end{aligned} \tag{2}$$

equation (1) gives

$$u = \frac{y}{h} U - \frac{h^2}{2\mu} \frac{dp}{dx} \frac{y}{h}\left(1 - \frac{y}{h}\right), \tag{3}$$

which gives the linear profile shown in Figure 4.1 if $dp/dx = 0$.

For a Poiseuille flow (see Figure 4.2) fluid enters a channel with a uniform velocity over the whole cross section. Thanks to the no–slip condition, the fluid next to the wall will be slowed down and boundary layers form on the channel walls. These boundary layers grow and ultimately meet producing the Poiseuille flow in the channel with a parabolic velocity profile.

The boundary conditions for a Poiseuille flow are

$$y = \pm b: \quad u = 0, \tag{4}$$

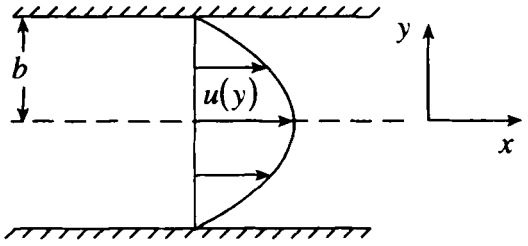

Figure 4.2. Poiseuille flow.

and equation (1) gives

$$u = -\frac{1}{2\mu}\frac{dp}{dx}\left(b^2 - y^2\right). \tag{5}$$

Decay of a Line Vortex

Consider the decay of a vortex filament in an incompressible fluid. Use the cylindrical coordinates and take the z–axis along the axis of the filament. The vorticity is governed by

$$\frac{\partial \zeta}{\partial t} = \nu\left(\frac{\partial^2 \zeta}{\partial r^2} + \frac{1}{r}\frac{\partial \zeta}{\partial r}\right), \tag{6}$$

where

$$\zeta \equiv \frac{\partial u_\theta}{\partial r} + \frac{u_\theta}{r}, \qquad \nu \equiv \frac{\mu}{\rho},$$

so that from equation (6) we obtain

$$\frac{1}{r}\frac{\partial^2 (ru_\theta)}{\partial r \partial t} = \nu\left[\frac{1}{r}\frac{\partial^3 (ru_\theta)}{\partial r^3} - \frac{1}{r^2}\frac{\partial^2 (ru_\theta)}{\partial r^2} + \frac{1}{r^3}\frac{\partial (ru_\theta)}{\partial r}\right]. \tag{7}$$

Nondimensionalize the various quantities using a reference length L and a reference time τ, so that

$$\frac{1}{r}\frac{\partial^2 (ru_\theta)}{\partial r \partial t} + \varepsilon\left[-\frac{1}{r}\frac{\partial^3 (ru_\theta)}{\partial r^3} + \frac{1}{r^2}\frac{\partial^2 (ru_\theta)}{\partial r^2} - \frac{1}{r^3}\frac{\partial^2 (ru_\theta)}{\partial r}\right] = 0, \tag{8}$$

where

$$\varepsilon \equiv \frac{\nu\tau}{L^2}.$$

The boundary conditions are

$$\left.\begin{aligned} r = 0: &\quad u_\theta = 0 \\ r \Rightarrow \infty: &\quad u_\theta \Rightarrow 0 \end{aligned}\right\} \quad \text{for } t > 0. \tag{9}$$

Let us seek a solution of equation (8) in the form of a straightforward expansion:

$$u_\theta^{(0)} = \sum_{n=0}^{\infty} \varepsilon^n u_{\theta n}^{(0)}(r,t), \qquad \varepsilon \ll 1. \tag{10}$$

Substituting in equation (8) and equating the coefficients of equal powers of ε, one obtains

$$\frac{1}{r}\frac{\partial^2 \left(ru_{\theta_0}^{(0)}\right)}{\partial r \partial t} = 0, \tag{11}$$

$$\frac{1}{r}\frac{\partial^2\left(ru_{\theta_1}^{(0)}\right)}{\partial r\partial t}=\frac{1}{r}\frac{\partial^3\left(ru_{\theta_0}^{(0)}\right)}{\partial r^3}-\frac{1}{r^2}\frac{\partial^2\left(ru_{\theta_0}^{(0)}\right)}{\partial r^2}+\frac{1}{r^3}\frac{\partial\left(ru_{\theta_0}^{(0)}\right)}{\partial r}. \tag{12}$$

From the nature of the equation (11) and (12), it is clear that their solutions cannot satisfy both of the boundary conditions (9), and one of them must be dropped.

Solving for the first two terms of (10) and requiring the satisfaction of the boundary conditions $u_\theta^{(0)} \Rightarrow 0$ as $r \Rightarrow \infty$, one finds

$$u_\theta^{(0)}=\frac{A}{r}+\frac{f(t)}{r}+\varepsilon\left[\frac{3A}{r^5}t\right]+\cdots. \tag{13}$$

Note $u_\theta^{(0)} \Rightarrow \infty$ at $r \Rightarrow 0$ so that the error in (10) is not uniform over $[0,\infty]$, and the expansion (10) breaks down at the axis. It is of interest to note that the higher-order terms in the expansion (10) introduce successively higher-order singularities at the axis. This simply implies that the problem (7) is of singular-perturbation type.

In order to understand further the nature of the nonuniformity, note the exact solution of equation (7),

$$u_\theta=\frac{\Gamma_0}{2\pi r}\left[1-\exp\left(-\frac{r^2}{4\varepsilon t}\right)\right], \tag{14}$$

which is in agreement with the first term in (13) and satisfies the boundary condition $u_\theta(\infty) \Rightarrow 0$ (Γ_0 can be shown to be the circulation of the vortex filament at time $t=0$). In order to understand what happens at the boundary $r=0$, write (14) in the form

$$u_\theta=\frac{\Gamma_0}{2\pi r}-\frac{\Gamma_0}{2\pi r}\exp\left(-\frac{r^2}{4\varepsilon t}\right).$$

The second term in the above is not negligible even as $\varepsilon \Rightarrow 0$ since we are interested in the region $r \Rightarrow 0$. Besides, in this form, the order of the error is uniform $[0,\infty]$. The behavior of u_θ is shown in Figure 4.3 together with the first term of $u_\theta^{(0)}$. Note that near $r=0$, the motion is a rigid-body rotation. It can be seen that for small ε, u_θ agrees with $u_\theta^{(0)}$ except in the small region near the axis where it changes rapidly in order to satisfy the boundary condition there which is about to be lost. Physically, this means that for small times there is a narrow vortex core near the axis, and the rest of the flow field is irrotational.

For $r \ll \sqrt{4\nu t}$, we have, from (14),

$$u_\theta \approx \frac{\Gamma_0}{8\pi\nu t}r,$$

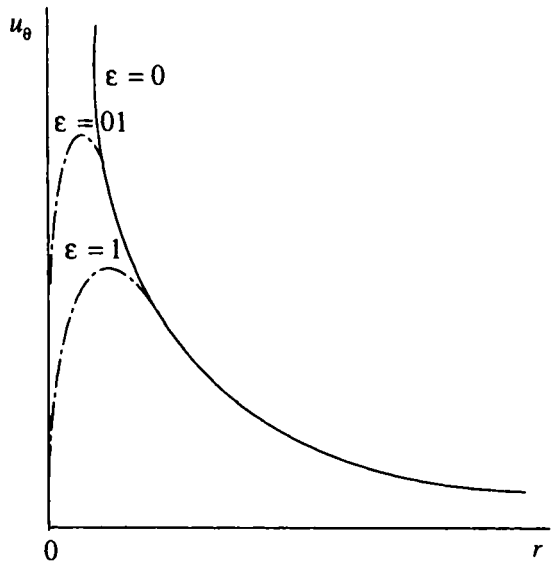

Figure 4.3. Velocity distribution in a vortex filament.

which corresponds to an almost rotation with angular velocity $\Gamma_0/8\pi\nu t$. The intensity of the vortex thus decreases with time as the *core* spreads radially outward.

Line Vortex in a Uniform Stream

Consider a uniform flow U_∞ parallel to the x–axis which is slightly perturbed by a unit line source of vorticity at the origin. One has

$$\frac{\partial \zeta}{\partial x} = \frac{\nu}{U_\infty} \nabla^2 \zeta . \tag{15}$$

When one puts

$$\zeta = e^{kx} f(x, y), \qquad k \equiv \frac{U_\infty}{2\nu}, \tag{16}$$

equation (15) gives

$$\nabla^2 f = k^2 f , \tag{17}$$

from which we have

$$f(r) = K_0(kr), \tag{18}$$

where $K_0(z)$ is the modified Bessel function of the second kind of order 0. Thus

$$\zeta = \exp(kr \cos\theta)\ K_0(kr). \tag{19}$$

For $kr \gg 1$, (19) gives

$$\zeta \approx \left\{\exp\left[-kr(1-\cos\theta)\right]\right\}\sqrt{\frac{\pi}{2kr}}; \tag{20}$$

and for $\theta \approx 0$, (20) gives

$$\zeta \sim \sqrt{\frac{\pi}{2kx}}\exp\left(-kx\frac{\theta^2}{2}\right), \tag{21}$$

which shows a wake region behind the line vortex.

Diffusion of a Localized Vorticity Distribution

It turns out that in the problem of diffusion of a localized vorticity distribution the nonlinear effects become negligible in what may be called the *final period*, (i.e., $t \Rightarrow \infty$). Further, the diffusion process in this limit turns out to be independent of the detailed nature of the initial condition.

The equation for the transport of vorticity ξ is

$$\frac{\partial \xi}{\partial t} + (\mathbf{v}\cdot\nabla)\xi = (\xi\cdot\nabla)\mathbf{v} + \nu\nabla^2\xi; \tag{22}$$

and for the axisymmetric case, in cylindrical coordinates, equation (22) tends to

$$\begin{aligned}
&\frac{\partial}{\partial t}\left(\frac{\partial u_\theta}{\partial z}\right) + \left(u_r\frac{\partial}{\partial r} + u_z\frac{\partial}{\partial z}\right)\frac{\partial u_\theta}{\partial z} \\
&\quad = \left[\left(\frac{\partial u_\theta}{\partial r} + \frac{u_\theta}{r}\right)\frac{\partial}{\partial z} + \frac{\partial u_\theta}{\partial z}\frac{\partial}{\partial r}\right]u_r \\
&\qquad + \nu\left(\frac{\partial^2}{\partial r^2} + \frac{1}{r}\frac{\partial}{\partial r} + \frac{\partial^2}{\partial z^2}\right)\frac{\partial u_\theta}{\partial z},
\end{aligned} \tag{23}$$

$$\begin{aligned}
&\frac{\partial}{\partial t}\left(\frac{\partial u_z}{\partial r} - \frac{\partial u_r}{\partial z}\right) + \left(u_r\frac{\partial}{\partial r} + u_z\frac{\partial}{\partial z}\right)\left(\frac{\partial u_z}{\partial r} - \frac{\partial u_r}{\partial z}\right) \\
&\quad = \left[\left(\frac{\partial u_\theta}{\partial r} + \frac{u_\theta}{r}\right)\frac{\partial}{\partial z} + \frac{\partial u_\theta}{\partial z}\frac{\partial}{\partial r}\right]u_\theta \\
&\qquad + \nu\left(\frac{\partial^2}{\partial r^2} + \frac{1}{r}\frac{\partial}{\partial r} + \frac{\partial^2}{\partial z^2}\right)\left(\frac{\partial u_z}{\partial r} - \frac{\partial u_r}{\partial z}\right),
\end{aligned} \tag{24}$$

$$\begin{aligned}
&\frac{\partial}{\partial t}\left(\frac{\partial u_\theta}{\partial r} + \frac{u_\theta}{r}\right) + \left(u_r\frac{\partial}{\partial r} + u_z\frac{\partial}{\partial z}\right)\left(\frac{\partial u_\theta}{\partial r} + \frac{u_\theta}{r}\right) \\
&\quad = \left[\left(\frac{\partial u_\theta}{\partial r} + \frac{u_\theta}{r}\right)\frac{\partial}{\partial z} + \frac{\partial u_\theta}{\partial z}\frac{\partial}{\partial r}\right]u_z \\
&\qquad + \nu\left(\frac{\partial^2}{\partial r^2} + \frac{1}{r}\frac{\partial}{\partial r} + \frac{\partial^2}{\partial z^2}\right)\left(\frac{\partial u_\theta}{\partial r} + \frac{u_\theta}{r}\right).
\end{aligned} \tag{25}$$

The continuity of mass gives

$$\frac{\partial u_r}{\partial r} + \frac{u_r}{r} + \frac{\partial u_z}{\partial z} = 0. \tag{26}$$

In order to study the behavior of equations (23)–(26) in the limit $t \Rightarrow \infty$, it is natural to introduce, for a fluid with small viscosity (such as air), the following renormalized variables:

$$\tau = \varepsilon t, \quad \tilde{r} = \sqrt{\varepsilon}\, r, \quad \varepsilon \equiv \frac{\nu}{LU} \ll 1, \tag{27}$$

where L, and U denote reference length and velocity, respectively. Let us consider a two–dimensional situation with no dependence on z. Then, equation (25) becomes

$$\varepsilon \frac{\partial \zeta_z}{\partial \tau} + \left(\sqrt{\varepsilon}\, u_r \frac{\partial}{\partial \tilde{r}}\right) \zeta_z = \left(\sqrt{\varepsilon}\, \zeta_r \frac{\partial}{\partial \tilde{r}}\right) u_z + \left[\varepsilon\left(\frac{\partial^2}{\partial \tilde{r}^2} + \frac{1}{\tilde{r}} \frac{\partial}{\partial \tilde{r}}\right)\right] \zeta_z, \tag{28}$$

where

$$\zeta_z \equiv \frac{\partial u_\theta}{\partial r} + \frac{u_\theta}{r}.$$

Seeking solutions of the form

$$\begin{aligned} \zeta_z(\tilde{r}, \tau; \varepsilon) &= \sum_{n=0}^{\infty} \varepsilon^n \zeta_z^{(n)}(\tilde{r}, \tau), \\ u_r(\tilde{r}, \tau; \varepsilon) &= \sum_{n=1}^{\infty} \varepsilon^n u_r^{(n)}(\tilde{r}, \tau), \\ u_z(\tilde{r}, \tau; \varepsilon) &= \sum_{n=1}^{\infty} \varepsilon^n u_z^{(n)}(\tilde{r}, \tau), \end{aligned} \tag{29}$$

we obtain from equation (28)

$$\left(\frac{\partial}{\partial \tau} - \left\{\frac{\partial^2}{\partial \tilde{r}^2} + \frac{1}{\tilde{r}} \frac{\partial}{\partial \tilde{r}}\right\}\right) \zeta_z^{(0)} = 0. \tag{30}$$

In order to solve equation (30), let us consider the initial–value problem:

$$\frac{\partial^2 \xi}{\partial x^2} + \frac{\partial^2 \xi}{\partial y^2} = \frac{1}{\nu} \frac{\partial \xi}{\partial t}, \tag{31}$$

$$t = 0: \quad \xi(x, y, t) = f(x, y). \tag{32}$$

Upon Fourier–transforming according to

$$\tilde{\xi}(k_1, k_2, t) = \frac{1}{2\pi} \int_{-\infty}^{\infty} \int_{-\infty}^{\infty} \xi(x, y, t)\, e^{-i(k_1 x + k_2 y)}\, dx dy, \tag{33}$$

$$\tilde{\xi}(x, y, t) = \frac{1}{2\pi} \int_{-\infty}^{\infty} \int_{-\infty}^{\infty} \tilde{\xi}(k_1, k_2, t)\, e^{i(k_1 x + k_2 y)} dk_1 dk_2, \tag{34}$$

equation (31) gives

$$-\left(k_1^2+k_2^2\right)\tilde{\xi}=\frac{1}{\nu}\frac{\partial\tilde{\xi}}{\partial t}; \tag{35}$$

and when one uses equation (32), equation (35) gives

$$\tilde{\xi}\left(k_1,k_2,t\right)=\phi\left(k_1,k_2\right)e^{-\left(k_1^2+k_2^2\right)\nu t}, \tag{36}$$

where

$$\begin{aligned}\tilde{\xi}\left(k_1,k_2,0\right)&=\frac{1}{2\pi}\int_{-\infty}^{\infty}\int_{-\infty}^{\infty}\xi(x,y,0)e^{-i\left(k_1x+k_2y\right)}\,dxdy\\&=\frac{1}{2\pi}\int_{-\infty}^{\infty}\int_{-\infty}^{\infty}f(x,y)e^{-i\left(k_1x+k_2y\right)}\,dxdy\\&\equiv\tilde{f}\left(k_1,k_2\right).\end{aligned} \tag{37}$$

Thus,

$$\begin{aligned}\xi(x,y,t)&=\int_{-\infty}^{\infty}\int_{-\infty}^{\infty}\frac{dk_1dk_2}{2\pi}e^{i\left(k_1x+k_2y\right)}\\&\quad\times\int_{-\infty}^{\infty}\int_{-\infty}^{\infty}dx'dy'f(x',y')e^{-i\left(k_1x'+k_2y'\right)-\left(k_1^2+k_2^2\right)\nu t}\\&=\int_{-\infty}^{\infty}\int_{-\infty}^{\infty}dx'dy'\,f(x',y')\frac{\exp\left[-\dfrac{(x-x')^2+(y-y')^2}{4\nu t}\right]}{4\pi\nu t}.\end{aligned} \tag{38}$$

Using equation (38), we obtain for equation (30), on reverting to the original variables, and letting

$$t=0:\quad\zeta_z^{(0)}=f(r),\qquad r<a, \tag{39}$$

the following solution:

$$\zeta_z(r,t)=\int_0^a 2\pi r'dr'f(r')G(r,t;r')+0(\varepsilon), \tag{40}$$

where the Green's function $G(r,t;t')$ is given by

$$G(r,t;t')=\frac{1}{2\pi}\int_{\theta}^{\theta+2\pi}\frac{\exp\left[-\dfrac{r^2+r'^2-2rr'\cos(\theta-\theta')}{4\nu t}\right]}{4\pi\nu t}\,d\theta'. \tag{41}$$

Note that because

$$\int_{\theta}^{\theta+2\pi} \exp\left[\frac{2rr'\cos(\theta-\theta')}{4\nu t}\right] d\theta' = 2\int_{0}^{\pi} \exp\left(\frac{rr'\cos\sigma}{2\nu t}\right) d\sigma = 2\pi I_0\left(\frac{rr'}{2\nu t}\right), \quad (42)$$

(41) becomes

$$G(r,t;r') = \frac{1}{4\pi\nu t} I_0\left(\frac{rr'}{2\nu t}\right) \exp\left(-\frac{r^2+r'^2}{4\nu t}\right), \quad (43)$$

where $I_0(z)$ is a modified Bessel function of the first order 0.

For a localized vorticity distribution, if the point of observation lies in the far field, one may expand the quantity

$$I_0\left(\frac{rr'}{2\nu t}\right)\exp\left(-\frac{r^2+r'^2}{4\nu t}\right)$$

as follows:

$$I_0\left(\frac{rr'}{2\nu t}\right)\exp\left(-\frac{r^2+r'^2}{4\nu t}\right) = \exp\left(-\frac{r^2}{4\nu t}\right) + \frac{r^2r'^2}{16\nu^2t^2}\exp\left(-\frac{r^2}{4\nu t}\right) + 0\left(\frac{1}{t^3}\right). \quad (44)$$

Then, (40) can be written as

$$\zeta_z(r,t) = \frac{\left[\int_0^a 2\pi r'dr'f(r')\right]}{4\pi\nu t}\exp\left(-\frac{r^2}{4\nu t}\right) + \frac{\left[\int_0^a 2\pi r'^3dr'f(r')\right]}{64\pi\nu^3t^3}\exp\left(-\frac{r^2}{4\nu t}\right) + 0\left(\frac{1}{t^4}\right), \quad (45)$$

so that $t \Rightarrow \infty$, the diffusion of a localized vorticity distribution corresponds to that of a line vortex filament at the origin with strength equal to the total vorticity. Further, in the limit $t \Rightarrow \infty$, any lack of symmetry does not show up at the leading term but in the higher–order terms.

Note that if one assumes then, in fact, only a single vortex filament at the origin, at $t = 0$, i.e.,

$$f(r) = \Gamma_0\delta(r), \quad (46)$$

where Γ_0 denotes the circulation about the sigle vortex filament, then in the limit $t \Rightarrow \infty$ we have from (45)

$$\zeta_z(r,t) = \frac{\Gamma_0}{4\pi\nu t}\exp\left(-\frac{r^2}{4\nu t}\right), \quad (47)$$

from which the circulation is given by

$$\Gamma(r,t) = 2\pi\int_0^r \zeta_z r dr = \Gamma_0\left[1-\exp\left(-\frac{r^2}{4\nu t}\right)\right]. \quad (48)$$

The azimuthal velocity is then given by

$$u_\theta(r,t)=\frac{\Gamma}{2\pi r}=\frac{\Gamma_0}{2\pi r}\left[1-\exp\left(-\frac{r^2}{4\nu t}\right)\right], \tag{49}$$

which is the same as that given in (14).

Flow Due to a Suddenly Accelerated Plane

Consider a semi-infinite region of stationary fluid which is bounded by a rigid plane given by $y=0$. The plane is suddenly given a velocity U in its own plane, and thereafter maintained at that velocity. The viscous stresses at the plane set the fluid into motion, which is governed by

$$\frac{\partial u}{\partial t}=\nu\frac{\partial^2 u}{\partial y^2} \tag{50}$$

with the following initial and boundary conditions:

$$t\le 0:\quad u=0 \tag{51}$$

$$\begin{aligned} t>0;\quad y=0:&\quad u=U\\ y\Rightarrow\infty:&\quad u\Rightarrow 0 \end{aligned} \tag{52}$$

where u is the fluid velocity component in the direction of motion of the plane.

When we introduce the similarity variables

$$u=Uf(\eta),\qquad \eta=\frac{y}{2\sqrt{\nu t}}, \tag{53}$$

(50)–(52) give

$$f''+2\eta f'=0, \tag{54}$$

$$\left.\begin{aligned} \eta=0:&\quad f=1,\\ \eta\Rightarrow\infty:&\quad f\Rightarrow 0. \end{aligned}\right\} \tag{55}$$

The boundary–value problem (54) and (55), has the solution

$$f(\eta)=1-\frac{2}{\sqrt{\pi}}\int_0^\eta e^{-\eta^2}d\eta. \tag{56}$$

Therefore,

$$u=U\left[1-\frac{2}{\sqrt{\pi}}\int_0^\eta e^{-\eta^2}d\eta\right]. \tag{57}$$

Note that the vorticity corresponding to this velocity field is given by

$$\zeta(y,t)=\frac{\partial u}{\partial y}\sim\frac{1}{\sqrt{\nu t}}\exp\left(-\frac{y^2}{4\nu t}\right). \tag{58}$$

If initially the vorticity is concentrated in a thin layer of thickness δ near the plane (which will be due to the discontinuity in the tangential velocity arising

near the boundary at $t = 0$), then from the conservation of vorticity in the flow we have

$$\zeta(0,t) \cdot \delta = \frac{\delta}{\sqrt{\nu t}} = \int_0^\infty \zeta(y,t)\, dy. \tag{59}$$

When one uses (58), (59) gives

$$\frac{\delta}{\sqrt{\nu t}} = \sqrt{\pi}, \tag{60}$$

from which

$$\frac{d\delta}{dt} = \frac{1}{2}\sqrt{\frac{\pi\nu}{t}}. \tag{61}$$

Equation (61) gives the rate at which the vorticity, initially concentrated near the plane, diffuses into the flow. Note that the rate of diffusion decreases at t increases, because the velocity gradient and its spatial rate of change becomes progressively smaller.

For the flow due to a plane set impulsively into an oscillation, we have the following initial and boundary conditions:

$$\begin{aligned} &t \le 0: \quad u = 0 \\ &t > 0;\ y = 0: \quad u = U\cos\omega t \\ &\qquad y \Rightarrow \infty: \quad u \Rightarrow 0. \end{aligned} \tag{62}$$

Equation (62), in conjunction with equation (50), leads to the following steady periodic state –

$$u(y.t) = U\exp\left(-\sqrt{\frac{\omega}{2\nu}}\, y\right)\cos\left(\omega t - \sqrt{\frac{\omega}{2\nu}}\, y\right). \tag{63}$$

Notice the phase lag in the fluid motion caused by the viscous effects. Equation (63) also exhibits clearly the intrinsic damping due to viscosity.

The Round Laminar Jet: Landau's Solution

We discuss here an exact solution for the case of axial symmetry. The calculated flow turns out to be a round laminar jet emerging from an orifice.

In spherical coordinates (r, θ, ϕ) with θ measured from the axis of the jet, one has

$$\frac{1}{r^2}\frac{\partial}{\partial r}\left(r^2 u\right) + \frac{1}{r\sin\theta}\frac{\partial}{\partial\theta}(\sin\theta \cdot v) = 0, \tag{64}$$

$$u\frac{\partial u}{\partial r} + \frac{v}{r}\frac{\partial u}{\partial\theta} - \frac{v^2}{r} = -\frac{1}{\rho}\frac{\partial p}{\partial r} + \nu\left(\nabla^2 u - \frac{2u}{r^2} - \frac{2}{r^2}\frac{\partial v}{\partial\theta} - \frac{2v\cot\theta}{r^2}\right), \tag{65}$$

$$u\frac{\partial v}{\partial r}+\frac{v}{r}\frac{\partial v}{\partial \theta}+\frac{uv}{r}=-\frac{1}{\rho r}\frac{\partial p}{\partial \theta}+\nu\left(\nabla^2 v+\frac{2}{r^2}\frac{\partial u}{\partial \theta}-\frac{v}{r^2\sin^2\theta}\right), \tag{66}$$

where the fluid velocity $\mathbf{v}$ has components $\mathbf{v}=(u,v,0)$, and

$$\nabla^2=\frac{1}{r^2}\frac{\partial}{\partial r}\left(r^2\frac{\partial}{\partial r}\right)+\frac{1}{r^2\sin\theta}\frac{\partial}{\partial \theta}\left(\sin\theta\frac{\partial}{\partial \theta}\right).$$

Let the stream function be written as

$$\Psi=\nu r f(\theta). \tag{67}$$

The fluid velocity components are then given by

$$\left.\begin{aligned} u&=\frac{1}{r^2\sin\theta}\frac{\partial \Psi}{\partial \theta}=-\frac{\nu}{r\sin\theta}f'(\theta),\\ v&=\frac{-1}{r\sin\theta}\frac{\partial \Psi}{\partial r}=-\frac{\nu}{r\sin\theta}f(\theta), \end{aligned}\right\} \tag{68}$$

so that

$$\left.\begin{aligned} \nabla^2 u&=\frac{1}{r^2\sin\theta}\frac{\partial}{\partial \theta}\left(\sin\theta\cdot\frac{\partial u}{\partial \theta}\right),\\ \nabla^2 v&=\frac{1}{r^2\sin\theta}\frac{\partial}{\partial \theta}\left(\sin\theta\cdot\frac{\partial v}{\partial \theta}\right), \end{aligned}\right\} \tag{69}$$

$$\frac{\partial u}{\partial r}=-\frac{u}{r},\qquad \frac{\partial v}{\partial r}=-\frac{v}{r}. \tag{70}$$

Using equations (68) and (69), we obtain from equation (64)

$$u+\frac{\partial v}{\partial \theta}+v\cot\theta=0. \tag{71}$$

When we use equations (68)–(71), equations (65) and (66) become

$$-\frac{u^2+v^2}{r}+\frac{v}{r}\frac{\partial u}{\partial \theta}=-\frac{1}{\rho}\frac{\partial p}{\partial r}+\frac{\nu}{r^2\sin\theta}\frac{\partial}{\partial \theta}\left(\sin\theta\cdot\frac{\partial u}{\partial \theta}\right), \tag{72}$$

$$\frac{v}{r}\frac{\partial v}{\partial \theta}=-\frac{1}{\rho r}\frac{\partial p}{\partial \theta}+\frac{\nu}{r^2}\frac{\partial u}{\partial \theta}. \tag{73}$$

We have from equation (73)

$$\frac{p-p_0}{\rho}=-\frac{v^2}{2}+\frac{\nu u}{r}+\frac{c_1}{r^2}, \tag{74}$$

where c_1 is an arbitrary constant.

When we use equation (74), equation (72) becomes

$$-\frac{u^2}{r}+\frac{v}{r}\frac{\partial u}{\partial \theta}=\frac{\nu}{r^2}\left[2u+\frac{1}{\sin\theta}\frac{\partial}{\partial \theta}\left(\sin\theta\cdot\frac{\partial u}{\partial \theta}\right)\right]+\frac{2c_1}{r^3}. \tag{75}$$

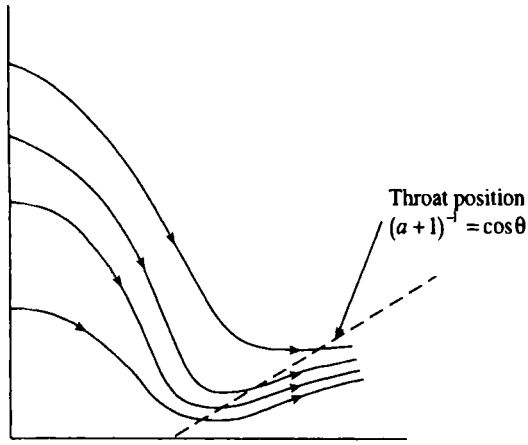

Figure 4.4. Steamline pattern for a jet issuing from a nozzle.

When we put

$$\mu = \cos\theta \tag{76}$$

and use equation (68), equation (75) gives

$$\left[f'(\mu)\right]^2 + f(\mu)f''(\mu) = 2f'(\mu) + \frac{d}{d\mu}\left[\left(1-\mu^2\right)f''(\mu)\right] - 2c_1. \tag{77}$$

Equation (77) can be integrated to give

$$ff' = 2f + \left(1-\mu^2\right)f'' - 2c_1\mu - c_2; \tag{78}$$

where c_2 is an arbitrary constant. Integrating equation (78) again, we obtain

$$f^2 = 4\mu f + 2\left(1-\mu^2\right)f' - 2\left(c_1\mu^2 + c_2\mu + c_3\right), \tag{79}$$

where c_3 is an arbitrary constant.

Now in order that the flow be free from singularities, one requires from (68) that

$$\mu \approx \pm 1 : f \sim \left(1 \mp \mu\right). \tag{80}$$

Using (80), we have from (79)

$$c_1, c_2, c_3 = 0 \tag{81}$$

Equation (79) then becomes

$$f = \frac{2\left(1-\mu^2\right)}{a+1-\mu} = \frac{2\sin^2\theta}{a+1-\cos\theta}, \tag{82}$$

where a is an arbitrary constant which determines the nature of the flow described by (67) and (82). Thus, when $a \gg 1$, the flow is symmetric about the plane $\theta = \pi/2$, and the flow becomes asymmetric about the latter plane when a is

reduced. Equation (82) can be interpreted as a jet (see Figure 4.4) issuing from a nozzle which coincides with one of the streamlines as far as its throat (whose position is given by $\cos\theta = 1/(a+1)$) and entraining slow-moving fluid outside the jet. In the limit, $a \ll 1$, the throat position corresponds to $\theta \approx 0$ so that the jet flow is sharply peaked around $\theta = 0$. In order to make this jet flow possible, it must be assumed, however, that a special frictional boundary condition is satisfied on the walls of the nozzle.

Ekman Layer at a Free Surface in a Rotating Fluid

Consider a fluid bounded by a horizontal free surface at which a uniform and constant stress μS is applied. This problem is of interest in connection with the drift at the surface of the sea due to wind blowing over it; the drift is found to occur somewhat to the right of the direction of the wind. Use a rectangular coordinate system rotating steadily with angular velocity Ω, with the z-axis along the vertical direction and with the x-axis in the direction of the stress applied at the surface. The fluid velocity associated with the flow generated by the latter can then be taken to lie in the horizontal plane everywhere and vary only in the vertical direction, so that the nonlinear convective derivative $(\mathbf{v}\cdot\nabla)\mathbf{v}$ vanishes identically. Then the equations of motion (see Section 2.6) give

$$-2v\Omega_z = -\frac{1}{\rho}\frac{\partial p}{\partial x} + \nu\frac{\partial^2 u}{\partial z^2}, \tag{83}$$

$$2u\Omega_z = -\frac{1}{\rho}\frac{\partial p}{\partial y} + \nu\frac{\partial^2 v}{\partial z^2}. \tag{84}$$

If geostropic flow prevails in the limit $z \Rightarrow -\infty$, we have from equation (83) and (84)

$$-2V\Omega_z = -\frac{1}{\rho}\frac{\partial p}{\partial x}, \tag{85}$$

$$2U\Omega_z = -\frac{1}{\rho}\frac{\partial p}{\partial y}. \tag{86}$$

Combining equations (85) and (86) with equations (83) and (84), we obtain

$$-2\hat{v}\Omega_z = \nu\frac{d^2 u}{dz^2}, \tag{87a}$$

$$2\hat{u}\Omega_z = \nu\frac{d^2 v}{dz^2}, \tag{87b}$$

where

$$\hat{u} \equiv u - U, \quad \hat{v} \equiv v - V.$$

The boundary conditions are

$$z=0:\quad \frac{d\hat{u}}{dz}=S,\quad \frac{d\hat{v}}{dz}=0,$$
$$z\Rightarrow-\infty:\quad \hat{u},\hat{v}\Rightarrow 0, \tag{88}$$

where Ω_z is the component of Ω along the z-axis.

One may write equation (87) and (88) in the form

$$\nu\frac{d^2(\hat{u}+i\hat{v})}{dz^2}=2i\Omega_z(\hat{u}+i\hat{v}), \tag{89}$$

from which

$$\hat{u}+i\hat{v}=\frac{S(1-i)}{2k}e^{k(1+i)z}, \tag{90}$$

where

$$k\equiv\sqrt{\frac{\Omega_z}{\nu}}.$$

We have from (90)

$$\left.\begin{aligned}\hat{u}&=\frac{S}{k\sqrt{2}}e^{kz}\cos\left(kz-\frac{\pi}{4}\right),\\ \hat{v}&=\frac{S}{k\sqrt{2}}e^{kz}\sin\left(kz-\frac{\pi}{4}\right),\end{aligned}\right\} \tag{91}$$

which are sketched in Figure 4.5.

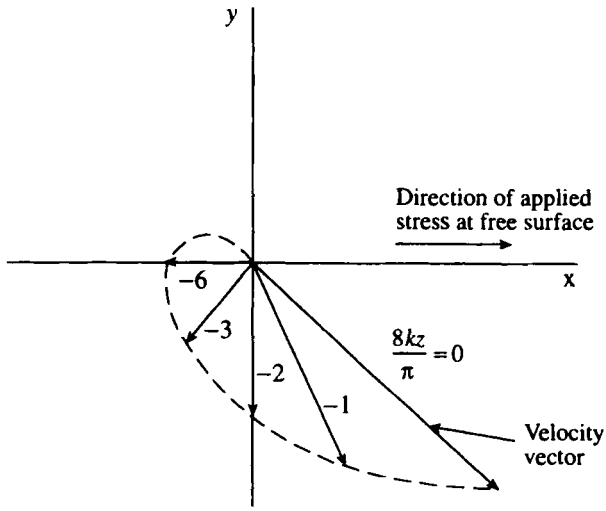

Figure 4.5. Variation of the velocity vector in the Ekman layer (from Batchelor, 1967).

Note that as the depth below the free surface increases, due to the Coriolis force, the direction of the velocity rotates uniformly in a clockwise sense (for $\Omega_z > 0$), and its magnitude falls off exponentially. This solution explains the observed discrepancy in movement between the sea current and floating pieces of ice.

Centrifugal Flow Due to a Rotating Disk

Consider a plane disk of large diameter which is made to rotate in its own plane with a steady angular velocity Ω in fluid which, at infinity, is rotating rigidly with a slightly smaller angular velocity Γ (the latter generalization is due to Batchelor). The relative motion of the disk and the fluid leads to viscous stresses, which tend to drag the fluid around with the disk. An exactly circular motion of fluid near the disk cannot occur because the enhanced centrifugal force near the disk is too great for the pressure gradient in the ambient fluid, and the fluid near the disk therefore spirals outward. This outward radial motion near the disk must lead to an axial motion toward the disk in order to ensure conservation of mass, and this prevents the vorticity generated at the boundary from spreading far from it. Thus, when the disk is rotating faster $(\Omega > \Gamma)$, the vorticity is confined to the vicinity of the rotating disk by convection toward the latter induced by the centrifugal action on the fluid near the disk.

Let us look for a solution of the form (an ansatz suggested by von Kármán)

$$\frac{u}{r}, \frac{v}{r}, w \sim \text{ functions of } z \text{ only}, \tag{92}$$

where (u, v, w) are velocity components parallel to the (r, φ, z) directions in a cylindrical coordinate system with $r = 0$ on the axis of the disk.

The equations of continuity and motion then give

$$\frac{2u}{r} + \frac{dw}{dz} = 0, \tag{93}$$

$$\frac{p}{\rho} = \nu \frac{dw}{dz} - \frac{1}{2} w^2 + \frac{1}{2} \Gamma r^2, \tag{94}$$

$$\left(\frac{u}{r}\right)^2 + w \frac{d(u/r)}{dz} - \left(\frac{v}{r}\right)^2 = \nu \frac{d^2(u/r)}{dz^2} - \Gamma^2, \tag{95}$$

$$\frac{2uv}{r^2} + w \frac{d(v/r)}{dz} = \nu \frac{d^2(v/r)}{dz^2}. \tag{96}$$

The boundary conditions are

$$\begin{aligned} z = 0: &\quad u = w = 0, \quad v = \Omega r, \\ z \Rightarrow \infty: &\quad u \Rightarrow 0, \quad v = \Gamma r. \end{aligned} \tag{97}$$

When we introduce the similarity variables

$$z=\left(\frac{\nu}{\Omega}\right)^{1/2}\zeta, \quad \frac{v}{r}=\Omega g(\zeta), \quad w=(\nu\Omega)^{1/2}h(\zeta), \tag{98}$$

equations (93)–(97) give

$$\frac{1}{2}h'^2-\frac{1}{2}hh''-g^2=-\frac{1}{2}h''-\left(\frac{\Gamma}{\Omega}\right)^2 \tag{99}$$

$$-gh'+g'h=g'', \tag{100}$$

$$\left.\begin{aligned}&\zeta=0: \quad h=h'=0, \quad g=1,\\ &\zeta\Rightarrow\infty: \quad h'\Rightarrow 0, \quad g\Rightarrow\frac{\Gamma}{\Omega},\end{aligned}\right\} \tag{101}$$

Let us look for solutions of the form

$$g=1+g_1, \quad |g_1|\ll 1; \tag{102}$$

we have, from equation (100), that

$$|h|\ll 1. \tag{103}$$

When we use (102) and (103) and linearize, equations (99)–(101) give

$$1+2g_1=\left(\frac{\Gamma}{\Omega}\right)^2+\frac{1}{2}h'', \tag{104}$$

$$-h'=g_1'', \tag{105}$$

$$\begin{aligned}&\zeta=0: \quad h=h'=g_1=0,\\ &\zeta\Rightarrow\infty: \quad h'\Rightarrow 0, \quad g_1\Rightarrow\frac{\Gamma}{\Omega}-1,\end{aligned} \tag{106}$$

from which

$$\left.\begin{aligned}g_1&=\frac{\Gamma-\Omega}{\Omega}\left(1-e^{-\zeta}\cos\zeta\right),\\ h'&=2\frac{\Gamma-\Omega}{\Omega}e^{-\zeta}\sin\zeta.\end{aligned}\right\} \tag{107}$$

Note from (107) that there is a net drift of fluid in the radial direction inwards when $\Gamma>\Omega$, and vice versa. Such a drift leads to an axial flow toward the disk if $\Gamma<\Omega$ and away from it if $\Gamma>\Omega$, as surmised before.[1]

In general, equations (99) and (100) in conjunction with the boundary conditions (101) may not have a solution (Evans) or have infinitely many solutions (Zandbergen and Dijkstra).

[1]Related to this problem is the so-called spin-up problem where an impulsive change in the rotation rate of a container of fluid leads to a boundary–layer–induced acceleration and inviscid pumping of the interior flow until a new steady state is attained.

Shock Structure: Becker's Solution

In Section 3.3, the theory of shock waves was given entirely in terms of an inviscid fluid. In a real fluid, as discussed in Section 3.7, however, the shock discontinuity gets spread out due to viscous and heat–conducting effects. Indeed, it turns out that the equations of conservation of mass, momentum, and energy for a perfect Newtonian gas (i.e., viscosity coefficient μ = constant) of Prandtl number $\Pr = \mu C_p / K = 3/4$ (K being the thermal conductivity) admit a smooth steady one–dimensional solution describing a shock transition in which the flow properties tend to the values corresponding to the uniform state at the limits $x \Rightarrow \pm\infty$.

The conservation equations for a one–dimensional flow are

$$\frac{d}{dx}(\rho u) = 0, \tag{108}$$

$$\rho u \frac{du}{dx} = -\frac{dp}{dx} + \frac{4\mu}{3}\frac{d}{dx}\left(\mu \frac{du}{dx}\right), \tag{109}$$

$$\rho u \frac{dh_0}{dx} = \frac{d}{dx}\left(K \frac{dT}{dx}\right) + \frac{4}{3}\frac{d}{dx}\left(\mu u \frac{du}{dx}\right), \tag{110}$$

where h_0 is the stagnation enthalpy fo the fluid. We have from equations (108)–(110)

$$\rho u = Q = \text{const.}, \tag{111}$$

$$\rho u^2 + p + \frac{4}{3}\mu \frac{du}{dx} = P = \text{const.}, \tag{112}$$

$$\left(h + \frac{1}{2}u^2\right)\rho u + \frac{4}{3}\mu u \frac{du}{dx} + K\frac{dT}{dx} = E = \text{const.} \tag{113}$$

When we use equation (111), equations (112) and (113) become

$$\frac{4}{3}\mu \frac{du}{dx} = P - Q\left(u + \frac{\gamma - 1}{\gamma}\frac{h}{u}\right), \tag{114}$$

$$\frac{K}{C_p}\frac{dh}{dx} + \frac{4}{3}\mu u \frac{du}{dx} = E - Q\left(h + \frac{1}{2}u^2\right). \tag{115}$$

If $\mu C_p / K = 3/4$, then (115) becomes

$$\frac{4}{3}\mu \frac{d}{dx}\left(h + \frac{1}{2}u^2\right) = E - Q\left(h + \frac{1}{2}u^2\right), \tag{116}$$

from which, on noting that

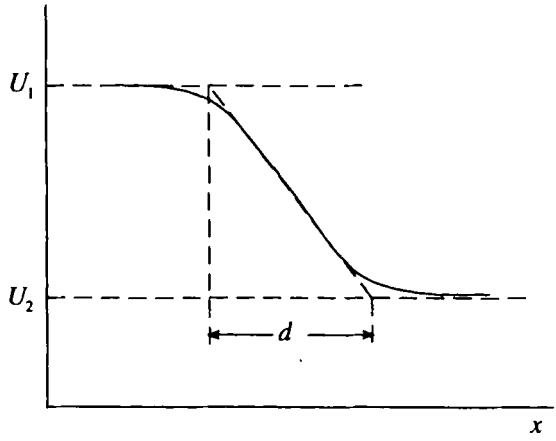

Figure 4.6. The shock structure.

$$x \Rightarrow \pm\infty : \frac{d}{dx}\left(h+\frac{1}{2}u^2\right) \Rightarrow 0,$$

we obtain

$$h+\frac{1}{2}u^2 = \frac{E}{Q}. \tag{117}$$

When we use (117), (114) becomes

$$\frac{4}{3}\mu\frac{du}{dx} = P - Q\left(\frac{\gamma+1}{2\gamma}u + \frac{\gamma-1}{\gamma}\frac{E}{Q}\frac{1}{u}\right). \tag{118}$$

Noting that

$$x \Rightarrow \pm\infty: \quad \frac{du}{dx} \Rightarrow 0,$$

we can write (115) as

$$\frac{4}{3}\mu\frac{du}{dx} = \frac{\gamma+1}{2\gamma}Q\frac{(u_1-u)(u-u_2)}{u}, \tag{119}$$

where

$$x \Rightarrow \pm\infty: \quad u \Rightarrow u_{1,2}.$$

On integration, (119) gives

$$u = \frac{1}{2}\left[(u_1+u_2)-(u_1-u_2)\tan h\left\{\frac{u_1-u_2}{\frac{3}{8}\left(\frac{\gamma+1}{\gamma}\right)\frac{Q}{\mu}}\left(x-\frac{u_1+u_2}{2}t\right)\right\}\right], \tag{120}$$

which is sketched in Figure 4.6. This solution describes a continuous variation between two asymptotic states

$$\left.\begin{aligned} x \Rightarrow -\infty: \quad u \Rightarrow u_1, \\ x \Rightarrow \infty \ : \quad u \Rightarrow u_2. \end{aligned}\right\}$$

Couette Flow of a Gas

Consider the plane flow of a viscous, heat–conducting gas between two infinite plates at $y = 0, L$, with the plate at $y = 0$ at rest and with the plate at $y = L$ moving with a constant velocity U_1 in its own plane.

Nondimensionalize the various flow variables as follows

$$\begin{aligned} &y' = \frac{y}{L}, \quad u' = \frac{u}{U_1}, \quad v' = \frac{v}{U_1}, \quad p' = \frac{p}{p_1}, \\ &T' = \frac{T}{T_1}, \quad \rho' = \frac{\rho}{\rho_1} = \frac{\rho}{p_1/RT_1}, \quad \mu' = \frac{\mu}{\mu_1}, \\ &C_p' = \frac{C_p}{C_{p_1}}, \quad K' = \frac{K}{K_1}, \end{aligned} \tag{121}$$

where the subscript 1 denotes the conditions at the wall at $y = L$.

The equations governing the flow are

$$\frac{d}{dy'}(\rho' v') = 0, \tag{122}$$

$$\frac{d}{dy'}\left(\mu' \frac{du'}{dy'}\right) = 0, \tag{123}$$

$$\frac{dp'}{dy'} = 0, \tag{124}$$

$$\frac{d}{dy'}\left(\frac{\mu' C_p'}{P_r}\frac{dT'}{dy'}\right) + (\gamma - 1) M_1^2 \mu' \left(\frac{du'}{dy'}\right)^2 = 0, \tag{125}$$

where $M_1^2 = U_1^2/\gamma RT_1$.

From equation (122), one obtains

$$v' \equiv 0; \tag{126}$$

from equation (124), one obtains

$$p' \equiv 1; \tag{127}$$

and from equation (123), one obtains

$$u' = \frac{\int_0^{y'} \frac{dy'}{\mu}}{\int_0^1 \frac{dy'}{\mu'}}. \tag{128}$$

When one uses equation (128), equation (125) gives

$$\frac{C_p'}{P_r}\frac{dT'}{dy'} + (\gamma - 1)\frac{M_1^2}{2}\frac{d(u'^2)}{dy'} = \frac{B'}{\mu'}, \tag{129}$$

from which

$$\frac{h'}{P_r} + \frac{(\gamma - 1)}{2} M_1^2 u'^2 = B_1 \int_0^{y'} \frac{dy'}{\mu'} + B_2. \tag{130}$$

When one uses the boundary conditions

$$\left.\begin{aligned} y' = 0: \quad & h' = h_\omega', \\ y' = 1: \quad & h' = h_1', \end{aligned}\right\} \tag{131}$$

equation (130) gives

$$h' = h_\omega' - \frac{(\gamma - 1)P_r M_1^2}{2} u'^2 + \left[(h_1' - h_\omega') + \frac{(\gamma - 1)}{2} M_1^2 P_r \right] u'. \tag{132}$$

EXERCISES

1. Calculate the steady flow between two infinitely long rotating circular cylinders of radii r_1, r_2 and angular speeds ω_1, ω_2.
2. Consider a fluid bounded by two rigid boundaries at $y = 0, d$, and initially at rest. The lower plate is suddenly brought to the steady velocity U in its own plane, the upper plate being held stationary. Calculate the subsequent motion of the fluid.
3. Calculate the motion generated from rest in the fluid contained within a circular cylinder of radius a, the cylinder being rotated with steady angular velocity Ω.

4.2. Flows at Low Reynolds Numbers

Motion of a body through a fluid at low Reynolds numbers, called *creeping flow*, is of relevance in many physical contexts, such as the settling of sediment in a liquid, and the fall of mist droplets in air. After all, high-school experiments use the Stokes formula to calculate the drag of an oil drop.

Dimensional Analysis

The Navier–Stokes equations for incompressible, viscous flows are

$$\nabla \cdot \mathbf{v} = 0, \tag{1}$$

$$\frac{D\mathbf{v}}{Dt} = -\frac{1}{\rho}\nabla p + \nu \nabla^2 \mathbf{v}. \tag{2}$$

The boundary conditions being that at a solid surface with which the fluid is in contact, there be a zero slip–velocity of the fluid relative to the solid surface.

Using the free–stream velocity U and a characteristic length L of the body placed in the flow, nondimensionalize the various flow variables as follows:

$$x^* = \frac{x}{L}, \quad t^* = \frac{tU}{L}, \quad \mathbf{v}^* = \frac{\mathbf{v}}{L}, \quad p^* = \frac{(p - p_\infty)L}{\mu U}, \tag{3}$$

where p_∞ is the free–steam pressure. Equations (1) and (2) then become

$$\nabla \cdot \mathbf{v}^* = 0, \tag{4a}$$

$$R_E \frac{D\mathbf{v}^*}{Dt^*} = -\nabla^* p^* + \nabla^{*2}\mathbf{v}^*, \tag{5}$$

where R_E is the Reynolds number:

$$R_E \equiv \frac{\rho UL}{\mu}.$$

Note from equation (5) that one has a low–Reynolds–number flow if the flow is very slow, if the body is very small, or if the fluid is very viscous. When $R_E \ll 1$ the viscous effects will dominate the convective effects, at least in the neighborhood of the body. On the mathematical side, note that such a limit also improves the solvability of the system (4) and (5), through the elimination of the nonlinear convective terms. Thus, in the limit $R_E \Rightarrow 0$, equations (4) and (5) describing the Stokes' flow become

$$\nabla \cdot \mathbf{v}^* = 0, \tag{4a}$$

$$\nabla^* p^* = \nabla^{*2}\mathbf{v}^*, \tag{6a}$$

and reverting to dimensional variables, we obtain

$$\nabla \cdot \mathbf{v} = 0, \tag{4b}$$

$$\nabla p = \mu \nabla^2 \mathbf{v}. \tag{6b}$$

Stokes' Flow Past a Rigid Sphere

Consider a uniform flow $-U\hat{i}_x$ past a rigid sphere of radius a centered at the origin. This problem is of interest in several physical contexts – e.g., the fall of mist droplets in air. Choose a coordinate system relative to which the fluid at

infinity is at rest and the origin of which instantaneously coincides with the center of the sphere; one then has the following boundary conditions

$$\mathbf{v} = U\hat{\mathbf{i}}_x \quad \text{at the body surface} \tag{7}$$
$$\mathbf{v} \Rightarrow \mathbf{0}, \qquad p - p_\infty \Rightarrow 0 \quad \text{at infinity.}$$

Note that $\mathbf{v}$ and $(p-p_\infty)/\mu$ must be symmetrical about the x–axis and that $\mathbf{v}$ lies in a plane through the x–axis. It follows that $(p-p_\infty)/\mu$ must be of the form $UxF(r^2/a^2)$, where $r = |\mathbf{x}|$. Noting from equations (4b) and (6b) that $(p-p_\infty)/\mu$ satisfies

$$\nabla^2\left(\frac{p-p_\infty}{\mu}\right) = 0, \tag{8}$$

and vanishes at infinity, it can be represented as a series of spherical solid harmonics of negative degree in r. Next, the only term of this series that is compatible with form $(p-p_\infty)/\mu = UxF(r^2/a^2)$ is of degree 2 (which corresponds to a *dipole*), so that

$$\frac{p-p_\infty}{\mu} = C\frac{Ux}{r^3}. \tag{9}$$

Further, noting from equation (6b) that the vorticity $\boldsymbol{\Omega} = \nabla \times \mathbf{v}$ satisfies

$$\nabla^2\boldsymbol{\Omega} = \mathbf{0} \tag{10}$$

and vanishes at infinity, and from equation (6b) that

$$\nabla p = \mu\nabla \times \boldsymbol{\Omega}, \tag{11}$$

we obtain

$$\boldsymbol{\Omega} = C\frac{U\hat{\mathbf{i}}_x \times \mathbf{x}}{r^3}. \tag{12}$$

Using a spherical–polar coordinate system (r, θ, ϕ) with the polar axis along the x–axis, we have

$$\Omega_\phi = \frac{1}{r}\frac{\partial(rv_\theta)}{\partial r} - \frac{1}{r}\frac{\partial v_r}{\partial \theta}, \tag{13}$$

where $\mathbf{v} = (v_r, v_\theta, v_\phi)$.

Introducing the stream function Ψ for the axisymmetric flow under consideration,

$$v_r = \frac{1}{r^2\sin\theta}\frac{\partial\Psi}{\partial\theta}, \quad v_\theta = -\frac{1}{r\sin\theta}\frac{\partial\Psi}{\partial r}, \tag{14}$$

and using (12), we obtain from (13)

$$\frac{\partial^2 \Psi}{\partial r^2} + \frac{\sin\theta}{r^2}\frac{\partial}{\partial \theta}\left(\frac{1}{\sin\theta}\frac{\partial \Psi}{\partial \theta}\right) = -C\frac{U\sin^2\theta}{r}. \tag{15}$$

When we put

$$\Psi = f(r)\cdot U\sin^2\theta, \tag{16}$$

equation (15) gives

$$\frac{d^2 f}{dr^2} - \frac{2f}{r^2} = -\frac{C}{r}, \tag{17}$$

from which

$$f(r) = \frac{1}{2}Cr + \frac{A}{r} + Br^2. \tag{18}$$

From (14) and (16), we then obtain

$$\boldsymbol{v} = U\hat{\boldsymbol{i}}_x\left(\frac{1}{r}\frac{df}{dr}\right) + \boldsymbol{x}\frac{Ux}{r^2}\left(\frac{2f}{r^2} - \frac{1}{r}\frac{df}{dr}\right). \tag{19}$$

The boundary conditions (7) give

$$\begin{aligned} r = a: \quad & v_r = U\cos\theta \\ & v_\theta = -U\sin\theta \\ r \Rightarrow \infty: \quad & v_r, v_\theta \Rightarrow 0. \end{aligned} \tag{20}$$

Equations (18)–(20) give

$$B = 0, \qquad A = \frac{a^3}{2} - \frac{Ca^2}{2}, \qquad C = \frac{3a}{2}. \tag{21}$$

Thus,

$$\Psi = Ur^2\sin^2\theta\cdot\left(\frac{3a}{4r} - \frac{a^3}{4r^3}\right), \tag{22}$$

from which

$$\begin{aligned} v_r &= -2\left(\frac{Ua^3}{4r^3} - \frac{3Ua}{4r}\right)\cos\theta, \\ v_\theta &= -\left(\frac{Ua^3}{4r^3} + \frac{3Ua}{4r}\right)\sin\theta. \end{aligned} \tag{23}$$

The streamline pattern given by (22) is shown in Figure 4.7. The steamlines are symmetric about the equatorial plane normal to the x–axis.

The resultant force acting on the surface of the sphere is, by symmetry, in the x–direction and is given by

$$F = 2\pi a^2 \int_0^\pi \tau_{rx}\sin\theta\cdot d\theta, \tag{24}$$

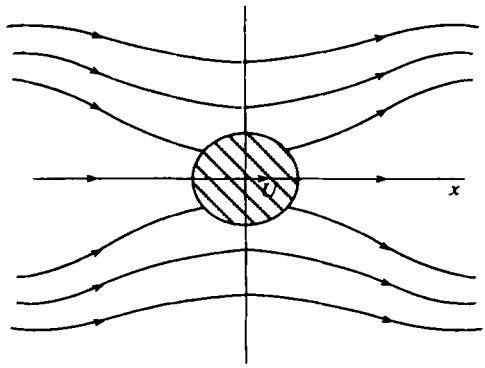

Figure 4.7. Stokes' flow past a sphere.

where

$$\tau_{rx} = \tau_{rr}\cos\theta - \tau_{r\theta}\sin\theta$$
$$= \left(-p + 4\mu\frac{\partial v_r}{\partial r}\right)\cos\theta - \mu\left[r\frac{\partial}{\partial r}\left(\frac{v_\theta}{r}\right) + \frac{1}{r}\frac{\partial v_r}{\partial \theta}\right]\sin\theta. \qquad (25)$$

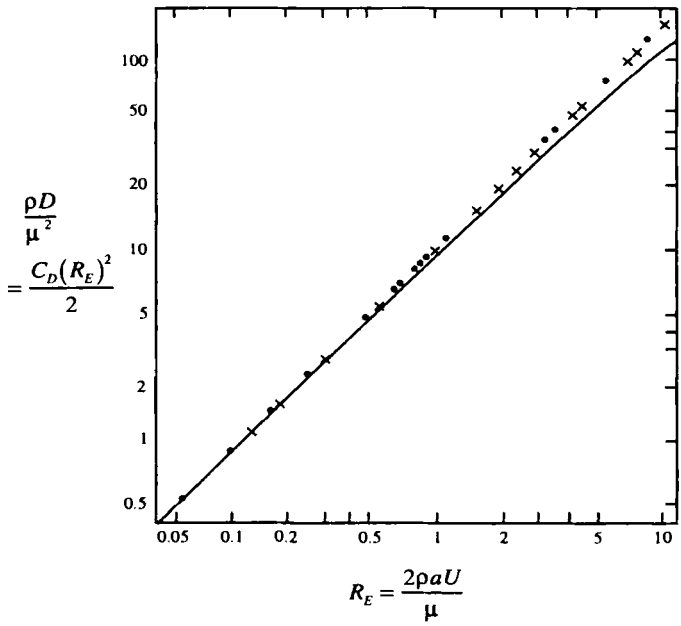

Figure 4.8. Drag on a sphere at low Reynolds numbers. Experimental points from Liebster (1927) (×) and Schmiedel (1928) (•), both using the falling sphere method. The line represents equation (26), plotted by Tritton (1988).

When we use (9), (21), (23), and (25), (24) gives

$$F = \frac{3}{2}\pi\mu a^5 U \int_0^{\pi} \left[\frac{\partial}{\partial r}\left(\frac{1}{r^3}\right)\right] \sin^3\theta \, d\theta = 6\pi\mu a U. \tag{26}$$

Figure 4.8 shows a comparison of (26) with experimental observations. Departures from Stokes' law (26) are observed to occur when the Reynolds number becomes high.

An obvious application of Stokes' formula (26) is in determining the coefficient of viscosity by measuring the drag of small spheres dropped in the fluid. Millikan's famous oil drop experiment to determine the charge on an electron was a case in point.

Stokes' Flow Past a Spherical Drop

Consider a spherical drop of radius a translating with velocity U in a fluid. We suppose that the two fluids are immiscible and that the surface tension at the interface is sufficiently strong to keep the drop approximately spherical against the deforming tendencies of viscous forces. Let the motion both outside and inside the drop occur at small Reynolds number. One determines the solution for the flow outside the drop as in the previous section except that the boundary conditions are now somewhat different. One has inside the drop (denoted by circumflex)

$$\nabla \cdot \hat{\mathbf{v}} = 0, \tag{27}$$

$$\nabla \hat{p} = \mu \nabla \times \hat{\boldsymbol{\Omega}}, \tag{28}$$

$$\nabla^2 \hat{p} = 0, \quad \nabla^2 \hat{\boldsymbol{\Omega}} = \mathbf{0}. \tag{29}$$

The boundary conditions are now

$$\hat{\mathbf{v}} \text{ and } (\hat{p} - p_\infty) \quad \text{finite inside the drop,} \tag{30}$$

$$r = a : \hat{\boldsymbol{n}} \cdot \mathbf{v} = \hat{\boldsymbol{n}} \cdot \hat{\mathbf{v}} = \hat{\boldsymbol{n}} \cdot \boldsymbol{U}, \tag{31}$$

$$\hat{\boldsymbol{n}} \times \mathbf{v} = \hat{\boldsymbol{n}} \times \hat{\mathbf{v}}, \tag{32}$$

$$\hat{\boldsymbol{n}} \times (\hat{\boldsymbol{n}} \cdot \boldsymbol{\tau}) = \hat{\boldsymbol{n}} \times (\hat{\boldsymbol{n}} \cdot \hat{\boldsymbol{\tau}}), \tag{33}$$

where $\hat{\boldsymbol{n}}$ denotes the unit normal to the drop. Equation (31) and (32) imply that there can be no relative motion of the two fluids at the interface. Equation (33) sets forth the fact that the tangential stresses at the interface on the two sides are equal and opposite.

We obtain from equations (28) and (29)

$$\frac{\hat{p} - p_\infty}{\mu} = \hat{C}\boldsymbol{U} \cdot \boldsymbol{x}, \qquad \hat{\boldsymbol{\Omega}} = -\frac{1}{2}\hat{C}\boldsymbol{U} \times \boldsymbol{x}. \tag{34}$$

Introducing the stream function Ψ,

$$\Psi = \hat{f}(r) \cdot U \sin^2 \theta, \tag{35}$$

and proceeding as in the previous section, we obtain

$$\hat{f}'' - \frac{2\hat{f}}{r^2} = \frac{1}{2}\hat{C}r^2, \tag{36}$$

from which

$$\hat{f} = \frac{1}{20}\hat{C}r^4 + \frac{\hat{A}}{r} + \hat{B}r^2. \tag{37}$$

Removal of the singularity at $r = 0$ requires $\hat{A} = 0$. Using (35) and (37), we then obtain from the kinematic condition (31)

$$\hat{B} = \frac{1}{2} - \frac{1}{20}\hat{C}a^2. \tag{38}$$

Thus,

$$\boldsymbol{v} = \boldsymbol{U} - \frac{1}{10}\hat{C}\left[\boldsymbol{U}\left(a^2 - 2r^2\right) + \boldsymbol{x}(\boldsymbol{U}\cdot\boldsymbol{x})\right]. \tag{39}$$

When we use (16), (19), (22), and (39), (32) gives

$$C - \frac{1}{2}a = \frac{1}{10}\hat{C}a^3 + a. \tag{40}$$

Next, the ith component of the force per unit area exerted on the drop at the position $\boldsymbol{x} = a\hat{\boldsymbol{n}}$ is given by

$$\begin{aligned}
\left(\hat{n}_j \tau_{ij}\right)_{r=a} &= \hat{n}_j\left[-p\delta_{ij} + \mu\left(\frac{\partial v_i}{\partial x_j} + \frac{\partial v_j}{\partial x_i}\right)\right]_{r=a} \\
&= \left[-p\hat{n}_i + \mu\hat{n}_i U\cdot\hat{n}\left(-\frac{f''}{r} + \frac{6f'}{r^2} - \frac{10f}{r^3}\right)\right. \\
&\qquad \left. + \mu U_i\left(\frac{f''}{r} - \frac{2f'}{r^2} + \frac{2f}{r^3}\right)\right]_{r=a} \\
&= n_i\left[-p_0 + 3\mu\frac{\boldsymbol{U}\cdot\hat{\boldsymbol{n}}}{a}\left(\frac{2C}{a} - 3\right)\right] + 3\mu\frac{U_i}{a}\left(1 - \frac{C}{a}\right).
\end{aligned} \tag{41}$$

Then, (33) gives

$$\frac{3\mu}{2}(a - C) = \frac{3}{10}\hat{\mu}a\hat{C}. \tag{42}$$

From (40) and (42), we obtain

$$C = \frac{1}{2}a\frac{2\mu + 3\hat{\mu}}{\mu + \hat{\mu}}, \quad \hat{C} = -\frac{5}{a^2}\frac{\mu}{\mu + \hat{\mu}}. \tag{43}$$

The drag force exerted on the drop by the external flow is then given by

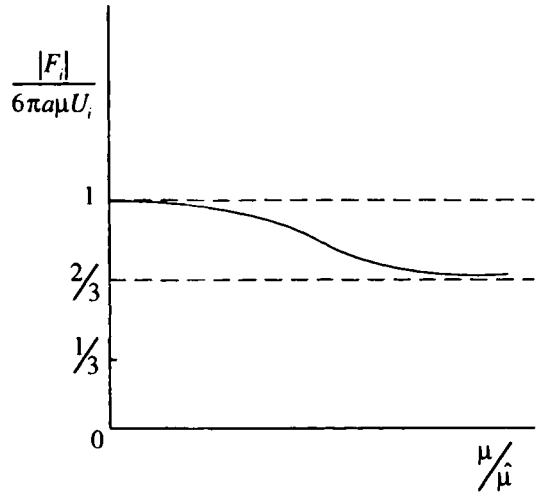

Figure 4.9. Variation of drag force with viscosity of the fluid in the drop.

$$F_i = \int_0^{2\pi} \hat{n}_j \left(\tau_{ij}\right)_{r=a} a d\theta$$

$$= -4\pi\mu U_i C = -6\pi a\mu U_i \left[\frac{1+\frac{2}{3}\left(\mu/\hat{\mu}\right)}{1+\left(\mu/\hat{\mu}\right)}\right]. \tag{44}$$

The dependence of $|F_i|$ on $(\mu/\hat{\mu})$ is sketched in Figure 4.9. Note that the case of the flow past a rigid sphere is recovered in the limit $\mu/\hat{\mu} \Rightarrow 0$. The case of a gas bubble moving through the liquid corresponds to $\mu/\hat{\mu} \Rightarrow \infty$.

Stokes' Flow Past a Rigid Circular Cylinder

Consider a circular cylinder of radius a moving with a velocity U in the x–direction normal to its axis in a fluid. The flow is now two–dimensional. Using the cylindrical–polar coordinates (r, θ), one has, like in equations (9) and (12),

$$\frac{p - p_\infty}{\mu} = C\frac{Ux}{r^2}, \qquad \boldsymbol{\Omega} = C\frac{U\hat{i}_x \times \boldsymbol{x}}{r^2}. \tag{45}$$

Then,

$$\Omega_z = \left[r\frac{\partial}{\partial r}\left(\frac{v_\theta}{r}\right) - \frac{\partial v_r}{r\partial\theta}\right] \tag{46}$$

gives upon using

$$v_r = \frac{\partial \Psi}{r \partial \theta}, \qquad v_\theta = -\frac{\partial \Psi}{\partial r}, \tag{47}$$

$$\Psi = f(r) \cdot U \sin\theta \tag{48}$$

the following equation for $f(r)$,

$$\frac{d^2 f}{dr^2} + \frac{1}{r}\frac{df}{dr} - \frac{f}{r^2} = -\frac{C}{r}, \tag{49}$$

from which

$$f(r) = -\frac{1}{2} Cr \ln r + Ar + \frac{B}{r}. \tag{50}$$

The boundary conditions are

$$r = a: \quad \frac{f}{r} = 1, \quad \frac{df}{dr} = 1, \tag{51}$$

$$r \Rightarrow \infty: \quad \frac{f}{r} \Rightarrow 0. \tag{52}$$

When one uses (50), (51) requires

$$A = 1 + \frac{C}{4} + \frac{C}{2} \ln a, \qquad B = -\frac{a^2 C}{4}. \tag{53}$$

But, when one uses (53) in (50), (52) shows that no choice of C satisfies the upstream–infinity condition. Thus the above solution is not valid at infinity. That is, for two–dimensional flow of an unbounded fluid past a body, solutions of the Stokes equations satisfying the proper conditions do not exist; this is called *Stokes' paradox*. This is simply due to the fact that the Stokes approximation (of ignoring the convective terms in equation (5)) is not valid uniformly in space. There is thus a region in which inertia forces are significant, and this region gets closer to the cylinder as the Reynolds number increases. The remedy for this is to go back and include the convective terms in equation (5) in at least some approximate form; one then obtains the so–called Oseen flow.

Oseen's Flow Past a Rigid Sphere

The Oseen equations are obtained by linearizing the Navier–Stokes equations (1) and (2) about the free–stream velocity say $\mathbf{v}_\infty = U\hat{i}_x$. (By constrast, the Stokes equations can be viewed as a linearization about zero velocity.) Therefore, Oseen's equations are more accurate than Stokes' equations in the region away from the sphere where the flow velocity is close to the free–stream velocity. (Stokes' equations are accurate on the region near the sphere where the flow velocity is close to zero.) Thus,

$$\nabla \cdot \mathbf{v} = 0, \tag{54}$$

$$\frac{\partial \mathbf{v}}{\partial t} + U\frac{\partial \mathbf{v}}{\partial x} = -\frac{1}{\rho}\nabla p + \nu\nabla^2\mathbf{v}. \tag{55}$$

Consider a sphere moving through a fluid with a velocity $U\hat{\mathbf{i}}_x$, and in the frame of reference moving with the body the flow is steady. One then has

$$\nabla \cdot \mathbf{v} = 0, \tag{56}$$

$$-U\frac{\partial \mathbf{v}}{\partial x} = -\frac{1}{\rho}\nabla p + \nu\nabla^2\mathbf{v}. \tag{57}$$

The boundary conditions are

$$\left.\begin{aligned} &r = a: \quad \mathbf{v} = U\hat{\mathbf{i}}_x, \\ &r \Rightarrow \infty: \quad \mathbf{v} \Rightarrow 0, \quad p - p_\infty \Rightarrow 0. \end{aligned}\right\} \tag{58}$$

We have from equations (56) and (57)

$$\nabla^2 p = 0. \tag{59}$$

When we put

$$\begin{aligned} p &= -\rho U\frac{\partial \phi}{\partial x}, \\ \mathbf{v} &= -\nabla\phi + \mathbf{v}', \end{aligned} \tag{60}$$

equations (57) and (59) give

$$\nabla^2\phi = 0, \tag{61}$$

$$\left(\nabla^2 + 2k\frac{\partial}{\partial x}\right)\mathbf{v}' = 0, \tag{62}$$

where

$$k \equiv \frac{U}{2\nu}.$$

Using the axisymmetric nature of the flow, we may write

$$\mathbf{v}' = \nabla\chi + 2k\chi\hat{\mathbf{i}}_x, \tag{63}$$

so that equation (62) gives

$$\nabla^2\chi = -2k\frac{\partial \chi}{\partial x}, \tag{64}$$

from which

$$\chi = \frac{C}{r}e^{k(r-x)}. \tag{65}$$

Let us now obtain an approximate solution by expanding ϕ and χ in series in descending powers of r. Thus we have from (65)

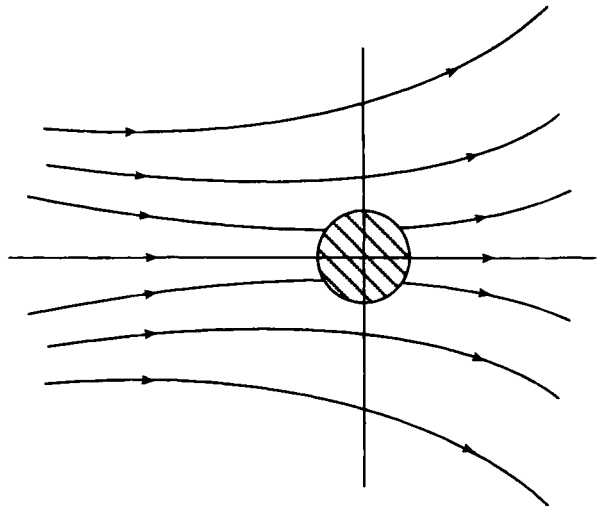

Figure 4.10. Oseen's flow past a sphere.

$$\chi = C\left(\frac{1}{r} + k - \frac{kx}{r} + \cdots\right), \tag{66}$$

and outside the sphere we obtain

$$\phi = \frac{A_0}{r} + \frac{A_1}{r^2} P_1(\cos\theta) + \frac{A_2}{r^3} P_2(\cos\theta) + \cdots \tag{67}$$

where the polar axis is taken along the direction of motion of the sphere, and

$$\cos\theta = \frac{x}{r}$$

and $P_n(\cos\theta)$ is Legendre's polynomial of order n.

Using (60), (63), (66), and (67) in (58), we obtain for $ka = Ua/2\nu \ll 1$

$$C = -\frac{3}{2}a\nu = A_0, \qquad A_1 = \frac{1}{4}Ua^3. \tag{68}$$

Noting

$$v_r = -\frac{\partial\phi}{\partial r} + \frac{\partial\chi}{\partial r} - 2k\chi\cos\theta,$$

$$\Psi = r^2 \int_0^\theta v_r \sin\theta \cdot d\theta \tag{69}$$

and using (65), (67), and (68), we obtain

$$\Psi = -\frac{Ua^3 \sin^2\theta}{4r} + \frac{3a\nu}{2}(1-\cos\theta)\left[1 - e^{-kr(1+\cos\theta)}\right]. \tag{70}$$

Near the sphere, where $kr \ll 1$, (70) gives

$$\Psi \approx \frac{3Ua}{4}\left(-\frac{a^2}{3r}+r\right)\sin^2\theta, \tag{71}$$

which agrees with the Stokes solution (22).

The streamline pattern given by (70) is sketched in Figure 4.10. Note that the streamlines are no longer symmetrical about the plane $\theta = \pi/2$. The flow tends to become radial far from the sphere as if it were created by a source of fluid at the sphere, except within a wake directly behind the sphere. Note that when $kr \gg 1$ the flow has different forms depending on whether as $(1+\cos\theta)$ is small or large compared with unity. For the latter case, we obtain from (70),

$$\Psi \sim Ua^2\frac{3}{4k}(1-\cos\theta), \tag{72}$$

which describes the radial flow from a source at the origin of strength $3\pi a^2 U/k$. For the former case (i.e., within the wake), we obtain from (70)

$$\Psi \sim \frac{3Ua^2}{2k}\left\{1-\exp\left[-\frac{r}{ka}(\pi-\theta)^2\right]\right\}. \tag{73}$$

Far from the sphere, the vorticity is zero in the source–flow region and is confined to the wake, whereas in the Stokes' approximation the vorticity diffuses out in all directions from the sphere.

Oseen's Approximation for Periodically Oscillating Wakes

Periodic oscillating flows are well described by von Kármán's classical theory of vortex sheets (see Section 2.4). In this theory, the motion of discrete vortices in a perfect fluid is considered. At considerable distances downstream, viscous forces must have had a significant influence on the vortices, so that Oseen's approximation may be applied.

Consider a small disturbance superposed on a uniform stream with velocity U. The linearized vorticity equation is

$$\frac{\partial\zeta}{\partial t}+U\frac{\partial\zeta}{\partial x}=\nu\left(\frac{\partial^2}{\partial x^2}+\frac{\partial^2}{\partial y^2}\right)\zeta, \tag{74}$$

where

$$\zeta \equiv (\partial v/\partial x)-(\partial u/\partial y).$$

Seeking solutions of the form

$$\zeta = f(x,y)e^{i\omega t}, \tag{75}$$

we obtain from equation (75)

$$\left(\frac{\partial^2}{\partial x^2}+\frac{\partial^2}{\partial y^2}\right)f=\frac{1}{\nu}\left(U\frac{\partial f}{\partial x}+i\omega f\right). \tag{76}$$

When we put

$$f(x,y)=e^{\alpha x}g(x,y), \tag{77}$$

where

$$\alpha\equiv\frac{U}{2\nu},$$

equation (76) gives

$$\left(\frac{\partial^2}{\partial x^2}+\frac{\partial^2}{\partial y^2}-k^2\right)g=0, \tag{78}$$

where

$$k^2\equiv\alpha^2(1+8\pi i\beta),\qquad \beta\equiv\frac{\nu\omega}{2\pi U^2}.$$

Thus,

$$g(x,y)=\sum_{n=0}^{\infty}\left(A_n\cos n\theta+B_n\sin n\theta\right)K_n(kr), \tag{79}$$

where

$$x=r\cos\theta,\qquad y=r\sin\theta;$$

and $K_n(kr)$ is the modified Bessel function, with

$$kr\Rightarrow\infty:\quad K_n(kr)\sim\sqrt{\frac{\pi}{2kr}}\,e^{-kr}.$$

When we use (77) and (79), (75) gives

$$\zeta(x,y,t)=e^{i\omega t+\alpha x}\sum_{n=0}^{\infty}K_n(kr)\left[A_n\cos n\theta+B_n\sin n\theta\right], \tag{80}$$

from which

$$kr\Rightarrow\infty:\quad \zeta(x,y,t)=\sqrt{\frac{\pi}{2kr}}\,e^{i\omega t+\alpha x-kr}\sum_{n=0}^{\infty}\left[A_n\cos n\theta+B_n\sin n\theta\right]. \tag{81}$$

This vorticity distribution vanishes very fast exponentially with increasing distance except when the real part of $(\alpha x-kr)$ is small. Now,

$$\mathrm{Re}(\alpha x-kr)\approx\alpha(x-r)=\alpha(\cos\theta-1)r$$

and is finite at large distances only for a parabolic region where θ is of the order of $\left(1/\sqrt{r}\right)$ – i.e., the wake. In this region, one may make the approximation

$$r \approx x, \quad \theta \approx \frac{y}{x}, \quad \alpha r(1-\cos\theta) \approx \frac{\eta^2}{2}, \quad \eta = y\sqrt{\frac{U}{2\nu x}},$$

so that (81) becomes

$$\zeta(x,y,t) = \frac{\exp\left(-\frac{\eta^2}{2}\right)}{\sqrt{x}} \exp\left[i\omega\left(t-\frac{x}{U}\right)\right]\left\{A + \frac{B\eta}{\sqrt{x}}\right\}. \tag{82}$$

Equation (82) has a symmetrical part

$$\zeta_s = \frac{A}{\sqrt{x}} \exp\left(-\frac{\eta^2}{2}\right) \exp\left[i\omega\left(t-\frac{x}{U}\right)\right]$$

and an antisymmetrical part

$$\zeta_a = \frac{B}{x}\,\eta \exp\left(-\frac{\eta^2}{2}\right) \exp\left[i\omega\left(t-\frac{x}{U}\right)\right].$$

We shall now discuss various flows represented by the superposition of such solutions.

1. For $\omega = 0$ the symmetrical part represents a steady shear flow with velocity difference

$$\Delta u = -\int_{-\infty}^{\infty} \zeta_s dy = -\sqrt{\frac{4\pi\nu}{U}}\, A$$

and

$$\Delta v \ll U.$$

2. For $\omega = 0$ the antisymmetrical part represents the wake solution with velocity distribution

$$u = \frac{B'}{\sqrt{x}} \exp\left(-\frac{\eta^2}{2}\right) \qquad B' = B\sqrt{\frac{2\nu}{U}}.$$

3. A double row of vortices arranged like the von Kármán vortex sheet may be represented by

$$\zeta = \frac{A}{\sqrt{x}} \exp\left[-\frac{1}{2}(\eta-\eta_0)^2\right]\left[1+\lambda \sin\omega\left(t-\frac{x}{U}\right)\right]$$
$$-\frac{A}{\sqrt{x}} \exp\left[-\frac{1}{2}(\eta-\eta_0)^2\right]\left[1-\lambda \sin\omega\left(t-\frac{x}{U}\right)\right],$$

where

$$\eta_0 = y_0\sqrt{\frac{U}{2\nu x}}.$$

For small values of x, the vortices are nearly discrete, and are located on the lines $y = \pm y_0$. The initial spacing between the two rows is

$$h_0 = 2y_0 = 2\eta_o \sqrt{\frac{2\nu x}{U}}.$$

Downstream it is

$$h = 2\eta \sqrt{\frac{2\nu x}{U}}.$$

Exercise

1. Show that in a slow, steady, two–dimensional flow of an incompressible viscous fluid, the stream function Ψ satisfies the biharmonic equation:

$$\nabla^4 \Psi = 0.$$

Further, deduce that $x\phi, y\phi$ and $\left(x^2 + y^2\right)\phi$ are solutions of this equation provided that $\phi(x, y)$ is a harmonic function.

2. Calculate the terminal velocity which a sphere would have when falling freely under gravity through a field.

3. Consider the low Reynolds number flow of a fluid between two parallel flat plates which are fixed at a small distance h apart (Hele–Shaw flow). Show that this flow is governed, to a leading approximation, by the following equations:

$$0 = -\frac{\partial p}{\partial x} + \nu \frac{\partial^2 u}{\partial z^2}$$

$$0 = -\frac{\partial p}{\partial y} + \nu \frac{\partial^2 v}{\partial z^2}$$

$$0 = \frac{\partial p}{\partial z}$$

$$\frac{\partial u}{\partial x} + \frac{\partial v}{\partial y} + \frac{\partial \omega}{\partial z} = 0,$$

with

$$z = 0 \text{ and } h: \quad u, v, \omega = 0.$$

Hence, show that

$$u = -\frac{1}{2\nu}\frac{\partial p}{\partial x} z(h - z), \quad v = -\frac{1}{2\nu}\frac{\partial p}{\partial y} z(h - z),$$

where

$$\frac{\partial^2 p}{\partial x^2} + \frac{\partial^2 p}{\partial y^2} = 0.$$

This leads to the mean velocity in the plane of the Hele–Shaw cell given by

$$\left.\begin{aligned} \bar{u} &= \int_0^h u\,dz = -\frac{h^2}{12\nu}\frac{\partial p}{\partial x}, \\ \bar{v} &= \int_0^h v\,dz = -\frac{h^2}{12\nu}\frac{\partial p}{\partial y}, \end{aligned}\right\}$$

which predicts that the mean velocity field for a Hele–Shaw flow corresponds to a potential flow in the two dimensions with the "mean" velocity potential given by $-h^3 p/12\nu$ satisfying the Laplace equation!

4.3. Flows at High Reynolds Numbers

For flows past streamlined bodies at large Reynolds numbers (i.e., in fluids of small viscosity), Prandtl proposed that one must recognize the effects of viscosity only in a thin layer–boundary layer adjacent to the body and that the rest of the flow may be considered inviscid. As a first approximtion, the inviscid–flow equations are solved with appropriate boundary conditions, ignoring the presence of the boundary layer. However, in general, the inviscid flow will not satisfy the condition of the no–slip of the fluid at the body, and it is necessary to introduce a boundary layer between the inviscid flow and the body to adjust the inviscid solution toward satisfying this condition on the body. Within the boundary layer, the flow is not irrotational since vorticity is generated along the surface of the body and is diffused across and convected along the boundary layer. Besides, the presence of the boundary layer helps one to explain the very common phenomenon of separation of flow at the rear of many bodies placed in the flow.

Prandtl's Boundary–Layer Concept

Certain qualitative features of boundary layers may be explained from considerations of the relative importance of convection and diffusion of vorticity generated at the surface of a body placed in a flow with velocity U. The mechanism for the generation of a sheet of concentrated vorticity at the surface of a body is provided by the no–slip condition at the body. This vorticity is convected downstream with a velocity of $0(U)$, and the problem of flow due to a suddenly accelerated plane (Section 4.1) showed that this vorticity will diffuse outward with an effective velocity $\sqrt{\nu/t}$. One may then expect that there will be an effective region of influence of vorticity called the boundary layer similar to the Mach cone in inviscid supersonic flows. The width of this region is approximately given by

$$\delta(x) \sim \frac{\sqrt{\nu/t}}{U}\, x \sim \frac{\sqrt{\nu U/x}}{U}\, x \sim \sqrt{\frac{\nu x}{U}}$$

or

$$\frac{\delta(x)}{L} \sim \sqrt{\frac{x}{L}}\sqrt{\frac{1}{R_E}},$$

where

$$R_E \equiv \frac{UL}{\nu}$$

and L is a characteristic length of body. Thus, for $R_E \gg 1$, the convective effects on the vorticity outweigh the diffusive effects on the latter, and consequently the vorticity layer is very thin relative to a typical dimension of the body. Such a layer is then called a boundary layer.

Downstream of the body the vorticity which has been carried by convection is essentially confined to a region called the wake, which at a distance d far downstream from the body has a width of $0(\sqrt{\nu d/U})$. Outside the wake and the vorticity layer near the body, the flow is essentially irrotational. Note that the boundary layer thickness δ increases as the square root of the distance from the leading edge of the plate because, as flow occurs past the plate, more and more fluid is retarded, besides there is no flow velocity component convecting vorticity toward the plate to counter diffusion of vorticity from it.

Prandtl's boundary–layer theory can be embedded in a systematic scheme of successive approximations via the method of matched asymptotic expansions. However, this solution, which is represented by an infinite series in powers of $R_E^{-1/2}$ (R_E being the Reynolds number), turns out to be asymptotic.

The Method of Matched Asymptotic Expansions

In cases where a small parameter multiplies the highest derivative in a differential equation there occurs a sharp change in the dependent variable in a certain region of the domain of the independent variable. In constructing a solution to the differential equaiton through uniformly valid expansions, one characterizes the sharp changes by a modified scale for the independent variable that is different from the scale characterizing the behavior of the dependent variable outside the *boundary–layer* regions. In other words, one represents the solution by two different asymptotic expansions using the independent variables x and x/ε, say; this is the method of matched asymptotic expansions. Since they are different asymptotic representations of the same function, they should be related to each other in a rational manner; this leads to the asymptotic matching principle (the latter makes also the two representations completely determinate).

Consider the problem

$$\varepsilon y'' + y' + y = 0, \quad 0 \le x \le 1, \quad \varepsilon \ll 1,$$
$$x = 0: \quad y = a,$$
$$x = 1: \quad y = b, \tag{1}$$

the exact solution of which is

$$y = \frac{\left(ae^{s_2} - b\right)e^{s_1 x} + \left(b - ae^{s_1}\right)e^{s_2 x}}{\left(e^{s_2} - e^{s_1}\right)}, \tag{2}$$

where

$$s_{1,2} = \frac{-1 \pm \sqrt{1 - 4\varepsilon}}{2\varepsilon}.$$

Equation (2) may be approximated by

$$y = be^{1-x} + (a - be)e^{x-(x/\varepsilon)} + 0(\varepsilon), \tag{3}$$

a form which is uniformly valid. Note that this expansion cannot be obtained keeping either x or x/ε fixed. In the former case, we obtain

$$y^{(0)} = be^{1-x} + 0(\varepsilon), \tag{4}$$

which is not valid in the boundary layer near $x = 0$ since

$$y^{(0)}(0) = be \neq a.$$

In the latter case, we obtain

$$y^{(i)}(1) = be + (a - be)e^{-x/\varepsilon} + 0(\varepsilon), \tag{5}$$

which is not valid as $x \Rightarrow 1$ since

$$y^{(i)}(1) = be \neq b;$$

$y, y^{(0)}$, and $y^{(i)}$ are sketched in Figure 4.11.

This suggests that we represent the solution by two different asymptotic expansions using the variables x and x/ε.

Thus, we seek an outer expansion

$$y^{(0)}(x;\varepsilon) = \sum_{n=0}^{N-1} \varepsilon^n y_n^{(0)}(x) + 0\left(\varepsilon^N\right), \tag{6}$$

where in accordance with the outer limit process we have

$$y_m^{(0)}(x) = \lim_{\substack{\varepsilon \Rightarrow 0 \\ x \text{ fixed}}} \frac{y^{(0)} - \sum_{n=0}^{m-1} \varepsilon^n y_n^{(0)}(x)}{\varepsilon^m}.$$

Substituting (6) in equation (1), and equating the coefficients of equal powers of ε, we obtain

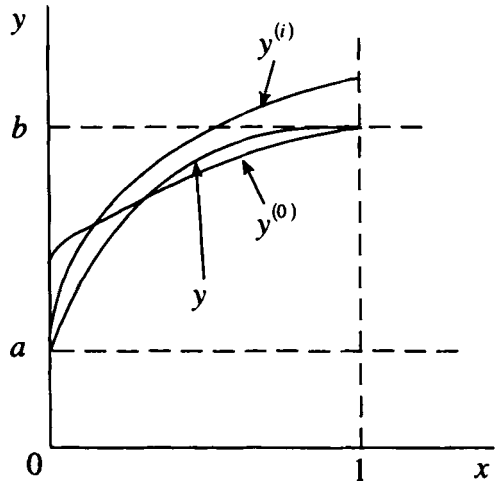

Figure 4.11. The inner, outer and composite solutions.

$$y_0^{(0)'} + y_0^{(0)} = 0$$
$$y_1^{(0)'} + y_1^{(0)} = -y_0^{(0)''}, \quad \text{etc.} \tag{7}$$

Notice that since a small parameter ε multiplies the highest derivative in equation (1), a regular perturbation scheme, such as (6), misses that derivative in the first approximation so that the order of the differential equation (1) is reduced. Therefore, the system (7) cannot, in general, take on both of the boundary conditions, and one of these boundary conditions, $y(0) = a$, should be dropped. This means that the outer solution (6) is valid everywhere except in the region $x = 0(\varepsilon)$, and we have

$$y_0^{(0)}(1) = b,$$
$$y_1^{(0)}(1) = 0, \quad \text{etc.} \tag{8}$$

Thus, we obtain

$$y_0^{(0)} = be^{1-x},$$
$$y_1^{(0)} = b(1-x)e^{1-x}, \quad \text{etc.}, \tag{9}$$

so that

$$y^{(0)} = b\left[1 + \varepsilon(1-x)\right] e^{1-x} + 0\left(\varepsilon^2\right). \tag{10}$$

For small ε this solution is close to the exact solution (3) everywhere, except in a small interval at $x = 0$, where the exact solution (3) changes rapidly (see Figure 4.11) in order to retrieve the boundary condition there which is about to be lost.

In order to determine an expansion valid in the boundary layer in $x = 0(\varepsilon)$, one magnifies the independent variable as

$$\xi = \frac{x}{\varepsilon}, \tag{11}$$

so that the size of the boundary–layer region then remains independent of ε as $\varepsilon \Rightarrow 0$ and the width of the boundary–layer region becomes of order unity. This artifice leads to the retention of the highest derivative in equation (1) as $\varepsilon \Rightarrow 0$, which is essential to represent the rapidly varying behavior of the solution in the boundary layer. When we use (11), equation (1) becomes

$$\frac{d^2y}{d\xi^2} + \frac{dy}{d\xi} + \varepsilon y = 0. \tag{12}$$

Now, let us seek an inner expansion,

$$y^{(i)}(\varepsilon\xi;\varepsilon) = \sum_{n=0}^{N-1} \varepsilon^n y_n^{(i)}(\xi) + 0(\varepsilon^N), \tag{13}$$

where, in accordance with the inner limit process, we have

$$y_m^{(i)}(\xi) = \lim_{\substack{\varepsilon \Rightarrow 0 \\ \xi \text{ fixed}}} \frac{y^{(i)} - \sum_{n=0}^{m-1} \varepsilon^n y_m^{(i)}(\xi)}{\varepsilon^m}. \tag{14}$$

Substituting (13) in equation (12) and equating the coefficients of equal powers of ε, we obtain

$$\begin{aligned} &\frac{d^2y_0^{(i)}}{d\xi^2} + \frac{dy_0^{(i)}}{d\xi} = 0, \\ &\frac{d^2y_1^{(i)}}{d\xi^2} + \frac{dy_1^{(i)}}{d\xi} = -y_0^{(i)}, \quad \text{etc.} \end{aligned} \tag{15}$$

Noting that the inner solution is valid only in the region $x = 0(\varepsilon)$, we have

$$\begin{aligned} &y_0^{(i)}(0) = a, \\ &y_1^{(i)}(0) = 0, \quad \text{etc.} \end{aligned} \tag{16}$$

Thus, we have

$$\begin{aligned} y_0^{(i)} &= a - A_0\left(1 - e^{-\xi}\right), \\ y_1^{(i)} &= A_1\left(1 - e^{-\xi}\right) - \left[a - A_0\left(1 + e^{-\xi}\right)\right]\xi, \quad \text{etc.}, \end{aligned} \tag{17}$$

so that

$$y^{(i)} = a - A_0\left(1 - e^{-\xi}\right) + \varepsilon\left[A_1\left(1 - e^{-\xi}\right) - \left\{a - A_0\left(1 + e^{-\xi}\right)\right\}\xi\right] + 0(\varepsilon^2). \tag{18}$$

Next, in order to relate the outer solution (10) and the inner solution (18) to each other, we presuppose the existence of an overlapping region where the two expansions are valid. One version of the asymptotic matching principle, due to Shivamoggi, states

$$\lim_{x \Rightarrow 0} y^{(0)} = \lim_{\xi \Rightarrow 0} y^{(i)}, \tag{19}$$

where the left–hand side, viz., the inner limit of the outer expansion, is essentially represented by a formal Laurent's series about the inner boundary. Thus, in the neighborhood of $x = 0$, we write

$$y^{(0)}(x) = y^{(0)}(0) + x y^{(0)'}(0) + 0(x^2)$$

or

$$y^{(0)}(x) = y_0^{(0)}(0) + \varepsilon\left[\frac{x}{\varepsilon} y_0^{(0)'}(0) + y_1^{(0)}(0)\right] + 0(\varepsilon^2)$$

and, written in terms of the inner variable ξ,

$$y^{(0)}(x) = y_0^{(0)}(0) + \varepsilon\left[\xi y_0^{(0)'}(0) + y_1^{(0)}(0)\right] + 0(\varepsilon^2). \tag{20}$$

Formally, this asymptotic matching principle may be enunciated as follows

$$\left\{\begin{array}{l}\text{The } n\text{ - term formal Laurent' s}\\ \text{series expansion of the outer}\\ \text{expansion about the inner}\\ \text{boundary written in terms of}\\ \text{the inner variable}\end{array}\right\} = \left\{\begin{array}{l}\text{The } n\text{ - term formal outer}\\ \text{limit of the inner expansion}\end{array}\right\}.$$

Using (10) and (18) in (19), we obtain

$$be + \varepsilon[be - be\xi] + 0(\varepsilon^2) = (a - A_0) + \varepsilon[A_1 - \{a - A_0\}\xi] + 0(\varepsilon^2),$$

from which we have

$$A_0 = a - be, \quad A_1 = be, \tag{21}$$

so that (18) becomes

$$y^{(i)} = be + (a - be)e^{-\xi} + \varepsilon\left\{be(1 - e^{-\xi}) - \left[be - (a - be)e^{-\xi}\right]\xi\right\} + 0(\varepsilon^2). \tag{22}$$

Location and Nature of the Boundary Layers

Consider an elliptic equation of the form

$$\varepsilon\left[\alpha_{11}\frac{\partial^2 u}{\partial x^2} + 2\alpha_{12}\frac{\partial^2 u}{\partial x \partial y} + \alpha_{22}\frac{\partial^2 u}{\partial y^2}\right] = a\frac{\partial u}{\partial x} + b\frac{\partial u}{\partial y} \tag{23}$$

where α_{ij}, a, and b are constants, $\varepsilon \ll 1$, and

$$\alpha_{12}^2 - \alpha_{11}\alpha_{22} < 0.$$

In order to determine a solution $u(x,y;\varepsilon)$ to equation (23) uniquely, it is sufficient to prescribe one boundary condition on u or its normal derivative, or a combination on a closed boundary.

Consider an interior boundary–value problem with $u = u_B(x_B)$ prescribed on a closed boundary curve (see Figure 4.12).

The curves

$$\xi = bx - ay = \text{const}. \tag{24}$$

are the characteristics of equation (23), in the limit $\varepsilon \Rightarrow 0$, and are called the sub–characteristics of equation (1) (Section 3.5).

When we introduce

$$\eta = ax + by \tag{25}$$

and transform the independent variables x, y to ξ, η, equation (23) becomes

$$\varepsilon\left[A_{11}u_{\xi\xi} + 2A_{12}u_{\xi\eta} + A_{22}u_{\eta\eta}\right] = u_\eta, \tag{26}$$

where

$$A_{11} = \frac{\alpha_{11}b^2 - 2\alpha_{12}ab + \alpha_{22}a^2}{a^2 + b^2},$$

$$A_{12} = \frac{\alpha_{11}ab + \alpha_{12}\left(b^2 - a^2\right) - \alpha_{22}ab}{a^2 + b^2},$$

$$A_{22} = \frac{\alpha_{11}a^2 + 2\alpha_{12}ab + \alpha_{22}b^2}{a^2 + b^2}.$$

Now, in equation (26), let

$$\lim_{\substack{\varepsilon \Rightarrow 0 \\ \xi,\eta \text{ fixed}}} u(\xi,\eta;\varepsilon) \Rightarrow u^{(0)}(\xi), \tag{27}$$

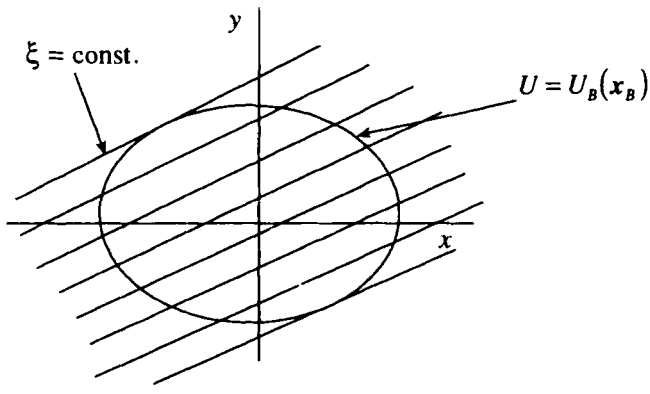

Figure 4.12. The subcharacteristics.

where the boundary condition on one side of the domain (see Figure 4.13) is sufficient to determine $u^{(0)}(\xi)$ uniquely in the whole domain, but $u^{(0)}(\xi)$ does not, in general, satisfy the boundary condition on the other side of the domain, so that one may expect a boundary layer to arise there. In order to study the latter region, we introduce

$$\eta^* = \frac{\eta - \eta_B(\xi)}{\delta(\varepsilon)} \tag{28}$$

and an associated limit process $\varepsilon \Rightarrow 0, \eta^*, \xi$ is held fixed. The retention of the highest–order derivatives in equation (26) then requires $\delta(\varepsilon) = \varepsilon^{1/2}$. When we seek an asymptotic solution of the form

$$u^*(\xi, \eta^*; \varepsilon) = u_0^*(\xi, \eta) + 0(\varepsilon), \tag{29}$$

equation (26) gives, in the limit $\varepsilon \Rightarrow 0$,

$$\kappa(\xi) u_{0\eta^*\eta^*} = u^*_{0\eta^*}, \tag{30}$$

where

$$\kappa(\xi) \equiv A_{11}\eta_{B\xi}^2 - 2A_{12}\eta_{B\xi} + A_{22}.$$

The elliptic nature of equation (26) ensures that $\kappa(\xi) > 0$.

We obtain from equation (30)

$$u_0^*(\xi, \eta^*) = A(\xi) + B(\xi)\exp\left(\frac{\eta^*}{\kappa(\xi)}\right). \tag{31}$$

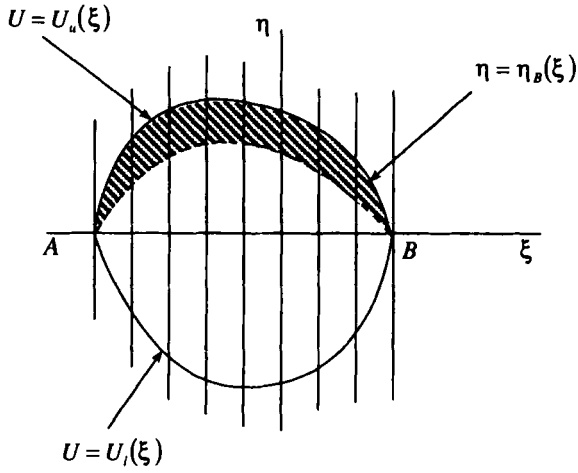

Figure 4.13. Production of a boundary layer on $u = u_u(\xi)$ (from Kevorkian and Cole, 1980).

(31) shows that the boundary layer occurs on the upper boundary. Matching (31) asymptotically to the interior solution $u_0^{(0)}(\xi)$, we obtain

$$u_0^*(\xi,\eta^*) = u_0^{(0)}(\xi) + \left[u_U(\xi) - u_0^{(0)}(\xi)\right] \exp\left(\frac{\eta^*}{\kappa(\xi)}\right),$$

where the subscript U refers to values on $\eta = \eta_B(\xi)$.

This solution breaks down for the case when the boundary is a sub-characteristic, say $\xi = \xi_s$. We then introduce

$$\xi^* = \frac{\xi - \xi_s}{\sqrt{\varepsilon}} \tag{32}$$

and assume an asymptotic expansion

$$u^*(\xi^*, \eta; \varepsilon) = u_0^*(\xi^*, \eta) + 0(\varepsilon) \tag{33}$$

with an associated limit process $\varepsilon \Rightarrow 0, \xi^*, \eta$ held fixed. Then equation (26) gives

$$A_{11} \frac{\partial^2 u_0^*}{\partial \xi^{*2}} = \frac{\partial u_0^*}{\partial \eta}. \tag{34}$$

Since $A_{11} > 0, \eta$ is a time-like coordinate, which means that one requires the prescription

$$\xi^* = \xi_s^*: \quad u = u_s(\eta). \tag{35}$$

Further, the requirement of matching of u_0^* with the interior solution $u_0^{(0)}$ gives

$$\xi^* \Rightarrow -\infty: \quad u_0^*(\xi^*, \eta) \Rightarrow u_0^{(0)}(\xi). \tag{36}$$

Thus, the boundary layers arising on the subcharacteristics are characterized by a diffusion-like behavior, which we also saw in Section 3.4.

For the problem of a viscous flow past a body, the boundary layer is along a streamline of the inviscid flow (since the body contour is such a streamline) – a subcharacteristic of the full problem. Now, the characteristic surfaces in general are the locus of possible discontinuities, and streamlines of an inviscid flow can support a discontinuity in vorticity. In the inviscid limit, in which the ambient flow is irrotational, such a discontinuity occurs at the surface of the body where the velocity component tangential to the body jumps so as to meet the no-slip condition at the surface of the body.

Incompressible Flow Past a Flat Plate

We consider here the problem of two-dimensional viscous incompressible flow past a flat plate. It turns out that the external inviscid flow is associated with an outer limit process and that the boundary layer is associated with an inner-limit process. The order of the differential equations is lowered in the outer limit, and

the boundary condition of no–slip of the flow at the plate is lost so that the problem under consideration is one of singular–perturbation type.

The Outer Expansion

Let x measure the distance along the plate from the leading edge, and let y measure the distance normal to the plate. In terms of the stream function $\Psi(x,y)$, the boundary–value problem in nondimensionalized flow variables is given by

$$\left(\Psi_y \frac{\partial}{\partial x} - \Psi_x \frac{\partial}{\partial y} - \frac{1}{R_E}\nabla^2\right)\nabla^2\Psi = 0, \tag{37}$$

$$\left.\begin{aligned} &y=0: \quad \Psi = 0, \quad \Psi_y = 0, \quad 0<x<1 \quad \text{or} \quad \infty, \\ &\text{upstream}: \quad \Psi \sim y, \end{aligned}\right\} \tag{38}$$

where

$$R_E \equiv \frac{\rho U L}{\mu}.$$

where U is the velocity of the fluid in the free stream. If the plate is semi–infinite, then there is no natural length in the problem, and the apparent difficulty is circumvented by choosing some reference length L.

Let us seek a straightforward asymptotic expansion, as $R_E \Rightarrow \infty$, of the form

$$\Psi(x,y;R_E) = \psi_1^{(0)}(x,y) + \delta_2^{(0)}(R_E)\psi_2^{(0)}(x,y) + \cdots \tag{39}$$

with the associated outer limit process $R_E \Rightarrow \infty, x, y$ fixed. Then, equation (37) gives

$$\left(\psi_{1y}^{(0)} \frac{\partial}{\partial x} - \psi_{1x}^{(0)} \frac{\partial}{\partial y}\right)\nabla^2\psi_1^{(0)} = 0, \tag{40}$$

from which

$$\nabla^2\psi_1^{(0)} = -\Omega_1^{(0)}\left(\psi_1^{(0)}\right). \tag{41}$$

If the oncoming stream is irrotational, equation (41) gives

$$\nabla^2\psi_1^{(0)} = 0 \tag{42}$$

with

$$\left.\begin{aligned} &y=0: \quad \psi_1^{(0)} = 0, \\ &\text{upstream}: \quad \psi_1^{(0)} \sim y. \end{aligned}\right\} \tag{43}$$

Note that the no–slip condition

$$y=0: \quad \psi_{1y}^{(0)} = 0$$

has been dropped since, in the outer limit, the order of the differential equation (37) has dropped.

From (42) and (43), we obtain

$$\psi_1^{(0)}(x,y) = y \tag{44}$$

so that, in the limit $R_E \Rightarrow \infty$, a flat plate causes no disturbance.

The Inner Expansion

Because of the loss of the no–slip condition, the basic inviscid solution is not valid close to the flat plate. Therefore, assume an inner expansion valid within the boundary layer

$$\psi^{(i)}(x,y;R_E) = \delta_1^{(i)}(R_E)\psi_1^{(i)}(x,Y) + \delta_2^{(i)}(R_E)\psi_2^{(i)}(x,Y) + \cdots \tag{45}$$

with the associated inner limit process $R_E \Rightarrow \infty, x, Y$ fixed, where

$$Y = \frac{y}{\delta_1^{(i)}(R_E)}.$$

Then, equation (37) gives

$$\left(\psi_{1Y}^{(i)}\frac{\partial}{\partial x} - \psi_{1x}^{(i)}\frac{\partial}{\partial Y}\right)\psi_{1YY}^{(i)} = \lim_{R_E \Rightarrow 0}\left[\frac{1}{R_E\delta_1^{(i)2}(R_E)}\right]\psi_{1YYYY}^{(i)}, \tag{46}$$

so that the retention of the highest derivative [the term on the right–hand side in (46)] requires

$$\delta_1^{(i)}(R_E) = \frac{1}{\sqrt{R_E}}. \tag{47}$$

Thus,

$$Y = \sqrt{R_E}\ y \tag{48}$$

and equation (46) becomes

$$\left(\frac{\partial^2}{\partial Y^2} - \psi_{1Y}^{(i)}\frac{\partial}{\partial x} + \psi_{1x}^{(i)}\frac{\partial}{\partial Y}\right)\psi_{1YY}^{(i)} = 0 \tag{49}$$

or

$$\frac{\partial}{\partial Y}\left(\psi_{1YYY}^{(i)} + \psi_{1x}^{(i)}\psi_{1YY}^{(i)} - \psi_{1Y}^{(i)}\psi_{1xY}^{(i)}\right) = 0, \tag{50}$$

from which we have

$$\psi_{1YYY}^{(i)} + \psi_{1x}^{(i)}\psi_{1YY}^{(i)} - \psi_{1Y}^{(i)}\psi_{1xY}^{(i)} = f(x), \tag{51}$$

where $f(x)$ is proportional to the pressure gradient impressed on the plate by the inviscid flow. Note that this implies that the pressure is almost constant across the boundary layer.

The asymptotic matching between the outer and the inner solutions gives

$$\psi_1^{(i)}(x,\infty) = Y\psi_{1y}^{(0)}(x,0) + \cdots,$$

from which

$$\psi_{1Y}^{(i)}(x,\infty) = \psi_{1y}^{(0)}(x,0), \tag{52}$$

which simply implies that the tangential velocity of the boundary–layer flow approaches the inviscid flow velocity $\psi_{1y}^{(0)}(x,0)$ at the outer edge of the boundary layer, $y \Rightarrow \infty$.

Using the outer inviscid solution, equation (51) becomes

$$\psi_{1YYY}^{(i)} + \psi_{1x}^{(i)}\,\psi_{1YY}^{(i)} - \psi_{1Y}^{(i)}\,\psi_{1xY}^{(i)} = -\psi_{1y}^{(0)}(x,0)\,\psi_{1xy}^{(0)}(x,0). \tag{53}$$

Notice that the boundary–layer equation is parabolic with x acting as a time–like variable, although the original Navier–Stokes equations were elliptic. This is in agreement with the result in the previous subsection that the boundary layers arising on the subcharacteristics are characterized by a diffusion–like behavior. This means that the upstream influence is lost so that the first–order boundary–layer solution on a flat plate is not affected by the trailing edge (if the plate is finite) and the wake beyond.

For a flat plate, equation (53) becomes

$$\psi_{1YYY}^{(i)} + \psi_{1x}^{(i)}\,\psi_{1YY}^{(i)} - \psi_{1Y}^{(i)}\,\psi_{1xY}^{(i)} = 0, \tag{54}$$

with the boundary conditions being

$$\left.\begin{aligned} &Y = 0: \quad \psi_1^{(i)} = 0, \quad \psi_{1Y}^{(i)} = 0 \quad \text{for} \quad 0 < x < 1 \text{ or } \infty, \\ &Y \Rightarrow \infty: \quad \psi_Y^{(i)} = 1. \end{aligned}\right\} \tag{55}$$

For a finite flat plate, the boundary layers at the top and bottom surfaces merge at the trailing edge and leave the plate as a wake without separating, so that the boundary–layer approximation continues to be valid in the wake. One then needs only replace the no–slip–of–the–flow at $y = 0$ by a symmetry requirement of the form

$$Y = 0: \quad \psi_{1YY}^{(i)} = 0, \quad x > 1. \tag{56}$$

Now, the problem given by (54) and (55) is invariant under the transformation

$$\psi_1^{(i)} \Rightarrow c\psi_1^{(i)}, \quad x \Rightarrow c^2 x, \quad Y \Rightarrow cY,$$

so that it is possible to look for solutions in which $\psi_1^{(i)}, x, y$ occur in certain combinations – self–similar solutions. This also reduces equation (54) to an ordinary differential equation. Thus, when we put

$$\psi_1^{(i)}(x,Y) = \sqrt{2x}\; f_1(\eta), \qquad \eta = \frac{Y}{\sqrt{2x}}, \tag{57}$$

(54) and (55) give

$$f_1''' + f_1 f_1'' = 0, \tag{58}$$

$$\left.\begin{aligned} \eta = 0: &\quad f_1 = 0,\ f_1' = 0, \\ \eta \Rightarrow \infty: &\quad f_1' \Rightarrow 1, \end{aligned}\right\} \tag{59}$$

where the primes denote differentiation with respect to η. Note that

$$u = f_1'(\eta), \qquad v = (\eta f_1' - f_1),$$

which implies that the velocity profile in the boundary layer is the same for all x except for the change of scale.

In order to find the asymptotic behavior of the solution of (58) and (59), note first that equation (58) admits solution of the form

$$f_1 \sim \frac{1}{\eta}. \tag{60}$$

This implies that equation (58) has the following scaling group

$$\bar{f}_1 = \alpha^{-1} f_1, \qquad \bar{\eta} = \alpha \eta. \tag{61}$$

We may therefore introduce the following canonical coordinates:

$$s = f_1 \eta, \qquad t = \eta^2 \frac{df_1}{d\eta}. \tag{62}$$

The transformation from (s,t) to (f,η) is given differentially by

$$\frac{ds}{t+s} = \frac{d\eta}{\eta}. \tag{63}$$

The transformation rules of the various derivatives are

$$\begin{aligned} \frac{d^2 f_1}{d\eta^2} &= -\frac{2}{\eta^3} t + \frac{1}{\eta^3} \frac{dt}{ds}(t+s), \\ \frac{d^3 f_1}{d\eta^3} &= \frac{6}{\eta^4} t - \frac{5}{\eta^4}(t+s)\frac{dt}{ds} + \frac{1}{\eta^4}\frac{d^2 t}{ds^2}(t+s)^2 + \frac{1}{\eta^4}\left(\frac{dt}{ds}\right)^2 (t+s). \end{aligned} \tag{64}$$

In terms of the new coordinates (s,t), the boundary–value problem (58) and (59) becomes

$$(t+s)^2 \frac{d^2 t}{ds^2} + (t+s)\left(\frac{dt}{ds} + 1\right)\frac{dt}{ds} - 5(t+s)\frac{dt}{ds} + 6t + \frac{s}{2}\left[-2t + (t+s)\frac{dt}{ds}\right] = 0, \tag{65}$$

$$\left.\begin{aligned} s = 0: &\quad t = 0, \\ s \Rightarrow \infty: &\quad t \Rightarrow \infty, \end{aligned}\right\}. \tag{66}$$

Near $s = 0$, equation (65) shows that

$$t \approx \lambda s, \tag{67}$$

with

$$(\lambda + 1)^2 - 5\lambda(\lambda + 1) + 6\lambda \approx 0 \tag{68a}$$

or

$$\lambda = 1, 2; \tag{68b}$$

$\lambda = 1$ turns out to be the spurious root. For $\lambda = 2$, we obtain from (63)

$$\frac{ds}{3s} \approx \frac{d\eta}{\eta}, \tag{69}$$

from which we have

$$s \approx \eta^3. \tag{70}$$

Hence, we have from (62)

$$\eta \Rightarrow 0: \quad f_1 = \eta^2. \tag{71}$$

Next, near $s \Rightarrow \infty$, equation (65) shows that

$$t \approx \lambda s, \tag{72}$$

with

$$-2\lambda + \lambda(\lambda + 1) \approx 0 \tag{73a}$$

or

$$\lambda = 1. \tag{73b}$$

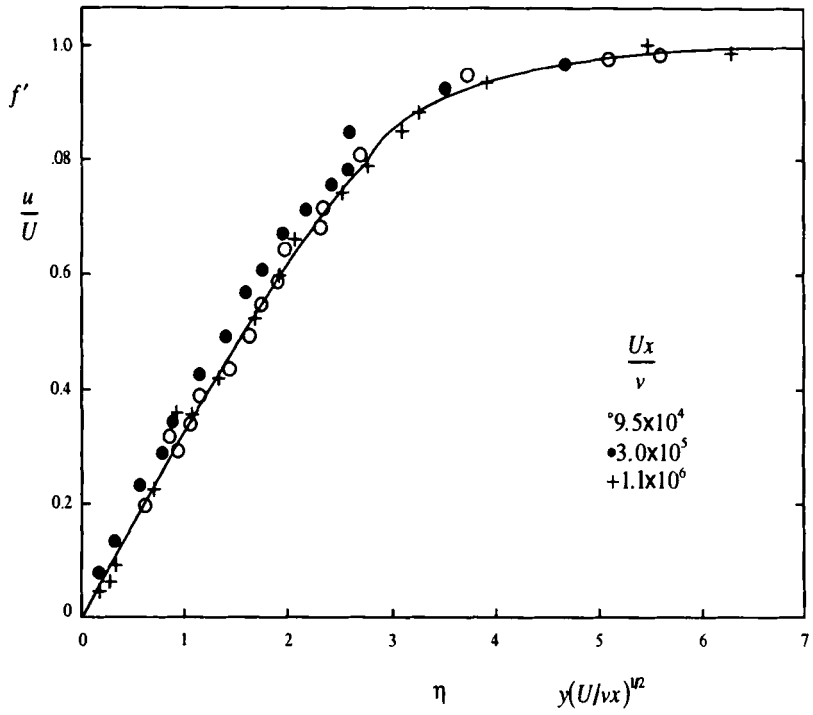

Figure 4.14. Theoretical Blasius profile (Schlichting, 1972) and experimental confirmation (Dhawan, 1952), plotted by Tritton (1988).

We then obtain from (63)

$$\frac{ds}{2s} \approx \frac{d\eta}{\eta}, \tag{74}$$

from which we have

$$s \approx \eta^2. \tag{75}$$

Hence, we have from (62)

$$\eta \Rightarrow \infty: \quad f_1 \approx \eta - \beta_1 \tag{76}$$

as expected! Here, β_1 is an arbitrary constant.

Figure 4.14 shows the numerical solution of equation (58) due to Schlichting compared with the experimental data for several values of Reynolds numbers. The agreement between the two shows the validity of the various approximations and assumptions made in the boundary–layer theory. Besides, the velocity profile is seen to preserve its shape as one moves downstream despite the fact that the boundary layer thickness is changing.

Flow Due to Displacement Thickness

When we use (39), (44), (45), (47), (54), (71), and (76), the asymptotic matching gives

$$\begin{aligned}
&0 + \delta_2^{(0)}(R_E)\psi_2^{(0)}(x,0) + \cdots + \frac{Y}{\sqrt{R_E}} + \cdots \\
&= \frac{1}{\sqrt{R_E}}\,\psi_1^{(i)}(x,\infty) + \cdots \\
&= \frac{1}{\sqrt{R_E}}\left[\sqrt{2x}\; f_1\left(\frac{Y}{\sqrt{2x}}\right)\right] + \cdots, \qquad \text{as} \quad Y \Rightarrow \infty \\
&= \frac{Y}{\sqrt{R_E}} - \frac{1}{\sqrt{2R_E}}\beta_1\sqrt{2x} + \cdots, \qquad \text{as} \quad Y \Rightarrow \infty.
\end{aligned} \tag{77}$$

Thus,

$$\begin{aligned}
&\delta_2^{(0)}(R_E) = \frac{1}{\sqrt{R_E}}, \\
&y = 0: \quad \psi_2^{(0)} = -\beta_2\sqrt{2x},
\end{aligned} \tag{78}$$

so that $\psi^{(0)} = 0$ at $y = \left(1/\sqrt{R_E}\right)\beta_1\sqrt{2x}$, which implies that the presence of boundary layer endows certain thickness to the plate, which then displaces the outer inviscid flow like a solid parabola of nose radius β_1^2/R_E.

For a semi–infinite flat plate, we then have

$$\nabla^2\psi_2^{(0)} = 0, \tag{79}$$

$$\left.\begin{aligned} y=0:\quad & \psi_2^{(0)}=0, \quad x<0, \\ & \psi_2^{(0)}=-\beta_1\sqrt{2x}, \quad x>0, \\ \text{upstream}:\quad & \psi_2^{(0)}=o(y), \end{aligned}\right\} \tag{80}$$

which corresponds to linearized flow for a body given by $y=\beta_1\left(\sqrt{2x/R_E}\right)$, and we have

$$\psi_2^{(0)}=-\beta_1 R_E\left[\sqrt{2(x+iy)}\right]. \tag{81}$$

Thus, even though the flow outside the wake and the boundary layer is essentially irrotational, it is not accurately described by the solution for potential flow past the given body. One has to take into account the apparent change of shape of the body caused by the displacement–thickness effect of the boundary layer.

Note that the foregoing theory is not valid within a distance of order ν/U from the leading edge of the plate where the thickness of the boundary layer is comparable with the distance from the leading edge.

Separation of Flow in a Boundary Layer: Landau's Theory

For streamlined bodies, one obtains a useful agreement between the inviscid theory and experimental results. Indeed, the mathematical results of irrotational flow associated with a rigid body moving in an otherwise stationary unbounded fluid may be applied directly to cases of flow at large Reynolds numbers in which a separation of flow does not occur in the boundary layer. For such flows, the boundary layers play a passive role by simply effecting a smooth transition between a given ambient flow and no–slip condition at the wall. However, sometimes the boundary layers can exert a controlling influence on the flow as a whole. One such case occurs with bodies of other shapes, especially those of blunt form such as cylinders, wherein an adverse pressure gradient arises (i.e., the pressure increases in the flow direction along the body). The retardation of the fluid particles under these circumstances leads to an abrupt thickening of the boundary layer which may then separate from the body. Mathematically, the only way in which this can happen is via a breakdown of the solution of the boundary–layer equations.[2]

---

[2]This may be seen mathematically by generalizing equation (58) to take account of a varying ambient velocity. If $\partial\psi_1^{(1)}/\partial y \Rightarrow U(x)$ as $y \Rightarrow \infty$ and $U(x) \sim x^m$, then a self-similar solution can still exist, with equation (58) replaced by

$$f_1''' + (m+1) f_1 f_1'' = 2m\left(f_1^2 - 1\right).$$

Numerical work (Schlichting, 1972) shows that this equation has a unique solution for $m > 0$, two solutions (one of which represents reverse flow) for $-0.0904 < m < 0$, and no solution for $m < -0.0904$.

Downstream of this point (or line) of breakaway, the original boundary–layer fluid passes over a region of recirculating flow. (Thus, separation involves the existence of a region in which the vorticity has opposite sign from that associated with the flow as a whole.) The point at which the thin boundary layer breaks away from the surface and which divides the region of downstream–directed flow from the region of recirculating flow is known as the *separation point.* (For two–dimensional steady flow over fixed walls, the point of vanishing shear coincides with the point of separation; but this is not true for two–dimensional steady flow over moving walls, two–dimensional unsteady flow, and three–dimensional steady flow.) Two different types of post–separation behavior are known to exist. In some cases, the original boundary layer passes over the region of recirculating fluid and reattaches to the body at some point downstream, trapping a bubble of recirculating fluid beneath it. In other cases, the original boundary–layer never reattaches to the body but passes downstream, mixing with recirculating fluid, to form a wake. It is obvious that the recirculating flow alters the effective body shape and hence the inviscid ambient flow about the body so that separation is the controlling feature of many fluid flows.

Consider a boundary layer on a plane wall. One has for the flow in the boundary layer,

$$\frac{\partial u}{\partial t} + u\frac{\partial u}{\partial x} + v\frac{\partial u}{\partial y} = -\frac{1}{\rho}\frac{dp}{dx} + \nu\frac{\partial^2 u}{\partial y^2}, \tag{82}$$

$$\frac{\partial u}{\partial x} + \frac{\partial v}{\partial y} = 0. \tag{83}$$

The flow near separation is controlled by the pressure gradient. In fact, equations (82) and (83) show that in the presence of an adverse pressure gradient $dp/dx > 0$, we have

$$\left.\frac{\partial^2 u}{\partial y^2}\right|_{y=0} > 0. \tag{84}$$

Consider now the flow upstream of the point at which $\partial u/\partial y\big|_{y=0} = 0$. Equation (84) then implies that the boundary–layer velocity profile must have an inflection point.

As one approaches the point (or line) of separation, the flow moves away from the boundary and toward the interior of the fluid. Then the velocity component normal to the wall ceases to be small compared with the velocity component tangential to the wall and is now of at least of the same order of magnitude. This implies an essentially unlimited magnification of normal velocity component as one goes toward the interior of the fluid from the point of separation, i.e., $\partial v/\partial y \Rightarrow \infty$ at the latter point. From equation (83), this means in turn that

$\partial u/\partial x \Rightarrow \infty$ at the same location. Thus, one may write in the neighborhood of the point of separation[3]

$$(x_0 - x) = (u_0 - u)^2 f(y,t) + 0(u_0 - u)^3, \tag{85}$$

where the subscript 0 denotes the conditions at the point of separation.

Equivalently, one may write

$$u(x,y,t) = u_0(\psi,t) + \frac{\partial \beta(\psi,t)}{\partial \psi}\sqrt{\chi} + \frac{\partial \beta_1(\psi,t)}{\partial \psi}\chi + \cdots, \tag{86}$$

where

$$\chi = x_0(t) - x \quad \text{and} \quad \psi = y - y_0(t).$$

One then finds from equation (83)

$$v(x,y,t) = \frac{\beta(\psi,t)}{2\sqrt{\chi}} + \beta_1(\psi,t) + \cdots. \tag{87}$$

When we use equations (86) and (87), equation (82) gives

$$\frac{\partial \beta}{\partial \psi}\frac{dx_0}{dt} - u_0\frac{\partial \beta}{\partial \psi} + \beta\frac{\partial u_0}{\partial \psi} = 0, \tag{88}$$

from which

$$\beta(\psi,t) = A(t)\left[u_0(\psi,t) - U_s(t)\right] \tag{89}$$

where

$$U_s(t) = \frac{dx_0}{dt}.$$

When we use equation (89), equations (86) and (87) become

$$u(x,y,t) = u_0(\psi,t) + A(t)\frac{\partial u_0(\psi,t)}{\partial \psi}\sqrt{\chi} + \frac{\partial \beta_1(\psi,t)}{\partial \psi}\chi + \cdots, \tag{90}$$

$$v(x,y,t) = A(t)\frac{\left[u_0(\psi,t) - U_s(t)\right]}{2\sqrt{\chi}} + \beta_1(\psi,t) + \cdots. \tag{91}$$

---

[3]In fact, differentiating equations (82) and (83), one obtains, when $y = 0$,

$$\frac{\partial}{\partial x}\left[\frac{1}{2}\left(\frac{\partial u}{\partial y}\right)^2\right] = \nu\frac{\partial^4 u}{\partial y^4}.$$

If $\partial^4 u/\partial y^4$ is nonzero at the point of separation, the above equation implies

$$\left.\frac{\partial u}{\partial y}\right|_{y=0} \sim -(x_0 - x)^{1/2},$$

in agreement with (85)!

Thus, at the point of separation we have

$$y = 0: \quad v_0 = 0, \quad \frac{\partial u_0}{\partial y} = 0, \quad u_0 = U_s. \tag{92}$$

Note that a point on the surface of the body, where $\partial u/\partial y = 0$, corresponds to the point of separation.

It should be noted that, for a satisfactory formulation of separated flows, one really needs an extension of classical boundary–layer theory incorporating the interaction between the ambient pressure gradient and the separating boundary layer. This is necessitated by the fact that the pressure gradient in the separated boundary layer is determined by the ambient flow which is, in turn, strongly influenced by the former.

Boundary Layers in Compressible Flows

The main differences between boundary layers in incompressible and compressible flows arise from thermal effects. In a compressible boundary layer flow the transport coefficients of the fluid (like viscosity and thermal conductivity) are functions of temperature T of the fluid which, because of viscous dissipation in the fluid and heat transport at the wall, vary considerably across the boundary layer. Consequently, the equations of motion and energy reduce to a pair of coupled equations whose solution is usually difficult.

However, the effect of the rise in temperature of the fluid is to diminish the density ρ of the fluid and increase the viscosity μ. These lead to a thickening of the boundary layer and a decrease in the velocity gradient in the boundary layer. The skin friction, given by

$$\tau_s = \mu \frac{\partial u}{\partial y}$$

consequently, changes slowly. It is actually independent of the free–stream Mach number M_∞ and the plate temperature, if $\mu \sim T$, and the free–stream speed $U_\infty = \text{const}$.

Further, there is no qualitative difference between supersonic and subsonic boundary layers as such, because unlike the inviscid flows, which change dramatically as the speed of sound is surpassed, the pressure is not the dominant force controlling the flow in the boundary. Nonetheless, since the free–stream Mach number M_∞ also enters the problem through the boundary conditions, differences in the interaction of the two boundary layers with the exterior inviscid flow are likely to occur. For example, regions of influence and domains of dependence take effect again via the displacement effect.

Consider a viscous, compressible, perfect gas flowing steadily past a body. The equations for the flow are

$$\frac{\partial}{\partial x}(\rho u)+\frac{\partial}{\partial y}(\rho v)=0, \tag{93}$$

$$\rho\left(u\frac{\partial u}{\partial x}+v\frac{\partial u}{\partial y}\right)=-\frac{\partial p}{\partial x}+\frac{\mu}{3}\frac{\partial}{\partial x}\left(\frac{\partial u}{\partial x}+\frac{\partial v}{\partial y}\right)-\frac{2}{3}\frac{\partial \mu}{\partial x}\left(\frac{\partial u}{\partial x}+\frac{\partial v}{\partial y}\right)$$
$$+2\frac{\partial \mu}{\partial x}\frac{\partial u}{\partial x}+\frac{\partial \mu}{\partial y}\left(\frac{\partial u}{\partial y}+\frac{\partial v}{\partial x}\right)+\mu\left(\frac{\partial^2 u}{\partial x^2}+\frac{\partial^2 u}{\partial y^2}\right), \tag{94}$$

$$\rho\left(u\frac{\partial v}{\partial x}+v\frac{\partial v}{\partial y}\right)=-\frac{\partial p}{\partial y}+\frac{\mu}{3}\frac{\partial}{\partial y}\left(\frac{\partial u}{\partial x}+\frac{\partial v}{\partial y}\right)-\frac{2}{3}\frac{\partial \mu}{\partial y}\left(\frac{\partial u}{\partial x}+\frac{\partial v}{\partial y}\right)$$
$$+2\frac{\partial \mu}{\partial y}\frac{\partial v}{\partial y}+\frac{\partial \mu}{\partial x}\left(\frac{\partial u}{\partial y}+\frac{\partial v}{\partial x}\right)+\mu\left(\frac{\partial^2 v}{\partial x^2}+\frac{\partial^2 v}{\partial y^2}\right), \tag{95}$$

$$\rho C_p\left(u\frac{\partial T}{\partial x}+v\frac{\partial T}{\partial y}\right)=u\frac{\partial p}{\partial x}+v\frac{\partial p}{\partial y}+\frac{\partial}{\partial x}\left(K\frac{\partial T}{\partial x}\right)+\frac{\partial}{\partial y}\left(K\frac{\partial T}{\partial y}\right)+\Phi, \tag{96}$$

$$p=\rho RT, \tag{97}$$

where Φ is the viscous dissipation term,

$$\Phi=2\mu\left(\frac{\partial u}{\partial x}\right)^2+2\mu\left(\frac{\partial v}{\partial y}\right)^2+\mu\left(\frac{\partial v}{\partial x}+\frac{\partial u}{\partial y}\right)^2-\frac{2}{3}\mu\left(\frac{\partial u}{\partial x}+\frac{\partial v}{\partial y}\right)^2,$$

R is the perfect–gas constant and K is the thermal conductivity of the fluid.

Following a procedure like the one in Section 4.4, one arrives from (94)–(96) at the following equations for the flow in the boundary layer

$$\rho\left(u\frac{\partial u}{\partial x}+v\frac{\partial u}{\partial y}\right)=-\frac{\partial p}{\partial x}+\frac{\partial}{\partial y}\left(\mu\frac{\partial u}{\partial y}\right), \tag{98}$$

$$0=-\frac{\partial p}{\partial y}, \tag{99}$$

$$\rho C_p\left(u\frac{\partial T}{\partial x}+v\frac{\partial T}{\partial y}\right)=u\frac{\partial p}{\partial x}+\frac{\partial}{\partial y}\left(K\frac{\partial T}{\partial y}\right)+\mu\left(\frac{\partial u}{\partial y}\right)^2 \tag{100}$$

Equations (93) and (97) remain unchanged.

The boundary conditions at the body are

$$y=0:\quad u,v=0,\quad \frac{\partial T}{\partial y}=0\quad \text{or}\quad T=T_w \tag{101}$$

depending on whether the wall is thermally insulated or isothermal. Next, as $y\Rightarrow\infty$, the boundary–layer solution must be matched to the inviscid–flow solution valid outside the boundary layer; i.e.,

$$y\Rightarrow\infty;\quad u\Rightarrow U(x),\quad T\Rightarrow T_\infty(x),\quad p\Rightarrow p_\infty(x). \tag{102}$$

Using (99), one obtains for the inviscid flow outside the boundary layer

$$-\frac{dp_\infty}{dx} = \rho_\infty U \frac{dU}{dx}. \tag{103}$$

If this inviscid flow is isoenergetic, then we have

$$C_p T_\infty + \frac{1}{2} U^2 = \text{const.} \tag{104}$$

Crocco's Integral

If

$$T = T(u), \tag{105}$$

then equation (100) becomes

$$\rho C_p T_u \left(u \frac{\partial u}{\partial x} + v \frac{\partial u}{\partial y} \right) = u \frac{\partial p}{\partial x} + \frac{\partial}{\partial y} \left(K T_u \frac{\partial u}{\partial y} \right) + \mu \left(\frac{\partial u}{\partial y} \right)^2, \tag{106}$$

When we use equation (98), equation (106) becomes

$$C_p T_u \left[-\frac{dp}{dx} + \frac{\partial}{\partial y} \left(\mu \frac{\partial u}{\partial y} \right) \right] = u \frac{dp}{dx} + T_u \frac{\partial}{\partial y} \left(K \frac{\partial u}{\partial y} \right) + \left(T_{uu} K + \mu \right) \left(\frac{\partial u}{\partial y} \right)^2,$$

from which

$$-\frac{dp}{dx} \left(C_p T_u + u \right) + T_u \left[C_p \frac{\partial}{\partial y} \left(\mu \frac{\partial u}{\partial y} \right) - \frac{\partial}{\partial y} \left(K \frac{\partial u}{\partial y} \right) \right] = \left(T_{uu} K + \mu \right) \left(\frac{\partial u}{\partial y} \right)^2. \tag{107}$$

For the case of flow over a flat plate, we obtain

$$\frac{dp}{dx} = 0$$

and

$$P_r = \frac{\mu C_p}{K} = 1, \tag{108}$$

and equation (107) gives

$$T_{uu} = -\frac{\mu}{K} = -\frac{1}{C_p}. \tag{109}$$

Equation (109) leads to

$$T = -\frac{u^2}{2C_p} + Au + B. \tag{110}$$

If we consider an insulated wall, for which the boundary conditions are

$$\left.\begin{aligned} &y = 0: \quad u = 0, \quad \frac{\partial T}{\partial y} = 0 \quad \text{or} \quad \frac{\partial T}{\partial u} = 0, \\ &y \Rightarrow \infty: \quad U \Rightarrow U, \quad T \Rightarrow T_\infty, \end{aligned}\right\} \tag{111}$$

(110) becomes

$$T = T_\infty + \frac{U^2 - u^2}{2C_p}. \tag{112}$$

On the other hand, if we consider an isothermal wall, for which the boundary conditions are

$$\left.\begin{aligned} y = 0: \quad & u = 0, \quad T = T_\omega, \\ y \Rightarrow \infty: \quad & u \Rightarrow U, \quad T \Rightarrow T_\infty, \end{aligned}\right\} \tag{113}$$

(110) becomes

$$T = -\left(T_\omega - T_\infty - \frac{U^2}{2C_p}\right)\frac{u}{U} + T_\omega - \frac{u^2}{2C_p}. \tag{114}$$

Note from (114) that, depending upon

$$T_\omega - T_\infty \gtrless \frac{U^2}{2C_p},$$

there is a heat transfer from the wall to the fluid or vice versa.

Flow Past a Flat Plate: Howarth–Dorodnitsyn Transformation

For the flow in a boundary layer on a flat plate, equations (93), (98), and (100) become

$$\frac{\partial}{\partial x}(\rho u) + \frac{\partial}{\partial y}(\rho v) = 0, \tag{115}$$

$$\rho\left(u\frac{\partial u}{\partial x} + v\frac{\partial u}{\partial y}\right) = \frac{\partial}{\partial y}\left(\mu\frac{\partial u}{\partial y}\right), \tag{116}$$

$$\rho\left(u\frac{\partial T}{\partial x} + v\frac{\partial T}{\partial y}\right) = \frac{1}{P_r}\frac{\partial}{\partial y}\left(\mu\frac{\partial T}{\partial y}\right) + \frac{\mu}{C_p}\left(\frac{\partial u}{\partial y}\right)^2. \tag{117}$$

When we introduce

$$y_1 = \int_0^y \frac{\rho}{\rho_\infty}dy, \qquad x_1 = x, \tag{118}$$

the stream-function relations obtained from equation (115)

$$\rho u = \rho_\infty \frac{\partial \Psi}{\partial y}, \qquad -\rho v = \rho_\infty \frac{\partial \Psi}{\partial x} \tag{119}$$

give

$$u = \frac{\partial \Psi}{\partial y_1}, \qquad \rho v = -\rho_\infty\left[\frac{\partial \Psi}{\partial x} + u\left(\frac{\partial y_1}{\partial x}\right)_y\right]. \tag{120}$$

When we use (118) and (120), equations (116) and (117) become

$$\frac{\partial \Psi}{\partial y_1}\frac{\partial^2 \Psi}{\partial x_1 \partial y_1} - \frac{\partial \Psi}{\partial x_1}\frac{\partial^2 \Psi}{\partial y_1^2} = \frac{\partial}{\partial y_1}\left(\frac{\mu\rho}{\rho_\infty}\frac{\partial^2 \Psi}{\partial y_1^2}\right), \tag{121}$$

$$\frac{\partial \Psi}{\partial y_1}\frac{\partial T}{\partial x_1}-\frac{\partial \Psi}{\partial x_1}\frac{\partial T}{\partial y_1}=\frac{1}{P_r}\frac{\partial}{\partial y_1}\left(\frac{\mu\rho}{\rho_\infty}\frac{\partial T}{\partial y_1}\right)+\frac{\mu\rho}{C_p\rho_\infty^2}\left(\frac{\partial^2\Psi}{\partial y_1^2}\right)^2. \tag{122}$$

When we put

$$\Psi=\sqrt{2Uv_\infty x_1}\ f(\eta),\qquad T=T(\eta),$$
$$\eta=y_1\sqrt{\frac{U}{2v_\infty x_1}}, \tag{123}$$

equations (121) and (122) give

$$ff''+\left[\left(\frac{\mu\rho}{\mu_\infty\rho_\infty}\right)f''\right]'=0, \tag{124}$$

$$\left[\left(\frac{\mu\rho}{\mu_\infty\rho_\infty}\right)T'\right]'+P_r fT'=-P_r\left(\frac{\mu\rho}{\mu_\infty\rho_\infty}\right)\frac{U^2}{C_p}(f'')^2. \tag{125}$$

The boundary conditions (101) and (102) give

$$\eta=0:\quad f,f'=0,\quad T=T_\omega,$$
$$\eta\Rightarrow\infty:\quad f'\Rightarrow 1,\quad T\Rightarrow T_\infty. \tag{126}$$

If the fluid behaves like a perfect gas and

$$\mu\sim T,\quad P_r=1,\quad T_\omega=\text{const.}, \tag{127}$$

then equations (124) and (125) become

$$ff''+f'''=0, \tag{128}$$

$$T''+fT'=-(\gamma-1)M_\infty^2T_\infty(f'')^2, \tag{129}$$

where

$$M_\infty^2=\frac{U^2}{\gamma RT_\infty},\qquad \gamma=\frac{C_p}{C_v}.$$

Note that equation (128) is the same as equation (58) for incompressible flows, and this establishes a correlation between the two boundary layers.

Equation (129) may be integrated to give, on using equation (126),

$$\frac{T}{T_\infty}=1+\frac{\gamma-1}{2}M_\infty^2(1-f'^2)+\left(\frac{T_\omega}{T_\infty}-1-\frac{\gamma-1}{2}M_\infty^2\right)(1-f'). \tag{130}$$

Flow in a Mixing Layer Between Two Parallel Streams

Consider the flow in a mixing layer between two parallel streams (see Figure 4.15).

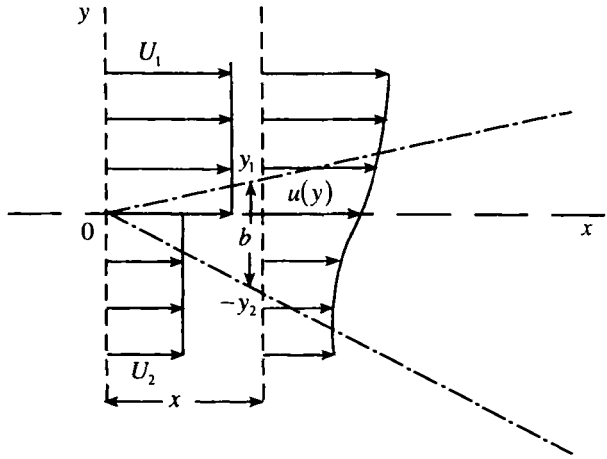

Figure 4.15. The mixing layer between two streams.

We adopt for this flow the boundary-layer model, so we make the following assumptions:

1. The change of velocity from that of one stream to the other takes place in a mixing region of small thickness as compared with the length of mixing,
2. The normal component of the velocity is small as compared with the component of velocity parallel to the main flow.

Note that there are only two apparent boundary conditions: viz.,

$$\left.\begin{aligned} y \Rightarrow \infty: \quad & u \Rightarrow U_1, \\ y \Rightarrow -\infty \quad : & u \Rightarrow U_2. \end{aligned}\right\} \tag{131}$$

The absence of a third boundary condition leads to the admission of an infinite number of solutions to the mixing layer. However, the difference between any two of the solutions is simply equivalent to a shift of the velocity profile as a whole in the y-direction. In other words, the location of the dividing streamline remains indeterminate to $0\left(1/\sqrt{R_E}\right)$ as $R_E \Rightarrow \infty$.

Consider the mixing flow for the case when $U_1 \approx U_2$. For this flow we have

$$\frac{\partial \Psi}{\partial y}\frac{\partial^2 \Psi}{\partial x \partial y} - \frac{\partial \Psi}{\partial x}\frac{\partial^2 \Psi}{\partial y^2} = \frac{1}{R_E}\frac{\partial^3 \Psi}{\partial y^3}. \tag{132}$$

When we put

$$\Psi = \sqrt{Uvx}\, f(\eta), \qquad \eta = y\sqrt{\frac{U}{vx}}, \tag{133}$$

where

$$U = \frac{U_1 + U_2}{2},$$

and use (133), equation (134) gives

$$ff'' + 2f''' = 0. \tag{134}$$

The boundary conditions (131) give

$$\eta \Rightarrow \pm\infty: \quad f' = 1 \pm \lambda, \tag{135}$$

where

$$\lambda = \frac{U_1 - U_2}{U_1 + U_2} \ll 1.$$

Putting the dividing streamline arbitrarily at $y = 0$, one has

$$\eta = 0: \quad f = 0. \tag{136}$$

When we seek solutions to (134)–(136) of the form

$$f = \eta + \lambda f_1 + \cdots, \tag{137}$$

(134)–(136) give

$$2f_1''' + \eta f_1'' = 0, \tag{138}$$

$$\left.\begin{aligned} \eta = 0: &\quad f_1 = 0, \\ \eta \Rightarrow \pm\infty: &\quad f_1' = \pm 1, \end{aligned}\right\} \tag{139}$$

from which we have

$$f_1' = \frac{2}{\sqrt{\pi}} \int_0^{\eta} e^{-\xi^2/4}\, d\xi. \tag{140}$$

When we use (137) and (140), (133) gives

$$u = \frac{U_1 + U_2}{2}\left[1 + \frac{U_1 - U_2}{U_1 + U_2}\frac{2}{\sqrt{\pi}} \int_0^{\eta} e^{-\xi^2/4}\, d\xi\right]. \tag{141}$$

Geometrical Characteristics of the Mixing Flow

The conservation of mass in the mixing layer (see Figure 4.15) gives

$$\frac{1}{b}\int_{-y_2}^{y_1} \rho u\, dy = \frac{1}{b}\left[\rho\left(U_1 y_1 - V_1 x\right) + \rho\left(-U_2 y_2 + V_2 x\right)\right], \tag{142}$$

where (U, V) are the velocity components in the (x, y)–directions, respectively.

The momentum conservation gives

$$\frac{1}{b}\int_{-y_2}^{y_1} \rho u^2\, dy = \frac{1}{b}\left[\rho U_1\left(U_1 y_1 - V_1 x\right) + \rho U_2\left(-U_2 y_2 + V_2 x\right)\right]. \tag{143}$$

Multiply (142) by U_1 and subtract from (143), so that

$$\int_{-y_2}^{y_1} \rho u(U_1 - u)\,dy = \rho(U_1 - U_2)(-U_2 y_2 + V_2 x). \tag{144}$$

Similarly, we have

$$\int_{-y_2}^{y_1} \rho u(u - U_2)\,dy = \rho(U_1 - U_2)(U_1 y_1 - V_1 x). \tag{145}$$

Now, noting that the momentum lost by one stream is equal to the momentum gained by the other, we have

$$\int_{-y_2}^{y_1} \rho u(U_1 - u)\,dy = \int_{-y_2}^{y_1} \rho u(u - U_2)\,dy. \tag{146}$$

When we use (144) and (145), (146) gives

$$-U_2 y_2 + V_2 x = U_1 y_1 - V_1 x. \tag{147}$$

When we use (147), (142) gives

$$\rho(-U_2 y_2 + V_2 x) = \rho(U_1 y_1 - V_1 x) = \frac{1}{2}\int_{-y_2}^{y_1} \rho u\,dy \equiv \frac{M}{2}, \tag{148}$$

from which we have

$$V_1 = \frac{1}{\rho x}\left(\rho U_1 y_1 - \frac{M}{2}\right)$$

and

$$V_2 = \frac{1}{\rho x}\left(\rho m U_1 y_2 + \frac{M}{2}\right), \tag{149}$$

where

$$m = \frac{U_2}{U_1}.$$

The transverse equilibrium of the mixing flow gives, on using (142) and (147),

$$\rho V_1(U_1 y_1 - V_1 x) = -\rho V_2(-U_2 y_2 + V_2 x), \tag{150}$$

from which

$$V_1 = -V_2. \tag{151}$$

When we use (147), (151) gives

$$y_1 = -m y_2 \tag{152}$$

or

$$|y_1| = m|y_2|$$

or

$$|y_1| < |y_2| \quad \text{if} \quad m < 1. \tag{153}$$

Equation (153) shows that the mixing layer penetrates more into the lower-speed stream than it does into the higher-speed stream. If one assumes $y = 0$ to be the dividing streamline, (152) implies the two streams contribute equally to the total amount of mass flux through the mixing layer.

Narrow Jets

Another example wherein a boundary-layer type flow occurs is a narrow jet, in which the steep gradients of velocity originate at an orifice, with the total change of velocity across the layer being zero. Consider a steady, two-dimensional jet discharged from an orifice in the form of a long slit. The pressure in the surrounding, nearly stationary, fluid is uniform and one obtains

$$u\frac{\partial u}{\partial x} + v\frac{\partial u}{\partial y} = \nu\frac{\partial^2 u}{\partial y^2}. \tag{154}$$

The x-axis is taken along the axis of the jet. The force acting on the fluid at the origin shows up as flux of momentum across a surface surrounding the origin and, at a section $x = \text{const.}$, is given by

$$F = \rho\int_{-\infty}^{\infty} u^2\, dy, \tag{155}$$

which is independent of x because of the momentum conservation of the jet as a whole. This follows from the fact that, on using equation (154), we have

$$\frac{dF}{dx} = 2\rho\int_{-\infty}^{\infty} u\frac{\partial u}{\partial x}dy = 2\rho\int_{-\infty}^{\infty}\left[-v\frac{\partial u}{\partial y} + \nu\frac{\partial^2 u}{\partial y^2}\right]dy$$

$$= -2\rho\int_{-\infty}^{\infty} u\frac{\partial u}{\partial x}dy + 2\rho\left[-uv + \nu\frac{\partial u}{\partial y}\right]_{-\infty}^{\infty} = 0.$$

Note, however, that the rate of efflux from the orifice, namely,

$$\frac{d}{dx}\int_{-\infty}^{\infty}\rho u\, dy > 0$$

so that the amount of the fluid transported downstream by the jet increases with distance downstream. This is caused by the entrainment of the ambient fluid by the jet.

When we introduce a stream function with the similarity form

$$\psi(x, y) \sim x^p f\left(\frac{y}{x^q}\right), \tag{156}$$

equations (154) and (155) give

$$p+q=1, \quad 2p-q=0 \tag{157}$$

or

$$p=\frac{1}{3}, \quad q=\frac{2}{3}. \tag{158}$$

Thus, we have

$$\psi = 6\nu x^{1/3} f(\eta), \quad \eta = \frac{y}{x^{2/3}}, \tag{159}$$

so

$$u = 6\nu x^{-1/3} f', \quad v = 2\nu x^{-2/3}(2\eta f' - f) \tag{160}$$

and equation (154) gives

$$f''' + 2ff'' + 2f'^2 = 0 \tag{161}$$

with the boundary conditions and symmetry conditions

$$\eta \Rightarrow \pm\infty: \quad f' \Rightarrow 0 \tag{162}$$

and

$$f'(\eta) = f'(-\eta). \tag{163}$$

The solution of (160)–(162) is

$$f = \alpha \tanh \alpha\eta, \tag{164}$$

from which

$$u = 6\nu x^{-1/3} \alpha \operatorname{sech}^2 \alpha\eta. \tag{165}$$

When we use (165), (155) becomes

$$F = 36\rho\nu^2\alpha^4 \int_{-\infty}^{\infty} \operatorname{sech}^4 \alpha\eta \, d\eta = 48\rho\nu^2\alpha^3. \tag{166}$$

It appears that a jet with an arbitrary initial velocity profile approaches asymptotically, as $x \Rightarrow \infty$, the similarity form (165). However, this form may not be observable because of instability of the jet flow.

Wakes

Wake refers to the region of vorticity on the downstream side of a body placed in an otherwise uniform flow. Although the velocity distribution in the wake is complicated near the body, for a steady flow far downstream the streamlines become nearly straight and parallel again, and a boundary–layer type flow prevails asymptotically. If we assume that the departures from the free–stream velocity U (taken in the x–direction) are small in this region, then for the asymptotic wake flow (i.e., as $x \Rightarrow \infty$) we have

$$U\frac{\partial u}{\partial x} = \nu\frac{\partial^2 u}{\partial y^2} \tag{167}$$

with the boundary conditions

$$y \Rightarrow \pm\infty: \quad u \Rightarrow U. \tag{168}$$

We have from equations (167) and (168)

$$x \Rightarrow \infty: \quad U_\infty - u \Rightarrow \frac{QU}{\sqrt{4\pi\nu x}} \exp\left(-\frac{Uy^2}{4\nu x}\right), \tag{169}$$

where

$$Q = \int_{-\infty}^{\infty} (U-u)\,dy = \text{const.}$$

Note that the total drag on the body giving rise to the wake is related to this velocity defect, and for a nonlifting body moving steadily through the fluid, it is given by

$$D = \rho U \int_{-\infty}^{\infty} (U-u)\,dy = \rho UQ. \tag{170}$$

Periodic Boundary-Layer Flows

In problems of unsteady motion of bodies through a fluid, viscous effects are generally limited to a thin boundary layer region only for small values of the time since the onset of motion. A low level of vorticity persists beyond the boundary layer, in general.

For a two-dimensional boundary-layer flow in the x-direction past the plane $y = 0$, we have

$$\frac{\partial u}{\partial x} + \frac{\partial v}{\partial y} = 0, \tag{171}$$

$$\frac{\partial u}{\partial t} + u\frac{\partial u}{\partial x} + v\frac{\partial u}{\partial y} = \frac{\partial U}{\partial t} + U\frac{\partial U}{\partial x} + \nu\frac{\partial^2 u}{\partial y^2}, \tag{172}$$

where $U(x,t)$ represents the ambient flow. If L denotes a representative length in the x-direction, U_∞ represents the reference velocity at infinity, and T is a representative time interval, the validity of equations (171) and (172) requires

$$\frac{TU_\infty}{L} \sim 0(1)$$

or

$$\frac{TU_\infty}{L(U_\infty L/\nu)} = \frac{\nu T}{L^2} \ll 1. \tag{173}$$

This means that vorticity will be confined to a thin boundary layer only within a comparatively small time interval from the onset of motion. It does not imply the complete breakdown of the boundary–layer approximations at large T, but only that vorticity has diffused or has been convected beyond the boundary–layer region, where it is no longer negligible.

Consider a periodic flow produced by the oscillations of an infinite plate parallel to itself in a fluid at rest at infinity. If the amplitude of the motion is assumed small, we may assume an expansion of the form

$$\left.\begin{aligned} u &= u_0 + \varepsilon u_1 + \varepsilon^2 u_2 + \cdots \\ v &= \varepsilon v_0 + \varepsilon^2 v_1 + \cdots \end{aligned}\right\} \quad \varepsilon \ll 1. \tag{174}$$

In the frame of reference moving with the plate, we have

$$U(x,t) = U_0(x) e^{i\sigma t}. \tag{175}$$

Let us assume that $\partial u/\partial x \sim 0(\varepsilon)$. Then, equation (172) gives

$$\frac{\partial u_0}{\partial t} - \nu \frac{\partial^2 u_0}{\partial y^2} = \frac{\partial U}{\partial t}, \tag{176}$$

$$\frac{\partial u_1}{\partial t} - \nu \frac{\partial^2 u_1}{\partial y^2} = U \frac{\partial U}{\partial x} - u_0 \frac{\partial u_0}{\partial x} - v_0 \frac{\partial u_0}{\partial y}, \tag{177}$$

etc., with

$$\begin{aligned} &y = 0: \quad u_0, u_1, \ldots = 0, \\ &y = \infty: \quad u_0 = U(x,t); \quad u_1, u_2, \ldots = 0. \end{aligned} \tag{178}$$

We may satisfy equation (171) identically by introducing

$$\left.\begin{aligned} &u_0 = \frac{\partial \psi_0}{\partial y}, \qquad v_0 = -\frac{\partial \psi_0}{\partial x}, \\ &\psi_0 = \sqrt{\frac{2\nu}{\sigma}}\, U_0(x) f_0(\eta) e^{i\sigma t}, \qquad \eta = y\sqrt{\frac{\sigma}{2\nu}}. \end{aligned}\right\} \tag{179}$$

Equation (176) then gives

$$if_0' - \frac{1}{2} f_0''' = i, \tag{180}$$

from which

$$f_0' = 1 - e^{-(1+i)\eta}. \tag{181}$$

Therefore,

$$u_0 = U_0(x)\left[\cos \sigma t - e^{-\eta} \cos(\sigma t - \eta)\right], \tag{182}$$

which shows that, at high frequencies, motion is in phase with that of the plate.

Next, let us introduce for the $0(\varepsilon)$ problem a stream function given by

$$\psi_1 = \sqrt{\frac{2\nu}{\sigma}}\, U_0 U_0' \frac{1}{\sigma}\left[f_1(\eta)e^{2i\sigma t} + g_1(\eta)\right], \tag{183}$$

so that equation (177) gives

$$2if_1' e^{2i\sigma t} - \frac{1}{2}\left(f_1''' e^{2i\sigma t} + g_1'''\right) = \mathrm{Re}\left(U_0 e^{i\sigma t}\right)\mathrm{Re}\left(U_0' e^{i\sigma t}\right) - \left[\mathrm{Re}\left(f_0' e^{i\sigma t}\right)\right]^2 + \mathrm{Re}\left(f_0 e^{i\sigma t}\right)\mathrm{Re}\left(f_0'' e^{i\sigma t}\right), \tag{184}$$

from which

$$2if_1' - \frac{1}{2}f_1''' = \frac{1}{2}\left(1 - f_0'^2 + f_0 f_0''\right),$$

$$\frac{1}{2}g_1''' = \frac{1}{2}\left(1 - f_0' f_0'^*\right) + \frac{1}{4}\left(f_0'' f_0^* + f_0 f_0^{*''}\right) \tag{185}$$

with

$$\left.\begin{aligned} \eta = 0: \quad & f_1, f_1' = 0, \\ & g_1, g_1' = 0, \\ \eta \Rightarrow \infty: \quad & f_1' \Rightarrow 0. \end{aligned}\right\} \tag{186}$$

Thus,

$$f_1' = -\frac{1}{2}ie^{-(1+i)\sqrt{2}\eta} + \frac{1}{2}ie^{-(1+i)\eta} - \frac{1}{2}(i-1)\eta e^{-(1+i)\eta} \tag{187}$$

$$g_1' = -\frac{3}{4} + \frac{1}{4}e^{-2\eta} + 2e^{-\eta}\sin\eta + \frac{1}{2}e^{-\eta}\cos\eta - \frac{1}{2}\eta e^{-\eta}(\cos\eta - \sin\eta). \tag{188}$$

Of significance is the existence of a steady component of velocity $U_0 U_0' g_1'(\eta)/\sigma$ induced by the oscillatory potential flow. Such a steady motion can lead to extensive migration of fluid elements in an apparently purely oscillatory system.

Exercises

1. Upon using x and Ψ as the independent variables instead of x and y, show that the boundary–layer equation can be reduced to a diffusion equation.
2. Consider a columnar jet formed by forcing a fluid through a small circular hole in a wall. Taking the x–axis along the axis of the jet, using cylindrical coordinates (r, θ, x), and making arguments concerning the relative sizes of velocity gradients in the jet, similar to those used for a two–dimensional jet, show that the equations of motion and continuity for the columnar–jet flow may be approximated by

$$\left.\begin{aligned} u\frac{\partial u}{\partial x}+v\frac{\partial u}{\partial r}&=\frac{\nu}{r}\frac{\partial}{\partial r}\left(r\frac{\partial u}{\partial r}\right),\\ \frac{\partial}{\partial x}(ru)+\frac{\partial}{\partial r}(rv)&=0, \end{aligned}\right\}$$

where u and v are the velocity components along the x, r–directions, respectively. The boundary conditions for this flow are

$$\left.\begin{aligned} r=0:&\quad v,\ \frac{\partial u}{\partial r}=0,\\ r\to\infty:&\quad u\to 0. \end{aligned}\right\}.$$

Show that the flux of momentum of the fluid forced through the hole, namely,

$$M=2\pi\rho\int_0^{\infty}u^2 r\,dr,$$

is constant. Introducing a Stokes stream function defined by

$$u=\frac{1}{r}\frac{\partial\Psi}{\partial r},\qquad v=-\frac{1}{r}\frac{\partial\Psi}{\partial x},$$

determine a similarity solution of the form $\Psi=x^p f\left(rx^q\right)$.

3. Consider the compressible flow in a boundary layer on a flat plate. Using Howarth–Dorodnitsyn transformation and assuming a constant–plate temperature, find the integral for the energy equaiton (i.e., the counterpart of (130)) for the case $P_r\neq 1$.

4. Consider a semifinite region of a stationary perfect gas which is bounded by a rigid plane. The plane is suddenly given a velocity U in its own plane and thereafter maintained at that velocity. Using Howarth–Dorodnitsyn transformation, calculate the ensuing flow.

4.4. Jeffrey–Hamel Flow

The so–called Jeffrey–Hamel flow refers to a two–dimensional flow in the region between two intersecting plane walls. The steady flow between the stationary walls is caused by the presence of a source or sink of fluid at the point of intersection of the walls. This example affords an impressive illustration of the combined effects of convection and diffusion of vorticity generated at a rigid boundary.

The Exact Solution

Let us use the cylindrical polar coordinates (r, θ) with the plane walls located at $\theta = \pm\alpha$ (Figure 4.16). We then have for this flow

$$\rho\left(u_r\frac{\partial u_r}{\partial r}+u_\theta\frac{\partial u_r}{r\partial\theta}-\frac{u_\theta^2}{r}\right)=-\frac{\partial p}{\partial r}+\mu\left[\nabla^2 u_r-\frac{u_r}{r^2}-2\frac{\partial u_\theta}{r^2\partial\theta}\right], \tag{1}$$

$$\rho\left(u_r\frac{\partial u_\theta}{\partial r}+u_\theta\frac{\partial u_\theta}{r\partial\theta}+\frac{u_r u_\theta}{r}\right)=-\frac{\partial p}{r\partial\theta}+\mu\left[\nabla^2 u_\theta-\frac{u_\theta}{r^2}+2\frac{\partial u_r}{r^2\partial\theta}\right], \tag{2}$$

$$\frac{\partial u_r}{\partial r}+\frac{u_r}{r}+\frac{1}{r}\frac{\partial u_\theta}{\partial\theta}=0, \tag{3}$$

where

$$\nabla^2=\frac{\partial^2}{\partial r^2}+\frac{1}{r}\frac{\partial}{\partial r}+\frac{\partial^2}{r^2\partial\theta^2}.$$

Let us look for a purely radial flow and put

$$u_r=\frac{f(\theta)}{r}, \qquad u_\theta\equiv 0, \tag{4}$$

so that equation (3) is identically satisfied, and equations (1) and (2) give

$$-\frac{f^2}{r^2}=-\frac{1}{\rho}\frac{\partial p}{\partial r}+\frac{\nu}{r^3}f'' \tag{5}$$

$$0=-\frac{1}{\rho r}\frac{\partial p}{\partial\theta}+\frac{2\nu}{r^3}f' \tag{6}$$

where the primes denote differentiation with respect to θ. The boundary conditions on f are

$$\theta=\pm\alpha: \quad f=0. \tag{7}$$

We obtain from equation (6)

$$\frac{p}{\rho}=\frac{2\nu}{r^2}f+F(r). \tag{8}$$

When we use equation (8), equation (5) gives

$$\nu f''+f^2+4\nu f=r^3\frac{dF}{dr}=\text{const.}=A, \tag{9}$$

from which

$$F(r)=-\frac{A}{r^2}+B, \tag{10}$$

where A and B are arbitrary constants.

Multiplying equation (9) by f', integrating between $\theta=-\alpha,\theta$, and using equation (7), we obtain

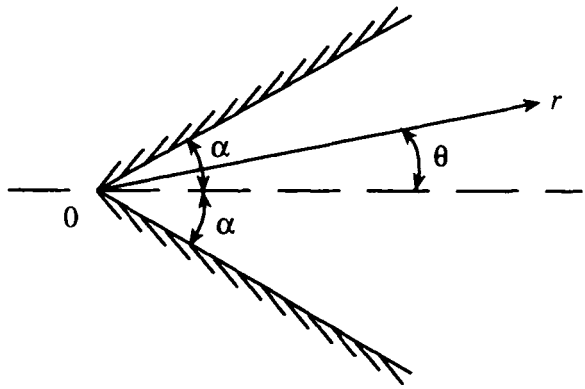

Figure 4.16. The Jeffrey–Hamel flow.

$$\frac{1}{3}f^3 + 2\nu f^2 + \frac{\nu}{2}f'^2 = Af + C_1, \tag{11}$$

where C_1 is an arbitrary constant. Rewriting (11), we have

$$f'^2 = -\frac{2}{3\nu}f^3 - 4f^2 + \frac{2Af}{\nu} + \frac{2}{\nu}C_1 \equiv -\frac{2}{3\nu}G(f), \tag{12}$$

from which

$$\theta = \pm\int \frac{df}{\sqrt{-\frac{2}{3\nu}G(f)}}. \tag{13}$$

Let us write

$$G(f) = (f - e_1)(f - e_2)(f - e_3). \tag{14}$$

We then have, from (12),

$$e_1 + e_2 + e_3 = -6\nu. \tag{15}$$

We now have two cases:

1. Only e_1 is real and positive; $G(f)$ then looks as shown in Figure 4.17. We then have pure outflow, and (13) becomes

$$\theta = \sqrt{\frac{3\nu}{2}}\int_f^{e_1} \frac{df}{\sqrt{-G(f)}}, \tag{16}$$

from which

$$f = \nu e_1 - \frac{3M^2\nu}{2}\frac{1 - cn(M\theta, \chi)}{1 + cn(M\theta, \chi)} \tag{17}$$

where

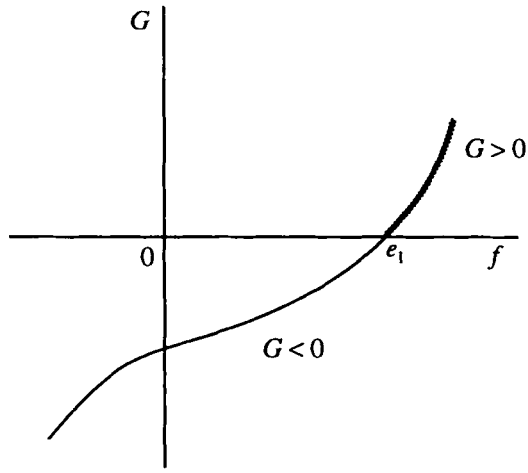

Figure 4.17. Variation of the function G with f for the case wherein only e_1 is real and positive.

$$M=\frac{2}{3}\left[(e_1-e_2)(e_1-e_3)\right]^{1/2},\quad \chi^2=\frac{1}{2}+\frac{e_1+2}{2M^2}.$$

2. e_1, e_2, and e_3 are real and distinct; $G(f)$ then looks as shown in Figure 4.18. For inflow we then have

$$\theta=\sqrt{\frac{3\nu}{2}}\int_{e_2}^{f}\frac{df}{\sqrt{-G(f)}}, \tag{18}$$

from which

$$f=\nu e_1-6\nu k^2m^2sn^2(K-m\theta,k), \tag{19}$$

where

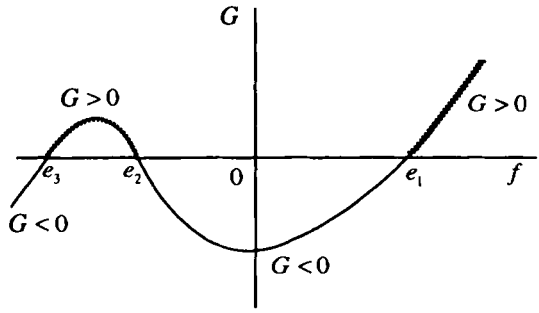

Figure 4.18. Variation of the function G with f for the case wherein e_1, e_2, and e_3 are real and distinct.

$$m^2 = \frac{e_1 - e_3}{6}, \qquad k^2 = \frac{e_1 - e_2}{e_1 - e_3}$$

and $K(k^2)$ is the complete elliptic integral of the first kind. For outflow,

$$\theta = \sqrt{\frac{3\nu}{2}} \int_f^{e_3} \frac{df}{\sqrt{-G(f)}}, \tag{20}$$

from which

$$f = \nu e_1 - 6k^2 m^2 sn^2(m\theta, k) \tag{21}$$

f and f' for cases 1 and 2 are sketched in Figures 4.19 and 4.20. Note that $f = f(\theta)$ is not periodic for case 1, while it is periodic with period $2(\beta + \alpha)$ for case 2, where

$$\beta = \int_0^{e_1} \frac{df}{\sqrt{-\frac{2}{3\nu} G(f)}}, \qquad \alpha = \int_{e_2}^{0} \frac{df}{\sqrt{-\frac{2}{3\nu} G(f)}}.$$

Using (7), we have 2β, $2\alpha < 2\pi$.

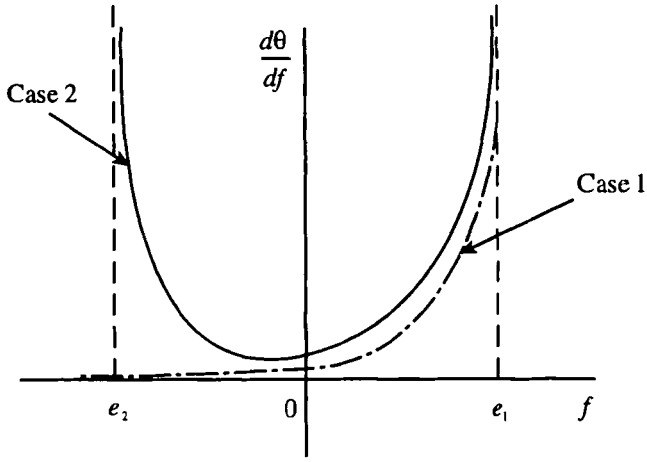

Figure 4.19. Variation of f' with f for the two cases illustrated in Figures 4.17 and 4.18.

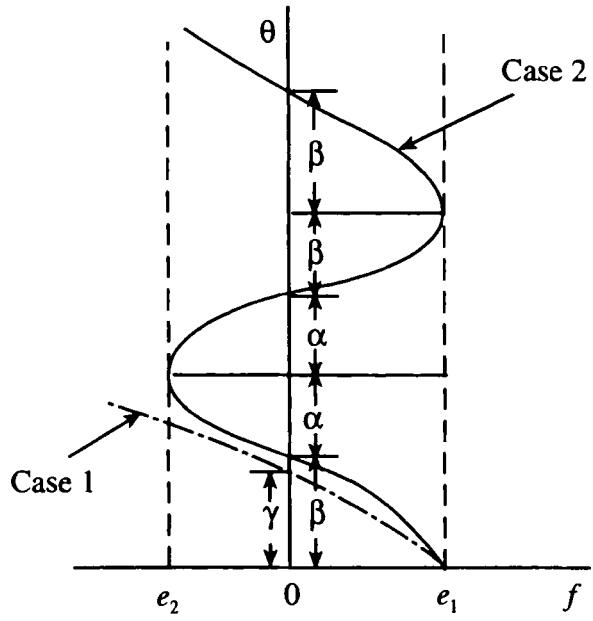

Figure 4.20. Variation of f with θ for the two cases illustrated in Figures 4.17 and 4.18.

The flows corresponding to cases 1 and 2 are shown in Figure 4.21. Note that

$$f(0) = \begin{cases} e_1, \\ e_2, \end{cases} \quad \text{if} \quad u_r \gtrless 0. \tag{22}$$

Note that the possibility of finding compound flows with zero values of f at $\theta = \pm\alpha$, increases as $\alpha f(0)/\nu$ increases.

Flows at Low Reynolds Numbers

When we nondimensionalize according to

$$\bar{f} = \frac{f}{f(0)}, \tag{23}$$

equation (9) becomes

$$\frac{d^2\bar{f}}{d\theta^2} + 4\bar{f} + R_E\bar{f}^2 = \frac{A}{\nu f(0)} \equiv \bar{A},$$

$$\theta = \pm\alpha: \quad \bar{f} = 0 \tag{24}$$

where

$$R_E = f(0)/\nu = e_{1,2}/\nu \ll 1.$$

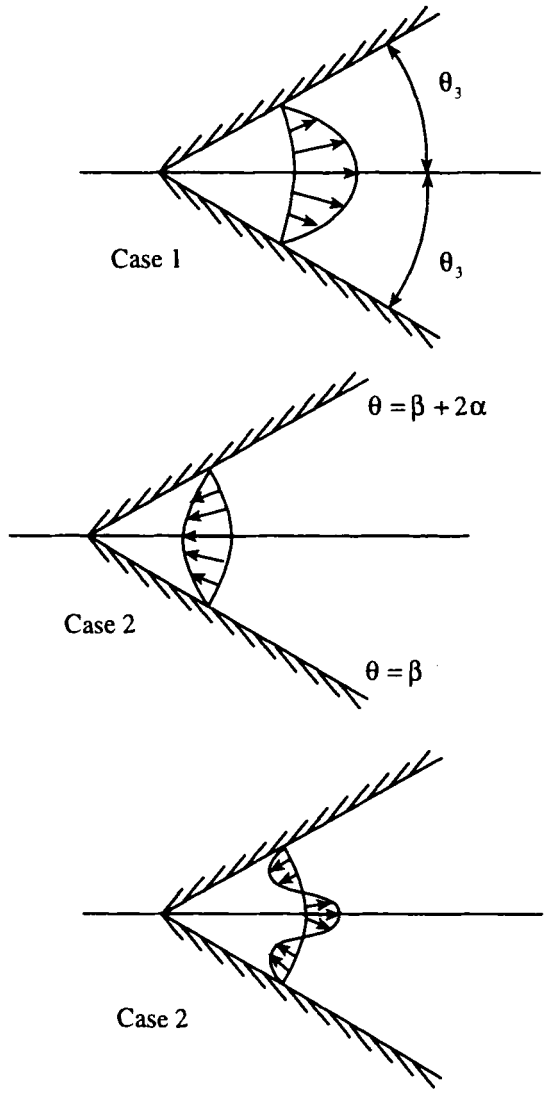

Figure 4.21. Diverging and converging flows at low Reynolds numbers.

Thus, the Reynolds number is based on the local maximum velocity and the local width of the region concerned.

Let us seek solutions of the form

$$\left.\begin{aligned} \bar{f}(\theta) &= \bar{f}_0(\theta) + R_E \bar{f}_1(\theta) + \cdots, \\ \overline{A} &= \overline{A}_0 + R_E \overline{A}_1 + \cdots, \end{aligned}\right\} \tag{25}$$

so that we have from (24) and (7)

$$\left.\begin{aligned} &\frac{d^2\bar{f}_0}{d\theta^2} + 4\bar{f}_0 = \bar{A}_0, \\ &\theta = \pm\alpha: \quad \bar{f}_0 = 0, \end{aligned}\right\} \tag{26}$$

$$\left.\begin{aligned} &\frac{d^2\bar{f}_1}{d\theta^2} + 4\bar{f}_1 = -\bar{f}_0^2 + \bar{A}_1, \\ &\theta = \pm\alpha: \quad \bar{f}_1 = 0, \end{aligned}\right\} \tag{27}$$

etc.

We have, from (26),

$$\bar{f}_0 = \frac{\bar{A}_0}{4}\left(1 - \frac{\cos 2\theta}{\cos 2\alpha}\right). \tag{28}$$

When $\bar{f}_0(0) = 1$, (28) gives

$$\frac{\bar{A}_0}{4} = \frac{1}{1 - \dfrac{1}{\cos 2\alpha}}. \tag{29}$$

When we use (29) to write (28) as

$$\bar{f}_0 = a(b - \cos 2\theta), \tag{30}$$

(27) becomes

$$\left.\begin{aligned} &\frac{d^2\bar{f}_1}{d\theta^2} + 4\bar{f}_1 = -a^2(b - \cos 2\theta)^2 + \bar{A}_1, \\ &\theta = \pm\alpha: \quad \bar{f}_1 = 0, \\ &\theta = 0: \quad \bar{f}_1 = 0. \end{aligned}\right\} \tag{31}$$

We have from (31)

$$\bar{f}_1(\theta) = C_2(\cos 2\theta - 1) + \frac{a^2b^2}{2}\,\theta \sin 2\theta + \frac{a^2}{24}(\cos 4\theta - 1), \tag{32}$$

where

$$C_2 = -\left[\frac{a^2b^2}{2}\,\alpha \sin 2\alpha + \frac{a^2}{24}(\cos 4\alpha - 1)\right]\frac{1}{\cos 2\alpha - 1}.$$

The solutions (25), (31), and (32) are sketched in Figure 4.22. Note that whereas for purely convergent flow, the effect of increasing R_ε is to produce a flatter velocity profile at the center of the channel with steep velocity gradients near the walls, the effect in purely divergent flow is to concentrate the flux of fluid at the center of the channel with smaller velocity gradients at the walls. This suggests that one may expect the boundary–layer flows to arise near the walls in purely convergent flows and not in purely divergents flows; this is verified in

detail below. Notice the occurrence of backflow in a diverging channel as R_E increases. In order to investigate this backflow, let us note from (12) that

$$C_1 = \frac{\nu}{2}\left[\left(\frac{df}{d\theta}\right)^2_{\theta=\pm\alpha}\right], \tag{33}$$

so that the onset of backflow is characterized by

$$C_1 = 0. \tag{34}$$

Using

$$\theta = 0: \quad f = e_1, \qquad f' = 0, \tag{35}$$

we have from (12)

$$e_1^3 + 6\nu e_1^2 - 3Ae_1 - 3C_1 = 0. \tag{36}$$

When we use (36), (12) becomes

$$f'^2 = \frac{2}{3\nu}(e_1 - f)\left[f^2 + f(6\nu + e_1) + \frac{3C}{e_1}\right], \tag{37}$$

from which corresponding to the onset of backflow (i.e., $C_1 = 0$) we obtain

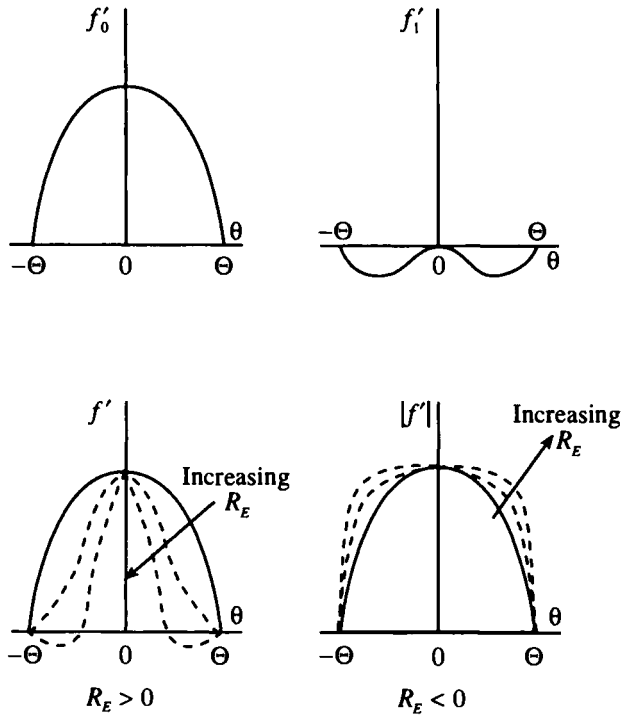

Figure 4.22. Diverging and converging flows at low Reynolds numbers.

$$\theta_{\text{Critical}} = \int_0^{e_1} \frac{df}{\sqrt{\frac{2}{3\nu}(e_1 - f)\left[f^2 + f(6\nu + e_1)\right]}},$$

$$= \sqrt{\frac{3\nu}{2e_1}} \int_0^1 \frac{dt}{\sqrt{t(1-t)\left[1 + \left(1 + \frac{6\nu}{e_1}\right)t\right]}},$$

$$= \sqrt{\frac{3\nu}{3\nu + e_1}}\, K\left[\frac{1}{2}\left(\frac{e_1}{3\nu + e_1}\right)\right]. \tag{38}$$

Flows at High Reynolds Numbers

We mentioned above that as the Reynolds number R_E becomes large, the flow tends to become uniform except for boundary layers near the walls. This may be seen by referring to (19); since m becomes large, it follows that so must be $K(k^2)$ or $k \sim 1$. Then $e_2 \approx e_3$, sn $t \sim \tanh t$, and $e_1 = -6\nu - 2e_2 \approx -2e_2$, so that

$$f = e_2\left[3\nu \tanh^2\left\{\sqrt{-\frac{e_2^2}{2}}(\alpha - \theta) + \beta\right\} - 2\right], \tag{39}$$

where

$$\beta = \tanh^{-1}\sqrt{\frac{2}{3\nu}}.$$

Thus f is approximately equal to e_2 except in the boundary layer of thickness proportional to $1/\sqrt{-e_2}$.

In order to verify these features in detail, write equation (24) as

$$\frac{d^3\bar{f}}{d\theta^3} + 4\frac{d\bar{f}}{d\theta} + 2R_E\bar{f}\frac{d\bar{f}}{d\theta} = 0. \tag{40}$$

In the limit $R_E \Rightarrow \infty$, i.e. corresponding to the outer core flow, equation (40) gives

$$\bar{f}^{(0)}\frac{d\bar{f}^{(0)}}{d\theta} = 0 \tag{41}$$

with

$$\theta = 0: \quad \bar{f}^{(0)} = 1. \tag{42}$$

We have from (41) and (42)

$$\bar{f}^{(0)} \equiv 1, \tag{43}$$

so that for $R_E \gg 1$ the radial velocity is nearly uniform over $\theta = (-\alpha, \alpha)$ except in boundary layers close to the wall.

In order to consider the flow near the wall, let us put

$$\Theta = \sqrt{|R_E|}\,(\alpha - \theta), \tag{44}$$

so that equation (40) becomes

$$\frac{d^3\bar{f}}{d\Theta^3} + \frac{4}{|R_E|^{3/2}}\frac{d\bar{f}}{d\Theta} + 2\frac{R_E}{|R_E|}\bar{f}\frac{d\bar{f}}{d\Theta} = 0. \tag{45}$$

In the limit $R_E \Rightarrow \infty$, equation (45) gives the following equation for the flow in a convergent channel:

$$\frac{d^2\bar{f}^{(i)}}{d\Theta^2} - \left(\bar{f}^{(i)}\right)^2 = -1. \tag{46}$$

For the flow in a divergent channel, equation (45) gives

$$\frac{d^2\bar{f}^{(i)}}{d\Theta^2} + \left(\bar{f}^{(i)}\right)^2 = 1. \tag{47}$$

Thus, putting

$$\bar{f}^{(i)} = 1 + \bar{h}^{(i)}(\Theta) \tag{48}$$

and noting that the boundary–layer nature of the flow near the wall requires $\bar{f}^{(i)}$ to match asymptotically with the outer–core flow, given by (43), we have

$$\Theta \Rightarrow \infty: \quad \bar{h}^{(i)} \Rightarrow 0. \tag{49}$$

From equations (46) and (47), we have for a convergent channel

$$\frac{d^2\bar{h}^{(i)}}{d\Theta^2} - 2\bar{h}^{(i)} = 0$$

or

$$\bar{h}^{(i)} = B_1 e^{-\sqrt{2}\,\Theta}, \tag{50}$$

and for a divergent channel we have

$$\frac{d^2\bar{h}^{(i)}}{d\Theta^2} + 2\bar{h}^{(i)} = 0$$

or

$$\bar{h}^{(i)} = D_1 \sin\sqrt{2}\,\Theta + D_2 \cos\sqrt{2}\,\Theta. \tag{51}$$

Therefore, it is obvious that there can be no boundary–layer flow in a divergent channel.

This page intentionally left blank

5

HYDRODYNAMIC STABILITY

5.1. Introduction to Hydrodynamic Stability

The equations of fluid dynamics admit some simple patterns of flow as stationary solutions which can exist only for certain ranges of the parameters characterizing them. This is traced to their inherent instability, i.e., in their inability to sustain themselves against any small perturbations acting on them. The objective of the theory of hydrodynamic stability is to examine the stability of admissible stationary solutions of the equations of fluid dynamics.

In the case of a dynamical system with a finite number degrees of freedom, a definition of stability of equilibrium or of steady motion can easily be given because the motion is determined by the initial conditions only. But, the case of a continuous medium renders this task difficult in that the determination of the motion requires a knowledge not only of the condition at time $t = 0$, but also the boundary conditions for $t > 0$.

Mathematically, the problem consists of following the subsequent career of a hydrodynamically possible disturbance which is superposed on the basic steady flow. If the disturbances vanish at $t \Rightarrow \infty$, the motion is stable, otherwise it is unstable.

In order to study the behavior of disturbances, one must follow the solution of a system of nonlinear partial differential equations which, in general, is very difficult. Sometimes, one assumes that the disturbances are small so that the equations governing the disturbances may be linearized, i.e., the terms quadratic or higher in the disturbances and their derivatives may be neglected. The resultant linear and homogeneous system of equations contains time t only through derivatives with respect to t, so that the solutions containing an exponential time factor e^{ct} may be expected. The boundary conditions for the disturbances (which require the vanishing of quantities like the disturbance velocities at the boundaries)

are normally homogeneous; consequently, we have a characteristic–value problem with c as the parameter. If all characteristic values of c have negative real parts, the motion is stable with respect to infinitesimal disturbances provided the characteristic functions form a complete set in terms of which any physically realizable initial state can be expanded. If some of the characteristic values of c have positive real parts, the motion is said to be unstable. However, it must be noted that such a linear instability does not necessarily lead to turbulence. It could lead to another, more stable state of laminar flow. Thus, linear stability theory is adequate if one is interested only in the onset of instability of a given basic state.

In the method of normal modes, one linearizes the governing equations for small perturbations about a stationary state of the system. Each disturbance is then resolved into dynamically independent wave components (which, because of linearity, do not interact with each other), and one examines the stability of the system with respect to each of these modes by posing a linear characteristic–value problem for a typical mode. The requirement that the governing equations for the normal modes allow nontrivial solutions satisfying the prescribed boundary conditions leads to a characteristic–value problem. The latter problem sometimes admits singular solutions with a continuous spectrum of characteristic values in addition to well–behaved solutions with a discrete spectrum.

5.2. Thermal Instability of a Layer of Fluid Heated from Below

Consider a horizontal layer of fluid in which an adverse temperature gradient is maintained by heating the underside. Due to thermal expansion, the fluid at the bottom will become lighter than the fluid at the top, so that this will be a potentially unstable top–heavy arrangement. This instability will cause the fluid to redistribute itself so as to remedy the weakness in the arrangement. However, since the fluid viscosity will inhibit this behavior, the adverse temperature gradient maintained in the fluid may be expected to exceed a certain value before the instability can manifest itself. When the instability sets in, it is found experimentally that the ensuing motions have a stationary cellular character.

The Characteristic–Value Problem

One has the following equations governing the motion of the fluid,

$$\frac{\partial \rho}{\partial t} + \frac{\partial}{\partial x_j}(\rho v_j) = 0, \tag{1}$$

$$\rho\left(\frac{\partial v_i}{\partial t} + v_j \frac{\partial v_i}{\partial x_j}\right) = \rho X_i - \frac{\partial p}{\partial x_i} + \frac{\partial}{\partial x_j}\left\{\mu\left(\frac{\partial v_i}{\partial x_j} + \frac{\partial v_j}{\partial x_i}\right) - \frac{2}{3}\mu\,\delta_{ij}\frac{\partial v_k}{\partial x_k}\right\}, \tag{2}$$

$$\rho\left\{\frac{\partial}{\partial t}\left(C_v T\right)+ v_j \frac{\partial}{\partial x_j}\left(C_v T\right)\right\}=\frac{\partial}{\partial x_j}\left(K\frac{\partial T}{\partial x_j}\right)-p\frac{\partial v_j}{\partial x_j}+\Phi, \tag{3}$$

where

$$\Phi=\mu\left[\left(\frac{\partial v_1}{\partial x_2}+\frac{\partial v_2}{\partial x_1}\right)^2+\left(\frac{\partial v_2}{\partial x_3}+\frac{\partial v_3}{\partial x_2}\right)^2+\left(\frac{\partial v_3}{\partial x_1}+\frac{\partial v_1}{\partial x_3}\right)^2\right]+,$$

$$+\frac{2}{3}\mu\left[\left(\frac{\partial v_1}{\partial x_1}-\frac{\partial v_2}{\partial x_2}\right)^2+\left(\frac{\partial v_2}{\partial x_2}-\frac{\partial v_3}{\partial x_3}\right)^2+\left(\frac{\partial v_3}{\partial x_3}-\frac{\partial v_1}{\partial x_1}\right)^2\right], \tag{4}$$

$$\rho=\rho_0\left[1-\alpha\left(T-T_0\right)\right]. \tag{5}$$

Based on experience in practice, one may treat ρ as a constant in all terms in the equations of motion except the one in the external force – the Boussinesq approximation. Then equations (1)–(3) give

$$\frac{\partial v_j}{\partial x_j}=0, \tag{6}$$

$$\frac{\partial v_i}{\partial t}+v_j\frac{\partial v_i}{\partial x_j}=-\frac{1}{\rho_0}\frac{\partial p}{\partial x_i}+\left(1+\frac{\delta\rho}{\rho_0}\right)X_i+\nu\nabla^2 v_i, \tag{7}$$

$$\delta\rho=-\rho_0\alpha\left(T-T_0\right), \tag{8}$$

$$\frac{\partial T}{\partial t}+v_j\frac{\partial T}{\partial x_j}=\hat{K}\nabla^2 T, \qquad \hat{K}\equiv\frac{K}{\rho_0 C_v}, \tag{9}$$

where $\delta\rho$ is the change in density, and the viscous heat generation Φ has been ignored.

Consider an infinite horizontal layer of fluid in which a steady adverse temperature gradient is maintained; further, let there be no motions initially. The initial state is given by

$$v_j\equiv 0, \qquad T\equiv T\left(\lambda_i x_i\right), \qquad x=\lambda_i x_i, \tag{10}$$

$$\frac{\partial p}{\partial x_i}=-\rho g\lambda_i, \tag{11}$$

$$\rho=\rho_0\left[1+\alpha\left(T_0-T\right)\right], \tag{12}$$

$$\nabla^2 T=0, \tag{13}$$

where $\lambda=(0,0,1)$ is a unit vector in the direction of the vertical. Equations (10)–(13) give

$$T=T_0-\beta\lambda_i x_i, \tag{14}$$

$$\rho = \rho_0\left(1 + \alpha\beta\lambda_i x_i\right), \tag{15}$$

$$p = p_0 - g\rho_0\left(\lambda_i x_i + \frac{1}{2}\alpha\beta\lambda_i\lambda_j x_i x_j\right). \tag{16}$$

Let v_j denote the velocity in the perturbed state; and let the altered temperature distribution be

$$T' = T_0 - \beta\lambda_i x_i + \theta \tag{17}$$

and let δp denote the change in pressure. Then, upon linearization, equations (6)–(9) give

$$\frac{\partial v_i}{\partial t} = -\frac{\partial}{\partial x_i}\left(\frac{\delta p}{\rho}\right) + g\alpha\theta\lambda_i + \nu\nabla^2 v_i, \tag{18}$$

$$\frac{\partial\theta}{\partial t} = \beta\lambda_j v_j + \hat{K}\nabla^2\theta, \tag{19}$$

$$\frac{\partial v_i}{\partial x_i} = 0. \tag{20}$$

Taking the curl of equation (18), one obtains for the vorticity Ω

$$\frac{\partial\Omega_i}{\partial t} = g\alpha\varepsilon_{ijk}\frac{\partial\theta}{\partial x_j}\lambda_k + \nu\nabla^2\Omega_i; \tag{21}$$

and taking the curl again, one obtains

$$\frac{\partial}{\partial t}\left(\nabla^2 v_i\right) = g\alpha\left(\lambda_i\nabla^2\theta - \lambda_j\frac{\partial^2\theta}{\partial x_i\partial x_j}\right) + \nu\nabla^4 v_i. \tag{22}$$

Multiplying equation (22) by λ_i, one obtains

$$\frac{\partial}{\partial t}\left(\nabla^2 w\right) = g\alpha\left(\frac{\partial^2\theta}{\partial x^2} + \frac{\partial^2\theta}{\partial y^2}\right) + \nu\nabla^4 w. \tag{23}$$

Equation (19) can be written as

$$\frac{\partial\theta}{\partial t} = \beta w + \hat{K}\nabla^2\theta, \tag{24}$$

where

$$w = \lambda_j v_j. \tag{25}$$

If the fluid is confined between the planes (assumed to be infinitely conducting) $z = 0, d$, one has the boundary conditions

$$z = 0, d: \quad w = 0, \qquad \theta = 0. \tag{26}$$

On a rigid surface, at $z = 0, d$, one must also have

$$u = 0, \qquad v = 0; \tag{27}$$

and from equation (20), equation (27) gives

$$\frac{\partial w}{\partial z} = 0. \tag{28}$$

On a free surface,

$$\frac{\partial u}{\partial z}, \quad \frac{\partial v}{\partial z} = 0; \tag{29}$$

and from equation (20), equation (29) gives

$$\frac{\partial^2 w}{\partial z^2} = 0. \tag{30}$$

Let us analyze the disturbances into normal modes, and look for solutions of the form

$$\left.\begin{aligned} w &= W(z)\, e^{i(k_x x + k_y y) + pt}, \\ \theta &= \Theta(z)\, e^{i(k_x x + k_y y) + pt}, \end{aligned}\right\} \tag{31}$$

so that equations (23) and (24) give

$$p\left(\frac{d^2}{dz^2} - k^2\right) W = -g\alpha k^2 \Theta + \nu \left(\frac{d^2}{dz^2} - k^2\right)^2 W, \tag{32}$$

$$p\Theta = \beta W + \hat{K}\left(\frac{d^2}{dz^2} - k^2\right)\Theta, \qquad k^2 \equiv k_x^2 + k_y^2. \tag{33}$$

The boundary conditions (26), (28), and (30) become

$$z = 0, d: \quad \Theta = 0, \qquad W = 0 \tag{34}$$

$$\left.\begin{aligned} &\text{on a rigid surface}: && \frac{dW}{dz} = 0, \\ &\text{on a free surface}: && \frac{d^2 W}{dz^2} = 0. \end{aligned}\right\} \tag{35}$$

Nondimensionalize various quantities using d, ν; then equations (32) and (33) become

$$\left(D^2 - a^2\right)\left(D^2 - a^2 - \sigma\right) W = \left(\frac{g\alpha}{\nu} d^2\right) a^2 \Theta, \tag{36}$$

$$\left(D^2 - a^2 - P\sigma\right)\Theta = -\left(\frac{\beta}{\hat{K}} d^2\right) W, \tag{37}$$

where

$$D \equiv \frac{d}{dz}, \qquad P = \frac{\nu}{\hat{K}}, \qquad a = kd, \qquad \sigma = \frac{pd^2}{\nu}.$$

One obtains from equations (36) and (37)

$$\left(D^2-a^2\right)\left(D^2-a^2-\sigma\right)\left(D^2-a^2-P\sigma\right)W=-R_A a^2 W, \tag{38}$$

where R_A is the Rayleigh number

$$R_A=\frac{g\alpha\beta}{\hat{K}\nu}d^4,$$

with

$$z=0,1,:W=0,\left(D^2-a^2\right)\left(D^2-a^2-\sigma\right)W=0, \tag{39}$$

$$\left.\begin{aligned}&\text{on a right surface}: \quad DW=0,\\ &\text{on a free surface}: \quad D^2W=0.\end{aligned}\right\}. \tag{40}$$

If at the onset of instability a stationary pattern of motions prevails, then one says that the principle of the exchange of stabilities is valid and that instability sets in as stationary cellular convection. In order to establish that the principle of the exchange of instabilities holds for the present problem (i.e., that σ is real and that the marginal states are characterized by $\sigma=0$), put

$$\left.\begin{aligned}G&=\left(D^2-a^2\right)W,\\ F&=\left(D^2-a^2\right)\left(D^2-a^2-\sigma\right)W=\left(D^2-a^2-\sigma\right)G,\end{aligned}\right\} \tag{41}$$

so that equations (38)–(40) give

$$\left(D^2-a^2-P\sigma\right)F=-R_A a^2 W, \tag{42}$$

$$z=0,1: \quad W=0, \qquad F=0. \tag{43}$$

Multiply equation (42) by F^* (the complex conjugate of F) and integrate between $z=0,1$; then one obtains

$$\int_0^1\left\{|DF|^2+\left(a^2+P\sigma\right)|F|^2\right\}dz=R_A a^2\int_0^1 WF^*dz. \tag{44}$$

Note

$$\begin{aligned}\int_0^1 WF^*dz&=\int_0^1 W\left(D^2-a^2-\sigma^*\right)G^*dz\\ &=\int_0^1 G^*\left\{\left(D^2-a^2\right)W-\sigma^*W\right\}dz\\ &=\int_0^1\left\{|G|^2+\sigma^*\left[|DW|^2+a^2|W|^2\right]\right\}dz.\end{aligned} \tag{45}$$

Using (45) in (44), the vanishing of the imaginary and real parts give

$$\mathrm{Im}(\sigma)\left\{P\int_0^1 |F|^2\,dz + R_A a^2 \int_0^1 \left[|DW|^2 + a^2|W|^2\right]dz\right\} = 0, \tag{46a}$$

$$\mathrm{Re}(\sigma) < 0 \quad \text{when} \quad R_A < 0. \tag{46b}$$

Equation (46b) is physically obvious, and equation (46a) gives

$$\mathrm{Im}(\sigma) = 0 \quad \text{when} \quad R_A > 0, \tag{47}$$

so that σ is real for $R_A > 0$.

Now, since σ is real for $R_A > 0$ (i.e., for all adverse temperature gradients), it follows that the transition from stability to instability must occur via a stationary state. Then, corresponding to a marginal state, (38)–(40) become

$$\left(D^2 - a^2\right)^3 W = -R_A a^2 W, \tag{48}$$

$$z = 0,1: \quad W = 0, \qquad \left(D^2 - a^2\right)^2 W = 0, \tag{49}$$

$$\left.\begin{aligned} &\text{on a right surface:} \quad DW = 0, \\ &\text{on a free surface:} \quad D^2 W = 0. \end{aligned}\right\} \tag{40}$$

One thus has a characteristic–value problem for R_A.[1] The minimum with respect to a^2 of the characteristic value so obtained is the critical Rayleigh number at which instability will manifest itself.

The Variational Problem

The characteristic–value problem for the marginal state is given by

$$\left(D^2 - a^2\right)F = -R_A a^2 W, \tag{50}$$

$$z = 0,1: \quad W = 0, \qquad F = 0, \qquad \text{and either} \quad DW = 0 \quad \text{or} \quad D^2 W = 0. \tag{51}$$

Let W_j be the characteristic solution corresponding to a characteristic value R_{A_j}; then, upon multiplying equation (50) by F_i and integrating over $(0,1)$,

$$\int_0^1 F_i\left(D^2 - a^2\right)F_j\,dz = -R_{A_j} a^2 \int_0^1 W_j\left(D^2 - a^2\right)G_i\,dz \tag{52}$$

or

$$\int_0^1 \left(DF_i \cdot DF_j + a^2 F_i F_j\right)dz = R_{A_j} a^2 \int_0^1 G_i G_j\,dz \tag{53}$$

[1] The characteristic values here are degenerate because, to each characteristic value R_A, there exist an infinite number of convection patterns with the same wavenumber a. This degeneracy is, of course, a consequence of the assumption that the fluid layer is of infinite extent in the horizontal plane.

and interchanging i and j, (53) becomes

$$\int_0^1 \left(DF_j \cdot DF_i + a^2 F_j F_i\right) dz = R_A a^2 \int_0^1 G_j G_i \, dz. \tag{54}$$

Upon subtracting (54) from (53), one obtains

$$\int_0^1 G_i G_j \, dz = 0 \quad \text{if} \quad i \neq j. \tag{55}$$

If $i = j$, then (53) gives

$$R_{A_j} = \frac{\int_0^1 \left[\left(DF_j\right)^2 + a^2 F_j^2\right] dz}{a^2 \int_0^1 G_j^2 \, dz}. \tag{56}$$

Indeed, the quotient

$$R_A = \frac{\int_0^1 \left[(DF)^2 + a^2 F^2\right] dz}{a^2 \int_0^1 G^2 \, dz} \equiv \frac{I_1}{a^2 I_2} \tag{57}$$

is stationary if $F = F_j$. In order to show this, use for W some arbitrary function $\tilde{W}$ that satisfies the boundary conditions. Let δR_A be the change in R_A consequent to the variation $\delta\tilde{W}$ in $\tilde{W}$, with $\delta\tilde{W}$ being compatible with the boundary conditions on $\tilde{W}$, i.e.,

$$\begin{aligned} z = 0,1: \quad \delta\tilde{W} = 0, \quad \delta\tilde{F} = 0, \quad \text{and either} \quad D\delta\tilde{W} = 0 \\ \text{or} \quad D^2\delta\tilde{W} = 0. \end{aligned} \tag{58}$$

Note that

$$\delta R_A = \frac{1}{a^2 I_2}\left(\delta I_1 - \frac{I_1}{I_2}\,\delta I_2\right) = \frac{1}{a^2 I_2}\left(\delta I_1 - R_A a^2 \delta I_2\right), \tag{59}$$

where

$$\delta I_1 = 2\int_0^1 \left(D\tilde{F} \cdot D\delta\tilde{F} + a^2 \tilde{F} \cdot \delta\tilde{F}\right) dz = -2\int_0^1 \delta\tilde{F} \cdot \left(D^2 - a^2\right)\tilde{F}\, dz \tag{60}$$

$$\delta I_2 = 2\int_0^1 \tilde{W}\left(D^2 - a^2\right)^2 \delta\tilde{W}\, dz = 2\int_0^1 \tilde{W}\delta\tilde{F}\, dz. \tag{61}$$

When we use (60) and (61), (59) becomes

$$\delta R_A = -\frac{2}{a^2 I_2}\int_0^1 \delta\tilde{F}\left\{\left(D^2 - a^2\right)\tilde{F} + R_A a^2 \tilde{W}\right\} dz, \tag{62}$$

so that

$$\delta R_A = 0 \tag{63}$$

if

$$\left(D^2 - a^2\right)\tilde{F} = -R_A a^2 \tilde{W}.$$

Conversely, if $\delta R_A = 0$ for any arbitrary $\delta\tilde{W}$ compatible with the boundary conditions of the problem, then $\tilde{W}$ is a characteristic solution. This analysis only established that R_A is stationary when $F = F_j$. It can be shown also that R_A is a minimum.

Physically, this implies that instability occurs at the minimum temperature gradient at which a balance can be steadily maintained between the kinetic energy dissipated by viscosity and the internal energy released by the buoyance force.

Example 1: As an illustration, consider the case with free boundaries. The boundary conditions are

$$z = 0, 1: \quad W = 0, \quad D^2 W = 0, \quad D^4 W = 0. \tag{64}$$

In order to satisfy (64), one may choose

$$W = A \sin n\pi z, \qquad n = 1, 2, \ldots. \tag{65}$$

When we use (65), (57) gives

$$R_A = \frac{\left(n^2\pi^2 + a^2\right)^3}{a^2}, \tag{66}$$

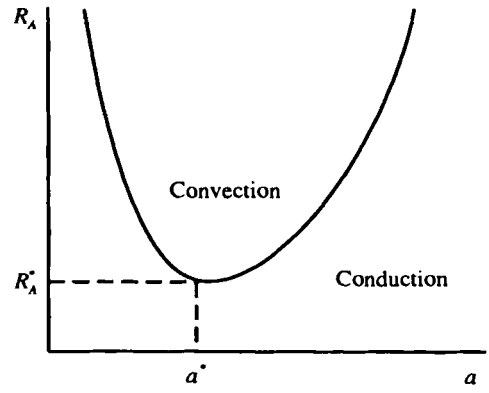

Figure 5.1. The marginal curve for the onset of thermal convection according to the linear theory.

the minimum value of which (corresponding to $n = 1$) is

$$R_A^* = \frac{\left(\pi^2 + a^2\right)^3}{a^2}. \tag{67}$$

The variation of R_A^* with a is shown in Figure 5.1. For Rayleigh numbers less than the critical value $R_{A_{cr}}^*$, only the basic state is possible in which the heat is conducted upwards in obeyance to Fourier's law, and the fluid rests in hydrostatic equilibrium. As the Rayleigh number increases through the critical value the static state becomes unstable. The new state consists of an interlocking pattern of steadily overturning cells, which can, under properly controlled conditions, be strikingly regular (see Figure 5.2.).[2] The solution for $n = 1$ corresponds to a convection roll that is almost as wide horizontally as the fluid is deep. The fluid in the cells draws heat from the lower boundary and, due to its resulting expansion, can rise by buoyancy to the upper boundary, where it gives up its heat, contracts and sinks to replenish its supply. These convective motions substantially enhance the efficiency of the layer in transporting heat.[3]

Observe from (66) that if the rolls are too wide compared with their height, i.e., $a/n \ll 1$, the convective motions are inhibited by enhanced viscous dissipation. On the other hand, if the rolls are too tall compared with their width,

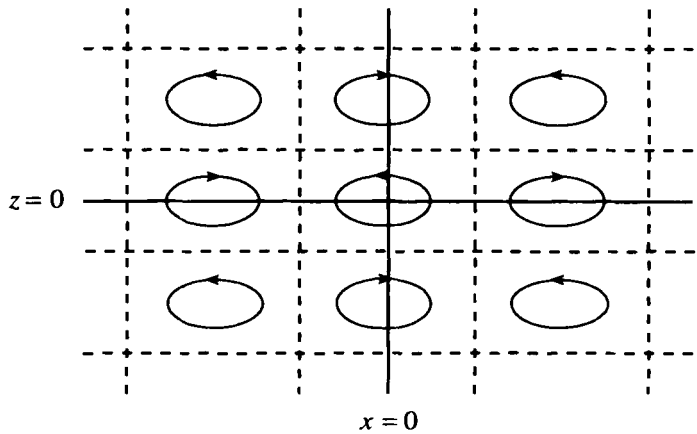

Figure 5.2. Periodic mode of convection visible in a cross-section through a body of fluid heated from below.

[2]The cellular pattern usually reflects the geometrical configuration of the side walls. In a rectangular fluid layer the rolls tend to align with the shorter sides while a circular lateral wall gives rise to a roll pattern in the form of concentric rings.

[3]It is to be noted that, in cases where the physical properties of the fluid layer are not symmetric with respect to the mid-plane, a hexagonal cellular pattern is preferred (Block). This is the case, as in the original experiments of Bénard, when the fluid layer has a free surface with the surface tension there being temperature-dependent. Hexagonal cellular patterns are of two types: one with upward motion and the other with downward motion in the center of the cells.

i.e., $a/n \gg 1$, convective motions are again inhibited by enhanced losses due to thermal conduction of the available free energy. Therefore, convective motions that arise first when the Rayleigh number is increased steadily from zero are those that correspond to the rolls with

$$\frac{a}{n} = \left(\frac{a}{n}\right)_* = \frac{1}{\sqrt{2}} \tag{68}$$

since this leads to a minimum value of the Rayleigh number in (67).

Experiments have confirmed that the onset of convection occurs for Rayleigh numbers at the critical values given by (67) and (68) to within a 3% margin of experimental error, provided that the horizontal extension of the fluid layer is large compared with the depth.

Nonlinear Effects

As the amplitude of the convection rolls becomes large, the mean temperature profile in the fluid layer is modified which will impede further growth of the perturbation.[4] Consequently, supercritical convective motions may be expected, as experiments have confirmed, to lead to steady and stable two–dimensional rolls.

There is another feature of convective motions that is produced by the nonlinear effects. As shown by Figure 5.1, for Rayleigh numbers greater than the critical value, a continuous spectrum of modes becomes unstable which would indicate a rather complicated convective flow pattern. However, experiments indicate a marked tendency toward a simple cellular pattern which is apparently attributable to nonlinear effects (though in a real experimental situation, the side walls may play an important role in this process).

One theoretical explanation of the observed phenomena near the linear instability threshold is based on the use of a two–dimensional model equation, due to Segel, that is much simpler than the full hydrodynamical equations and yet correctly describes the development of the supercritical equilibrium. This model equation is

$$-W_t + \Delta^3 W - R_A \Delta_1 W = \left(W W_z\right)_{zz}, \tag{69}$$

where

$$\Delta W \equiv \Delta_1 W + W_{zz}, \quad \Delta_1 W \equiv W_{xx} + W_{yy}$$

and subscripts denote the derivative. The boundary conditions are

[4]For large-amplitude convective motions, the mean temperature gradient becomes sharp near the boundaries while that in the interior of the fluid layer can even reverse. The latter aspect merely reflects the efficiency of the convective heat transfer which can supersede even a reversed conductive heat flux.

$$\left.\begin{aligned} &z=0,1: \quad W, W_{zz} \text{ and } W_{zzzz}=0, \\ &x^2+y^2 \Rightarrow \infty: \quad W \text{ bounded.} \end{aligned}\right\} \tag{70}$$

For supercritical Rayleigh numbers, one may seek the steady solution by using a perturbation method (Gorkov; Malkus and Veronis). In this method, the physical variable W as well as the Rayleigh number R_A are expanded in power series in a small parameter ε, which is a measure of the amplitude of the convective motion:

$$\left.\begin{aligned} W(x,y,z;\varepsilon) &= \sum_{n=1}^{\infty} \varepsilon^n W_n(x,y,z), \\ R_A(\varepsilon) &= R_A^* + \sum_{n=1}^{\infty} \varepsilon^n R_{A_n}. \end{aligned}\right\} \tag{71}$$

The unknown constants R_{A_n} are successively determined by the solvability conditions applied to the sequence of inhomogeneous linear partial differential equations for the W_n.

Substituting (71), (69), and (70) give,

$$\left(\Delta^3 - R_A^* \Delta_1\right) W_1 = 0, \tag{72}$$

$$\left(\Delta^3 - R_A^* \Delta_1\right) W_2 = \left(\frac{1}{2} W_1^2\right)_{zzz} + R_{A_1} \Delta_1 W_1, \tag{73}$$

$$\left(\Delta^3 - R_A^* \Delta_1\right) W_3 = \left(W_1 W_2\right)_{zzz} + R_{A_1} \Delta_1 W_2 + R_{A_2} \Delta_1 W_1, \tag{74}$$

etc.,

with boundary conditions

$$z=0,1: \quad W_n, \left(W_n\right)_{zz} \text{ and } \left(W_n\right)_{zzzz} = 0. \tag{75}$$

Consider a roll pattern given by

$$W_1 = \cos ax \cdot \sin \pi z, \tag{76}$$

which satisfies equation (72), provided that

$$R_A^* = \frac{\left(\pi^2 + a^2\right)^3}{a^2}. \tag{77}$$

Equation (77) is the same as (67), so that the model equation (69) incorporates the principal qualitative aspects underlying the full hydrodynamical equations governing the thermal convection problem in the Boussinesq approximation.

Now, equation (73) will have a solution, provided that its right–hand side is orthogonal to the solution W_1 of the corresponding homogeneous solution. This leads to

$$R_{A_1} = -\frac{\left[W_1, \left(\frac{1}{2} W_1^2\right)_{zzz}\right]}{\left[W_1, \Delta_1 W_1\right]}, \tag{78}$$

where $[f,g]$ denotes the inner product,

$$[f,g] \equiv \int_0^1 \int_0^{2\pi/a} f\, g\, dx\, dz .$$

When we use (76), (78) leads to

$$R_{A_1} = 0. \tag{79}$$

Therefore, equation (73) has the solution

$$W_2 = (A + B \sin 2\pi z) \cdot \cos 2ax, \tag{80}$$

where

$$A = \frac{1}{64\pi^3}, \quad B = \frac{\pi^3}{60\left(\pi^2 + a^2\right)^3}.$$

Next, the solvability condition for equation (74) leads to

$$R_{A_2} = -\frac{\left[W_1, (W_1 W_2)_{zzz}\right]}{\left[W_1, \Delta_1 W_1\right]}. \tag{81}$$

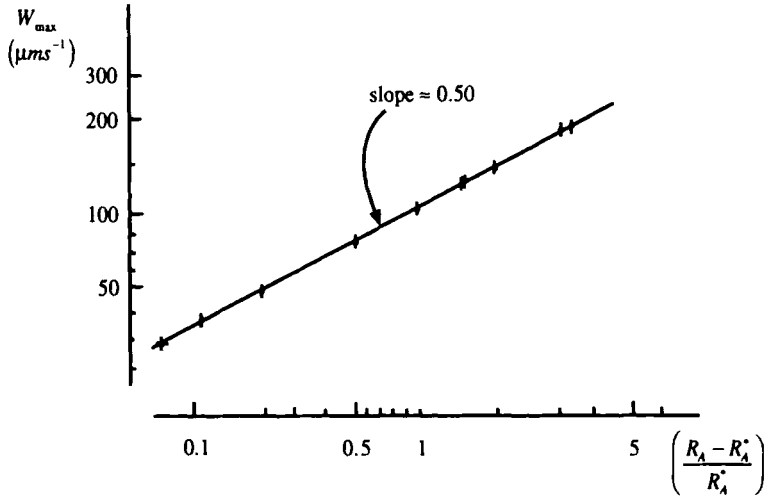

Figure 5.3. Dependence of the maximum vertical velocity component on $\left(R_A - R_A^*\right)$ (from Dubois and Berge, 1978).

When we use (76) and (80), (81) gives

$$R_{A_2} = \frac{\pi^3(2A+B)}{4a^2}. \tag{82}$$

When we use (79) and (82), (71) then implies, for the supercritical equilibrium state, the following behavior[5]:

$$\varepsilon \sim \left(R_A - R_A^*\right)^{1/2}. \tag{83}$$

Experimental measurements (Dubois and Berge) of the maximum amplitude of the vertical component of the velocity showed very good agreement with this result (see Figure 5.3).

Instability of the Roll Pattern

Theoretical work (Clever and Busse) has shown that, as the Rayleigh number increases beyond the supercritical value, the roll pattern becomes unstable and develops a wavy shape. However, the experimental evidence for this does not seem to be conclusive (Koschmieder).

EXERCISE

1. Study the effect of uniform rotation about the z–axis on the thermal stability of a layer of fluid heated from below. Assume free boundaries.

5.3. Stability of Couette Flow

The origin of instabilities here is a potentially unstable arrangement of flow resulting from a prevailing adverse gradient of angular momentum. The simplest example of such instability occurs in Couette flow, i.e., in the steady circular flow of a liquid between two rotating coaxial cylinders. Experiments show that this instability leads to a secondary flow in the form of toroidal vortices (with opposite circulations in adjacent vortices) which are regularly spaced along the axis of the cylinders (see Figure 5.4). This secondary flow tends to redistribute the angular momentum of the basic flow in such a way as to reduce the adverse angular momentum gradient.

Inviscid Couette Flow: Rayleigh Criterion

Heuristic Derivation

For axisymmetric flows of an incompressible inviscid fluid, one has the following governing equations:

[5]This is reminiscent of the mean-field result for the order parameter for continuous, second-order phase transitions in statistical mechanics.

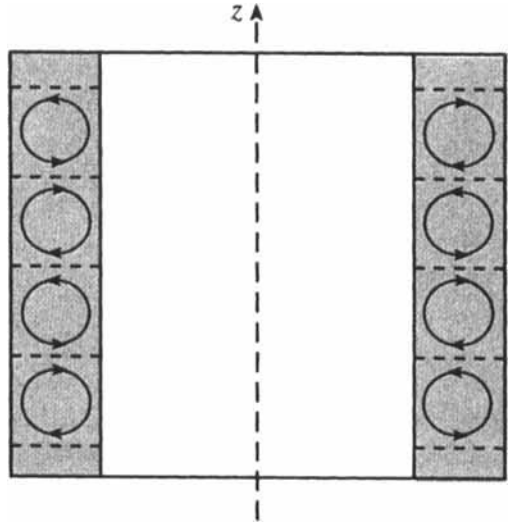

Figure 5.4. The secondary circulation resulting from the instability of Couette flow between two rotating coaxial cylinders.

$$\frac{\partial v_r}{\partial r} + \frac{v_r}{r} + \frac{\partial v_z}{dz} = 0, \tag{1}$$

$$\frac{\partial v_r}{\partial t} + v_r \frac{\partial v_r}{\partial r} + v_z \frac{\partial v_r}{\partial z} = \frac{v_\theta^2}{r} - \frac{\partial}{\partial r}\left(\frac{p}{\rho}\right), \tag{2}$$

$$\frac{\partial v_\theta}{\partial t} + v_r \frac{\partial v_\theta}{\partial r} + v_z \frac{\partial v_\theta}{\partial z} + \frac{v_\theta v_r}{r} = 0, \tag{3}$$

$$\frac{\partial v_z}{\partial t} + v_r \frac{\partial v_z}{\partial r} + v_z \frac{\partial v_z}{\partial z} = -\frac{\partial}{\partial z}\left(\frac{p}{\rho}\right). \tag{4}$$

One obtains from equation (3)

$$\frac{d}{dt}\left(r v_\theta\right) = \frac{d}{dt}\left(r^2 \Omega\right) = 0, \tag{5}$$

so that

$$\alpha = r^2 \Omega = \text{const.} \tag{6}$$

Corresponding to the force v_θ^2/r that arises in the radial motion, one may associate a potential energy $\rho\alpha^2/2r^2$. Consider now the interchange of fluid contained in two elementary rings of equal heights and masses at $r = r_1, r_2, (r_2 > r_1)$, so that $2\pi r_1 dr_1 = 2\pi r_2 dr_2$. The change in the potential energy consequent to such an interchange is given by

$$\left\{\left(\frac{\alpha_2^2}{r_1^2}+\frac{\alpha_1^2}{r_2^2}\right)-\left(\frac{\alpha_1^2}{r_1^2}+\frac{\alpha_2^2}{r_2^2}\right)\right\}2\pi r_1 dr_1=\left(\alpha_2^2-\alpha_1^2\right)\left(\frac{1}{r_1^2}-\frac{1}{r_2^2}\right)2\pi r_1 dr_1, \tag{7}$$

so that for stability one requires $\alpha_2 > \alpha_1$. Therefore, if one introduces

$$\Phi(r)=\frac{1}{r^3}\frac{d}{dr}\left(r^2\Omega\right)^2=\frac{2}{r}\Omega\frac{d}{dr}\left(r^2\Omega\right), \tag{8}$$

then one has for stability

$$\Phi(r)>0: \quad \text{Rayleigh's criterion.} \tag{9}$$

Rigorous Derivation

Consider the stability of a stationary state given by

$$v_r=0, \qquad v_z=0, \qquad v_\theta=V(r)=r\Omega(r). \tag{10}$$

Let the perturbed state be described by

$$v_r, V+v_\theta, v_z, \tilde{\omega}\left(=\frac{\delta p}{\rho}\right). \tag{11}$$

The linearized equations governing these perturbations are

$$\frac{\partial v_r}{\partial t}-2\frac{V}{r}v_\theta=-\frac{\partial\tilde{\omega}}{\partial r}, \tag{12}$$

$$\frac{\partial v_\theta}{\partial t}+\left(\frac{V}{r}+\frac{dV}{dr}\right)v_r=0, \tag{13}$$

$$\frac{\partial v_z}{\partial t}=-\frac{\partial\tilde{\omega}}{\partial z}, \tag{14}$$

$$\frac{\partial v_r}{\partial r}+\frac{v_r}{r}+\frac{\partial v_z}{\partial z}=0. \tag{15}$$

Seek solutions to equations (12)–(15) of the form

$$q\sim q(r)e^{i(kz+pt)}, \tag{16}$$

so that equations (12)–(15) give

$$ipv_r-2\Omega v_\theta=-\frac{d\tilde{\omega}}{dr}, \tag{17}$$

$$ipv_\theta+\left[\Omega+\frac{d}{dr}(r\Omega)\right]v_r=0, \tag{18}$$

$$ipv_z=-ik\tilde{\omega}, \tag{19}$$

$$\frac{dv_r}{dr}+\frac{v_r}{r}+ikv_z=0. \tag{20}$$

Introduce

$$v_r = ip\xi_r, \quad v_\theta = ip\xi_\theta - r\frac{d\Omega}{dr}\xi_r, \quad v_z = ip\xi_z, \tag{21}$$

so that equations (17)–(20) become

$$\left(p^2 - 2r\Omega\frac{d\Omega}{dr}\right)\xi_r + 2i\Omega p\xi_\theta = \frac{d\tilde{\omega}}{dr}, \tag{22}$$

$$p^2\xi_\theta - 2i\Omega p\xi_r = 0, \tag{23}$$

$$p^2\xi_z = ik\tilde{\omega}, \tag{24}$$

$$\frac{d\xi_r}{dr} + \frac{\xi_r}{r} + ik\xi_z = 0, \tag{25}$$

from which one derives

$$\left(p^2 - 2r\Omega\frac{d\Omega}{dr}\right)\xi_r - 4\Omega^2\xi_r = \frac{d\tilde{\omega}}{dr}$$

or

$$\left[p^2 - \Phi(r)\right]\xi_r = \frac{d\tilde{\omega}}{dr} \tag{26}$$

and

$$p^2\left(\frac{d\xi_r}{dr} + \frac{\xi_r}{r}\right) = \tilde{\omega}$$

or

$$\frac{1}{r}\frac{d}{dr}(r\xi_r) = \frac{k^2}{p^2}\tilde{\omega}. \tag{27}$$

The boundary conditions are

$$r = R_1, R_2: \quad \xi_r = 0, \tag{28}$$

where R_1 and R_2 are the radii of the inner and outer cylinders, respectively.

From equations (26) and (27), we have

$$\frac{d}{dr}\left[\frac{1}{r}\frac{d}{dr}(r\xi_r)\right] - k^2\xi_r = -\frac{k^2}{p^2}\Phi(r)\xi_r \tag{29}$$

with

$$r = R_1, R_2: \quad \xi_r = 0,$$

which constitutes the classical Sturm–Liouville characteristic–value problem. And thus the characteristic values of k^2/p^2 are all positive if $\Phi(r)$ is everywhere positive and vice versa.

From (29), indeed, we have, on using (28),

$$\frac{p^2}{k^2} = \frac{\int \Phi(r) r\xi_r^2 \, dr}{\int \left[\left\{ \frac{d}{dr}(r\xi_r) \right\}^2 \frac{1}{r} + k^2 r \xi_r^2 \right] dr}, \tag{30}$$

which sets forth the variational character of the problem. Rayleigh's stability criterion (9) follows from (30) immediately.

Couette Flow with Axial Velocity: Howard–Gupta Theory

Consider the stability of a stationary state, with an axial flow $W(r)$, given by

$$v_r = 0, \qquad v_z = W(r), \qquad v_\theta = V(r) = r\Omega(r). \tag{31}$$

Let the perturbed state be described by

$$v_r, V + v_\theta, W + v_z, \tilde{\omega}\left(= \frac{\delta p}{\rho} \right). \tag{32}$$

The linearized equations governing these perturbations are

$$\frac{\partial v_r}{\partial t} + W \frac{\partial v_r}{\partial z} - 2\frac{V}{r} v_\theta = -\frac{\partial \tilde{\omega}}{\partial r}, \tag{33}$$

$$\frac{\partial v_\theta}{\partial t} + W \frac{\partial v_\theta}{\partial z} + \left(\frac{V}{r} + \frac{dV}{dr} \right) v_r = 0, \tag{34}$$

$$\frac{\partial v_z}{\partial t} + W \frac{\partial v_z}{\partial z} = -\frac{\partial \tilde{\omega}}{\partial z}, \tag{35}$$

$$\frac{\partial v_r}{\partial r} + \frac{v_r}{r} + \frac{\partial v_z}{\partial z} = 0. \tag{36}$$

Seek solutions to equations (33)–(36) of the form

$$q \sim q(r) e^{i(kz + pt)}, \tag{16}$$

so that equations (33)–(36) give

$$i\sigma v_r - 2\Omega v_\theta = -\frac{d\tilde{\omega}}{dr}, \tag{37}$$

$$i\sigma v_\theta + \left[\Omega + \frac{d}{dr}(r\Omega) \right] v_r = 0, \tag{38}$$

$$i\sigma v_z = -ik\tilde{\omega}, \tag{39}$$

$$\frac{dv_r}{dr} + \frac{v_r}{r} + ik v_z = 0, \tag{40}$$

where

$$\sigma \equiv p + kW.$$

When we introduce

$$v_r = i\sigma\xi_r,\ v_\theta = i\sigma\xi_\theta - r\frac{d\Omega}{dr}\xi_r,\ v_z = i\sigma\xi_z \tag{41}$$

equations (37)–(40) become

$$\left(\sigma^2 - 2r\Omega\frac{d\Omega}{dr}\right)\xi_r + 2i\Omega\sigma\xi_\theta = \frac{d\tilde{\omega}}{dr}, \tag{42}$$

$$\sigma^2\xi_\theta - 2i\Omega\sigma\xi_r = 0, \tag{43}$$

$$\sigma^2\xi_z = ik\tilde{\omega}, \tag{44}$$

$$\frac{d\xi_r}{dr} + \frac{\xi_r}{r} + ik\xi_z = 0, \tag{45}$$

from which we derive

$$\left(\sigma^2 - 2r\Omega\frac{d\Omega}{dr}\right)\xi_r - 4\Omega^2\xi_r = \frac{d\tilde{\omega}}{dr}$$

or

$$\left[\sigma^2 - \Phi(r)\right]\xi_r = \frac{d\tilde{\omega}}{dr} \tag{46}$$

and

$$\sigma^2\left(\frac{d\xi_r}{dr} + \frac{\xi_r}{r}\right) = k^2\tilde{\omega}$$

or

$$\frac{\sigma^2}{k^2}\frac{1}{r}\frac{d}{dr}(r\xi_r) = \tilde{\omega}. \tag{47}$$

We have from equations (46) and (47)

$$\frac{d}{dr}\left[\left(W + \frac{p}{k}\right)^2\frac{1}{r}\frac{d}{dr}(r\xi_r)\right] - k^2\left(W + \frac{p}{k}\right)^2\xi_r = -\Phi(r)\xi_r. \tag{48}$$

The boundary conditions are

$$r = R_1, R_2: \quad \xi_r = 0. \tag{28}$$

Suppose that the boundary–value problem (48) and (28) has a nontrivial solution ξ_r with $\mathrm{Im}(p) > 0$. Then, since $\left(W + \frac{p}{k}\right)$ does not vanish on $[R_1, R_2]$, one may consider a square root $\left(W + \frac{p}{k}\right)^{1/2}$ which is as smooth as W is. We assume W to be continuous and piecewise continuously differentiable. When we put

$$G = \left(W + \frac{p}{k}\right)^{1/2}\xi_r \tag{49}$$

equation (48) becomes

$$\frac{d}{dr}\left[\left(W+\frac{p}{k}\right)\frac{1}{r}\frac{d}{dr}(rG)\right]+\frac{1}{2}\left(\frac{1}{r}\frac{dW}{dr}-\frac{d^2W}{dr^2}\right)G$$
$$-\frac{1}{4}\left(\frac{dW}{dr}\right)^2\frac{G}{W+\frac{p}{k}}-k^2\left(W+\frac{p}{k}\right)G+\Phi\frac{G}{W+\frac{p}{k}}=0. \tag{50}$$

Multiplying equation (50) by rG^* and integrating over (R_1, R_2), we obtain

$$\int_{R_1}^{R_2}\left(W+\frac{p}{k}\right)\left[\left|\frac{1}{r}\frac{d}{dr}(rG)\right|^2+k^2|G|^2\right]r\,dr$$
$$+\frac{1}{2}\int_{R_1}^{R_2}\left(r\frac{d^2W}{dr^2}-\frac{dW}{dr}\right)|G|^2 r\,dr$$
$$+\int_{R_1}^{R_2}\left(W+\frac{p^*}{k}\right)\left[\frac{1}{4}\left(\frac{dW}{dr}\right)^2-\Phi\right]\left|\frac{G}{W+\frac{p}{k}}\right|^2 r\,dr=0. \tag{51}$$

If $\mathrm{Im}(p)>0$, the imaginary part of equation (51) gives

$$\int_{R_1}^{R_2}\left[\left|\frac{1}{r}\frac{d}{dr}(rG)\right|^2+k^2|G|^2\right]r\,dr$$
$$+\int_{R_1}^{R_2}\left[\Phi-\frac{1}{4}\left(\frac{dW}{dr}\right)^2\right]\left|\frac{G}{W+\frac{p}{k}}\right|^2 r\,dr=0, \tag{52}$$

which is impossible if $\Phi \geq 1/4\,(dW/dr)^2$ everywhere. Thus, a sufficient condition for stability is that

$$\Phi \geq \frac{1}{4}\left(\frac{dW}{dr}\right)^2 \tag{53}$$

everywhere.

Viscous Couette Flow: Synge's Theory

The Navier–Stokes equations for an axisymmetric viscous incompressible flow are

$$\frac{\partial v_r}{\partial t}+(\mathbf{v}\cdot\nabla)v_r-\frac{v_\theta^2}{r}=-\frac{\partial}{\partial r}\left(\frac{p}{\rho}\right)+\nu\left(\nabla^2 v_r-\frac{v_r}{r^2}\right), \tag{54}$$

$$\frac{\partial v_\theta}{\partial t}+(\mathbf{v}\cdot\nabla)v_\theta+\frac{v_r v_\theta}{r}=\nu\left(\nabla^2 v_\theta-\frac{v_\theta}{r^2}\right), \tag{55}$$

$$\frac{\partial v_z}{\partial t} + (\mathbf{v}\cdot\nabla)\, v_z = -\frac{\partial}{\partial z}\left(\frac{p}{\rho}\right) + \nu\nabla^2 v_z, \tag{56}$$

and

$$\frac{\partial v_r}{\partial r} + \frac{v_r}{r} + \frac{\partial v_z}{\partial z} = 0, \tag{57}$$

where

$$\mathbf{v}\cdot\nabla = v_r\frac{\partial}{\partial r} + v_z\frac{\partial}{\partial z},$$

$$\nabla^2 = \frac{\partial^2}{\partial r^2} + \frac{1}{r}\frac{\partial}{\partial r} + \frac{\partial^2}{\partial z^2}.$$

Equations (34)–(37) allow a stationary solution of the form

$$v_r = 0, \qquad v_z = 0, \qquad v_\theta = V(r), \tag{10}$$

provided that one has

$$\frac{d}{dr}\left(\frac{p}{\rho}\right) = \frac{V^2}{r} \tag{58}$$

and

$$\nu\left(\nabla^2 V - \frac{V}{r^2}\right) = \nu\frac{d}{dr}\left(\frac{d}{dr} + \frac{1}{r}\right) V = 0 \tag{59}$$

from which we obtain

$$V = Ar + \frac{B}{r} \tag{60}$$

where

$$A = -\Omega_1\eta^2\,\frac{1-\mu/\eta^2}{1-\eta^2}, \qquad B = \Omega_1\frac{R_1^2(1-\mu)}{1-\eta^2}$$

$$\mu = \frac{\Omega_2}{\Omega_1}, \qquad \eta = \frac{R_1}{R_2}.$$

Let the perturbed state be described by

$$v_r,\ V + v_\theta,\ v_z,\ \frac{\delta p}{\rho} = \tilde{\omega}. \tag{61}$$

For the axisymmetric case, one then obtains the linearized equations from equations (54)–(57)

$$\frac{\partial v_r}{\partial t} - 2\frac{V}{r}v_\theta = -\frac{\partial\tilde{\omega}}{\partial r} + \nu\left(\nabla^2 v_r - \frac{v_r}{r^2}\right) \tag{62}$$

$$\frac{\partial v_\theta}{\partial t} + \left(\frac{dV}{dr} + \frac{V}{r}\right) v_r = \nu\left(\nabla^2 v_\theta - \frac{v_\theta}{r^2}\right), \tag{63}$$

$$\frac{\partial v_z}{\partial t} = -\frac{\partial \tilde{\omega}}{\partial z} + \nu \nabla^2 v_z, \tag{64}$$

$$\frac{\partial v_r}{\partial r} + \frac{v_r}{r} + \frac{\partial v_z}{\partial z} = 0, \tag{65}$$

where

$$\nabla^2 = \frac{\partial^2}{\partial r^2} + \frac{1}{r}\frac{\partial}{\partial r} + \frac{\partial^2}{\partial z^2}.$$

Let us analyze the disturbance into normal modes and seek solutions of the form

$$\left.\begin{aligned} v_r &= u(r) e^{pt} \cos kz, \\ v_\theta &= v(r) e^{pt} \cos kz, \\ v_z &= w(r) e^{pt} \sin kz, \\ \tilde{\omega} &= \tilde{\omega}(r) e^{pt} \cos kz, \end{aligned}\right\} \tag{66}$$

so that equations (62)–(65) give

$$\nu\left(DD_* - k^2 - \frac{p}{\nu}\right) u + 2\frac{V}{r} v = \frac{d\tilde{\omega}}{dr}, \tag{67}$$

$$\nu\left(DD_* - k^2 - \frac{p}{\nu}\right) v - (D_* V) u = 0, \tag{68}$$

$$\nu\left(D_* D - k^2 - \frac{p}{\nu}\right) w = -k\tilde{\omega}, \tag{69}$$

$$D_* u = -kw, \tag{70}$$

where

$$\nabla^2 = D_* D - k^2 = DD_* + \frac{1}{r^2} - k^2,$$

$$D \equiv \frac{d}{dr}, \qquad D_* \equiv \frac{d}{dr} + \frac{1}{r}.$$

From equations (67)–(70) we derive

$$\frac{\nu}{k^2}\left(DD_* - k^2 - \frac{p}{\nu}\right)\left(DD_* - k^2\right) u = 2\frac{V}{r} v, \tag{71}$$

$$\nu\left(DD_* - k^2 - \frac{p}{\nu}\right) v = (D_* V) u. \tag{72}$$

When we measure r in units of the radius R_2 of the outer cylinder and write

$$k^2 = \frac{a^2}{R_2^2}, \qquad \sigma = \frac{pR_2^2}{\nu}, \qquad u\frac{2AR_2^2}{\nu} \Rightarrow u, \tag{73}$$

equations (71) and (72) become

$$\left(DD_* - a^2 - \sigma\right)\left(DD_* - a^2\right)u = -Ta^2\left(\frac{1}{r^2} - N\right)v, \tag{74}$$

$$\left(DD_* - a^2 - \sigma\right)v = u, \tag{75}$$

where T is the Taylor number

$$T \equiv -\frac{4AB}{\nu^2}R_2^2 = \frac{4\Omega_1^2 R_1^4}{\nu^2}\frac{(1-\mu)\left(1-\mu/\eta^2\right)}{\left(1-\eta^2\right)^2}$$

and

$$N \equiv -\frac{AR_2^2}{B} = \frac{1-\mu/\eta^2}{1-\mu}.$$

The boundary conditions are

$$r = 1, \eta: u = 0, \qquad v = 0, \qquad Du = 0. \tag{76}$$

Note that if $f(r)$ and $g(r)$ are any two functions and if

$$r = 1, \eta: f(r) = 0, \tag{77a}$$

then

$$\int_\eta^1 rfDD_*g\,dr = -\int_\eta^1\left(r\frac{df}{dr}\frac{dg}{dr} + \frac{fg}{r}\right)dr; \tag{77b}$$

and if

$$r = 1, \eta: f(r) = 0, \qquad f'(r) = 0, \tag{78a}$$

then

$$\int_\eta^1 rfDD_*g\,dr = \int_\eta^1 rgDD_*f\,dr. \tag{78b}$$

When we multiply equation (74) by u^*, the complex conjugate of u, and integrate from η to 1, then

$$\int_\eta^1 ru^*\left\{\left(DD_* - a^2\right)^2 u - \sigma\left(DD_* - a^2\right)u\right\}dr = -Ja^2\int_\eta^1 r\phi(r)\,vu^*\,dr, \tag{79}$$

where

$$J = \frac{T}{1-\mu} = \frac{4\Omega_1^2 R_1^4}{\nu^2}\frac{\left(1-\mu/\eta^2\right)}{\left(1-\eta^2\right)^2}, \qquad \phi = (1-\mu)\left(\frac{1}{r^2} - N\right).$$

Using (77) and (78), note that

$$\int_\eta^1 ru^*\left\{\left(DD_* - a^2\right)^2 u - \sigma\left(DD_* - a^2\right)u\right\} dr$$

$$= \int_\eta^1 r\left|\left(DD_* - a^2\right)u\right|^2 dr + \sigma\int_\eta^1 \left\{r\left|\frac{du}{dr}\right|^2 + \left(\frac{1}{r} + a^2 r\right)|u|^2\right\} dr \tag{80}$$

and

$$\int_\eta^1 r\phi(r)\upsilon u^* dr = \int_\eta^1 r\phi(r)\upsilon\left(DD_* - a^2 - \sigma^*\right)v^* dr$$

$$= -\left(a^2 + \sigma^*\right)\int_\eta^1 \phi(r) r|\upsilon|^2 dr + \int_\eta^1 r\phi(r)\upsilon DD_* v^* dr$$

$$= -\left(a^2 + \sigma^*\right)\int_\eta^1 \phi(r) r|\upsilon|^2 dr$$

$$-\int_\eta^1 \phi(r)\left(r\left|\frac{d\upsilon}{dr}\right|^2 + \frac{|\upsilon|^2}{r}\right)dr + 2(1-\mu)\int_\eta^1 \frac{\upsilon}{r^2}\frac{dv^*}{dr} dr. \tag{81}$$

When we use (80) and (81), (79) becomes

$$\sigma I_1 + I_2 = Ja^2\left\{\left(a^2 + \sigma^*\right)I_3 + I_4\right\}, \tag{82}$$

where

$$I_1 = \int_\eta^1 \left\{r\left|\frac{du}{dr}\right|^2 + \left(\frac{1}{r} + a^2 r\right)|u|^2\right\} dr,$$

$$I_2 = \int_\eta^1 \left|\left(DD_* - a^2\right)u\right|^2 r\, dr,$$

$$I_3 = \int_\eta^1 \phi(r) r|\upsilon|^2 dr,$$

$$I_4 = \int_\eta^1 \phi(r)\left(r\left|\frac{d\upsilon}{dr}\right|^2 + \frac{|\upsilon|^2}{r}\right)dr - 2(1-\mu)\int_\eta^1 \frac{\upsilon}{r^2}\frac{dv^*}{dr} dr.$$

Note that I_1 and I_2 are positive definite and that

$$\phi = (1-\mu)\left(\frac{1}{r^2} - N\right) = \begin{cases} \dfrac{\mu}{\eta}\left(1-\eta^2\right) & \text{for } r = 1, \\ \dfrac{1}{\eta^2}\left(1-\eta^2\right) & \text{for } r = \eta, \end{cases} \tag{83}$$

so that $\mu > 0$ implies

$$\phi > 0; \tag{84}$$

then I_3 is also positive definite. Next, note that

$$\mathrm{Re}(I_4) = \int_{\eta}^{1} r\phi(r)\left|\frac{dv}{dr} - \frac{v}{r}\right|^2 dr. \tag{85}$$

When we use (83)–(85), (82) gives

$$\mathrm{Re}[\sigma]\left(I_1 - Ja^2 I_3\right) + I_2 - Ja^2\left(a^2 I_3 + \mathrm{Re}[I_4]\right) = 0, \tag{86}$$

from which, noting that $J < 0$ when $\mu > \eta^2$, we have that

$$\mathrm{Re}[\sigma] < 0 \text{ when } \mu > \eta^2, \tag{87}$$

and then the flow is stable, as before.

Next, the imaginary part of equation (82) gives

$$\mathrm{Im}(\sigma)\cdot\left[I_1 + Ja^2 I_3\right] = -2Ta^2\,\mathrm{Im}\left(\int_{\eta}^{1}\frac{v}{r^2}\frac{dv^*}{dr}dr\right). \tag{88}$$

But, no general conclusion can be drawn from this equation. In order to be able to obtain some definitive information about $\mathrm{Im}(\sigma)$, let us consider the case wherein the gap $(R_2 - R_1)$ between the two cylinders is small compared to their mean radius $1/2\,(R_2 + R_1)$. Then

$$D_* \approx D, \qquad V = \Omega_1 r\left[1 - (1-\mu)\frac{r - R_1}{R_2 - R_1}\right]. \tag{89}$$

Let us measure radial distances from the surface of the inner cylinder in the unit $d = R_2 - R_1$. Further, when we put

$$\zeta = \frac{r - R_1}{d}, \qquad k = \frac{a}{d}, \qquad \sigma = \frac{pd^2}{\nu}, \tag{90}$$

equations (71) and (72) become

$$\left(D^2 - a^2 - \sigma\right)\left(D^2 - a^2\right)u = \frac{2\Omega_1 d^2}{\nu}a^2\left[1 - (1-\mu)\zeta\right]v, \tag{91}$$

$$\left(D^2 - a^2 - \sigma\right)v = \frac{2Ad^2}{\nu}u. \tag{92}$$

Let us replace

$$u \text{ by } \frac{2\Omega_1 d^2 a^2}{\nu}u, \tag{93}$$

so that equations (91) and (92) become

$$\left(D^2 - a^2 - \sigma\right)\left(D^2 - a^2\right)u = \left(1 + \alpha\zeta\right)v, \tag{94}$$

$$\left(D^2 - a^2 - \sigma\right) v = -Ta^2 u, \tag{95}$$

where the Taylor number T is now given by

$$T = -\frac{4A\Omega_1 d^4}{\nu^2}$$

and

$$\alpha = -(1-\mu).$$

The boundary conditions (96) are

$$\zeta = 0,1: \quad u, v, Du = 0. \tag{96}$$

Let us consider the case $\mu \approx 1$ so that we may ignore the term linear in ζ on the right-hand side in equation (94.)[6] Multiply equation (94) by u^* and integrate over the range of ζ; one then obtains

$$\int_0^1 v u^* d\zeta = \int_0^1 u^* \left[\left(D^2 - a^2\right)^2 - \sigma\left(D^2 - a^2\right)\right] u \, d\zeta$$

$$= \int_0^1 \left|\left(D^2 - a^2\right) u\right|^2 d\zeta + \sigma \int_0^1 \left(|Du|^2 + a^2 |u|^2\right) d\zeta. \tag{97}$$

Now, multiply the complex conjugate of equation (95) by v and integrate over the range of ζ; one then obtains

$$-Ta^2 \int_0^1 v u^* d\zeta = \int_0^1 v\left(D^2 - a^2 - \sigma^*\right) v^* d\zeta$$

$$= -\int_0^1 \left[|Dv|^2 + \left(a^2 + \sigma^*\right)|v|^2\right] d\zeta. \tag{98}$$

One obtains from equations (97) and (98)

$$Ta^2 \left[\int_0^1 \left|\left(D^2 - a^2\right) u\right|^2 d\zeta + \sigma \int_0^1 \left(|Du|^2 + a^2 |u|^2\right) d\zeta\right]$$

$$= \int_0^1 \left(|Dv|^2 + a^2 |v|^2\right) d\zeta + \sigma^* \int_0^1 |v|^2 \, d\zeta, \tag{99}$$

the imaginary part of which gives

$$\mathrm{Im}(\sigma) \cdot \left[Ta^2 \int_0^1 \left(|Du|^2 + a^2 |u|^2\right) d\zeta + \int_0^1 |v|^2 \, d\zeta\right] = 0 \tag{100}$$

---

[6] In this limit, equations (94) and (95) are identical (following a minor redefinition of the variables) to equations (36) and (37) describing the thermal instability of a fluid layer heated from below in Section 5.2! This, of course, reflects the similarity between the instability mechanisms of the two systems.

so that

$$\mathrm{Im}(\sigma) = 0. \tag{101}$$

This shows that the marginal state is stationary. Indeed experiments show that the instability sets in as a secondary stationary flow.

Nonlinear Effects

The exponential growth of disturbances predicted by the linear theory is modified by the nonlinear effects when the critical Taylor number T^* has been exceeded. In particular, the amplitude growth of supercritical toroidal vortices (called the Taylor vortices) tapers off once the amplitude reaches an equilibrium value. The theoretical work of Stuart and Davey et al. on weakly nonlinear Taylor vortex flow between infinite cylinders has shown that this equilibrium amplitude is proportional to $\left(T - T^*\right)^{1/2}$ as in the case of the thermal instability of a fluid layer heated from below (Section 5.2). This result was confirmed in a qualitative manner by the experiments of Donnelly and Schwarz and later by Gollub and Freilich.

Instability of the Toroidal Vortices

As the Taylor number increases beyond the supercritical value, the toroidal vortices become unstable and develop a wavy pattern. However, experiments (Coles) have shown that the spatial structure is nonunique: different axial and azimuthal wavenumbers are observed at the same Taylor number and the wavy pattern depends on the manner in which the Taylor number increases or decreases and on the initial conditions of the experiment.

EXERCISE

1. Consider a cylindrical column of liquid of radius rotating about its axis with a uniform angular velocity Ω. Show that the frequencies of oscillations are given by

$$\frac{n}{\Omega_0} = \pm \frac{2i}{\left(1 + \alpha^2/a^2\right)^{1/2}} - im,$$

where $a = kR_0$, and α is a root of the equation

$$\alpha J_m'(\alpha) \pm m\left(1 + \alpha^2/a^2\right)^{1/2} J_m(\alpha) = 0,$$

with $J_m(x)$ being the Bessel's function of the first kind (Chandrasekhar).

5.4. Rayleigh–Taylor Instability of Superposed Fluids

The instability the interface between two fluids having different densities and accelerated toward each other is called the Rayleigh–Taylor instability. A static state, in which an incompressible fluid of variable density subject to a vertical acceleration is arranged in horizontal strata and the pressure and the density ρ are functions of the vertical coordinate z only, is obviously a kinematically realizable one. However, whether this state is also a dynamically realizable is related to the issue of stability with respect to small disturbances.

If viscosity is neglected, the flow can be assumed to be irrotational and the velocity potential of each fluid satisfies the Laplace equation. The difficulty in solving this type of problem, however, arises from the nonlinear boundary conditions at an unknown interface. On the other hand, if one assumes the disturbance amplitude to be infinitesimal, the boundary conditions can be linearized and a solution to the linear problem can be readily obtained. For the linear problem of two different inviscid and incompressible fluids in contact and subject to an acceleration directed from the heavier fluid toward the lighter one, it turns out, for the case of zero surface tension, that any slight disturbance in the plane interface grows exponentially with time. The effect of the surface tension in the linear problem is to produce a critical wavenumber k_c, so that the interface is unstable or stable depending on whether the wavenumber is less or greater than k_c. The surface tension, therefore, has a stabilizing effect on the interface, at sufficiently short wavelengths.

The Linear Problem

The two fluids are taken to be inviscid and incompressible, and if the motion of the whole system is supposed to start from rest, it may be assumed to be irrotational. The applied acceleration g' is directed from heavier to lighter fluid (see Figure 5.5). Initially, the interface is taken to be disturbed according to a simple sinusoidal standing wave with an amplitude a' and a wavelength λ'.

If $y = \eta$ denotes the disturbed shape of the interface, then one has with the velocity potentials, Φ_j, such that $\mathbf{v} = -\nabla\Phi$,

$$y \lessgtr \eta: \quad \nabla^2\Phi_j = 0; \qquad j = 1,2. \tag{1}$$

Further, one has the following boundary conditions at the interface:

1. *Kinematic Condition*: This expresses the fact that a fluid particle initially on the interface must stay on the interface during the course of perturbation. This requires

$$y = \eta: \quad \eta_t - \eta_x\Phi_{jx} + \Phi_{jy} = 0, \qquad j = 1,2. \tag{2}$$

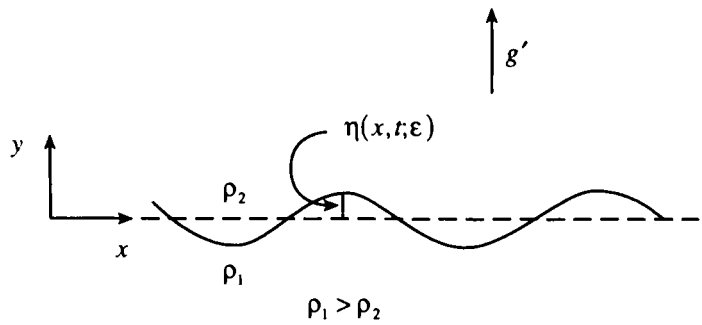

Figure 5.5. The interface accelerated normally and subjected to a perturbation.

2. *Dynamic Condition*: This refers to the force balance across the interface. In order to derive the dynamic condition, note that in the presence of a surface tension T', at the interface, for equilibrium, the normal stresses acting on the two sides of an interfacial element dS' must differ by an amount given by

$$\left[\left(-p'\delta_{ik}\right)_1 - \left(-p'\delta_{ik}\right)_2\right]\hat{n}_k = -T'\left(\frac{1}{R_1'}\right),$$

where p' is the normal pressure exerted by the fluid, $\hat{n}_k$ is the outward normal to dS', and R_1' is the principal radius of curvature of dS'. The convention regarding signs is that (see Section 1.2) R_1' is to be considered positive if the corresponding center of curvature lies on side 1 of dS'. For the case under consideration, note that

$$\frac{1}{R_1'} = \eta'_{x'x'}\left(1+\eta_{x'}'^2\right)^{-3/2}.$$

Using the Bernoulli integral, the dynamic condition at the interface becomes

$$y=\eta:\ \Phi_{1t} - \frac{1}{2}\left(\nabla\Phi_1\right)^2 + \eta - s\left[\Phi_{2t} - \frac{1}{2}\left(\nabla\Phi_2\right)^2 + \eta\right] = -k^2\eta_{xx}\left(1+\eta_x^2\right)^{-3/2}, \quad (3)$$

where

$$k^2 \equiv \left(\frac{2\pi}{\lambda'}\right)\frac{T'}{\rho_1' g'}, \qquad s = \frac{\rho_2'}{\rho_1'},$$

and the initial conditions are

$$t=0:\ \eta = \varepsilon\cos x, \qquad \eta_t = 0, \quad (4)$$

where

$$\varepsilon \equiv a'\left(2\pi/\lambda'\right).$$

The conditions at infinity are

$$y \to (-1)^j\infty:\ \Phi_{jy} \to 0. \quad (5)$$

All quantities in equations (1)–(5) have been nondimensionalized with respect to a reference length $\lambda'/2\pi$, a time $(\lambda'/2\pi g')^{1/2}$, where primes denote dimensional quantities.

Make a change of variable

$$\tau = \sigma t \tag{6}$$

so that (1)–(3) become

$$y \lessgtr \eta: \quad \nabla^2 \Phi_j = 0; \qquad j = 1,2 \tag{7}$$

$$y = \eta: \quad \sigma \eta_\tau - \eta_x \Phi_{jx} + \Phi_{jy} = 0 \tag{8}$$

$$y = \eta: \quad \sigma \Phi_{1\tau} - \frac{1}{2}(\nabla \Phi_1)^2 + \eta - s\left[\sigma \Phi_{2\tau} - \frac{1}{2}(\nabla \Phi_2)^2 + \eta\right] = -k^2 \eta_{xx}(1+\eta_x^2)^{-3/2}. \tag{9}$$

When we linearize the system (7)–(9), (4) and (5) becomes

$$y \lessgtr 0: \quad \nabla^2 \phi_j = 0; \qquad j = 1,2 \tag{10}$$

$$y = 0: \quad \sigma \eta_\tau + \phi_{jy} = 0 \tag{11}$$

$$y = 0: \quad \sigma \phi_{1\tau} + \eta - s(\sigma \phi_{2\tau} + \eta) + k^2 \eta_{xx} = 0 \tag{12}$$

$$y \to (-1)^j \infty: \quad \phi_{jy} \to 0 \tag{13}$$

$$\tau = 0: \quad \eta = \cos x, \qquad \eta_\tau = 0. \tag{14}$$

From (10), (11), (13), and (14), one obtains

$$\eta(x,\tau) = \cos x \cdot \cos \tau, \tag{15}$$

$$\phi_j(x,y,\tau) = -(-1)^j \cos x \cdot \sin \tau \cdot e^{-(-1)^j y}. \tag{16}$$

When we use (15) and (16), (12) gives the dispersion relation

$$\sigma^2 = \frac{k^2 + s - 1}{s+1}. \tag{17}$$

Note from (17) that:

1. In the absence of the surface tension, the interface is stable or unstable depending on $\rho_1' \lessgtr \rho_2'$,

2. In the presence of the surface tension, the interface is stable or unstable according as $k' \gtrless k_c'$, where

$$k_c' = \sqrt{\left(\frac{g'(\rho_1' - \rho_2')}{T'}\right)}, \tag{18}$$

indicating a stabilizing effect of the surface tension at sufficiently short wavelengths.

The Nonlinear Problem

When the interface is unstable according to the linear theory, the evolution of the interface quickly gets out of the linear regime because the predicted growth is exponential. It turns out that the nonlinear problem of instability of a vertically accelerated horizontal two–dimensional interface between two different fluids is one of singular perturbation type. One may therefore use the method of strained parameters to develop a uniformly valid solution for the above problem for wave numbers near the linear cutoff value. The density ratio of the fluids is now found to have a significant role in the stability or growth of the interface. Further, the interfacial waves are found to grow even at $k = k_c$ despite the cutoff predicted by the linear theory so that the instability in question is a subcritical instability.

Seek solutions to equations (7)–(9), (4), and (5), of the form, for wavenumbers near the linear cutoff value k_c,

$$\Phi_j(x, y, \tau; \varepsilon) = \sum_{n=1}^{\infty} \varepsilon^n \phi_j^{(n)}(x, y, \tau), \tag{19}$$

$$\eta(x, \tau; \varepsilon) = \sum_{n=1}^{\infty} \varepsilon^n \eta_n(x, \tau), \tag{20}$$

$$\sigma(k; \varepsilon) = \sum_{n=1}^{\infty} \varepsilon^{n-1} \sigma_n(k), \tag{21}$$

$$k^2(\varepsilon) = k_c^2 + \varepsilon^2 K + 0(\varepsilon^3). \tag{22}$$

In (22), one could include an $0(\varepsilon)$ term on the right–hand side, but it turns out to be zero anyway.

Upon substitution of (19)–(22) into (7)–(9), (4), and (5), one obtains

$0(\varepsilon)$:

$$y \lessgtr 0: \quad \phi_{jxx}^{(1)} + \phi_{jyy}^{(1)} = 0, \tag{23}$$

$$y = 0: \quad \sigma_1 \eta_{1\tau} + \phi_{jy}^{(1)} = 0, \tag{24}$$

$$y = 0: \quad \sigma_1 \phi_{1\tau}^{(1)} + \eta_1 - s\left(\sigma_1 \phi_{2\tau}^{(1)} + \eta_1\right) + k_c^2 \eta_{1xx} = 0, \tag{25}$$

$$y \to (-1)^j \infty: \quad \phi_{jy}^{(1)} \to 0, \tag{26}$$

$$\tau = 0: \quad \eta_1 = \cos x, \qquad \eta_{1\tau} = 0; \tag{27}$$

$0(\varepsilon^2)$:

$$y \lessgtr 0: \quad \phi_{jxx}^{(2)} + \phi_{jyy}^{(2)} = 0, \tag{28}$$

$$y = 0: \quad \sigma_1 \eta_{2\tau} + \phi_{jy}^{(2)} = \eta_{1x} \phi_{jx}^{(1)} - \phi_{jyy}^{(1)} \eta_1 - \sigma_2 \eta_{1\tau}, \tag{29}$$

$$y=0:\ \sigma_1\phi_{1\tau}^{(2)}+\eta_2-s\left(\sigma_1\phi_{2\tau}^{(2)}+\eta_2\right)+k_c^2\eta_{2xx}=\frac{1}{2}\left[\left(\phi_{1x}^{(1)}\right)^2+\left(\phi_{1y}^{(1)}\right)^2\right]$$
$$-s\frac{1}{2}\left[\left(\phi_{2x}^{(1)}\right)^2+\left(\phi_{2y}^{(1)}\right)^2\right]-\sigma_1\phi_{1\tau y}^{(1)}\eta_1-\sigma_2\phi_{1\tau}^{(1)}$$
$$+s\left(\sigma_1\phi_{2\tau y}^{(1)}\eta_1+\sigma_2\phi_{2\tau}^{(1)}\right), \tag{30}$$

$$y\to(-1)^j\infty:\ \phi_{jy}^{(2)}\to 0, \tag{31}$$

$$\tau=0:\ \eta_2=0,\qquad \eta_{2\tau}=0. \tag{32}$$

$0(\varepsilon^3)$:

$$y\lesseqgtr 0:\ \phi_{jxx}^{(3)}+\phi_{jyy}^{(3)}=0, \tag{33}$$

$$y=0:\ \sigma_1\eta_{3\tau}+\phi_{jy}^{(3)}=-\phi_{jyy}^{(1)}\eta_2-\phi_{jyy}^{(2)}\eta_1-\frac{1}{2}\phi_{jyyy}^{(1)}\eta_1^2+\phi_{jx}^{(2)}\eta_{1x}$$
$$+\phi_{jxy}^{(1)}\eta_1\eta_{1x}+\phi_{jx}^{(1)}\eta_{2x}-\sigma_2\eta_{2\tau}-\sigma_3\eta_{1\tau}, \tag{34}$$

$$y=0:\ \sigma_1\phi_{1\tau}^{(3)}+\eta_3-s\left(\sigma_1\phi_{2\tau}^{(3)}+\eta_3\right)+k_c^2\eta_{3xx}=-\sigma_2\left(\phi_{1\tau}^{(2)}+\phi_{1\tau y}^{(1)}\eta_1\right)$$
$$-\sigma_3\phi_{1\tau}^{(1)}-\sigma_1\left(\phi_{1\tau y}^{(2)}\eta_1+\phi_{1\tau y}^{(1)}\eta_2+\frac{1}{2}\phi_{1\tau yy}^{(1)}\eta_1^2\right)+s\left[\sigma_2\left(\phi_{2\tau}^{(2)}+\phi_{2\tau y}^{(1)}\eta_1\right)\right.$$
$$\left.-\sigma_3\phi_{2\tau}^{(1)}-\sigma_1\left(\phi_{2\tau y}^{(2)}\eta_1+\phi_{2\tau y}^{(1)}\eta_2+\frac{1}{2}\phi_{2\tau yy}^{(1)}\eta_1^2\right)\right]+\left(\phi_{1x}^{(1)}\phi_{1x}^{(2)}\right.$$
$$+\phi_{1x}^{(1)}\phi_{1xy}^{(1)}\eta_1+\phi_{1y}^{(1)}\phi_{1y}^{(2)}+\phi_{1y}^{(1)}\phi_{1yy}^{(1)}\eta_1\Big)-s\left(\phi_{2x}^{(2)}\phi_{2x}^{(2)}+\phi_{2x}^{(1)}\phi_{2xy}^{(1)}\eta_1\right.$$
$$\left.+\phi_{2y}^{(1)}\phi_{2y}^{(2)}+\phi_{2y}^{(1)}\phi_{2yy}^{(1)}\eta_1\right)+\frac{3}{2}k_c^2\eta_{1xx}\eta_{1x}^2-K\eta_{1xxx}, \tag{35}$$

$$y\to(-1)^j\infty:\phi_{jy}^{(3)}\to 0, \tag{36}$$

$$\tau=0:\ \eta_3=0,\qquad \eta_{3\tau}=0. \tag{37}$$

One obtains for the $0(\varepsilon)$ problem, as before for the linearized problem,

$$\eta_1(x,\tau)=\cos x\cdot\cos\tau, \tag{38}$$

$$\phi_j^{(1)}(x,y,\tau)=-(-1)^j\cos x\cdot\sin\tau\cdot e^{-(-1)^j y}, \tag{39}$$

$$\sigma_1^2=\frac{k_c^2+s-1}{s+1}. \tag{40}$$

The linear cutoff wavenumber k_c is given by

$$\sigma_1^2=0\quad\text{or}\quad k_c^2+s-1=0. \tag{18}$$

One may expect to construct uniformly valid solutions only for wavenumbers larger than k_c. But it turns out, upon a consideration of the nonlinear problem in

the following, that this is possible only for wavenumbers greater than k_c by a definite amount, namely, $\varepsilon^2 K$.

For wavenumbers near k_c, using (38) and (39), the system (28)–(32) becomes

$$y \lessgtr 0: \quad \phi_{jxx}^{(2)} + \phi_{jyy}^{(2)} = 0, \tag{41}$$

$$y = 0: \quad \phi_{jy}^{(2)} = \sigma^2 \cos x \cdot \sin \tau, \tag{42}$$

$$y = 0: \quad (1-s)\eta_2 + k_c^2 \eta_{2xx} = 0, \tag{43}$$

$$y \to (-1)^j \infty: \quad \phi_{jy}^{(2)} \to 0, \tag{44}$$

$$\tau = 0: \quad \eta_2 = 0, \qquad \eta_{2\tau} = 0, \tag{45}$$

from which

$$\eta_2(x, \tau) = \cos x \cdot (1 - \cos \tau), \tag{46}$$

$$\phi_j^{(2)}(x, y, \tau) = -(-1)^j \sigma_2 \cos x \cdot \sin \tau \cdot e^{-(-1)^j y}, \tag{47}$$

where σ_2 is now nonzero but is arbitrary in the $0(\varepsilon^2)$ problem.

Next, using (38), (39), (46), and (47), the system (33)–(37) becomes

$$y \lessgtr 0: \quad \phi_{jxx}^{(3)} + \phi_{jyy}^{(3)} = 0, \tag{48}$$

$$y = 0: \quad \phi_{jy}^{(3)} = -\frac{\sigma_2}{2} \cos 2x \cdot \sin 2\tau - (\sigma_2 - \sigma_3) \cos x \cdot \sin \tau, \tag{49}$$

$$y = 0: \quad (1-s)\eta_3 + k_c^2 \eta_{3xx} = \left[-(1+s)\sigma_2^2 + K - \frac{3}{8}(1-s) \right] \cos x \cdot \cos \tau, \tag{50}$$

$$y \to (-1)^j \infty: \quad \phi_{jy}^{(3)} \to 0, \tag{51}$$

$$\tau = 0: \quad \eta_3 = 0, \qquad \eta_{3\tau} = 0. \tag{52}$$

The removal of the secular terms in (50) requires

$$(1+s)\sigma_2^2 - K + \frac{3}{8}(1-s) = 0$$

or

$$\sigma_2 = \pm \left[\frac{K - \frac{3}{8}(1-s)}{1+s} \right]^{1/2}, \tag{53}$$

so that one has

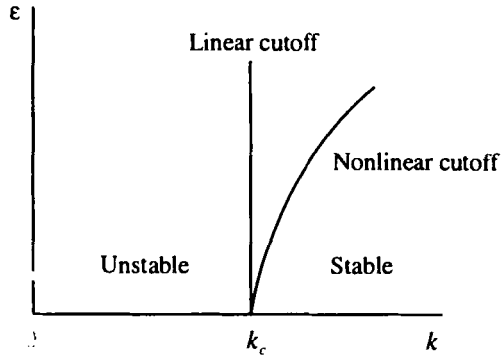

Figure 5.6. Linear and nonlinear cutoffs for Rayleigh–Taylor instability.

$$\left.\begin{aligned} K &< \frac{3}{8}(1-s): \text{ instability,} \\ K &= \frac{3}{8}(1-s): \text{ neutral stability,} \\ K &> \frac{3}{8}(1-s): \text{ stability} \end{aligned}\right\}$$

and corresponding to neutral stability, one has

$$k^2 = k_c^2 + \frac{3}{8}(1-s)\varepsilon^2 + 0(\varepsilon^3), \tag{54}$$

which is graphically represented in Figure 5.6.

It is to be noted that the interfacial waves grow even at $k = k_c$ despite the cut–off predicted by the linear theory. On the other hand, the onset of instability even below the linear stability threshold when the disturbance has finite amplitude implies that this instability is a subcritical instability.

EXERCISE

1. Study the effect of uniform rotation about the y–axis on the Rayleigh–Taylor instability of the interface between two fluids having different densities.

5.5. Kelvin–Helmholtz Instability

When two superposed fluids of different densities flow one over the other with a relative velocity parallel to the plane interface, the instability of the plane interface between the two fluid is called the Kelvin–Helmholtz instability.

The Stratified Fluid in Nonuniform Streaming

Consider the character of equilibrium of an incompressible, inviscid, stratified fluid when the different layers are in relative motion with velocity $U(z)$ in the x-direction. The assumption that the fluid is inviscid allows one to choose for U any arbitrary function of z. The equations governing linearized disturbances superposed on this flow are

$$\rho\left(\frac{\partial u}{\partial t}+U\frac{\partial u}{\partial x}+w\frac{\partial U}{dz}\right)=-\frac{\partial \delta p}{\partial x}, \tag{1}$$

$$\rho\left(\frac{\partial v}{\partial t}+U\frac{\partial v}{\partial x}\right)=-\frac{\partial \delta p}{\partial y}, \tag{2}$$

$$\rho\left(\frac{\partial w}{\partial t}+U\frac{\partial w}{\partial x}\right)=-\frac{\partial \delta p}{\partial z}-g\delta\rho, \tag{3}$$

$$\frac{\partial \delta\rho}{\partial t}+U\frac{\partial \delta\rho}{\partial x}+w\frac{d\rho}{dz}=0, \tag{4}$$

$$\frac{\partial u}{\partial x}+\frac{\partial v}{\partial y}+\frac{\partial w}{\partial z}=0. \tag{5}$$

Analyzing the disturbances into normal modes, one seeks solutions of the form

$$q\sim q(z)e^{i(k_x x+k_y y+nt)}. \tag{6}$$

Equations (1)–(5) then give

$$i\rho(n+k_xU)u+\rho(DU)w=-ik_x\delta p, \tag{7}$$

$$i\rho(n+k_xU)v=-ik_y\delta p, \tag{8}$$

$$i\rho(n+k_xU)w=-D\delta p-g\delta\rho, \tag{9}$$

$$i(n+k_xU)\delta\rho+wD\rho=0, \tag{10}$$

$$i(k_xu+k_yv)+Dw=0, \tag{11}$$

where

$$D\equiv\frac{d}{dz}.$$

Multiply equation (7) by $-ik_x$ and equation (8) by $-ik_y$, add and use equation (11), so that

$$i\rho(n+k_xU)Dw-i\rho k_x(DU)w=-k^2\delta p, \tag{12}$$

where

$$k^2=k_x^2+k_y^2.$$

From equations (9) and (10), one obtains, on the other hand,

$$i\rho(n+k_xU)w = -D\delta p - ig\cdot D\rho\cdot\frac{w}{n+k_xU}. \tag{13}$$

Eliminating δp between equations (12) and (13), one obtains

$$D\{\rho(n+k_xU)Dw - \rho k_x\cdot DU\cdot w\} - k^2\rho(n+k_xU)w = gk^2\cdot D\rho\cdot\frac{w}{n+k_xU}. \tag{14}$$

If ρ and U change discontinuously at some point $z = z_s$, then one may obtain from equation (14) a jump condition at $z = z_s$ by integrating equation (14) over an infinitesimal element $(z_s-\varepsilon,\ z_s+\varepsilon)$ and passing to the limit $\varepsilon \Rightarrow 0$. Noting, from the kinematic condition at such an interface, that

$$\frac{w}{n+k_xU} \text{ is continuous at } z = z_s, \tag{15}$$

one thus obtains

$$[\rho(n+k_xU)Dw - \rho k_x\cdot DU\cdot w] = gk^2[\rho]\cdot\left(\frac{w}{n+k_xU}\right)_{z=z_s}, \tag{16}$$

where the rectangular brackets denote the jump of the contents at $z = z_s$.

The Case of Two Uniform Fluids in Relative Motion Parallel to the Plane Interface

Consider two uniform fluids of densities ρ_1,ρ_2 and constant velocities U_1,U_2 separated by the plane $z = 0$ (Figure 5.7). Let $\rho_2 < \rho_1$ so that in the absence of streaming, the arrangement is a stable one. Equation (14) then becomes

$$z\gtrless 0:\ \ (D^2 - k^2)w = 0, \tag{17}$$

from which, upon using (15),

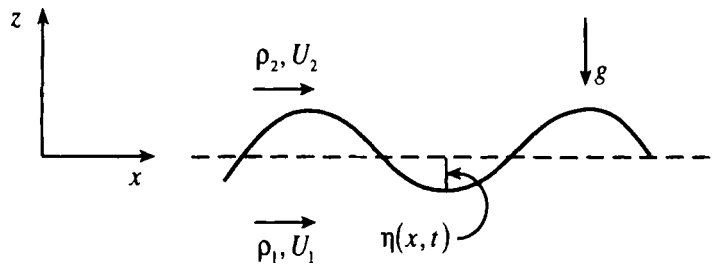

Figure 5.7. The interface between two streams accelerated normally and subjected to a perturbation.

$$z<0 : w_1 = A(n+k_x U_1)e^{kz}, \tag{18a}$$

$$z>0 : w_2 = A(n+k_x U_2)e^{-kz}. \tag{18b}$$

When one uses (18), (16) gives

$$\rho_2(n+k_x U_2)^2 + \rho_1(n+k_x U_1)^2 = gk(\rho_2 - \rho_1), \tag{19}$$

from which

$$n = -k_x(\alpha_1 U_1 + \alpha_2 U_2) \pm \left[gk(\alpha_1 - \alpha_2) - k_x^2 \alpha_1 \alpha_2 (U_1 - U_2)^2\right]^{1/2}, \tag{20}$$

where

$$\alpha_{1,2} = \frac{\rho_{1,2}}{\rho_1 + \rho_2}.$$

From (20), one has for stability

$$k < \frac{g(\alpha_1 - \alpha_2)}{\alpha_1 \alpha_2 (U_1 - U_2)^2}, \tag{21}$$

so that in the presence of streaming, a statically stable arrangement becomes unstable when there are disturbances of sufficiently small wavelengths.

A Shear Layer in a Stratified Fluid

Consider a shear layer given by

$$U = U_0 \tan h \frac{z}{d} \tag{22}$$

in a stratified fluid.

For disturbances propagating along the direction of streaming (i.e., $k_y = 0$, $k_x \neq 0$), equation (14) becomes

$$\left(\frac{n}{k} + U\right)(D^2 - k^2)w - D^2 U \cdot w - g\frac{D\rho}{\rho}\frac{w}{U + n/k} = 0. \tag{23}$$

When we

$$\rho = \rho_0 e^{-\beta z}, \qquad \beta = \text{const.}, \tag{24}$$

equation (23) becomes

$$(U-c)(D^2 - k^2)w - D^2 U \cdot w + J\frac{w}{U-c} = 0, \tag{25}$$

where the length and velocity have been nondimensionalized using d and U_0, respectively, and

$$c = -\frac{n}{kU_0}, \qquad J = \frac{g\beta d^2}{U_0^2}.$$

Next, note that, if $w(z)$ is a characteristic function of equation (25) with $c = c_r + ic_i$ $(c_i > 0)$, then, $w(-z)$ is also a characteristic function with the same α but with $c = -c_r + ic_i$, since $U(z)$ is odd. Since there can be only one unstable mode for a given α, one requires $c_r = 0$. Thus, for neutrally stable disturbances, equation (25) becomes

$$U\left(D^2 - k^2\right)w - D^2U \cdot w + J\frac{w}{U} = 0. \tag{26}$$

One transforms equation (26) using U as the independent variable, an elegant idea due to Drazin; noting that

$$\frac{dU}{dz} = \sec h^2 z = 1 - U^2, \quad \frac{d^2U}{dz^2} = -2U\left(1 - U^2\right),$$

equation (26) becomes

$$\frac{d}{dU}\left[\left(1-U^2\right)\frac{dw}{dU}\right] + \left[2 - \frac{k^2}{1-U^2} + \frac{J}{U^2\left(1-U^2\right)}\right]w = 0 \tag{27}$$

with the boundary conditions

$$U = \pm 1: \quad w = 0. \tag{28}$$

The singular points of equation (27) are at $U = \pm 1, 0$. In order to determine the behavior of the solutions of equation (27) at the singular points $U = \pm 1$, put

$$U = 1 \pm y, \qquad y \ll 1, \tag{29}$$

so that equation (27) becomes

$$y\frac{d^2w}{dy^2} + \frac{dw}{dy} + \frac{1}{4y}\left(J - k^2\right)w = 0, \tag{30}$$

from which

$$w \sim y^{\nu}, \nu^2 = \frac{1}{4}\left(k^2 - J\right). \tag{31}$$

Therefore, a solution of equation (27) regular at $U = \pm 1$ must have the behavior

$$U = \pm 1: \quad w \sim \left(1 - U^2\right)^{\nu}, \tag{32}$$

and it is necessary that $\mathrm{Re}(\nu) \geq 0$.

Similarly, the behavior of w at $U = 0$ is

$$w \sim U^{\mu}, \mu = \frac{1}{2} + \frac{1}{2}\sqrt{1 - 4J}. \tag{33}$$

Equation (32) and (33) suggest that one seek a solution of the form

$$w = U^{\mu}\left(1 - U^2\right)^{\nu}\chi, \tag{34}$$

where χ is regular at $U = \pm 1$. Equation (27) then gives

$$\frac{d^2\chi}{dU^2}+\left\{\frac{\mu}{U}-\frac{2(\nu+1)U}{(1-U^2)}\right\}\frac{d\chi}{dU}-\frac{(2\nu+\mu+2)(2\nu+\mu-1)}{1-U^2}\chi=0. \tag{35}$$

Equation (35) admits a solution $\chi = \text{const}$, provided that

$$(2\nu+\mu+2)(2\nu+\mu-1)=0. \tag{36}$$

Note from (31) and (33) that

$$2\nu+\mu+2=\frac{5}{2}+\sqrt{k^2-J}+\frac{1}{2}\sqrt{1-4J}\neq 0. \tag{37}$$

Equation (36) gives

$$2\nu+\mu-1=\sqrt{k^2-J}-\frac{1}{2}+\frac{1}{2}\sqrt{1-4J}=0, \tag{38a}$$

from which

$$J=k^2(1-k^2). \tag{38b}$$

When we use (37), (31) and (33) give

$$\nu=\frac{1}{2}k^2, \qquad \mu=1-k^2, \tag{39}$$

so that corresponding to the characteristic value given by (38b) the characteristic solution is

$$w\sim(1-U^2)^{k^2/2}U^{(1-k^2)}$$

or

$$w\sim(\operatorname{sech}hz)^{k^2}\cdot(\tanh hz)^{(1-k^2)}. \tag{40}$$

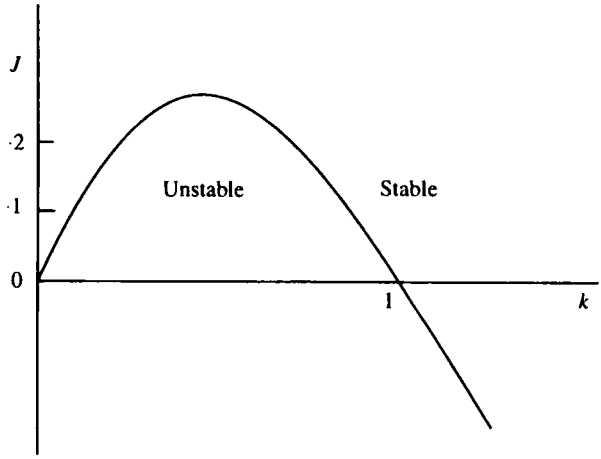

Figure 5.8. The marginal stability curve for a shear layer in a stratified fluid.

The curve of marginal stability, given by (38), is sketched in Figure 5.8. Note that one has $J_{max} = 1/4$ corresponding to $k^2 = 1/2$, and the flow is stable for $J > 1/4$. In the latter case, the stabilizing effect of gravity (associated with the density decreasing with height) is sufficient to overcome the destabilizing effect of the shear.

Stability of an Interface Between a Liquid and Gas Stream

We consider here the stability of the wave motion at the interface between a liquid layer and a gas stream adjacent to it. It turns out that the nature of the waves generated at the interface depends markedly upon the state of flow of the gas. For supersonic gas flow, the gas pressure at the interface is out of phase with the surface tension so that a purely oscillatory constant-amplitude motion of the interface is not possible. For a subsonic gas flow, however, the stabilizing effect of the surface tension gives rise to cutoff frequencies.

We consider a body force directed toward the liquid, and the effects of the surface tension of the liquid. The liquid is assumed to be initially quiescent and of infinite depth whose mean level of contact with a gas flowing past it is the horizontal surface $y = 0$ (see Figure 5.9). Both the liquid and the gas are assumed to be inviscid, and the effects of the viscous boundary layer at the interface are ignored. If the motion of the whole system is supposed to start from rest, it may be assumed to be irrotational. If a typical interfacial disturbance is characterized by a sinusoidal traveling wave with an amplitude a' and wavelength λ', then all the quantities in the following are nondimensionalized with respect to a reference length $\lambda'/2\pi$ and a time $(\lambda'/2\pi g')^{1/2}$, and the inertial effects of the gas motion are characterized by the ratio of the wave speed to the gas speed. The gas density ρ_g' is small so that the corresponding body force is negligible. The potential function of the motions of the liquid and the gas are taken to be, respectively,

$$(g')^{1/2}\left(\frac{\lambda'}{2\pi}\right)^{3/2}\varphi(x,y,t) \quad \text{and} \quad U_\infty'\left[x+\phi(x,y,t)\right]\left(\frac{\lambda'}{2\pi}\right). \tag{41}$$

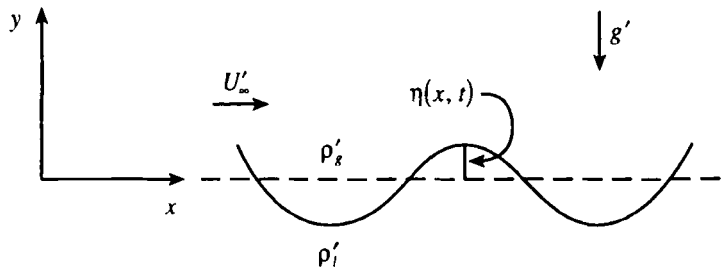

Figure 5.9. The interface between a gas stream and a liquid.

We consider here a linearized problem; the latter is governed by the following equations

$$y < \eta: \quad \varphi_{xx} + \varphi_{yy} = 0, \tag{42}$$

$$y > \eta: \quad \phi_{yy} - \left(M_\infty^2 - 1\right)\phi_{xx} - M_\infty^2\left(2\delta\phi_{xt} + \delta^2\phi_{tt}\right) = 0, \tag{43}$$

where

$$\delta = \left(\frac{\lambda' g'}{2\pi}\right)^{1/2} \frac{1}{U_\infty'} \sim \frac{\text{wave speed}}{\text{gas speed}} \ll 1.$$

Here, $y = \eta(x,t)$ denotes the disturbed shape of the interface, and U_∞' and M_∞ are the ambient gas velocity and the Mach number. One has the following boundary conditions at the interface

(1) *kinematic condition*

$$y = 0: \quad \varphi_y = \eta_t, \tag{44}$$

$$y = 0: \quad \phi_y = \delta\eta_t + \eta_x; \tag{45}$$

(2) *dynamic condition*

$$y = 0: \quad \varphi_t + \eta = k^2\eta_{xx} - \frac{\sigma}{2}kC_p, \tag{46}$$

where

$$k^2 = \left(\frac{2\pi}{\lambda'}\right)^2 \frac{T'}{\rho_\ell' g'}, \qquad \sigma = \frac{\rho_g' U_\infty'^2}{\sqrt{\rho_\ell' g' T'}},$$

$$C_p = -2\phi_x - 2\delta\phi_t,$$

and T' denotes the surface tension.

The infinity conditions are

$$y \Rightarrow -\infty: \quad \varphi_y \Rightarrow 0, \tag{47}$$

$$y \Rightarrow \infty: \quad \phi_y \Rightarrow 0 \quad \text{if the gas flow is subsonic.} \tag{48}$$

Since we are looking for traveling waves, let us introduce

$$\xi = x - ct, \tag{49}$$

so that (42)–(47) become

$$y < 0: \quad \varphi_{\xi\xi} + \varphi_{yy} = 0, \tag{50}$$

$$y > 0: \quad \gamma^2\phi_{\xi\xi} + \phi_{yy} = 0, \tag{51}$$

$$y = 0: \quad \varphi_y = -c\eta_\xi, \tag{52}$$

$$y = 0: \quad \phi_y = (1 - \delta c)\eta_\xi, \tag{53}$$

$$y = 0: \quad \eta = c\varphi_\xi + k\sigma(1 - \delta c)\phi_\xi + k^2\eta_{\xi\xi}, \tag{54}$$

$$y \Rightarrow -\infty: \quad \varphi_y \Rightarrow 0, \tag{55}$$

$$y \Rightarrow \infty: \quad \phi_y \Rightarrow 0 \quad \text{if the flow is subsonic,} \tag{56}$$

where

$$\gamma^2 \equiv 1 - M_\infty^2 + 2\delta c M_\infty^2.$$

Subsonic Gas Flow

Let

$$\eta(\xi) = A \cos \xi; \tag{57}$$

then from (50)–(53), (55), and (56), one obtains

$$\varphi(\xi, y) = Ace^{y} \sin \xi, \tag{58}$$

$$\phi(\xi, y) = \frac{A}{\gamma}(1 - \delta c)e^{-\gamma y} \sin \xi. \tag{59}$$

Using (57)–(59) in (54), one obtains the dispersion relation

$$c^2 + \frac{k\sigma(1 - 2\delta c)}{\gamma} - (1 + k^2) = 0, \tag{60}$$

from which

$$c = k\sigma\delta\left(\frac{1}{m} + \frac{M_\infty^2}{2m^3}\right) \pm \Delta, \tag{61}$$

where

$$\Delta = \sqrt{k^2 - \frac{k\sigma}{m} + 1}, \qquad m = \sqrt{1 - M_\infty^2}.$$

It is obvious that the inertial effects of the gas motion lead to overstability (because $\mathrm{Re}(c) \neq 0$ when $\mathrm{Im}(c) = 0$).

The cutoff wavenumbers correspond to

$$k_{c_{1,2}} = \frac{\sigma}{2m} \mp \sqrt{\frac{\sigma^2}{4m^2} - 1}. \tag{62}$$

Thus, thanks to the stabilizing effect of the surface tension, there are two cut-off wavenumbers, and all disturbances with wavenumbers above or below these values propagate without growth or decay.

Supersonic Gas Flow

Let

$$\eta(\xi) = Ae^{i\xi}; \tag{63}$$

then from (50)–(53), and (55), one obtains

$$\phi(\xi, y) = -\frac{iA}{\Delta}(1 - \delta c)e^{i(\xi - \Delta y)}, \tag{64}$$

$$\varphi(\xi, y) = -iAce^{y + i\xi}, \tag{65}$$

where

$$\Delta^2 \equiv M_\infty^2 - 1 - 2\delta c M_\infty^2.$$

Using (63)–(65) in (54), one obtains the dispersion relation

$$1 = c^2 + \frac{ik\sigma(1-\delta c)^2}{\Delta} - k^2, \tag{66}$$

from which

$$c = \frac{ik\sigma\delta}{2m^3}\left(M_\infty^2 - 2\right) \pm \Sigma, \tag{67}$$

where

$$\Sigma = \sqrt{k^2 - \frac{ik\sigma}{m} + 1}, \qquad m = \sqrt{M_\infty^2 - 1}.$$

It is seen that the physical condition is always one of instability, regardless of the presence of surface tension. The inertial effects of the gas motion worsen this instability. However, interestingly enough, note that the inertial effects of the gas motion disappear in the linear model at $M_\infty^2 = 2$!

EXERCISES

1. Deduce the variational characterization of the problem corresponding to $U = 0$. Show, hence or otherwise, that if $D\rho < 0$ throughout the flow, all the values of n^2 are positive (so the flow is stable), and vice versa.
2. Show that the stability criterion $J > 1/4$ in Section 5.3 holds for more general velocity profiles as well (Miles' criterion).

5.6. Capillary Instability of a Liquid Jet

We study here the linear stability of a cylindrical column of an ideal fluid, of circular cross section, under the action of surface tension. A columnar jet of circular cross section is formed when a liquid issues under pressure through a small circular orifice into the air when the gravity effect may be neglected. Since surface tension tries to minimize surface area the jet may become unstable under a small disturbance. The instability causes the jet to disintegrate into drops since the latter have smaller surface area.

The jet fluid is assumed to be inviscid and incompressible and has density ρ_1' and axial velocity U' (which is constant). The undisturbed jet is assumed to be circular with radius R'. The jet is surrounded by a stagnant fluid which is also

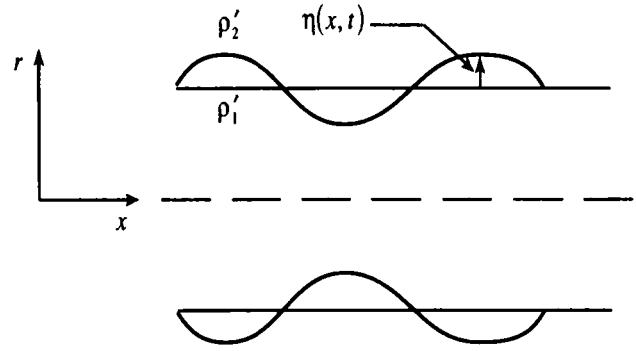

Figure 5.10. The liquid jet.

inviscid and incompressible and has density ρ_2' (Figure 5.10). The disturbances are taken to be axisymmetric (the jet turns out to be more stable relative to nonaxisymmetric disturbances, see Exercise 1), and they are considered to be sinusoidal waves propagating along the jet axis with wavenumber kR' and amplitude a' (which is small). The various quantities are nondimensionalized using a characteristic length R' and a characteristic time $\left(\rho' R'^3/T'\right)$, where T' denotes the surface tension at the interface. Here, primes denote dimensional quantities.

The flow is assumed to start from rest so that it can be represented by velocity potentials

$$V'R'\left[Ux+\phi(x,r,t)\right] \quad \text{and} \quad V'R'\varphi(x,r,t), \tag{1}$$

where

$$V' = \frac{T'}{\rho' R'^2}$$

for the jet–fluid and the surrounding fluid, respectively. If $r-1=\eta(x,t)$ denotes the disturbed shape of the interface, one has

$$r<1+\eta: \quad \phi_{rr}+\frac{\phi_r}{r}+\phi_{xx}=0, \tag{2}$$

$$r>1+\eta: \quad \varphi_{rr}+\frac{\varphi_r}{r}+\varphi_{xx}=0. \tag{3}$$

The boundary conditions at the interface are:

(1) *kinematic condition*

$$r=1+\eta: \quad \phi_r=\eta_t+\left(U+\phi_x\right)\eta_x \tag{4}$$

$$r=1+\eta: \quad \varphi_r=\eta_t+\varphi_x\,\eta_x. \tag{5}$$

(2) *dynamic condition*

$$r=1+\eta:\quad \left[\phi_t+U\phi_x+\frac{1}{2}\left(\phi_x^2+\phi_r^2\right)\right]-s\left[\varphi_t+\frac{1}{2}\left(\varphi_x^2+\varphi_r^2\right)\right]$$
$$=1+\eta_{xx}\left(1+\eta_x^2\right)^{-3/2}-(1+\eta)^{-1}\left(1+\eta_x^2\right)^{-1/2}, \tag{6}$$

where

$$s=\frac{\rho_2'}{\rho_1'}.$$

In order to derive an initial condition, consider an initially sinusoidal disturbance (called a varicose deformation) which preserves rotational symmetry about the x–axis,

$$r=R+\varepsilon\cos kx,\qquad \varepsilon=\frac{a'}{R'}. \tag{7}$$

From the conservation of mass of a column of liquid of length π/k and volume π^2/k, one obtains

$$\frac{\pi^2}{k}=\int_0^{\pi/k}\pi(R+\varepsilon\cos kx)^2\,dx, \tag{8}$$

from which

$$R=\left(1-\frac{\varepsilon^2}{2}\right)^{1/2}, \tag{9}$$

so that one has the initial condition

$$t=0:\quad \eta=\left(1-\frac{\varepsilon^2}{2}\right)^{1/2}-1+\varepsilon\cos kx,\qquad \eta_t=0. \tag{10}$$

Linearize the system (4(–(6) and (10), and look for traveling waves by introducing

$$\xi=x-ct \tag{11}$$

so that (2)–(6), and (10) give

$$r<1:\quad \phi_{rr}+\frac{\phi_r}{r}+\phi_{\xi\xi}=0, \tag{12}$$

$$r>1:\quad \varphi_{rr}+\frac{\varphi_r}{r}+\varphi_{\xi\xi}=0, \tag{13}$$

$$r=1:\quad \phi_r=(U-c)\eta_\xi, \tag{14}$$

$$r=1:\quad \varphi_r=-c\eta_\xi, \tag{15}$$

$$r=1:\quad (U-c)\phi_\xi+sc_0\varphi_\xi=\eta+\eta_{\xi\xi}, \tag{16}$$

$$\xi=x:\quad \eta=\cos kx,\qquad \eta_\xi=0. \tag{17}$$

One obtains from (12)–(15),

$$\eta = \cos k\xi, \tag{18}$$

$$\phi = -(U-c)\left[\frac{I_0(kr)}{I_1(k)}\right]\sin k\xi, \tag{19}$$

$$\phi = -c\left[\frac{K_0(kr)}{K_1(k)}\right]\sin k\xi, \tag{20}$$

where I_n and K_n are modified Bessel functions of first kind and second kind, respectively, and order n.

Using (18)–(20) in (16), one obtains the dispersion relation

$$(U-c)^2 \alpha k + sc^2 \beta k = k^2 - 1, \tag{21}$$

where

$$\alpha = \frac{I_0(k)}{I_1(k)}, \qquad \beta = \frac{K_0(k)}{K_1(k)}.$$

From (21),

$$c = \left(\frac{\alpha}{\alpha + s\beta}\right) U \pm \sqrt{\frac{(k^2-1)}{k(\alpha+s\beta)} - \frac{s\alpha\beta}{(\alpha+s\beta)^2} U^2}. \tag{22}$$

Note, from (22), that:

1. In the absence of an axial flow in the jet, the jet is stable or unstable with respect to an axisymmetric disturbance depending upon whether its wavelength is less or greater than the circumference of the jet,

2. The physically significant effects of the axial flow on the linear-stability characteristics of the jet arise only in the presence of a fluid surrounding the jet.

3. The linear cutoff wavenumber corresponds to the positive root k_c of

$$k^2 - \left(\frac{s\alpha\beta U^2}{\alpha + s\beta}\right)k - 1 = 0 \tag{23}$$

and the destabilizing effect of the axial flow is obvious by observing from (23) that $k_c > 1$, while $k = 1$ is the linear cutoff value corresponding to the case $U = 0$.

4. In the absence of the axial flow, on the other hand, it is clear that the presence of the fluid surrounding the jet has no effect on the stability criterion for the interface, but merely reduces the frequencies of oscillation by a certain amount.

The nonlinear problem of capillary instability of a liquid jet is also one of singular perturbation type. However, despite many attempts, a fully satisfactory perturbatory treatment of the problem for wavenumbers near the linear cutoff value $k_c = 1$ does not seem to be available yet. Nonetheless, the instability in

question appears to be a subcritical instability, like the Rayleigh–Taylor instability.

EXERCISE

1. Show that the jet is more stable with respect to nonaxisymmetric disturbances.

5.7. Stability of Parallel Flows

The most extensive discussion of hydrodynamic stability has been the study of inertial instabilities in parallel flows. The physical cause of instability of parallel flows is a bit suble compared with several other kinds of instability such as thermal instability, interfacial instability, etc., we considered before. The basic premise of the theory that the stability or instability of infinitesimal disturbances depends only on their frequency or wavelength and on the Reynolds number was confirmed by the experiments of Schubauer and Skramstad showing that the transition to turbulence was preceded by this instability.

The subject of hydrodynamic stability of parallel flows remains, however, well known for its controversial nature. The effect of viscosity in parallel flows is one such example. Intuition would suggest that viscosity is essentially dissipative in nature and therefore provides a mechanism for damping out the disturbances. If one further observes that instability generally occurs at large Reynolds numbers, one might reason that the principal features of the mechanism of instability may be obtained by first neglecting the viscous effects and then incorporating them later as a stabilizing influence.

But experiments show that viscous effects can also serve as a cause of instability. In the case of plane Poiseuille flow, Rayleigh's criterion would certainly indicate stability in the absence of viscosity. The theory does show that the flow is stable with respect to disturbances of a given wavelength, provided that the Reynolds number is high enough. However, experiments show that, for wavelengths beyond a certain lower limit, there is always a finite range of Reynolds number for which the motion is unstable. This is so since, by some means, viscosity also promotes the transfer of energy from the basic laminar flow to the disturbance, which is thereby amplified. Physically, the dual action of viscosity is connected with the fact that its effects are diffusive as well as dissipative in character; consequently, it can assist in spreading any local concentration of vorticity to neighboring parts of the fluid. This diffusive action materializes since the theory shows that the supposed regions of concentrated vorticity do exist in the disturbed flow. (Indeed, Rayleigh believed that an investigation in which viscosity is altogether ignored may not be applicable to the limiting case of a viscous fluid when the viscosity approaches zero.)

The Orr–Sommerfeld Equation

Consider two–dimensional flows of an incompressible fluid between parallel planes. Let x denote the distance parallel to the flow, y the distance normal to the planes, and z the distance normal to the flow, but coplanar with the bounding planes. Let (u, v, w) be the corresponding velocity components. Let the various flow variables be nondimensionalized using a reference length L and a reference velocity U and mass density ρ. The Navier–Stokes equations are then

$$\frac{\partial u}{\partial t} + u\frac{\partial u}{\partial x} + v\frac{\partial u}{\partial y} + w\frac{\partial u}{\partial z} = -\frac{\partial p}{\partial x} + \frac{1}{R_E}\nabla^2 u, \tag{1}$$

$$\frac{\partial v}{\partial t} + u\frac{\partial v}{\partial x} + v\frac{\partial v}{\partial y} + w\frac{\partial u}{\partial z} = -\frac{\partial p}{\partial y} + \frac{1}{R_E}\nabla^2 v, \tag{2}$$

$$\frac{\partial w}{\partial t} + u\frac{\partial w}{\partial x} + v\frac{\partial w}{\partial y} + w\frac{\partial w}{\partial z} = -\frac{\partial p}{\partial z} + \frac{1}{R_E}\nabla^2 w, \tag{3}$$

$$\frac{\partial u}{\partial x} + \frac{\partial v}{\partial y} + \frac{\partial w}{\partial z} = 0, \tag{4}$$

where

$$\nabla^2 = \frac{\partial^2}{\partial x^2} + \frac{\partial^2}{\partial y^2} + \frac{\partial^2}{\partial z^2}, \qquad R_E = \frac{UL\rho}{\mu}.$$

Consider perturbations about a mean parallel flow $\bar{u}(y)$ parallel to the x–axis,

$$u = \bar{u} + u', \qquad v = v', \qquad w = w', \qquad p = \bar{p} + p'. \tag{5}$$

When we use (5) and linearize the perturbations, equations (1)–(4) give

$$\frac{\partial u'}{\partial t} + \bar{u}\frac{\partial u'}{\partial x} + v'\frac{d\bar{u}}{dy} = -\frac{\partial p'}{\partial x} + \frac{1}{R_E}\nabla^2 u', \tag{6}$$

$$\frac{\partial v'}{\partial t} + \bar{u}\frac{\partial v'}{\partial x} = -\frac{\partial p'}{\partial y} + \frac{1}{R_E}\nabla^2 v', \tag{7}$$

$$\frac{\partial w'}{\partial t} + \bar{u}\frac{\partial w'}{\partial x} = -\frac{\partial p'}{\partial z} + \frac{1}{R_E}\nabla^2 w', \tag{8}$$

$$\frac{\partial u'}{\partial x} + \frac{\partial v'}{\partial y} + \frac{\partial w'}{\partial z} = 0. \tag{9}$$

In the theory of normal–modes, one looks for solutions of the form

$$\{u', v', w', p'\} = \{u'(y), v'(y), w'(y), p'(y)\}e^{i(\alpha x + \beta z - \alpha c t)}, \tag{10}$$

where α and β are real, and $c = c_r + ic_i$ so that the disturbances grow or die away in time like $e^{\alpha c_i t}$. When we use (10) and eliminate p', equations (6)–(9) give

$$(\bar{u}-c)\left(D^2-\gamma^2\right)v'-v'D^2\bar{u}=-\frac{i}{\alpha R_E}\left(D^2-\gamma^2\right)^2 v', \tag{11}$$

$$(\bar{u}-c)(\beta u'-\alpha w')-\frac{i\beta}{\alpha}v'D\bar{u}=-\frac{i}{\alpha R_E}\left(D^2-\gamma^2\right)(\beta u'-\alpha w'), \tag{12}$$

$$i\alpha u'+i\beta w'+Dv'=0, \tag{13}$$

where

$$D\equiv\frac{d}{dy}, \qquad \gamma^2\equiv\alpha^2+\beta^2.$$

The boundary conditions for a flow bounded by rigid planes at $y=0,1$ are

$$y=0,1: \quad u',v',w'=0 \tag{14a}$$

or, using (13),

$$y=0,1: \quad v', Dv'=0. \tag{14b}$$

From equation (12), note that it is possible to make the transformation

$$\beta u'-\alpha w'=\gamma\tilde{u}', \alpha R_E=\gamma\tilde{R}_E \tag{15}$$

to arrive at an equivalent two–dimensional problem $(\beta=0)$. Thus, the three–dimensional evolution of a disturbance at a Reynolds number R_E is equivalent to the two–dimensional evolution of the disturbance at a lower Reynolds number $\tilde{R}_E$ (because it is only the component of the mean flow in the direction of propagation of the disturbance that matters). In the case of neutral disturbances $(c_i=0)$, therefore, the minimum critical Reynolds number occurs for a two–dimensional disturbance, so that in seeking a sufficient criterion for instability one may consider only the two–dimensional disturbances, which greatly simplifies the analysis. This is the so–called Squire's Theorem. (Alternatively, one may also show that in an unstable parallel flow, the disturbance with the greatest rate of amplification αc_i at a given value of R_E is two–dimensional.) However, Squire's Theorem does not imply that the most dangerous disturbance at any Reynolds number about the critical value necessarily two–dimensional.

Using Squire's Theorem and introducing

$$u'=\frac{\partial\phi}{\partial y}, \qquad v'=-i\alpha\phi, \tag{16}$$

where ϕ is the amplitude of a stream function

$$\psi=\phi(y)e^{i\alpha(x-ct)}, \tag{17}$$

equation (11) gives the Orr–Sommerfeld equation

$$(u-c)(\phi''-\alpha^2\phi)-u''\phi=-\frac{i}{\alpha R_E}(\phi''''-2\alpha^2\phi''+\alpha^4\phi), \tag{18}$$

where the bar over u has been dropped without causing further ambiguity, and the primes now denote differentiation with respect to y.

The boundary conditions (14) become

$$y=0,1:\ \phi,\phi'=0. \tag{19}$$

The characteristic–value relation for this problem then takes the form

$$F(\alpha,c,R_E)=0.$$

In the usual temporal stability problem, in which one considers the growth of a disturbance in time, one takes α and R_E to be real and given. The characteristic–value relation above then defines a discrete set of characteristic values $c_j,(j=1,2,\ldots)$. If one writes

$$c=c_r(\alpha,R_E)+ic_i(\alpha,R_E),$$

then the curves of neutral stability are given by $c_i(\alpha,R_E)=0$.

The Inviscid Solutions

In the inviscid limit, (18) and (19) become

$$(u-c)(D^2-\alpha^2)\phi-D^2u\cdot\phi=0, \tag{20}$$

$$y=0,1:\quad \phi=0, \tag{21}$$

where u is now an arbitrary function of y.

Note that, in the inviscid limit, the order of the equation for ϕ has dropped by two, so one needs to drop the boundary condition of no–slip at the walls.

Next, note that unless

$$(u'')_{u=c}=0$$

the point $y=y_c$, where $u=c$, in the complex y–plane is a regular singularity of equation (20). Otherwise, the inviscid system (20) and (21) would have a well–defined characteristic–value problem. The singular nature of equation (20) is also one of the chief difficulty in constructing uniformly valid asymptotic solutions to equation (18). Besides, if $c_i=0$ or $c_i<0$, it turns out that a regular solution of equation (20) satisfying the boundary conditions (21) does not exist if $0<y_c<1$.

Corresponding to $\alpha=0$, equation (20) has two solutions:

$$\left.\begin{aligned}\phi_{10}&=u-c,\\ \phi_{20}&=(u-c)\int_0^y\frac{dy}{(u-c)^2}.\end{aligned}\right\}. \tag{22}$$

Seeking solutions to equation (20), then, in ascending powers of α^2,

$$\left.\begin{aligned}\phi_1 &= \phi_{10} + \alpha^2\phi_{11} + \cdots,\\ \phi_2 &= \phi_{20} + \alpha^2\phi_{21} + \cdots,\end{aligned}\right\} \tag{23}$$

and noting that equation (20) can be written as

$$\left[\left\{\frac{\phi_{n1}}{u-c}\right\}'(u-c)^2\right]' = (u-c)\phi_{n0}, \qquad n = 1,2,$$

one obtains

$$\phi_{n_1} = (u-c)\int_0^y \frac{dy}{(u-c)^2}\int_0^y (u-c)\phi_{n_0}\,dy, \qquad n = 1,2. \tag{24}$$

Now, in order that ϕ_1, ϕ_2 may be valid approximations to the regular solution of equation (18) all along the path of integration between the point $y = 0$ and $y = y$ on the real axis, that path must lie wholly in a region in which the asymptotic expansions of the regular solutions for large values of R_E are valid. But, within the framework of the inviscid problem alone, it is not obvious in the normal-mode approach how should one negotiate the point $y = y_c$, particularly when c is real.

An efficient way to resolve this difficulty is to pose the problem of stability as an initial-value problem. (Another advantage of the latter approach is the revelation that the singularity at $u = c$ leads to a continuous spectrum of characteristic values that are in addition to the discrete spectrum of characteristic values, which may be real or complex.) Consideration of the initial-value problem (see below) or the viscous problem (see below) shows that the path of integration from $y = 0$ to y is continued around the critical point $y = y_c$ (when c is real) from below the real axis in the complex y-plane, when $u_c' > 0$, and vice versa.

Next, let us obtain two linearly independent solutions in the neighborhood of the point $y = y_c$. First, write $(u-c)$ as a Taylor-series expansion around the point $y = y_c$,

$$u - c = u_c' \cdot \eta + \frac{u_c''}{2!}\eta^2 + \cdots, \tag{25}$$

where

$$\eta \equiv y - y_c$$

so that equation (20) becomes

$$\eta\phi'' - \left(\frac{u_c''}{u_c'} + \alpha^2\eta\right)\phi = 0. \tag{26}$$

Since $\eta = 0$ is a regular singular point of equation (26), seek a solution of equation (26) of the form (Frobenius' method)

$$\phi_1 = \eta^m \sum_{n=0}^{\infty} a_n \eta^n, \qquad \eta > 0. \tag{27}$$

By substituting (27), equation (26) gives

$$\sum_{n=-1}^{\infty} a_{n+1}(m+n)(m+n+1)\eta^{m+n} - \frac{u_c''}{u_c'} \sum_{n=0}^{\infty} a_n \eta^{m+n} - \alpha^2 \sum_{n=1}^{\infty} a_{n-1}\eta^{m+n} = 0,$$

from which

$$[a_0(m-1)m]\eta^{m-1} + \left[a_1(m+1)m - \frac{u_c''}{u_c'} a_0\right]\eta^m + \sum_{n=1}^{\infty}\left[a_{n+1}(m+n)(m+n+1) - \frac{u_c''}{u_c'}a_n - \alpha^2 a_{n-1}\right]\eta^{m+n} = 0. \tag{28}$$

Equating the coefficient of each power of η to zero, one obtains from (28), first, the indicial equation

$$a_0(m-1)m = 0, \tag{29}$$

from which, since $a_0 \neq 0$,

$$m = 1 \text{ or } 0. \tag{30}$$

Next, one obtains from (28)

$$a_1 = \frac{a_0}{2}\frac{u_c''}{u_c'}, \tag{31}$$

so that

$$\phi_1(\eta) = a_0\left[\eta + \frac{1}{2}\frac{u_c''}{u_c'}\eta^2 + \cdots\right]. \tag{32}$$

Now, note that since the two roots of the indicial equation (29) differ by an integer, the other linearly independent solution is given by

$$\phi_2(\eta) = a\phi_1(\eta)\ln\eta + \eta^0\left[\sum_{n=0}^{\infty} b_n \eta^m\right]. \tag{33}$$

By substituting (33), equation (26) gives

$$\eta\left[a\left\{a_0\frac{u_c''}{u_c'}+\cdots\right\}\ln\eta+2a\,a_0\left\{1+\frac{u_c''}{u_c'}\eta+\cdots\right\}\frac{1}{\eta}\right.$$

$$-a\,a_0\left\{\eta+\frac{1}{2}\frac{u_c''}{u_c'}\eta^2+\cdots\right\}\frac{1}{\eta^2}$$

$$\left.+\sum_{n=0}^{\infty}b_n n(n-1)\eta^{n-2}\right]-a\,a_0\frac{u_c''}{u_c'}\left\{\eta+\frac{1}{2}\frac{u_c''}{u_c'}\eta^2+\cdots\right\}$$

$$-\frac{u_c''}{u_c'}\sum_{n=0}^{\infty}b_n\eta^n-\alpha^2\sum_{n=0}^{\infty}b_n\eta^{n+1}=0. \tag{34}$$

Equating the coefficient of the term η^0 to zero, one obtains

$$-\frac{u_c''}{u_c'}b_0+a\,a_0=0. \tag{35}$$

By using (35), (33) may be rewritten as

$$\phi_2(\eta)=\left(\frac{u_c''}{u_c'}\ln\eta\right)\phi_1(\eta)+\left[1+\sum_{n=1}^{\infty}b_n\eta^n\right]. \tag{36}$$

Note that because of the singular nature of $\phi_2(\eta)$ at least in the neighborhood of y_c (where it is discontinuous and multivalued), it cannot be a uniformly valid asymptotic approximation to any solution of equation (18). Further, the main problem here is to decide the proper branch to be taken in connection with the logarithmic singularity at y_c. This reduces to the determination of the domain of the complex y–plane (excluding the neighborhood of y_c) in which (36) is asymptotic to a solution of equation (18). If one assumes the neutral modes as the limit of unstable modes, then one has the following analytical continuation for $\ln\eta$:

$$\ln\eta\sim\begin{cases}\ln\eta, & \eta>0,\\ \ln|\eta|-i\pi, & \eta<0.\end{cases}$$

The Initial–Value Problem: Case–Dikii Theory

In the normal–mode approach, each disturbance is resolved into dynamically independent components and each mode of perturbation is assumed to be of the form $e^{i\alpha(x-ct)}$ times an amplitude function of y. One then searches for those values of c for which the linearized equations of the flow with appropriate boundary conditions possess nontrivial solutions. If there are admissible values of c with $\mathrm{Im}(c)>0$, the perturbed basic flow is said to be unstable. Otherwise, it is stable.

One may seek to justify the normal-mode procedure by following the subsequent time evolution of a small perturbation, introduced, say at $t=0$, through a normal-mode expansion (assuming that the normal modes are complete). If any of the normal modes have $\mathrm{Im}(c)>0$, the perturbation would grow, and one may then claim instability in the physical sense. But this also indicates that the problem of hydrodynamic stability is really an initial-value problem and should be, strictly speaking, posed as such. In particular, one really wants to know whether an initial perturbation grows in time. In most problems the initial-value-problem approach gives results that complement those due to the normal-mode approach. It turns out, for instance, that in an initial-value-problem analysis, one cannot miss the modes associated with a continuous spectrum of characteristic values unlike that in a normal-mode analysis. But, a notable merit of the initial-value-problem approach is its ability to resolve some of the difficulties that arise (as we saw previously) in the course of a normal-mode analysis, without having to go outside the inviscid model for a fluid.

Such considerations are not peculiar to fluid dynamics. A classical example in other fields is that of longitudinal plasma oscillations in plasma physics. The ambiguities that arise in a straightforward Fourier-transform approach are resolvable readily when one poses the issue as an initial-value problem, as Landau did.

The initial-value problem corresponding to (20) and (21) is

$$\left(u-\frac{i}{\alpha}\frac{\partial}{\partial t}\right)\left(\frac{\partial^2}{\partial y^2}-\alpha^2\right)\phi-u''\phi=0 \tag{37}$$

with the boundary conditions

$$y=0,1: \quad \phi=0 \tag{21}$$

and the initial conditions, say,

$$t=0: \quad \phi=\phi_0. \tag{38}$$

Upon Laplace transforming, according to

$$\bar{\phi}(y)=\int_0^\infty e^{-st}\phi(y,t)\,dt,$$

(37), (38), and (21) give

$$\left(u-\frac{is}{\alpha}\right)\left(\frac{d^2}{dy^2}-\alpha^2\right)\bar{\phi}-u''\bar{\phi}=g(y), \tag{39}$$

where

$$g(y)\equiv-\frac{i}{\alpha}\left(\phi_0''-\alpha^2\phi_0\right).$$

One may construct an explicit solution to (39), using the Green-function method:

$$\bar{\phi}(y) = \int_0^y \frac{\bar{\psi}_1(y)\bar{\psi}_2(\xi)}{\left[u(\xi) - \frac{is}{\alpha}\right] W(\bar{\psi}_1, \bar{\psi}_2)} g(\xi)\, d\xi$$

$$+ \int_y^1 \frac{\bar{\psi}_1(\xi)\bar{\psi}_2(y)}{\left[u(\xi) - \frac{is}{\alpha}\right] W(\bar{\psi}_1, \bar{\psi}_2)} g(\xi)\, d\xi, \tag{40}$$

where

$$\left.\begin{aligned} &\left[\left(u - \frac{is}{\alpha}\right)\left(\frac{d^2}{dy^2} - \alpha^2\right) - u''\right]\bar{\psi}_{1,2} = 0, \\ &\bar{\psi}_1(0) = 0, \qquad \bar{\psi}_2(1) = 0, \\ &W(\bar{\psi}_1, \bar{\psi}_2) \equiv \bar{\psi}_1(y)\bar{\psi}_2'(y) - \bar{\psi}_1'(y)\bar{\psi}_2(y). \end{aligned}\right\}$$

One may construct $\bar{\psi}_1, \bar{\psi}_2$ from the two linearly independent solutions $\bar{\phi}_1, \bar{\phi}_2$ as follows:

$$\left.\begin{aligned} \bar{\psi}_1 &= \bar{\phi}_1(y)\bar{\phi}_2(0) - \bar{\phi}_1(0)\bar{\phi}_2(y), \\ \bar{\psi}_2 &= \bar{\phi}_1(y)\bar{\phi}_2(1) - \bar{\phi}_1(1)\bar{\phi}_2(y). \end{aligned}\right\}$$

Thus,

$$W(\bar{\psi}_1, \bar{\psi}_2) = -W(\bar{\phi}_1, \bar{\phi}_2) \cdot \Delta,$$

where

$$\Delta \equiv \begin{vmatrix} \bar{\phi}_1(0) & \bar{\phi}_2(0) \\ \bar{\phi}_1(1) & \bar{\phi}_2(1) \end{vmatrix}.$$

The solution to (37), (38), and (21) is, then, given on inversion,

$$\phi(y,t) = \frac{1}{2\pi i} \int_{-i\infty+\delta}^{i\infty+\delta} \bar{\phi}(y) e^{st}\, ds. \tag{41}$$

The path of integration in (41) corresponds to the Bromwich contour, which lies to the right of all the singularities of $\bar{\phi}(y)$. In the absence of singularities other than the one at $u = is/\alpha$ on the imaginary axis, one may push the path of integration along the imaginary axis $(\delta \Rightarrow 0)$ and continue around the pole at $u = is/\alpha$ from the right, if $u_c' > 0$, and vice versa.

In the normal-mode formulation, $s \Rightarrow -i\alpha c$, this would imply that the path of integration is continued around the critical point $y = y_c$ (when c is real) from

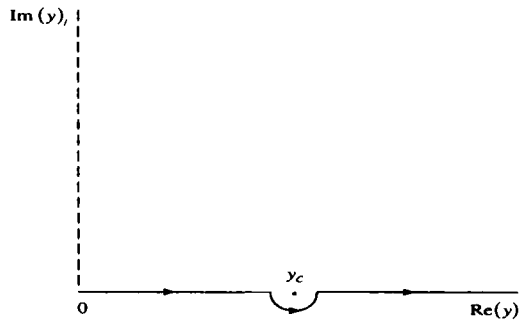

Figure 5.11. Indentation of contour of integration at $y = y_c$.

below the real axis in the complex y–plane when $u_c' > 0$, and vice versa (see Figure 5.11).

Other poles of $\bar{\phi}(y)$ arise at

$$\overline{W}(\overline{\psi}_1, \overline{\psi}_2) = 0 \quad \text{or} \quad \Delta = 0 \quad \text{for} \quad \text{Re}(s) > 0,$$

which is simply the characteristic–value relation for the discrete spectrum of normal modes with $\text{Im}(c) > 0$.

Thus, one obtains from (41)

$$\phi(y,t) = \frac{1}{2\pi i} \int_{-i\infty+\delta}^{i\infty+\delta} \bar{\phi}(y) e^{st} ds + \sum_{\substack{\text{discrete} \\ \text{spectrum}}} \left(\text{exponentials growing like } e^{\alpha[\text{Im}(c)]t}\right). \tag{42}$$

Consider the asymptotic behavior of the first term on the right–hand side in (42). The integral picks up contributions from the poles at $u = is/\alpha = c$. Recall, from (32) and (36), that ϕ_1 and ϕ_2 in the neighborhood of the singular point $y = y_c$ are given by

$$\left.\begin{aligned} \phi_1(y) &= (y - y_c) + \frac{1}{2}\left(\frac{u_c''}{u_c'}\right)(y - y_c)^2 + \cdots, \\ \phi_2(y) &= \left[\frac{u_c''}{u_c'} \cdot \ln(y - y_c)\right] \phi_1(y) + \left[1 + \sum_{n=1}^{\infty} b_n \cdot (y - y_c)^n\right]. \end{aligned}\right\} \tag{43}$$

Thus, the contributions to the integral come from a simple pole at $u = c$ and from the logarithmic term in ϕ_2. Upon inversion, this simple pole produces a simple exponential $e^{i\alpha ct}$ (c real), while the logarithm produces a term behaving like $1/t$. Therefore, for large t, the dominant contribution to the solution will come from the discrete spectrum, if there is one, and from the term growing like

$e^{\alpha[\mathrm{Im}(c)]t}$ for the largest value of $\alpha[\mathrm{Im}(c)]$, with $\mathrm{Im}(c) > 0$. This means that the continuous spectrum does not correspond to instability, and the discrete spectrum alone is associated with instability. Thus, in seeking a criterion for instability, one may use the method of normal modes and ignore the continuos spectrum.

Example 1: As an example of the initial–value problem approach, consider a plane Couette flow between infinite parallel plates at $y = 0$ and 1, with

$$u(y) = y. \tag{44}$$

(1) *The Normal Mode Approach*: For the present case, one has in the normal–mode approach

$$\phi'' - \alpha^2 \phi = 0 \tag{45}$$

$$y = 0,1: \quad \phi = 0. \tag{21}$$

The solution is

$$\phi \equiv 0. \tag{46}$$

This does not mean, however, that an inviscid plane Couette flow has no nontrivial solutions. In going from equation (20) to equation (45) we have eliminated the modes corresponding to a continuous spectrum of characteristic values. These can be recovered by posing an initial–value problem.

(2) *The Initial–Value Problem Approach*: Fourier transforming in x, and Laplace transforming in t, as

$$\bar{\phi}(\alpha, y, s) = \int_0^\infty e^{-st} dt \int_{-\infty}^{\infty} e^{-i\alpha x} \psi(x, y, t) dx, \tag{47}$$

one obtains from (45) and (21)

$$\bar{\phi}'' - \alpha^2 \bar{\phi} = \frac{\phi_0'' - \alpha^2 \phi_0}{s + i\alpha y}, \tag{48}$$

$$y = 0,1: \quad \phi = 0, \tag{21}$$

where

$$t = 0: \quad \phi = \phi_0. \tag{38}$$

Upon inverting the Laplace transform, equation (48) gives

$$\phi'' - \alpha^2 \phi = e^{-i\alpha y t} \left(\phi_0'' - \alpha^2 \phi_0 \right). \tag{49}$$

Since there are no nonzero ϕ_0, such that

$$\left.\begin{aligned} &\phi_0'' - \alpha^2 \phi_0 = 0, \\ &y = 0,1: \quad \phi_0 = 0, \end{aligned}\right\} \tag{50}$$

the right-hand side in equation (49) cannot be identically zero. What is giving us relief now is exactly what caused us dismay in the normal-mode approach!

In order to solve equation (49) with the boundary conditions(21), let us use the Green-function method; let

$$\left.\begin{aligned} &\left(\frac{\partial^2}{\partial y^2}-\alpha^2\right)G(y,\tilde{y})=\delta(y-\tilde{y}),\\ &y=0,1:\quad G(y,\tilde{y})=0,\\ &y=\tilde{y}:\quad [G]=0,\quad \left[\frac{\partial G}{\partial y}\right]=1, \end{aligned}\right\} \tag{51}$$

where the rectangular brackets denote the jump of their contents at $y=\tilde{y}$. Thus,

$$G(y,\tilde{y})=\begin{cases} -\dfrac{\sin h\alpha\tilde{y}\cdot\sin h\alpha(1-y)}{\alpha\sin h\alpha}, & \tilde{y}<y,\\ -\dfrac{\sin h\alpha y\cdot\sin h\alpha(1-\tilde{y})}{\alpha\sin h\alpha}, & \tilde{y}>y. \end{cases} \tag{52}$$

Then

$$\phi(\alpha,y,t)=\int_0^1 G(y,\tilde{y})e^{-i\alpha\tilde{y}t}\left(\frac{d^2\phi_0}{d\tilde{y}^2}-\alpha^2\phi_0\right)d\tilde{y}. \tag{53}$$

Consider the case wherein

$$\frac{d^2\phi_0}{dy^2}-\alpha^2\phi_0=\delta(y-y_0). \tag{54}$$

Since the vorticity is given by

$$\zeta=-\frac{i}{\alpha}\left(\frac{d^2\phi}{dy^2}-\alpha^2\phi\right), \tag{55}$$

(54) corresponds to introduction of a concentrated vorticity at $y=y_0$ at $t=0$. When we use (54), (53) gives

$$\phi(\alpha,y,t)=\begin{cases} -\dfrac{\sin h\alpha y_0\cdot\sin h\alpha(1-y)}{\alpha\sin h\alpha}e^{-i\alpha y_0 t}, & y_0<y,\\ -\dfrac{\sin h\alpha y\cdot\sin h\alpha(1-y_0)}{\alpha\sin h\alpha}e^{-i\alpha y_0 t}, & y_0>y. \end{cases} \tag{56}$$

Upon inverting the Fourier transform, one obtains

$$\psi(x,y,t)=\frac{1}{2\pi}\int_{-\infty}^{\infty}e^{i\alpha x}\phi(\alpha,y,t)\,d\alpha. \tag{57}$$

Closing the contour of integration along the real axis by an infinite semicircle in the lower half plane, the contributions come from the poles at

$$\alpha = -in\pi, \qquad n = 1,2,3,....$$

Thus, one obtains from (56) and (57)

$$\psi(x,y,t) = \begin{cases} \sum_{n=1}^{\infty} \dfrac{\sin n\pi y_0 \cdot \sin n\pi(1-y)}{n\pi} e^{n\pi(x-y_0 t)}, & y_0 < y, \\ \sum_{n=1}^{\infty} \dfrac{\sin n\pi y \cdot \sin n\pi(1-y_0)}{n\pi} e^{n\pi(x-y_0 t)}, & y_0 > y. \end{cases} \tag{58}$$

Since y_0 can take any value between 0 and 1, (58) represents a set of continuum modes. Note that as $t \Rightarrow \infty$, these continuum modes decay exponentially and not as a power of t.

However, the above continuum modes are not normal modes (associated with a discrete spectrum of characteristic values). And it should be noted that whereas a well-behaved initial perturbation will decay according to a power law, special singular solutions, like the one above, can behave differently.

Let us reconsider what has happened. Corresponding to

$$(y-c)\left(\frac{d^2\phi}{dy^2} - \alpha^2\phi\right) = 0, \tag{59}$$

two classes of solutions occur.

(1) Discrete solutions, which satisfy

$$\left.\begin{aligned} &\frac{d^2\phi}{dy^2} - \alpha^2\phi = 0 \\ &y = 0,1 : \phi = 0 \end{aligned}\right\}. \tag{60}$$

This class is empty for a plane Couette flow.

(2) Continuum solutions, which satisfy

$$\frac{d^2\phi}{dy^2} - \alpha^2\phi = \delta(y-c),$$

$$y = 0,1 : \phi = 0, \tag{61}$$

from which

$$\phi = G(y,c) \tag{62}$$

with a continuum spectrum of characteristic values c, running between 0 and 1. The normal-mode approach recognizes only the first possibility and ignores the second possibility and therefore produces only a trivial result for a plane Couette flow.

Inviscid Stability Theory

Discontinuities in the Mean Flow

Note that for the basic flow we have

$$\mu \frac{d^2u}{dy^2} = \frac{dp}{dx},$$

where dp/dx = constant. Thus, the class of strictly parallel flows is rather limited since u can at most be quadratic in y. However, for an inviscid fluid, $u(y)$ can be an arbitrary function of y and even discontinuities are admissible. Thus, if u or u' is discontinuous at y_0, say, then the pressure must be continuous at the material interface with mean position at $y = y_0$. Therefore, noting that

$$(u-c)\phi'' - u''\phi = \{(u-c)\phi' - u'\phi\}' = \{p\}',$$

one has

$$[(u-c)\phi' - u'\phi] = 0 \tag{63}$$

at $y = y_0$, where the square brackets denote the jump of their contents at such a discontinuity. Also, the normal velocity of the fluid must be continuous at the material interface. Let this interface be represented by

$$y = y_0 + \xi(x,t), \tag{64}$$

where

$$\xi(x,t) \sim e^{i\alpha(x-ct)}.$$

Then, one has

$$v' = \frac{D\xi}{dt} = \frac{\partial \xi}{\partial t} + u\frac{\partial \xi}{\partial x} = i\alpha(u-c)\xi. \tag{65}$$

Noting $v' = \alpha\varphi$, one obtains

$$\left[\frac{\phi}{u-c}\right] = 0 \tag{66}$$

at $y = y_0$.

Explicit solutions of the characteristic–value problem of (20), (21) are difficult to find in practice for smoothly varying functions $u(y)$. However, when $u(y)$ is a piecewise linear function, the situation is tractable, and one can then join up such solutions by using conditions (63) and (66). As an illustration, consider the Kelvin–Helmholtz instability problem of two uniform fluids in relative horizontal motion separated by a horizontal boundary.

Example 2: Let two uniform fluids of velocities U_1, U_2 be separated by a horizontal boundary at $y = 0$. One has

$$y \gtrless 0 : \phi_{1,2}'' - \alpha^2\phi_{1,2} = 0, \tag{67}$$

from which, noting that

$$y \Rightarrow \pm\infty: \quad \phi_{1,2} \Rightarrow 0$$

and using (66), one obtains

$$\left.\begin{aligned} y>0: \quad & \phi_1 = A(U_1 - c)e^{-\alpha y}, \\ y<0: \quad & \phi_2 = A(U_2 - c)e^{\alpha y}. \end{aligned}\right\} \tag{68}$$

When one uses (68), (63) gives the dispersion relation

$$(U_1 - c)^2 + (U_2 - c)^2 = 0, \tag{69a}$$

from which

$$-\alpha c = \frac{1}{2}(U_1 + U_2) \pm \frac{i\alpha}{2}|U_1 - U_2|, \tag{69b}$$

so that such an interface is always unstable.

It is possible to effect some inhibition of the instability of such an interface by introducing a vorticity appropriately in the two streams. Let us introduce a constant vorticity ω (along the z–direction) in the two streams. The velocity distribution in the two streams in the steady state is, then, given by

$$y \gtrless 0: \quad u_{1,2} = U_{1,2}\left[1 - \frac{\omega y}{U_{1,2}}\right]. \tag{70}$$

When one uses (68) and (70), (63) gives the dispersion relation

$$(U_1 - c)^2 + (U_2 - c)^2 - \omega\alpha(U_1 - U_2) = 0, \tag{71a}$$

from which

$$-\alpha c = \frac{1}{2}(U_1 + U_2) \pm \frac{1}{2}\left[\frac{2\omega}{\alpha}(U_1 - U_2) - (U_1 - U_2)^2\right]^{1/2}, \tag{71b}$$

which shows that if the ambient shear is opposite in sign to that of the interfacial shear, it is possible to inhibit the instability of such an interface. In order to understand this result physically, let us recall that the instability of an interface between two streams is caused by the relative motion of the fluids tangential to the interface – in other words, an interfacial shear. One may then expect that any agent, such as an ambient shear, that opposes the interfacial shear, effectively, reduces the relative motion of the fluids at the interface, and hence, would inhibit the instability of the latter.

Odd and Even Solutions

Next, the solutions for the disturbances exhibit certain symmetries when the basic flow is symmetric, i.e., say the flow domain is transformed from $(0,1)$ to $(-1,1)$, and $u(y)$ is an even function. In that case, if $\phi(y)$ is a characteristic function for a given α, it follows that the even part

$$\phi_e = \frac{1}{2}[\phi(y) + \phi(-y)] \tag{72}$$

and the odd part

$$\phi_0 = \frac{1}{2}\left[\phi(y) - \phi(-y)\right] \tag{73}$$

of ϕ are also characteristic functions for the same c, α. It can be shown further that either ϕ_0 or ϕ_e is identically zero. In order to see this, multiply equation (1) for ϕ_e by ϕ_0 and subtract ϕ_e times the corresponding equation for ϕ_0. Then, one obtains

$$\phi_e \phi_0'' - \phi_0 \phi_e'' = 0 \tag{74}$$

where $u \neq c$. Therefore,

$$\phi_e \phi_0' - \phi_0 \phi_e' = \text{const.} = 0. \tag{75}$$

Thus, in general, ϕ_0 and ϕ_e are linearly dependent, which is possible only if one of them is identically zero. Thus, it follows that a characteristic function is either odd or even, except when c is real.

In fact, both even and odd characteristic functions can be found for the same basic symmetric flow, but they have different characteristic values of c for each α. The oddness and evenness of ϕ allows one to reduce the effective field of flow to the half domain, $0 \leq y \leq 1$, applying the symmetry condition $\phi' = 0$ (or $\phi = 0$) at $y = 0$ and the original boundary condition $\phi = 0$ at $y = 1$.

Next, suppose that the basic flow profile is antisymmetric, with the flow domain $(0,1) \Rightarrow (-1,1)$ and odd $u(y)$. Then, for each characteristic function ϕ with a characteristic value c, there is a characteristic function $\phi^*(-y)$ with a characteristic value $c^* = -c_r + ic_i$ for the same α. When the characteristic solution is unique, the Hermitian symmetry implies that $c_r = 0$, as we saw in Section 5.5, and $\phi^*(-y) = \phi(y)$. Otherwise, there may be a pair of characteristic solutions with phase velocities $\pm c_r(\alpha)$ and the same $c_i(\alpha)$, with one function being the Hermitian conjugate of the other.

Self-Excited and Damped Disturbances

It would appear that, for the inviscid problem (20) and (21), it is meaningless to distinguish between self-excited and damped disturbances, because for each characteristic function with characteristic value c, for a given α, there is another complex conjugate characteristic function ϕ^* with characteristic value $c^* = c_r - ic_i$ for the same α. (This is evident by taking the complex conjugate of (20) and (21).) Thus to each amplified wave there would be a damped wave and vice versa, which merely signifies the time symmetry of the problem, comprising periodic motion of inviscid fluid with steady boundaries. However, this is not correct since the inviscid equations have meaning only as the limiting case of the complete viscous equations, and the latter are not invariant under complex conjugation unlike the inviscid problem.

Local and Global Necessary Conditions for the Existence of Non-neutral and Neutral Modes

THEOREM: If the flow possesses a non-neutral mode of disturbance with a finite wavelength, the mean velocity profile has an inflection point at some point $y = y_s$, where $0 \le y \le 1$, i.e., it satisfies a local necessary condition

$$(u'')_{y=y_s} = 0.$$

Furthermore, in the case of a neutral mode, one must have $u(y_s) = c$, $c = c_r$.

PROOF: Multiply equation (20) by ϕ^*, the complex conjugate of ϕ, and integrate from 0 to 1; then, using (21), one obtains

$$-\int_0^1 \left[|\phi'|^2 + \alpha^2 |\phi|^2 \right] dy = \int_0^1 \frac{u''}{u-c} |\phi|^2 dy. \tag{76}$$

The imaginary part of equation (76) gives

$$c_i \int_0^1 \frac{u''}{|u-c|^2} |\phi|^2 dy = 0. \tag{77}$$

If $c_i \neq 0$, it follows that u'' must change sign at one or more points in the flow field. Assuming that u'' is continuous for $0 \le y \le 1$, there must be at least one point in the interval $(0,1)$, where one has

$$(u'')_{y=y_s} = 0. \tag{78}$$

Next, in order to show, in the case of a neutral mode, that one must have $u(y_s) = c$, $c = c_r$, multiply equation (20), written in the form

$$\phi'' - \left[\frac{u''}{u-c} - \alpha^2 \right] \phi = 0, \tag{79}$$

by ϕ^* and subtract from the resulting equation its complex conjugate, and then there follows

$$\frac{d}{dy}\left(\phi'\phi^* - \phi^{*\prime}\phi \right) - (c - c^*)\left(\frac{u''}{|u-c|^2} \right) |\phi|^2 = 0. \tag{80}$$

When we introduce the Wronskian,

$$W \equiv \frac{i}{2}\left(\phi\phi^{*\prime} - \phi'\phi^* \right), \tag{81}$$

equation (80) gives

$$\frac{dW}{dy} - c_i \left(\frac{u''}{|u-c|^2} \right) |\phi|^2 = 0. \tag{82}$$

If we let $c_i \Rightarrow 0$ in equation (82), we obtain results corresponding to neutral disturbances. Thus,

$$W = \text{const.} \tag{83}$$

except possibly at the critical point y_c (where $u = c$, $c = c_r$), which may now lie in the real interval $(0,1)$. If it does (we shall soon show that it must), W has a discontinuity at the point. Integrate equation (82) from y_c^- to y_c^+, then

$$W\left(y_c^+\right) - W\left(y_c^-\right) = \int_{u_c^-}^{u_c^+} \frac{u'' \cdot |\phi|^2 c_i du}{u'\left\{\left(u - c_r\right)^2 + c_i^2\right\}}, \tag{84}$$

where the subscript c refer to the values at the point u_c. Note that this is of the form

$$I\left(x,0^+\right) = \lim_{\substack{y \Rightarrow 0^+ \\ \varepsilon \Rightarrow 0}} \int_{x-\varepsilon}^{x+\varepsilon} \frac{h(\xi)}{y\left[1 + \dfrac{(x-\xi)}{y^2}\right]}\, d\xi. \tag{85a}$$

Let

$$\mu = \frac{x - \xi}{y}$$

so that

$$I\left(x,0^+\right) = h(x) \lim_{\substack{y \Rightarrow 0^+ \\ \varepsilon \Rightarrow 0}} \int_{-\varepsilon/y}^{\varepsilon/y} \frac{d\mu}{1 + \mu^2}$$

or

$$I\left(x,0^+\right) = 2h(x)\left\{\lim_{\substack{y \Rightarrow 0^+ \\ \varepsilon \Rightarrow 0}} \left[\tan^{-1}\frac{\varepsilon}{y}\right]\right\}.$$

Taking the limits $y \Rightarrow 0^+$, $\varepsilon \Rightarrow 0$ in such a way that $\varepsilon/y \Rightarrow \infty$, one finds

$$I\left(x,0^+\right) = \pi h(x). \tag{85b}$$

Thus, as $c_i \Rightarrow 0$, equation (84) gives

$$W\left(y_c^+\right) - W\left(y_c^-\right) = [W]_c = \pi \frac{u_c''}{u_c'} |\phi_c|^2 \tag{86}$$

provided in this limit, $c_i > 0$, and $u_c^+ > u_c^-$. Equation (86) shows that if a neutral mode is to exist, there are two possibilities:

(1) either all the jumps $[W]_c = 0$, i.e., $u'' = 0$ at all points where $u = c$, $c = c_r$; or

(2) several of the jumps $[W]_c$ cancel out, then u'' changes sign at the various points where $u = c$, $c = c_r$.

If the mean flow profiles are monotonic, then, the first possibility prevails. In this case, equation (20) has regular solutions which are physically possible in the absence of viscous effects.

Application of this result to plane Poiseuille flow $u(y) = 1 - y^2$ shows that the latter is globally stable. For plane Couette flow $u(y) = y$, equation (76) shows that $\phi \equiv 0$. Thus, in the inviscid case, plane Poiseuille and Couette flows are stable to linear disturbances.

A Global Necessary Condition: We next deduce a *global* necessary condition for the existence of a non–neutral or neutral mode.

The real part of equation (76) gives

$$\int_0^1 (u - c_r) \frac{u''}{|u - c|^2} |\phi|^2 dy = -\int_0^1 \left[|\phi'|^2 + \alpha^2 |\phi|^2 \right] dy. \tag{87}$$

Adding

$$(c_r - u_s) \int_0^1 \frac{u''}{|u - c|^2} |\phi|^2 dy = 0$$

to the left–hand side of equation (87), one obtains

$$\int_0^1 \frac{u'' \cdot (u - u_s)}{|u - c|^2} |\phi|^2 dy = -\int_0^1 \left[|\phi'|^2 + \alpha^2 |\phi|^2 \right] dy, \tag{88}$$

from which we obtain a *global* necessary condition for the existence of a non–neutral or neutral mode

$$u'' \cdot (u - u_s) < 0 \tag{89}$$

where, for $0 \le y \le 1$,

$$(u'')_{y=y_s} = 0 \tag{90}$$

and

$$u_s = u(y_s).$$

In particular, if $u(y)$ is a monotonic function, and u'' vanishes only once in the flow field, $0 \le y \le 1$, a combined *local* and *global* necessary condition for instability is that

$$u'' \cdot (u - u_s) \le 0 \tag{91}$$

throughout the flow field $0 \le y \le 1$, with equality valid only where $y = y_s$ (Fjortoft's Theorem). Physically, this means that the magnitude of vorticity $|u'|$, at the point of inflection, y_s, must be a maximum.

It is not difficult to find a counterexample to the sufficiency of the above necessary condition for instability involving an inflection point in the mean velocity profile.

Example 3: Consider a mean flow given by (Drazin and Howard)

$$y_1 \le y \le y_2: \quad u = \sin y \tag{92}$$

for which

$$D^2 u = 0 \qquad \text{when } y = y_s = n\pi; \qquad n = 0, \pm 1, \pm 2, \ldots. \tag{93}$$

If there is no value y_s in the interval (y_1, y_2), the flow is certainly stable by the above necessary condition for instability. If there is at least one value, one may suppose $y_s = 0$ without loss of generality, so $y_1 \le 0 \le y_2$. Since $u(y)$ is odd, for each characteristic function $\phi(y)$ with a characteristic value c, there is a characteristic function $\phi(-y)$ with a characteristic value $\tilde{c} = -c_r + ic_i$, for the same α. The uniqueness of the characteristic solution again implies that $c_r = 0$. Thus, one has for the odd solution, from equation (20),

$$D^2\phi + (1 - \alpha^2)\phi = 0, \tag{94}$$

$$y = y_1, y_2: \quad \phi = 0, \tag{21}$$

from which

$$\phi = \sin \frac{n\pi(y - y_1)}{y_2 - y_1} \tag{95}$$

where

$$\alpha = \left[1 - \frac{n^2\pi^2}{(y_2 - y_1)^2}\right]^{1/2} \tag{96}$$

for each positive integer $n < (y_2 - y_1)/\pi$. It then follows that the flow is unstable if $(y_2 - y_1) > \pi$, but stable otherwise, although the point of inflexion lies at $y = 0$ in the field of flow. This problem also illustrates the stabilizing effect of the walls on the flow.

Howard's Semicircle Theorem

We next deduce a Semicircle Theorem for non-neutral disturbances. First construct a function $g(y)$, which is regular in the interval $(0,1)$:

$$g(y) = \frac{\phi(y)}{u(y) - c}. \tag{97}$$

Then, equation (20) becomes

$$\frac{d}{dy}\left[(u-c)^2 g'\right] - \alpha^2 (u-c)^2 g = 0. \tag{98}$$

Multiply equation (97) by g^*, where g^* is the complex conjugate of g, and integrate between $(0,1)$, then

$$\int_0^1 (u-c)^2 \left\{ |g'|^2 + \alpha^2 |g|^2 \right\} dy = 0, \tag{99}$$

where we have transformed the first part by partial integration.

THEOREM: If $c_i \neq 0$, c_r must lie within the range of u.

PROOF: The real and imaginary parts of equation (99) give

$$\int_0^1 \left\{ (u-c_r)^2 - c_i^2 \right\} \left\{ |g'|^2 + \alpha^2 |g|^2 \right\} dy = 0 \tag{100}$$

and

$$c_i \int_0^1 (u-c_r) \left\{ |g'|^2 + \alpha^2 |g|^2 \right\} dy = 0. \tag{101}$$

Equation (101) shows that c_r must lie within the range of u if $c_i \neq 0$.

THEOREM: The complex wave velocity for a self-excited mode lies inside the semicircle in the upper half of the c-plane, which has the range of u for its diameter along the real axis.

PROOF: From equation (101), for $c_i \neq 0$,

$$\int_0^1 u \left\{ |g'|^2 + \alpha^2 |g|^2 \right\} dy = \int_0^1 c_r \left\{ |g'|^2 + \alpha^2 |g|^2 \right\} dy. \tag{102}$$

When one uses equation (102), equation (100) becomes

$$\int_0^1 u^2 \left\{ |g'|^2 + \alpha^2 |g|^2 \right\} dy = \int_0^1 \left(c_r^2 + c_i^2 \right) \left\{ |g'|^2 + \alpha^2 |g|^2 \right\} dy. \tag{103}$$

Using (102) and (103) in the inequality,

$$0 \geq \int_0^1 (u - u_{\min})(u - u_{\max}) \left\{ |g'|^2 + \alpha^2 |g|^2 \right\} dy \tag{104}$$

one obtains

$$\int_0^1 \left\{ |g'|^2 + \alpha^2 |g|^2 \right\} \left[\left(c_r^2 + c_i^2 \right) - \left(u_{\min} + u_{\max} \right) c_r + u_{\min} u_{\max} \right] dy \leq 0, \tag{105}$$

from which we have

$$c_r^2 + c_i^2 - (u_{\min} + u_{\max}) c_r + u_{\min} u_{\max} \le 0$$

or

$$\left[c_r - \frac{1}{2}(u_{\min} + u_{\max}) \right]^2 + c_i^2 \le \frac{1}{2}\left[\frac{1}{2}(u_{\max} - u_{\min}) \right]^2 \tag{106}$$

which shows that the complex wave velocity for a self–excited mode must lie inside the semicircle in the upper half of the complex c–plane, which has the range of u for its diameter along the real axis.

Sufficient Conditions for the Existence of Self–Excited and Neutral Modes

Once the *global* necessary condition in the form

$$-\frac{u''}{u(y) - u(y_s)} \ge 0, \qquad 0 < y < 1$$

holds, we turn to the question of sufficient conditions for the existence of self–excited and neutral modes. Toward this we first exhibit the variational character of the inviscid problem for monotonic symmetrical type of mean flow and then use the Sturm–Liouville Theorem to show that there exists a neutrally stable characteristic solution with $c = c_r = u_s$, and then we construct unstable solutions that are contiguous with the neutral modes, i.e., $c \Rightarrow u_s$, as $c_i \Rightarrow 0^+$.

THEOREM: Regular neutral modes, i.e.,

$$\phi = \phi_s, \qquad \alpha = \alpha_s, \qquad c = c_s = u_s, \tag{107}$$

are possible if the mean flow profiles are monotonic, and if there is satisfied in the flow field

$$(u'')_{y=y_s} = 0.$$

PROOF: First, write equation (20) as

$$\phi'' + K(y)\phi + \lambda\phi = 0, \tag{108}$$

where

$$\lambda \equiv -\alpha^2, \quad K(y) \equiv -\frac{u''}{u - c_s}.$$

Let there be a point $y = y_s$, such that

$$(u'')_{y=y_s} = 0$$

and

$$(u')_{y=y_s} \neq 0.$$

In addition, let $u(y) > 0$ for $0 < y < 1$ and assume that $K(y)$ is a regular function for $0 < y < 1$. Then, equation (108) is a real nonsingular equation which makes up a Sturm–Liouville problem with boundary condition (21). This characteristic-value problem possesses an infinite sequence of characteristic values. In order to show that there is a characteristic value α for which a neutral mode exists with $c = u(y_s)$, where $c = c_r$, we have to identify λ with $-\alpha^2$, i.e., we must show that at least one of the characteristic values of equation (108) is negative.

Multiply equation (108) by ϕ^* and integrate from 0 to 1, and using the boundary conditions (21), one obtains

$$\lambda = \frac{\int_0^1 \left[|\phi'|^2 - K|\phi|^2 \right] dy}{\int_0^1 |\phi|^2 dy}; \tag{109}$$

as we shall presently see, this is a characteristic value problem for the parameter $\lambda = -\alpha^2$ and is associated with the variational principle

$$\delta \int_0^1 \left[|\phi'|^2 - K|\phi|^2 \right] dy = 0$$

subject to

$$\int_0^1 |\phi|^2 dy = \text{const.} \tag{110}$$

We now show that the variational principle associated with equation (108) gives the least characteristic value (109). In particular, if ϕ really satisfies equation (108) as well as the boundary conditions (21), then λ is determined from equation (109) by noting that λ is stationary, if ϕ is given a slight variation $\delta\phi$ satisfying only the boundary conditions (21). If $\delta\lambda$ corresponds to $\delta\phi$, then

$$\delta\lambda = \frac{2I \int_0^1 (\phi' \delta\phi' - K\phi\delta\phi)\, dy - 2J \int_0^1 \phi\delta\phi\, dy}{I^2}, \tag{111}$$

where

$$I \equiv \int_0^1 |\phi|^2 dy, \qquad J \equiv \int_0^1 \left[|\phi'|^2 - K|\phi|^2 \right] dy.$$

Noting

$$\int_0^1 \phi' \delta\phi'\, dy = -\int_0^1 \phi'' \delta\phi\, dy$$

since

$$\delta\phi' = (\delta\phi)',$$

we see that equation (111) becomes

$$-\frac{I}{2}\delta\lambda = \int_0^1 [\phi'' + K\phi + \lambda\phi]\delta\phi\, dy. \tag{112}$$

Equation (112) implies, on using equation (108),

$$\delta\lambda = 0. \tag{113}$$

Conversely, if $\delta\lambda$ vanishes for all variations $\delta\phi$ satisfying the boundary conditions and possessing a derivative which, like ϕ, is square–integrable, then equation (112) shows that the corresponding function ϕ satisfies equation (108). Equation (125) merely shows that the characteristic value λ is stationary; in order to show that λ is a minimum, note that when $c_i \neq 0$, the real part of equation (76) gives

$$-\int_0^1 \left[|\phi'|^2 - \lambda_1|\phi|^2\right] dy = \int_0^1 \frac{(u-c_s)}{|u-c|^2}\, u''|\phi|^2 dy.$$

Thus,

$$\int_0^1 \left[|\phi'|^2 - \lambda_1|\phi|^2\right] dy = \int_0^1 \frac{(u-c_s)^2}{|u-c|^2}\, K|\phi|^2 dy < \int_0^1 K|\phi|^2 dy,$$

from which

$$-\lambda_1 < \frac{\int_0^1 \left[-|\phi'|^2 + K|\phi|^2 dy\right]}{\int_0^1 |\phi|^2 dy}$$

or

$$-\lambda_1 < -\lambda$$

or

$$\lambda < \lambda_1.$$

Thus,

$$\lambda = \min(\lambda_1),$$

where

$$\lambda_1 = \frac{\int_0^1 \left[|\chi'|^2 + \frac{u''}{u-c} |\chi|^2 \right] dy}{\int_0^1 |\chi|^2 dy}, \tag{114}$$

where χ is any function possessing a square–integrable derivative and satisfying the boundary conditions (21).

Replace χ by the test function u, and recalling that $K(y) > 0$, one obtains from (114)

$$I_1 \lambda = \int_0^1 \frac{u'' \cdot u u_s}{u - u_s} dy = -\int_0^1 K u u_s dy < 0, \tag{115}$$

where

$$I_1 \equiv \int_0^1 u^2 dy \neq I,$$

provided that $u(y) > 0$. Therefore, λ is negative, and α real and positive, for which there is a neutrally stable mode.

Next we deduce the existence of a self–excited mode in the neighborhood of the neutral disturbance, i.e., unstable modes whose limit as $c_i \Rightarrow 0^+$ is the neutral mode. If

$$(u'')_{u=c=c_r} = 0 \tag{78}$$

holds somewhere within the flow field, one ensures the existence of neutral disturbances. If the conditions at such a point are denoted by a subscript s, one has a solution $c_s = u$ (where c_s is real).

That the neutral solution has a neighboring self–excited solution will be shown here by considering the dependence of c on $\lambda = -\alpha^2$ in the characteristic value problem of equation (20). Recalling that there is a characteristic function ϕ_s corresponding to the characteristic value $c = c_s$, $-\alpha_s^2 = \lambda_s$, one has

$$\phi_s'' - \frac{u''}{u - c_s} \phi_s + \lambda_s \phi_s = 0. \tag{116}$$

Multiply equation (20) by ϕ_s, multiply equation (116) by ϕ, and subtract, so that

$$\frac{d}{dy}\left[\phi_s \phi' - \phi_s' \phi\right] + (\lambda - \lambda_s)\, \phi \phi_s - \left[\frac{u''}{u-c} - \frac{u''}{u-c_s} \right] \phi \phi_s = 0. \tag{117}$$

Integrating between $(0,1)$, one obtains

$$(\lambda-\lambda_s)\int_0^1 \phi\phi_s dy=\int_0^1\left[\frac{u''}{u-c}-\frac{u''}{u-c_s}\right]\phi\phi_s\,dy,$$

which, in the limit $\lambda \Rightarrow \lambda_s$, $c \Rightarrow c_s$, $\phi \Rightarrow \phi_s$ gives

$$\left(\frac{d\lambda}{dc}\right)_{\alpha=\alpha,\,0}\int_0^1 |\phi_s|^2 dy=\lim_{c\Rightarrow c_s}\int_0^1 \frac{u''}{u-c_s}\cdot\frac{|\phi_s|^2}{u-c}\,dy. \tag{118}$$

The right-hand side of equation (118) is

$$\int_0^1 \frac{|\phi_s|^2}{u-c}\left[-\frac{u''}{u-c_s}\right]dy=\int_0^1 \frac{\left[-\dfrac{u''}{u-c_s}\right](u-c_r)}{|u-c|^2}|\phi_s|^2 dy$$
$$+i\int_0^1 \frac{\left[-\dfrac{u''}{u-c_s}\right]c_i}{|u-c|^2}|\phi_s|^2 dy.$$

The limit of the real part becomes the principal value of the integral

$$\int_0^1 \frac{\left[\dfrac{u''}{u-c_s}\right]}{u-c_s}|\phi_s|^2 dy.$$

The imaginary part tends to the limit

$$\pi\left[-\frac{u''}{u_s'(u-c_s)}\right]|\phi_s|^2>0$$

as $c_i \Rightarrow 0^+$. Equation (118) gives, then, an equation of the form

$$-\frac{d\lambda}{dc}=A+iB, \qquad B>0$$

or

$$-\frac{dc}{d\lambda}=\frac{dc}{d(\alpha^2)}=\frac{A-iB}{A^2+B^2}. \tag{119}$$

If α^2 decreases slightly, equation (119) shows that c_i becomes positive, which proves the existence of a self-excited disturbance in the neighborhood of the neutral disturbance. In other words, when viscosity is neglected, if the flow can execute a small neutral oscillation of finite wavelength, it can also execute self-excited oscillation of longer wavelengths and execute damped oscillation of shorter wavelengths.

Viscous Theory

Because the situations of interest correspond to large values of the Reynolds number, the asymptotic methods of analysis should play an important role in the theory. In the asymptotic theory, the sacrifice of the uniformity of approximation is compensated by greater simplicity.

We shall now construct asymptotic solutions to equation (18) using a WKBJ method. Thus, seek solutions to equation (18) of the form

$$\phi = e^{\int g(y)\,dy} \tag{120}$$

so that equation (18) gives

$$\begin{aligned}(u-c)\left\{\left(g^2+g'\right)-\alpha^2\right\}-u'' = -\frac{i}{\alpha R_E}\left\{g''''+6g^2g'+3g'^2+4gg''+g''''\right.\\ \left.-2\alpha^2\left(g^2+g'\right)+\alpha^4\right\}.\end{aligned} \tag{121}$$

Let us solve equation (121) by expanding $g(y)$ in powers of αR_E, as

$$g(y) = (\alpha R_E)^{1/2} g_0(y) + g_1(y) + (\alpha R_E)^{-1/2} g_2(y) + \cdots, \tag{122}$$

so that equation (121) gives

$$(u-c)g_0^2 = -ig_0^4, \tag{123}$$

$$(u-c)\left(g_0' + 2g_0g_1\right) = -i\left(4g_0^3g_1 + 6g_0^2g_0'\right), \tag{124}$$

etc.,

from which

$$g_0 = \pm\sqrt{i(u-c)}, \tag{125}$$

$$g_1 = -\frac{5}{2}\frac{g_0'}{g_0}, \tag{126}$$

etc.

Thus,

$$\phi(y) = (u-c)^{5/4} e^{\pm\int_0^y \sqrt{i\alpha R_E(u-c)}\,dy}. \tag{127}$$

The domain of validity and the proper branch of the multiple-valued asymptotic solutions (122) can be revealed again by a careful examination of the manner in which the latter represent valid asymptotic approximations to the exact solution of equation (18).

Note that the WKBJ solutions (127) are not valid in a domain of the complex y-plane that contains the critical point $u = c$, nor do they give the boundary values of the solutions sufficiently accurate if $|y - y_c| \sim (\alpha R_E)^{-1/3}$. The point $u = c$ appears in the inviscid solutions as a logarithmic branch point. Here, it

appears as an algebraic point. Again the determination of the correct branch so as to achieve the analytical continuation of the functions across the point $u = c$ should be such that (127) yields a valid asymptotic solution of equation (18) all along the path. This is necessary *a fortiori* if the critical point y_c lies below or on the real axis joining $(0,1)$ where the boundary conditions are to be satisfied. One must therefore take a path from 0 to 1 in the complex y–plane such that the real part of $\int_0^y \sqrt{i\alpha R_E(u-c)}\, dy$ increases monotonically. It turns out that if one takes a path below the critical point y_c, one is then always in a region in the complex y–plane where the above asymptotic solutions are valid (see Figure 5.12).

In order to determine the location of the point y_c as a function of the sign of c_i in the complex y–plane, let us write $y = y_r + iy_i$, and analytically continue the velocity field $u(y)$ in the complex y–plane. Then, $u = u(y)$ will be an analytical function. One has $u(y) \to u(y_r)$ as $y_i \to 0$ and the equation $u(y) = c$ must have a solution, namely, $u(y_{r_c}) = c$. In order to determine y_c, let $y_c = y_{r_c} + iy_i$. Separating the relation

$$u(y_{r_c} + iy_i) = c \tag{128}$$

into real and imaginary parts, one has

$$u(y_{r_c} + iy_i) = u_r + iu_i = c_r + ic_i, \tag{129}$$

from which

$$u_r = c_r, \qquad u_i = c_i. \tag{130}$$

For small y_i, one may write (130) as

$$c_i = u_i(y_{r_c}) + \frac{\partial u_i}{\partial y_i}(y_{r_c}) \cdot y_i. \tag{131}$$

When we use the Cauchy–Riemann conditions

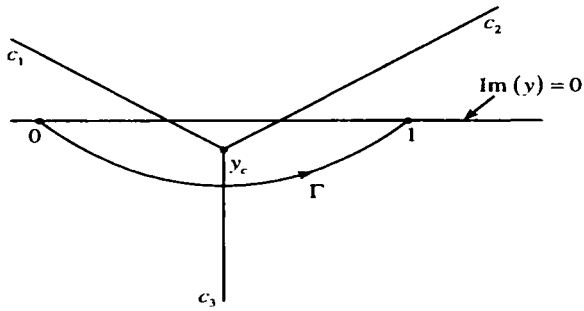

Figure 5.12. Path of integration to ensure validity of the asymptotic solutions.

$$\frac{\partial u_r}{\partial y_r} = \frac{\partial u_i}{\partial y_i}, \tag{132}$$

(131) becomes

$$c_i = u_i\left(y_{r_c}\right) + \frac{\partial u_r}{\partial y_r}\left(y_{r_c}\right) \cdot y_i. \tag{133}$$

Since $u_i \to 0$ as $y_i \to 0$, (133) implies that if $u_c' > 0$ and $c_i > 0$, the point y_c lies above the real axis in the complex y–plane. Likewise, if $u_c' > 0$ and $c_i < 0$, then the point y_c lies below the real axis in the complex y–plane.

Thus, if $c_i > 0$ and $u_c' > 0$, the point y_c lies above the real axis, and the asymptotic solutions (127) are valid all along the real axis of y. If $c_i = 0$, the point y_c lies on the real axis of y where the asymptotic solutions (127) cease to be valid. If $c_i < 0$, the point y_c lies below the real axis of y, and one may use the asymptotic solutions (127) only along the part of the real axis of y and their analytic continuation must be determined by a path circling below the critical point. The two inner viscous layers for damped disturbances, therefore, coalesce into one in the case of neutral disturbances and disappear altogether for self–excited disturbances. Consequently, for the self–excited disturbances, the viscous solutions tend to the corresponding inviscid solutions throughout the part of the real axis of the complex y–plane corresponding to the flow field, as $R_E \Rightarrow \infty$. For the damped disturbances, the viscous solutions do not tend to the corresponding inviscid solutions along the whole of the real axis of the complex y–plane corresponding to the flow field.

Let us now deduce two viscous solutions which are valid in a complex neighborhood of the critical point y_c. First, note that the quantity $1/R_E$ multiplies the highest derivative in equation (18), so that a straightforward expansion in terms of the parameter $1/R_E$ will not be uniformly valid. An alternative method is to choose a small parameter ε related to $\left(\alpha R_E\right)^{-1/3}$ and make a transformation

$$y - y_c = \varepsilon\eta, \qquad \varepsilon = \left(\alpha R_E u_c'\right)^{-1/3}. \tag{134}$$

Expanding $(u - c)$ in powers of $\left(y - y_c\right)$ and putting

$$\phi = \chi_0 + \varepsilon\chi_1 + \varepsilon^2\chi_2 + \cdots, \tag{135}$$

one obtains from equation (18)

$$i\frac{d^4\chi_0}{d\eta^4} + \eta\frac{d^2\chi_0}{d\eta^2} = 0, \tag{136}$$

$$i\frac{d^2\chi_1}{d\eta^4} + \eta\frac{d^2\chi_1}{d\eta^2} = \frac{u_c''}{u_c'}\chi_0 - \frac{1}{2}\frac{u_c''}{u_c'}\eta^2\frac{d^2\chi_0}{d\eta^2}, \tag{137}$$

etc.

The four basic solutions of equation (136) are

$$\chi_0^{(1)} = 1,$$

$$\chi_0^{(2)} = \eta,$$

$$\chi_0^{(3)} = \int_{-\infty}^{\eta} d\eta \int_{-\infty}^{\eta} \eta^{1/2} H_{1/3}^{(1)}\left[\frac{2}{3}(i\eta)^{3/2}\right] d\eta,$$

$$\chi_0^{(4)} = \int_{-\infty}^{\eta} d\eta \int_{-\infty}^{\eta} \eta^{1/2} H_{1/3}^{(2)}\left[\frac{2}{3}(i\eta)^{3/2}\right] d\eta, \tag{138}$$

where $H_{1/3}^{(1)}$ and $H_{1/3}^{(2)}$ denote Hankel functions of order 1/3. The solutions $\chi_0^{(1)}$ and $\chi_0^{(2)}$ correspond to the terms of lowest powers of η in the inviscid solutions ϕ_1 and ϕ_2 of (32) and (36). On the other hand, $\chi_0^{(3)}$ and $\chi_0^{(4)}$ are viscous solutions. By using the asymptotic properties of the Hankel functions, it can be shown that for large values of η, $\chi_0^{(3)}$ tends to zero for large positive η, and $\chi_0^{(4)}$ tends to zero for large negative η. If one assumes that u_c' is positive, then ε is positive, so that η is negative at the wall (assuming the wall to be at $y = 0$) and positive on the other side of y_c. Consequently, $\chi_0^{(3)}$ is the physically realistic solution in representing the boundary layer at the wall.

Thanks to the idea of a composite approximation which is commonly used in connection with the method of matched asymptotic approximations, one may continue the foregoing approximations to form composite approximations which are valid in domains that do not shrink to zero as $\varepsilon \to 0$. The WKBJ solutions are valid provided that $|y - y_c| \gg \varepsilon$. Thus, if $|\varepsilon| \ll |y - y_c|$ and $-7/6\pi <$ Phase $(y - y_c) < 5/6\pi$, then one has from (127)

$$\phi \sim C_2 \left[u_c' \cdot (y - y_c)\right]^{-5/4} \exp\left[-\frac{2}{3}(y - y_c)^{3/2}\left(i\alpha R_E u_c'\right)^{1/2}\right]. \tag{139a}$$

The inner solutions (135) are valid, provided that $|y - y_c| \ll |\varepsilon|^{3/5}$. Thus, if $1 \ll |\eta| \ll |\varepsilon|^{-2/5}$ and $|\text{Phase}(\eta)| < \pi$, $\chi_0^{(3)}$ becomes

$$\chi_0^{(3)}(\eta) \sim \frac{1}{2\sqrt{\pi}}\, \eta^{-5/4} e^{-\frac{2}{3}\eta^{3/2}}. \tag{140}$$

If these limiting forms are both valid in the overlap domain $|\varepsilon| \ll |y - y_c| \ll |\varepsilon|^{3/5}$, with $|\text{Phase}(\eta)| < \pi$, their matching gives

$$C_2 = \frac{1}{2\sqrt{\pi}}\left(\varepsilon u_c'\right)^{5/4}. \tag{139b}$$

Heisenberg Criterion

For boundary-layer type of flows, the boundary conditions are

$$y = 0, \infty: \quad \phi = \phi' = 0. \tag{141}$$

The required solution is given by a linear combination of the solutions $\tilde{\phi}$ of equation (20) and $\hat{\phi}$ of equation (18), and the boundary condition at $y = 0$ leads to the characteristic–value equation

$$\frac{\tilde{\phi}'(0)}{\tilde{\phi}(0)} = \frac{\hat{\phi}'(0)}{\hat{\phi}(0)}. \tag{142}$$

Now, from (127), one has

$$\frac{\hat{\phi}'(y)}{\hat{\phi}(y)} = -\left[i\alpha R_E (u-c)\right]^{1/2} - \frac{5}{4}\frac{u'}{u-c} + \cdots, \tag{143}$$

from which

$$\frac{c}{u_0'}\frac{\hat{\phi}'(0)}{\hat{\phi}(0)} = -Z^{3/2} e^{-i\pi/4} + \frac{5}{4}, \tag{144}$$

where

$$Z = \left(\frac{\alpha R_E c^3}{u_0'^2}\right)^{1/3}, \qquad u'(0) = u_0'.$$

When we write

$$W = \left[1 + \frac{u_0'}{c}\frac{\tilde{\phi}(0)}{\tilde{\phi}'(0)}\right]^{-1}, \tag{145}$$

equation (142) becomes

$$\frac{W-1}{W} = G(Z), \tag{146}$$

where

$$G(Z) \equiv \left(Z^{3/2} e^{-i\pi/4} - \frac{5}{4}\right)^{-1}$$

or

$$Z^{3/2} = \left[\frac{1}{G(Z)} + \frac{5}{4}\right] e^{i\pi/4}. \tag{147}$$

Also, note that

$$G(Z) = \begin{cases} -\dfrac{4}{5}\left[1 + \dfrac{4}{5} e^{-i\pi/4} Z^{3/2} + \cdots\right], & Z \Rightarrow 0 \\ \dfrac{e^{i\pi/4}}{Z^{3/2}}\left[1 + \dfrac{5}{4}\dfrac{e^{i\pi/4}}{Z^{3/2}} + \cdots\right], & Z \Rightarrow \infty \end{cases}. \tag{148}$$

Some general stability characteristics in a viscous fluid can now be deduced by means of the asymptotic behavior of the above expressions.

The inviscid solutions are (see (36))

$$\tilde{\phi}_2(z)=\begin{cases}1+\ldots+\left[\dfrac{u_c''}{u_c'}\tilde{\phi}_1(z)\right]\left[\ln|z|-i\pi\right], & z<0,\\ 1+\ldots+\left[\dfrac{u_c''}{u_c'}\tilde{\phi}_1(z)\right]\left[\ln z\right], & z>0,\end{cases} \tag{149}$$

where

$$\tilde{\phi}_1(\eta)=\eta+\frac{1}{2}\frac{u_c''}{u_c'}\eta^2+\cdots, \quad \eta=y-y_c. \tag{32}$$

For real values of $c=c_s$, one finds from equation (146)

$$\mathrm{Im}\left[G(\eta)\right]=-\pi\frac{(u'')_{u=c_s}}{c_s}. \tag{150}$$

When we use (150), (147) gives

$$\mathrm{Im}[c]=\left(\frac{u_0'^2}{\alpha_s R_E}\right)^{1/3}\left[\frac{\pi}{c_s}(u'')_{u=c_s}+\frac{5}{4}\right]e^{i\pi/4}. \tag{151}$$

If we restrict ourselves to cases where α and c do not approach zero along the neutral curve as $R_E\Rightarrow\infty$ (i.e., $\alpha=\alpha_s\neq 0$, $c=c_s\neq 0$), one finds from equation (151) that

$$c_i>0$$

or that the disturbance $\alpha=\alpha_s$, neutrally stable $(c=c_s)$ in the inviscid case, is unstable when viscosity comes into the picture. One therefore has the Heisenberg criterion: *If a parallel flow has an inviscid neutral disturbance with* $\alpha=\alpha_s\neq 0$ *and* $c=c_s\neq 0$, *the disturbance* $\alpha=\alpha_s$ *is unstable in the real fluid for sufficiently large values of the Reynolds number (when viscous effects appear).*

Thus, for boundary-layer flows, instability prevails for large Reynolds numbers, no matter whether the inviscid instability criterion

$$(u'')_{u=c}=0$$

is satisfied or not.

General Characteristics of the Neutral-Stability Curve

A brief discussion of the significance of the neutral stability curve (see Figure 5.13) is in order:

1. The region bounded by the two asymptotic branches of the curve signifies instability.

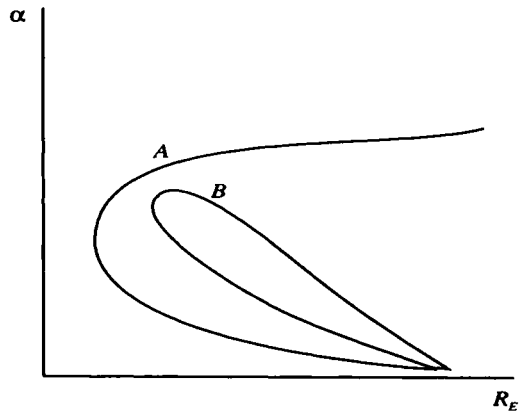

Figure 5.13. Neutral–stability curves for free shear–layer flows (A) and boundary–layer flows (B).

2. For free shear–layer flows, the two branches of the curve approach two different asymptotes $\alpha = 0$ and $\alpha = \alpha_s$, leaving a finite unstable region for $R_E \Rightarrow \infty$. For boundary–layer flows, the two branches approach the same asymptote $\alpha \Rightarrow 0$, so that one has only the disturbance $\alpha \Rightarrow 0$ at $R_E \Rightarrow \infty$. The lowest Reynolds number on each curve is the critical Reynolds number, R_{E_c}.

3. One may conjecture that the neutral stability curve could also correspond to cases of minimum damping with stable regions on both sides of it. In order to clarify this, we have to show that $c_i > 0$ in the neighborhood of the neutral curve. Indeed, if we regard c as a function of the two independent parameters α and $\alpha R_E = R'_E$, we need only show that

$$\frac{\partial c_i}{\partial R'_E} < 0$$

for the upper branch of the neutral curve. Note that this is simply analogous to the viscous stability criterion we have enunciated in the foregoing.

From equation (146), we have

$$G - 1 = -\frac{1}{W}. \tag{152}$$

Regard now α as fixed and consider the variation of R'_E and Z with c. Taking the logarithmic derivatives of both sides of equation (146), one finds

$$\frac{G'}{G-1} = \frac{W'}{W}. \tag{153}$$

Now, the characteristic value equation (153) involves the inviscid solutions only in the combination $\tilde{\phi}'/\tilde{\phi}$, and the latter can be directly found. It is also convenient to determine the asymptotic behavior of the neutral curve. In the case

of boundary-layer type of flows, $\alpha \Rightarrow 0$ along both branches of the neutral curve, as $\alpha R_E \Rightarrow \infty$, and it is then natural to seek an approximation to W that is valid for small values of α.

When we put

$$H = \frac{\bar{\phi}'}{\bar{\phi}}, \tag{154}$$

(20) gives a Riccati equation

$$H' + H^2 = \frac{u''}{u-c} + \alpha^2. \tag{155}$$

Consider the boundary-layer flows for which the velocity profiles are monotonically increasing, and let

$$y \Rightarrow \infty: \quad \frac{\bar{\phi}'}{\bar{\phi}} \Rightarrow -\alpha. \tag{156}$$

Then, from (154), one has

$$y \Rightarrow \infty: \quad H(y) \Rightarrow -\alpha. \tag{157}$$

Seek a solution to equation (155) of the form

$$H(y) = -\alpha + H_2(y) + \cdots. \tag{158}$$

Upon substituting this expression into equation (155), one obtains

$$H_2(y) = e^{-2\alpha y} \int_{\infty}^{y} \frac{u''}{u-c} e^{2\alpha y'} dy'. \tag{159}$$

From equations (145) and (154), one obtains

$$W = \left[1 + \frac{u_0'}{c} \frac{1}{H(0)}\right]^{-1}$$

or

$$W \approx 1 - \frac{u_0'}{c} \frac{1}{H(0)}. \tag{160}$$

Using (160), one obtains from equation (146)

$$G(Z) = 1 - \frac{cH(0)}{u_0'} + \left[\frac{cH(0)}{u_0'}\right]^2 + \cdots \tag{161}$$

Noting that on the upper branch of the neutral curve, $Z \Rightarrow \infty$, and using (148) and (161), one obtains

$$\left(\frac{\partial c}{\partial R_E'}\right)_\alpha = \frac{-\frac{1}{2}\frac{e^{i\pi/4}}{Z^{3/2}}\frac{c}{R_E}}{\left[\frac{u_0'/c}{1+u_0'/c}+\frac{3}{2}\frac{e^{i\pi/4}}{Z^{3/2}}\right]}, \tag{162}$$

from which, for small c_i (i.e., for the neighborhood of the neutral curve), one has

$$\left(\frac{\partial c_i}{\partial R_E'}\right)_\alpha < 0. \tag{163}$$

Note, however, that only for the particular disturbance $\alpha \Rightarrow 0$, for which one is on the lower branch of the neutral curve, a decrease of R_E promotes stability, so that for this particular case, viscosity is in the nature of stabilizing the flow.

Computation of the Neutral Stability Curve

Since equation (18) is of the fourth order, the solution consists of a linear combination of four basic solutions:

$$\phi = C_1\phi_1 + C_2\phi_2 + C_3\phi_3 + C_4\phi_4, \tag{164}$$

where C_1, C_2, C_3, and C_4 are arbitrary constants. The functions ϕ_1 and ϕ_2 are the inviscid solutions, and ϕ_3 and ϕ_4 are the viscous solutions. The viscous effects become important both near the critical point $u = c$ and near a rigid wall. When considering a rigid wall, one of the viscous solutions (ϕ_3) decreases exponentially with distance from the wall and is the one which is physically realistic, while the other (ϕ_4) increases exponentially with distance from the wall.

For plane Poiseuille flow, u is an even function of y, so that the general solution, ϕ, of equation (18) may be split into odd and even solutions. If one considers only the even solution, corresponding to an antisymmetric disturbance, one may focus attention on the half–channel $y = -1$ to $y = 0$. If one ignores the solution which increases exponentially with distance from the wall, one has the following three boundary conditions:

$$\left.\begin{aligned} y = -1: &\quad \phi, \phi' = 0, \\ y = 0: &\quad \phi' = 0. \end{aligned}\right\} \tag{165}$$

For a boundary–layer flow near a flat plate, one may assume that the viscous effects are negligible for the disturbance at the edge of, and outside, the boundary layer. Since the flow velocity u is constant in this region, the two inviscid solutions will be proportional to $e^{\pm\alpha y}$, of which only $e^{-\alpha y}$ is physically realistic. Thus, the three boundary conditions appropriate for boundary–layer flows are

$$\left.\begin{aligned} y = 0: &\quad \phi, \phi' = 0, \\ y \to \infty: &\quad \phi' + \alpha\phi = 0. \end{aligned}\right\} \tag{166}$$

For plane Poiseuille flow, (165) results in the following characteristic–value relation:

$$\frac{\phi_{3w}}{\phi'_{3w}} = \frac{\phi_{1w}\phi'_{2o} - \phi_{2w}\phi'_{1o}}{\phi'_{1w}\phi'_{2o} - \phi'_{2w}\phi'_{1o}}, \tag{167}$$

where the second subscript, w or o, denotes conditions at the wall or at the center of the channel, respectively.

For the boundary–layer flow, (167) results in the following characteristic–value relation:

$$\frac{\phi_{3w}}{\phi'_{3w}} = \frac{\phi_{1w}\Phi_{2\infty} - \phi_{2w}\Phi_{1\infty}}{\phi'_{1w}\Phi_{2\infty} - \phi'_{2w}\Phi_{1\infty}}, \tag{168}$$

where $\Phi_{n\infty} \equiv \phi'_{n\infty} + \alpha\phi_{n\infty}$, and the second subscript, w or ∞, denotes the wall or the edge of the boundary layer, respectively.

The right–hand sides of (167) and (168) can be calculated by using the inviscid solutions. The left–hand sides can be calculated by using $\phi_3 = \chi_0^{(3)}$. If $y = y_1$ denotes the wall ($y_1 = -1$ for plane Poiseuille flow and o for the boundary layer), (167) becomes

$$F(Y) = \frac{1}{y_1 - y_c}\left[\frac{\phi_{1w}\phi'_{2o} - \phi_{2w}\phi'_{1o}}{\phi'_{1w}\phi'_{2o} - \phi'_{2w}\phi'_{1o}}\right] \tag{169}$$

and (168) becomes

$$F(Y) = \frac{1}{y_1 - y_c}\left[\frac{\phi_{1w}\Phi_{2\infty} - \phi_{2w}\Phi_{1\infty}}{\phi'_{1w}\Phi_{2\infty} - \phi'_{2w}\Phi_{1\infty}}\right], \tag{170}$$

where

$$Y \equiv -(\eta)_{\text{wall}} = (\alpha R_E u'_c)^{1/3}(y_c - y_1),$$

$$F(Y) \equiv \frac{-\int_{-\infty}^{-y} d\eta \int_{-\infty}^{\eta} \eta^{1/2} H_{1/3}^{(1)}\left[\frac{2}{3}(i\eta)^{3/2}\right] d\eta}{Y\int_{-\infty}^{y} \eta^{1/2} H_{1/3}^{(1)}\left[\frac{2}{3}(i\eta)^{3/2}\right] d\eta}.$$

The function $F(Y)$ has been tabulated.

The characteristic–value relation, (169) or (170), depends on α, c_r, and R_E. Since it is a complex relation, it may be separated into two real relations. If c_r is eliminated, then one has a relation between α and R_E. The neutral–stability curve is the result of plotting α against R_E (Figure 5.13).

In general, the relation $\alpha = \alpha(R_E)$ must be obtained through computer calculations (Orszag), although (for large Reynolds numbers) several analytical

representations are known in the form of uniform approximations (Lakin et al.) and triple–deck approximations (Hall and Smith).

The linear theory predicts the critical Reynolds number of 5772 for plane Poiseuille flow which is far above the observed value 1000 for typical transition to turbulence.[7] The linear theory prediction for plane Couette flow is even worse because no instability is indicated for the latter.

Nonlinear Theory

The first paper to appear with really definite and coherent predictions about the effects of nonlinearity on instability was that of Landau. Although Landau's work appeared to be conjectural in part, many of the ideas advanced there have later been justified more rigorously (Stuart).

If R_E slightly exceeds R_{E_c}, only a narrow band of wavemember modes around α_c will be amplified, producing a wavepacket consisting of a modulated carrier wave with wavenumber α_c. In the nonlinear theory for $R_E \gtrsim R_{E_c}$, one therefore considers a perturbation of the form $A(t)\,\phi(y)\,e^{i\alpha(x-c_p t)}$ where c_p is real and $\phi(y)$ shows that the same spatial structure as the linear mode; $A(t)$ is found to satisfy an equation of the form

$$\frac{dA}{dt} = \alpha c_i A + kA|A|^2, \tag{171}$$

where αc_i is the growth rate determined by the linear characteristic–value relation. Solving equation (171), one obtains

$$A^2 = \frac{\alpha c_i c\, e^{2\alpha c_i t}}{1 - kc\, e^{2\alpha c_i t}}. \tag{172}$$

Equation (172) shows that:

1. If $k < 0$, the solution $A = 0$ is unstable for $\alpha c_i > 0$ and then A approaches $(-\alpha c_i/k)^{1/2}$ as $t \to \infty$; this new steady–state solution is called a supercritical equilibrium.
2. If $k > 0$ and $\alpha c_i < 0$, then the solution $A = 0$ is stable for $A^2(0) < (-\alpha c_i/k)$ but is unstable for $A^2(0) > (-\alpha c_i/k)$; this instability is called a subcritical instability.

In the case of a supercritical equilibrium $(R_E > R_{E_c})$, the nonlinear effects bring an exponentially growing disturbance to a new equilibrium state (see Figure 5.14a);

[7] Instability of plane Poiseuille flow at transitional Reynolds numbers appears to be explainable in terms of a three-dimensional linear instability of two-dimensional secondary flows (Orszag and Patera).

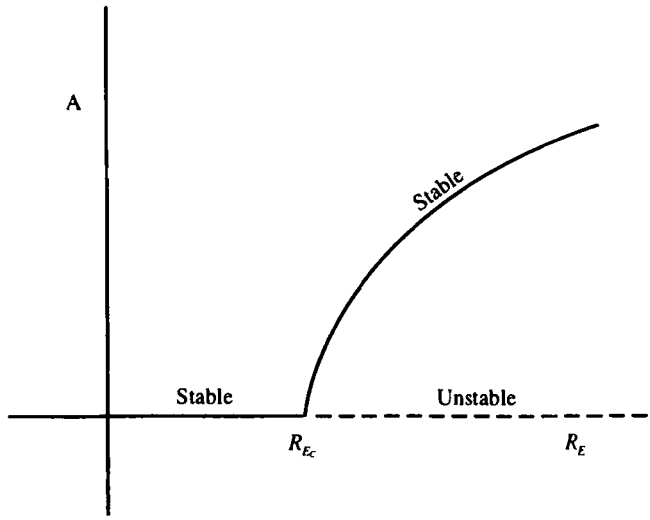

Figure 5.14a. Supercritical equilibrium.

in the case of a subcritical instability $\left(R_E < R_{E_c}\right)$, the nonlinear effects produce instability if the amplitude exceeds a threshold (see Figure 5.14b). Experiments (Nishioka and Asai) have shown that in plane Poiseuille flow transition to turbulence occurs at Reynolds numbers well below the critical value, so that a subcritical instability appears to be operational here. The other nonlinear scenario takes effect in the thermal convection problem and the Couette flow problem where a steady cellular patter comes into being when the Rayleigh/Taylor number becomes supercritical.

Arnol'd Stability Approach

In the normal mode method, discussed in the foregoing, one keeps track of each disturbance mode satisfying the linearized equations of motion and the boundary conditions. This approach is valid if the discrete spectrum alone is associated with instability. It also leaves open the question of stability with respect to arbitrary disturbances.

In the Liapunov stability method, one identifies a functional, say $\mathscr{L}$, of the perturbation field that is a dynamical invariant ($\mathscr{L}$ could be the second variation of the Hamiltonian). If $\mathscr{L}$ can then be shown to be positive definite for all possible perturbations, then stability with respect to the given norm is established. The advantage of the Liapunov stability method over the normal–mode method is that the former also covers algebraic instabilities, if any, and establishes an explicit norm that measures the growth of perturbations without regard to their initial form.

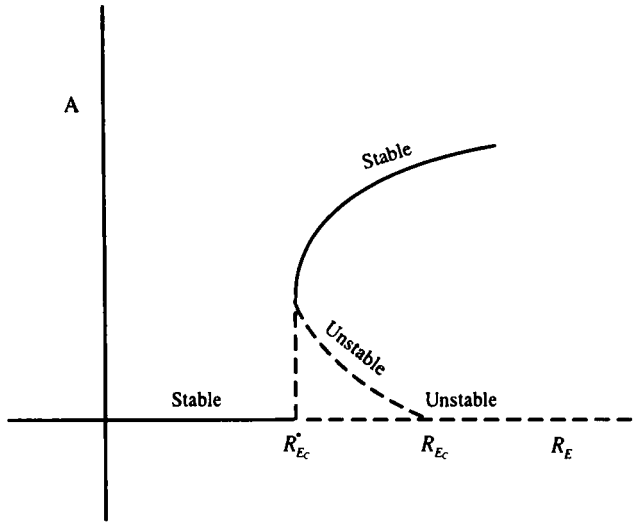

Figure 5.14b. Subcritical instability.

The Arnol'd stability method extends the Liapunov stability method from finite–dimensional to infinite–dimensional systems and seeks to establish sufficient conditions for stability.

Nonlinear stability theory seeks to establish stability of a steady state by showing that it is a local extremum of energy with respect to finite–amplitude, Casimir–preserving perturbations. But, Arnol'd type stability Theorems may turn out to be too powerful for some cases: The hypotheses required to establish the convexity estimates generally prove *global* stability, so that the extremum is actually *global* rather than just *local*. This implies that there can be at most one state satisfying an Arnol'd–type stability Theorem, while one may expect the existence of *local* extrema of energy. On the other hand, it becomes difficult to find nontrivial stable states satisfying Arnol'd–type stability criteria.

Consider a constrained conditional extremum $u = U$ of a noncanonical Hamiltonian system given by

$$\delta(\mathcal{H}+\mathcal{C}) = 0, \tag{173}$$

where $\mathcal{H}$ is the Hamiltonian and $\mathcal{C}$ is a Casimir invariant. In order to determine the stability of this extremum, one tests the sign–definiteness of the second variation $\delta^2(\mathcal{H}+\mathcal{C})$.[8]

[8]Here $1/2\ \delta^2(\mathcal{H}+\mathcal{C})$ is a Hamiltonian for the dynamics of

$$u_t = J\frac{\delta \mathcal{H}}{\delta u}$$

linearized about

$$\delta(\mathcal{H}+\mathcal{C}) = 0.$$

For finite–dimensional systems, where all norms are equivalent, this so–called formal stability, namely,

$$\delta\left(\mathcal{H}+\mathcal{C}\right)=0 \text{ and } \delta^2\left(\mathcal{H}+\mathcal{C}\right)\neq 0 \quad \forall\ \delta u, \tag{174}$$

implies normed stability to finite–amplitude perturbations (Liapunov stability), namely, $\forall \varepsilon > 0$, $\exists \delta > 0$ such that

$$\|u(0)\| < \delta \rightarrow \|u(t)\| < \varepsilon \quad \forall\ t.$$

Note that a criterion for stability with respect to norm places a definite constraint on the fully nonlinear evolution of the system, in the sense that the system is required to remain close to a stable state if it starts there.

For infinite–dimensional systems, on the other hand, formal stability does not, in itself, prove normed stability. Here, one must, instead, examine the sign of the exact invariant

$$\Delta \mathcal{I} \equiv \mathcal{H}(u)+\mathcal{C}(u)-\left[\mathcal{H}(U)+\mathcal{C}(U)\right] \tag{175}$$

to which the second variation $1/2\ \delta^2(\mathcal{H}+\mathcal{C})$ is only the small–amplitude approximation. One must, in particular, show that $\Delta \mathcal{I}$ can be sandwiched between two norms, which involves establishing certain convexity estimates on the functional $\mathcal{I}(u)$ (which ensure that the functional $\mathcal{I}(u)$ is convex in a small but finite neighborhood of the extremum U). One looks *a priori* for constants c_1 and c_2 (both positive) and some norm $\|\cdot\|$ such that

$$\|u(t)\| < c_1 \Delta \mathcal{I}(t) = c_1 \Delta \mathcal{I}(0) < c_1 c_2 \|u(0)\| \quad \forall\ t.$$

The Arnol'd stability method then consists of implementation of the following program: Suppose the system in question conserves both the energy and an infinite family of Casimir invariants (see Chapter 1). The Arnol'd invariant, which is a conserved quadratic integral of the linearized equations for a perturbation, is constructed by taking the sum (or the difference) of the energy and a suitable Casimir invariant. (The first–order terms in the perturbation in this invariant cancel if the zeroth–order solution is stationary.) If this invariant is positive or negative definite, then it can be used to define a norm, and the stationary solution is stable in this norm. (The energy extremum is then isolated under variations that conserve all Casimir invariants.)

Hamiltonian Formulation of Two-Dimensional Incompressible Flows

Consider a two–dimensional incompressible flow in $D \subseteq R^2$. The governing equations are

$$\frac{\partial \zeta}{\partial t} + \partial(\psi, \zeta) = 0, \tag{176}$$

where

$$\left.\begin{aligned} &\mathbf{v} = \hat{\mathbf{i}}_z \times \nabla\psi,\ \zeta = \hat{\mathbf{i}}_z \cdot \nabla \times \mathbf{v} = \nabla^2\psi, \\ &\partial(\psi, \zeta) \equiv \psi_x \zeta_y - \psi_y \zeta_x. \end{aligned}\right\}.$$

The Hamiltonian for this system is

$$\mathcal{H} = -\frac{1}{2}\iint_D \psi\zeta \, dxdy, \tag{177}$$

assuming that $\psi = 0$ on the boundary ∂D which is taken to be simply connected.

If one chooses ζ to be the canonical (Darboux) variable and takes the skew–symmetric operator J to be

$$J = -\partial(\zeta, \cdot),^9 \tag{178}$$

Hamilton's equation is

$$\frac{\partial \zeta}{\partial t} = J\frac{\delta \mathcal{H}}{\delta \zeta} = -\partial\left(\zeta, (-\psi)\right) = -\partial(\psi, \zeta), \tag{179}$$

which is just equation (176)!

The Casimir invariants for this problem are the solutions of

$$J\frac{\delta \mathcal{C}}{\delta \zeta} = -\partial\left(\zeta, \frac{\partial \mathcal{C}}{\partial \zeta}\right) = 0, \tag{180}$$

which implies, for some function $F(\zeta)$,

$$\frac{\delta \mathcal{C}}{\delta \zeta} = F'(\zeta). \tag{181}$$

Thus, the Casimir invariant is

---

[9]The Poisson bracket for this problem is given by

$$\begin{aligned} [\mathcal{F}, \mathcal{G}] &= \iint_D \left(\frac{\delta \mathcal{F}}{\delta \zeta}, J\frac{\delta \mathcal{G}}{\delta \zeta}\right) dxdy \\ &= -\iint_D \frac{\delta \mathcal{F}}{\delta \zeta}\partial\left(\zeta, \frac{\delta \mathcal{G}}{\delta \zeta}\right) dxdy \\ &= \iint_D \zeta\partial\left(\frac{\delta \mathcal{F}}{\delta \zeta}, \frac{\delta \mathcal{G}}{\delta \zeta}\right) dxdy. \end{aligned}$$

$$\mathcal{C} = \iint_D F(\zeta)\, dxdy. \tag{182}$$

Equation (182) may be understood by noting from equation (176) that material fluid elements carry their values of vorticity with them so that vorticity is actually a Lagrangian invariant. Consequently, any integral function of vorticity would be conserved.

Note that

$$\frac{\partial \mathcal{H}}{\partial t} = \left(\frac{\delta \mathcal{H}}{\delta \zeta}, J \frac{\delta \mathcal{H}}{\delta \zeta} \right) = -\left(J \frac{\delta \mathcal{H}}{\delta \zeta}, \frac{\delta \mathcal{H}}{\delta \zeta} \right) = 0. \tag{183}$$

In fact, translational symmetry with respect to time implies the existence of an invariant $\mathcal{M}$ satisfying

$$J \frac{\partial \mathcal{M}}{\partial \zeta} = -\partial \left(\zeta, \frac{\delta \mathcal{M}}{\delta \zeta} \right) = -\zeta_t = -\partial(\psi, \zeta), \tag{184}$$

which implies

$$\frac{\delta \mathcal{M}}{\delta \zeta} = \psi. \tag{185}$$

Thus,

$$\mathcal{M} = \iint_D \psi \zeta \, dxdy = -2\,\mathcal{H}. \tag{186}$$

So, $\mathcal{M}$ is indeed proportional to $\mathcal{H}$!

If this system has translational symmetry along the x–direction, according to Noether's Theorem (which provides conservation laws associated with the symmetry groups), there exists an invariant $\mathcal{M}$ given by

$$J \frac{\delta \mathcal{M}}{\delta \zeta} = -\frac{\partial \zeta}{\partial x}, \tag{187}$$

which implies that

$$\mathcal{M} = \iint y \zeta \, dxdy. \tag{188}$$

Equation (188) is simply the x–component of Kelvin's impulse.

On the other hand, translational symmetry along the x–direction also implies that

$$\zeta(x, y, t) = \zeta(x - ct, y), \tag{189}$$

which means, in turn,

$$-c \frac{\partial \zeta}{\partial x} = \frac{\partial \zeta}{\partial t}. \tag{190}$$

Thus,

$$cJ\frac{\delta \mathcal{M}}{\delta \zeta} = J\frac{\delta \mathcal{H}}{\delta \zeta} \tag{191}$$

or

$$J\frac{\delta(\mathcal{H} - c\mathcal{M})}{\delta \zeta} = 0. \tag{192}$$

Therefore, translationally symmetric states correspond to extremizing $(\mathcal{H} - c\mathcal{M})$ under variations that preserve the Casimir invariants.

Example 4. Consider a two–dimensional flow with a steady–state solution given by

$$\zeta \equiv \nabla^2 \psi = \mu(\psi + Vy).$$

Then, the quantity

$$\mathcal{I} = \mathcal{H} + \frac{1}{\mu}\mathcal{C},$$

where $\mathcal{H}$ and $\mathcal{C}$ are the perturbation energy and enstrophy, respectively,

$$\mathcal{H} = \iint_D (\nabla \psi)^2 \, dxdy,$$

$$\mathcal{C} = \iint_D (\nabla^2 \psi)^2 \, dxdy,$$

is an invariant.

Consider the linear instability of a plane wave of wavenumber m produced by a triadic interaction with two other plane waves of wavenumbers l and n (Carnevale et al.). Let this interaction be described by

$$\left.\begin{aligned} \dot{x} &= ayz, \\ \dot{y} &= bzx, \\ \dot{z} &= cxy, \end{aligned}\right\}$$

where

$$a = n^2 - m^2, \quad b = l^2 - n^2, \quad c = m^2 - l^2.$$

This system conserves energy

$$\mathcal{H} \equiv x^2 + y^2 + z^2$$

and enstrophy,

$$\mathcal{C} \equiv l^2 x^2 + m^2 y^2 + n^2 z^2.$$

In order to investigate the stability of the plane wave with wavenumber m, consider the invariant

$$\mathcal{I} \equiv \mathcal{H} - \frac{1}{m^2}\mathcal{C} = \frac{\left(cx^2 - az^2\right)}{m^2}.$$

Note that $\mathcal{I}$ is of definite sign if a and c are of opposite signs (i.e., $ca < 0$), which implies that m must be either the largest or the smallest of the three wavenumbers. This simply reflects the fact that one cannot conserve both energy and enstrophy by transferring energy in one direction only. On the other hand, $\mathcal{I}$ is of indefinite sign if a and c are of the same sign (i.e., $ca > 0$), which implies that m is intermediate in size between l and n. Then, the plane wave with wavenumber m is unstable and the instability proceeds by transferring energy both to larger and smaller scales.

Arnol'd Stability of Two-Dimensional Incompressible Flows

(a) Linear Stability: The stationary state is a stationary point of the functional

$$\mathcal{I}(\psi) = \mathcal{H}(\psi) + \mathcal{C}(\psi) = \iint_D \left\{\frac{1}{2}(\nabla\psi)^2 + F(\zeta)\right\} dxdy \tag{193}$$

and is given by the first variation of $\mathcal{I}(\psi)$,

$$\delta\mathcal{I}(\psi) = \iint_D \left\{-\overline{\psi} + F'(\zeta)\right\}\delta\zeta \; dxdy = 0, \tag{194}$$

from which

$$\overline{\psi} = F'(\zeta) \text{ or } \overline{\zeta} = P(\overline{\psi}). \tag{195}$$

Next, the second variation of $\mathcal{I}(\psi)$ is given by

$$\delta^2\mathcal{I} = \iint_D \left\{(\delta\nabla\psi)^2 + \frac{1}{2}F''(\overline{\zeta})(\delta\zeta)^2\right\} dxdy. \tag{196}$$

A sufficient condition for linear stability in the Liapunov sense is that $\delta^2\mathcal{I}$ is positive (or negative) definite for all variations $\delta\psi$ and $\delta\zeta$. This requires, from (192), that

$$F''(\overline{\zeta}) \geq 0, \quad \forall (x,y) \in D \tag{197}$$

and leads to the following Theorem.

THEOREM: The steady state $(\overline{\psi}, \overline{\zeta})$ is linearly stable in the Liapunov sense with respect to the perturbation norm

$$\|(\delta\psi, \delta\zeta)\| = \left\{\delta^2\mathcal{I}(\psi)\right\}^{\frac{1}{2}} \tag{198}$$

if the Casimir function F, given by (182), satisfies

$$F''(\overline{\zeta}) \geq 0, \quad \forall (x,y) \in D. \tag{199}$$

Example 2: If the system has translational symmetry along the x–direction, (197) may be rewritten as

$$P'(\overline{\psi} + cy) = \frac{\partial \overline{\zeta}/\partial y}{(\partial \overline{\psi}/\partial y + c)} \geq 0$$

or

$$(\overline{u} - c)\frac{\partial \overline{\zeta}}{\partial y} \leq 0.$$

Consider the case of parallel shear flows, $\overline{u} = \overline{u}(y)$; the stability criterion then reduces to Fjortoft's Theorem:

$$(\overline{u} - c)\frac{\partial^2 \overline{u}}{\partial y^2} \geq 0.$$

Note that the stability criterion is applicable to an arbitrary perturbation ψ which allows $\mathcal{I}(\psi)$ to exist. Thus, Fjortoft's Theorem is generalizable to arbitrary perturbations and implies even the normed stability!

(b) Nonlinear Stability: For infinite–dimensional systems, the positive (or negative) definiteness of the second variation of the functional $\mathcal{I}$ does not imply nonlinear stability (unlike finite–dimensional Hamiltonian systems) because of topological difficulties besetting infinite–dimensional function spaces. For this purpose, one needs to examine the sign of the exact invariant

$$\Delta \mathcal{I}(\psi) = \mathcal{I}(\psi) - \mathcal{I}(\overline{\psi}) \tag{200}$$

to which the second variation $1/2\ \delta^2 \mathcal{I}$ is only the small–amplitude approximation. If this invariant is positive (or negative) definite, then it can be used to define a perturbation norm, and the steady state is nonlinearly stable in this norm. This requires imposition of additional convexity conditions on the functional $\mathcal{I}(\psi)$ in order to ensure that the functional $\mathcal{I}(\psi)$ is convex in a small but finite neighborhood of the steady state $\overline{\psi}$.

Let us write the functional $\Delta \mathcal{I}(\psi)$ as follows:

$$\Delta \mathcal{I}(\hat{\psi}) = \mathcal{I}(\overline{\psi} + \hat{\psi}) - \mathcal{I}(\overline{\psi}), \tag{201}$$

where $\hat{\psi}$ is the finite–amplitude perturbation imposed on the steady state $\overline{\psi}$.

Using (193) in (201) , we have

$$\Delta \mathcal{I}(\hat{\psi}) = \frac{1}{2}\iint_D (\nabla \hat{\psi})^2\, dxdy - \iint_D F'(\overline{\zeta})\hat{\zeta}\, dxdy + \iint_D \left[F(\overline{\zeta} + \hat{\zeta}) - F(\overline{\zeta})\right] dxdy. \tag{202}$$

Observe that if (202) is Taylor–expanded about the steady state $\overline{\psi}$, the leading–order term is just the second variation $1/2\ \delta^2 \mathcal{S}$, given by (196)!

Suppose that the Casimir function $F(\zeta)$ satisfies the convexity condition[10]

$$0 < \alpha_1 < F''(\zeta) < \beta_1 < \infty, \ \forall \zeta, \tag{203}$$

where α_1 and β_1 are real numbers. Condition (203) implies

$$\frac{1}{2}\alpha_1 \hat{\zeta}^2 < \left[F\left(\overline{\zeta} + \hat{\zeta}\right) - F\left(\overline{\zeta}\right) - F'\left(\overline{\zeta}\right)\hat{\zeta} \right] < \frac{1}{2}\beta_1 \hat{\zeta}^2. \tag{204}$$

Using (204) in (202), we have

$$\frac{1}{2}\iint_D \left[\left(\nabla \hat{\psi}\right)^2 + \alpha_1 \hat{\zeta}^2 \right] dxdy < \Delta \mathcal{S}\left(\hat{\psi}\right) < \frac{1}{2}\iint_D \left[\left(\nabla \hat{\psi}\right)^2 + \beta_1 \hat{\zeta}^2 \right] dxdy. \tag{205}$$

(205) shows that the convexity condition (203) is sufficient to establish the positive (or negative) definiteness of $\Delta \mathcal{S}\left(\hat{\psi}\right)$.

If one defines a perturbation norm by

$$\left\| \hat{\psi} \right\| = \left\{ \Delta \mathcal{S}^*\left(\hat{\psi}\right) \right\}^{\frac{1}{2}}, \tag{206}$$

where

$$\Delta \mathcal{S}^*\left(\hat{\psi}\right) = \frac{1}{2}\iint_D \left[\left(\nabla \hat{\psi}\right)^2 + \alpha_1 \hat{\zeta}^2 \right] dxdy,$$

then (205) shows that this norm is bounded from above. We thus have the following Nonlinear Stability Theorem:

THEOREM: Suppose that the Casimir function F satisfies the following convexity condition

$$0 < \alpha_1 < F''(\zeta) < \beta_1 < \infty, \ \forall \zeta \tag{207}$$

for some real constants α_1 *and* β_1. Then, the steady state $\overline{\psi}$, determined by F through the relation (195), is nonlinearly stable in the Liapunov sense with respect to the perturbation norm:

$$\left\| \hat{\psi} \right\| = \left\{ \Delta \mathcal{S}^*\left(\hat{\psi}\right) \right\}^{\frac{1}{2}}. \tag{208}$$

It may be mentioned that there are some restrictions on the direct applicability of the Arnol'd stability method for many problems. One such restriction is placed by Andrews' Theorem, which states that the Arnol'd stable flows of a system

---

[10] A function $f(x)$ is convex if

$$f\left(\frac{x+y}{2}\right) \le \frac{1}{2}\left[f(x) + f(y)\right]$$

for $\forall x, y$ in the domain of f.

must have the same symmetry properties as the system. This property places significant limitations on the utility of the Arnol'd stability method. Thus, this method runs into difficulties in handling translationally invariant or steadily translating structures.

EXERCISE

1. For the type of mean–flow profiles that lead to the satisfaction of the *global* necessary condition (108) in the flow field, show that there can be no more than $(n-1)$ linearly–independent unstable characteristic function of equation (120) if $\alpha^2 \geq -\lambda_n$; $\lambda_1, \lambda_2, \ldots$ being the increasing sequence of characteristic values of equation (120). (In other words, the number of distinct unstable modes cannot exceed the number of neutral modes associated with the points where $(u'')_{u=c} = 0$.)

This page intentionally left blank

6

TURBULENCE

6.1. The Origin and Nature of Turbulence

Usually, in flows which are originally laminar, turbulence arises from the onset of instabilities at large Reynolds numbers. The details of the mechanism of transition of laminar flow to turbulence are not well understood at present. Much of the theory of instabilities in fluid flow, as discussed in Chapter 5, is a linear formalism that is valid only for very small disturbances. And the mechanism of transition is not contained within the framework of such a linear theory.

Among the characteristics of turbulence are:

(1) large fluctuations of the flow properties about the mean values (similar to the thermal motion of the molecules in a gas) at any point;

(2) increased diffusivity which causes rapid mixing and enhanced rates of momentum, heat, and mass transport;

(3) when three–dimensional, the presence of vortex–stretching cascade mechanism that creates motion at ever smaller scales;

(4) the existence of some energy sources, such as shear, in flow to sustain turbulence (in the absence of energy sources, turbulence decays).

Fourier analysis of the turbulent velocity field shows that wave fluctuations in a range of frequencies and wavenumbers are present, with the width of the range changing with certain flow parameters like the Reynolds number. The various component motions interact through the nonlinear terms in the equations of motion, and the observed properties of the turbulence are thought of as being the statistical result of such interactions.

Mathematically, the description of these interactions should center on invariant measures. Although there is no rigorous theory about the existence of strictly invariant measures in turbulence, experimental observations strongly support the idea that turbulence at small scales organizes itself into a statistically stationary universal state. Apparently, as the Reynolds number of the flow becomes infinite,

all the invariance properties of the Navier–Stokes equations, possibly broken by the mechanisms producing the turbulence, are recovered asymptotically at small scales in a statistical sense. Thus, Kolmogorov argued that the small–scale structure has a scale–invariant and universal character in turbulence at high Reynolds numbers of the flow. This implies that there exists, for large wavenumbers, an inertial range where the statistical properties of the small–scale components are isotropic, uniquely determined by the average energy dissipation rate ε and the kinematic viscosity ν, and independent of the detailed form of the large–scale features of the flow.

Statistical theories of the turbulence can be viewed as models which have in common with the original problem several structural properties like energy conservation and Galilean invariance. They can give information about energy transfer and turbulent transport coefficients. However, the basic problem in the description of turbulent flows, when treated in terms of the time average of the dynamical variables and their correlations, is that an open–ended hierarchy of formally exact moment equations results from a systematic treatment of the equations governing the flow. This so–called closure problem is due to the nonlinearity of the Navier–Stokes equations and refers to the fact that the evolution of second–order moments involves triple correlations, and so on. This problem is just one manifestation of the intractable nature of turbulent flows, and it is usually overcome by making some hypothesis to complement the averaged equations. But, as in many statistical problems, it is not possible to directly check this hypothesis, so only its consequences are open for experimental verification. In the phenomenological approach, one addresses oneself only to a study of the mean flow and formulates the effects of turbulence on the mean flow in some statistical fashion rather than attending to the enormously detailed structure of turbulence. Typically, a phenomenological approach is based on a superficial resemblance between the way momentum and heat are transferred by the molecular motions and turbulent velocity fluctuations and thus recognizes the existence of suitable transport coefficients for the latter. However, the concept of transport coefficients can be systematically justified only when there is motion on widely separated scales, whereas in turbulent flows the dominant interactions are believed to occur among contiguous, rather than widely separated scales. Besides, the turbulent transport is a complex process which is dependent among others on the history of flow dynamics (because flow elements retain their identity over long intervals of time) and cannot be simply related to the local functionals of the mean–flow properties unlike the molecular transport. Besides, whereas molecular viscosity is a property of fluids, turbulence is a characteristic of flows. In the following we shall avoid the phenomenological approach and take instead the statistical approach. (It may be mentioned that there is also a dynamical systems approach (Frisch) which provides new methods of characterizing turbulent behavior.)

6.2. Three-Dimensional Turbulence

A Statistical Formalism

A characteristic feature of turbulence at fairly large Reynolds numbers is the presence of an extremely irregular temporal variation of the velocity at each point. The velocity continually fluctuates about some mean value, and the amplitude of this variation is in general not small in comparison with the magnitude of the velocity itself. This amplitude distribution is Gaussian, i.e., the number of times during a long time interval that a given magnitude of fluctuation is reached varies with the magnitude according to the *error* curve.[1] Even though an exact description of the temporal variation of the velocity distribution in the fluid requires prescription of the initial conditions, the actual initial conditions cease to have any effect after sufficiently long intervals of time. Besides, since the detailed velocity pattern of a turbulent flow is always changing and never repeats, even if one could measure the complete sequence of changes, the measurements would relate only to that particular experiment. Therefore, one may attach general significance only to the statistical specifications of the velocity field in turbulence, i.e., to the joint probability distribution function which determines the probability of occurrence of a given combination of velocities at a point in space at a given time. However, it turns out to be feasible to consider only a few moments of this probability distribution function, which are usually mean values of some flow properties.

In the statistical studies of random processes, one does not investigate the individual realizations $\xi^{(k)}(t)$ of the random function $\xi(t)$ but the characteristics of a whole set of ensemble of realizations by means of suitable averages which are reproducible from experiment to experiment. The classical theory of turbulence tacitly assumes that individual realizations of a turbulent flow are sensitive to initial conditions and that averages do not exhibit such sensitivity because the fluctuations become uncorrelated before too long.

If the ergodic theorem is valid, at least in some weak sense, then the time averages of the flow field are interpreted as ensemble average, i.e., averages over a large number of flow realizations prepared under nearly identical initial and boundary conditions. A distribution function can then be defined at each point for any given flow variable at a given time, as the ratio of the number of times the given variable is observed to occur to the total number of observations made in

---

[1] However, the joint probability distributions have been shown experimentally to be of a more general type. If ΔV_ℓ represent the velocity difference between two points a distance ℓ apart, laboratory experiments and numerical simulations show that the probability distribution function $P(\Delta V_\ell)$ differs significantly from Gaussian, being reduced for small values of ΔV_ℓ and enhanced for large values. This means that the statistical properties are dominated by sparsely distributed large fluctuation amplitudes showing the presence of spatial intermittency.

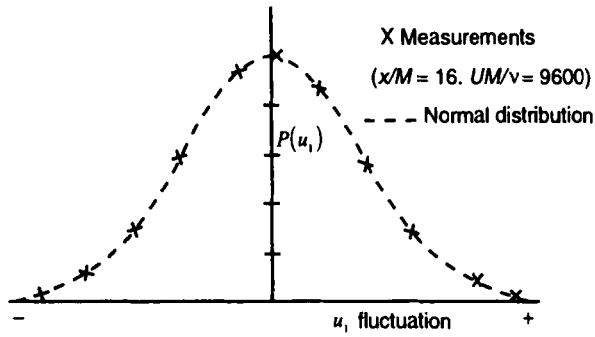

Figure 6.1. Probability density function of the velocity component u_1 in the direction of the stream for the turbulence generated by a square–mesh grid in a wind tunnel measured by Townsend (1947).

the limit, with the latter tending to infinity. However, averaging results in loss of information and the lost information must somehow be replaced empirically!

The mathematical formulation of the problem can be given as follows: 'One has a flow realization satisfying the Navier–Stokes equations

$$\nabla \cdot \mathbf{v} = 0, \tag{1}$$

$$\frac{\partial \mathbf{v}}{\partial t} + (\mathbf{v} \cdot \nabla)\mathbf{v} = -\frac{1}{\rho}\nabla p + \nu \nabla^2 \mathbf{v}, \tag{2}$$

and at some initial instant the velocity of the fluid is a random function of position described by certain probability laws which are independent of position. The problem is to determine the probability laws that describe the motion of the fluid at subsequent times.' This problem is not trivial because one has to solve the nonlinear equations to find statistical information at any point within the domain, which are required to satisfy initial and boundary conditions that are given only statistically.

Since the initial conditions are random functions of position, the broad range of variation of initial conditions renders the investigation of particular sets of initial conditions virtually useless. However, thanks to the large degrees of freedom of the system which are coupled to each other, such a system is likely to approach a statistical state which is independent of the initial conditions. Hence, rather than investigating the motion consequent to a particular set of initial conditions, one explores the solutions which are asymptotic in the sense that they change very little with further passage of time.

The Probability Density

In order to investigate how fluctuations are distributed around an average value,

one introduces the probability density and its Fourier transform – the characteristic function. Let us restrict ourselves to fluctuating quantities that are statistically steady (or stationary), i.e., their mean values are not functions of time. One introduces probability density $B(u)$ as the probability of finding $u(t)$ between u and $u+\Delta u$; note that

$$B(u) \geq 0, \qquad \int_{-\infty}^{\infty} B(u)\,du = 1. \tag{3}$$

The mean value of a quantity $f(u)$ is then given by

$$\langle f \rangle = \int_{-\infty}^{\infty} f(u)\,B(u)\,du. \tag{4}$$

If

$$u = \langle u \rangle + u', \tag{5}$$

then $\langle u' \rangle = 0$ (the prime denotes the fluctuations). Any lack of symmetry in $B(u)$ does not contribute to $\langle u'^2 \rangle$ (the variance), but only that contributes to $\langle u'^3 \rangle$ (the skewness).

Let us next introduce the Fourier transform of the probability density – the characteristic function

$$\phi(k) = \frac{1}{\sqrt{2\pi}} \int_{-\infty}^{\infty} e^{iku'} B(u')\,du' \tag{6a}$$

with

$$B(u') = \frac{1}{\sqrt{2\pi}} \int_{-\infty}^{\infty} e^{-iku'} \phi(k)\,dk. \tag{6b}$$

The moments of u' are related to $\phi(k)$ in a simple manner

$$\langle u'^n \rangle = \frac{1}{i^n} \frac{1}{\sqrt{2\pi}} \left(\frac{d^n \phi(k)}{dk^n} \right)_{k=0}, \tag{7}$$

so that

$$\phi(k) = \sqrt{2\pi} \sum_{n=0}^{\infty} \frac{(ik)^n}{n!} \langle u'^n \rangle. \tag{8}$$

Note that

$$\phi(k) = \frac{1}{\sqrt{2\pi}} \int_{-\infty}^{\infty} \cos ku' \cdot B(u')\,du' + \frac{i}{\sqrt{2\pi}} \int_{-\infty}^{\infty} \sin ku' \cdot B(u')\,du', \tag{9}$$

so that $\phi(k)$ is real if $B(u')$ is symmetric.

Note further that

$$|\phi(k)| = \left| \frac{1}{\sqrt{2\pi}} \int_{-\infty}^{\infty} e^{iku'} B(u')\, du' \right|$$

$$\leq \frac{1}{\sqrt{2\pi}} \int_{-\infty}^{\infty} \left| e^{iku'} \right| \left| B(u')\, du' \right| = \frac{1}{\sqrt{2\pi}} \int_{-\infty}^{\infty} B(u')\, du' = \frac{1}{\sqrt{2\pi}}, \tag{10a}$$

where we have used Schwartz's inequality. So,

$$|\phi(k)| \leq \phi(0) = 1. \tag{10b}$$

Note also that if $B(u')$ is broad, $\phi(k)$ is narrow and vice versa.

Note that if $B(u')$ has a discontinuity, then from

$$\phi(k) = -\frac{1}{\sqrt{2\pi}} \int_{-\infty}^{\infty} \frac{e^{iku'}}{k} \frac{dB(u')}{du'}\, du \tag{11}$$

one concludes, when the spike in $dB(u')/du'$ is infinitely narrow at $u' = s$, that

$$\phi(k) \sim \frac{e^{iks}}{k} \text{ for large } k. \tag{12}$$

Consider two functions $f(x)$ and $g(x)$ with Fourier transforms $F(k)$ and $G(k)$, respectively. Then, one has Parseval's relation

$$\int_{-\infty}^{\infty} f(x)\, g^*(x)\, dx = \int_{-\infty}^{\infty} F(k) G^*(k)\, dk, \tag{13}$$

where the star denotes a complex conjugate.

In order to see how an operation carried out on a function affects its Fourier transform, consider the averaging of $f(x)$ over an interval $-X \leq x \leq X$. This requires a choice

$$g^*(x) = \begin{cases} \dfrac{1}{2X}, & -X \leq x \leq X, \\ 0, & \text{otherwise.} \end{cases} \tag{14}$$

As $g^*(x)$ becomes wider, $G^*(k)$ becomes narrower (see Figure 6.2); thus (13) gives

$$\frac{1}{2X} \int_{-X}^{X} f(x)\, dx = \frac{F(0)}{2\pi} \left\{ \int_{-\infty}^{\infty} G^*(k)\, dk \right\}, \tag{15}$$

which implies that average of a function is related only to its Fourier component at zero frequency.

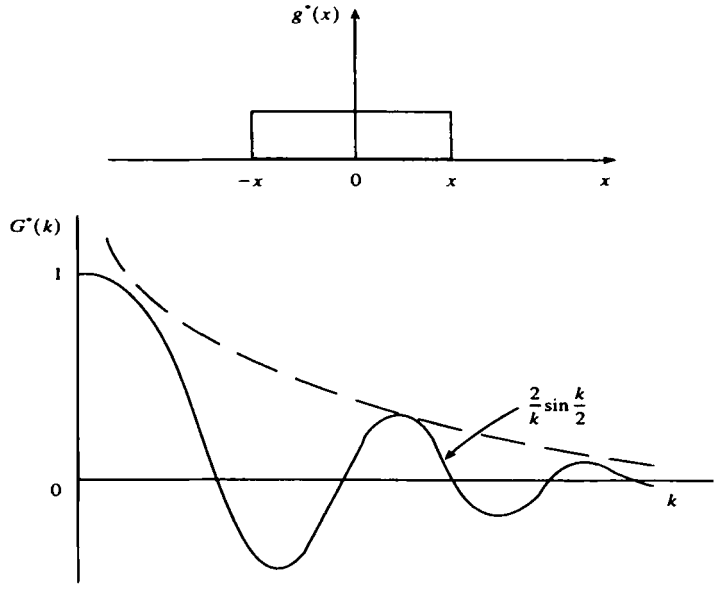

Figure 6.2. A double–step function and its Fourier transform (from Tennekkes and Lumley, 1973).

The Autocorrelation

In order to examine how adjacent fluctuations (in space and time) are related to each other, one introduces the autocorrelation and its Fourier transform – the energy spectrum. Consider the probability density for two variables u' and v', with zero mean, simultaneously. One introduces the joint probability density $B(u',v')$ as the probability of finding $u'(t)$ and $v'(t)$ simultaneously between u' and $u'+\Delta u'$, v' and $v'+\Delta v'$, respectively. Note that

$$B(u',v') \geq 0, \qquad \int_{-\infty}^{\infty}\int_{-\infty}^{\infty} B(u',v')\,du'\,dv' = 1$$

and

$$\int_{-\infty}^{\infty} B(u',v')\begin{pmatrix} du' \\ dv' \end{pmatrix} = \begin{pmatrix} B_{v'}(v') \\ B_{u'}(u') \end{pmatrix}, \tag{16}$$

where $B_{u'}(u')$ and $B_{v'}(v')$ are the individual probability densities for u' and v'. Note that if u' and v' are statistically independent, one has

$$B(u',v') = B_{u'}(u')\,B_{v'}(v'). \tag{17}$$

The correlation between u' and v' is given by

$$\langle u'v' \rangle = \int_{-\infty}^{\infty}\int_{-\infty}^{\infty} u'v'\,B(u',v')\,du'\,dv'. \tag{18}$$

Note that the correlation is a measure of asymmetry of $B(u', v')$.

The autocorrelation $\langle u'(t)u'(t')\rangle$ describes evolution of a fluctuating function $u'(t)$. For stationary variables, the autocorrelation must be a symmetric function of $\tau = t' - t$. Further, note that

$$\langle u'^2(t)\rangle = \langle u'^2(t')\rangle = \text{constant} = \langle u'^2\rangle. \tag{19}$$

Thus, one introduces an autocorrelation coefficient

$$\rho(\tau) = \frac{\langle u'(t)u'(t')\rangle}{\langle u'^2\rangle}. \tag{20}$$

From Schwartz inequality, one has

$$\left|\langle u'(t)u'(t')\rangle\right| \leq \left|\langle u'^2(t)\rangle\langle u'^2(t')\rangle\right|^{1/2}, \tag{21}$$

so there follows

$$\left|\rho(\tau)\right| \leq \rho(0) = 1. \tag{22}$$

Note that ρ is real, symmetric and vanishes faster than $1/\tau$ (see Figure 6.3).

Expanding ρ in a Taylor series about the origin, one obtains

$$\rho(\tau) \approx 1 - \frac{\tau^2}{\lambda^2}, \tag{23}$$

where λ is the microscale defined by

$$\left(\frac{d^2\rho}{d\tau^2}\right)_{\tau=0} \equiv -\frac{2}{\lambda^2}.$$

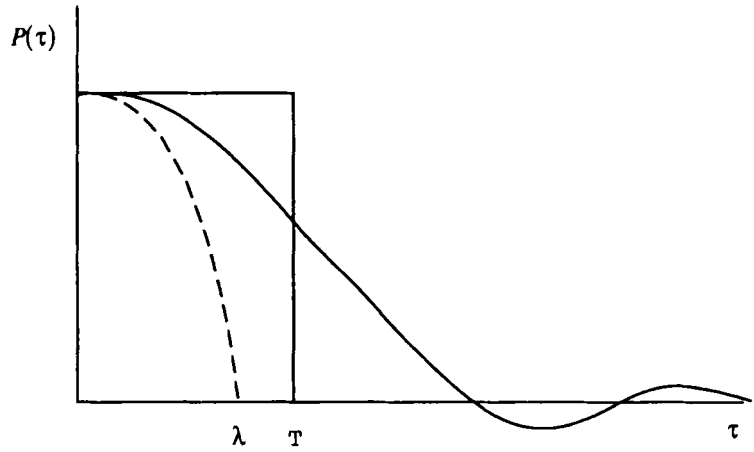

Figure 6.3. The autocorrelation coefficient (from Tennekkes and Lumley, 1973).

Further, note that

$$\frac{d^2}{dt^2}\langle u'^2\rangle = 0 = \left\langle 2u'\frac{d^2u'}{dt^2}\right\rangle + 2\left\langle\left(\frac{du'}{dt}\right)^2\right\rangle, \tag{24}$$

from which, on using (23), one obtains

$$\left\langle\left(\frac{du'}{dt}\right)^2\right\rangle = \frac{2\langle u'^2\rangle}{\lambda^2}. \tag{25}$$

Consider now the average value of $u(t)$ over a finite interval:

$$U_T \equiv \frac{1}{T}\int_0^T u(t)\,dt. \tag{26}$$

Then, the difference between U_T and the true mean value U is given by

$$U_T - U = \frac{1}{T}\int_0^T [u(t) - U]\,dt = \frac{1}{T}\int_0^T u'(t)\,dt, \tag{27}$$

from which the mean square error is given by

$$\left\langle (U_T - U)^2\right\rangle = \frac{\langle u'^2\rangle}{T^2}\int_0^T\int_0^T \rho(t'-t)\,dt\,dt' = \frac{2\langle u'^2\rangle}{T}\int_0^T\left(1-\frac{\tau}{T}\right)\rho(\tau)\,d\tau. \tag{28}$$

If $T \gg I$, where I is the integral scale,

$$I \equiv \int_0^\infty \rho(\tau)\,d\tau, \tag{29}$$

so that $\tau/T \approx 0$ in the range of values of τ where $\rho(\tau) \neq 0$ (see Figure 6.3), then (28) gives

$$\left\langle (U_T - U)^2\right\rangle \approx 2\langle u'^2\rangle\frac{I}{T}. \tag{30}$$

Thus, the difference between the time average of u and its true mean is due to the existence of a correlation of u with itself.

The requirement that a time average should converge to a mean value, i.e., that the error should become smaller as the integration time increases and that the mean value found this way should always be the same, is called *ergodicity*. An ergodic variable thus becomes uncorrelated with itself at large time differences.

Introduce the Fourier transform of $\rho(\tau)$ – the energy spectrum:

$$S(\omega) = \frac{1}{\sqrt{2\pi}}\int_{-\infty}^{\infty} e^{-i\tau\omega}\rho(\tau)\,d\tau$$

with

$$\rho(\tau) = \frac{1}{\sqrt{2\pi}} \int_{-\infty}^{\infty} e^{i\tau\omega} S(\omega)\, d\omega. \tag{31}$$

Note that the condition on the behavior of the correlation at large time separations may be translated into a condition on the behavior of the spectrum near the origin – the derivatives of the spectrum near the origin are the moments of the correlation coefficient. Further, $S(\omega)$ is real because $\rho(\tau)$ is symmetric, and $S(\omega)$ is symmetric because $\rho(\tau)$ is real; note from (22) and (29) that

$$\frac{1}{\sqrt{2\pi}} \int_{-\infty}^{\infty} S(\omega)\, d\omega = 1, \qquad S(0) = \sqrt{\frac{2}{\pi}}\, I. \tag{32}$$

If

$$\tilde{u}'_T(\omega, t) \equiv \frac{1}{T} \frac{1}{\sqrt{2\pi}} \int_{t}^{t+T} e^{i\omega t'} u'(t')\, dt', \tag{33}$$

then

$$\lim_{T \to \infty} T \left\langle \left| \tilde{u}'_T(\omega, t) \right|^2 \right\rangle = \frac{\langle u'^2 \rangle}{\sqrt{2\pi}}\, S(\omega); \tag{34}$$

hence the name energy spectrum for $S(\omega)$.

The Central Limit Theorem

It turns out that the probability density of a group of stationary variables is independent of the probability densities of the individual variables and tends to a limit when the number of the latter becomes very large.

Consider N statistically independent quantities $x_n(t)$. Assume that all $x_n(t)$ have identical probability densities and that their mean values are zero. Let us introduce a normalized sum variable,

$$w(t) = \frac{1}{\sqrt{N}} \sum_{n=1}^{N} x_n(t). \tag{35}$$

The variance of w is given by

$$w^2 = \frac{1}{N} \sum_{n=1}^{N} x_n^2 \equiv \sigma^2, \tag{36}$$

where σ^2 is the variance of x_n, which is the same for each x_n because they have identical probability densities, and the double sum becomes a single sum because x_n and $x_m (n \neq m)$ are uncorrelated. Note that the presence of the factor $1/\sqrt{N}$ in $w(t)$ leads to the independence of the variance of $w(t)$ on N.

The characteristic function $\phi_w(k)$ of $w(t)$ is given by

$$\phi_w(k) = \frac{1}{\sqrt{2\pi}} \exp\langle ikw(t)\rangle = \frac{1}{\sqrt{2\pi}} \exp\left\langle \left[\frac{ik}{\sqrt{N}} \sum_{n=1}^{N} x_n(t) \right] \right\rangle$$

$$= \frac{1}{\sqrt{2\pi}} \left[\frac{1}{\sqrt{2\pi}} \phi\left(\frac{k}{\sqrt{N}} \right) \right]^N, \tag{37}$$

where

$$\phi\left(\frac{k}{\sqrt{N}} \right) \equiv \frac{1}{\sqrt{2\pi}} \exp\left\langle \left[\frac{ik}{\sqrt{N}} x_n(t) \right] \right\rangle$$

is the same for all $x_n(t)$ since they have identical probability densities, and the factorization became possible because $x_n(t)$ are statistically independent.

If the first few moments of the probability density of x_n exist, then $\phi\left(k/\sqrt{N}\right)$ may be expanded in a Taylor series

$$\phi\left(\frac{k}{\sqrt{N}} \right) = 1 - \frac{k^2\sigma^2}{2N} + 0\left(\frac{k}{\sqrt{N}} \right)^3. \tag{38}$$

So, as $N \Rightarrow \infty$, (37) gives

$$\phi_w(k) = \lim_{N\Rightarrow\infty} (2\pi)^{N/2} \left(1 - \frac{k^2\sigma^2}{2N} \right)^N \approx (2\pi)^{N/2} \exp\left(-\frac{k^2\sigma^2}{2} \right), \tag{39}$$

from which the probability distribution function of the sum is given by

$$B(w) = \frac{1}{\sqrt{2\pi\sigma^2}} \exp\left(-\frac{w^2}{2\sigma^2} \right). \tag{40}$$

Thus, we have the following result (Central Limit Theorem).

THEOREM: The sum of a large number of identically distributed statistically independent variables has a Gaussian probability density, regardless of the shape of the density of the variables themselves.

Example 1: Consider an integral of $u'(t)$ over a time interval T. If $u'(t)$ is a stationary random variable, this integral will also be a stationary random variable. Now, an integral is like a sum, so that under suitable conditions the Central Limit Theorem becomes applicable in finding its probability distribution. If the integration time T is large compared with the integral scale I, the integral may be divided into sections of length larger that $2I$ so as to render the sections approximately independent (recall that I is a measure of the time over which $u'(t)$ is correlated with itself):

$$\int_0^T u'(t)\,dt = \int_0^{nl} u'(t)\,dt + \int_{nl}^{2nl} u'(t)\,dt + \cdots. \tag{41}$$

As n increases, the sections of integral become more nearly independent because neighboring sections depend on each other only near the ends. Noting that nl is the length of each section and T/nl is the number of sections, it is possible to choose n such that both nl and T/nl go to infinity as $T \Rightarrow \infty$. We then have more and more sections and they become more and more nearly independent so that the probability distribution of the given integral becomes Gaussian.

Let us use this result to analyze the motion of a marked fluid particle in stationary, homogeneous turbulence without mean velocity – a problem which is of relevance in the spreading of a spot of dye injected into a turbulent fluid. Let $\boldsymbol{V}(\boldsymbol{a},t)$ be a Lagrangian velocity at time t of a moving point which was at the point $\boldsymbol{x}=\boldsymbol{a}$ at $t=0$. $\boldsymbol{V}(\boldsymbol{a},t)$ is a stationary function. The position of the wandering point is given by

$$\boldsymbol{X}(\boldsymbol{a},t) = \boldsymbol{a} + \int_0^t \boldsymbol{V}(\boldsymbol{a},t')\,dt'. \tag{42}$$

Since $\boldsymbol{V}$ is stationary, the application of Central Limit Theorem shows that $(\boldsymbol{X}-\boldsymbol{a})_k$ asymptotically has a Gaussian probability density, with variance (or dispersion) given by

$$\begin{aligned}
\left\langle (X-a)_k^2 \right\rangle &= \int_0^t dt' \int_0^t dt'' \left\langle V_k(a,t')\,V_k(a,t'') \right\rangle \\
&= 2\int_0^t dt' \int_0^{t'} dt'' \left\langle V_k(a,t')\,V_k(a,t'') \right\rangle \\
&= 2\int_0^t dt' \int_0^{t'} d\tau \left\langle V_k(a,t')\,V_k(a,t'-\tau) \right\rangle \\
&= 2\left\langle V_k^2 \right\rangle \int_0^t dt' \int_0^{t'} d\tau\, \rho_{kk}(\tau) \\
&= 2\left\langle V_k^2 \right\rangle t \int_0^t \left(1-\frac{\tau}{t}\right) \rho_{kk}(\tau)\,d\tau,
\end{aligned} \tag{43}$$

which gives the root mean square (rms) dispersion of a marked fluid particle in terms of the Lagrangian velocity autocorrelation coefficient $\rho_{kk}(\tau)$, defined by

$$\rho_{kk}(\tau) \equiv \frac{1}{\left\langle V_k^2 \right\rangle} \left\langle V_k(a,t)\,V_k(a,t-\tau) \right\rangle.$$

For long times, (43) gives the result corresponding to the classical random walk of discontinuous movements:

$$\left\langle (X-a)_k^2 \right\rangle \approx 2\left\langle V_k^2 \right\rangle t\, I_{kk},$$

where I_{kk} is the Lagrangian integral scale defined by

$$I_{kk} \equiv \int_0^t \rho_{kk}(\tau)\, d\tau.$$

Thus, for long times, the dispersion increases as if there were a constant "eddy diffusivity" of $\left\langle V_k^2 \right\rangle I_{kk}$ showing that the concept of diffusion is valid in this limit. (In general, the concept of a diffusion coefficient is, however, a crude approximation because the variation of statistical properties of interest in turbulent diffusion occurs over scales comparable to that of the turbulent motion itself.)

For short times, $\rho_{kk} \approx 1$ so that, according to (43), the dispersion goes like t^2 (as in free steaming) and the probability density of $(X-a)_k$ is still nearly Gaussian because V is Gaussian distributed.

Symmetry Conditions

The infinite field of turbulent motion is determined statistically by the complete system of joint probability distributions of the values of the velocities at any n points of space–time. The statistical properties of this flow field at different times are uniquely related by the equations of continuity and momentum. Analysis becomes simpler if fields of turbulence satisfy certain symmetry conditions in a statistical sense. These symmetry conditions are imposed on the joint probability distribution of the values of the velocity at n points of space at a given time. For a spatially homogeneous case, the joint probability distribution is independent of arbitrary spatial translations of the configuration formed by the n points, for an isotropic case, it is independent also of arbitrary rigid body rotations of the configuration relative to the fluid.[2]

Now, the axes to which the velocities are referred must rotate with the configuration of n points so that one may consider the joint probability distribution of the velocity components in specified directions at the n points. In order to determine the consequences of the above symmetry conditions, note that the typical member (of order m, $m \geq n$) of the set of mean values of the velocity product derived from the joint probability distribution of the velocities at n points is

$$Q^{(m)}_{ij\ldots p}(r,s,\ldots,t) = \left\langle u_i(x_1,t)\, u_j(x_2,t) \ldots u_p(x_m,t) \right\rangle, \tag{44}$$

where

---

[2]The concept of homogeneous and isotropic turbulence is introduced in order to separate individual macroscopic effects connected with the geometry of the particular system and the mechanism of turbulence generation from the more universal behavior at small scales.

$$r = x_2 - x_1, \quad s = x_3 - x_2, \quad \text{etc.}$$

The invariance of the joint probability distribution function with respect to arbitrary translations and rigid–body rotations and reflections of the configuration formed by $r,s,\ldots$ implies that $Q^{(m)}_{ij\ldots p}(r,s,\ldots,t)$ can be expressed in terms of the fundamental invariants, under the same operation, of $r,s,\ldots$. Therefore,

$$Q^{(m)}_{ij\ldots p}(r,s,\ldots,t) = \sum A\left(r^2, s^2, r\cdot s, \ldots\right) r_i s_j \ldots \tag{45}$$

In particular,

$$\begin{aligned} Q_i(r) &= A r_i, \\ Q_{ij}(r) &= A r_i r_j + B\delta_{ij}, \\ Q_{ijk}(r) &= A r_i r_j r_k + B r_i \delta_{jk} + C r_j \delta_{ki} + D r_k \delta_{ij}, \\ &\text{etc.,} \end{aligned} \tag{46}$$

where the scalar functions A, B, C, D, etc., are all even functions of r.

$u_k(x,t)$ is said to be a stationary random variable if the associated many–time probability distribution depends only on the differences between measuring times and not on their absolute values.

Spectral Theory

According to the cascade process advanced by Richardson, large vortices in turbulence break up via the mechanism of vortex stretching into smaller vortices which themselves break up into still smaller scales, and so on until viscous effects take over and turbulence is damped out.

Fourier analysis of the velocity field, when it is a stationary random function of position, affords a convenient identification of the scales of motion with Fourier modes and a view of the turbulent motion as comprised of the superposition of motions of a large number of components of different length scales. These Fourier components contribute additively to the total energy and interact with each other according to the nonlinear inertial terms in the equations of flow. The observed properties of the turbulent field are thought of as being the statistical result of such interactions. It should be noted that Fourier representation is natural for infinitely extended homogeneous turbulent fields but not for inhomogeneous flows for which there is only a weak relation between the structure in real space and the Fourier modes.

It is convenient to work with the Fourier components in a box of side L and apply periodic boundary conditions. One may then express the flow properties at any point x at time t, as a superposition of plane waves of the form

$$\left.\begin{aligned} \boldsymbol{v}(\boldsymbol{x},t) &= \sum_{\boldsymbol{k}} \boldsymbol{V}(\boldsymbol{k},t)\, e^{i\boldsymbol{k}\cdot\boldsymbol{x}}, \\ \frac{1}{\rho}\, p(\boldsymbol{x},t) &= \sum_{\boldsymbol{k}} P(\boldsymbol{k},t)\, e^{i\boldsymbol{k}\cdot\boldsymbol{x}}, \end{aligned}\right\} \tag{47}$$

where the summation is over all wavenumbers permitted by the cyclic boundary conditions. If L is finite, the wavevector $\boldsymbol{k}$ is an infinite but countable sequence, while if L is infinite, $\boldsymbol{k}$ will be a continuous variable. Note that $\boldsymbol{v}$ and p are actually measurable so that

$$\boldsymbol{V}(-\boldsymbol{k}) = \boldsymbol{V}^*(\boldsymbol{k}), \qquad P(-\boldsymbol{k}) = P^*(\boldsymbol{k}).$$

Here, and in the following, we are dropping the argument t for convenience.

When we use equation (47), equations (1) and (2) give

$$k_\alpha V_\alpha(-\boldsymbol{k}) = 0, \tag{48}$$

$$\left(\frac{\partial}{\partial t} + \nu k^2\right) V_\alpha(\boldsymbol{k}) = -ik_\alpha P(\boldsymbol{k}) - ik_\beta \sum_j V_\alpha(\boldsymbol{k}-\boldsymbol{j}) V_\beta(\boldsymbol{j}). \tag{49}$$

Multiplying equation (49) by k_α, summing over α and using equation (48), we obtain

$$k^2 P(\boldsymbol{k}) = -k_\alpha k_\beta \sum_j V_\alpha(\boldsymbol{k}-\boldsymbol{j}) V_\beta(\boldsymbol{j}). \tag{50}$$

When we use equation (50), equation (49) becomes

$$\left(\frac{\partial}{\partial t} + \nu k^2\right) V_\alpha(\boldsymbol{k}) = \frac{1}{i} D_{\alpha\gamma}(\boldsymbol{k}) k_\beta \sum_j V_\beta(\boldsymbol{j}) V_\gamma(\boldsymbol{k}-\boldsymbol{j}), \tag{51}$$

where $D_{\alpha\gamma}(\boldsymbol{k})$ is the transverse projection operator,

$$D_{\alpha\gamma}(\boldsymbol{k}) \equiv \delta_{\alpha\gamma} - \frac{k_\alpha k_\gamma}{|\boldsymbol{k}|^2}.$$

Now, the symmetry of the right-hand side in equation (52) with respect to the indices β and γ may be made explicit by introducing the symmetrized transverse projection operator $M_{\alpha\beta\gamma}(\boldsymbol{k})$:

$$M_{\alpha\beta\gamma}(\boldsymbol{k}) \equiv \frac{1}{2i}\left[k_\beta D_{\alpha\gamma}(\boldsymbol{k}) + k_\gamma D_{\alpha\beta}(\boldsymbol{k})\right].$$

Equation (51) may then be rewritten as

$$\left(\frac{\partial}{\partial t} + \nu k^2\right) V_\alpha(\boldsymbol{k}) = M_{\alpha\beta\gamma}(\boldsymbol{k}) \sum_j V_\beta(\boldsymbol{j}) V_\gamma(\boldsymbol{k}-\boldsymbol{j}). \tag{52}$$

Now, note that

$$\left\langle V_\alpha(k) V_\beta(k') \right\rangle = \frac{1}{L^6} \int\int dx\, dx' \left\langle V_\alpha(x,t) V_\beta(x',t) \right\rangle e^{-ik\cdot x - ik'\cdot x'}.$$

If the turbulence is spatially homogeneous, then we obtain

$$\left\langle V_\alpha(x,t) V_\beta(x',t) \right\rangle = Q_{\alpha\beta}(r,t),\ r = x - x'$$

so that

$$\left\langle V_\alpha(k) V_\beta(k') \right\rangle = \frac{1}{L^6} \int\int dx\, dr\ Q_{\alpha\beta}(r)\, e^{-i(k+k')\cdot x + ik'\cdot r}$$

$$= \left(\frac{2\pi}{L}\right)^3 \delta_{k+k',0}\ Q_{\alpha\beta}(k). \tag{53a}$$

Similarly,

$$\left\langle V_\alpha(k) V_\beta(k') V_\gamma(k'') \right\rangle = \left(\frac{2\pi}{L}\right)^6 \delta_{k+k'+k'',0}\ Q_{\alpha\beta\gamma}(k,k'). \tag{53b}$$

Taking the average of equation (52) and using equation (53), we have

$$\left(\frac{\partial}{\partial t} + \nu k^2\right) \left\langle V_\alpha(k) \right\rangle = \left(\frac{2\pi}{L}\right)^3 M_{\alpha\beta\gamma}(k)\, \delta_{k,0} = 0,$$

which is apparent since, for a spatially homogeneous turbulence, the mean velocity is either zero or constant over all space.

Next, when we multiply equation (52) by $V_\sigma(-k)$ and a similar equation for $V_\sigma(-k)$ by $V_\alpha(k)$, add the two, and take the average, we obtain

$$\left(\frac{\partial}{\partial t} + 2\nu k^2\right) \left\langle V_\alpha(k) V_\sigma(-k) \right\rangle = M_{\alpha\beta\gamma}(k) \sum_j \left\langle V_\beta(j) V_\gamma(k-j) V_\sigma(-k) \right\rangle$$

$$+ M_{\sigma\beta\gamma}(-k) \sum_j \left\langle V_\beta(j) V_\gamma(-k-j) V_\alpha(k) \right\rangle$$

or

$$\left(\frac{\partial}{\partial t} + 2\nu k^2\right) Q_{\alpha\sigma}(k) = M_{\alpha\beta\gamma}(k) \sum_j Q_{\beta\gamma\sigma}(j, k-j)$$

$$+ M_{\sigma\beta\gamma}(-k) \sum_j Q_{\beta\gamma\alpha}(j, -k-j). \tag{54a}$$

Observe, from equation (54a) that the equation for the spectral density tensor $Q_{\alpha\beta}$ involves $Q_{\alpha\beta\gamma}$. Similarly, the equation for $Q_{\alpha\beta\gamma}$ involves $Q_{\alpha\beta\gamma\sigma}$, and so on. Thus, the equations for cumulants form an open–ended hierarchy (the closure problem). This hierarchy of equations is, therefore, useless until a suitable closure scheme is prescribed to reduce the problem to a finite set of equations.

Heisenberg's Theory

Setting $\sigma = \alpha$, we have, from equation (54a),

$$\left(\frac{\partial}{\partial t} + 2\nu k^2\right) E(\boldsymbol{k}) = \sum_{\boldsymbol{k}'} W(\boldsymbol{k},\boldsymbol{k}'), \tag{54b}$$

where

$$\left.\begin{aligned} E(\boldsymbol{k}) &\equiv \frac{1}{2}\left|V(\boldsymbol{k})\right|^2, \\ W(\boldsymbol{k},\boldsymbol{k}') &\equiv M_{\alpha\beta\gamma}(\boldsymbol{k})\, Q_{\beta\gamma\alpha}(\boldsymbol{k}',\boldsymbol{k}-\boldsymbol{k}') + M_{\alpha\beta\gamma}(-\boldsymbol{k})\, Q_{\beta\gamma\alpha}(\boldsymbol{k}',-\boldsymbol{k}-\boldsymbol{k}'). \end{aligned}\right\}$$

Equation (54b) describes the transport of the turbulent kinetic energy in the wavenumber space.

The nonlinear inertial transfer term $W_{\alpha\beta\gamma}(\boldsymbol{k},\boldsymbol{j})$ only redistributes energy in wavenumber space so that we have

$$\frac{\partial}{\partial t}\sum_{\boldsymbol{k}} E(\boldsymbol{k}) + \sum_{\boldsymbol{k}} 2\nu k^2 E(\boldsymbol{k}) = \sum_{\boldsymbol{k}}\sum_{\boldsymbol{k}'} W(\boldsymbol{k},\boldsymbol{k}') = 0.$$

Therefore, the turbulent energy dissipation rate ε is given by

$$\varepsilon = \sum_{\boldsymbol{k}} 2\nu k^2\, E(\boldsymbol{k}).$$

Now, the vortex stretching process is believed to cause the amplification of enstrophy (which is the mean square of vorticity) and the associated spectral flux of energy toward small scales. If viscosity is very small, this leads to an unlimited enstrophy explosion at infinitely small scales. Nonetheless, since the viscous dissipation of energy, ε, is given by the product of viscosity and enstrophy, it remains finite even in the limit $\nu \Rightarrow 0$. This leads to the property of inviscid dissipation of energy in three–dimensional turbulence. As a result, three–dimensional turbulence is strongly dissipative even in fluids with negligible viscosity.

Note that

$$W(\boldsymbol{k},\boldsymbol{k}') = -W(\boldsymbol{k}',\boldsymbol{k}); \tag{55}$$

thus if

$$\boldsymbol{k}' < \boldsymbol{k}: \quad W > 0,$$

then

$$\boldsymbol{k}' > \boldsymbol{k}: \quad W < 0$$

and vice versa. This is physically understood by noting that W is the contribution to the energy increase of the $\boldsymbol{k}$th mode due to nonlinear interaction with all other modes. Thus, $W > 0$ for interactions with modes of smaller wavenumbers and vice versa. Let us write

$$\sum_{k'} W(\boldsymbol{k},\boldsymbol{k}') = \sum_{k'<k} W^{(1)}(\boldsymbol{k},\boldsymbol{k}') - \sum_{k'>k} W^{(2)}(\boldsymbol{k}',\boldsymbol{k}), \tag{56a}$$

where $W^{(1)}$ denotes the energy gained from the modes with smaller wavenumbers, and $W^{(2)}$ denotes the energy loss to the modes with larger wavenumbers. Equation (56a) describes a cascade process by which energy is passed from the smallest–wavenumber modes to the largest–wavenumber modes which lose their energy by dissipation.[3]

When the volume of the flow region becomes very large, one may replace the Fourier sum by a Fourier integral. Thus, one may write

$$\sum_{k'} W(\boldsymbol{k}',\boldsymbol{k}) \equiv \int T(k',k)\,dk', \tag{56b}$$

where $T(k',k)\,dk'$ is the net energy gain by modes of wavenumber k from all modes in the range k' to $k'+dk'$. Equation (54), then, becomes

$$\left(\frac{\partial}{\partial t} + 2\nu k^2\right) E(k) = \int T(k',k)\,dk'. \tag{57}$$

Now, instead of dealing with modes of wide–ranging wavenumbers, it may be more useful to "integrate out" the modes with large wavenumbers to obtain a coarse–grained description of the flow at the integral scale. This coarse–graining leads to a renormalization of the molecular transport coefficients to include the effect of modes with large wavenumbers and is accomplished by making some assumption about the nonlinear transfer of energy across the spectrum. If one assumes, then, that the latter is of the same form as that for molecular transport (at least for modes with large wavenumbers or small eddies), then one may write

$$T(k',k) = \begin{cases} 2AE(k')k'^2\sqrt{\dfrac{E(k)}{k^3}}, & k' < k, \\ -2AE(k)k^2\sqrt{\dfrac{E(k')}{k'^3}}, & k' > k, \end{cases} \tag{58}$$

where A is a constant. Using (58) in equation (57), the rate of energy loss by modes with wavenumbers less than some value k is given by

---

[3]One assumes sometimes, as in the Kolmogorov theory, that the nonlinear interaction among the various Fourier modes is local, i.e., $|\boldsymbol{k}|, |\boldsymbol{k}'|$ and $|\boldsymbol{k}-\boldsymbol{k}'|$ are comparable. On the other hand, numerical simulations (Ohkitani and Kida) have now confirmed that the most energetic interactions are nonlocal. However, while some distant interactions transfer large amounts of energy into a certain wavenumber, other distant interactions remove equally large amounts of energy from that wavenumber. Consequently, local interactions apparently still make a dominant contribution to the net energy transfer at a particular wavenumber, thereby validating the assumption of the statistical independence of the large- and small-scale modes in the Kolmogorov theory.

$$\int_0^k \frac{\partial E(k'')}{\partial t}\, dk'' = -2\nu \int_0^k E(k'')k''^2 dk''$$

$$-2\int_0^k dk''\, E(k'')k''^2 \int_k^\infty A\sqrt{\frac{E(k')}{k'^3}}\, dk'$$

$$= -2(\nu + \tilde{\nu}_k)\int_0^k E(k'')k''^2\, dk'', \tag{59}$$

where $\tilde{\nu}_k$ is the 'eddy viscosity' given by

$$\tilde{\nu}_k \equiv \int_k^\infty A\sqrt{\frac{E(k')}{k'^3}}\, dk'.$$

Equations (57) and (59) imply that the transfer of energy from one mode to another mode at a higher wavenumber is a cascade process which can be visualized in terms of a suitably defined eddy viscosity $\tilde{\nu}_k$. The analogy with molecular viscosity is imperfect, however, because of the presence of continuous scales of motion in a turbulent flow.

Let us now replace

$$\int_0^k \frac{\partial E(k'')}{\partial t}\, dk''$$

by the total rate of decay of energy ε if only a negligible amount of energy is contained in wavenumbers greater than k. Equation (59) then becomes

$$\varepsilon = 2\left[\nu + A\int_k^\infty \sqrt{\frac{dH(k')}{dk'}\frac{dk'}{k'^5}}\, dk'\right] H(k), \tag{60}$$

where

$$H(k) \equiv \int_0^k k''^2 E(k'')\, dk''.$$

One obtains, from equation (60),

$$\frac{dH(k)}{dk} = \frac{4A^2}{\varepsilon^2}\frac{[H(k)]^4}{k^5}. \tag{61}$$

Noting, from equation (60), that

$$k \Rightarrow \infty: \quad H \Rightarrow \frac{\varepsilon}{2\nu}, \tag{62}$$

equation (61) can be solved to give

$$[H(k)]^{-3} = \frac{3A^2}{\varepsilon^2 k^4} + \left(\frac{2\nu}{\varepsilon}\right)^3. \tag{63}$$

Therefore,

$$E(k) = \frac{\dfrac{dH(k)}{dk}}{k^2} = \left(\frac{8\varepsilon}{2A}\right)^{2/3} k^{-5/3}\left[1 + \frac{8\nu^3}{3A^2\varepsilon} k^4\right]^{-4/3}. \tag{64}$$

Equation (64) shows that for small wavenumbers we obtain

$$E(k) \sim k^{-5/3}, \tag{65}$$

whereas for large wavenumbers we have

$$E(k) \sim k^{-7}. \tag{66}$$

Equation (65) holds in the so–called inertial subrange (see below). However, (66) is not quite acceptable because it leads to the divergence of higher–order moments of the spectrum.

Kolmogorov's Universal Equilibrium Theory

We have seen that inertial effects cause a transfer of energy from modes with small wavenumbers to modes with large wavenumbers wherein this energy is dissipated by viscous damping. If the Reynolds number of the turbulent motion is sufficiently high, the viscous effects occur selectively in small–scale modes whereas the large–scale modes become independent of viscosity and are influenced only by the boundary conditions on the flow. If the energy–containing and dissipation ranges of the spectrum are widely separated so that the detailed statistical information about the large scales is degraded in the cascade, one may think of a range of wavenumbers near the upper end of the spectrum which have little connection with the details of the large–scale structure of the motion and are governed by

(1) the removal of energy by viscous dissipation chiefly at the upper end of this range;

(2) the supply of energy ε by inertial effects at the lower end of the range.

This reasoning led Kolmogorov to postulate that this range of wavenumbers will have a statistically steady, universal and isotropic structure that is determined by the parameters ε and ν. If one defines the basis length and velocity parameters

$$\eta = \left(\frac{\nu^3}{\varepsilon}\right)^{1/4}, \qquad V = (\nu\varepsilon)^{1/4} \tag{67}$$

and expresses all lengths in units of η and all velocities in units of V, the motion associated with the equilibrium[4] range of wavenumbers will have a universal statistical form.

One may then write for the correlation function

$$\left\langle \left(u_1' - u_2'\right)^2 \right\rangle \sim (\nu\varepsilon)^{1/2} G(r/\eta) \tag{68}$$

where $G(r/\eta)$ has a universal form for small values of r. If the Reynolds number is very large, Kolmogorov argued that, there is a range of r, called the *inertial subrange*, at the upper end of the universal range where the viscous effects do not play an explicit role. Equation (68), then, gives in this inertial subrange

$$\left\langle \left(u_1' - u_2'\right)^2 \right\rangle \sim (\varepsilon r)^{2/3}. \tag{69}$$

Thus, the energy spectrum is given by

$$E(k) \sim V^2 \eta H(k\eta), \tag{70}$$

where $H(k\eta)$ has a universal form for large values of k. This implies that the energy spectrum for different kinds of turbulence collapses into a single curve at large k, if it is normalized according to the similarity law. In the inertial subrange, (70) reduces to

$$E(k) \sim \varepsilon^{2/3} k^{-5/3} f(k\eta), \tag{71}$$

where the scaling function $f(x)$ is constant for small x and decays rapidly for large x.

The Kolmogorov law (71) has been verified remarkably well in experiments[5] (see Figure 6.4). The range of scales over which the Kolmogorov law (71) holds is found to increase with the Reynolds number. So, this scaling appears to be a universal asymptotic property of very–high–Reynolds–number turbulence for which the energy–containing and dissipation wavenumbers are widely separated.

Equilibrium Statistical Mechanics: Lee's Theory

Let us consider a three–dimensional turbulence within a box which can be expanded into an infinite series of discrete wave vectors $\boldsymbol{k}_n$ with velocity

---

[4]The equilibrium range is not in equilibrium in the usual statistical mechanical sense because there is no detailed balance. On the other hand, thanks to viscosity, the equilibrium range continually dissipates energy with a stationary state maintained due to the shortness of the characteristic time scales compared with large-scale evolutionary times so that the high-wavenumber modes adjust themselves rapidly to changing conditions in the mean flow.

[5]Experiments are typically limited to a one-dimensional surrogate for the local energy dissipation given by

$$\varepsilon = 15\nu\left(\frac{\partial u}{\partial x}\right)^2.$$

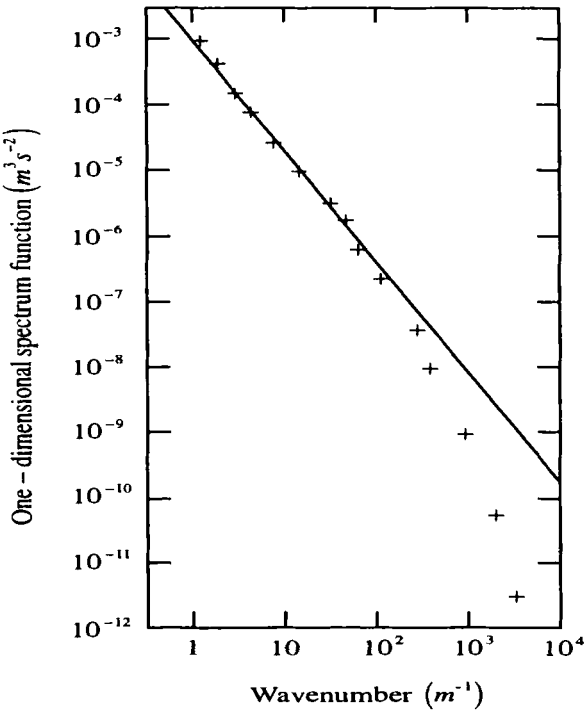

Figure 6.4. One–dimensional spectrum measured in a tidal channel; line has slope of $-5/3$. Data from Grant el al. (1962) plotted by Tritton (1988).

amplitudes $\boldsymbol{V}(\boldsymbol{k}_n, t)$ related by Euler's equations in Fourier space. These equations are truncated[6] by retaining the modes lower than a cutoff wavenumber $k_{\max}$ (so as to preserve the validity of the inviscid model) and are suitably normalized to give for the velocity amplitude

$$\frac{\partial}{\partial t} V_i(\boldsymbol{k}) = -\frac{i}{2} P_{ijm} \sum_{\boldsymbol{k}=\boldsymbol{k}'+\boldsymbol{k}''} V_j(\boldsymbol{k}', t) V_m(\boldsymbol{k}'', t), \tag{51}$$

where

$$P_{ijm} \equiv k_j \left(\delta_{im} - \frac{k_i k_m}{k^2} \right).$$

Let $y_{n_1}(t)$ and $y_{n_2}(t)$ be the real and imaginary parts of each mode $\boldsymbol{V}(\boldsymbol{k}_n)$. Then, if the truncated system contains N wave vectors, the system can be

[6]Thanks to the detailed balance relations for the triadic interactions satisfying $\boldsymbol{k} = \boldsymbol{k}' + \boldsymbol{k}''$ the quadratic invariants like the kinetic energy are sufficiently robust or "rugged" to survive this truncation.

represented by a point of $4N$ coordinates $y_{n_i}(t)$ $(i=1,2)$ in a phase space determined by $y_\alpha(t)(\alpha=1,\ldots,4N)$.

Equation (51) conserves the kinetic energy

$$\frac{1}{2}\sum_{k_n}\left|V(k_n)\right|^2=\frac{1}{2}\sum_{\alpha=1}^{4N}y_\alpha^2(t), \tag{72}$$

which implies that the system evolves ergodically in the phase space on a sphere of radius equal to the initial kinetic energy. Let us consider a collection of such systems which is represented at each instant of time by a cluster of points in the phase space of density $\rho(y_1,\ldots,y_{4N},t)$ in the phase space. Since the total number of such systems and hence the volumes are preserved as they wander around in the phase space, we have the Liouville Theorem:

$$\frac{\partial\rho}{\partial t}+\sum_{\alpha=1}^{4N}\frac{dy_\alpha}{dt}\frac{\partial\rho}{\partial y_\alpha}=0. \tag{73}$$

The Liouville Theorem is crucial to the statistical formulation since it determines the measure in the phase space.

Ergodicity on surfaces of constant kinetic energy implies that an arbitrary smooth initial ensemble on this surface converges weakly (i.e., finite–order moments of the distribution converge) to a uniform distribution over the energy surface. The distribution does not itself become uniform everywhere but rather develops a fine–grained structure. The typical approach of statistical mechanics is to explain the statistical behavior of a system in terms of its structural properties, like the conservation of energy, which specify representative ensembles pertinent to the system. This would allow one to study the equilibrium spectra of three–dimensional turbulence from the viewpoint of canonical ensemble averages.

By the elementary Gibbsian methods of statistical mechanics, equilibrium solutions of equation (73) are constructed as functions of the conserved quantities and are given by the Boltzmann–type distribution, which will be uniform over the surface of constant total energy given by (72),

$$P(y_1,\ldots,y_{4N})=\frac{1}{Z}\,e^{-\frac{1}{2}\sigma\sum_{\alpha=1}^{4N}y_\alpha^2}, \tag{74}$$

where σ is a positive constant and Z is the partition function of the system

$$Z=\int\cdots\int e^{-\frac{1}{2}\sigma\sum_{\alpha=1}^{4N}y_\alpha^2}dy_1\ldots dy_{4N}. \tag{75}$$

One then assumes that the canonical ensemble average $\langle\rho(y_1,\ldots,y_{4N},t)\rangle$ of an ensemble of given systems $\rho(y_1,\ldots,y_{4N},t)$ obeying equations (52) and (73) will eventually relax toward the equilibrium distribution (74) over the entire region of phase space permitted by the total energy constant (72).

The mean variance of the mode "α" of the velocity is given by

$$\left\langle y_\alpha^2(t)\right\rangle = \frac{1}{Z}\int\cdots\int y_\alpha^2\, e^{-\frac{1}{2}\sigma\sum_{\beta=1}^{4N} y_\beta^2}\, dy_1 \ldots dy_{4N} = \frac{1}{\sigma} \tag{76}$$

which turns out to be independent of α. Thus, there is an equipartition of energy among the modes $\alpha = 1,\ldots,4N$. Since the number of modes is, in three dimensions proportional to $4\pi k^2$, the energy spectrum $E(k)$ is proportional to k^2. This shows an accumulation of energy at $k_{\max}$ and an ultraviolet catastrophe in the absence of a high wavenumber cut–off.

Though an inviscid finite system has here been seen to evolve towards an equipartition of energy among all Fourier modes, real flows behave quite differently and evolve toward the Kolmogorov scaling law

$$E(k) \sim k^{-5/3} \tag{71}$$

in the energy cascade. Thus, truncation of the modes acts as a barrier preventing possible cascades and can produce a significant alteration in the statistical properties of the system.

Homogeneous, Isotropic Turbulence: Taylor's Correlation Theory

We consider here a turbulence with zero mean so that the primes are unnecessary. The velocity correlation tensor for two points separated by a distance $\boldsymbol{r}$ is

$$R_{ij}(\boldsymbol{r}) = \left\langle u_i(x)u_j(x+r)\right\rangle. \tag{77}$$

In a homogeneous turbulence, one has

$$R_{ij}(\boldsymbol{r}) = R_{ji}(-\boldsymbol{r}). \tag{78}$$

The energy spectrum tensor $\Phi_{ij}(\boldsymbol{k})$ is the Fourier transform of the correlation tensor

$$\Phi_{ij}(\boldsymbol{k}) = \int R_{ij}(\boldsymbol{r})e^{-i\boldsymbol{k}\cdot\boldsymbol{r}}\frac{d\boldsymbol{r}}{\left(8\pi^3\right)^{1/2}}, \tag{79}$$

where

$$R_{ij}(\boldsymbol{r}) = \int \Phi_{ij}(\boldsymbol{k})e^{-i\boldsymbol{k}\cdot\boldsymbol{r}}\frac{d\boldsymbol{k}}{\left(8\pi^3\right)^{1/2}}.$$

Note that $\Phi_{ij}(\boldsymbol{k})$ possesses Hermitian symmetry

$$\Phi_{ij}(\boldsymbol{k}) = \Phi_{ji}(-\boldsymbol{k}) = \Phi_{ji}^*(\boldsymbol{k}). \tag{80}$$

Further,

$$R_{ij}(0) = \left\langle u_i(x)u_j(x)\right\rangle = \int \Phi_{ij}(\boldsymbol{k})\frac{d\boldsymbol{k}}{\left(8\pi^3\right)^{1/2}} \tag{81}$$

so that $\Phi_{ij}(\boldsymbol{k})$ represents a density in the wavenumber space of contributions to $\langle u_i(\boldsymbol{x})u_j(\boldsymbol{x})\rangle$ and thus describes a distribution of kinetic energy over the Fourier spectrum, and is, therefore, called the *energy spectrum tensor.*

In isotropic turbulence, note, from (46), that

$$R_{ij}(\boldsymbol{r}) = F(r)r_i r_j + G(r)\delta_{ij}. \tag{82}$$

The solenoidal condition on the velocity field then gives

$$\frac{\partial R_{ij}}{\partial r_i} = r_j\left(4F + rF' + \frac{1}{4}G'\right) = 0$$

or

$$4F + rF' + \frac{1}{4}G' = 0 \tag{83}$$

where primes denote differentiation with respect to the argument.

Introduce longitudinal and lateral velocity correlation coefficients (see Figure 6.5)

$$\left.\begin{aligned} f(r) &= \frac{1}{\langle u_p^2\rangle}\langle u_p(\boldsymbol{x})u_p(\boldsymbol{x}+\boldsymbol{r})\rangle, \\ g(r) &= \frac{1}{\langle u_n^2\rangle}\langle u_n(\boldsymbol{x})u_n(\boldsymbol{x}+\boldsymbol{r})\rangle, \end{aligned}\right\} \tag{84}$$

where u_p and u_n are the velocity components parallel and perpendicular to r, and $\langle u_p^2\rangle = \langle u_n^2\rangle = u^2$. Note, from (77) and (82), that

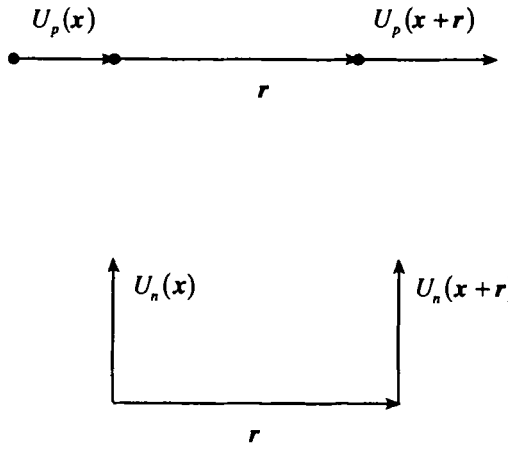

Figure 6.5. Longitudinal and lateral velocity correlations.

$$\left.\begin{aligned}\langle u_p(\boldsymbol{x})u_p(\boldsymbol{x}+\boldsymbol{r})\rangle &= r^2F(r)+G(r)=u^2f(r),\\ \langle u_n(\boldsymbol{x})u_n(\boldsymbol{x}+\boldsymbol{r})\rangle &= G(r)=u^2g(r).\end{aligned}\right\}. \tag{85}$$

When we use (85) and (83), (82) becomes

$$R_{ij}(r)=u^2\left(\frac{f-g}{r^2}\,r_ir_j+g\delta_{ij}\right)=u^2\left[-\frac{f'}{2r}r_ir_j+\left(f+\frac{1}{2}rf'\right)\delta_{ij}\right]. \tag{86}$$

Now, the homogeneity condition

$$\frac{\partial}{\partial x_j}\left(\langle u_i^2\rangle\right)=0 \tag{87}$$

implies that $f(r)$ is an even function of r. Let us expand $f(r)$ and $g(r)$ as a Taylor series in powers of r, about $r=0$, where they reach their maxima:

$$\left.\begin{aligned}f(r)&=1+\frac{1}{2}f_0''\cdot r^2+\cdots,\\ g(r)&=1+\frac{1}{2}g_0''\cdot r^2+\cdots,\end{aligned}\right\} \tag{88}$$

where the subscript 0 refers to values at $r=0$, and

$$f_0'', g_0''<0.$$

Note, from (85) and (83), that

$$\int_0^\infty r^m g(r)\,dr=\int_0^\infty r^m\left(f+\frac{1}{2}rf'\right)dr=\left(\frac{1-m}{2}\right)\int_0^\infty r^m f(r)\,dr, \tag{89}$$

where we assumed that $f(r)$ vanishes rapidly enough as $r\Rightarrow\infty$. Thus,

$$\int_0^\infty rg(r)\,dr=0, \tag{90}$$

$$m>1:\quad \int_0^\infty r^m g(r)\,dr<0. \tag{91}$$

This leads to a graphical representation in Figure 6.6.

Next, one has for the energy spectrum tensor

$$\Phi_{ij}(k)=A(k)k_ik_j+B(k)\delta_{ij}. \tag{92}$$

Then, the condition (49) gives

$$k_j\Phi_{ij}=0. \tag{93}$$

When we use (92), (93) gives

$$B=-k^2A \tag{94}$$

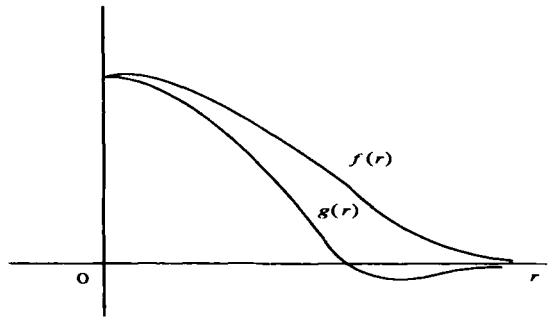

Figure 6.6. Scalars characterizing longitudinal and lateral velocity coefficients (from Batchelor, 1953).

so that the density in the wavenumber space of contributions to the total energy is

$$\frac{1}{2}\Phi_{ii}(k) = -k^2 A(k). \tag{95}$$

The contribution to the total energy from that part of wavenumber space between spheres of radii k and $k + dk$ is $E(k)\,dk$, so

$$E(k) = 4\pi k^2 \cdot \frac{1}{2}\Phi_{ii}(k) = -4\pi k^4 A(k). \tag{96}$$

When we use (94) and (96), equation (92) becomes

$$\Phi_{ij}(k) = \frac{E(k)}{4\pi k^4}\left(k^2\delta_{ij} - k_i k_j\right), \tag{97}$$

from which

$$\Phi_{ii}(k) = \frac{E(k)}{2\pi k^2} = \frac{1}{\left(8\pi^3\right)^{1/2}} \int R_{ii}(r) e^{-ik\cdot r}\, dr. \tag{98}$$

If $R_{ii}(r) = 2R(r)$, then (98) gives

$$E(k) = (32\pi)^{1/2} \int_0^\infty R(r)\, kr \sin kr\, dr, \tag{99a}$$

$$R(r) = \frac{1}{\left(8\pi^3\right)^{1/2}} \int_0^\infty E(k) \frac{\sin kr}{kr}\, dk. \tag{99b}$$

Since from (86) and (85) we obtain

$$R_{ii}(r) = u^2(f + 2g) = u^2(3f + rf'), \tag{100}$$

(99a) gives

$$E(k) = (4\pi)^{1/2} \int_0^\infty u^2 f(r) k^2 r^2 \left(\frac{\sin kr}{kr} - \cos kr \right) dr, \tag{101a}$$

$$u^2 f(r) = \frac{1}{(4\pi^3)^{1/2}} \int_0^\infty E(k) \frac{1}{k^2 r^2} \left(\frac{\sin kr}{kr} - \cos kr \right) dk. \tag{101b}$$

The longitudinal one–dimensional spectrum function, on using (97), becomes

$$\phi(k_1) = \frac{1}{\sqrt{2\pi}} \int_{-\infty}^\infty R_{11}(r_1, 0, 0) e^{-ik_1 r_1} dr_1 = \frac{1}{\sqrt{2\pi}} \int_{-\infty}^\infty u^2 f(r_1) \cos k_1 r_1 dr_1$$

$$= \frac{1}{2\pi} \int_{-\infty}^\infty \int_{-\infty}^\infty \Phi_{11}(k_1, k_2, k_3)\, dk_2 dk_3 = \frac{1}{4\pi} \int_{k_1}^\infty \left(1 - \frac{k_1^2}{k^2} \right) \frac{E(k)}{k} dk. \tag{102}$$

Next, the lateral one–dimensional spectrum function is similarly calculated as

$$\psi(k_1) = \frac{1}{\sqrt{2\pi}} \int_{-\infty}^\infty R_{22}(r_1, 0, 0) e^{-ik_1 r_1} dr_1 = \frac{1}{\sqrt{2\pi}} \int_{-\infty}^\infty u^2 g(r_1) \cos k_1 r_1 dr_1$$

$$= \frac{1}{2\pi} \int_{-\infty}^\infty \int_{-\infty}^\infty \Phi_{22}(k_1, k_2, k_3) dk_2 dk_3 = \frac{1}{8\pi} \int_{k_1}^\infty \left(1 + \frac{k_1^2}{k^2} \right) \frac{E(k)}{k} dk$$

$$= \frac{\phi(k_1)}{2} - \frac{k_1}{2} \cdot \frac{d\phi(k_1)}{dk_1}. \tag{103}$$

Note the relation between the derivatives of $E(k)$ at $k = 0$ and the integral moments of $R(r)$ (use (99) and (100)):

$$\left(\frac{d^{2m} E(k)}{dk^{2m}} \right)_{k=0} = 8m\sqrt{2\pi}\, (-1)^{m+1} \int_0^\infty r^{2m} R(r) dr, \qquad m = 1, 2, \ldots$$

$$= 8m\sqrt{2\pi}\, (m-1)(-1)^m u^2 \int_0^\infty r^{2m} f(r) dr. \tag{104}$$

Note, from (99)–(101), that

$$\int_0^\infty R(r) dr = u^2 \int_0^\infty f(r) dr = \frac{\pi}{2} \int_0^\infty \frac{E(k)}{k} dk, \tag{105}$$

$$u^2 \int_0^\infty r^2 f(r) dr = \pi \int_0^\infty \frac{E(k)}{k^3} dk. \tag{106}$$

Recall, from (96), that

$$E(k) = Ck^4 + 0(k^6), \tag{107}$$

where C is a constant. Using (107), (104) gives

$$C = \frac{2}{3}\sqrt{2\pi}\, u^2 \int_0^\infty r^4 f(r)\, dr. \tag{108}$$

Next, one obtains from (100) and (101)

$$\left[\frac{d^{2m}R(r)}{dr^{2m}}\right]_{r=0} = \frac{1}{2}(2m+3)u^2\left[\frac{\partial^{2m}f(r)}{\partial r^{2m}}\right]_{r=0}$$

$$= \frac{(-1)^m}{2m+1}\frac{1}{\left(8\pi^3\right)^{1/2}}\int_0^\infty k^{2m}E(k)\, dk, \tag{109}$$

from which

$$-\left(\frac{d^2 f}{dr^2}\right)_{r=0} = \frac{2}{15u^2}\frac{1}{\left(8\pi^3\right)^{1/2}}\int_0^\infty k^2 E(k)\, dk, \tag{110}$$

which shows how the dispersion of the energy in wavenumber space determines the radius of curvature of the correlation curves at $r = 0$.

Consider, finally, the third–order correlation tensor

$$S_{ijl}(\boldsymbol{r}) = \left\langle u_i(\boldsymbol{x})u_j(\boldsymbol{x})u_l(\boldsymbol{x}+\boldsymbol{r})\right\rangle. \tag{111}$$

For isotropic turbulence, one has from (46)

$$S_{ijl}(\boldsymbol{r}) = Ar_i r_j r_l + B\left(r_i\delta_{jl} + r_j\delta_{il}\right) + Dr_l\delta_{ij}. \tag{112}$$

The solenoidal condition on the velocity field gives

$$\frac{\partial S_{ijl}}{\partial r_l} = 0. \tag{113}$$

Using (112), this gives, in turn,

$$\left(5A + rA' + \frac{2}{r}B'\right)r_i r_j + \left(2B + 3D + rD'\right)\delta_{ij} = 0, \tag{114}$$

from which

$$5A + rA' + \frac{2}{r}B' = 0, \tag{115}$$

$$2B + 3D + rD' = 0. \tag{116}$$

Now, note that S_{iil} is a first–order isotropic tensor so that, from (46), it may be written as

$$S_{iil} = A(r)r_l. \tag{117}$$

Thus the solenoidal condition on the velocity field gives

$$\frac{\partial}{\partial r_l} S_{iil} = 0. \tag{118}$$

When we use (117), (118) gives

$$3A + rA' = 0, \tag{119}$$

from which

$$A = \frac{C}{r^3}, \tag{120}$$

where C is a constant. In order to have a smooth behavior, one then has to prescribe $C = 0$. Therefore,

$$S_{iil} \equiv 0. \tag{121}$$

When we use (112), (121) gives

$$r^2 A + 2B + 3D = 0. \tag{122}$$

When we solve (115), (116), and (122), one obtains

$$A = \frac{1}{r} D', \qquad B = -\frac{1}{2}(3D + rD'). \tag{123}$$

Introduce a specific third–order correlation (see Figure 6.7)

$$\left\langle u_n^2(\boldsymbol{x}) u_p(\boldsymbol{x}+\boldsymbol{r}) \right\rangle \equiv u^3 h(\boldsymbol{r}); \tag{124}$$

then, from (101), one has

$$u^3 h(\boldsymbol{r}) = rD(\boldsymbol{r}). \tag{125}$$

When we use (123) and (125), (112) becomes

$$S_{ijl} = u^3 \left[\frac{rh' - h}{r^3} r_i r_j r_l - \frac{rh' + 2h}{2r} \left(r_j \delta_{il} + r_i \delta_{jl} \right) + \frac{h}{r} r_l \delta_{ij} \right] \tag{126}$$

The experimentally measured double and triple correlations are shown in Figure 6.8.

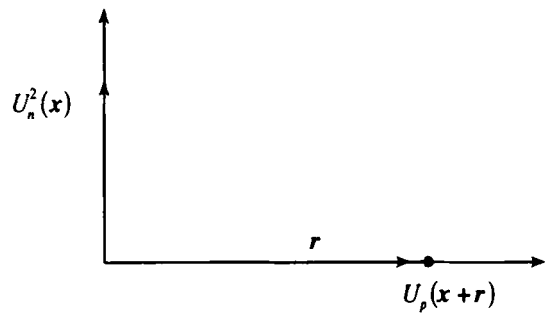

Figure 6.7. A third–order velocity correlation.

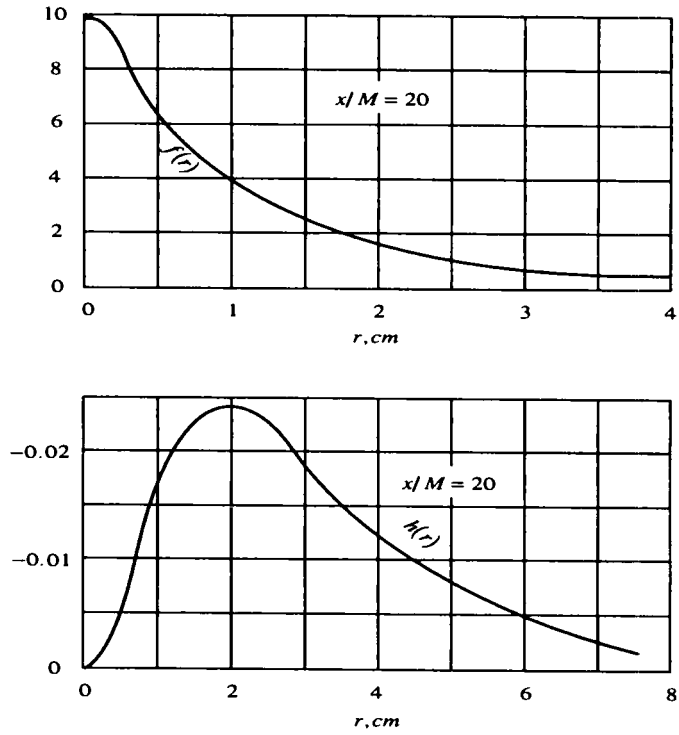

Figure 6.8. Top, double, and triple correlation functions involving velocity fluctuation u behind a heated grid set perpendicular to a uniform air stream (from Kistler et al., 1956). Here, x and r denote distance in the direction of the stream, and M is the mesh width of the grid.

Introduce the Fourier transforms of $S_{ijl}(\boldsymbol{r})$:

$$Y_{ijl}(k) = \frac{1}{8\pi^3} \int S_{ijl}(\boldsymbol{r}) e^{-i\boldsymbol{k}\cdot\boldsymbol{r}} d\boldsymbol{r}. \tag{127}$$

Then, from equation (113), one obtains

$$k_l Y_{ijl}(k) = 0. \tag{128}$$

Using (128), one may express $Y_{ijl}(\boldsymbol{k})$ as

$$Y_{ijl}(\boldsymbol{k}) = iY(k)\left[k_i k_j k_l - \frac{1}{2}k^2 k_i \delta_{jl} - \frac{1}{2}k^2 k_j \delta_{il}\right]. \tag{129}$$

Noting, from (126), that

$$S_{iji}(\boldsymbol{r}) = -u^3\left(h' + 4\frac{h}{r}\right)r_j = \frac{1}{2}H(r)r_j, \text{ say,} \tag{130}$$

one has

$$Y_{iji}(k) = \frac{1}{\left(32\pi^3\right)^{1/2}} \int H(r) r_j e^{-ik\cdot r} dr$$

$$= \frac{i}{\left(32\pi^3\right)^{1/2}} \frac{\partial}{\partial k_j} \left[\int H(r) e^{-ik\cdot r} dr\right]$$

$$= \frac{i}{\sqrt{2\pi}} \frac{\partial}{\partial k_j} \left[\int_0^\infty H(r)\, r^2 \frac{\sin kr}{kr}\, dr\right]$$

$$= -\frac{i}{\sqrt{2\pi}} \frac{k_j}{k^2} \int_0^\infty \frac{\partial\left(r^3 H\right)}{\partial r} \frac{\sin kr}{kr}\, dr. \tag{131}$$

Using (129), one then obtains

$$Y(k) = \frac{1}{\sqrt{2\pi}} \frac{1}{k^6} \int_0^\infty \left(r\frac{\partial}{\partial r} + 3\right) H(r) kr \sin kr\, dr. \tag{132}$$

The von Kármán–Howarth Equation

We have just seen that the correlations of the components of the velocities at two points and three points can each be expressed in terms of single scalar functions when the turbulence is isotropic. We shall see below that the Navier–Stokes equation provides a differential equation connecting these two scalar functions.

Let us here use the notation

$$u_i' \equiv u_i(x + r).$$

Multiply equation (2) for u_i by u_i', and vice versa, average, and add the two; one then obtains

$$\frac{\partial}{\partial t}\left\langle u_i u_j' \right\rangle + \frac{\partial}{\partial x_k}\left\langle u_i u_k u_j \right\rangle + \frac{\partial}{\partial x_k'}\left\langle u_i u_j' u_k' \right\rangle$$

$$+ \frac{1}{\rho}\left(\left\langle u_j' \frac{\partial p}{\partial x}\right\rangle + \left\langle u_i \frac{\partial p'}{\partial x_j'}\right\rangle\right) = \nu\left(\left\langle u_i \nabla'^2 u_j' \right\rangle + \left\langle u_j' \nabla^2 u_i \right\rangle\right), \tag{133}$$

which may be written as

$$\frac{\partial}{\partial t} R_{ij} = T_{ij} + P_{ij} + 2\nu\nabla^2 R_{ij}, \tag{134}$$

where

$$\left.\begin{aligned} T_{ij} &= -\frac{\partial}{\partial x_k}\left\langle u_i u_k u_j' \right\rangle - \frac{\partial}{\partial x_k'}\left\langle u_i u_j' u_k' \right\rangle = \frac{\partial}{\partial r_k}\left\langle u_i u_k u_j' - u_i u_j' u_k' \right\rangle, \\ P_{ij} &= -\frac{1}{\rho}\left(\left\langle u_j' \frac{\partial p}{\partial x_i}\right\rangle + \left\langle u_i \frac{\partial p'}{\partial x_j'}\right\rangle\right) = \frac{1}{\rho}\left[\frac{\partial}{\partial r_i}\left\langle p u_j' \right\rangle - \frac{\partial}{\partial r_j}\left\langle p' u_i \right\rangle\right]. \end{aligned}\right\}$$

Now $\left\langle p u_j' \right\rangle$ is a solenoidal first–order isotropic tensor, so, as in (121), it is identically zero. Therefore,

$$P_{ij} \equiv 0. \tag{135}$$

Next, note from (130) that

$$T_{ii} = \frac{\partial}{\partial r_k}\left[S_{iki}(\boldsymbol{r}) - S_{iki}(-\boldsymbol{r})\right] = 2\frac{\partial}{\partial r_k} S_{iki}(\boldsymbol{r}) = \left(rH' + 3H\right). \tag{136}$$

Let

$$\nabla^2 R_{ij} = u^2\left[\left(s + \frac{1}{2}rs'\right)\delta_{ij} - \frac{1}{2r}\, s' r_i r_j\right] \tag{137}$$

so that

$$\nabla^2 R_{ii} = u^2\left(3s + rs'\right). \tag{138}$$

But, from (100), one has

$$\nabla^2 R_{ii} = u^2 \frac{1}{r^2}\frac{\partial}{\partial r}\left[r^2 \frac{\partial}{\partial r}\left(3f + rf'\right)\right]. \tag{139}$$

Comparing (138) with (139), one obtains

$$s = f'' + \frac{4}{r} f'. \tag{140}$$

Then, contracting the subscripts i and j in equation (134), using (100), (135), (136), and (138), one obtains

$$\frac{\partial}{\partial t}\left[u^2\left(3f + rf'\right)\right] = \left(3H + rH'\right) + 2\nu u^2\left(3s + rs'\right). \tag{141}$$

An obvious first integral of equation (141) is

$$\frac{\partial}{\partial t}\left(u^2 f\right) = H + 2\nu u^2 s. \tag{142}$$

On using (130) and (140), equation (142) becomes

$$\frac{\partial}{\partial t}\left(u^2 f\right) = -2u^3\left(h' + \frac{4}{r}h\right) + 2\nu u^2\left(f'' + \frac{4}{r}f'\right), \tag{143}$$

which is the von Kármán–Howarth equation. Noting that equation (143) can be written as

$$\frac{\partial}{\partial t}\left(u^2 f\right)+2u^3\frac{1}{r^4}\frac{\partial}{\partial r}\left(r^4 h\right)=2\nu u^2\frac{1}{r^4}\frac{\partial}{\partial r}\left(r^4\frac{\partial f}{\partial r}\right), \tag{144}$$

we have

$$\frac{\partial}{\partial t}\left(u^2\int_0^\infty r^4 f(r)\,dr\right)=0$$

and hence the integral invariant –

$$u^2\int_0^\infty r^4 f(r)\,dr=\text{const.}, \tag{145}$$

which is called *Loitsiansky's invariant*. From (107) and (108), physically, this implies the permanence of the spectral density at very low wavenumbers.

6.3. Two–Dimensional Turbulence

A principal reason for interest in two–dimensional turbulence is the possibility of applying the theory to planetary boundary layers. Strictly two–dimensional flow in a layer of fluid requires that the velocity vector everywhere lie in a given plane and that there be no variation of the velocity field perpendicular to that plane. On a global scale, the earth's atmosphere and oceans are a very thin layer so that it is reasonable to expect two–dimensional motion on scales large compared with the layer thickness. Besides, the rotation of the earth plays a crucial role in preserving the two–dimensional nature of the motion. (This follows from the Taylor–Proudman Theorem (see Section 2.5), which shows that uniform rotation of a plane layer of fluid about an axis, say z–axis, perpendicular to the plane tends to lock the fluid into two–dimensional motion independent of z.)

Two inertial ranges become possible in a two–dimensional turbulence: the energy subrange in which energy propagates to larger scales, and the enstrophy subrange in which enstrophy cascades to smaller scales. Kraichnan and Batchelor invoked arguments similar to those used in Kolmogorov's theory of three–dimensional isotropic hydrodynamic turbulence to surmise that if the Reynolds number is sufficiently high the large–scale components are influenced only by the boundary conditions on the system. The statistical properties of the small–scale components of velocity and vorticity fields in the inertial range were assumed to have some universality and to be uniquely determined by the mean energy and enstrophy dissipation rates ε and τ, respectively, and the kinematic viscosity ν and to depend only weakly on the large–scale features of these fields. By using dimensional arguments, $k^{-5/3}$ and k^{-3} power laws were derived for the spectrum of kinetic energy density of the fluctuations in the stationary state for the energy subrange and enstrophy subrange, respectively (see below).

Conserved Quantities for a Two-Dimensional Flow

The Navier–Stokes equations for an incompressible fluid are

$$\nabla \cdot \mathbf{v} = 0, \tag{1}$$

$$\frac{\partial \mathbf{v}}{\partial t} + (\mathbf{v} \cdot \nabla)\mathbf{v} = -\nabla\left(\frac{p}{\rho}\right) + \nu \nabla^2 \mathbf{v}. \tag{2}$$

Equations (1) and (2) are known to be well–posed in the following sense. If the initial vorticity field is Hölder continuous and the initial velocity is C^n, then the velocity field will remain so for all finite time. Taking the curl of equation (2) and using equation (1), we find that the vorticity $\boldsymbol{\Omega} = \nabla \times \mathbf{v}$ obeys

$$\frac{\partial \boldsymbol{\Omega}}{\partial t} + (\mathbf{v} \cdot \nabla)\boldsymbol{\Omega} = (\boldsymbol{\Omega} \cdot \nabla)\mathbf{v} + \nu \nabla^2 \boldsymbol{\Omega}. \tag{3}$$

For a two–dimensional flow, taking the scalar product of equation (2) and (3) with $\mathbf{v}$ and $\boldsymbol{\Omega}$, respectively, we obtain

$$\frac{\partial}{\partial t}\left(\frac{\mathbf{v}^2}{2}\right) + \nabla \cdot \left(\mathbf{v}\frac{\mathbf{v}^2}{2} + \mathbf{v}\frac{p}{\rho}\right) \equiv \nu \nabla \cdot (\mathbf{v} \times \boldsymbol{\Omega}) - \nu \boldsymbol{\Omega}^2, \tag{4a}$$

$$\frac{\partial}{\partial t}\left(\frac{\boldsymbol{\Omega}^2}{2}\right) + \nabla \cdot \left(\frac{\boldsymbol{\Omega}^2}{2}\mathbf{v}\right) = \nu \nabla \cdot [\boldsymbol{\Omega} \times (\nabla \times \boldsymbol{\Omega})] - \nu (\nabla \times \boldsymbol{\Omega})^2. \tag{4b}$$

If the fluid is surrounded by a rigid boundary so that the normal component of velocity vanishes on the boundary, we have from equations (4)

$$\frac{\partial W}{\partial t} \equiv \frac{\partial}{\partial t}\int \frac{\mathbf{v}^2}{2}\, dx = \oint (\mathbf{v} \times \boldsymbol{\Omega}) \cdot ds - \int \nu \boldsymbol{\Omega}^2\, dx,^{7} \tag{5a}$$

$$\frac{\partial U}{\partial t} \equiv \frac{\partial}{\partial t}\int \frac{\boldsymbol{\Omega}^2}{2}\, dx = \oint \nu \boldsymbol{\Omega} \times (\nabla \times \boldsymbol{\Omega}) \cdot ds - \int \nu (\nabla \times \boldsymbol{\Omega})^2\, dx. \tag{5b}$$

In the absence of viscous dissipation ($\nu = 0$), equation (5) gives the conservations of the total energy E and the total enstrophy U (which is the mean square vorticity):

$$E = \text{const.}, \qquad U = \text{const.} \tag{6a,b}$$

Thus, in two–dimensional turbulence, there are two conserved quantities: the energy and the enstrophy.[8] (Due to a finite viscosity, however, the enstrophy is dissipated at a nonnegligible rate; therefore, the maintenance of a stationary state requires an external source since the vortex stretching, which acts like a source of

---

[7] Note that the energy balance equation (5) does not show any contribution from the nonlinear term in equation (2). This is because the nonlinear term merely redistributes energy among the various scales of motion without affecting the global energy balance.

[8] Vorticity itself is a Lagrangian invariant, because, according to equation (3), material fluid elements carry their values of vorticity with them. Thus, any integral function of vorticity is conserved.

vorticity, is inoperative here unlike the three–dimensional turbulence. However, energy dissipation will tend to zero as $\nu \Rightarrow 0$, so that two–dimensional turbulence, unlike its three–dimensional counterpart is almost nondissipative as $\nu \Rightarrow 0$.) Therefore, there are two types of inertial ranges: one for energy and one for enstrophy.

If the enstrophy vanishes during the direct cascade, equation (5) shows that $\partial E/\partial t \Rightarrow 0$ even in the presence of a viscous dissipation. This implies that the system will evolve toward a state of minimum enstrophy with constant energy. Thus, there exists a selective dissipation process among the conserved quantities in a two–dimensional flow when dissipation is introduced: The enstrophy decays faster than the energy.

The evolution of the system toward a state of minimum enstrophy with constant energy implies that

$$\delta\left[\int \Omega^2 dx + \lambda \int |\nabla \psi|^2 dx\right] = 0, \tag{7}$$

which yields

$$\nabla^2 \Omega = -\lambda \Omega$$

or

$$\Omega \sim \psi. \tag{8}$$

However, laboratory experiments on dipole vortices (van Heijst and Flor) have shown that the relation between Ω and ψ is not linear, as predicted by (8), and is given by

$$\Omega \sim \sin h\psi.^9 \tag{9}$$

Fourier Analysis of the Turbulent Velocity Field

Let us express the flow properties at any point x at time t, as a superposition of plane waves of the form

$$v(x,t) = \sum_k V(k,t) e^{ik \cdot x}, \qquad \frac{1}{\rho} p(x,t) = \sum_k P(k,t) e^{ik \cdot x}. \tag{10}$$

Since V and P are actually measurable, they must be real so that

$$V^*(k) = V(-k), \; P^*(k) = P(-k).$$

We have dropped the argument t for convenience. We then obtain from equations (1) and (2) the following equation:

---

[9]Consider the mechanical analogy of a membrane clamped at its edge, in which stream function is displacement and vorticity is load. The minimum-energy arrangement of the load is then achieved by moving it as close as possible to the edge so that the support bears its weight. The maximum-energy configuration is found by placing the load in the middle of the membrane as far as possible from the edge.

$$\left(\frac{\partial}{\partial t}+\nu k^2\right)V_j(k)=-ik_m\left(\delta_{jl}-\frac{k_jk_l}{k^2}\right)\sum_{k'}V_m(k')V_l(k-k'), \tag{11}$$

which describes the mode coupling among different Fourier components.

In terms of the stream function ψ, defined by

$$\mathbf{v}=\nabla\psi\times\hat{\boldsymbol{i}}_z, \tag{12}$$

we have for the vorticity $\boldsymbol{\Omega}$

$$\boldsymbol{\Omega}=\nabla\times\mathbf{v}=-\nabla^2\psi\hat{\boldsymbol{i}}_z, \tag{13}$$

and equation (3) becomes

$$\frac{\partial}{\partial t}\nabla^2\psi+\left(\nabla\psi\times\hat{\boldsymbol{i}}_z\right)\cdot\nabla\left(\nabla^2\psi\right)=\nu\nabla^4\psi. \tag{14}$$

Upon Fourier analyzing $\psi(\boldsymbol{x},t)$ according to

$$\psi(\boldsymbol{x},t)=\sum_{\boldsymbol{k}}\Psi(\boldsymbol{k},t)e^{i\boldsymbol{k}\cdot\boldsymbol{x}}, \tag{15}$$

equation (14) becomes

$$\left(\frac{\partial}{\partial t}+\nu k^2\right)\Psi(\boldsymbol{k})=\sum_{\boldsymbol{k}=\boldsymbol{k}'+\boldsymbol{k}''}\Lambda^{\boldsymbol{k}}_{\boldsymbol{k}',\boldsymbol{k}''}\Psi(\boldsymbol{k}')\Psi(\boldsymbol{k}''), \tag{16}$$

where

$$\Lambda^{\boldsymbol{k}}_{\boldsymbol{k}',\boldsymbol{k}''}=\frac{1}{k^2}(\boldsymbol{k}'\times\boldsymbol{k}'')\cdot\hat{\boldsymbol{i}}_z\left(k'^2-k''^2\right),$$

and we have again dropped the argument t for convenience. Λ becomes large when $\boldsymbol{k},\boldsymbol{k}'$, and $\boldsymbol{k}''$ have comparable magnitudes so that the modal cascade is dominated by local interactions in $\boldsymbol{k}$–space.

Energy and Enstrophy Cascades

Consider a source in the spectral space at $k=k_s$ with energy $E_s=E(k_s)$ (the omnidirectional energy spectrum $E(k)$ is defined such that $\int E(k)\,dk=\sum|V(\boldsymbol{k})|^2$ gives the total energy).

Through mode–mode coupling this source would decay into two modes with wavenumbers k_1 and k_2 with energies E_1 and E_2, ($k<k_s$ corresponds to the inertial range for energy and $k>k_s$ corresponds to the inertial range for enstrophy.) Since energy and enstrophy are conserved, we have

$$E_s=E_1+E_2, \tag{17}$$

$$k_s^2E_s=k_1^2E_1+k_2^2E_2, \tag{18}$$

from which the energy is partitioned as

$$\left.\begin{aligned} E_1 &= \frac{k_2^2 - k_s^2}{k_2^2 - k_1^2} E_s, \\ E_2 &= \frac{k_s^2 - k_1^2}{k_2^2 - k_1^2} E_s. \end{aligned}\right\} \tag{19}$$

This implies that

$$k_2^2 > k_s^2 > k_1^2 \tag{20}$$

so that the mode with wavenumber k_s decays into a mode with wavenumber $k_1 < k_s$ and to another mode with wavenumber $k_2 > k_s$.

Let us assume that a mode k_s first decays into modes $k_1\left(k_1 = \sqrt{p}\, k_s\right)$ and $k_2\left(k_2 = \sqrt{1+p}\; k_s;\, p<1\right)$, with corresponding energies $E_1 = pE_s$ and $E_2 = (1-p)E_s$ and enstrophies $U_1 = k_s^2\, p^2\, E_s$ and $U_2 = k_s^2\left(1-p^2\right)E_s$. In the next step of the cascade, the mode k_1 decays into a mode $\sqrt{p}\, k_1 = pk_s$ and another mode $\sqrt{1+p}\; k_1 = \sqrt{p(1+p)}\; k_s$, while the mode k_2 decays into a mode $\sqrt{p}\, k_2 = \sqrt{p(1+p)}\, k_s$ and another mode $\sqrt{1+p}\, k_2 = (1+p)k_s$. The energies for the modes pk_s, $\sqrt{p(1+p)}\; k_s$ and $(1+p)k_s$ are p^2E_s, $2p(1-p)E_s$ and $(1-p)^2 E_s$, respectively. Thus, at the nth step of the cascade, the energy is given by

$$E\left(k^2 = p^{n-r}(1+p)^r k_s^2\right) = \binom{n}{r} p^{n-r}(1-p)^r E_s. \tag{21}$$

Now, by the de Moivre–Laplace approximation, we have for the binomial distribution, as $n \Rightarrow \infty$,

$$\binom{n}{r} p^{n-r}(1-p)^r \approx \frac{1}{\sqrt{2\pi np(1-p)}}\, e^{-\frac{(n-r-np)^2}{2\pi p(1-p)}} \tag{22}$$

so that the binomial distribution in (21) peaks at $r/n \approx 1-p$ as $n \Rightarrow \infty$. The corresponding wavenumber is

$$\begin{aligned} k_*^2 &= \lim_{n\Rightarrow\infty} p^{n-r}(1+p)^r k_s^2 = \lim_{n\Rightarrow\infty}\left[p^{1-\frac{r}{n}}(1+p)^{\frac{r}{n}}\right]^n k_s^2 \\ &= \lim_{n\Rightarrow\infty}\left[p^p(1+p)^{1-p}\right]^n k_s^2. \end{aligned} \tag{23}$$

Since, for $0 < p < 1$, $p^p(1+p)^{1-p} < 1$, we obtain $k_*^2 \approx 0$. This means that the peak of the energy distribution moves to $k \Rightarrow 0$, as $n \Rightarrow \infty$. Hence, the energy cascades inversely and condensates at $k \Rightarrow 0$ (or at the longest wavelength permissible for the system).

Next, the enstrophies for the modes pk_s, $\sqrt{p(1+p)}\,k_s$ and $(1+p)k_s$ are $k_s^2 p^4 E_s$, $2k_s^2 p^2(1-p^2)E_s$ and $k_s^2(1-p^2)^2 E_s$, respectively. Thus, at the nth step of the cascade, the enstrophy is given by

$$U\left(k^2 = p^{n-r}(1+p)^r k_s^2\right) = \binom{n}{r} p^{2(n-r)}(1-p^2)^r k_s^2 E_s. \tag{24}$$

The binomial distribution in (24) peaks at $r/n \approx 1-p^2$ as $n \Rightarrow \infty$. The corresponding wavenumber is

$$\begin{aligned} \tilde{k}_*^2 &= \lim_{n\Rightarrow\infty} p^{n-r}(1+p)^r k_s^2 \\ &= \lim_{n\Rightarrow\infty}\left[p^{1-\frac{r}{n}}(1+p)^{\frac{r}{n}}\right]^n k_s^2 \\ &= \lim_{n\Rightarrow\infty}\left[p^{p^2}(1+p)^{1-p^2}\right]^n k_s^2. \end{aligned} \tag{25}$$

Since, for $0 < p < 1$, $p^{p^2}(1+p)^{1-p^2} > 1$, we obtain $\tilde{k}_*^2 \approx \infty$. This means that the peak of the enstrophy distribution moves to $k \Rightarrow \infty$, as $n \Rightarrow \infty$. Hence, the enstrophy cascades directly and condensates at $k \Rightarrow \infty$ (where strong viscous dissipation sets in).

Self-Organization and Self-Degradation in Two-Dimensional Flows

The energy cascade to lower wavenumbers has the result that random excitation at intermediate wavenumbers drives the (necessarily coherent) largest spatial scales of the system. Thus, two-dimensional flows seem to have a self-organizing character. The smooth structure of the stream function is expected to evolve toward a smooth structure as a consequence of the inverse cascade of the energy to large wavelengths, while the vorticity is expected to evolve toward a convoluted structure as a result of the enstrophy cascading to smaller wavelengths.

In order to understand the self-degradation of vorticity, consider equations (12)–(14) in the inviscid limit,

$$\left[\frac{\partial}{\partial t} + L(t)\right]\Omega(t) = 0, \tag{26}$$

$$\nabla^2\psi(t) = -\Omega(t), \tag{27}$$

where the operator $L(t)$ is given by

$$L(t) \equiv \nabla\psi(t) \times \hat{i}_z \cdot \nabla$$

and we have omitted showing the dependence on x explicitly.

Let us split the operator $L(t)$ into a mean part $\bar{L}(t)$ and a fluctuating part $L'(t)$ as follows:

$$L(t) = \bar{L}(t) + L'(t). \tag{28}$$

Upon averaging, equation (26) gives

$$\left[\frac{\partial}{\partial t} + \bar{L}(t)\right] \bar{\Omega}(t) = -\langle L'(t)\Omega'(t)\rangle, \tag{29}$$

where the bars overhead (or $\langle\ \rangle$) refer to the average, and the primes refer to the fluctuation, and

$$\Omega(t) = \bar{\Omega}(t) + \Omega'(t).$$

Upon subtracting equation (29) from equation (26), we obtain

$$\left[\frac{\partial}{\partial t} + \bar{L}(t)\right] \Omega'(t) = -L'(t)\bar{\Omega}(t) + \langle\langle L'(t)\Omega'(t)\rangle\rangle, \tag{30}$$

where

$$\langle\langle Q\rangle\rangle \equiv \langle Q\rangle - Q.$$

If we introduce Green's function $\bar{G}(t,t')$ for the operator $\left[\frac{\partial}{\partial t} + \bar{L}(t)\right]$, defined by

$$\left[\frac{\partial}{\partial t} + \bar{L}(t)\right]^{-1} H(t) = \int \bar{G}(t,t')H(t')dt', \tag{31}$$

the solution of equation (30) can be written formally as

$$\Omega'(t) = \int G(t,t')\left[\langle L'(t')\Omega'(t')\rangle - L'(t')\bar{\Omega}(t')\right] dt' \tag{32a}$$

and, on iteration, as the Neumann series:

$$\Omega'(t) = -\int \bar{G}(t,t')L'(t')\bar{\Omega}(t')dt' - \int \bar{G}(t,t')\left\langle\left\langle L'(t')\int \bar{G}(t',t'')L'(t'')\bar{\Omega}(t'')dt''\right\rangle\right\rangle dt' + \cdots. \tag{32b}$$

As a first approximation we will retain only the first term on the right–hand side of equation (32). Thus, equation (29) and the fluctuating part of equation (27) become

$$\left[\frac{\partial}{\partial t} + \bar{L}(t)\right] \bar{\Omega}(t) = \int dt' \langle L'(t)\bar{G}(t,t')L'(t')\rangle \bar{\Omega}(t'), \tag{33}$$

$$\nabla^2 \psi'(t) = \int dt'\, \bar{G}(t,t')L'(t')\bar{\Omega}(t'). \tag{34}$$

If we now suppose that the integrand on the right in equation (33) peaks near $t' = t$ for a short period of time of the order of τ_c, the correlation time of the

fluctuations (or the eddy turnover time), and that $\overline{\Omega}(t)$ is sufficiently smooth and does not change significantly during this period, we may ignore the nonlocal character of the diffusion operator in equation (33) – Markovianization. The latter, then, becomes the Fokker–Planck equation,

$$\left(\frac{\partial}{\partial t}+\overline{\mathbf{v}}\cdot\nabla\right)\overline{\Omega}(x,t)=\frac{\partial}{\partial x}\cdot D(x,t)\cdot\frac{\partial\overline{\Omega}(x,t)}{\partial x}, \tag{35}$$

and equation (34) becomes

$$\left[\nabla\times\mathbf{v}'(x,t)\right]\cdot\hat{i}_z=-\frac{\partial\overline{\Omega}(x,t)}{\partial x}\cdot\int dt'\,\overline{G}(t,t')\mathbf{v}'(x,t'). \tag{36}$$

Here, assuming that the fluctuations are stationary, the diffusion coefficient D is given by

$$D(x,t)=\int dt'\left\langle\mathbf{v}'(x,t)\overline{G}(t,t-t')\mathbf{v}'(x,t-t')\right\rangle, \tag{37}$$

which embodies the Kubo's Fluctuation–Dissipation Theorem.

Equation (35) signifies the self–degradation of vorticity and implies that the evolution of vorticity in two–dimensional turbulence can be considered to be a Markov process. This is plausible if we note that when the vorticity has evolved for a time long compared with the correlation time of the enstrophy cascade the enstrophy–transfer process would have completed a large number of steps in the cascade, each of which produces a small random contribution.

Batchelor–Kraichnan Theory of the Inertial Ranges

Komogorov's theory of the inertial range occupies a central place in the theory of three–dimensional turbulence. As we saw in Section 6.2, Kolmogorov argued that there exists a certain range, called the *inertial range*, in the wavenumber space which is in a state of statistical equilibrium in the sense that there is neither a source nor a sink of energy. The energy spectrum is assumed to cascade here smoothly through nonlinear processes in a stationary state. Furthermore, the energy spectrum $E(k)$ in the inertial range is assumed to depend only on the wavenumber k and on the rate ε at which energy is cascaded per unit mass. Dimensional arguments then imply that $E(k)$ has the form

$$E(k)=C\varepsilon^{2/3}k^{-5/3}, \tag{38}$$

where C is a dimensionless constant.

In two–dimensional turbulence the existence of two conserved quantities, energy and enstrophy, imply the possibility of two cascades with inertial ranges of the Kolmogorov type. Using dimensional arguments, Kraichnan and Batchelor gave for the inertial–range energy spectrum $E(k)$, the following form in the energy cascade:

$$E(k)=C_1\varepsilon^{2/3}k^{-5/3}; \tag{39}$$

and they gave the following form in the enstrophy cascade:

$$E(k) = C_2 \tau^{2/3} k^{-3}. \tag{40}$$

Here ε and τ are the rate of transfer of energy and enstrophy per unit area, respectively, and C_1, C_2 are dimensionless constants.

The energy spectrum (40) in the enstrophy range leads to violation of locality in the latter range. In order to see this, note that the eddy turnover time $T(k)$ for a scale k is given, on dimensional grounds, by

$$T(k) \sim \frac{E(k)k^3}{\tau}; \tag{41}$$

and note that on using (40), (41) becomes

$$T(k) \sim \tau^{-1/3}. \tag{42}$$

According to (42), $T(k)$ does not decrease with decreasing scale, so that the characteristic timescales of the small eddies will not be small compared with that of the large eddies, and the small eddies will not remain in equilibrium with the latter. Kraichnan suggested a phenomenalogical solution to the nonlocality in the enstrophy range by taking the eddy turnover time $T(k)$ to be, instead,

$$T(k) \sim \left[\int_{k_0}^{k} p^2 E(p)\,dp\right]^{-1/2}, \tag{43}$$

which then leads to the log–corrected spectrum:

$$E(k) \sim \tau^{2/3} k^{-3} \left[ln\left(k/k_0\right)\right]^{-1/3}. \tag{44}$$

Here, k_0 is the scale at which forcing is introduced.

Equilibrium Statistical Mechanics: Kraichnan's Theory

Let us consider a two–dimensional turbulence within a square which can be expanded into an infinite series of discrete wave vectors $\boldsymbol{k}_n$ with velocity amplitudes $V(\boldsymbol{k}_n, t)$ related by Euler's equations in Fourier space. These equations are truncated by retaining the modes lower than a cutoff wavenumber k_{max} (so as to preserve the validity of the inviscid model) and are suitably normalized to give for the stream function ψ (recall equation (16)):

$$\frac{d\Psi(k)}{dt} = \frac{1}{2} \sum_{k=k'+k''} \Lambda^k_{k',k''}\, \Psi(k')\, \Psi(k''). \tag{45}$$

Let $y_{n1}(t)$ and $y_{n2}(t)$ be the real and imaginary parts of each mode $\Psi(\boldsymbol{k}_n)$. Then, if the truncated system contains N wave vectors, the system can be represented by a point of $2N$ coordinates $y_{n_i}(t)(i = 1,2)$ in a phase space determined by $y_\alpha(t)(\alpha = 1, \ldots, 2N)$. Equation (45) conserves the kinetic energy

$$\frac{1}{2}\sum_{k_n} k_n^2 \left|\Psi(k_n)\right|^2 = \frac{1}{2}\sum_{\alpha=1}^{2N} k_\alpha^2 y_\alpha^2(t) \tag{46}$$

and the enstrophy[10]

$$\frac{1}{2}\sum_{k_n} k_n^4 \left|\Psi(k_n)\right|^2 = \frac{1}{2}\sum_{\alpha=1}^{2N} k_\alpha^4 y_\alpha^2(t), \tag{47}$$

which implies that the system evolves ergodically in the phase space on the intersection of the kinetic energy sphere and the enstrophy ellipsoid. Let us consider a collection of systems which is represented at each instant of time by a cluster of points in the phase space of density $\rho(y_1,\ldots,y_{2N},t)$ in the phase space. Since the total number of such systems and hence the volumes are preserved as they wander around in the phase space, we have the Liouville Theorem:

$$\frac{\partial\rho}{\partial t} + \sum_{\alpha=1}^{2N} \frac{dy_\alpha}{dt}\frac{\partial\rho}{\partial y_\alpha} = 0. \tag{48}$$

By the elementary Gibbsian methods of statistical mechanics, equilibrium solutions of equation (48) are constructed as functions of the conserved quantities, and are given by the Boltzmann type distribution

$$P(y_1,\ldots,y_{2N}) = \frac{1}{Z}\, e^{-\frac{1}{2}\sum_{\alpha=1}^{2N}\left(\sigma k_\alpha^2 y_\alpha^2 + \mu k_\alpha^4 y_\alpha^2\right)}, \tag{49}$$

where σ and μ are two positive constants, and Z is the partition function of the system

$$Z = \int\cdots\int e^{-\frac{1}{2}\sum_{\alpha=1}^{2N}\left(\sigma k_\alpha^2 y_\alpha^2 + \mu k_\alpha^4 y_\alpha^2\right)} dy_1 \ldots dy_{2N}. \tag{50}$$

One then assumes that the microcanonical ensemble average $\langle\rho(y_1,\ldots,y_{2N},t)\rangle$ of an ensemble of given systems $\rho(y_1,\ldots,y_{2N},t)$ obeying equations (45) and (48) will eventually relax toward the equilibrium distribution (49) over the entire region of phase space permitted by the total energy and the total enstrophy constants (46) and (47).

The mean variance of the mode α of the stream function is given by

$$\left\langle y_\alpha^2(t)\right\rangle = \frac{1}{Z}\int\cdots\int y_\alpha^2\, e^{-\frac{1}{2}\sum_{\beta=1}^{2N} k_\beta^2(\sigma+\mu k_\beta^2) y_\beta^2} dy_1\ldots dy_{2N} = \frac{1}{k_\alpha^2\left(\sigma+\mu k_\alpha^2\right)}. \tag{51}$$

Thus,

$$\left\langle\left|\Psi(k)\right|^2\right\rangle = \frac{2}{k_\alpha^2\left(\sigma+\mu k_\alpha^2\right)} \tag{52}$$

---

[10]Note again that only the quadratic invariants (energy and enstrophy) survive the spectral truncation because they are conserved by an interacting triad.

and the energy spectrum is then given by

$$E(k) = \pi k^3 \left\langle \left| \Psi(k) \right|^2 \right\rangle \sim \frac{k}{\sigma + \mu k^2}. \tag{53}$$

Equation (53) shows that for the case $\sigma < 0$, high–energy states are statistically favored relative to the low–energy states and the energy spectrum is dominated by the contributions form the largest wavelengths $\left(k = k_{min} \approx \sqrt{-\sigma/\mu}\right)$. This again implies that the energy cascades toward large scales and leads to coalescence of vortices of the same sign which represent states of high–energy. Observe further that for $k \Rightarrow 0$ (this also corresponds to abandoning the enstrophy conservation condition) (53) gives the spectrum of equipartition of kinetic energy among the modes:

$$E(k) \sim k. \tag{54}$$

Thus, an inviscid finite system evolves toward an equipartition of energy among all Fourier modes. However, as we saw before, the situation is quite different for real flows (with infinite degrees of freedom), which evolve toward the Batchelor–Kraichnan scaling laws:

$$E(k) \sim k^{-5/3} \tag{55}$$

in the inverse energy cascade and

$$E(k) \sim k^{-3} \tag{56}$$

in the direct enstrophy cascade. Thus, truncation of the modes acts as a barrier preventing possible cascades and can produce a significant alteration of the statistical properties of the system.

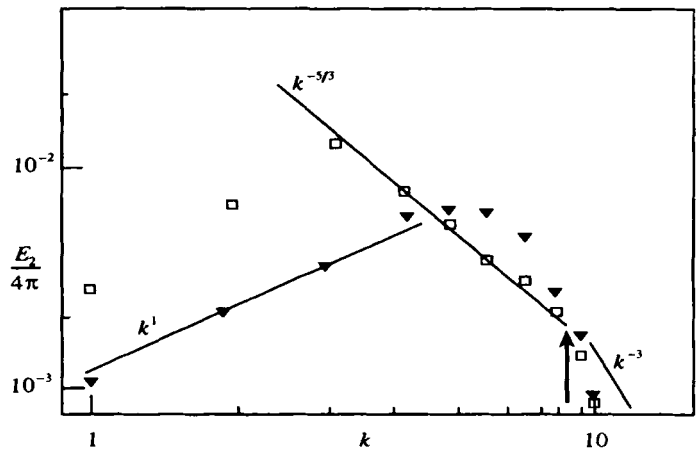

Figure 6.9. Experimentally observed energy spectra in a two–dimensional turbulence (from Sommeria, 1986). Arrow indicates the injection wavenumber.

The whole theory of two–dimensional turbulence had, until recently, remained almost an academic exercise, notwithstanding its possible connections with atmospheric and oceanic large–scale flows. Recently, truly two–dimensional flows were produced to a close approximation in laboratory experiments. Experimental evidence of the existence of inverse energy cascade was first obtained by Couder on this liquid soaps films, then by Sommeria in a shallow mercury layer immersed in a strong normal magnetic field.

The inverse energy cascade in a statistically steady forced two–dimensional turbulence (without forcing, the inverse cascade cannot develop), experimentally investigated by Sommeria, showed a $k^{-5/3}$ behavior at large wavenumbers and a k^{1} behavior corresponding to an equilibrium energy equipartition spectrum at small wavenumbers (Figure 6.9).

6.4. Turbulent Dispersion: Lin's Theory

While the theory of turbulence is usually developed in the Eulerian description, the dispersion process requires Lagrangian viewpoint because it is concerned with relative motion between neighboring particles.

Let us analyze the one–dimensional relative motion of two particles which are close to each other and have essentially the same initial velocity but have different initial accelerations, if the distance between the particles exceeds the range of Eulerian correlation of pressure gradient. Such particles will begin to have different velocities and will consequently drift apart.

Let $Z_1(t)$ and $Z_2(t)$ be the position of two particles which were close to each other at $t = 0$. Then,

$$Z_1(0) = Z_2(0) = 0. \tag{1}$$

If $W_1(t)$ and $W_2(t)$ are their respective velocities, then we have

$$W_1(0) = W_2(0). \tag{2}$$

Let their relative displacement at time t be

$$z(t) = Z_2(t) - Z_1(t) \tag{3}$$

and their relative velocity be

$$w(t) = W_2(t) - W_1(t). \tag{4}$$

Then, the initial conditions (1) and (2) can be reexpressed as

$$z(0) = 0, \qquad w(0) = 0. \tag{5}$$

Let the relative acceleration of the two particles be

$$a(t) = \dot{W}_2(t) - \dot{W}_1(t). \tag{6}$$

Then

$$a(0) \neq 0.$$

From the relations

$$w = \frac{dz}{dt} \quad \text{and} \quad a = \frac{dw}{dt} \tag{7}$$

and using (5), we obtain

$$w(t) = \int_0^t a(t')\,dt, \tag{8}$$

$$z(t) = \int_0^t (t - t')\,a(t')\,dt'. \tag{9}$$

Multiplying each of these equations by $a(t)$ and averaging over an ensemble of pairs of such particles, we obtain

$$\frac{1}{2}\frac{d}{dt}\left\langle w^2(t)\right\rangle = \int_0^t \left\langle a(t)\,a(t')\right\rangle dt', \tag{10}$$

$$\frac{1}{2}\frac{d^2}{dt^2}\left\langle z^2(t)\right\rangle = \left\langle w^2(t)\right\rangle + \int_0^t (t - t')\left\langle a(t)\,a(t')\right\rangle dt'. \tag{11}$$

If we now assume the acceleration to be stationary, we may then write

$$\left\langle a(t)\,a(t')\right\rangle = a_*^2\,R(\tau), \qquad \tau = t' - t. \tag{12}$$

The correlation coefficient $R(\tau)$ satisfies the following asymptotic properties:

$$\left.\begin{aligned} &R(0) = 1, \\ &\lim_{\tau \to \infty} R(\tau) = 0. \end{aligned}\right\} \tag{13}$$

The first property follows from the definition of $R(\tau)$, while the second expresses the obvious physical fact that events which are widely separated in time become uncorrelated.

We then have from (10) and (11)

$$\frac{1}{2}\frac{d}{dt}\left\langle w^2(t)\right\rangle = a_*^2 \int_0^t R(\tau)\,d\tau, \tag{14}$$

$$\frac{1}{2}\frac{dt^2}{dt^2}\left\langle z^2(t)\right\rangle = \left\langle w^2(t)\right\rangle + a_*^2 \int_0^t \tau\,R(\tau)\,d\tau. \tag{15}$$

We obtain from (14) and (15)

$$\left\langle w^2(t)\right\rangle = 2a_*^2 \int_0^t (t - \tau)\,R(\tau)\,d\tau, \tag{16}$$

$$\langle z^2(t)\rangle = \frac{2a_*^2}{3}\int_0^t (t-\tau)^3 R(\tau)\,d\tau + a_*^2\int_0^t (t-\tau)^2\tau R(\tau)\,d\tau$$

$$= \frac{2a_*^2}{3}\left[t^3\int_0^t R(\tau)\,d\tau - \frac{3}{2}t^2\int_0^t \tau R(\tau)\,d\tau + \frac{1}{2}\int_0^t \tau^3 R(\tau)\,d\tau\right]. \tag{17}$$

Since $R(\tau)$ vanishes rapidly for large value of τ, we have approximately

$$\int_0^t R(\tau)\,d\tau = \int_0^T R(\tau)\,d\tau, \quad \text{for} \quad t > T. \tag{18}$$

Also for such large values of t, we have

$$t \gg \frac{\left[\int_0^t \tau R(\tau)\,d\tau\right]}{\left[\int_0^t R(\tau)\,d\tau\right]}, \qquad t^3 \gg \frac{\left[\int_0^t \tau^3 R(\tau)\,d\tau\right]}{\left[\int_0^t R(\tau)\,d\tau\right]}. \tag{19}$$

Under such conditions, (16) and (17) yield the following approximate relations

$$\langle z^2(t)\rangle = \frac{2}{3}Bt^3, \tag{20}$$

$$\langle w^2(t)\rangle = 2Bt, \tag{21}$$

where

$$B \equiv a_*^2\int_0^T R(\tau)\,d\tau.$$

Equation (20) is called the Richardson's law.

Note that the validity of the above formulation requires that the time involved in the correlation of the forces be very short compared with the time scale of the observations. Indeed, the function describing the dependence of force as a function of time should resemble a δ–function. Thus, one may visualize that the fluid particle has been subjected to successive small impulsive forces, like those experienced by a Brownian particle, i.e., the particles are moving almost freely and subjected only to "small" random forces having a very short–ranged correlation.

If we define a dispersion coefficient by

$$D \equiv \frac{1}{2}\frac{d}{dt}\left(\langle z^2\rangle\right) \tag{22}$$

then we have from (19)

$$D = Bt^2 = \left(\frac{3}{2}\right)^{\frac{2}{3}} B\left[\langle z^2(t)\rangle\right]^{\frac{2}{3}}. \tag{23}$$

Equation (23) implies that the dispersion coefficient increases as the 4/3 power of scale. Such a relationship was earlier discovered by Richardson from a purely empirical analysis of atmospheric dispersion.

BIBLIOGRAPHY

My indebtedness to information and benefit received from many sources in connection with this undertaking cannot be adequately documented. In particular, I have extensively consulted the following books in addition to the several papers mentioned below:

Batchelor, G.K.: *Theory of Homogeneous Turbulence*, Cambridge Univ. Press (1953).

Batchelor, G.K.: *Introduction to Fluid Dynamics*, Cambridge Univ. Press (1967).

Bisplinghoff, R.L., Ashley, H., and Halfman, R.L.: *Introduction to Aeroelasticity*, Addison-Wesley Publishing Co. (1955).

Chandrasekhar. S.: *Hydrodynamic and Hydromagnetic Stability*, Clarendon Press (1961).

Chorin, A.J. and Marsden, J.E.: *A Mathematical Introduction to Fluid Mechanics*, Springer-Verlag (1990).

Drazin, P.G. and Howard, L.N.: Hydrodynamic Stability in Parallel Flows of Inviscid Fluid in *Advances in Applied Mechanics*, Vol. 9 (1966).

Drazin, P.G. and Johnson, R.S.: *Solitons*, Cambridge Univ. Press (1989).

Faber, T.E.: *Fluid Dynamics for Physicists*, Cambridge Univ. Press (1995).

Fung, Y.C.: *Aeroelasticity*, Dover Publications (1955).

Greenspan, H.P.: *Theory of Rotating Fluids*, Cambridge Univ. Press (1968).

Karamcheti, K.: *Principles of Ideal Fluid Aerodynamics*, Wiley (1966).

Kevorkian, J. and Cole, J.D.: *Perturbation Methods in Applied Mathematics*, Springer-Verlag (1980).

Liepmann, H.W. and Pucket, A.E.: *Aerodynamics of a Compressible Fluid*, John Wiley and Sons (1949).

Liepmann, H.W. and Roshko, A.: *Elements of Gas Dynamics*, John Wiley and Son (1957).

Lighthill, M.J., *Waves in Fluids*, Cambridge Univ. Press (1978).

Lin, C.C.: *Theory of Hydrodynamic Stability*, Cambridge Univ. Pres (1955).

Tennekkes, H. and Lumley, J.L., *A First Course in Turbulence*, M.I.T. Press (1973).

O'Neil, M.E. and Chorlton, F,: *Ideal and Incompressible Fluid Dynamics*, Ellis Horwood (1986).

O'Neil, M.E. and Chorlton, F.: *Viscous and Compressible Fluid Dynamics*, Ellis Horwood (1987).

Reid, W.H.: The Stability of Parallel Flows in *Basic Developments in Fluid Dynamics*, Ed. Holt, M., Academic Press (1965).

Rutherford, D.E.: *Fluid Dynamics*, Oliver & Boyd (1959).

Schlichting, H.: *Boundary Layer Theory*, McGraw Hill Publishing Co. (1972).

Tritton, D.J.: *Physical Fluid Dynamics*, Clarendon Press (1988).

Van Dyke, M.D.: *Perturbation Methods in Fluid Mechanics*, Parabolic Press (1975).

Whitham, G.B.: *Linear and Nonlinear Waves*, Wiley-Interscience (1974).

Review of Basic Concepts and Equations

Cauchy, A.: Mem. Acad. Sci. *1* (1827).
Moffatt, H.K.: J. Fluid Mech. *35*, 117 (1969).
Navier, L.M.H.: Ibid, *6*, 389 (1822).
Olver, P.J.: J. Math. Anal. Applics. *89*, 233 (1982).
Poisson, S.D.: Journ. de l'Ecole Polytech. *13*, 1 (1829).
Saint-Venant, B.: Comptes Rendus *17*, 1240 (1843).
Salmon, R.: Ann. Rev. Fluid Mech. *20*, 225 (1988).
Shepherd, T.G.: Adv. Geophys. *32*, 287 (1990).
Stokes, G.G.: Trans. Camb. Phil. Soc. *8*, 287 (1845).
Truesdell, C.: Proc. Roy. Soc. (Lond.) *A226*, 389 (1954).

Potential Flows

Blasius, H.: Z. Math. Phys. *58*, 90 (1910).
Helmholtz, H. von: Crelle J. *55* (1858).
Kelvin, Lord: Math. Phys. Papers *1*, 107, (1849). Ibid. *4*, 13, 49, and 52 (1869).
LaGally, M.: Z. Angew. Math. Mech. *2*, 409 (1922).
Ludford, G.S.S., Martinek, J. and Yeh, G.C.K.: Proc. Camb. Phil. Soc. *51*, 389 (1955).
Milne-Thomson, L.M.: Ibid, *36*, 246 (1940).
Plesset, M. and Prosperetti, A.: Ann. Rev. Fluid Mech. *9*, 145 (1977).
Rankine, W.J.M.: Phil. Trans. Roy. Soc. *267* (1871).

Rotating Flows

Dickinson, R.E.: Ann. Rev. Fluid Mech. *10*, 159 (1978).

Fultz, D.: J. Meteor, *16*, 199 (1959).
Gortler, H.: Proc. V Midwestern Conf. Fluid. Mech. *1* (1957).
Haurwitz, B.: J. Mar. Res. *3*, 254 (1940).
Lighthill, M.J.: J. Fluid Mech. *26*, 411 (1966).
Long, R.R.: J. Meteor, *10*, 197 (1953).
Longuet-Higgins, M.S.: Proc. Roy. Soc. (Lond.) *A279*, 446, (1964). Ibid. *A284*, 40 (1965).
Morrison, J.A. and Morgan, G.W.: Tech. Rep. *8*, Divn. Appl. Math., Brown Univ. (1956).
Phillips, O.M.: Phys. Fluids *6*, 513 (1963).
Proudman, J.: Proc. Roy. Soc. (Lond.) *A92*, 408 (1916).
Rao, A.R.: J. Fluid Mech. *58*, 161 (1973).
Rossby, C.G.: J. Mar. Res. *2*, 38 (1939).
Shivamoggi, B.K.: Acta Mech. *62*, 29 (1986).
Stewartson, K.: Q.J. Mech. Appl. Math. *11*, 39 (1958).
Taylor, G.I.: Proc. Roy. Soc. (Lond.) *A100*, 114, (1921). Ibid. *A102*, 180 (1922). Ibid. *A104*, 213 (1923).

Vortex Flows

Benjamin, T.B.: J. Fluid Mech. *14*, 593 (1962).
Biot, J.B. and Savart, F.: J. Phys. (Paris) *91*, 151 (1820).
Bossel, H.H.: Phys. Fluids *12*, 498 (1969).
Hall, M.G.: Ann. Rev. Fluid Mech. *1*, 195 (1972).
Hall, M.G.: In *Proc. 1976 Heat Tr. Fluid Mech. Inst.*, 319, Stanford Univ. Press.
Harvey, J.K.: J. Fluid Mech. *14*, 585 (1962).
Hill, M.J.M.: Phil. Trans. Roy. Soc. *A185* (1894).
Leibovich, S.: Ann. Rev. Fluid Mech. *10*, 221 (1978).
Moore, D.W.: Mathematika *23*, 35 (1976).
Moore, D.W. and Saffman, P.G.: In *Aircraft Wake Turbulence*, Eds. Olsen, J., Goldburg, H. and Rogers, M., Plenum (1971). Phil. Trans. Roy. Soc. *272*, 403 (1972). Proc. Roy. Soc. (Lond.) *A333*, 509 (1973).
Orszag, S.A. and Crow, S.C.: Studies Appl. Math. *49*, 167 (1970).
Randall, J.D. and Leibovich, S.: J. Fluid Mech. *18*, 481 (1973).
Shivamoggi, B.K.: Nuovo Cimento D *13*, 105 (1991).
Shivamoggi, B.K.: Phys. Scripta *53*, 703 (1996).
Shivamoggi, B.K. and Uberoi, M.S.: Acta Mech. *41*, 211 (1981).
Uberoi, M.S., Shivamoggi, B.K. and Chen, S.S.: Phys. Fluids *22*, 214 (1979).
Widnall, S.E., Bliss, D.B. and Tsai, C.Y.: J. Fluid Mech. *66*, 35 (1974).

Water Waves

Benjamin, T.B.: Proc. Roy. Soc. (Lond.) *A299*, 59 (1967).
Benjamin, T.B.: Ibid. *A328*, 153 (1972).
Benjamin, T.B. and Feir, J.E.: J. Fluid Mech. *27*, 417 (1967).
Benjamin, T.B. and Lighthill, M.J.: Proc. Roy. Soc. (Lond.) *A224*, 448 (1954).
Benney, D.J.: J. Fluid Mech. *14*, 577 (1962).
Bretherton, F.P.: Ibid. *20*, 457 (1964).
Byatt-Smith, J.G.B.: Ibid. *48*, 33 (1971).

Dodd, R.K., Eilbeck, J.C., Gibbon, J.D. and Morris, H.C.: *Solitons and Nonlinear Wave Equations*, Academic Press (1982).
Hasselmann, K.: Ibid. *12*, 481 (1962). Ibid. *15*, 273 and 385 (1963).
Hirota, R.: Phys. Rev. Lett. *27*, 1192 (1971).
Janssen, P.A.E.M.: Phys. Fluids *24*, 23 (1981).
Jeffrey, A. and Kakutani, T.: SIAM Rev. *14*, 582 (1972).
Kadomtsev, B.B. and Petviashvili, V.I.: Sov. Phys. Dokl. *15*, 539 (1970).
Korteweg, D.J. and de Vries, G.: Phil. Mag. (5) *39*, 422 (1895).
Lake, B.M., Yuen, H.C., Rungaldier, H., and Fergusson, W.E.: J. Fluid Mech. *83*, 49 (1977).
Lighthill, M.J.: Phil. Trans. Roy. Soc. *A252*, 397 (1960) J. Inst. Math. Applics. *1*, 1 and 269 (1965). J. Fluid Mech. *27*, 725 (1967).
Lighthill, M.J. and Whitham, G.B.: Proc. Roy. Soc. (Lond.) *A229*, 281 (1955).
Longuet-Higgins, M.S.: J. Fluid Mech. *12*, 321, (1962). Phil. Trans. Roy. Soc. *A260*, 317, (1966); Proc. Roy. Soc. (Lond.) *A331*, 445 (1972).
McGoldrick, L.F.: J. Fluid Mech. *21*, 305 (1965). Ibid. *42*, 193 (1972).
Miles, J.: Ibid. *13*, 145 (1962); *79*, 157 (1977).
Oikawa, M., Satsuma, J. and Yojima, N.: J. Phys. Soc. Japan *35*, 511 (1974).
Phillips, O.M.: Ibid. *9*, 193 (1960).
Segur, H. and Finkel, A.: Stud. Appl. Math. *73*, 183 (1985).
Shivamoggi, B.K.: J. Phys. A *23*, 4289 (1990).
Shivamoggi, B.K. and Rollins, D.K.: Phys. Scripta *43*, 236 (1991). J. Math. Phys. *35*, 4779 (1994).
Simmons, W.F.: Proc. Roy. Soc. (Lond.) *A309*, 551 (1969).
Stoker, J.J.: Comm. Pure Appl. Math. *1*, 1 (1948). *Water Waves*, Wiley-Interscience (1957).
Whitham, G.B.: Proc. Roy Soc. (Lond.) *A283*, 238 (1965). Ibid. *A299*, 6 (1967). J. Fluid Mech. *27*, 399 (1967).
Zabusky, N.J. and Kruskal, M.D.: Phys. Rev. Lett. *15*, 240 (1965).
Zakharov, V.E.: J. Appl. Mech. Tech. Phys. (U.S.S.R.) *2*, 190 (1968).

Aerodynamics of an Incompressible Fluid

Glauert, M.B.: Proc. Roy. Soc. (Lond.) *A242*, 108 (1957).
Helmholtz, H. von: J. Reine Angew. Math. *55*, 25 (1858).
Joukowski, N.E.: Trans. Phys. Soc., Imp. Soc. Friends Natl. Sci. Moscow *23* (1906).
Kirchoff, G.: J. Reine Angew. Math. *70*, 289 (1869).
Kutta, W.M.: Ill. Aero. Mitt. *6*, 133 (1902).
Magnus, G.: Poggendorf's Ann. der Phys. U. Chemie *88*, 1 (1853).
Prandtl, L.: J. Roy. Aero. Soc. *31*, 730 (1927).
Theodorsen, T.: NACA Rep. 411, (1932). NACA Rep. 496 (1935).

Nonlinear Acoustic Waves

Crighton, D.G.: Ann. Rev. Fluid Mech. *11*, 11 (1979).
Crow, S.C.: Studies Appl. Math. *49*, 21 (1970).
Curle, N.: Proc. Roy. Soc. (Lond.) *A231*, 505 (1955).
Fox, P.A.: J. Math. and Phys. *34*, 133 (1955).

Fubini-Ghiron: Alta Frequenza *4*, 530 (1935).
Lighthill, M.J.: Ibid. *A211*, 564 (1952).
Lin, C.C.: J. Math. and Phys. *33*, 117 (1954).
Pan, Y.S.: J. Acoust. Soc. Am. *58*, 794 (1975).
Riemann, B.: *Collected Works*, p. 156, Dover (1953).
Sears, W.R.: AIAA J. *7*, 577 (1969).
Shivamoggi, B.K.: J. Sound Vib. *51*, 303 (1977). Ibid. *54*, 603 (1977). Ibid. *55*, 594 (1977). Ibid. *57*, 453 (1978). Ibid. *58*, 592 (1978). Arch. Mech. *33*, 603 (1981). Phys. Scripta *40*, 302 (1989). J. Sound Vib. *176*, 271 (1994).

Shock Waves

Becker, R.: Z. Phys. *8*, 321 (1922).
Burgers, J.M.: Trans. Roy. Neth. Acad. Sci. *17*, 1, (1939). Proc. Roy. Neth. Acad. Sci. *43*, 2 (1940). Adv. Appl. Mech. *1*, 171 (1948).
Chapman, D.L.: Phil. Mag. *47*, 90 (1899).
Cole, J.D.: Q. Appl. Math. *9*, 225, (1951).
Collins, R. and Holt, M.: Phys. Fluids *11*, 701 (1968).
Friedrichs, K.O.: Comm. Pure Appl. Math. *1*, 211 (1948).
Hayes, W.D.: J. Aero. Sci. *21*, 720 (1954).
Hopf, E.: Comm. Pure Appl. Math. *3*, 201, (1950).
Hugoniot, H.: J. Ecole Polytech. (1) *57*, 1 (1887). Ibid. (1) *58*, 1 (1889).
Laumbach, D.D. and Probstein, R.F.: J. Fluid Mech. *35*, 53 (1969).
Lighthill, M.J.: Phil. Mag. *11*, 1202 (1949). In *Surveys in Mechanics*, Eds. Batchelor, G.K. and Davies, R.M., Camb. Univ. Press (1956). J. Fluid Mech. *1*, 290 (1956).
Mott-Smith, H.M.: Phys. Rev. *82*, 885 (1951).
Rankine, W.J.M.: Phil. Trans. Roy. Soc. *160*, 277 (1870).
Sedov, L.I.: Dokl. Akad. Nauk. SSSR *52*, 17 (1946).
Taylor, G.I.: Proc. Roy. Soc. (Lond.) *A84*, 371 (1910). Ibid. *A201*, 159 (1950).
Truesdell, C.: J. Ratl. Mech. Anal. *1*, 125 (1952). Ibid. *2*, 593 (1953).

Subsonic Flows

Busemann, A.: Z. Angew. Math. Mech. *12*, 73 (1937).
Chaplygin, S.A.: NACA TM-1063 (1944).
Glauert, H.: Proc. Roy. Soc. (Lond.) *A118*, 113 (1928).
Hayes, W.D.: J. Aero. Sci. *22*, 284 (1955).
Kármán, T. von: Ibid. *21*, 647 (1954).
Kármán, T. von and Tsien, H.S.: Ibid. *6*, 399 (1939).
Lighthill, M.J.: Proc. Roy. Soc. *A191*, 341 and 352 (1947).
Molenbrock, P.: Arch. Math. Phys. *9*, 157 (1890).
Possio, C.: Aerotecnica *18*, 441 (1938).
Ringleb, F.: Z. Angew. Math. Mech. *20*, 185 (1940).
Shivamoggi, B.K.: AIAA J. *16*, 1310 (1978).
Tsien, H.S.: J. Aero Sci. *6*, 399 (1939).
Van Dyke, M.D.: Ibid. *21*, 647 (1954). NACA Rep. 1081 (1952).

Transonic Flows

Hosokawa, I.: J. Phys. Soc. Japan *15*, 149 (1960).
Landahl, M.T.: In *Symp. Transonicum* II, Ed. Oswatitsch, K., Springer (1976).
Murmon, E.M. and Cole, J.D.: AIAA J. *9*, 114 (1971).
Nixon, D.: Ibid. *16*, 976 (1978).
Oswatitsch, K.: Ingen. Archiv. *8*, 282 (1954). Ibid. *10*, 359 (1956).
Shivamoggi, B.K.: Mec. Appliquee *25*, 661 (1980). Arch. Mech. *35*, 5 (1983). Rozprawy Inzynierskie: Engineering Trans. *31*, 27 (1983).
Spreiter, J.R. and Alksne, A.Y.: NACA Rep. 1359 (1958).
Stahara, S.S. and Spreiter, J.R.: NASA CR-2258 (1973).
Tidjeman, H. and Seebass, R.: Ann. Rev. Fluid Mech. *12*, 181 (1980).

Supersonic Flows

Ackeret, J.: Helv. Phys.Acta *1*, 301 (1928). NACA TM-317 (1925).
Busemann, A.: Lufthrtforschung *12*, 210 (1935).
Crocco, L.: Z. Angew. Math. Mech. *17*, 1 (1937).
Kármán, T. von: J. Aero. Sci. *8*, 337 (1941).
Laitone, E.V.: Ibid. *17*, 250 (1950).
Munk, M.M.: NACA TN-1032 (1946).
Prandtl, L.: Lufthrtforschung *13*, 313 (1936).
Prandtl, L. and Busemann, A.: Stodola Festschrift *85* (1929).
Reissner, E.: NACA TN-1815 (1949).
Sears, W.: Q. Appl. Math. *4*, 191 (1946). Ibid. *5*, 89 (1947).
Stewartson, K.: Q.J. Mech. Appl. Math. *3*, 182 (1950).
Taylor, G.I. and Macoll, J.W.: Proc. Roy. Soc. (Lond.) *A159*, 459 (1937).
Tsien, H.S.: J. Aero. Sci. *5*, 480 (1938).
Tsien, H.S. and Lees, L.: Ibid. *12*, 173 (1945).
Ward, G.N.: Q.J. Mech. Appl. Math. *2*, 75 (1949).
Whitham, G.B.: Comm. Pure Appl. Math. *5*, 301 (1952).

Viscous Flows: Exact Solutions

Batchelor, G.K.: Q.J. Mech. Appl. Math. *4*, 29 (1951).
Benton, E.R. and Clark, A.: Ann. Rev. Fluid Mech. *6*, 257 (1974).
Cochran, W.G.: Proc. Camb. Phil. Soc. *30*, 365 (1934).
Ekman, V.W.: Ark. Mat. Astr. Fys. *2*, 1 (1905).
Evans, D.J.: Q. J. Mech. Appl. Math. *22*, 467 (1969).
Hagen, G.: Poggendorf's Ann. Phys. U. Chemie (2) *46*, 423 (1839).
Kármán, T. von: Z. Angew. Math. Mech. *4*, 29 (1951).
Landau, L.D.: Dokl. Acad. Sci. URSS *43*, 286 (1944).
Poiseuille, J.L.M.: Comptes Rendus *11*, 961 and 1041 (1840).
Shivamoggi, B.K.: Mec. Appliquee *27*, 101 (1982).
Squire, H.B.: Q.J. Mech. Appl. Math. *4*, 321 (1951).
Zandbergen, P.J. and Dijkstra, D.: J. Eng. Math. *11*, 167 (1977).

Stokes and Oseen Flows

Chester, W.: J. Fluid Mech. *13*, 557 (1962).
Hadamard, J.: Comptes Rendus *152*, 1735 (1911).
Kaplun, S. and Lagerstrom, P.A.: J. Math. Mech. *6*, 585 (1957).
Lamb, H.: Phil. Mag. (6) *21*, 112 (1911).
Oseen, C.W.: Ark. Mat. Abstr. Fys. *6*, 29 (1910).
Proudman, I. and Pearson, J.R.A.: J. Fluid Mech. *2*, 237 (1957).
Stokes, G.G.: Trans. Camb. Phil. Soc. *9*, 8 (1851).

Boundary–Layer Theory

Alden, H.L.: J. Math. Phys. *27*, 91 (1948).
Banks, W.H.H. and Drazin, P.G.: J. Fluid Mech. *58*, 763 (1973).
Blasius, H.: Z. Math. Phys. *56*, 1 (1908).
Busemann, L.: Z. Angew. Math. Mech. *15*, 23 (1935).
Crocco, L.: Aero. Res. Council Rep. *4*, 582 (1939).
Dean, W.R.: Mathematika *1*, 143 (1955).
Dhawan, S.: NACA Tech. Note 2567 (1952).
Goldstein, S.: Proc. Camb. Phil. Soc. *35*, 538 (1939).
Howarth, L.: Proc. Roy. Soc. (Lond.) *A194*, 16 (1948).
Kaplun, S.: Z. Angew. Math. Phys. *5*, 111 (1954).
Kármán, T. von and Tsien, H.S.: J. Aero. Sci. *5*, 227 (1938).
Lagerstrom, P.A. and Cole, J.D.: J. Ratl. Mech. Anal. *4*, 817 (1955).
Liebster, H.: Ann. Phys. *82*, 541 (1927).
Lock, R.C.: Q.J. Mech. Appl. Math. *4*, 42 (1951).
Mises, R. von: Z. Angew. Math. Mech. *7*, 425 (1927).
Prandtl, L.: Proc. III Inter. Math. Congr., Heidelberg (1904). NACA TM-452 (1928).
Schlichting, H.: *Boundary Layer Theory*, McGraw-Hill (1979).
Schmiedel, J.: Z. Phys. *29*, 593 (1928).
Shivamoggi, B.K.: Z. Angew. Math. Mech. *58*, 354 (1978).
Stewartson, K.: Proc. Roy. Soc. (Lond.) *A200*, 84 (1949).
Van Dyke, M.D.: J. Fluid Mech. *14*, 161, and 281 (1962); Ann. Rev. Fluid Mech. *1*, 265 (1969).

Separation of Boundary–Layer Flow

Brown, S.N.: Phil. Trans. Roy. Soc. *A257*, 409 (1965).
Brown, S.N. and Stewartson, K.: Ann. Rev. Fluid Mech. *1*, 45 (1969).
Goldstein, S.: Q.J. Mech. Appl. Math. *1*, 43 (1948).
Goldstein, S. and Rosenhead, L.: Proc. Camb. Phil. Soc. *32*, 392 (1936).
Landau, L.D.: *Collected Works*, Pergamon Press (1965).
Prandtl, L.: Nachr. Ges. Wiss. Gottingen Math. Phys. Klasse *177* (1914).
Sears, W.R. and Telonis, D.P.: SIAM J. Appl. Math. *28*, 215 (1975).
Stewartson, K.: Proc. Camb. Phil. Soc. *50*, 454 (1954). J. Fluid Mech. *12*, 117 (1962). Fluid Dyn. Trans. *3*, 127, Warsaw (1967). Q.J. Mech. Appl. Math. *11*, 399 (1958).
Williams, J.C.: Ann. Rev. Fluid Mech. *9*, 113 (1977).

Oscillatory Boundary Layer Flows

Lighthill, M.J.: Proc. Roy. Soc. (Lond.) *A224*, 1 (1954).
Longuet-Higgins, M.S.: Phil. Trans. Roy. Soc. *A245*, 535 (1953).
Schlichting, H.: Phys. Zeit. *33*, 327 (1932).
Shivamoggi, B.K.: Acta Mech. *33*, 303 (1979).
Stuart, J.T.: J. Fluid Mech. *24*, 673 (1966).

Jeffrey–Hamel Flow

Fraenkel, L.E.: Proc. Roy. Soc. (Lond.) *A233*, 506 (1956).
Hamel, G.: Jahresbericht der Deutschen Mathematicker Vereinigung *25*, 34 (1927).
Millsaps, K. and Pohlhaussen, K.: J. Aero. Sci. *36*, 246 (1940).
Rosenhead, L.: Proc. Roy. Soc. (Lond.) *A175*, 436 (1940).

Thermal Instability of a Fluid Layer Heated from Below

Bénard, H.: Rev. Gen. Sci. Pure Appl. *11*, 1261 and 1309 (1900).
Block, M.J.: Nature *178*, 650 (1956).
Busse, F.H.: J. Math. Phys. *46*, 140 (1967). J. Fluid Mech. *65*, 625 (1974).
Boussinesq, J.: Theorie Analytique de la Chaleur, II. p. 172, Gauthier Villars (1903).
Clever, R.M. and Busse, F.H.: J. Fluid Mech. *176*, 403 (1987).
Dubois, M. and Berge, P.: J. Fluid Mech. *85*, 641 (1978).
Gorkov, L.P.: Soviet Phys. JETP *6*, 311 (1957).
Jeffreys, H.: Phil. Mag. (7) *2*, 833 (1926).
Koschmieder, E.L.: Beitr. Phys. Atmos. *39*, 1 (1966).
Koschmieder, E.L.: *Bénard Cells and Taylor Vortices*, Cambridge University Press (1993).
Malkus, W.V.R. and Veronis, G.: J. Fluid Mech. *4*, 225 (1958).
Mihaljan, J.M.: Astrophys J. *136*, 1126 (1962).
Palm, E.: J. Fluid Mech. *8*, 183 (1960). Ibid. *30*, 651 (1967).
Palm, E.: Ann. Rev. Fluid Mech. *7*, 39 (1975).
Pellew, A. and Southwell, R.V.: Proc. Roy. Soc. (Lond.) *A176*, 312 (1940).
Reid, W.H. and Harris, D.L.: Phys. Fluids *1*, 102 (1958).
Segel, L.A.: In *Non-Equilibrium Thermodynamics*, Eds. Donelly, R.J., Herman R., and Prigogine, I. Univ. of Chicago Press (1966).
Schluter, A., Lortz, D., and Busse, F.: J. Fluid Mech. *23*, 129 (1965).
Spiegel, E.A. and Veronis, G.: Astrophys. J. *131*, 442 (1960).
Stork, K. and Muller, U.: J. Fluid Mech. *54*, 299 (1972).
Stuart, J.T.: Ibid. *18*, 481 (1964).

Stability of a Couette Flow

Chandrasekhar, S.: Mathematika *1*, 5 (1954).
Chossat, P. and Iooss, G.: *The Couette–Taylor Problem*, Springer-Verlag (1992).
Coles, D.: J. Fluid Mech. *21*, 385 (1965).
Davey, A.: Ibid. *14*, 336 (1962).

Davey, A., DiPrima, R.C. and Stuart, J.T.: Ibid. *31*, 17 (1968).
DiPrima, R.C.: Ibid. *6*, 462 (1959). Phys. Fluids *4*, 751 (1961).
Duty, R.L. and Reid, W.H.: J. Fluid Mech. *20*, 81 (1964).
Donnelly, R.J. and Schwarz, K.W.: Proc. Roy. Soc. (Lond.) *A283*, 531 (1965).
Gollub, J.P. and Freilich, M.H.: Phys. Fluids *19*, 618 (1976).
Howard, L.N. and Gupta, A.S.: Ibid. *14*, 463 (1962).
Hughes, T.H. and Reid, W.H.: Z. Angew. Math. Phys. *15*, 573 (1964).
Krueger, E.R. and DiPrima, R.C.: Phys. Fluids *5*, 1362 (1962).
Meksyn, D.: Proc. Roy. Soc. (Lond.) *A187*, 115 and 480 (1946).
Rayleigh, Lord: Ibid. *A93*, 148 (1917).
Reid, W.H.: J. Math. Anal. Applics. *1*, 411 (1960).
Synge, J.L.: Trans. Roy. Soc. Can. *27*, 1 (1933). Proc. Roy. Soc. (Lond.) *A167*, 250 (1938).
Taylor, G.I.: Phil. Trans. Roy. Soc. *A223*, 289 (1923). Proc. Roy. Soc. (Lond.) *A157*, 546, and 565 (1936).

Rayleigh–Taylor Instability

Chandrasekhar, S.: Proc. Camb. Phil. Soc. *51*, 162 (1955).
Goldstein, S.: Proc. Roy. Soc. (Lond.) *A132*, 524 (1931).
Lewis, D.J.: Ibid. *A117*, 81 (1950).
Plesset, M.S. and Hsieh, D.Y.: Phys. Fluids *7*, 1099 (1964).
Sharp, D.H.: Physica *12D*, 3 (1984).
Shivamoggi, B.K.: Acta Mech. *31*, 301 (1979).
Taylor, G.I.: Proc. Roy. Soc. (Lond.) *A132*, 449 (1931). Ibid. *A201*, 192 (1950).
Van der Voort, P.: Astrophys. J. *134*, 699 (1961).
Wesson, J.: Phys. Fluids *13*, 761 (1970).

Kelvin–Helmholtz Instability

Alterman, Z.: Phys. Fluids *4*, 1177 (1961).
Chang, I.D. and Russell, P.E.: Ibid. *8*, 1018 (1965).
Drazin, P.G.: J. Fluid Mech. *3*, 214 (1958).
Nayfeh, A.H. and Saric, W.S.: J. Fluid Mech. *46*, 209 (1971).
Shivamoggi, B.K.: Arch. Mech. *33*, 153 and 691 (1981).

Capillary Instability of a Liquid Jet

Bogy, D.B.: Ann. Rev. Fluid Mech. *11*, 207 (1979).
Rayleigh, Lord: Proc. Roy. Soc. (Lond.) *A29*, 71 (1879). Phil. Mag. (5) *34*, 177 (1892).
Uberoi, M.S., Chow, C.Y. and Narain, J.P.: Phys. Fluids *15*, 1718 (1972).
Wang, D.P.: J. Fluid Mech. *34*, 299 (1968).

Stability of Parallel Flows

Andrews, D.G.: Geophys. Astrophys. Fluid Dyn. *28*, 243 (1984).
Arnol'd, V.I.: Dokl. Akad. Nauk. SSSR *162*, 975 (1965).
Arnol'd, V.I.: Uchebn. Zaved. Matematika *54*, 3 (1966).

Banks, W.H.H., Drazin, P.G., and Zaturska, M.D.: J. Fluid Mech. *75*, 149 (1976).
Betchov, R. and Szewczyk, A.: Phys. Fluids *6*, 1391 (1963).
Bickley, W.G.: Phil. Mag. (7) *23*, 727 (1937).
Blumen, W.: J. Fluid Mech. *40*, 769 (1970).
Bouthier, M.: J. Mecanique *11*, 599 (1972). Ibid. *12*, 75 (1973).
Carnevale, G.F., Vallis, G.K., Purini, R. and Briscolini, M.: Phys. Fluids *31*, 2567 (1988).
Case, K.M.: Ibid. *3*, 143 (1960). Proc. Symp. Appl. Math. *13*, 25 (1962).
Curle, N.: Aero. Res. Council Rep. 18426, FM2400 (1956).
Davey, A.: J. Fluid Mech. *57*, 369 (1973).
Deardorff, J.W.: Ibid. *15*, 623 (1963).
DeVilliers, J.M.: Phil. Trans. Roy. Soc. *A280*, 171 (1975).
Dikii, L.A.: Sov. Phys. Dokl. *5*, 1179 (1961). J. Appl. Math. Mech. *28*, 479 (1964).
DiPrima, R.C.: J. Math. Phys. *33*, 249 (1954).
Drazin, P.A.: J. Fluid Mech. *3*, 214 (1958).
Drazin, P.A. and Howard, L.N.: Ibid. *14*, 257 (1962). Adv. Appl. Mech. *7*, 1 (1966).
Fjortoft, R.: Geofys. Publ. *17*, 1 (1950).
Friedrichs, K.O.: *Fluid Dynamics*, Brown Univ. (1942).
Gaster, M.: J. Fluid Mech. *32*, 173, (1968). Proc. Roy. Soc. *A347*, 271 (1975).
Hall, P. and Smith, F.T.: Studies Appl. Math. *66*, 241 (1982).
Heisenberg, W.: Ann. Phys. *74*, 517 (1924).
Helmholtz, H. von: Phil. Mag. (4) *36*, 337 (1868).
Howard, L.N.: J. Math. Phys. *37*, 283 (1959). J. Fluid Mech. *10*, 509 (1961). J. Mechanique *3*, 433 (1964).
Joseph, D.D.: J. Fluid Mech. *33*, 617 (1968). Ibid. *36*, 721 (1969).
Kelvin, Lord: Math. Phys. Papers *4*, 76 and 166 (1910).
Lakin, W.D., Ng, B.S. and Reid, W.H.: Phil. Trans. Roy. Soc. (London) *289*, 347 (1978).
Lamb, H.: *Hydrodynamics*, Cambridge Univ. Press (1932).
Landau, L.D.: Sov. Phys. Dokl. *44*, 139 (1944). J. Phys. USSR *10*, 25 (1946).
Lin, C.C.: Q. Appl. Math. *3*, 117, 218, and 277 (1946). J. Fluid Mech. *10*, 42, (1961).
Ling, C.H. and Reynolds, W.C.: Ibid. *59*, 571 (1973).
McKoen, C.H.: Aero. Res. Council Rep. 17952, FM 2313 (1955).
Michalke, A.: J. Fluid Mech. *19*, 543 (1964).
Miles, J.W.: Ibid. *3*, 185 (1957). Ibid. *4*, 538 (1958). Ibid. *10*, 496 (1961).
Orr, W.M.F.: Proc. Roy. Irish Acad. 27A, 9 (1907).
Orszag, S.A.: J. Fluid Mech. *50*, 689 (1971).
Orszag, S.A. and Patera, A.T.: in *Chaotic Behavior of Deterministic Systems*, Eds. Iooss, G. Helleman, R.H.G. and Stork, R. North-Holland (1983).
Pekeris, C.L.: Proc. Camb. Phil. Soc. *32*, 55 (1936).
Rayleigh, Lord: Proc. Lond. Math. Soc. *11*, 57 (1880). Ibid. *14*, 170 (1883). Phil. Mag. (5) *34*, 59 (1892). Proc. Roy. Soc. (Lond.) *A86*, 208 (1912). Phil. Mag. (6) *26*, 776 (1913). Ibid. (6) *28*, 609 (1914).
Reid, W.H.: Studies Appl. Math. *51*, 341 (1972). Ibid. *53*, 91 and 217 (1974). Ibid. *61*, 83 (1979).

Saric, W.S. and Nayfeh, A.H.: Phys. Fluids *18*, 945 (1975).
Schubauer, G.B. and Skramstad, H.K.: J. Aero. Sci. *14*, 69 (1947).
Shivamoggi, B.K.: J. Mecanique *16*, 227 (1977). J. Fluid Mech. 79, 745 (1977). Proc. Indian Acad. Sci. *A87*, 107 (1978). Acta Mech. *30*, 197 (1978). Z. Angew. Math. Mech. *59*, 405 (1979). Mec. Appliquee *25*, 353 (1980). Acta Mech. *44*, 137, 237, and 327 (1982).
Smith, F.T.: Proc. Roy. Soc. (Lond.) *A366*, 91 (1979).
Sommerfeld, A.: Proc. IV Inter. Congr. Math. Rome, 116 (1908).
Squire, H.B.: Proc. Roy. Soc. (Lond.) *A142*, 621 (1933).
Synge, J.L.: Semi. Cent. Publ. Am. Math. Soc. 2, 227 (1938).
Tam, K.K.: J. Fluid Mech. *34*, 145 (1968).
Tatsumi, T. and Gotoh, K.: Ibid. *7*, 433 (1960).
Tatsumi, T. and Kakutani, T.: Ibid. *4*, 261 (1958).
Tollmien, W.: NACA TM-792 (1936).

Nonlinear Stability Theory

Benney, D.J.: Proc. Symp. Appl. Math. *13*, 1 (1962).
Benney, D.J. and Bergeron, R.F.: Studies Appl. Math. *48*, 181 (1969).
Benney, D.J. and Lin, C.C.: Phys. Fluids *3*, 656 (1960).
Benney, D.J. and Maslowe, S.A.: Studies Appl. Math. *54*, 181 (1975).
Busse, F.H.: J. Fluid Mech. *23*, 129 (1965). Ibid. *30*, 625 (1967). Ibid. *47*, 305 (1971). Ibid. *52*, 97 (1972). Ibid. *91*, 319 (1979).
Davey, A., Hocking, L.M. and Stewartson, K.: Ibid. *63*, 529 (1974).
Dikii, L.A.: J. Appl. Math. Mech. *29*, 1009 (1965).
Greenspan, H.P. and Benney, D.J.: J. Fluid Mech. *15*, 133 (1963).
Haberman, R.: Studies Appl. Math. *51*, 139 (1972).
Hasselmann, K.: J. Fluid Mech. *30*, 737 (1967).
Joseph, D.D.: *Stability of Fluid Motions*, Springer-Verlag (1976).
Maslowe, S.A.: Ibid. *79*, 689 (1977).
Meksyn, D. and Stuart, J.T.: Proc. Roy. Soc. (Lond.) *A208*, 517 (1951).
Nishioka, M. and Asai, M.: J. Fluid Mech. *150*, 441 (1985).
Reynolds, W.C. and Potter, M.C.: Ibid. *27*, 465 (1967).
Smith, F.T.: Proc. Roy. Soc. (Lond.) *A368*, 573 (1979).
Stewartson, K. and Stuart, J.T.: J. Fluid Mech. *48*, 529 (1971).
Stuart, J.T.: Ibid. *4*, 1 (1958). Ibid. *9*, 353 (1960); Ann. Rev. Fluid Mech. *3*, 347 (1971).
Watson, J.: Ibid. *9*, 371 (1960).

Turbulence

Batchelor, G.K.: J. Aero. Sci. *17*, 441 (1950). Phys. Fluids Suppl. II, 233 (1969).
Boussinesq, J.: *Theorie de l'écoulement tourbillonant*, Paris (1897).
Frisch, U.: *Turbulence*, Cambridge University Press (1995).
Grant, H.L., Stewart, R.W. and Moilliet, A.: J. Fluid Mech. *12*, 241 (1962).
Hasegawa, A.: Adv. Phys. *34*, 1 (1985).
Heisenberg, W.: Z. Phys. *124*, 628 (1948).
Kármán, T. von and Howarth, L.: Proc. Roy. Soc. (Lond.) *A164*, 192 (1938).

Kistler, A.L., O'Brien, V. and Corrsin, S.: J. Aero. Sci. *23*, 96 (1956).
Kolmogorov, A.N.: C.R. Acad. Sci. URSS *30*, 301 (1941). Ibid. *31*, 538 (1941). Ibid. *32*, 16 (1941). J. Fluid Mech. *13*, 82 (1962).
Kraichnan, R.H.: J. Fluid Mech. *5*, 497 (1959); Phys. Fluids *7*, 1030 (1964); Ibid. *10*, 1417 (1967). J. Fluid Mech. *67*, 155 (1975).
Lee, T.D.: Q. Appl. Math. *10*, 69 (1952).
Lin, C.C.: Proc. Nat. Acad. Sci. *46*, 566 and 1147 (1960).
Loitsiansky, L.G.: NACA TM-1079 (1945).
Obukov, A.M.: C.R. Acad. Sci. URSS *32*, 19 (1941).
Ohkitani, K. and Kida, S.: Phys. Fluids *A4*, 794 (1992).
Reynolds, O.: Phil. Trans. Roy. Soc. *171*, 935 (1883). Ibid. *174*, 177 (1886).
Richardson, L.F.: Proc. Roy. Soc. (Lond.) *A110*, 709 (1926).
Shivamoggi, B.K.: Helv. Phys. Acta *64*, 1112 (1991). Ann. Phys. (N.Y.) *243*, 169 and 177 (1995). Ibid. *253*, 265 (1997). Europhys. Lett.*38*, 657 (1997).
Sommeria, J.: J. Fluid Mech. *170*, 139 (1986).
Taylor, G.I.: Proc. Lond. Math. Soc. (2) *20*, 196 (1921). Proc. Roy. Soc. (Lond.) *A151*, 421 (1935). Ibid. *A154*, 476 (1938).
Townsend, A.A.: Proc. Camb. Phil. Soc. *43*, 560 (1947).
Van Heijst, G.J.F. and Flor, J.B.: Nature *340*, 212 (1989).

SUBJECT INDEX